The Technology of Tang Sancai Glaze



Yun Zhang

Linacre College

University of Oxford

Thesis, submitted for the degree of

Doctor of Philosophy in Archaeological Science

Trinity 2023

For my parents, Dongxia Li and Yanqiang Zhang,

who have encouraged and supported me to explore the world,

and always kept a light on, waiting for me to come home.

Acknowledgement

I wish to begin by expressing my deepest gratitude to my dedicated supervisors, Prof. Mark Pollard, and Dr Chris Doherty. My appreciation for Mark knows no bounds as he provided invaluable help, unwavering support, endless inspiration, and encouragement, especially during the pivotal decision to change the thesis topic in my third year at Oxford. Mark's patient guidance and steadfast companionship enabled me to explore this new research area and complete this seemingly insurmountable thesis within just two years. I owe a debt of gratitude to him that words cannot fully convey. I would also like to extend my thanks to my second supervisor, Chris Doherty, for the memorable moments spent observing samples in the charming yet dimly lit SEM room.

My heartfelt thanks extend to my collaborators in China – Mr. Hui Li, Mr. Yongqing Hu, Ms. Yunhua Heng and Ms. Xin Liu from the Henan Provincial Institute of Cultural Heritage and Archaeology, and Ms. Xiaomeng Wang and Ms. Menghe Cui from the Shaanxi Academy of Archaeology. Their generosity in offering their assistance and support granted me access to analyse the precious Sancai samples unearthed from the Gongyi and Liquanfang kilns.

Furthermore, I wish to express my gratitude to Prof. Rui Wen, Dr Dong Wang, Yulai Chen, Yulong Li, and Kun Cao at Northwest University, and Kai Cao at Nanjing University for their unwavering assistance during my fieldwork and laboratory research in China.

My sincere appreciation goes out to my besties – Naihui Wang at Max Planck Institutes in Germany, Xintong Li at Fudan University in China, and Rubi Wu, Siyi Wu,

Xuyang Gao, Dr Quan Zhang, Dr Yinghong Wang, Dr Lili Yang, and Dr Xi Chen at the University of Oxford in the UK. Throughout our respective PhD journeys, we were not just companions but pillars of support for each other. Despite being in different countries and cities now, I hold firm to the belief that women empower and uplift each other, forever.

I am also appreciative of my examiners, Prof. Nigel Wood, and Prof. Shadreck Chirikure, for their insightful comments and valuable guidance throughout the examination process.

Finally, I reserve the deepest part of my gratitude for my parents, Dongxia Li and Yanqiang Zhang. Despite facing financial hardships that prevented my parents from pursuing higher education in their own youth, they worked tirelessly to support me both financially and emotionally in my pursuit of my dream at Oxford. My family remains my everlasting source of happiness.

Abstract

Tang Sancai has long been attributed to the peak of the Chinese lead glaze tradition and the beginning of the use of cobalt blue on Chinese ceramics. However, the Sancai glaze rarely preserves mineral grains of raw materials after glaze firing. The author collected 66 raw (unfired) glazed sherds from two official excavations of the Gongyi kiln in 2002-4 and 2015, which offered the first and a rare opportunity to find direct evidence for the technology of Sancai glaze from the raw glaze. This thesis aims to reveal the raw materials and manufacturing techniques of Tang Sancai glaze by analysing raw glazes in the optical microscope (OM), energy dispersive X-ray fluorescence spectroscopy (EDXRF) and scanning electron microscopy with energy dispersive spectroscopy (SEM-EDS).

The unfired colours of raw clear white, iron-brown, copper-green, and cobalt-blue glazes are similar by visual observation – various shades of brown. The first research question is to establish a classification standard for raw glazes. Seventeen pieces were selected and fired in the muffle furnace at 850℃. The standard is established by comparing the chemical data and colour changes of raw and fired glazes. Based on this classification, the core research questions – colourant types and origins, glaze recipe and processing methods, were discussed. This research reveals that the raw clear glaze is the shared base of raw coloured glaze. Raw brown, green and blue glazes were produced by adding iron, copper, and cobalt colourants into the clear glaze (stock glaze). The iron-brown colourant is ore powder made of hematite. Copper-green colourants include malachite and chrysocolla. These green minerals also might be supplied with a

bag of mixed copper minerals. Startlingly, the cobalt material is likely to be powdered cobalt glass which was fluxed by Mg or Mg and K together. The original cobalt ore of this glass might be a low-iron, trace-manganese (high-Fe_2O_3/MnO), low-copper, uncertain-arsenic, no-nickel, no-zinc cobalt ore. Some characteristics of the ore of this cobalt glassy pigment are similar to the Yuan-Dynasty (1271-1368 CE) blue-and-white porcelain but the cobalt mine used in Tang Sancai might be not in Kāshān. The hematite colourant is relatively coarse, but the copper and cobalt colourants are very fine powder. The contents added of hematite is around 3%, and those of copper minerals and cobalt glass are both about 1%.

The clear glaze (stock glaze) was made from kaolinitic clay, quartz (flint and sand), high-Ca-and-P material and white lead. The local kaolinitic clay was exploited and directly added to the stock glaze after physical grinding to provide Al and some Si. The flint and sand both brought in a considerable quantity of silica. They were heated followed by rapid cooling to break up into small particles. Si and Al act as the framework of the glaze. Ca, P and Pb work as the flux. Pb was made from white lead which refers to $PbCO_3$ and $2PbCO_3 \cdot Pb(OH)$. It was also ground into fine powder to be added to the glaze. Regarding the sources of Ca and P, further analysis is required due to current scientific limitations. The presence of certain textural characteristics of some remains suggests the potential use of wood ash, although the high P_2O_5 levels cannot be explained solely by wood ash. Whether XRF instrumentation limitations inflated phosphorus content or other phosphorus-rich materials were employed in Sancai glazes remains an open question. If wood ash was introduced by potters, calcium and phosphorus content may have been contributed by limestone and unidentified wood sources, which were calcinated together to create the wood ash. The proportions of

these four main ingredients are approximately one-part kaolinitic clay, two-part quartz (flint and sand), three-part white lead, and some calcium and phosphorus-rich material, with the latter likely present in lower quantities compared to white lead.

Contents

List of Figures ..... **i**

List of Tables ..... **xix**

Glossary of Terms ..... **xxi**

Chapter 1 Introduction **1**

1.1 Lead Glazes 1

1.1.1 Beginning of Lead Glaze in the Warring States (475-221 BCE) 1

1.1.2 Evolution of Lead Glaze in the Han Dynasty (202 BCE-220 CE) 4

1.1.3 Breakthrough of Lead Glaze in the Northern Dynasties (420 CE - 589 CE) 7

1.1.4 Glory of Lead Glaze in the Tang Dynasty (618 – 907 CE) 10

1.1.5 Survival of Lead Glaze in the Liao (916-1125 CE), Song (960-1279 CE), and Jin (1115-1234 CE) Dynasties 18

1.1.6 Transformation of Lead Glaze in the Yuan Dynasty (1271-1368 CE) 24

1.2 Tang Sancai Kilns 29

1.2.1 Gongyi Kiln 30

1.2.2 Liquanfang Kiln 33

1.2.3 Gongyi and Liquanfang: Related Kiln Sites? 37

1.3 Why Tang Sancai and Why Gongyi? 42

Chapter 2 Samples and Methodology **45**

2.1 Samples 45

2.1.1 Archaeological Investigations of the Gongyi Kiln 46

2.1.2 Sample Collection and Description 47

2.2 Scientific Methods 56

2.2.1 Optical Microscopy (OM) 57

2.2.2 Energy Dispersive X-ray Fluorescence Spectroscopy (EDXRF).....57

2.2.3 Scanning Electron Microscopy with Energy Dispersive Spectrometry (SEM-EDS).....60

Chapter 3 Colours.....**63**

3.1 Experimental Glaze Firing.....63

3.2 Standards of Raw Coloured Glazes.....68

3.2.1 Colour Changes of Experimental-fired Samples.....68

3.2.2 Establishment of Standards.....81

3.3 Classification of Raw Glazes.....87

3.3.1 Special Samples.....87

3.3.2 Raw Coloured Glazes.....91

Chapter 4 Colourants.....**95**

4.1 Iron Brown.....95

4.2 Copper Green.....114

4.3 Cobalt Blue.....131

4.3.1 Cobalt Glass.....132

Smalt or not?.....132

Base and flux.....140

Possible ore type.....142

Mn.....143

Fe.....148

As.....154

Cu.....155

4.3.2 Colouring and Weathering.....163

4.3.3 Manufacturing and Applying.....164

Chapter 5 Glazes.....**167**

5.1 Stock Glaze Recipe 167

5.1.1 Clay or Feldspar? 169

5.1.2 Flint and Sand? 193

5.1.3 Ash or Mineral? 207

5.1.4 Which Lead? 225

5.2 Glaze Making 234

5.2.1 From Raw Materials to Stock Glaze 234

5.2.2 From Stock Glaze to Coloured Glazes 238

Chapter 6 Conclusions and Future Work 240

Bibliography 244

Appendices 263

Appendix 1 Description of samples unearthed from the Gongyi kiln site (II and III areas) in 2002-2004 263

Appendix 2 Description of samples unearthed from the Gongyi kiln site in 2015 267

Appendix 3 The scientific methods of Tang Sancai in publications 287

Appendix 4 Two tests of corning glasses B, C and D 293

Appendix 5 EDXRF testing areas of samples for experimental glaze firing 296

Appendix 6 Chemical compositions of samples for experimental glaze firing 299

Appendix 7 Chemical compositions of bodies 306

Appendix 8 Chemical compositions of clear glazes 312

Appendix 9 Chemical compositions of brown glazes 323

Appendix 10 Chemical compositions of green glazes 343

Appendix 11 Chemical compositions of blue glazes 347

Appendix 12 Chemical compositions of special samples 350

Appendix 13 Chemical compositions of slips 354

List of Figures

Figure 1. 1 (a) Photo of a Warring-States glazed pottery jar (H. 9.5cm) with highly weathered lead glazes, obtained from Wood (1999, p.190). The original glaze colours would have been red, yellow and blue on a white-glaze ground. The jar is collected in the British Museum in UK. (b) Photo of a Warring-States glazed bead (L. 2 cm) with stonepaste body and red, blue and yellow glazes on a white ground, obtained from Wood (1999, p.191). The bead is collected by the British Museum. (c) Photo of an Eastern-Zhou-dynasty glazed pottery Lei (H. 27 cm), obtained from Chen (2021). This Lei was found in Luoyang and collected in the Nelson- Atkins Museum of Art in USA. (d) Photo of a Warring-States bronze Lei, from Lang and Cui (2017). It was excavated in Linzi. 3

Figure 1. 2 (a) Map of Qi, a state of Zhou dynasty in ancient China. Qi was variously reckoned as a vassal state, duchy, and independent kingdom which was founded 1046 BCE and was replaced by Qin in 221 BCE. The extent of the Qi state changed over time. The yellow area in the map presents the border of Qi in 260 BCE and the red spot marks the location of capital of Qi, Linzi. The map is from https://en.wikipedia.org/wiki/Qi_(state)#/media/File:EN-QI260BCE.jpg (b) Photo of one of the glazed pottery Lei (H. 27cm) excavated from an elite tomb of Qi state in Linzi, from Chen (2021). 4

Figure 1. 3 (a) Photo of a brown-glaze oven model found in Jiyuan, Henan province. (b) Photo of a green-glaze food container found in Nanchang, Jiangxi province. (c) Photo of a two-coloured glazed Zun (Chinese: 樽). Photos were from Wang and Tian (2010). 6

Figure 1. 4 (a) Photo of Han glazed pottery excavated from Yan'an, Shaanxi: (1–8) Hu; (9–11) Ding; (12–15) Zao; (16–20) Cang; (21) Fang; (22) Zun; (23) Guan; (24) flattened Hu; (25) Boshan incense burner; (26) incense burner; (27) Pan; (28) Xiao Hu; (29) duck-shaped Hu; (30) pig-shaped glazed pottery, cited from Chen et al. (2020). The white /silver motifs on the surfaces of wares were caused by weathering. The original colour is green. According to the author's introduction, No.6, 7, and 27 are monochrome wares, and others are two-coloured wares. (b) Map of the distribution and locations of archaeological findings of two-coloured glazed potteries in the Han dynasty, developed from Wang (2018). The black spots present the locations of findings of two-coloured glazed potteries. And the circles present the distribution

areas. (c) Box plot of PbO, BaO, CuO and Fe_2O_3 of Han-dynasty glazes, obtained from Chen et al. (2020). 7

Figure 1. 5 (a) Photo of polychrome bowl excavated from Lou Rui tomb (570 CE), from http://kaogu.cssn.cn/zwb/xsdt/xsdt_3347/xsdt_3348/202205/t20220516_5408447.shtml. (b) Photo of green-and-white flask unearthed from Fan Cui tomb (575 CE), from http://www.chnmus.net/sitesources/hnsbwy/page_pc/bwzl/yyhxzzjd/cpsx/article62aab56cfb474ef8b5%200a046b23c815b0.html. (c) Photo of the green-and-yellow jar (H. 23.5 cm) found in Li Yun tomb (576 CE), from https://www.dpm.org.cn/collection/ceramic/226731.html?hl. (d and f) Photos of dark green and brown glazed inkstone (H. 6.9-7.2cm) and jar (H. 24 cm) unearthed from Li Yi couple tomb (534 CE), obtained from Shen et al. (2015). (e and g) Photos of dark green glazed dog figure (H. 10cm) and human figures (H. 20.8 cm) found in a Northern-Wei tomb in Datong, Shanxi province, from Zhang et al. (2022). 10

Figure 1. 6 Photos of (a) Sancai heavenly guardian (118cm), (b) Sancai tomb guardian beast (H. 80.5cm), (c) Sancai horse figure (H. 76.5cm), (d) Sancai horseman figure and (e) a model for a female figure. Sancai figures (a), (b) and (c) are collected in the Palace Museum and photos are from (a) https://www.dpm.org.cn/collection/ceramic/227537.html, (b) https://www.dpm.org.cn/collection/sculpture/233434.html, and (c) https://www.dpm.org.cn/collection/ceramic/227486.html. (d) The figure riding a horse was excavated from Yide Prince tomb, and its face was painted by pigments after glaze firing. (e) Mould unearthed from the Liquanfang kiln site. (d) and (e) Photos were from Wang (2018). 12

Figure 1. 7 Photos of blue Sancai: (a) female figure (H. 45 cm) excavated from Zhongbaocun tomb in Xi'an, taken by the author; (b) camel-carrying-musicians figure (H. 58.4 cm) found in Xianyu Tinghui tomb (Ma and Zhang, 1958), from http://kgzg.cn/a/396228.html; (c) acrobatic figure (H. 40.8 cm) contained in tomb M31 in southern outskirts in Xi'an, obtained from Sun et al. (2004); (d) pot (H. 14.7 cm) from Yangjia Weiqiang Tomb, obtained from Guan et al. (2012). (e) Sancai cover button (D. 2.8 cm, H. 3 cm) from Zheng Rentai tomb, taken by the author; (f) blue-and-white Sancai bowl excavated from the Gongyi kiln site, obtained from Henan Provincial Institute of Cultural Heritage and Archaeology et al. (2016a, p.230); (g) blue Deng (lamp) (H. 33.6 cm) unearthed from Gonglin, obtained from Wang (2011). 13

Figure 1. 8 Photo of glass beads from Xujialing Site, obtained from Gan (2016, p.274). 16

Figure 1. 9 Photos of Tang blue-and-white: (a-f) sherds found in the Gongyi kiln, obtained from Henan Provincial Institute of Cultural Heritage and Archaeology et al. (2009, pp.165-167) and Henan Provincial Institute of Cultural Heritage and Archaeology et al. (2005, p. 145); (g) sherd unearthed in Siraf, a port city of Persian Gulf, from Spataro et al. (2019); (h) plate uncovered from the Belitung Shipwreck and collected in Asian Civilisations Museum in Singapore, taken by the author.....17

Figure 1. 10 Photos of typical Samarra-type pottery: (a) white glaze with cobalt blue decoration (the Metropolitan Museum of Art, acc. no. 63.159.4); (b) white glaze with cobalt blue and green decoration (Freer and Sackler Galleries, acc. no. F2000.2); (c) splash glazed (the Metropolitan Museum of Art, acc. no.30.112.46), obtained from Matin (2016, p.8).....17

Figure 1. 11 Photos of Nara Sancai, obtained from Zi (2011).....17

Figure 1. 12 Photos of Bohai Sancai excavated in Longhai royal tomb of Bohai state, cited from Wang and Yang (2021). 18

Figure 1. 13 Map of (a) Liao (Khitan) (purple area) and Song (orange area) dynasties in 1111 CE, (b) Jin (blue area) and Song (orange area) dynasties in (1141 CE), from (a) https://en.wikipedia.org/wiki/Administrative_divisions_of_the_Liao_dynasty#/media/File:Song-Liao-Xixia-1111.png and (b) http://en.wikipedia.org/wiki/Jin_dynasty_(1115%E2%80%9 21

Figure 1. 14 Photos of Song Sancai: (a) and (b) human figures, (c) animal figures, (d) and (f) pillows (f-1 H. 9 cm, f-2 H.10.3 cm, f-3 H. 9.6 cm), and (e) bowl (H. 6.5 cm). Photos (a), (b) and (c) were from Li (2011), (d) was obtained from Wang (2011), and (e) and (f) cited from Yang and Zhao (2015). 22

Figure 1. 15 Photos of Jin Sancai: (a) pillows, from Li (2011); (b) vase, bowl and censer, from Zhang and Ma (2000); (c) Deng (lamps), from Zhang and Zhang (2020). 23

Figure 1. 16 Photos of Liao Sancai: (a) figure of Buddha, Deng (lamp) and plate, obtained from Yao (2017); (b) plate, animal-shaped pot, and heat retainer, from Shan (2019). 23

Figure 1. 17 Photo of Song blue-and-white sherds excavated from the foundation of Jinsha Pagoda in Longquan, southern China, obtained from Zhejiang Provincial Museum (https://www.zhejiangmuseum.com/Collection/ExcellentCollection/602zonghepingtaiexhibit/

602zonghepingtaiexhibit). This image only shows both sides of two sherds from two bowls. Two fragments on the left are regarded as one joint sherd because they belong to one bowl (Ruan, 1990; Zhu, 1980). 24

Figure 1. 18 Photos of Yuan 'Sancai' plates and pillows, obtained from Wang (2012). 26

Figure 1. 19 Photos of blue glazed (a-c) vase, pots, and (d-h) figures. Blue vessels were excavated from DZXM29 tomb in Zhenzishan which was the biggest cemetery situated about nine kilometres as the crow flies to the southeast of Shangdu Site of the Yuan dynasty (Wei, 2008a, p.328). The colour of (a) and (c) was described as black (Wei, 2008a, pp.396-397), however the photos show dark blue (Wei, 2008b, p.216). (d-h) Blue figures unearthed in a Yuan-dynasty tomb, from Ji (2001). According to Ji (2001)'s description in the report, the blue area was outlined by blue lines. 27

Figure 1. 20 (a-c) Photos of glazed tile sherds excavated from Grand Bao'en Temple in Nanjing, obtained from Tang et al., (2022). (d) Photo presents the roof of some halls in the Palace Museum, from https://www.dpm.org.cn/building/talk/225255.html. (e) Photo of a tile fragment of Shenwu Gate in the Palace Museum, from Kang et al. (2013). 28

Figure 1. 21 Map of Tang Empire around 660s CE and the locations of six Sancai kilns (green spots), and two capital cities of Tang Empire – Chang'an (618-683 CE and 705-904 CE) and Luoyang (664-705 CE and 904-907 CE) (red stars), developed from https://en.wikipedia.org/wiki/Tang_dynastwordy#/media/File:Tang_circuits_660.png. 30

Figure 1. 22 Map of the Gongyi kiln sites and locations of Gongyi and its towns, developed from Henan Provincial Institute of Cultural Heritage and Archaeology et al. (2016b, p.2) and Li et al. (2017). The red star presents the location of Luoyang, the eastern capital city of Tang Empire. And the green spots present the locations of Gongyi city and its towns. Black triangular symbols show the excavation sites of the Gongyi kiln. 33

Figure 1. 23 (a) Map of Chang'an city during the Tang dynasty showing the location of Liquanfang, which refers to the block (yellow area) and the Liquanfang kiln (red triangle in the yellow area), developed from Shaanxi Provincial Institute of Archaeolog (2008, p.5). 36

Figure 1. 24 Structure of two kilns in the Huangye and Liquanfang kiln sites, obtained from Henan Provincial Institute of Cultural Heritage and Archaeology et al. (2016b, p.5) and Shaanxi Provincial Institute of Archaeology (2008, p.18). 39

Figure 1. 25 (a-d) Photos of Huangye products and (e-h) Liquanfang products, obtained from (a-d) Henan Provincial Institute of Cultural Heritage and Archaeology et al. (2005, p.108, 133, 141 and 143), and (e-h) Shaanxi Provincial Institute of Archaeology (2008, p.5, picture list 11, 26, 29). 40

Figure 1. 26 Map of the Sui-Tang Canal, developed from https://en.wikipedia.org/wiki/Grand_Canal_(China)#/media/File:ChinaGrand_canal,_Sui_and_Tang.svg. Two red stars represent capitals, and the orange spot and two blue spots mark the locations of Yangzhou and two kilns producing blue Sancai wares.....40

Figure 1. 27 Image of the simplified development of lead glazes from the Warring States to Yuan dynasty and of blue-and-white porcelain from the Tang to Yuan dynasties. The colour of spots presents the colour of glazes, and the blue squares presents cobalt pigment. 43

Figure 2. 1 Manufacturing process of Tang Sancai, source of photos of kaolinitic clay: https://www.britannica.com/science/kaolin and https://en.wikipedia.org/wiki/Kaolinite. 49

Figure 2. 2 Maps of the archaeological excavation in 2002-2004 (left) and in 2015 (right). Left: image was obtained from Henan Provincial Institute of Cultural Heritage and Archaeology et al. (2016b, p.9). Yellow areas show the location of sample collection. Right: the map is provided by a local excavator and archaeologist, Mr Hui Li. Yellow circle presents the excavation in 2015 and the sample collection area as well. 49

Figure 2. 3 Photos of the inside of 8 samples from the Gongyi kiln in 2002-2004, taken by the author. 50

Figure 2. 4 Photos of the outside of 8 samples from the Gongyi kiln in 2002-2004, taken by the author. 50

Figure 2. 5 Photos of the inside of 32 samples (HY-38 – HY-147) from the Gongyi kiln in 2015, taken by the author. 51

Figure 2. 6 Photos of the inside of 26 samples (HY-148 – HY-188) from the Gongyi kiln in 2015, taken by the author. 52

Figure 2. 7 Photos of the outside of 32 samples (HY-38 –HY-147) from the Gongyi kiln in 2015, taken by the author. 53

Figure 2. 8 Photos of the outside of 26 samples (HY-148 – HY-188) from the Gongyi kiln in 2015, taken by the author. 54

Figure 2. 9 Photo of Corning glasses B, C and D, taken by the author. 59

Figure 2. 10 Comparison between mean values and real values of three Corning glasses..... 60

Figure 3. 1 Photo of samples before experimental glaze firing 66

Figure 3. 2 Left: Photo of the muffle furnace in Northwest University. Right: Photo of samples and inside of the muffle furnace. Photos were taken by the author in the Key Laboratory of Cultural Heritage Study and Conservation at Northwest University, China. 66

Figure 3. 3 Line chart of scheduled heating procedure of the experimental glaze firing by the muffle furnace. 66

Figure 3. 4 Photo of samples after experimental glaze firing, taken by the author. 67

Figure 3. 5 Photo of unfired and fired samples (one side), taken by the author. Black labels mark samples before experimental glaze firing and red labels represent sherds after firing... 71

Figure 3. 6 Photo of unfired and fired samples (the other side), taken by the author. Black labels mark samples before experimental glaze firing and red labels represent sherds after firing... 73

Figure 3. 7 Photos of unchanged samples after the experimental glaze firing, obtained from observation by the optical microscope. Black labels mark samples before experimental glaze firing and red labels represent sherds after firing. 73

Figure 3. 8 Photos of special changes of three re-fired pieces, obtained from observation by the optical microscope. Black labels mark samples before experimental glaze firing and red labels represent sherds after firing. The white numbers in the photo of HY-149 and HY-136 present the thickness of dark layers. 74

Figure 3. 9 Colour changes of clear glazes before and after the experimental glaze firing, obtained from observation by the optical microscope. Font colours mark samples before experimental glaze firing (black colour) and after firing (red colour). 77

Figure 3. 10 Colour changes of brown glazes before and after the experimental glaze firing, obtained from observation by the optical microscope. Font colours mark samples before experimental glaze firing (black colour) and after firing (red colour). 78

Figure 3. 11 Colour changes of green glazes (HY-38 and HY-132) and before and after the experimental glaze firing. Font colours mark samples before experimental glaze firing (black colour) and after firing (red colour). Photos were obtained from observation by the optical microscope. 79

Figure 3. 12 Colour changes of blue glazes (HY-43) before and after the experimental glaze firing. Font colours mark samples before experimental glaze firing (black colour) and after firing (red colour). Photos were obtained from observation by the optical microscope..... 79

Figure 3. 13 Hypothesis of glaze-making technology. 80

Figure 3. 14 Bar chart of Fe_2O_3 in raw glazes and fired glazes. 84

Figure 3. 15 Bar chart of CoO in raw and fired glaze..... 84

Figure 3. 16 Bar chart of CuO in raw and fired glaze..... 85

Figure 3. 17 Box plot of Fe_2O_3/CuO in raw glazes..... 85

Figure 3. 18 Bar chart of percentages of Fe_2O_3, CuO and CoO in raw glazes. 85

Figure 3. 19 Flow chart of raw glaze classification. 86

Figure 3. 20 Special samples covered by unknown red materials. Photos of sherds were taken by the author and photos of surfaces were obtained from observation by the optical microscope. 89

Figure 3. 21 Other special samples. Photos of sherds were taken by the author and photos of surfaces were obtained from observation by the optical microscope. 91

Figure 3. 22 Colours of all glazes on HY-43 sherd, photos taken by the author. 92

Figure 3. 23 (a) Bar chart of glaze classification. (b) Bar chart of colour combinations of raw glazes..... 94

Figure 4. 1 Test bar, showing the effect of adding red iron oxide (Fe_2O_3) in 1% increments to a high-lead glaze, source from Wood (1999, p.161). In these quantities, Fe_2O_3 dissolved in the molten glaze to give Fe^{3+} ions, was fired to 1060℃ in oxidation. 96

Figure 4. 2 Box plot of Fe_2O_3 in raw glazes 97

Figure 4. 3 BSE (left), SE (centre) and chemical mapping (right) images of Fe-O-associated particles (yellow circles) in raw brown glazes, obtained from the ESEM.....99

Figure 4. 4 BSE (left), SE (mid-left), chemical mapping (mid-right) images and line scan charts (right) of Fe-O-associated particles (yellow circles) in the raw brown glaze of HY-43, HY-92 and HY-129, obtained from the ESEM.....100

Figure 4. 5 Test areas of Fe-O-associated particles in raw brown glazes. BSE images were obtained from the ESEM. 100

Figure 4. 6 Photos of raw brown glazes in dark red colour, obtained from observation by the optical microscope. 103

Figure 4. 7 Sizes of iron particles in raw brown glazes, obtained from the ESEM. 104

Figure 4. 8 BSE (left), SE (centre) and chemical mapping (right) images of Fe-Mg-Si-Al-O-associated particles in raw brown glazes of HY-136, HY-121, HY-38, obtained from the ESEM. 105

Figure 4. 9 BSE (top left), SE (bottom left), chemical mapping (centre) images and line scan charts (right) of the Fe-Mg-Si-Al-O-associated particle in the brown glaze of HY-123, obtained from the ESEM. 106

Figure 4. 10 BSE (top left), SE (bottom left), chemical mapping (centre) images and line scan charts (right) of the Fe-Mg-Si-Al-O-associated particle in the brown glaze of HY-151, obtained from the ESEM. 106

Figure 4. 11 BSE (top left), SE (bottom left), chemical mapping (centre) images and line scan charts (right) of the Fe-Mg-Si-Al-K-O-associated particle in the brown glaze of HY-152, obtained from the ESEM. 107

Figure 4. 12 Test areas of iron particles in raw brown glazes, obtained from the ESEM. The area labelled with spec 9 of HY-151 presented a Na-Al-Si-associated particle. 107

Figure 4. 13 BSE (top left), SE (bottom left), chemical mapping (centre) images and line scan charts (right) of the Fe-Mg-Si-Al-K-O-associated particle in the clear glaze of HY-59, obtained from the ESEM. 109

Figure 4. 14 BSE (top left), SE (bottom left), chemical mapping (centre) images and line scan charts (right) of the Fe-Mg-Si-Al-O-associated particle in the clear glaze of HY-123, obtained from the ESEM. 109

Figure 4. 15 BSE (top left), SE (bottom left), chemical mapping (centre) images and line scan charts (right) of the Fe-Mg-Si-Al-K-O-associated particle (green circles) in the green glaze of HY-38, obtained from the ESEM. 110

Figure 4. 16 BSE (top left), SE (bottom left), chemical mapping (centre) images and line scan charts (right) of Fe-Mg-Si-Al-O-associated particle (green circles) in the green glaze of HY-136, obtained from the ESEM. 110

Figure 4. 17 BSE (top left), SE (bottom left), chemical mapping (centre) images and line scan charts (right) of Fe-Mg-Si-Al-K-O-associated particles in the blue glaze of HY-43, obtained from the ESEM. 111

Figure 4. 18 BSE (top left), SE (bottom left) and mapping (centre) images and line scan charts (right) of the Fe-Mg-Si-Al-O-associated particles (blue circles) in the blue glaze of HY-43, obtained from the ESEM. 112

Figure 4. 19 Scatter diagrams of (a) Al_2O_3 and Fe_2O_3 in raw glazes, and of (b) SiO_2 and Fe_2O_3 in raw glazes. 112

Figure 4. 20 Test areas of Fe-Mg-Si-Al-(K)-O-associated particles in raw clear, green and blue glazes, obtained from the ESEM. 112

Figure 4. 21 Box plot (left)) of CuO in raw glazes and photos (centre and right) of azurite, malachite and atacamite. This azurite ore is from Anhui in China, and malachite ore is from Zaire in Africa. Photos of azurite and malachite ores were obtained from Driscoll et al. (2011). Photo of atacamite presents sparking deep green crystallised atacamite covering a green malachite matrix, from https://en.wikipedia.org/wiki/Atacamite#/media/File:Atacamite_on_malachite_-_Mt_Gunson_mines,_South_Australia.jpg. 114

Figure 4. 22 BSE (left), SE (centre left), chemical mapping (centre right) images and line scan charts (right) of Cu-O-associated particles (green circles) in the raw green glazes of HY-166, obtained from the ESEM. 116

Figure 4. 23 BSE (left), SE (centre) and chemical mapping (right) images of Cu-O-associated particle (green circles) in the raw green glaze of HY-166, obtained from the ESEM.....116

Figure 4. 24 Texture of Cu-O-associated particles in green glazes of HY-166, obtained from the ESEM.....117

Figure 4. 25 Texture of malachite crystals, from (a) Woods and Garrels (1986), (b) and (c) Bublikova et al. (2022), (d) and (e) https://www.alexstrekeisen.it/english/meta/malachite.php#:~:text=Malachite%20is%20a%20green%2C%20very,as%20mammillary%20aggregates%20as%20well.....118

Figure 4. 26 Photos of green grains (green circles) in the raw green glaze of HY-166 and HY-132, obtained from the optical microscope.....118

Figure 4. 27 BSE (top left), SE (bottom left), chemical mapping (centre) images and line scan charts (right) of the Cu-Si-Al-K-O-associated particle in the raw green glaze of HY-136, obtained from the ESEM. 120

Figure 4. 28 BSE (top left), SE (top right), chemical mapping (bottom left) images and the line scan chart (bottom right) of a pure Cu particle in the raw green glaze of HY-136, obtained from the ESEM.....121

Figure 4. 29 BSE (top left), SE (top right), chemical mapping (bottom left) images and the line scan chart (bottom right) of a pure Cu particle in the raw green glaze of HY-136, obtained from the ESEM.....121

Figure 4. 30 BSE (top left), SE (top right), chemical mapping (bottom left) images and line scan charts (centre and bottom right) of Cu-V-Pb-associated particles in the raw brown glaze of HY-38, obtained from the ESEM. The Cu-V-Pb-rich areas cannot be distinguished from the high lead areas, which are both very light in the BSE image. The chemical mapping of Cu and V can show the Cu-V-rich ‘shells’.....123

Figure 4. 31 BSE (top let), SE (bottom left), chemical mapping (centre) images and line scan charts (right) of Cu-V-Pb-associated areas in the raw brown glaze of HY-38, obtained from the ESEM.....124

Figure 4. 32 Test area (left) and bar chart (right) of Cu, V and Pb in raw green glazes of HY-38. The image and compositional data were obtained from the ESEM.....124

Figure 4. 33 BSE (top left), SE (top right), chemical mapping (bottom left) images and line scan charts (centre and bottom right) of a pure Cu particle in the raw green glaze of HY-38, obtained from the ESEM. 125

Figure 4. 34 Sizes of Cu-rich particles in raw green glazes, obtained from the ESEM. 127

Figure 4. 35 Test areas of Cu-rich particles in raw green glazes, obtained from the ESEM. 127

Figure 4. 36 Estimated colours of all raw glazes of HY-43. The colours are predicted based on the compositional results by EDXRF. The small photos in the bottom left present original appearance of HY-43 sherd. Photos were taken by the author. 132

Figure 4. 37 BSE (top left), SE (bottom left), chemical mapping (centre) images and line scan charts (right) of Co-O-Si-Al-Mg associated particles in raw blue glazes of HY-43, obtained from the ESEM. 134

Figure 4. 38 BSE (top left), SE (bottom left), chemical mapping (centre) images and line scan charts (right) of Co-O-Si-Al-Mg associated particles (blue circles) in raw blue glazes of HY-43, obtained from the ESEM. 135

Figure 4. 39 BSE (top left), SE (top right), chemical mapping (bottom left) images and line scan charts (centre and bottom right) of Co-O-Si-Al-Mg associated particles (blue circles) in raw blue glazes of HY-43, obtained from the ESEM. 135

Figure 4. 40 BSE (top left), SE (top right), chemical mapping (bottom left) images and line scan charts (centre and bottom right) of Co-O-Si-Al-Mg associated particles (blue circles) in raw blue glazes of HY-43, obtained from the ESEM. 136

Figure 4. 41 BSE (top left), SE (top right), and chemical mapping (bottom) images the Co-O-Si-Al-K-Mg-associated particle of HY-43, obtained from the ESEM. 137

Figure 4. 42 BSE (top left), SE (top right), chemical mapping (bottom left) images and line scan charts (centre and bottom right) of Co-O-Si-Al-Mg-Fe-associated particles (blue circles) in raw blue glazes of HY-43, obtained from the ESEM. 138

Figure 4. 43 BSE (top left), SE (top right), chemical mapping (bottom left) images and line scan charts (centre and bottom right) of Co-O-associated particles in raw blue glazes of HY-43, obtained from the ESEM. 138

Figure 4. 44 Texture of Co-rich particles in raw blue glazes of HY-43, obtained from the ESEM. 139

Figure 4. 45 Photo (left) and BSE image (right) of a smalt pigment and lead white in oil in sixteenth- and eighteenth-century paintings, source from (Kugler et al., 2013). The red arrow points to the area of the smalt particle that was analysed and discussed in that paper (Kugler et al., 2013). 139

Figure 4. 46 SE images of smalt particles, source from Xia et al. (2019). 139

Figure 4. 47 BSE and chemical mapping images of smalt in oil paint, source from Spring et al. (2005). 141

Figure 4. 48 Photos, SE, BSE, and mapping images of smalt in wall paintings in Cyprus, source from Daniilia and Minopoulou (2009). 141

Figure 4. 49 BSE image of a weathered smalt grain with line scan of Si, K and Co, source from Daniilia and Minopoulou (2009). 142

Figure 4. 50 BSE (top left), SE (top right), chemical mapping (bottom left) images and line scan charts (centre and bottom right) of Co-O-Mn-associated particles (blue circles) in raw blue glazes of HY-43, obtained from the ESEM. 146

Figure 4. 51 Scatter diagrams of (a) MnO/CoO and (b) Fe_2O_3/MnO ratios, and (c) Fe_2O_3, (d) MnO and (e) CoO contents of blue glaze of Sancai and cobalt pigments used in blue-and-white porcelains from Tang to Ming dynasties. The purple, green and red circles present Song and two Yuan blue-and-white porcelains found in Zhejiang, which were made from local cobalt ore rather than imported material. 147

Figure 4. 52 Box plots of (a) CoO and (b) Fe_2O_3 in raw glazes of HY-43 and (c) Fe_2O_3 in different-colour raw glazes of all samples 148

Figure 4. 53 Bar chart of Fe content (atomic weight) of Co-rich particles (cross-striped bars) and in the surrounded background (clear-coloured bars). The compositional data was obtained from ESEM. 149

Figure 4. 54 Scatter diagrams of (a) Fe_2O_3/MnO values, and of (b) Fe_2O_3/CoO values of cobalt pigment of raw blue glaze and blue pigments of blue-and-white porcelains. Bar chart of (c) Fe and Co (atomic weight) in cobalt particles. 152

Figure 4. 55 Bar chart of Fe_2O_3 content of raw and fired glazes of the same sherd. The examination was run in the locations of HY-43 before and after glaze firing, and data obtained from XRF analysis 153

Figure 4. 56 BSE, SE, mapping images and line scan charts of the Co-Ti-Fe-O-associated particle (blue circles) in the raw blue glaze of HY-43, obtained from the ESEM.....153

Figure 4. 57 BSE (top left), SE (bottom left), chemical mapping (centre) images and line charts of the Co-As-O-associated particle in the blue glaze of HY-43, obtained from the ESEM. .155

Figure 4. 58 Bar chart of (a) As levels in Co-rich particles and surrounded background. Scatter diagram of (b) As and Co of cobalt particles. The compositional data was obtained from ESEM. 155

Figure 4. 59 Box plots of (a) CuO in raw glazes of HY-43 and of (b) all raw glazes of all samples.....156

Figure 4. 60 Bar chart of (a) Cu of Co-rich particles and of surrounding areas where the particles are located in. Scatter diagram of (b) Cu and Co of cobalt particles. The compositional data was obtained from ESEM. 157

Figure 4. 61 Percentage relationships of CoO, Fe_2O_3, MnO, and CuO of (a) raw blue glaze and of cobalt pigments used in blue ceramics, and of (b) estimated blue colourant of raw blue glaze and cobalt of cobalt pigments used in blue ceramics.....159

Figure 4. 62 Test areas of Co-rich particles in raw blue glaze, obtained from the ESEM. ...159

Figure 4. 63 Colours of raw blue glazes, obtained by the optical microscope. 163

Figure 4. 64 Sizes of Co-rich particles in raw blue glazes, obtained from the ESEM. 166

Figure 4. 65 Details of blue decorations on ceramics: (a-d) Tang Sancai, from Henan Provincial Institute of Cultural Heritage and Archaeology et al. (2016a, p.130, 160, 232, 262); (e) and (f) Tang blue-and-white porcelains, taken by the author; (g) Yuan blue-and-white porcelain, from https://www.dpm.org.cn/collection/ceramic/227179.html; (h) Ming blue-and-white porcelain, from https://www.dpm.org.cn/collection/ceramic/226869.html.....166

Figure 5. 1 BSE (the first column), SE (the second column), and mapping images (other columns) of Si-Al-K-O-associated particles in raw glazes, obtained from the ESEM.....171

Figure 5. 2 BSE (the first column), SE (the second column) and mapping images (other columns) of Si-Al-Na-O-associated particles in raw glazes, obtained from the ESEM. 171

Figure 5. 3 BSE (the first column), SE (the second column) and mapping (other columns) images of Si-Al-O-associated particles in raw glazes, obtained from the ESEM. 172

Figure 5. 4 Test areas of Si-Al-(K/Na)-O-associated particles in raw glazes, obtained from ESEM. 172

Figure 5. 5 Scatter diagrams of Al_2O_3 to SiO_2 of (a) all raw glazes, (b) raw clear glaze, (c) raw brown glaze and (d) raw green glaze, data from XRF. The data in red triangle belongs to the high-Si group. 176

Figure 5. 6 Scatter diagrams of (a) Na_2O to Al_2O_3 and (b) K_2O to Al_2O_3 of raw glazes. 176

Figure 5. 7 Scatter diagrams of (a) Fe_2O_3 to Al_2O_3 and (b) TiO_2 to Al_2O_3 of raw glazes. 177

Figure 5. 8 Scatter diagrams of (a) Fe_2O_3 to K_2O and (b) TiO_2 to K_2O of raw glazes. 177

Figure 5. 9 SEM (the first column), SE (the second column) and mapping (other columns) images of Si-O-associated particles in raw glazes, obtained from ESEM. 178

Figure 5. 10 Box plots of (a) m (K_2O), (b) m' (K_2O) and (c) Δm (K_2O) of raw glazes. The calculation is based on hypothesis 1: feldspar. 180

Figure 5. 11 Box plots of (a) m (SiO_2), (b) m' (SiO_2) and (c) Δm (SiO_2) of raw glazes. The calculation is based on hypothesis 2: kaolinitic clay. 181

Figure 5. 12 Box plots of (a) m (SiO_2), (b) m' (SiO_2) and (c) Δm (SiO_2) of raw glazes. The calculation is based on hypothesis 3: body material. 182

Figure 5. 13 Box plots of (a) Δm (K_2O), (b) ΔTiO_2 and (c) ΔFe_2O_3 of all raw glazes and of blue, clear and brown glazes of HY-43 184

Figure 5. 14 (a) Box plot of Fe_2O_3 and TiO_2 of raw glazes and of fired bodies. (b) Scatter diagram of TiO_2 to Fe_2O_3 of raw clear, green and blue glazes. Box plots of (c) Fe_2O_3/TiO_2 ratios, (d) Fe_2O_3/Al_2O_3 ratios and (e) TiO_2/Al_2O_3 ratios of raw clear, green, blue glaze and fired bodies. 186

Figure 5. 15 BSE (the first and third rows) and SE (the second and fourth rows) images of Fe-Si-Al-O-associated particles and Fe-Mg-Si-Al-K-O-associated particles in raw glazes, obtained from ESEM. 187

Figure 5. 16 BSE (left), SE (centre left) and mapping (right) images of Fe-Ti-associated particle in blue glaze of HY-43.....187

Figure 5. 17 BSE (left column), SE (central column) and mapping (right column) images of Ti-rich particles in raw glazes, obtained from the ESEM.....188

Figure 5. 18 Test areas of Ti-rich particles in raw glazes, obtained from the ESEM.....188

Figure 5. 19 Photo of kaolinitic clay in a modern Sancai kiln in Luoyang, taken by the author. Luoyang is situated about 54 kilometres as the crow flies to the west of Gongyi.....191

Figure 5. 20 (a and d) Test areas, (b and e) BSE and (c and f) SE images of kaolinitic clay, obtained from the ESEM. 192

Figure 5. 21 BSE (the first column), SE (the second column) and mapping (other columns) images of Si-O-associated particles in raw glazes, obtained from ESEM.....193

Figure 5. 22 Test areas of Si-O-associated particles in raw glazes, developed from ESEM. 194

Figure 5. 23 BSE (a-c) and SE (d-f) images of possible flint grains in raw clear glaze of HY-38, obtained from ESEM. 196

Figure 5. 24 (a-c) BSE and (c-f) SE images of possible flint grains in raw brown glaze of HY-130, obtained from ESEM. 196

Figure 5. 25 (a-c) BSE and (c-f) SE images of possible flint grains in raw green glaze of HY-38, obtained from ESEM. 197

Figure 5. 26 (a-c) BSE and (c-f) SE images of possible flint grains in raw blue glaze of HY-43, obtained from ESEM. 197

Figure 5. 27 Photo of a flint, from Hamer and Hamer, 2015 (p.142). 198

Figure 5. 28 Photos of possible black flint grains in raw brown glazes, obtained from the optical microscope. 198

Figure 5. 29 (a-c) BSE and (c-f) SE images of sand grains in raw clear glaze of HY-101, obtained from ESEM. 201

Figure 5. 30 (a-c) BSE and (c-f) SE images of sand grains in raw brown glaze of HY-130, obtained from ESEM. 201

Figure 5. 31 (a-c) BSE and (c-f) SE images of sand grains in raw green glaze of HY-38, obtained from ESEM. 202

Figure 5. 32 (a-c) BSE and (c-f) SE images of sand grains in raw blue glaze of HY-43, obtained from ESEM. 202

Figure 5. 33 Photos of flint and sand in raw glaze. The arrows identify flint and sand grains in the raw glazes, developed from the optical microscope. 203

Figure 5. 34 Test areas of high-Al particles in raw brown and blue glazes, obtained from ESEM. 203

Figure 5. 35 Sizes of flint and sand grains in raw glazes, developed from ESEM. 204

Figure 5. 36 BSE (top) and SE (bottom) images of clear glaze layer of HY-38, obtained from ESEM. 205

Figure 5. 37 BSE (top) and SE (bottom) images of brown glaze layer of HY-38, obtained from ESEM. 205

Figure 5. 38 BSE (top) and SE (bottom) images of green glaze layer of HY-38, obtained from ESEM. 206

Figure 5. 39 BSE (top) and SE (bottom) images of blue glaze layer of HY-43, obtained from ESEM. 206

Figure 5. 40 Box plots of (a) PbO, (b) CaO, (c) P_2O_5 of raw glazes 210

Figure 5. 41 BSE (the first column), SE (the second column) and mapping (the other columns) images of glaze layers. Yellow circle presents the high-lead area. Images obtained from ESEM. 210

Figure 5. 42 (a) Scatter diagram of CaO to P_2O_5 of raw glazes. (b) Box plot of n(CaO)/n(P_2O_5) ratios of raw glazes 212

Figure 5. 43 BSE (left) and SE (right) images of unknow curl materials in the raw brown glaze of HY-62, obtained from ESEM. 215

Figure 5. 44 BSE (top left), SE (top right), mapping (centre) and line scan (bottom) images of unknown curl 'grains' in raw brown glaze of HY-62, obtained from ESEM. 215

Figure 5. 45 BSE (top left), SE (top right), mapping (centre) and line scan (bottom) images of unknown curl 'grains' in raw brown glaze of HY-62, obtained from ESEM. 216

Figure 5. 46 BSE (A, B and F) and SE (C, D and E) images of (A and B) archaeological wood, (C, D and E) charcoal fossils, and (F and G) special remains in raw glazes of Gongyi Sancai. Variable pressure scanning electron microscope images of (A) a tangential longitudinal section of mineral-replaced wood, and (B) a tangential longitudinal section of desiccated wood from a funerary Table in a Jericho Bronze Age tomb. A and B are cited from Cartwright (2015). SE images of (C, D and E) charcoal fossils of from Ludford Lane, obtained from Glasspool et al. (2004). 217

Figure 5. 47 Mapping (the first and fourth row), BSE (the second and fifth row) and SE (the third and sixth) images of Ca-rich particles in raw glazes, obtained from ESEM. 221

Figure 5. 48 BSE (the first one from the left), SE (the second one from the left) and mapping (the others) images of possible CaCO3 particles, obtained from ESEM. 222

Figure 5. 49 BSE (top left), SE (bottom left), mapping (centre), line scan (right) images of Ca-Mg-C-O-associated particles in clear glaze of HY-123, obtained from ESEM. 222

Figure 5. 50 BSE (top left), SE (top right) and mapping (bottom) images of Ca-Mg-C-O-associated particles in raw green glaze of HY-106, obtained from ESEM. 223

Figure 5. 51 Scatter diagrams of MgO to CaO of raw glazes. 223

Figure 5. 52 (a) Box plot of m(CaO), m'(CaO) and Δm(CaO) of raw glazes. Scatter diagrams of (b) P_2O_5 to Δm (CaO) and (c) P_2O_5 to CaO of raw glazes. 224

Figure 5. 53 Test areas of Ca-rich particles in raw glazes, obtained from ESEM. 224

Figure 5. 54 Photos of (a) a potter who is decorating a Sancai body in a traditional Sancai kiln in Henan and of (b-e) lead oxides and lead. Photo (a) was taken by the author, (b) is from https://en.wikipedia.org/wiki/Lead(II,IV)_oxide#/media/File:Red_lead.jpg, (c) is from

https://en.wikipedia.org/wiki/Lead_dioxide#/media/File:Lead_dioxide.jpg, (d) is from https://en.wikipedia.org/wiki/Lead(II)_oxide#/media/File:Oxid_olovnat%C3%BD.JPG, and (e) is from https://en.wikipedia.org/wiki/Lead#/media/File:Lead_electrolytic_and_1cm3_cube.jpg.....227

Figure 5. 55 BSE (top) and SE (bottom) images of the green-glaze surface of HY-166, obtained from ESEM. 228

Figure 5. 56 BSE (the first column), SE (the second column) and mapping (the other columns) images of high-Pb areas of clear glazes of HY-101 and HY-130.....229

Figure 5. 57 Photos of colours of different raw glaze.....231

Figure 5. 58 Photos of cerussite and hydrocerussite, from https://www.mindat.org/min-934.html and from https://www.mindat.org/min-1969.html 231

Figure 5. 59 Test areas of high-Pb areas in raw glazes, developed from ESEM.....232

Figure 5. 60 BSE (the first and third rows) and SE (the second and fourth rows) images of high-Pb areas (light areas) of raw glazes, obtained from ESEM. 233

Figure 5. 61 Box plots of (a) weight percentage of stock glaze, (b) the sum of SiO_2 and Al_2O_3, (c) P_2O_5 and CaO, and (d) PbO of raw glazes. 235

Figure 5. 62 Ternary plot of PbO, the sum of P_2O_5 and CaO, and the sum of SiO_2 and Al_2O_3 of raw glazes.....236

Figure 5. 63 Box plot of main ingredients of stock glaze. 238

Figure 5. 64 The manufacturing process of stock glaze. 238

Figure 5. 65 Manufacturing process of coloured glazes. 239

List of Tables

Table 1. 1 Comparison of production of the Huangye and Liquanfang kilns in different periods 41

Table 2. 1 Strata of samples 55

Table 2. 2 Samples observed and analysed by ESEM-EDS 62

Table 3. 1 Classification of samples 93

Table 3. 2 Colour combinations of samples.....93

Table 4. 1 Chemical compositions of Fe-O-associated particles in raw brown glazes by ESEM 101

Table 4. 2 Chemical compositions of Fe-Mg-Si-Al-O-associated particles in brown glazes by ESEM.....108

Table 4. 3 Chemical compositions of Fe-Mg-Si-Al-(K)-O-associated particles in clear, green and blue glazes by ESEM 113

Table 4. 4 Chemical compositions of Cu-rich particles in green glazes by ESEM.....128

Table 4. 5 Chemical compositions of cobalt particles/tested areas 160

Table 5. 1 Mean values of main elements of raw glazes. 168

Table 5. 2 Mean values of trace elements and colourant elements of raw glazes. 168

Table 5. 3 Chemical compositions of Si-Al-(K/Na)-O-associated particles in raw glazes by ESEM.....173

Table 5. 4 Chemical compositions of Si-Al-(K/Na)-O-associated particles by calculation (PbO removed and re-normalised) 174

Table 5. 5 Chemical compositions of Ti-rich particles in raw glazes.....189

Table 5. 6 Chemical compositions of Ti-rich particles (remove Pb and re-normalised) in raw glaze 189

Table 5. 7 Chemical compositions of kaolinitic clay collected in Luoyang by ESEM 192

Table 5. 8 Chemical compositions of Si-O-associated particles in raw glazes by ESEM.....194

Table 5. 9 Calculated compositions of Si-O-associated particles of raw glazes by ESEM. The data was normalised after decreasing P_2O_5 and PbO.....194

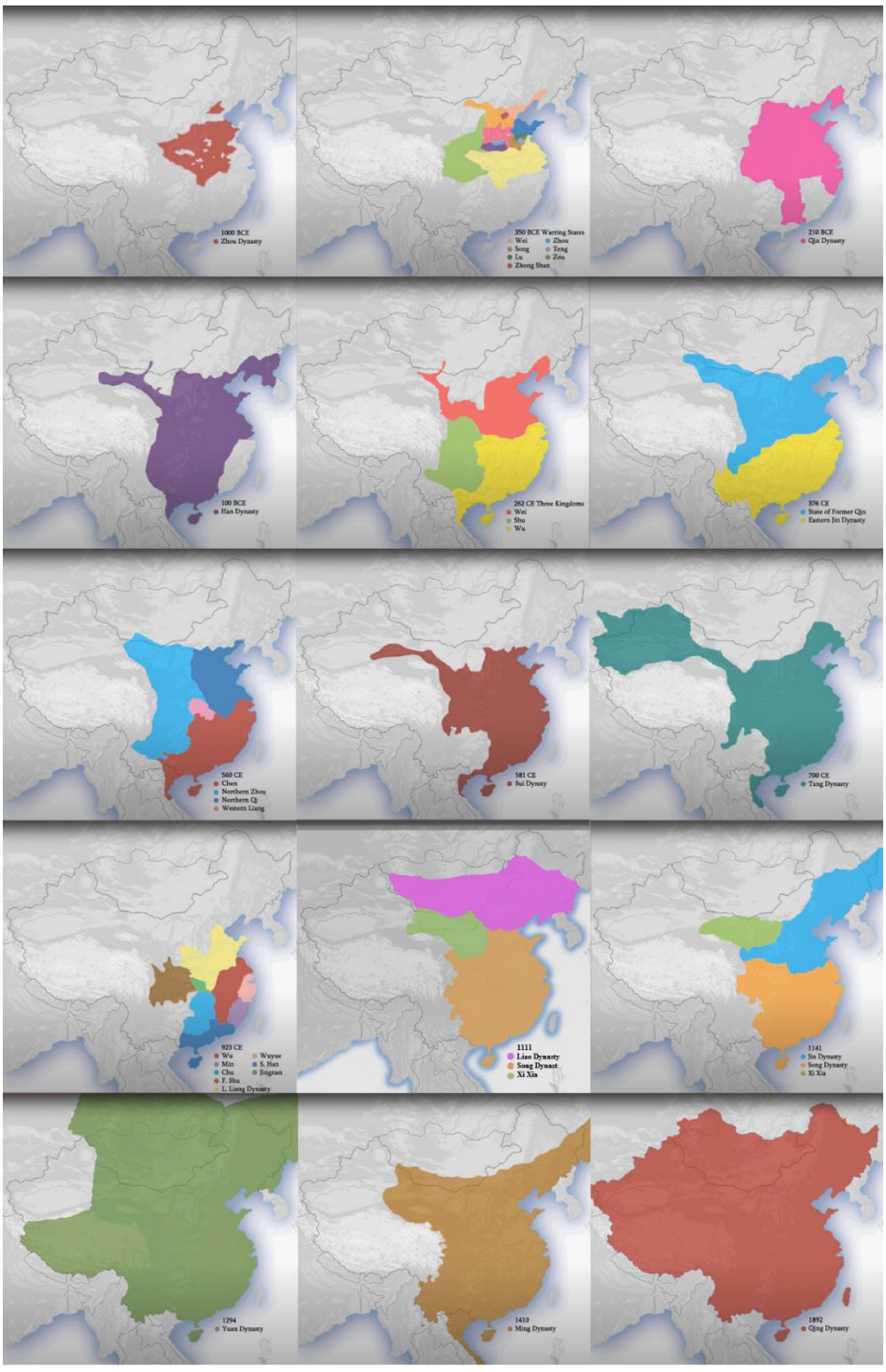
Table 5. 10 Chemical compositions of high-Al particles in raw brown and blue glazes by ESEM 204

Table 5. 11 Chemical compositions of Ca-rich particles in raw glazes by ESEM. 225

Table 5. 12 Chemical compositions of high-Pb areas in raw glazes by ESEM.....232

Glossary of Terms

Chinese dynasties Dynasties in Chinese history from first millennium BCE to second millennium CE. These dynasties are mentioned in this thesis.



Images were developed from

https://www.youtube.com/watch?v=zdHkY3XYHKA and

https://en.wikipedia.org/wiki/Administrative_divisions_of_the_Liao_dynasty#/media/File:Song-Liao-Xixia-1111.png

Timeline of dynasties (1046 BCE -1912 CE) is as follows:

Zhou Dynasty: 1046 -256 BCE (Western Zhou: 1046 - 771 BCE; Eastern Zhou: 771- 256 BCE (Spring and Autumn: 770 – 476 BCE; Warring States: 475 – 221 BCE))

Qin Dynasty: 221 - 207 CE

Han Dynasty: 206 BCE - 220 CE (Western Han: 206 - 9 BCE; Xin: 9 - 23 CE; Eastern Han: 25 - 220 CE)

Three Kingdoms: 220 - 280 CE

Jin Dynasty: 266 - 420 CE (Western Jin: 266 -316 CE; Eastern Jin: 317 - 420 CE)

Sixteen Kingdoms: 304 - 439 CE

Northern and Southern Dynasties: 420 - 589 CE

Sui Dynasty: 581 - 618 CE

Tang Dynasty: 618 - 907 CE

Five Dynasties and Ten Kingdoms: 907 - 979 CE

Liao Dynasty: 916 - 1125 CE

Song Dynasty: 960 - 1279 CE (Northern Song: 960 - 1127 CE; Southern Song: 1127 - 1279 CE)

Jin Dynasty: 1115 - 1234 CE

Yuan Dynasty: 1271 - 1368 CE

	Ming Dynasty: 1368 - 1644 CE
	Qing Dynasty: 1636 - 1912 CE
Tang dynasty	An imperial dynasty of China from 618 to 907 CE. Historians generally regard the Tang as a high point in Chinese civilisation, and a golden age of cosmopolitan culture.
Glaze	A layer of glass which is fused into place on a pottery body.
Lead glaze	A glaze fluxed by lead oxide.
Sancai	A type of lead-glazed earthenware. 'San' (Chinese: 三) means three and cai (Chinese: 彩) means colour in Chinese. 'Sancai' (Chinese: 三彩) refers to tri-coloured decoration. This lead-glazed earthenware includes monochrome and polychrome wares as well as three-coloured wares. The polychrome effect was obtained by using colouring oxides – copper (which turns green), iron (which turns yellow/brown), and cobalt (which turns blue). The body of it is made of white clay (kaolinitic clay), coated with lead glaze(s). It needs two firings, biscuit firing with about 1100℃ for body and glaze firing at about 800℃.
Blue Sancai	Tang Sancai wares which include cobalt-blue decoration, either alone or in combination with other colours.
Ordinary Sancai	Tang Sancai wares without cobalt-blue decoration.
Archetypal/typical blue-and-white porcelain	A tyle of high-fired porcelain decorated with underglaze cobalt pigment and covered by lime glaze. The whole vessel is fired once around 1250℃.

	Its production and use boomed in the Yuan (1271-1368 CE), Ming (1368-1644 CE) and Qing (1644-1912 CE) dynasties.
Tang blue-and-white porcelain	Blue-and-white porcelain produced in the Tang dynasty. Compared with archetypal blue-and-white porcelain, Tang blue-and-white wares show some primitive characteristics decoratively and technically.
Raw glaze	Unfired glaze. The finished Sancai needs two firings – high firing for the body and lower firing for the glaze. In this thesis, the samples are semi-finished Sancai. Their bodies were biscuit fired but the glazes on the bodies are unfired.
Experimental glaze firing	A firing of the raw glaze in the lab at Northwest University. Some samples with the raw (unfired) glaze on the fired body were selected and fired in the muffle furnace at 850℃. This experimental firing is the refiring of the sherd, but first firing of the glaze.
Raw colour	Colours of raw glazes.
Fired colour	Colours of fired glazes.
Coloured glaze	Fired brown, green, and blue glazes.
Stock glaze	The base of glazes without any colourant. The clear, brown, green, and blue glazes might share the same stock glaze.
Smalt	Potash silicate blue glassy pigment coloured with cobalt. It was an important and popular blue pigment in the 16th and 17th centuries CE in Europe.

Chapter 1 Introduction

In the Tang Dynasty, the glaze became a shining, colourful, glassy coating on ceramics. It gives ceramics exquisite appearances and pleasant properties. In the history of Chinese ceramic, two different glaze technologies were developed – lime glaze and lead glaze. Based on these two traditions, many sub-branches were innovated. All these various glazes make China the country of china. The lime glaze is fluxed by calcium oxide, sometimes with alkaline oxides with a relatively high maturing temperature above 1200℃. In contrast, lead acts as a flux for the low-fired lead glaze, maturing around 700-900℃. Based on the current archaeological findings (Wang and Cui, 2008; Lang and Cui, 2017), the beginning of lead glaze in China was a few glazed earthenware in the Warring States (475-221 BCE). The technology of lead glaze developed in the Han dynasty (202 BCE-220 CE) and matured in the Tang dynasty (618-907 CE). This low-fired glaze was carried down from generations of potters in early China to modern craftsmen over the past two thousand years.

1.1 Lead Glazes

1.1.1 Beginning of Lead Glaze in the Warring States (475-221 BCE)

The earliest Chinese low-fire glazes so far found seem to have been those used on some rare Warring States earthenware jars decorated with relief rosettes of dotted glaze (Wood, 1999,

p.189). Before the excavation of an elite tomb in Linzi in 2006 (Wang and Cui, 2008) only four examples of Warring-States lead glazed vessels were known. One is in the collection of the British Museum, London (Figure 1. 1a); two more are in the USA (Figure 1. 1c); and one is in the National Museum in Tokyo (Wood, 1999, p.189). In 2006, an elite tomb of Qi state in Anledian Village of Xindian Township of Linzi in Shandong province was excavated (Figure 1. 2a). Two glazed Lei (罍, jar with narrowed mouth and neck, and large belly) with brownish green glaze were buried in this tomb (Wang and Cui, 2008) (Figure 1. 2b). Generally, this shape was used for bronze vessels (Figure 1. 1d) - the bronze Lei was popular from the Shang dynasty (1600 -1045 BCE) to the Eastern Zhou dynasty (771-256 BCE). The jar collected by the Nelson- Atkins Museum of Art in America looks very similar to this Lei found in Linzi (Figure 1. 1c and Figure 1. 2b). The only difference is that the jar collected in America has two ears, but the Lei found in Linzi has four ears. The colours of them are both very dull. However, the jar collected in Britain has different glaze characteristics. It is a polychrome object and was decorated with regular dotted and striped patterns. The original colours would have been iron-red, iron-yellow, and Chinese-blue ($BaO{\cdot}CuO{\cdot}4SiO_2$) on a white-glaze ground (Wood, 1999, p.190). This glaze might make use of similar technologies to the contemporary glass beads (Figure 1. 1b) (Wood, 1999, pp.190-191).

Compositionally, the analysis of the Lei excavated from Linzi by XRF (X-ray fluorescence) shows that the PbO reaches 61.18-62.44%. It is a high-lead glaze. However, the jar collected in Britain used relatively low PbO, around 20% (Wood, 1999, p.191), and the white glaze on the jar might be opacified by barium disilicate, the usual opacifier in very early white Chinese glass (Wood, 1999, p.190). But the content of BaO in the monochrome glaze of the Lei is only 0.01-0.02% which is close to the analytical limit of XRF. It can be assumed that the brownish-green lead glaze of the Lei found in Linzi does not contain barium. This suggests that two types

of lead glaze existed in the Warring States. Besides, the iron colourant of the high-lead glaze of the Lei gives a brownish green colour, which contains 4.12-4.41% Fe_2O_3. By contrast, the iron colourant in the glazes of the jar collected in Britain shows red and yellow colours. This might suggest that the firing atmosphere was different. Oxidation of iron gives red and yellow, whereas reduction produced green. In summary, the high-lead and low-lead glazes used different technologies. Whether these two technologies had different origins, relating to two independent origins of early Chinese lead glaze, are still live issues.



Figure 1. 1 (a) Photo of a Warring-States glazed pottery jar (H. 9.5cm) with highly weathered lead glazes, obtained from Wood (1999, p.190). The original glaze colours would have been red, yellow, and blue on a white-glaze ground. The jar is collected in the British Museum in UK. (b) Photo of a Warring-States glazed bead (L. 2 cm) with stonepaste body and red, blue, and yellow glazes on a white ground, obtained from Wood (1999, p.191). The bead is collected by the British Museum. (c) Photo of an Eastern-Zhou-dynasty glazed pottery Lei (H. 27 cm), obtained from Chen (2021). This Lei was found in Luoyang and collected in the Nelson- Atkins Museum of Art in USA. (d) Photo of a Warring-States bronze Lei, from Lang and Cui (2017). It was excavated in Linzi.



Figure 1. 2 (a) Map of Qi, a state of Zhou dynasty in ancient China. Qi was variously reckoned as a vassal state, duchy, and independent kingdom which was founded 1046 BCE and was replaced by Qin in 221 BCE. The extent of the Qi state changed over time. The yellow area in the map presents the border of Qi in 260 BCE and the red spot marks the location of capital of Qi, Linzi. The map is from https://en.wikipedia.org/wiki/Qi_(state)#/media/File:EN-QI260BCE.jpg (b) Photo of one of the glazed pottery Lei (H. 27cm) excavated from an elite tomb of Qi state in Linzi, from Chen (2021).

1.1.2 Evolution of Lead Glaze in the Han Dynasty (202 BCE-220 CE)

A great majority of burial lead-glazed ceramics were found in the Han-dynasty tombs. These lead glazes can be divided into three groups by decoration – monochrome yellow/brown glaze, monochrome green glaze, and two-coloured glaze (Figure 1. 3). The monochrome brown glaze took the dominant position among these three groups. In the late Eastern Han dynasty (about 2nd – 3rd century CE), green glaze became popular (Wang and Tian, 2010). The two-coloured glaze was prevalent around the 1st - 2nd century CE (Du, 2011). The production of all these ceramics almost stopped in the 3rd - 4th century CE.

The differences of the Warring States and Han-dynasty glazed ceramics are the colours and colourants. The iron colourant in the lead glaze of Warring-states objects shows red, yellow, and brownish green colours. The red and brown were produced by iron fired in an oxidising atmosphere. This technology was also used in Han-dynasty lead glaze. However, Han-dynasty potters did not employ iron in a reducing atmosphere to make the green colour. They added copper colourant into the glaze and fired it in an oxidising atmosphere to produce the green glaze, which was a new product. Moreover, the white glaze did not appear in Han-dynasty wares. The white ground of the Warring-States glaze jar was opacified either by undissolved quartz or perhaps by barium disilicate (Figure 1. 1a) (Wood, 1999, p.190). This technology of opacified white glaze was not utilised in Han-dynasty vessels.

The significant innovation of the Han-dynasty lead glaze is the two-coloured decoration. This style refers to the brown, iron-red or -yellow colour working as the ground and the green and blue glazes being used to paint simple patterns (Figure 1. 3c and Figure 1. 4a). One hundred and sixty-seven two-coloured wares were found in Han-dynasty tombs in Baoji, Yan'an and Jiyuan (Figure 1. 4b) Nine tombs in Baojin contained 40 objects. In Jiyuan, eighty-one vessels were unearthed from six tombs, and forty-six wares were excavated from Yan'an. These three areas can be regarded as the centres of the two-coloured glazed ceramic production in the Han dynasty, but there are also a few of these wares found in other places (Figure 1. 4b). Two types of lead glaze, high-lead glaze, and lead-barium glaze were both found in the Han-dynasty ceramics (Figure 1. 4c). Surprisingly, the scientific analysis of two-coloured glazes showed that the lead glaze (red, yellow, and brown glazes) and the lead-barium glaze (green and blue glazes) were applied on the same vessel (Chen et al., 2020).



Figure 1. 3 (a) Photo of a brown-glaze oven model found in Jiyuan, Henan province. (b) Photo of a green-glaze food container found in Nanchang, Jiangxi province. (c) Photo of a two-coloured glazed Zun (Chinese: 樽). Photos were from Wang and Tian (2010).



Figure 1. 4 (a) Photo of Han glazed pottery excavated from Yan'an, Shaanxi: (1–8) Hu; (9–11) Ding; (12–15) Zao; (16–20) Cang; (21) Fang; (22) Zun; (23) Guan; (24) flattened Hu; (25) Boshan incense burner; (26) incense burner; (27) Pan; (28) Xiao Hu; (29) duck-shaped Hu; (30) pig-shaped glazed pottery, cited from Chen et al. (2020). The white /silver motifs on the surfaces of wares were caused by weathering. The original colour is green. According to the author's introduction, No.6, 7, and 27 are monochrome wares, and others are two-coloured wares. (b) Map of the distribution and locations of archaeological findings of two-coloured glazed potteries in the Han dynasty, developed from Wang (2018). The black spots present the locations of findings of two-coloured glazed potteries. And the circles present the distribution areas. (c) Box plot of PbO, BaO, CuO and Fe_2O_3 of Han-dynasty glazes, obtained from Chen et al. (2020).

1.1.3 Breakthrough of Lead Glaze in the Northern Dynasties (420 CE - 589 CE)

The number of the Northern-dynasties lead glazed ceramics is much lower than in the Han dynasty. As the typical wares, ceramics found in three tombs with specific years have been paid much archaeological attention. They are polychrome glazed vessels from Lou Rui tomb (570 CE), Fan Cui Tomb (575 CE) and Li Yun Tomb (576 CE) (Figure 1.5) (Zhou, 1964; Li, 1972; Henan Provincial Institute of Cultural Heritage and Archaeology, 1972). These glazed wares had white bodies, with clear white, bright green and yellow glazes. Noticeably, the green glazes of the vessels unearthed from Lou Rui Tomb (570 CE), Fan Cui (575 CE) and Li Yun tomb (576 CE) is apple green rather than the moss green of the Han-dynasty wares (Figure 1.5) (Hai, 2015; Wang, 2018).

The breakthrough is the use of the kaolinitic white body. Kaolinite ($Al_2O_3 \cdot 2SiO_2 \cdot 2H_2O$) has high silicate and aluminium, and it needs a high temperature, around 1100℃, to mature and harden. However, the lead glaze can melt from 700℃. This suggests that the Northern-dynasties glazed wares were fired twice, once for the body and again for the lead glaze. This was the first time that a kaolinite-based white body was employed for lead-glazed potteries. The Warring States and Han-dynasty lead glazes were both applied to the red body (Figure 1. 1a-c and Figure 1. 3b) which was produced using a high-iron clay. The white body can offer a whiter ground for the lead glaze and allow the transparent/semi-transparent glazes to show bright colours. This development is based on the technological advancements of kaolinitic clay exploitation, materials purification, and kiln firing technology. Synchronously, monochrome dark green and brown glazes were also produced in this period - for example, the green inkstone and brown jar from Li Yi couple tomb (534 CE) and dark green figures found in a Northern-Wei tomb (Shen et al., 2015, Zhang et al., 2022). The figures (Figure 1. 5 e and g) were new shapes in the Northern dynasties, and no lead-glazed figures have been found in Han-dynasty tombs.

Unfortunately, these complete vessels and figures have not been analysed compositionally. However, seven sherds including clear (white), green and brown glazes were examined by optical microscopy, XRF and dilatometry (Wang et al., 2011). This scientific analysis shows that the white body belongs to the high-Al and low-Fe-and-Ti family. The alumina is above 20%, and the highest level is 26.95%. Fe_2O_3 in the body is around 2-3% and TiO_2 is only about 1%. The firing temperatures of these bodies are 960℃ and 1048℃, which is increased

compared to the Han-dynasty glazed wares (900-1000°C[1]). For the glazes, no BaO was found and the PbO reached to 70.97-75.37%, except for one sample containing 47.42%. This revealed that the Northern-dynasties lead glazes can be classified as high-lead glazes. The production of monochrome dark-green and -brown glazed wares and the innovation of a white body and bright colours suggests that Northern-dynasties potter inherited the previous technology of lead glaze from the Han dynasty, but also pioneered the new products, even though the Northern dynasties was generally a chaotic period which was divided into different dynasties and states with many wars.



[1] The high lead glaze begins to melt at 650°C, and supplies good lead glazes in the 900-1000°C range (Wood, 1999, p.192)

Figure 1. 5 (a) Photo of polychrome bowl excavated from Lou Rui tomb (570 CE), from http://kaogu.cssn.cn/zwb/xsdt/xsdt_3347/xsdt_3348/202205/t20220516_5408447.shtml. (b) Photo of green-and-white flask unearthed from Fan Cui tomb (575 CE), from http://www.chnmus.net/sitesources/hnsbwy/page_pc/bwzl/yyhxzzjd/cpsx/article62aab56cfb474ef8b5%200a046b23c815b0.html. (c) Photo of the green-and-yellow jar (H. 23.5 cm) found in Li Yun tomb (576 CE), from https://www.dpm.org.cn/collection/ceramic/226731.html?hl. (d and f) Photos of dark green and brown glazed inkstone (H. 6.9-7.2cm) and jar (H. 24 cm) unearthed from Li Yi couple tomb (534 CE), obtained from Shen et al. (2015). (e and g) Photos of dark green glazed dog figure (H. 10cm) and human figures (H. 20.8 cm) found in a Northern-Wei tomb in Datong, Shanxi province, from Zhang et al. (2022).

1.1.4 Glory of Lead Glaze in the Tang Dynasty (618 – 907 CE)

In 1905 CE, some Tang-dynasty tombs were damaged by the construction of a railway in Mang Mountain near Luoyang. Many exquisite glazed human figures, animal figures and vessels were found (Wang, 2018). Since these wares were decorated with elegant splashed white, brown, and green glazes, they were named ‘Tang Sancai’. ‘Sancai’ (三彩) means three colours in Chinese. Afterwards, with more and more Sancai found, people recognised that a variety of colours, such as brown, green, white, red, blue etc., were used on these ceramics, either alone or in combination with other colours. Thus, Sancai also includes lead-glazed monochrome and two-coloured wares prevailing in Tang China. Most of the Tang Sancai wares were buried in tombs, but some Sancai objects were also collected and dedicated by Buddhist temples. For example, a Sancai plate holding a Sancai pumpkin was excavated from the chamber of Dagoba in Qingshan Temple in Lintong, near Xi’an (Zhao, 1985). Also, two sherds of a Sancai figure

of Buddha were unearthed from the hall site in Qinglong Temple in Xi'an (The Institute of Archaeology CASS, 1974).

Undoubtedly, the production and use of Chinese lead glaze peaked in the Tang dynasty. Based on an analysis of around 4,100 Tang tombs, this author found that more than 200 tombs contained about 2,500 Sancai wares[2]. Besides mass production and widespread use, there are two key innovations. The first one is the making of various figures, especially large figures (Figure 1. 6 a, b, and c). For instance, the height of the Sancai heavenly guardian in Figure 1. 6 is 118cm. In addition, the technology of shaping and sculpture of Sancai is very advanced. The expressions on human figures are extremely vivid (Figure 1. 7 d and e). Although a few figures had been produced before the Tang dynasty, such as the human figures and dog figure from the Northern-Wei tomb (Figure 1.5 e and g), they are much smaller than Tang Sancai, and much less life-like.

[2] This section takes a largely numerical approach, using data from published archaeological reports of Tang tombs between 1934 and 2022. However, due to the word limitation, this quantitative study and discussions cannot be included in this thesis. The author is preparing this part for an independent paper which groups tombs by different tags, such as time, location, the status of owners, distance to Sancai kilns etc. And it will discuss the availability of ordinary Sancai (Sancai without blue decoration) and blue Sancai (Sancai wares which include cobalt-blue decoration, either alone or in combination with other colours), the social hierarchy of owners of Sancai, the evolution of decorations and colours, and the relation of Sancai and blue-and-white porcelain.



Figure 1. 6 Photos of (a) Sancai heavenly guardian (118cm), (b) Sancai tomb guardian beast (H. 80.5cm), (c) Sancai horse figure (H. 76.5cm), (d) Sancai horseman figure and (e) a model for a female figure. Sancai figures (a), (b) and (c) are collected in the Palace Museum and photos are from (a) https://www.dpm.org.cn/collection/ceramic/227537.html, (b) https://www.dpm.org.cn/collection/sculpture/233434.html, and (c) https://www.dpm.org.cn/collection/ceramic/227486.html. (d) The figure riding a horse was excavated from Yide Prince tomb, and its face was painted by pigments after glaze firing. (e) Mould unearthed from the Liquanfang kiln site. (d) and (e) Photos were from Wang (2018).



Figure 1. 7 Photos of blue Sancai: (a) female figure (H. 45 cm) excavated from Zhongbaocun tomb in Xi'an, taken by the author; (b) camel-carrying-musicians figure (H. 58.4 cm) found in Xianyu Tinghui tomb (Ma and Zhang, 1958), from http://kgzg.cn/a/396228.html; (c) acrobatic figure (H. 40.8 cm) contained in tomb M31 in southern outskirts in Xi'an, obtained from Sun et al. (2004); (d) pot (H. 14.7 cm) from Yangjia Weiqiang Tomb, obtained from Guan et al. (2012). (e) Sancai cover button (D. 2.8 cm[3], H. 3 cm) from Zheng Rentai tomb, taken by the

[3] The diameter was measured by the author. The archaeological report showed 2.5 cm (Shaanxi Provincial Institute of Archaeology, 1972).

author; (f) blue-and-white Sancai bowl excavated from the Gongyi kiln site, obtained from Henan Provincial Institute of Cultural Heritage and Archaeology et al. (2016a, p.230); (g) blue Deng (lamp) (H. 33.6 cm) unearthed from Gonglin, obtained from Wang (2011).

Furthermore, another crucial innovation was created on Sancai by Tang-dynasty potters – the use of cobalt-blue glaze (Figure 1. 7). The blue glaze was applied to various shaped bodies, either alone or in combination with white, green, and brown colours. Why was this application so crucial? Cobalt material was one of the earliest pigments used by humans. As early as the Eighteenth Dynasty (1479-1424 BCE) in the New Kingdom of Egypt, cobalt blue colourant was used in glass to give it a beautiful dark blue colour. The source of this cobalt was cobalt ferrous alum from the Western Oases of Egypt (Abe et al., 2012). In China, the earliest evidence for cobalt pigment used in vitreous materials is the glass eye beads from the Xujialing Tomb Site (the Warring States Period 475-221 BCE) in Henan province (Figure 1. 8) (Gan et al., 2009; Gan, 2016). However, it is uncertain whether the original of the blue colourant was a local mine or imported material. Cobalt pigment was only used in glass and did not become a popular blue pigment for a long time in early China.

This situation changed in the Tang dynasty (618-907 CE). The Tang potters employed cobalt pigment as a blue colourant on ceramics to produce Tang Sancai. The earliest known example is a button on the cover of a container from Zheng Rentai tomb (664 CE) (Shaanxi Provincial Institute of Archaeology, 1972) (Figure 1. 7e). From then on, the style of the cobalt-blue motif against a white background was created and was widely used in ceramics (Figure 1. 7e and f). Tang blue-and-white was one of these ceramics (Figure 1. 9). A scientific comparison study revealed that these two blue-decorated ceramics (Sancai and blue-and-white porcelain) shared the same imported cobalt pigment (Zhang and Pollard, 2022). The biggest difference between Tang blue-and-white and Sancai is that Tang blue-and-white employed a high-firing lime glaze,

whereas Sancai is a low-fired lead-glazed ware. Thirty-nine Tang blue-and-white sherd/vessels have been found in and outside China – twenty-eight from two port cities (twenty-seven sherds from Yangzhou in China and one sherd from Siraf in Iran), six sherds from the Gongyi kiln, two intact jars from a tomb in Zhengzhou, and three complete plates from the Belitung shipwreck (Zhang and Pollard, 2022). The excavation of the Gongyi kiln confirmed that blue Sancai and blue-and-white porcelain were produced in the same kiln during the Tang dynasty, and the production of Sancai was earlier than blue-and-white (Henan Provincial Institute of Cultural Heritage and Archaeology et al., 2009, p.11; Henan Provincial Institute of Cultural Heritage and Archaeology et al., 2016b, p.17). Six Tang blue-and-white sherds have been unearthed at this site (Figure 1. 9 a-f), and one sherd found at Siraf was also produced there (Spataro et al., 2019) (Figure 1. 9g). Accordingly, the archaeological and scientific findings both prove that blue Sancai was the predecessor of the Chinese blue-and-white porcelain. Therefore, the foundations of the prosperity of blue-and-white porcelain in China and the global trade from the Yuan (1271–1368 CE) to Ming (1368–1644 CE) and Qing (1644–1912 CE) dynasties originated from Tang Sancai.

At a similar time, the cobalt-blue decoration was also popular in Islamic areas. A considerable number of glazed pottery sherds with blue decorations have been excavated in Iraq, Egypt, and Syria (Allan, 1991; Watson, 2014; Spataro et al., 2019). Islamic potters also painted blue motifs by using cobalt pigment on a white ground (Figure 1. 10), and the splashed effect also appeared on the Islamic pottery (Figure 1. 10c). Iraqi imitations of Chinese Sancai wares were found at Samarra (Wood et al., 2009). All these findings suggest that Chinese and Islamic ceramics had some connection, interaction, and exchange. Additionally, there was also trade and interactions between Tang China and her neighbour countries – Japan, Korea, and Russia (Gelman, 2006; Wang and Yang, 2021; Chang et al., 2023). They learned the

technology of Tang Sancai and produced local products, such as Nara Sancai (Figure 1. 11) (Zi, 2011; Chang et al., 2023) and Bohai Sancai (Figure 1. 12) (Gelman, 2006; Wang and Yang, 2021; Buravlev et al., 2022). To summarise, if the history of Chinese ceramics was likened to a river, Sancai can be regarded as an intersection which received water from the upstream, exchange water with other rivers, and broadens its width and depth to accumulate much 'new water' for the downstream.



Figure 1. 8 Photo of glass beads from Xujialing Site, obtained from Gan (2016, p.274).

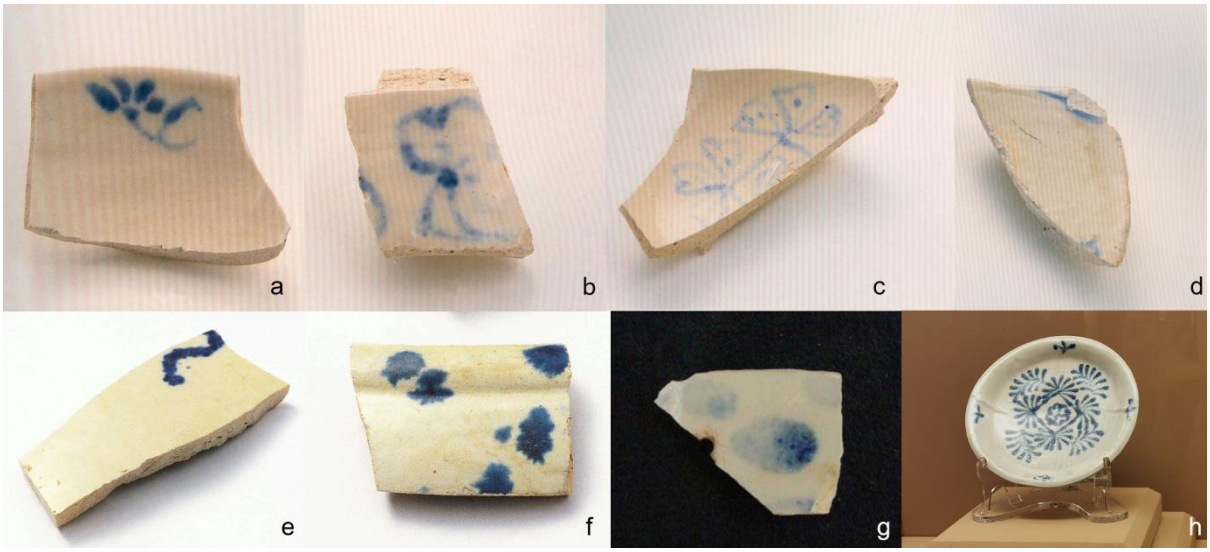


Figure 1. 9 Photos of Tang blue-and-white: (a-f) sherds found in the Gongyi kiln, obtained from Henan Provincial Institute of Cultural Heritage and Archaeology et al. (2009, pp.165-167) and Henan Provincial Institute of Cultural Heritage and Archaeology et al. (2005, p. 145); (g) sherd unearthed in Siraf, a port city of Persian Gulf, from Spataro et al. (2019); (h) plate uncovered from the Belitung Shipwreck and collected in Asian Civilisations Museum in Singapore, taken by the author.



Figure 1. 10 Photos of typical Samarra-type pottery: (a) white glaze with cobalt blue decoration (the Metropolitan Museum of Art, acc. no. 63.159.4); (b) white glaze with cobalt blue and green decoration (Freer and Sackler Galleries, acc. no. F2000.2); (c) splash glazed (the Metropolitan Museum of Art, acc. no.30.112.46), obtained from Matin (2016, p.8).



Figure 1. 11 Photos of Nara Sancai, obtained from Zi (2011).



Figure 1. 12 Photos of Bohai Sancai excavated in Longhai royal tomb of Bohai state, cited from Wang and Yang (2021).

1.1.5 Survival of Lead Glaze in the Liao (916-1125 CE), Song (960-1279 CE), and Jin (1115-1234 CE) Dynasties

The Liao dynasty (or Great Liao, Khitan Empire) was an imperial dynasty of China that ruled the north and northeast of China between 916-1125 CE (Figure 1. 13a). The Jin dynasty or Great Jin gradually replaced some places of the Liao and Song in the northeast of China from 1115 to 1234 CE (Figure 1. 13b). These two dynasties co-existed with the Song in different periods. After the collapse of the Tang Empire, the Sancai was not as glorious as before, but the wares were still popular. Various kinds of Sancai were found in these dynasties (Figure 1. 14, Figure 1. 15 and Figure 1. 16). In the Song dynasty, the political and economic centres shifted from the north to the south of China. The centre of Sancai making and use became the southwest instead of Chang'an and Luoyang in the Tang dynasty. Song Sancai was also used as grave ceramics. For example, the Song tomb in Pujiang (Sichuan province, southwest in China), dated to 1072 CE, contained 86 Sancai figures and four Sancai drums, which is the Song tomb with the most Sancai objects (Chen and Liao, 1986). But generally, Song-dynasty

Sancai figures are much smaller than Tang figures. The heights of most of the figures in the Pujiang tomb are around 29-39 cm. Only a few figures in the Song dynasty were tall. For instance, the height of soldier figures in Figure 1. 14b unearthed in Chengdu was above 1 m. Compared with the Tang Sancai figures, the shapes, and colours of Song Sancai are relatively inferior. The use of Liao Sancai was different from Tang and Song Sancai. It acted commonly as daily-life utensils rather than as burial ceramics (Sun, 2006).

In the Tang dynasty, figures and vessels were both popular shapes. However, in the Song, Liao and Jin dynasties, the proportion of vessels became much greater, and the proportion of figures decreased considerably. Various vessels, such as pots, plates, jars, trays, vases, Deng etc., were found in Song, Liao, and Jin dynasties (Figure 1. 14, Figure 1. 15 and Figure 1. 16). But the types of vessels of these Sancai are fewer than those of Tang Sancai. Moreover, the bodies of Song and Liao Sancai are greyish or yellowish, so the potters applied a white slip to them. All these characteristics indicated that the technology of the body took a step backwards. However, remarkably, Sancai ceramic pillows achieved unprecedented success and became the most popular products of all Sancai in the Song and Jin dynasties. The shapes and decorations were various (Figure 1. 14 d and f, and Figure 1. 15).

There are two differences in decoration between Tang and later Sancai. In terms of colours, Tang Sancai exploited more colours, including white, green, yellow, brown, red, and blue etc. The common colours of Song Sancai were green, yellow, and brown. White was used rarely, and no blue decoration has been found. Liao Sancai were decorated with white, green, and yellow. Also, the cobalt-blue decoration was not applied to Jin Sancai. In other words, the use of cobalt on low-fired ceramics stopped after the Tang dynasty. Surprisingly, however, cobalt pigment was still used in high-fired blue-and-white porcelain in the Song dynasty. Seven Song

blue-and-white wares have been found in two pagodas, and one kiln site. Four sherds[4] were discovered in the rammed earth layer of two pagoda foundations – Jinsha Pagoda in Longquan, and Huancui Pagoda in Shaoxing (Zhu, 1980; Ruan, 1990), both in the Zhejiang province of southern China (Figure 1. 17). Three sherds from the Jinsha Pagoda and one sherd from the Huancui Pagoda were produced at or before 977 CE and 1265 CE respectively[5]. Furthermore, two blue-and-white sherds and one plate were found in the Jizhou kiln in southern China by an early archaeological survey (Tang, 1980). Their date was inferred to be Song or early Yuan. However, no more evidence for Song blue-and-white has been found by any recent excavation at this kiln.

The other difference is the glazing and painting techniques. The beauty of Tang Sancai is the bright colours with splash effect, whereas the preferred style of later Sancai was a regular pattern made by filling glazes after scraping motifs onto the body. Scraping motifs on the body is like drawing the outline on paper. For example, the potters carved several shallow lines on the unfired body with a hard tool (like an iron needle or bamboo stick etc.) to show a leaf and then covered the leaf by the green glaze. This technique was employed for many vessels, especially Sancai pillows (Figure 1. 14d and Figure 1. 15a). The splashed effect gave Tang

[4] Three big sherds were unearthed from Jinsha Pagoda and one sherd from Huancui Pagoda. Those three big sherds were thirteen small fragments when they were uncovered. And the excavator found that these fragments were from three different bowls after piecing them together (Zhu, 1980).

[5] Some tower bricks of Jinsha Pagoda were carved with Chinese characters '太平兴国二年' (Taiping Xingguo ernian) which corresponds to 977 CE, the second year of the reign of the second emperor in the Song dynasty, Taizong (reigned 976-997 CE).

A stele was excavated from the foundation of Huancui in 1970, which was carved with twenty-eight characters '岁次咸淳乙丑六月念八日辛未建景斌僧竟叅舍己财干造宝塔□座' which means a Buddhist monk donated private property to build the pagoda on the 28th of June in 1265 CE'.

Sancai a dynamic sense of beauty. In contrast, the scraping-and-filling made it possible for Song, Liao, and Jin Sancai to present complex and detailed patterns. Thus, fine flowers (Figure 1. 14d, Figure 1. 15 a and b), animals (Figure 1. 14d and Figure 1. 15b) and playing children (Figure 1. 15a) patterns, etc., became popular and creative styles of Song, Liao, and Jin Sancai wares.

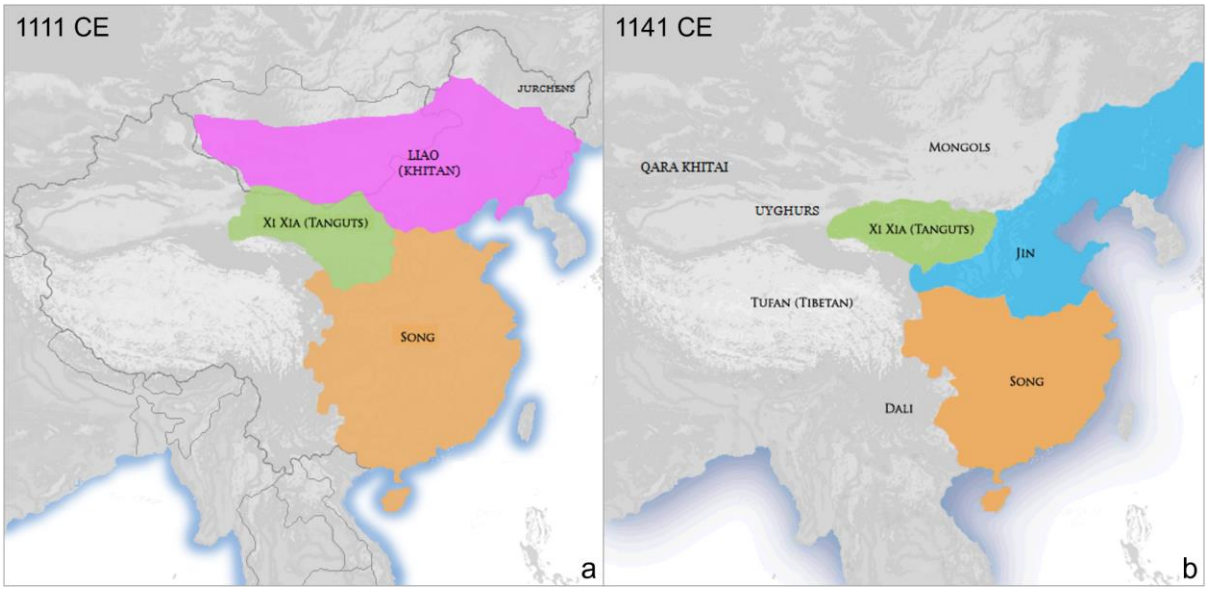


Figure 1. 13 Map of (a) Liao (Khitan) (purple area) and Song (orange area) dynasties in 1111 CE, (b) Jin (blue area) and Song (orange area) dynasties in (1141 CE), from (a) https://en.wikipedia.org/wiki/Administrative_divisions_of_the_Liao_dynasty#/media/File:Song-Liao-Xixia-1111.png and (b) http://en.wikipedia.org/wiki/Jin_dynasty_(1115%E2%80%931234)#/media/File:Jin_Dynasty_1141_(no_borders).png.



Figure 1. 14 Photos of Song Sancai: (a) and (b) human figures, (c) animal figures, (d) and (f) pillows (f-1 H. 9 cm, f-2 H.10.3 cm, f-3 H. 9.6 cm), and (e) bowl (H. 6.5 cm). Photos (a), (b) and (c) were from Li (2011), (d) was obtained from Wang (2011), and (e) and (f) cited from Yang and Zhao (2015).



Figure 1. 15 Photos of Jin Sancai: (a) pillows, from Li (2011); (b) vase, bowl, and censer, from Zhang and Ma (2000); (c) Deng (lamps), from Zhang and Zhang (2020).



Figure 1. 16 Photos of Liao Sancai: (a) figure of Buddha, Deng (lamp) and plate, obtained from

Yao (2017); (b) plate, animal-shaped pot, and heat retainer, from Shan (2019).

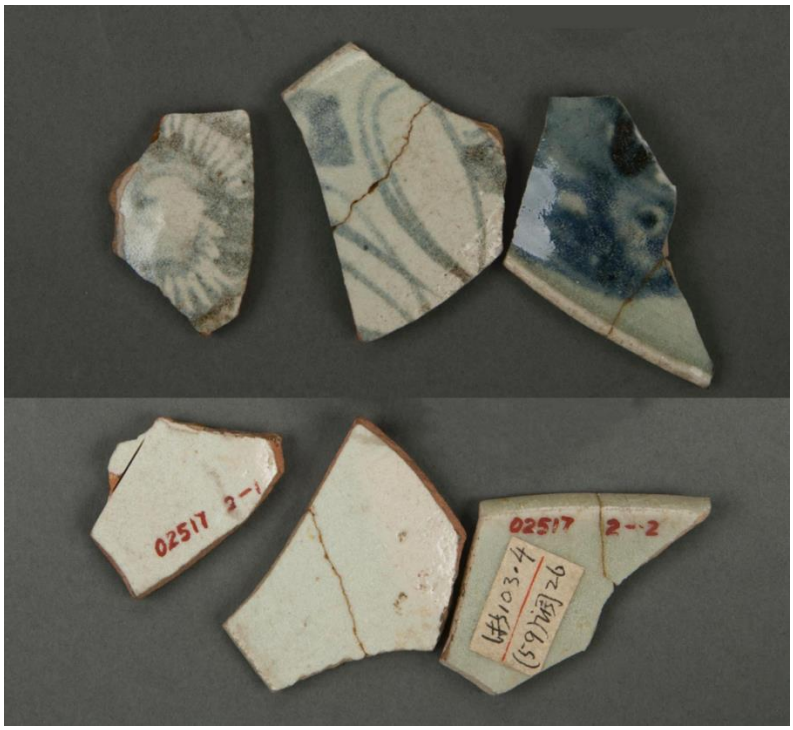


Figure 1. 17 Photo of Song blue-and-white sherds excavated from the foundation of Jinsha Pagoda in Longquan, southern China, obtained from Zhejiang Provincial Museum (https://www.zhejiangmuseum.com/Collection/ExcellentCollection/602zonghepingtaiexhibit/602zonghepingtaiexhibit). This image shows both sides of two sherds from two bowls. Two fragments on the left are regarded as one joint sherd because they belong to one bowl (Ruan, 1990; Zhu, 1980).

1.1.6 Transformation of Lead Glaze in the Yuan Dynasty (1271-1368 CE)

Although a few polychrome lead-glazed wares were still found in Yuan-dynasty tombs and sites (Figure 1. 18), its production and use declined considerably. Remarkably, some monochrome dark blue vessels were found in tombs near the Shangdu Site (the summer capital) of the Yuan dynasty (Figure 1. 19 a-c) (Wei, 2008a, pp.396-397), and a few polychrome blue

figures were found in Hebei (Figure 1. 19 d-h) (Ji, 2001). The use of blue glaze distinguished the Yuan-dynasty lead glaze from Song-, Liao- and Jin-dynasties glazes. The dark-blue colour of these monochrome blue vessels is the same as the cobalt-blue glaze of Tang Sancai. Probably, its colourant is cobalt. However, these vessels have not been analysed. Obviously, there are a lot of questions to be answered about the material – is it cobalt blue? And if it is, is it the same cobalt blue as the Yuan-dynasty blue pigment of blue-and-white porcelain in Jingdezhen[6]? The boom of Yuan blue-and-white porcelain proved that potters could obtain cobalt pigment in the Yuan dynasty, but no scientific analysis of these blue lead glazes has been carried out. Thus, it cannot yet be concluded that the Yuan-dynasty blue glaze was coloured with cobalt pigment. If these Yuan-dynasty blue glazed wares used cobalt pigment, they still cannot be grouped into Sancai, since their body was made of red clay rather than kaolinitic clay, therefore, it might be fired with glaze together at low temperatures around 700-900℃. In contrast, Tang Sancai employed kaolinitic clay to make the white body that needs twice firing – biscuit firing for hardening the body and low firing for maturing the lead glaze. The body material and firing are the key differences between Sancai and other lead-glazed pottery.

The big and significant transformation of lead glaze in this period was the mass production and wide distribution of lead-glazed tile. It had a specific name - Liuli (琉璃 in Chinese). This word was used to describe glass in early ancient Chinese literature, but from the Northern Wei dynasty (286-534 CE), it referred to the glazed tiles of buildings (Jiang, 1959). In the Tang dynasty, lead glaze was also applied to the roof of buildings, but only for the ridge tiles. The Yuan, Ming and Qing dynasties witnessed the prosperity of these lead-glazed tiles. For instance,

[6] Jingdezhen is a small city in the south of China. It was famous for its ceramic industry from the Yuan to Qing dynasties and was best known as China's porcelain capital.

many glazed tile fragments were found in the Site of Xanadu of the Yuan dynasty (Shi et al., 2021). Ming-dynasty Grand Bao'en Temple site in Nanjing contained more than 16,000 glazed sherds (Figure 1. 20 a-c) (Tang et al., 2022). The most famous and direct evidence is the golden roof of the Palace Museum (Figure 1. 20 d and e). From the beginning of lead glaze in the Warring States to the end of Qing dynasty, the production and use of lead glazes had many innovations, changes, inclines, declines and stops. This tradition has provided abundant invaluable treasure, but also many unanswered questions.



Figure 1. 18 Photos of Yuan 'Sancai' plates and pillows, obtained from Wang (2012).

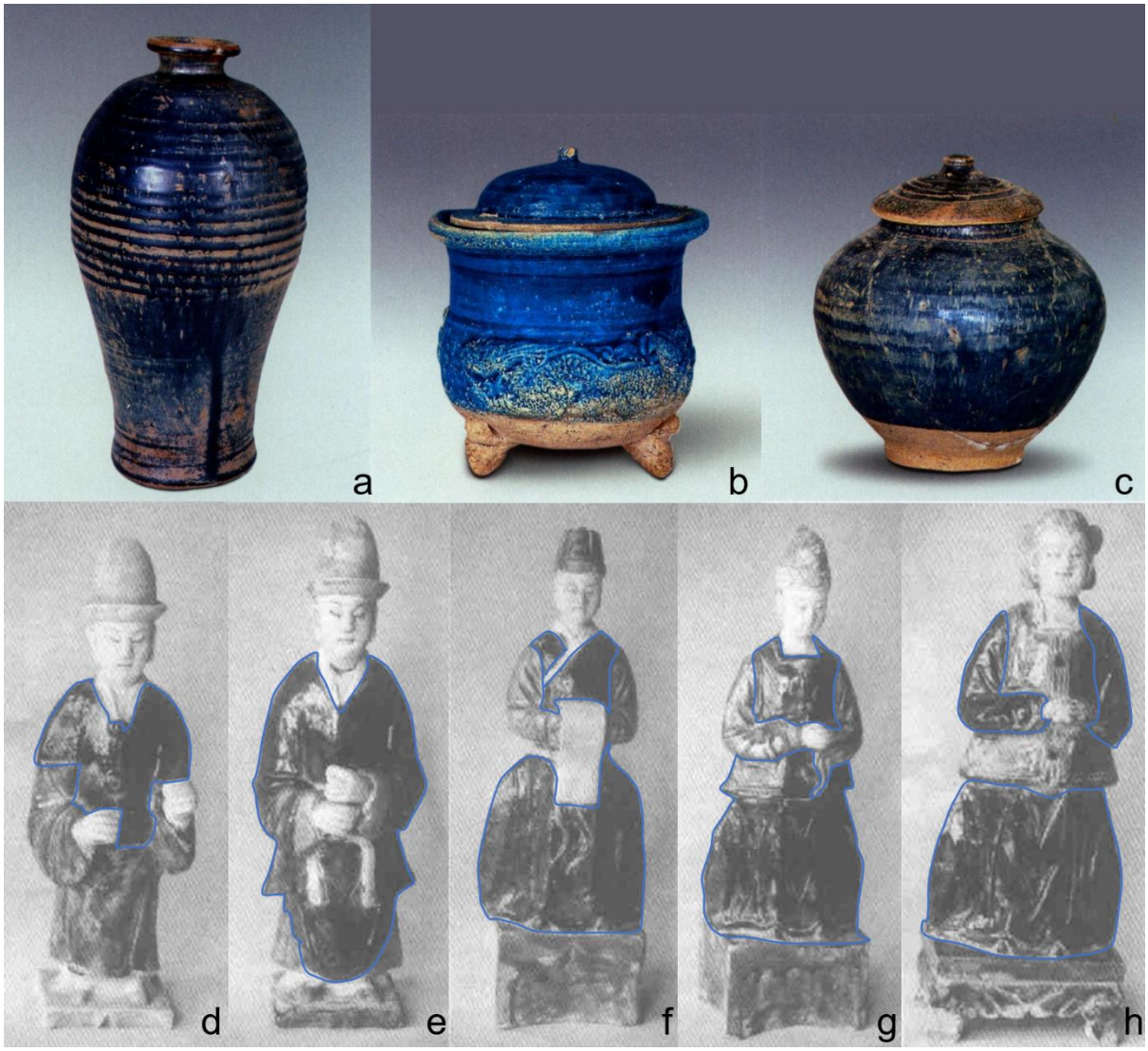


Figure 1. 19 Photos of blue glazed (a-c) vase, pots, and (d-h) figures. Blue vessels were excavated from DZXM29 tomb in Zhenzishan which was the biggest cemetery situated about nine kilometres as the crow flies to the southeast of Shangdu Site of the Yuan dynasty (Wei, 2008a, p.328). The colour of (a) and (c) was described as black (Wei, 2008a, pp.396-397), however the photos show dark blue (Wei, 2008b, p.216). (d-h) Blue figures unearthed in a Yuan-dynasty tomb, from Ji (2001). According to Ji (2001)'s description in the report, the blue area was outlined by blue lines.

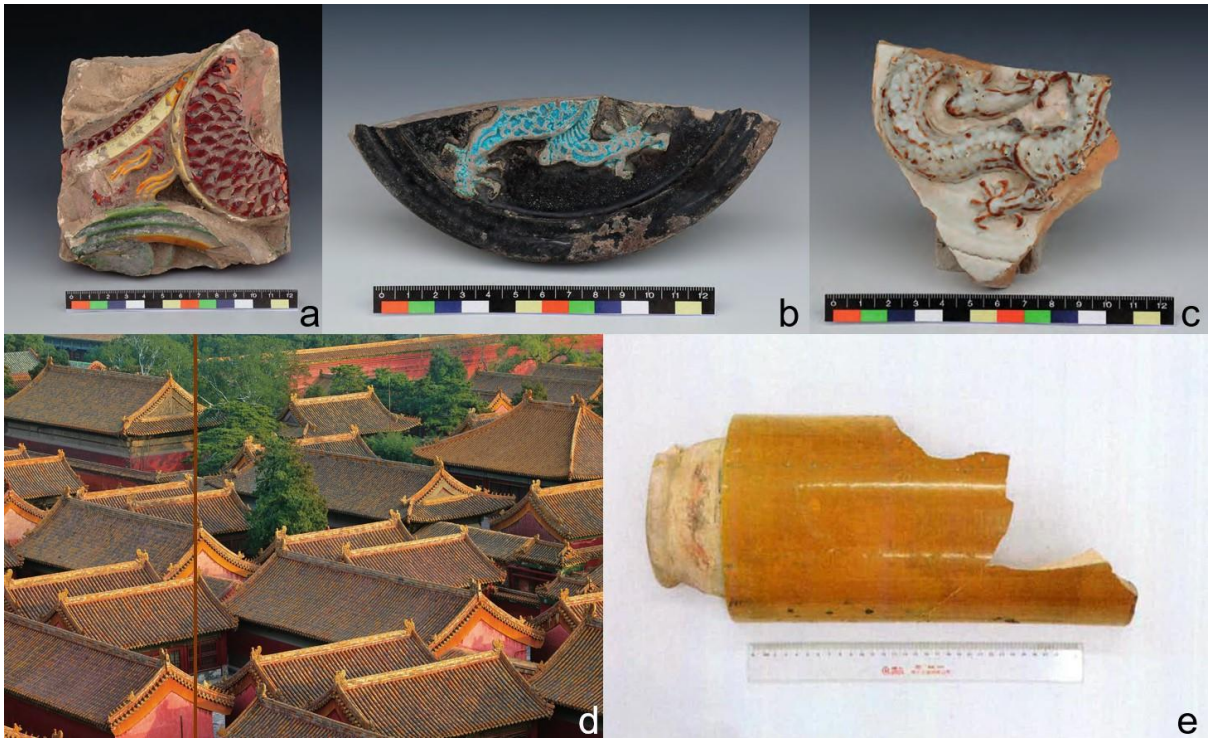


Figure 1. 20 (a-c) Photos of glazed tile sherds excavated from Grand Bao'en Temple in Nanjing, obtained from Tang et al., (2022). (d) Photo presents the roof of some halls in the Palace Museum, from https://www.dpm.org.cn/building/talk/225255.html. (e) Photo of a tile fragment of Shenwu Gate in the Palace Museum, from Kang et al. (2013).

1.2 Tang Sancai Kilns

Archaeological excavation has identified the provenance of Tang Sancai to six kiln sites (Figure 1. 21) - the Huangbao (also known as 'Huangbu' and 'Yaozhou') (Xue, 2002) and the Liquanfang kilns in Shaanxi (Shaanxi Provincial Institute of Archaeology, 2008), the Gongyi kiln (also known as 'Gongxian') in Henan (Henan Provincial Institute of Cultural Heritage and Archaeology et al., 2016b), the Xing kiln in Hebei (Jia and Jia, 1987), the Hunyuan kiln (or Jiezhuang kiln) in Shanxi (Tian, 2002) and the Qionglai kiln (or Qiong kiln) in Sichuan (Li, 2013). Except for Qionglai which is situated in southwest China, other Sancai kilns are in north China. The Liquanfang, Huangbao, Gongyi and Xing kiln sites were big ceramic factories in the Tang dynasty (618-907 CE) with abundant products and archaeological findings but only Liquanfang and Gongyi produced blue Sancai[7].

[7] Tang Sancai wares which include cobalt-blue decoration, either alone or in combination with other colours.



Figure 1. 21 Map of Tang Empire around 660s CE and the locations of six Sancai kilns (green spots), and two capital cities of Tang Empire – Chang'an (618-683 CE and 705-904 CE) and Luoyang (664-705 CE and 904-907 CE) (red stars), developed from https://en.wikipedia.org/wiki/Tang_dynastwordy#/media/File:Tang_circuits_660.png.

1.2.1 Gongyi Kiln

Gongyi (or Gongxian[8]) was famous for its ceramic industry in the Tang dynasty and is situated about 54 kilometres as the crow flies to the east of Luoyang (Figure 1. 22), the eastern capital

[8] Gongxian had been the official name of this city before 1991. And the kiln was named by the city so there is an ambiguity about the name. Although the official name has been confirmed as 'Gongyi kiln' in 2006, 'Gongxian kiln' still is used in some publications. In this thesis, I only use current official name -- 'Gongyi'.

city during 664-705 CE and 904-907 CE, and the second-largest city of the Tang Empire (Schafer, 1963, p.46). Rich coal and kaolin clay deposits benefit the industry of ceramic production. The Gongyi kiln site refers to two joint kiln sites and related smaller sites (Figure 1. 22), called Huangye and Baihe by Chinese archaeologists, which are about four kilometres apart and have similar products. The Huangye kiln site was the first known Sancai production site, found in 1957 and investigated officially five times from 1972 to 1984 (Henan Provincial Institute of Cultural Heritage and Archaeology et al., 2016b, pp.3-7). Henan Provincial Institute of Cultural Heritage and Archaeology organised a professional excavation in 2002-04. More than 5000 complete vessels (after repairing) and 800,000 sherds were unearthed from ten kilns, 162 ash pits and 20 other sites, such as ash trenches, filter tanks, elutriation pools and wells, etc (Henan Provincial Institute of Cultural Heritage and Archaeology et al., 2016b, p.29). The excavation shows that the production in this kiln site lasted around 300 years from the Sui dynasty (581-618 CE) to the end of the Tang (618-907 CE). These findings indicate that the Huangye kiln was quite a large factory producing ceramics in the Tang dynasty.

The other kiln site of the Gongyi kiln is Baihe which is a little smaller than the Huangye kiln site. Based on the excavation from 2005 to 2008, six kilns, more than 100 ash pits and other sites have been uncovered (Zhao, 2011). It has been found that this kiln was established in the Wei dynasty (386-534 CE) to produce white porcelains and celadons. The previous opinion had been that the Baihe kiln focused on producing white porcelains in the Tang dynasty. However, the excavation modified this consensus. Tang Sancai was mass-produced here even though fine white porcelains were the main products.

The Gongyi kiln site (Huangye and Baihe) was not only one of the producers of ordinary Sancai[9] and blue Sancai, but also the sole manufacturer of Tang blue-and-white porcelain. Four Tang blue-and-white sherds were found in the Baihe site, and two sherds were excavated from the Huangye site. The Baihe blue-and-white sherds have a clearer glaze, purer cobalt pigment, and finer blue motifs than the Huangye products. The production of blue Sancai started earlier and lasted for a longer period than that of blue-and-white porcelain. Blue Sancai was made from the seventh to the end of the ninth century CE and blue-and-white porcelain was developed in the late ninth century CE at this kiln (Henan Provincial Institute of Cultural Heritage and Archaeology et al., 2016b, pp.299-305). The analysis of Tang blue-and-white sherds found in Yangzhou and Siraf, two port cities in the south of China and Persian Gulf, revealed that they were produced in the Gongyi kiln in the late Tang, around the late ninth century CE. If future scientific analysis could confirm that the three complete blue-and-white plates in the Belitung shipwreck were produced by the Gongyi kiln, it would prove that this kiln started to make Tang blue-and-white porcelain in 826 CE or before. The manufacture of Song blue-and-white was not at Gongyi kiln and its provenance has not yet been found.

In summary, the Baihe and Huangye sites are like twins, and share similar experiences. They were both established near the same river in the Northern Wei dynasty (386-534 CE) and the Sui dynasty (581-619 CE) respectively (Henan Provincial Institute of Cultural Heritage and Archaeology et al., 2009, p.8; Henan Provincial Institute of Cultural Heritage and Archaeology et al., 2016b, p.304). Subsequently, their production peaked in the Tang dynasty, with a similar catalogue of wares, such as Sancai, celadon, whitewares[10], black wares, brown wares, blue-

[9] Tang Sancai wares without cobalt-blue decoration

[10] Most Gongyi celadons and whitewares are stoneware-bodied, but some translucent Gongyi whitewares are true porcelains in the English terminology as they are both white and translucent.

and-white wares etc. Specifically, the Huangye kiln is regarded as a specialist Sancai kiln, and Baihe is more famous for its white porcelain. However, all these productions were halted with the collapse of the Tang Empire (618-907 CE).

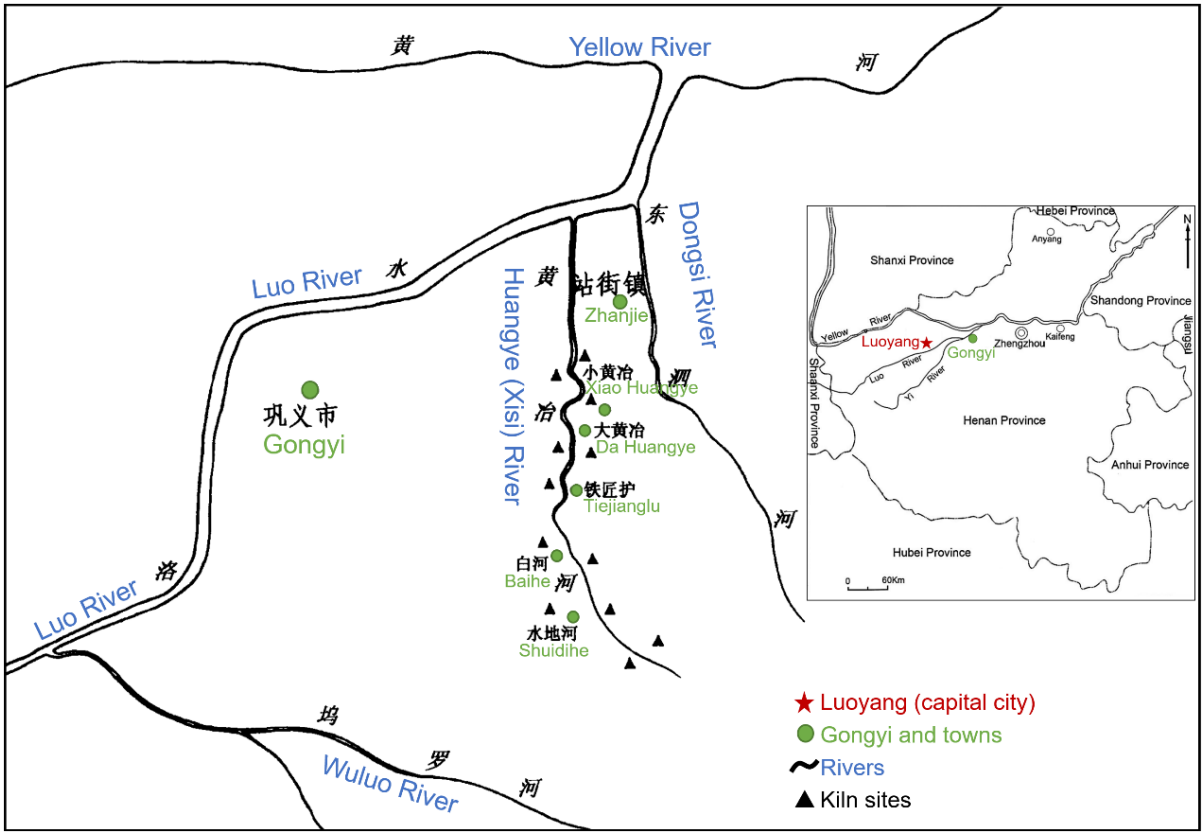


Figure 1. 22 Map of the Gongyi kiln sites and locations of Gongyi and its towns, developed from Henan Provincial Institute of Cultural Heritage and Archaeology et al. (2016b, p.2) and Li et al. (2017). The red star presents the location of Luoyang, the eastern capital city of Tang Empire. And the green spots present the locations of Gongyi city and its towns. Black triangular symbols show the excavation sites of the Gongyi kiln.

1.2.2 Liquanfang Kiln

The other maker of blue Sancai was the Liquanfang kiln in Chang'an (modern Xi'an) (Figure 1. 23), the capital of the Tang Empire (618-683 CE and 705-904 CE). Shaanxi Provincial

Institute of Archaeology organised the excavation in 1999 and found four kilns, ten ash pits and 12982 ceramics (intact wares and sherds). More than 97% of them are Sancai and fired Sancai body before glazing. Others are white and black porcelains (335) and pottery (352) (Henan Provincial Institute of Cultural Heritage and Archaeology et al., 2016b, p.112). In other words, Liquanfang was a professional Sancai kiln, which was different from Huangye and Baihe. Compared with the various products and the long history of the Gongyi kiln, the ceramic industry in the Liquanfang kiln had a smaller scale over a shorter period - only around 30 years in 730-760 CE, and blue Sancai was only a small part of its production (Shaanxi Provincial Institute of Archaeolog, 2008, pp.112-114). The main colours of Sancai bodies of Liquanfang products are red or pink, not as white as Gongyi Sancai. In contrast to the Gongyi kiln which was producing blue Sancai and blue-and-white porcelain, the Liquanfang potters only used cobalt-blue decoration on Sancai, but not for blue-and-white porcelain.

The important point about the Liquanfang kiln site was its location. It was named by its location, Liquan block ('fang 坊' means urban block in Chinese). This kiln site was built in the block which was one of the largest blocks in Chang'an city, the size of which was 838×1032 metres (Shaanxi Provincial Institute of Archaeolog, 2008, p.4). Around 1700 households, 10,000 inhabitants, lived there (Shaanxi Provincial Institute of Archaeolog, 2008, p.9). Yong'an Canal and Cao Canal were built in the east and south of this block (Figure 1. 23). The developed waterway connected this block to the Imperial Garden and the Wei River, which is the largest tributary of the Yellow River. The Liquan block was near to the Imperial City and close to the West Market, one of the biggest and busiest commercial areas, the start of the Silk Road. All these advantages could offer an easy market for Liquanfang products, and convenient transportation for raw materials. Moreover, the unique location may suggest a relationship between its products and the life of the city, perhaps even the imperial life of the Tang Empire.

Additionally, another special characteristic of this block is that many places of worship were gathered here, such as Buddhist temples, Taoist temples, Zoroastrian (fire-worship) temples etc, which distinguished it from other blocks in Chang'an. The Persian Temple, which was located in the south of the Liquanfang kiln site, was built in 677 CE by the Persian prince, Peroz III, who was son of Yazdegerd III, the last Sasanian King of Kings of Iran from 632 CE to 651 CE. Peroz III fled to Chang'an in 674 CE and served as a Tang general and the head of the Governorate of Iran, an exiled extension of the Sassanid court. Chinese archaeologists inferred that the Persian Temple and Liquan block became the gathering place for Persian people in Chang'an from that time. It has been unclear whether the deep religious life and assemblage of Persian people affected the production of the Liquanfang kiln, or not.

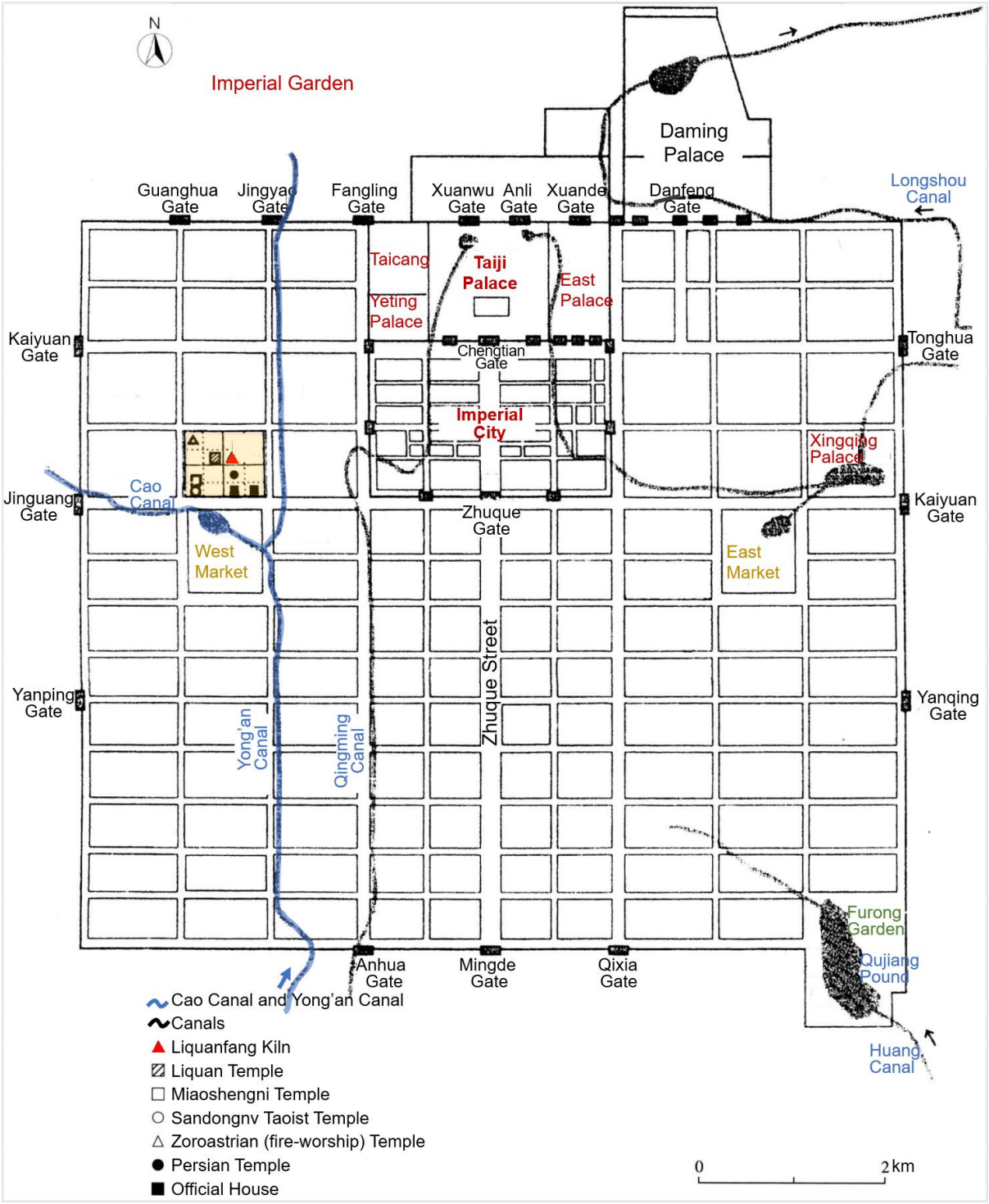


Figure 1. 23 (a) Map of Chang'an city during the Tang dynasty showing the location of Liquanfang, which refers to the block (yellow area) and the Liquanfang kiln (red triangle in the yellow area), developed from Shaanxi Provincial Institute of Archaeolog (2008, p.5).

1.2.3 Gongyi and Liquanfang: Related Kiln Sites?

The Gongyi and Liquanfang kilns were the only two makers of blue Sancai. What are the similarities and differences in technology and materials in Gongyi and Liquanfang products? Did technology and/or material exchange exist between them in the Tang dynasty? Firstly, the firing technology of the Gongyi and Liquanfng kilns were the same. The excavations have revealed 17 Tang-dynasty kilns sites in Gongyi and Liquanfang – one kiln in Baihe, ten kilns in Huangye and six kilns in Liquanfang respectively. All kilns in Gongyi and Liquanfang are cross-draught mantou kiln and the cross-section is hoof-shaped (Figure 1. 24). This design could offer a high temperature. The sizes of kilns in these two sites are similar. The width of the kiln chamber of the largest kiln Y6 in the Huangye kiln site is 1.58 m and the smallest one is 1.15 m (Henan Provincial Institute of Cultural Heritage and Archaeology et al., 2016b, pp.29-38). The width of the kiln chambers in the Liquanfang site are from 1.16 m to 1.58 m (Shaanxi Provincial Institute of Archaeolog, 2008, pp.15-19). The kilns in Liquanfang were built on the ground, but some kilns in Huangye were carved into small cliffs. Many Sancai (with fired glazes), fired Sancai body, black porcelain, brown porcelain sherds and vessels were discovered in Y6 of the Huangye site. This suggests that the Sancai body and porcelains shared the same high-temperature technology and used the same kiln. Also, body firing and glaze firing of Sancai used the same kiln but employed a different process. The biscuit firing temperature of the Huangye Sancai body was around 1000-1200℃ (Li et al., 2017) but glaze firing is about 800-900℃. The high-temperature kilns and high-quality raw materials ensure the success of hard and pure bodies, especially for the white body of the Huangye kiln site.

The body materials of Gongyi and Liquanfang had some differences. One of the advantages of Gongyi Sancai is the white body. Kaolinitic clay, the raw material of the body, in Gongyi was of high quality. However, at least two types of body materials were used in the Liquanfang

kiln: local loess-type earthenware clay to produce red or pink bodies, and stoneware clay for the white body. The archaeological and scientific analysis both found that this pure white body material was transported from Gongyi (Yong et al., 2005; Shaanxi Provincial Institute of Archaeolog, 2008; Ma et al., 2014; Henan Provincial Institute of Cultural Heritage and Archaeology et al., 2008, p.113, pp. 136-137; 2016b, p.310). Gongyi and Liquanfang kilns were conveniently connected to each other by natural and man-made rivers (Figure 1. 23 and Figure 1. 24), which made it possible to exchange technology and material. The distance between the two cities was not great, being about 380 km as the crow files.

Another significant connection was the use of cobalt material. Liquanfang blue wares had a similar cobalt-blue decoration to the Gongyi products (Figure 1. 25). The patterns are almost the same. The Gongyi potters decorated both Sancai and Tang blue-and-white porcelain by cobalt pigment, but this blue was only used on Sancai in the Liquanfang kiln. It is unknown whether the cobalt material of Liquanfang was transported from Gongyi or not. To summarise, the Gongyi kiln worked as a main centre which produced high-quality Sancai and dominated the production and design of Tang blue-decorated ceramics, blue Sancai and blue-and-white porcelain during the whole Tang dynasty for around 300 years (Table 1.1). The Liquanfang kiln was more likely to be a temporary workshop that produced red/pink-body Sancai and imitated the Gongyi blue Sancai for a period of 30 years, from around 730-760 CE. This workshop was constructed in a unique and advantageous location which connected Liquanfang Sancai directly to the imperial life of the Tang Empire and made those products ready for the international ceramic trade.

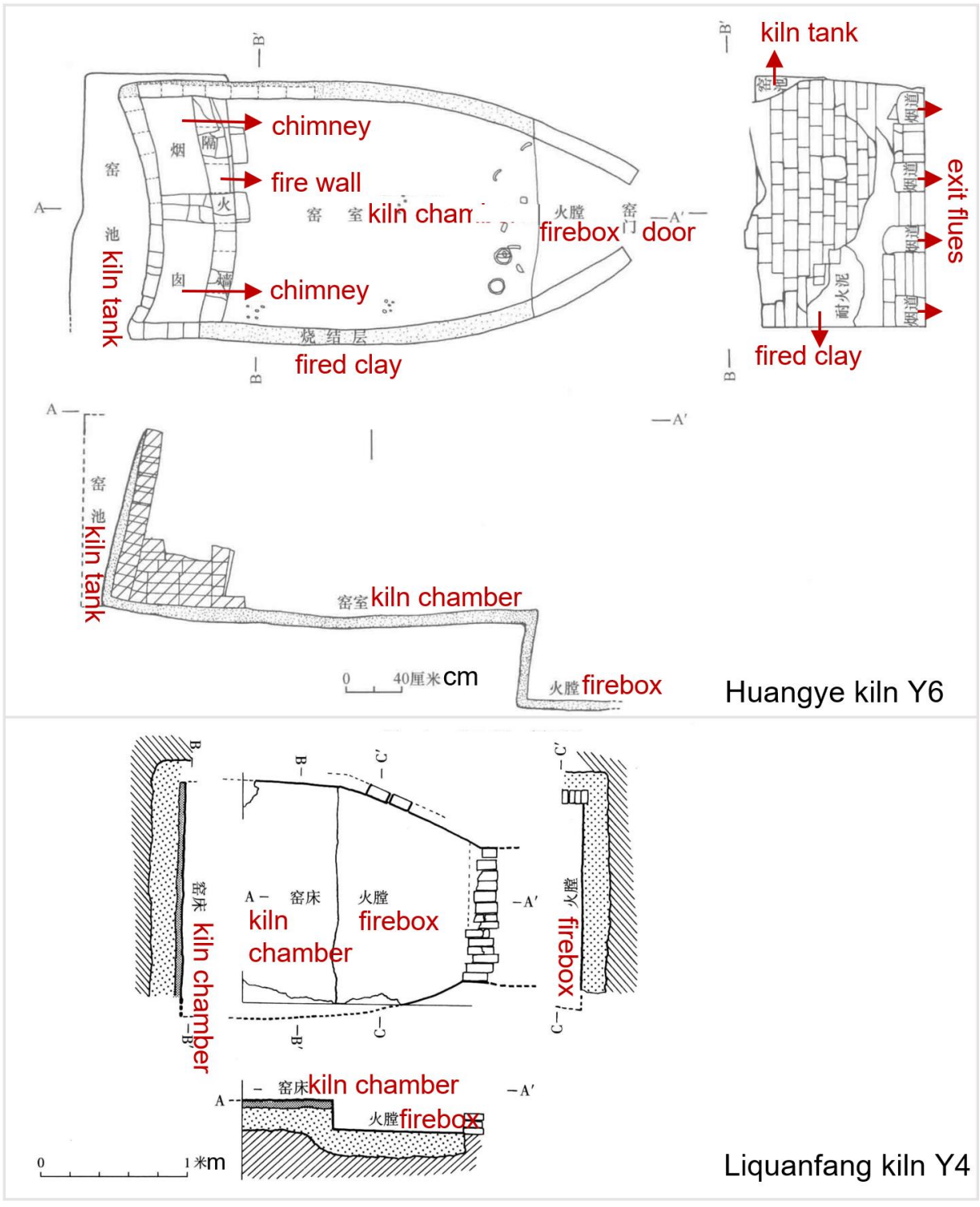


Figure 1. 24 Structure of two kilns in the Huangye and Liquanfang kiln sites, obtained from Henan Provincial Institute of Cultural Heritage and Archaeology et al. (2016b, p.5) and Shaanxi Provincial Institute of Archaeology (2008, p.18).

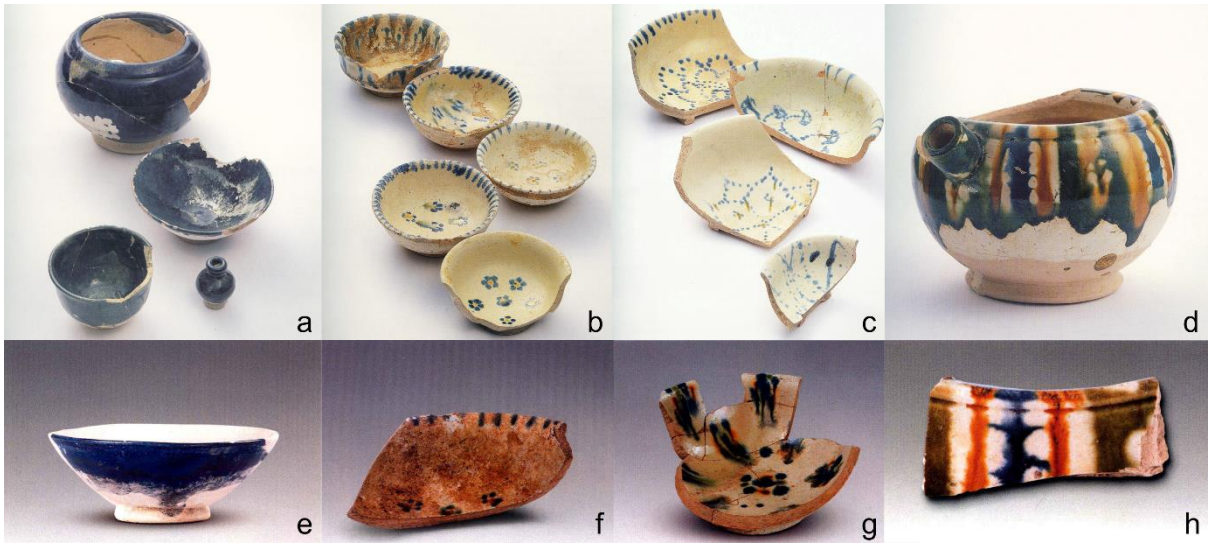


Figure 1. 25 (a-d) Photos of Huangye products and (e-h) Liquanfang products, obtained from (a-d) Henan Provincial Institute of Cultural Heritage and Archaeology et al. (2005, p.108, 133, 141 and 143), and (e-h) Shaanxi Provincial Institute of Archaeology (2008, p.5, picture list 11, 26, 29).



Figure 1. 26 Map of the Sui-Tang Canal, developed from https://en.wikipedia.org/wiki/Grand_Canal_(China)#/media/File:ChinaGrand_canal,_Sui_and_Tang.svg. Two red stars represent capitals, and the orange spot and two blue spots mark the

locations of Yangzhou and two kilns producing blue Sancai wares.

Table 1. 1 Comparison of production of the Huangye and Liquanfang kilns in different periods

Huangye kiln	Liquanfang kiln
581-618 CE (birth period): Celadon>white porcelain	No products
618-684 CE (development period): White porcelain>black porcelain>ordinary Sancai without blue decoration (no celadon)	
684-840 CE (prosperity period): Sancai (around 95%)>white porcelain>black porcelain; 70% ceramics are three-/four-colour Sancai (yellow, green, blue and white); 25% ceramics are two-colour (green-and-white, blue-and-white Sancai) and monochrome (yellow, green, white and blue)	730-760s: Sancai: 2863 (monochrome 1533), 8901 Sancai bodies; Others: 352 potteries, 335 porcelains, 531 ceramic-making tools, 17 glass: 17(fragments), 1 crucible, 11 ores, 336 bones (332fragments), 5 copper tools (knife etc.) and coins
841-907 CE (collapse period): Sancai: quality decreased but quantity increased; Main products: two colour (green-and-white, blue-and-white Sancai) and monochrome yellow Sancai; Several Tang blue-and-white porcelain sherds	No products

1.3 Why Tang Sancai and Why Gongyi?

Why was Tang Sancai selected as a research topic and why samples from Gongyi? As Figure 1. 27 shows, the technology of lead-glazed ceramics peaked during the Tang dynasty. Lead glazed wares were first made in the Warring States, but the number was very few and the colours were dark. The colourants inluded iron and copper but copper-green was not applied. In the Han dynasty, the production increased but the colours were still dark, and the technology of making clear glaze disappeared. Later, Northern-dynasties potters created kaolinite-based white body ceramics that gave the pottery a whiter ground, and the colours became brighter, but cobalt-blue glazes did not appear until the Tang dynasty. Finally, based on the white body, lead glaze, iron and copper colourants, and the newly imported cobalt pigment, Tang Sancai was made creatively, produced on a massive scale, traded intenationally, and variously imitated. The technology of lead glaze peaked in this period.

The current archaeological findings have discovered six Tang Sancai kilns in China. Gongyi and Liquanfang produced ordinary Sancai and blue Sancai together. The other four kilns only made ordinary Sancai. The manufacture of Sancai in Gongyi lasted the whole of the Tang dynasty, but only around thirty years in Liquanfang. More importantly, the Gongyi kiln is the sole known provenance of Tang blue-and-white. Blue Sancai and Tang blue-and-white were both produced here in the mid/late Tang. In other words, Gongyi potters gave birth to Chinese blue-and-white porcelain by transferring the technology of blue Sancai to Tang blue-and-white. Subsequently, blue-and-white porcelain replaced the use of Sancai, and boomed from the Yuan to the Qing dynasties. To summarise, the Gongyi kiln had the most various products, advanced technology and massive production amongst the six Sancai kilns in the Tang dynasty.

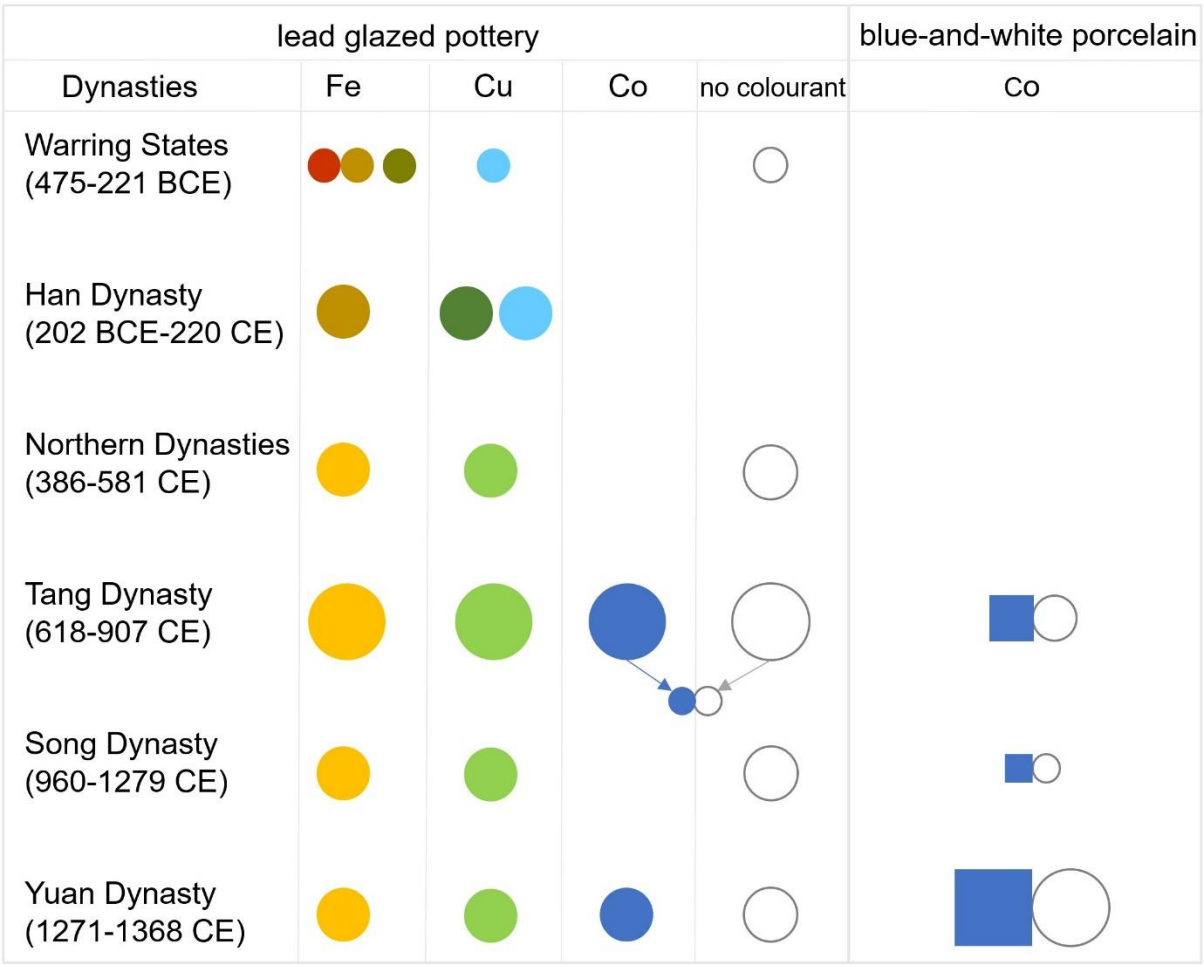


Figure 1. 27 Image of the simplified development of lead glazes from the Warring States to Yuan dynasty and of blue-and-white porcelain from the Tang to Yuan dynasties. The colour of spots presents the colour of glazes, and the blue squares presents cobalt pigment.

The key research question for Tang Sancai study is the technology. Until now, analysis of fired Sancai has been the only way to explore the raw materials, glaze recipe and processing methods, etc. This author got access to partially unfired (raw) glazes which offered the first and rare opportunity to look at the technology of Sancai in detail. Raw glaze samples were analysed and observed scientifically. Chapter 2 provides an overview of the methodology used in this research. Due to the similar colours of raw glazes, a reliable classification of these compositional data for all samples obtained from scientific analysis is necessary. Chapter 3

addresses this aim by the experimental glaze firing, and the observation and analysis of raw and fired glazes. Following this classification, the central research questions – colourants and glazes, of this thesis are addressed in Chapters 4 and 5 respectively. The possible types and origins of iron, copper and cobalt colourants of Sancai glazes are discussed in Chapter 4. Chapter 5 seeks to reveal the recipe, ingredients and manufacturing method of Sancai glaze. In summary, this thesis aims to understand the technology of the Tang Sancai glaze in detail by analysing rare raw glazes. This research also provides reference and clues for the study of other lead glazes.

Chapter 2 Samples and Methodology

As outlined in Chapter 1 (Introduction), this thesis aims to understand the technology of Tang Sancai glaze in detail by analysing raw glazed sherds excavated from the Gongyi kiln. This chapter provides an overview of the samples and methods employed in this research. The excavations, collections and descriptions of samples are presented in section 2.1. Following this, section 2.2 introduces three methods of instrumental analyses used in the lab work.

2.1 Samples

The archaeological findings of Tang Sancai are from tombs, temples (The Institute of Archaeology CASS, 1974) and palace sites (Gong and He, 2003). Sancai wares unearthed from these tombs and sites are finished products. However, kiln sites provide different sets of samples. Because they are the sites of manufacture, they can provide evidence of the raw materials used, partially finished samples, failed examples, as well as the finished products themselves. Accordingly, the collection of kiln samples is particularly useful in studying the technology of Sancai.

Based on the archaeological investigations, the Gongyi and Liquanfang kilns provide the most extensive range of Sancai products in the Tang dynasty, among all six Sancai kilns (the Gongyi, Liquanfang, Yaozhou, Xing, Hunyuan and Qionglai kilns). These two kilns produced clear, brown, green, and blue glazes. Other kilns, however, only made the first three glazes, but

not blue. The production of the Gongyi kiln was on a much larger scale than that of Liquanfang over a longer period. The Gongyi products have the greatest possibility to answer the core questions about Tang Sancai production, such as identification of raw materials and the processing techniques used to make Sancai glazes. Therefore, samples unearthed from the Gongyi kiln were selected carefully for this thesis.

2.1.1 Archaeological Investigations of the Gongyi Kiln

Gongyi city is located in central Henan Province, adjacent to the Yellow River to the north and 76 kilometres from Luoyang to the west. The Gongyi kiln sits 5-7 km east of Gongyi city. 'Gongyi kiln' is a collective name which refers to a series of kiln sites on both sides of the Huangye River (also known as the Xisi River), such as Huangye, Baihe and Tiejianglu etc., (Figure 1.22) rather than being a single archaeological site. The earliest archaeological investigation of the Gongyi kiln was carried out by Feng Xianming in 1957 (Feng, 1959). Feng and his colleagues investigated three towns in Gongyi and collected many Sancai, celadon and ceramic-making tools from there. Following this finding, many archaeological investigators from local institutes did a lot of field surveys, test-pitting, and sample collections from 1972-1987 (Henan Provincial Institute of Cultural Heritage and Archaeology et al., 2016b, pp.4-5). The most important large-scale excavation project of the Gongyi kiln was organised in 2002-2004 by the Henan Provincial Institute of Cultural Relics and Archaeology. This excavation covered 1570 square meters. Ten kilns, five workshops and caves, two wells, three tanks, twelve trenches and one hundred and sixty-two pits have been uncovered. More than 5000 restorable wares and 800,000 ceramic sherds have been found in this excavation (Henan Provincial Institute of Cultural Heritage and Archaeology et al., 2016b, pp.6-8). After that,

there was a salvage excavation in 2015, but not as large as the former one. The official report of this has not yet been published.

2.1.2 Sample Collection and Description

The manufacture of Sancai can be summarised into four procedures (Figure 2. 1): 1) using prepared kaolinitic clay to shape the body; 2) firing the body at a high temperature to toughen it; 3) decorating the fired body with raw glaze(s); 4) maturing the glaze by a low temperature firing. The published scientific analysis of Gongyi Sancai has focused on studying finished products, whether the discussion is about Sancai bodies or glazes (Cui et al., 2010a; Cui et al., 2010b; Ma et al., 2014; Shen et al., 2019; Chang et al., 2020; Chang et al., 2021). Undoubtedly, the research on semi-finished products could reveal more facts about the raw materials and technologies of Sancai. However, these samples are extremely rare and hard to be found and analysed. So far, no scientific analysis of raw glazes has been published. To understand more about the materials and technologies of Sancai glazes, I did a lot of fieldwork in Gongyi and

Zhengzhou[11] to find semi-finished Sancai. Finally, sixty-six raw glazed samples[12] were selected and analysed based on two excavation projects in 2002-2004 and 2015 (Figure 2. 2): eight sherds from the 2002-2004 excavation project (Figure 2. 3 and Figure 2. 4) and fifty-eight sherds from the 2015 project (Figure 2. 5 - Figure 2. 8).

These sixty-six samples were conserved with approximately tens of thousands other excavated samples in the storerooms of the Gongyi Museum and the Henan Provincial Institute of Archaeology. Based on the records of the excavation and excavator's notes (Appendices 1 and 2), the detailed information about the stratum of sixty-six samples is described in Table 2. 1. All samples were excavated from the middle-Tang and late-Tang strata but a more precise date than this period cannot be confirmed based on current excavation.

[11] Henan Provincial Institute of Cultural Relics and Archaeology organised the excavations of the Gongyi kiln in 2002-2004 and 2015. All samples and records of 2002-2004 project and some intact Sancai wares of 2015 project are stored in this institute in Zhengzhou. Other samples found from 2015 excavation are stored in Gongyi. The collection and analysis of Gongyi Sancai is based on the collaboration between Research Laboratory for Archaeology and the History of Art in Oxford University and Henan Provincial Institute of Cultural Relics and Archaeology. The collaboration agreement was signed in 14/11/2019. And Party A (Henan Provincial Institute of Cultural Relics and Archaeology) and Party B (RLAHA of Oxford University) acknowledge that Yun Zhang is a DPhil student at Party B and is undertaking the project as part of her DPhil studies. As such, nothing in this Agreement shall prevent: 1) the submission by Yun Zhang for a degree of Party B of a thesis or dissertation based on the results of the project, including the analysis of the samples, and the examination of such a thesis or dissertation by examiners appointed by Party B; 2) the deposit of such a thesis or dissertation in the library of Party B.

[12] Raw glazed ware/sherd refers to a type of semi-finished Sancai product. The body of this product is biscuit fired but the glaze decorating on the body is unfired and raw. The low-temperature glaze firing was not accepted by this product due to unknown reasons.

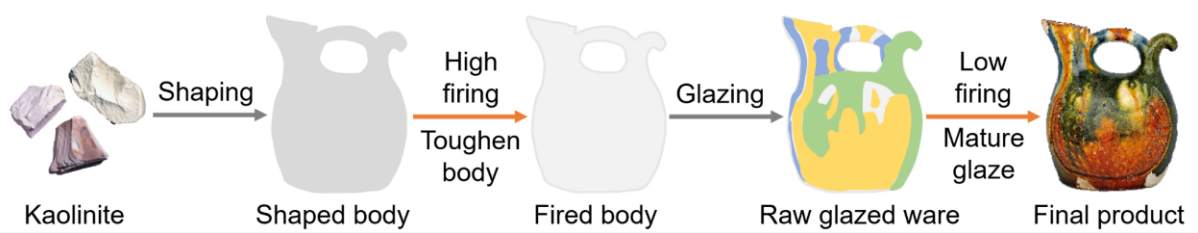


Figure 2. 1 Manufacturing process of Tang Sancai, source of photos of kaolinitic clay: https://www.britannica.com/science/kaolin and https://en.wikipedia.org/wiki/Kaolinite.

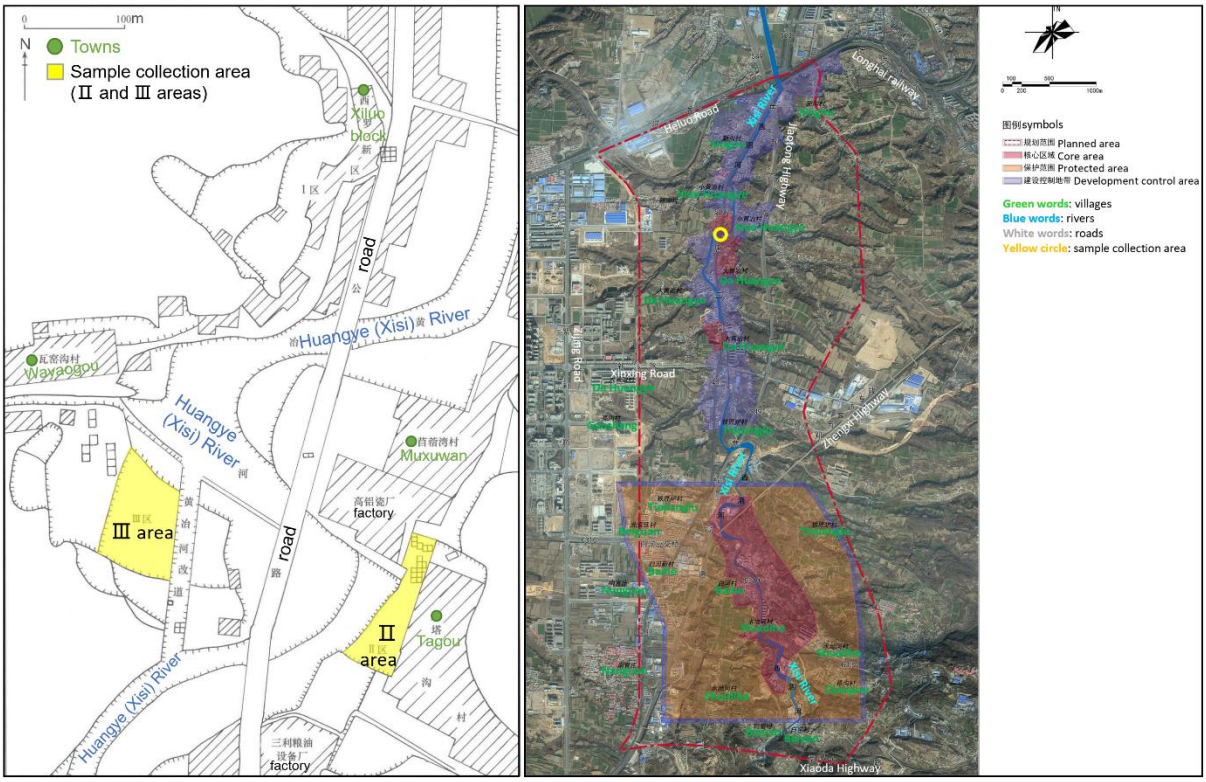


Figure 2. 2 Maps of the archaeological excavation in 2002-2004 (left) and in 2015 (right). Left: image was obtained from Henan Provincial Institute of Cultural Heritage and Archaeology et al. (2016b, p.9). Yellow areas show the location of sample collection. Right: the map is provided by a local excavator and archaeologist, Mr Hui Li[13]. Yellow circle presents the

[13] Hui Li is a Chinese archaeologist and excavator who works in Henan Provincial Institute of Cultural Relics and Archaeology, He led the archaeological excavation project of the Huangye kiln site in 2015.

excavation in 2015 and the sample collection area as well.



Figure 2. 3 Photos of the inside of 8 samples from the Gongyi kiln in 2002-2004, taken by the author.



Figure 2. 4 Photos of the outside of 8 samples from the Gongyi kiln in 2002-2004, taken by the author.

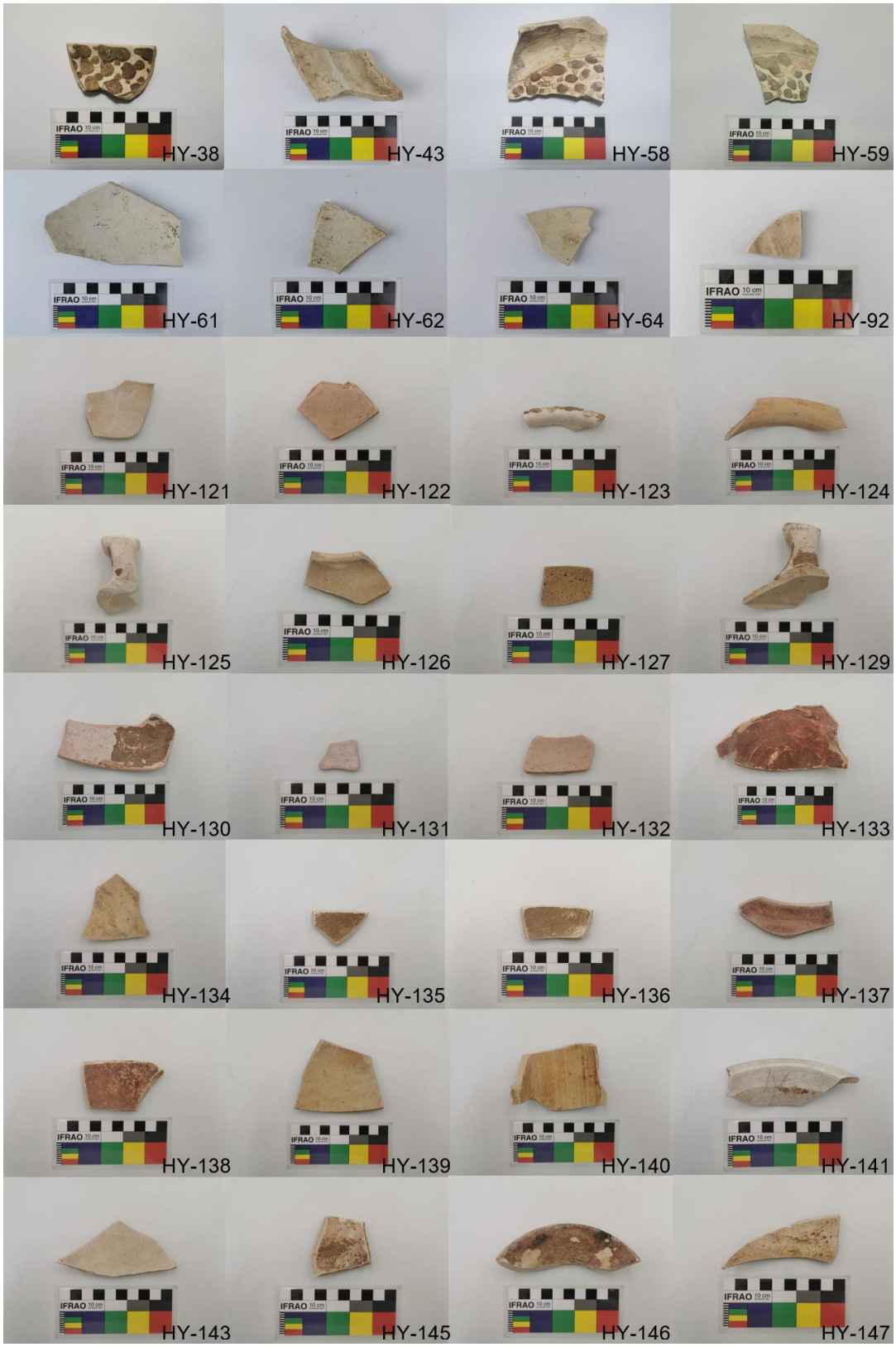


Figure 2. 5 Photos of the inside of 32 samples (HY-38 – HY-147) from the Gongyi kiln in 2015, taken by the author.

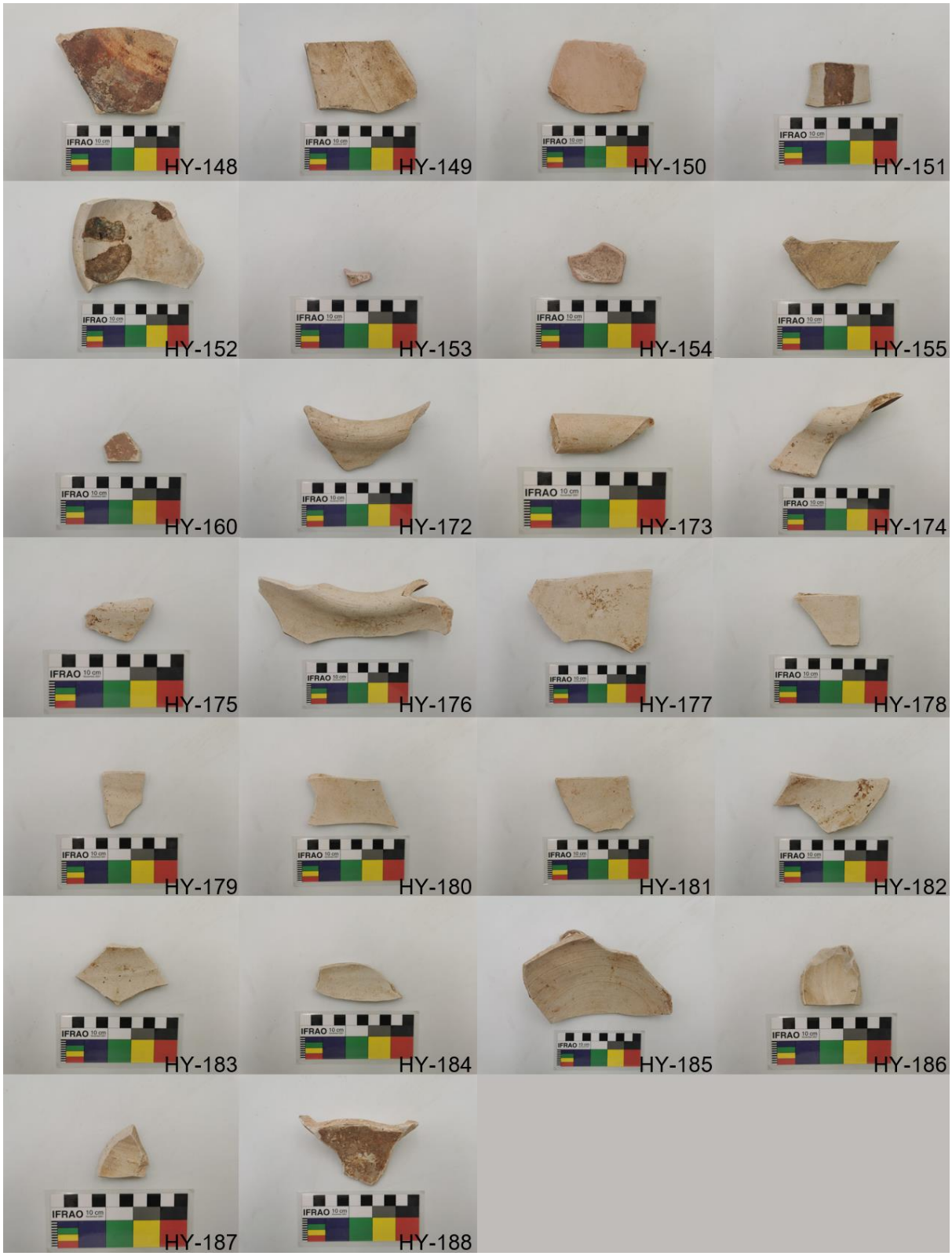


Figure 2. 6 Photos of the inside of 26 samples (HY-148 – HY-188) from the Gongyi kiln in 2015, taken by the author.



Figure 2. 7 Photos of the outside of 32 samples (HY-38 –HY-147) from the Gongyi kiln in 2015, taken by the author.



Figure 2. 8 Photos of the outside of 26 samples (HY-148 – HY-188) from the Gongyi kiln in 2015, taken by the author.

Table 2. 1 Strata of samples

Projects	Strata	Samples
2002-2004	II T4H15	HY-101, 102, 106, 115, 119
	II T6(0706)H81	HY-116, 117, 118
2015	T0131: ①	HY-127, 153, 154, 155, 166
	T0131: ⑥	HY-64, 129, 130, 172, 173, 174, 175, 176, 177, 178, 179, 180, 181, 182, 183, 184, 185, 186, 187, 188
	T0131: ⑭	HY-121, 122, 123
	T0231: ⑥	HY-43
	T0231:⑦	HY-38, 58, 59, 133, 134
	T0231:⑨	HY-137, 138
	T0236: ③	HY-126
	T0331: ⑥	HY-124
	T0331: ⑧	HY-146, 147, 148
	T0331: ⑧下	HY-149, 150, 151, 152
	T0332: ⑥	HY-135, 136
	T0131 北	HY-141, 143
	T0332H7	HY-61, 62
	T0331	HY-92
	T0237	HY-125, 139, 140
	T0 333C1	HY-131, 132
Unknown		HY-145

2.2 Scientific Methods

The analytical methods employed in the published articles on Sancai wares mainly include compositional analysis, isotope study and microstructure observation (Appendix 3). In most studies, X-ray fluorescence spectrometry (XRF) (Ma et al., 2014; Chang et al., 2020; Buravlev et al., 2022), inductively coupled plasma mass spectrometry (ICP-MS) (Li et al., 2005; Li et al., 2006; Chang et al., 2021), inductively coupled plasma atomic emission spectroscopy (ICP-AES) (Cui et al., 2010b) and instrumental neutron activation analysis (INAA) (Miao and Luo, 2001; Lei et al., 2007) are widely used to examine bodies and glazes of Tang Sancai. INAA has been utilised to test trace elements and identify elemental abundance patterns of Sancai bodies. Lei and his colleagues have done a considerable amount of work to distinguish Sancai products from different kilns and find the provenance of tomb figures and vessels by this method (Lei et al., 2004; Lei et al., 2005; Lei, 2007; Lei et al., 2007). ICP-AES and ICP-MS both are useful methods for studying trace elements and ICP-MS also could be employed to test for isotopes. Sancai glazes are analysed for lead isotopes as recently reported by Chang et al. (2021), Shen et al. (2019), and Cui et al. (2010a). These research aim to distinguish the different sources of lead raw materials and explore the possible exchange between kilns. Sr and Nd isotope analysis has been employed to discuss characteristics of body materials (Li et al., 2005; Li et al., 2006). Admittedly, these analyses are not non-destructive, and the cost is relatively high. In comparison, there is no special requirement for the XRF test. Any-size samples could be analysed compositionally within five minutes for every test. It is much simpler, safer, cheaper, and more rapid than others.

For microstructure observation, an optical microscope (OM) and scanning electron microscopy (SEM) both are significant methods. OM equipped with a functional magnifying

lens can show the detailed appearance of samples in natural colours and measure the thickness of glaze layers. It is generally accepted as the first-step observation. SEM plays an important role in subsequent analysis. It can be used to observe details of samples and examine compositions of tiny grains when it is associated with energy dispersive spectrometry (EDS). Besides these common instruments, some new methods have been employed in the study of Sancai. Dong et al. (2015) attempted to use optical coherence tomography (OCT) to explore the thin splashed Sancai glaze. Taking in to account the applicability, availability, and efficiency, XRF, OM and SEM-EDS were selected to explore the raw glazed samples in this study.

2.2.1 Optical Microscopy (OM)

Before the first-step observation, a detailed cleaning by absolute ethanol is necessary. When the dirt and disruptive contamination were removed, the appearances, surfaces, colours, motifs etc. of raw glazed sherds were all observed by two optical microscopes -- HIROX KH-7700 optical microscope in the Key Laboratory of Cultural Heritage Study and Conservation at Northwest University and ZEISS Smartzoom 5 Automated Digital Microscope in Shaanxi Academy of Archaeology. The magnification power of these microscopes is from 50x – 1000x and 10x – 1011x respectively. Both have measurement tools for length and area. The thickness of the glazes and the diameter of identifiable particles in the glazes were measured.

2.2.2 Energy Dispersive X-ray Fluorescence Spectroscopy (EDXRF)

The chemical compositions of all samples were obtained by the BRUKER ARTAX 400 μ-XRF in the Key Laboratory of Cultural Heritage Study and Conservation at Northwest University,

China. All the surfaces of the test area were cleaned with absolute ethyl alcohol before testing. If the contaminations adhere to ceramic sherds tightly, gentle grinding of the surface with fine papers is acceptable. These preparations can uncover the relatively fresh and original appearance of raw glazed sherds. The voltage used was 30kv and the current was 900μA. High-purity helium gas (99.9995%) was used to reduce the absorption of the secondary X-rays. The diameter of the beam was 1.5 mm, and the counting time was 300s. For most elements, the detection limit was 0.01-0.02%.

The Corning glass standards (Corning glass B, C and D) (Figure 2. 9) were used for calibration and calculation. Corning B is soda-lime silicate glass, Corning C is a high-lead and high-barium glass, and Corning D is a potash-lime silicate glass (Adlington, 2017). Twenty oxides – Na_2O, MgO, Al_2O_3, SiO_2, P_2O_5, K_2O, CaO, TiO_2, V_2O_5, MnO, Fe_2O_3, CoO, NiO, CuO, ZnO, SrO, SnO_2, Sb_2O_3, BaO, PbO were semi-quantitatively analysed by the Corning glass standards and using ARTAX software. The elements in samples were presented as these oxides. It does not indicate the stoichiometric formula of the oxides. For instance, iron in the samples might be Fe (II), Fe(III) or a mixture of them, but the compositional data obtained from EDXRF presents Fe_2O_3. Since the examination was run from April to June 2021, to be certain of the stability of the EDXRF and estimate the instrumental errors during the periods of lab work, I tested the three corning glasses (B, C and D) and calculated the data by the same standard (corning glass standard) on the 14th of April and 25th of June (Appendix 4). The comparison between the mean values and real values of three glasses shows that the data obtained from duplicate tests in April and June are stable (Figure 2. 10). And the relative errors between real value and analytical results are acceptable. To summarise, this instrument worked well during this lab work and the selection of corning glass standard is suitable for Sancai glazes.

Admittedly, XRF is not a perfect method as each method has its advantages and drawbacks.

The elements lighter than Na in periodic table cannot be detected by EDXRF. Sodium is the lightest element capable of being detected by EDXRF analysis, but the result is not accurate. Thus, the discussion and conclusion of raw glazes in this thesis cannot be certain about sodium. Besides, the content of Sb of corning glass B and D, and Ba of Corning glass C are not as accurate as other elements (Figure 2. 10). This might result from the voltage used (30kV). Heavier elements need higher energy to be excited. But these elements are not the main compositions of the Sancai glaze. Also, these results can be double-checked by SEM-EDS results. Thus, the XRF results are reliable in this study.

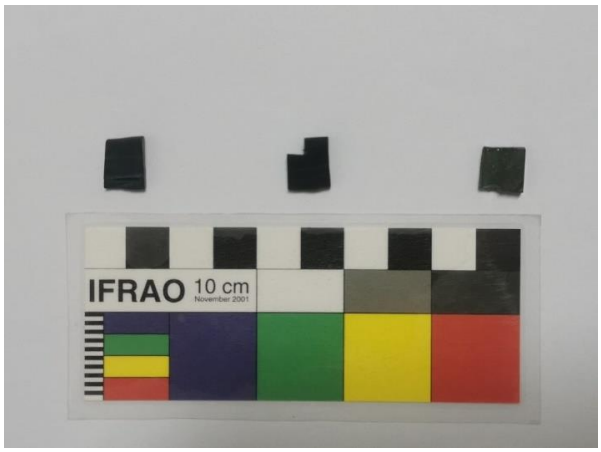


Figure 2. 9 Photo of Corning glasses B, C and D, taken by the author.

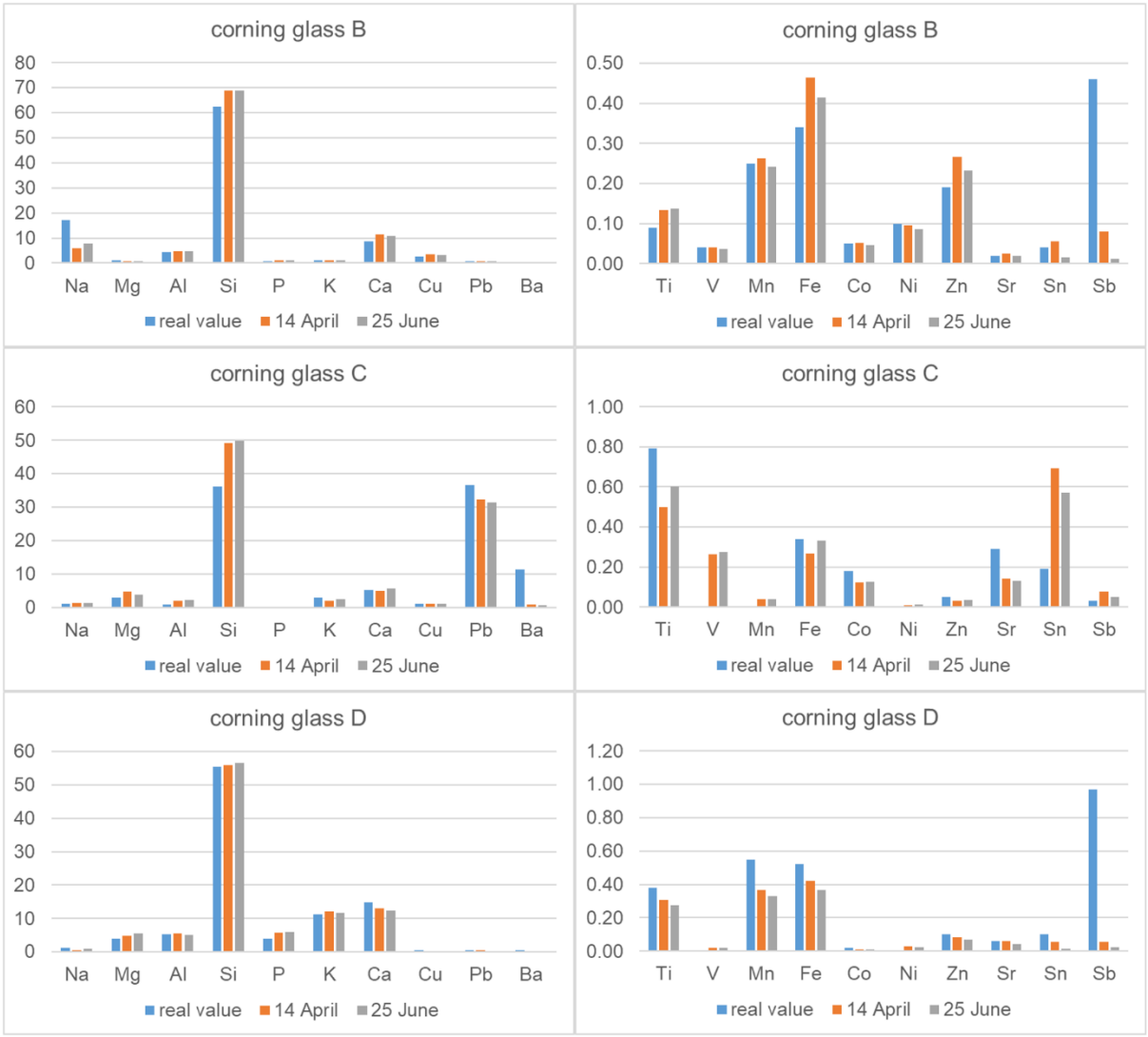


Figure 2. 10 Comparison between mean values and real values of three Corning glasses.

2.2.3 Scanning Electron Microscopy with Energy Dispersive Spectrometry (SEM-EDS)

To explore the raw glazed samples from different angles and answer the research questions based on more solid evidence, some samples were also observed and tested by scanning electron microscopy with energy dispersive spectroscopy (SEM-EDS). This is one of the most common analytical methods for archaeological ceramics, but it is not widely used in many Sancai studies to explore the raw materials because the fired lead glaze is very homogeneous

and highly melted. Mineral grains of raw materials cannot remain in fired glazes. However, these raw glazed samples could avoid this traditional disadvantage. The decision to use SEM-EDS was based on its many advantages. For instance, images of microstructure and chemical data of test areas could be obtained together by this instrument. And large magnification power and various analysis modes, such as spot, line scan, mapping etc., are quite helpful to explore raw glazes. This instrument also has limitations. Boron cannot be detected by this method, and carbon is too light to be tested accurately. Thus, if a carbonate mineral was used in the raw glaze, the SEM-EDS analysis cannot provide reliable and direct evidence.

The traditional sample preparation of archaeological ceramics for SEM-EDS study includes four steps: 1) get pieces by cutting; 2) put pieces into resin to make blocks; 3) grind and polish the blocks to expose samples and obtain even surfaces; 4) coat the surfaces by carbon to make samples conductive. However, the raw glaze is not as hard and well consolidated as the fired glaze. It is relatively soft and vulnerable and contains many particles which have different sizes and hardness. The general preparation possibly leads to scuffs and marks on the surfaces or a loss of many important particles, even the whole glaze layer. Moreover, there are many tiny cracks, holes and bumps on surfaces, the carbon particles cannot be removed totally after coating. It will change the appearance and affect later observation. For this reason, using conductive tapes to fix the samples on the specimen holder and coating some important sherds after careful selection were both accepted (Table 2. 2).

The SEM-EDS observation and examination were carried out using HITACHI TM4000Plus Tabletop Microscope with Oxford Instrument EDS in Research Laboratory for Archaeology and the History of Art at Oxford University. The EDS detector is Si(Li), and the system was operated at 5-20 kV accelerating voltage with selectable measuring time for all EDS analyses. Glaze microstructures were studied and recorded in vacuum mode by backscattered electron

(BSE) and mix (backscattered electron + secondary electron) images, in which the different phases present could be distinguished based on their atomic number contrast. The results are presented in Chapters 3, 4 and 5.

Table 2. 2 Samples observed and analysed by ESEM-EDS

Conduction	Samples	Total number of samples
Conductive tape	HY-38, 43, 58, 59, 61, 62, 64, 92, 101, 102, 106, 118, 123, 126, 127, 129, 132, 134, 136, 139, 151, 152, 166	23
Carbon coating	HY-38, 43, 101, 115, 126, 127, 130, 151	8

Chapter 3 Colours

As described and shown in Chapter 2.1, most of the samples shared similar colours. However, these raw (unfired) glazes cannot be grouped into brown, green, blue and clear by visual observation. Therefore, the aim of this chapter is to establish a classification standard of different-colour glazes by comparing the colours and compositions of some raw glazes and of fired glazes after the experimental glaze firing. Chapter 3.1 shows the design and process of experimental glaze firing, and Chapter 3.2 presents the establishment of the classification standard of raw clear, brown, green, and blue glazes. Following this standard, all raw glazes are classified in Chapter 3.3. The firing and classification laid the foundation for further analysis and discussion in Chapters 4 and 5.

3.1 Experimental Glaze Firing

Prior to the compositional examination of all samples, accurately inferring the matured colours of raw glazes after glaze firing is fundamental for all comparison and discussion. The major problem of observation is that the predominant colour of all raw glazes is brown, even though the details are different. There are reddish, yellowish, dark and pale brown. Therefore, finding a reliable method to classify the raw glazes by their matured colours is a prime task. An experimental glaze firing should be an appropriate choice.

Preparing experimental-firing samples is the first step. I selected some samples and obtained small pieces by cutting them to be the experimental-firing samples (the criteria of the selection were discussed below). Next, the raw glazes on these samples are analysed compositionally (details can be found in Chapter 2.2.2). Particularly, the chemicals of the main colourants – iron, copper, and cobalt, are significant. The third step is to fire samples in a muffle furnace under oxidation. When the glaze firing is finished, I used the same compositional analysis method to obtain the compositions of the same glaze. The last step is to confirm the compositional standards of classification of different raw glazes by comparing the chemical data and colour changes.

The limitation of this experiment is that the firing is irreversible. The cutting is a little destructive and the cut pieces could not show original information either from the appearance or inner microstructure when the firing is finished. To reduce the destructive processes and to ensure the validity of the experiment, the selection of samples is significant. There are three requirements. Firstly, this selection should cover all types of raw glaze colours identified by observation including reddish, yellowish, dark and pale brown raw glazes. Additionally, samples decorated by typical patterns should be involved because motifs and colours work together to show specific decoration generally. For example, HY-38 and HY-58 (Figure 2.5) both are typical products decorated by spots. Those different-size spots were painted regularly and repeatedly on the Sancai body, which might show a traditional pattern. And HY-101 is covered by raw glaze except for the foot area. Possibly, this sample is a monochrome Sancai after glaze firing. Also, a few special samples should be selected because the appearance cannot be predicted based on compositional analysis, such as HY-149 (Figure 2.8) covered by a confusing black material. According to these three standards, seventeen pieces were obtained from sixteen raw glazed sherds (Figure 3. 1).

The experimental glaze firing was carried out using a muffle furnace (Figure 3. 2) in the Key Laboratory of Cultural Heritage Study and Conservation at Northwest University, China[14]. There are different descriptions of the firing temperature of the Sancai glaze. Wood (1999, p.206) and Li (1998, p.467) proposed 900-100℃. Feng et al. (2005) 's opinion is that the high lead glaze could be melted thoroughly when fired at 800℃. Ye (2011, p.193) supported a lower temperature from 750℃ to 850℃. The samples are very tiny (Figure 3. 1 and Figure 3. 2 right) and the high-fluidity glaze might be lost if the temperature is too high. Thus 850℃ was set as the temperature of experimental glaze firing (Figure 3. 3). Figure 3. 4 shows the samples after experimental firing.



[14] Based on the regulation of labs in Northwest University and of students in Oxford University, the muffle furnace was operated by the professional assistant. The author designed and took photos. The whole process is safe and guaranteed.

Figure 3. 1 Photo of samples before experimental glaze firing



Figure 3. 2 Left: Photo of the muffle furnace in Northwest University. Right: Photo of samples and inside of the muffle furnace. Photos were taken by the author in the Key Laboratory of Cultural Heritage Study and Conservation at Northwest University, China.

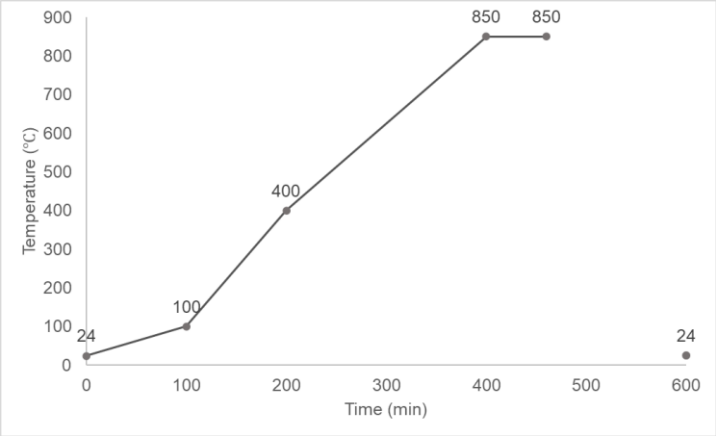


Figure 3. 3 Line chart of scheduled heating procedure of the experimental glaze firing by the muffle furnace.



Figure 3. 4 Photo of samples after experimental glaze firing, taken by the author.

3.2 Standards of Raw Coloured Glazes

3.2.1 Colour Changes of Experimental-fired Samples

The predominant tone of the raw glazes is brown with various shades even though they should show clear, brown, green and blue colours after the glaze firing. To establish the correspondence between raw glazes and fired glazes, 17 pieces were obtained from 16 samples by cutting and fired at 850°C using a muffle furnace. All selected samples were tested for composition by XRF before experimental firing, and, for best comparability, the same areas were examined again after the glaze firing by using the same instrument, parameters, and standards (Appendix 5). Sample selection and furnace setting have been shown in Chapter 2.3.

Eleven specimens – HY-38, -43 (a and b), -58, -59, -64, -92, -101, -118, -132 and HY-152 were fired successfully. The glazes of them show bright colours and vitreous lustre after experimental firing. However, the other six pieces – HY-61, -62, -127, -136, -138, and -149, became failed fired samples (Figure 3. 5 and Figure 3. 6). After firing, the black material on the HY-149 disappeared completely from the surface, while the appearance of the other five pieces was almost unchanged. The reason for these failures can be deduced from an analysis of their composition. HY-61 and HY-62 both have very low PbO, 9.20% (HY-61) and 8.27% (HY-62) respectively (Appendix 6). The low flux content cannot mature the raw lead glazes at 850℃. The PbO of HY-127 is also very low (6.10%), but it is not the only reason for the failed glaze.

The other reason is the high SiO_2 (66.87%) and Al_2O_3 (12.00%) which raise the melting temperature of the glaze. The sums of SiO_2 and Al_2O_3 of HY-61 and -62 are much lower than HY-127, around 10%. That is why some glazes in a few small areas on HY-61 and HY-62 were

matured and could show vitreous lustre after the firing (Figure 3. 5). High silica and alumina and low lead content should account for the unchanged appearance of HY-127 at 850℃. Such high silica and high alumina are characteristics of porcelain glaze rather than Sancai lead glaze. But if HY-127 is a porcelain sherd, its glaze should not contain such high PbO (6.1%). This is the result of a Sancai glaze mixing error or of a failed try for creating a new product. The specific reason cannot be explained based on current evidence. It is also worth noting that this glaze contains 1.91% Fe_2O_3 and 4.31% CuO, and the colour is dark green (Figure 3. 7). If the firing temperature can meet the demand of maturing the glaze, perhaps 1100-1200℃, what would be the matured colour? Copper-red or dark green? The answer to this question needs further experiments and is worth exploring in the future.

The PbO of HY-138 is much lower than that of HY-127, only at 0.74%. However, the SiO_2 and Al_2O_3 are up to 50.03% and 25.65%. At the same time, the alkali metal oxide – MgO, CaO and K_2O, are very high. The colouring element Fe_2O_3 is 6.83%. Accordingly, this sherd might be celadon. But celadon is supposed to be fired once at a high temperature, around 1200℃. Why is the body of it biscuit-fired but the glaze is unmatured? These questions require more experiments and discussions to explore in future work.

Before firing, HY-149 was covered by a very thin layer (42.43μm) of black material (Figure 3. 8), almost free of PbO (0.05%) which is probably not a lead glaze. The black material disappeared, and its composition was almost unchanged after firing. Presumedly, it might be a thin layer of carbon remaining from smoking. The carbon is oxidised to carbon dioxide and disappear at high temperatures. Two findings, however, contradict this supposition. If the black material is smoked carbon which cannot be detected by XRF, the test results from the surface would be the same as that of the body. However, the compositions show that the unfired black material contains higher K_2O and CaO than the body, 5.14% and 6.74% in the black material

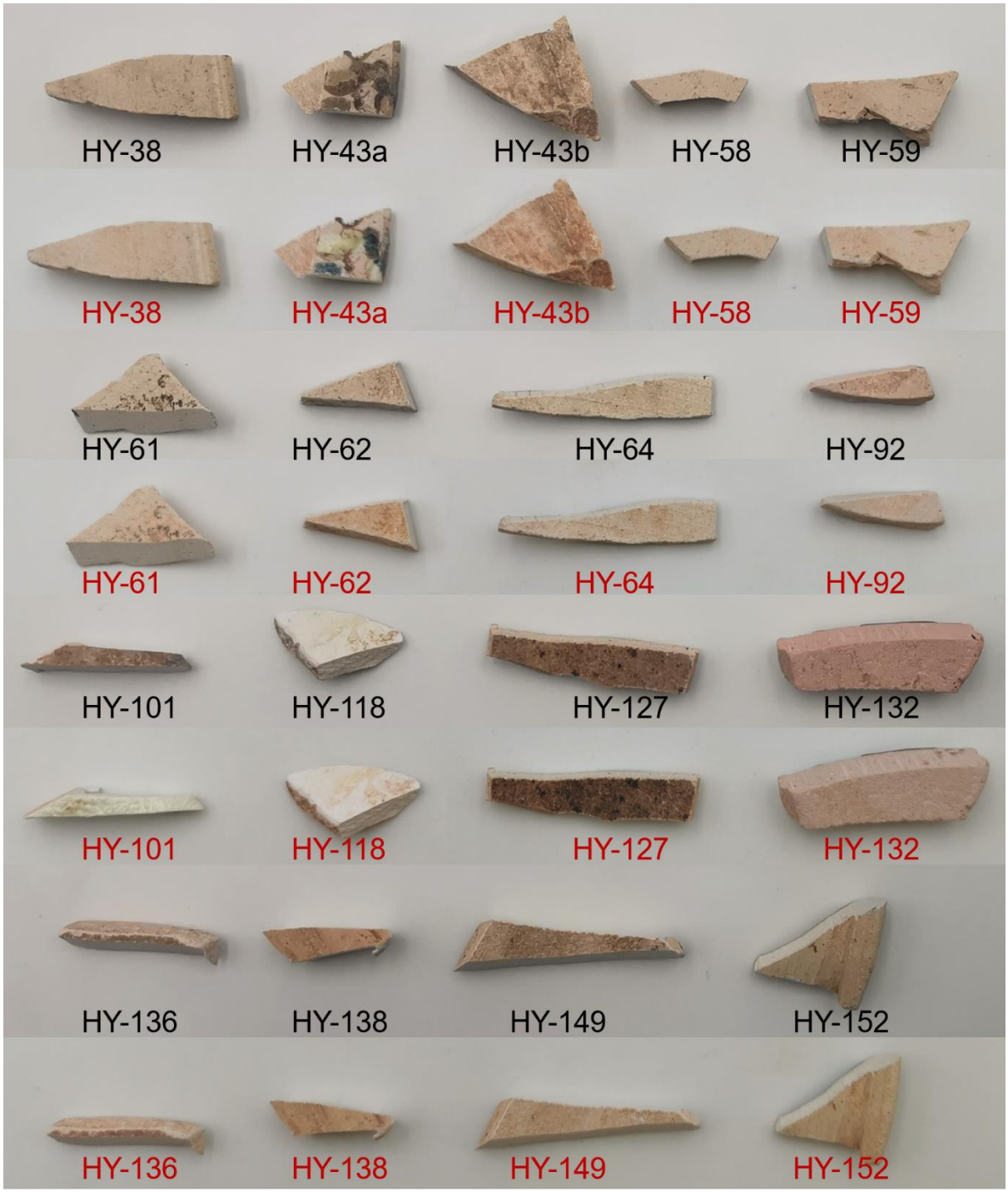
and 2.17% and 0.64% in the body (Appendices 6 and 7). The other finding is that a very thin layer of shiny glaze can be seen on some areas of the surface after firing by microscope (Figure 3. 8). Therefore, perhaps, the black material is a thin-layer residual glaze after the removing of the whole layer of glaze.

The compositions of HY-64-1 and HY-136 show that they should be tri-coloured glazes. The PbO contents are 21.43% and 25.58%, and the sum of SiO_2 and Al_2O_3 is 30-40%. But the raw glaze did not show vitreous lustre after experimental firing. In contrast, the other raw glazes of HY- 64-2 (Figure 3. 8) were successfully fired, forming a glaze with a dark brown colour and a vitreous lustre. The compositions of HY-64-1 and HY-64-2 are very similar (Appendix 6) which suggests that the temperature is sufficient to mature the glaze in this experiment and that the lack of a glossy glaze was most likely due to the flaking of the glaze or the too-thin layer of glaze. HY-136 shared a similar condition with HY-64. The thickness of the glaze on HY-136 only is 39.69μm. Although some of these questions have not yet been definitively answered, they are worthy to explore in the future. The Gongyi kiln was a major factory producing both Sancai and various types of porcelains at the same time. The study of these failed fired samples may provide evidence for the connections between different ceramics in terms of materials and technologies in Gongyi. Significantly, the classification standard of raw glazes can be established based on the analysis of those successfully fired samples. All 66 sherds collected for this thesis would be grouped into raw Sancai, raw porcelain, raw/fired special ceramics (such as semi-porcelain-semi-pottery etc.), unglazed sherds etc. Raw Sancai lead glazes were selected and examined by XRF and ESEM.



Figure 3. 5 Photo of unfired and fired samples (one side), taken by the author. Black labels

mark samples before experimental glaze firing and red labels represent sherds after firing.[15]



[15] A raised brown glaze spot appeared on HY-64 after experimental firing. It was preserved well during the XRF analysis (Appendices 5 and 6). However, this brown glaze ball was broken before taking this photo. Therefore, the same sample in Figure 3.5 (HY-64) and Appendix 5 (brown glaze) looks different.

Figure 3. 6 Photo of unfired and fired samples (the other side), taken by the author. Black labels mark samples before experimental glaze firing and red labels represent sherds after firing.

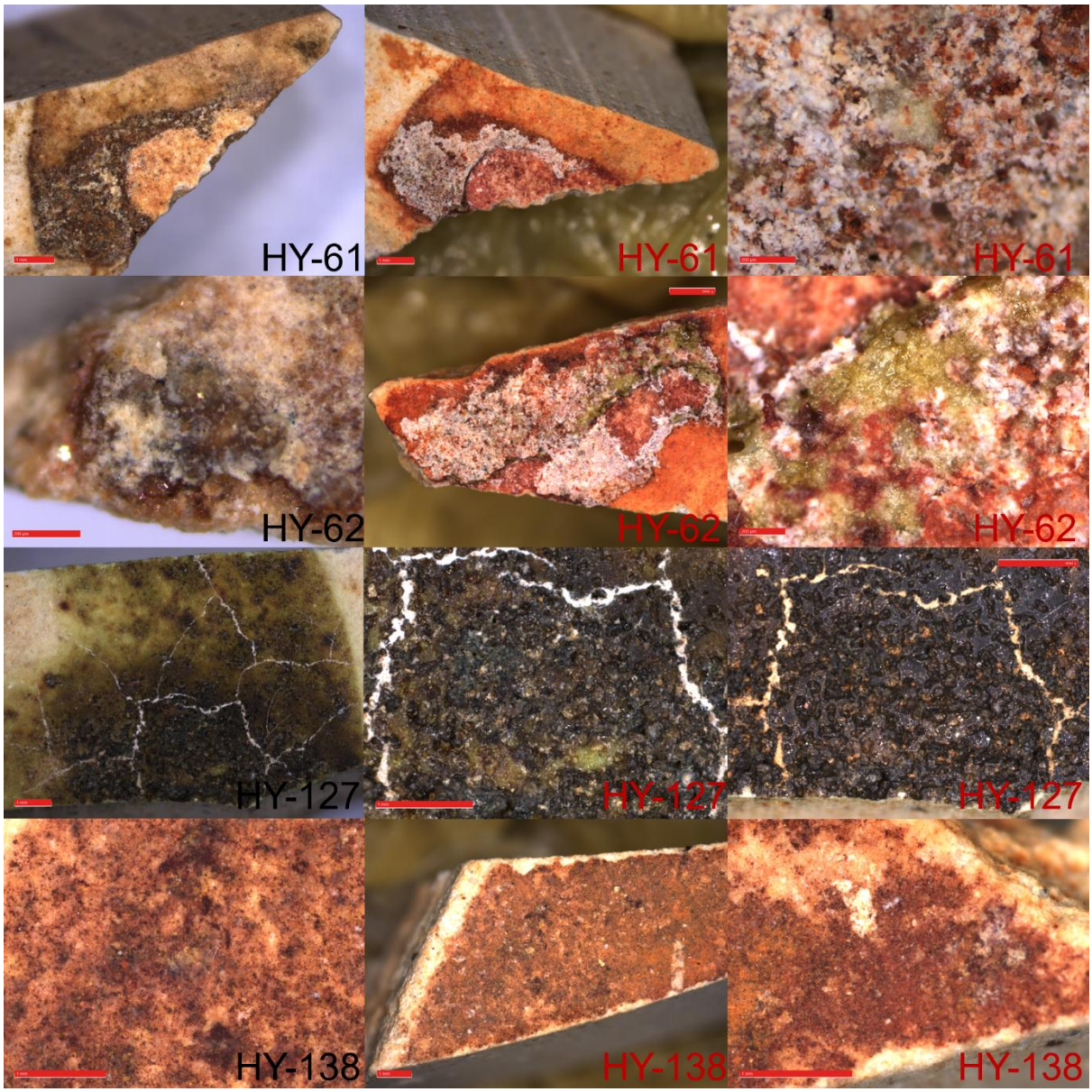


Figure 3. 7 Photos of unchanged samples after the experimental glaze firing, obtained from observation by the optical microscope. Black labels mark samples before experimental glaze firing and red labels represent sherds after firing.

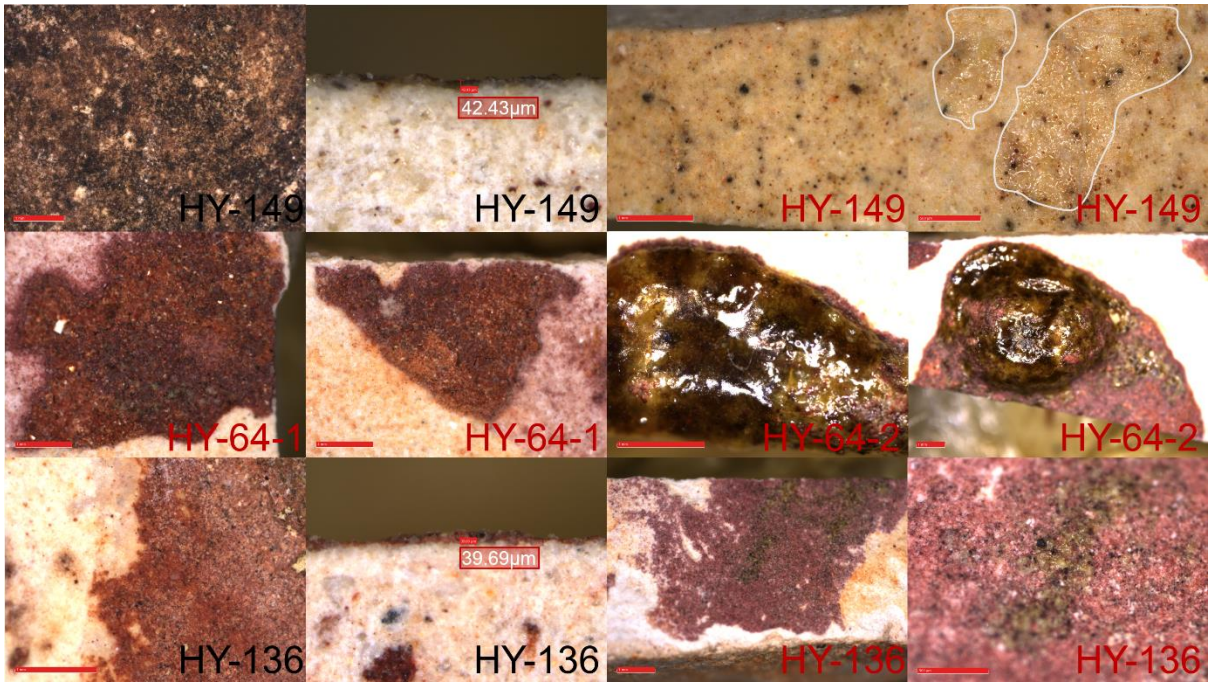


Figure 3. 8 Photos of special changes of three re-fired pieces, obtained from observation by the optical microscope. Black labels mark samples before experimental glaze firing and red labels represent sherds after firing. The white numbers in the photo of HY-149 and HY-136 present the thickness of dark layers.

For the 10 samples successfully fired - HY-38, 43, 58, 59, 64, 92, 101, 118, 132, 152 - the colour of the raw glazes can be classified as blackish brown, reddish brown, yellowish brown and white/pale yellow. Following this finding, a very important question is raised: do the colours of the raw glazes correspond to the colours of the fired glazes? If a one-to-one correspondence exists and the white/pale yellow raw glaze became clear after firing, the three coloured glazes are most likely to be made by the same stock glaze. The colourless clear glaze might work as the stock glaze. Although the colourants changed the shades of raw colours, the addition is too small to transform the predominant tone (brown) of the unfired glaze. If sherds which shared the same raw colour, such as reddish brown, show different colours after firing, it could be confirmed that the same main ingredients were used for all raw glazes. Although

the colourants are various, the addition of them is too small to affect the shades of raw colours. The different browns – blackish, reddish, or yellowish brown, were caused by different production batches. For example, potters obtained raw materials from place A in Gongyi during several years and the colour of this glaze material was yellowish brown. When these materials were depleted, potters started to use raw materials in place B in Gongyi. The colour of that material might become reddish brown or blackish brown. In other words, those colours might relate to the date of production which can be revealed by the stratum of excavation. The last hypothesis is that the correspondence is neither one-to-one nor one-to-all, but rather cross-correspondence. This complex correspondence may indicate the combination of the former two hypotheses. The observation of colour changes after experimental firing is an essential premise to establish the classification standards and can clue the discussion of the manufacturing process and making methods of the Sancai glaze.

The clear glazes were mostly yellowish brown before firing, such as HY-43, -59, -118 and -101, but in different shades (Figure 3. 9). Clear glaze on the HY-43 was very dark brown before firing, while the raw colour of HY-101 was very light, almost yellow. The most unusual sample is HY-58 which showed white colour before firing by the optical microscope. The brown Sancai glazes were all reddish-brown colour before firing (Figure 3. 10). Some of the reddish-brown colours are very dark, such as HY-43. This colour is difficult to be distinguished from the blackish brown. The green-glazed samples are yellowish brown before firing, and darker than the typical clear glaze samples (HY-59, -101, and -118) (Figure 3. 11). There is only one blue glaze sample, HY-43, which shows a different characteristic from all the other glazes. The colour of it was blackish brown, the darkest one among all raw glazes (Figure 3. 12). Overall, the clear glaze covered most kinds of colours before firing – from the lightest white and yellow to yellowish brown and brown. Other coloured glazes (brown, green and blue) show the one-

to-one correspondence of raw colours and fired colours. After firing, raw reddish brown became brown/yellow; raw dark brown and yellowish brown showed green; raw blackish brown matured to blue. These features imply a possibility that all raw glazes shared a base or a stock glaze. The one-to-one correspondence between raw colours and fired colours suggests that the iron, copper, and cobalt colourants determined different colour tones in the raw glazes. Based on this possibility, two hypotheses of glaze making can be proposed (Figure 3. 13). The first one is that raw clear glaze worked as the base of stock glaze of all raw coloured glazes. Iron, copper, and cobalt colourants were added to the clear glaze to make coloured glazes. The other hypothesis is that four raw glazes shared the same stock glaze. Colourants of coloured glazes and an unknown material of clear glaze were mixed up with the stock glaze to produce four raw glazes. These hypotheses and more key procedures of glaze-making techniques will be discussed in Chapter 4.

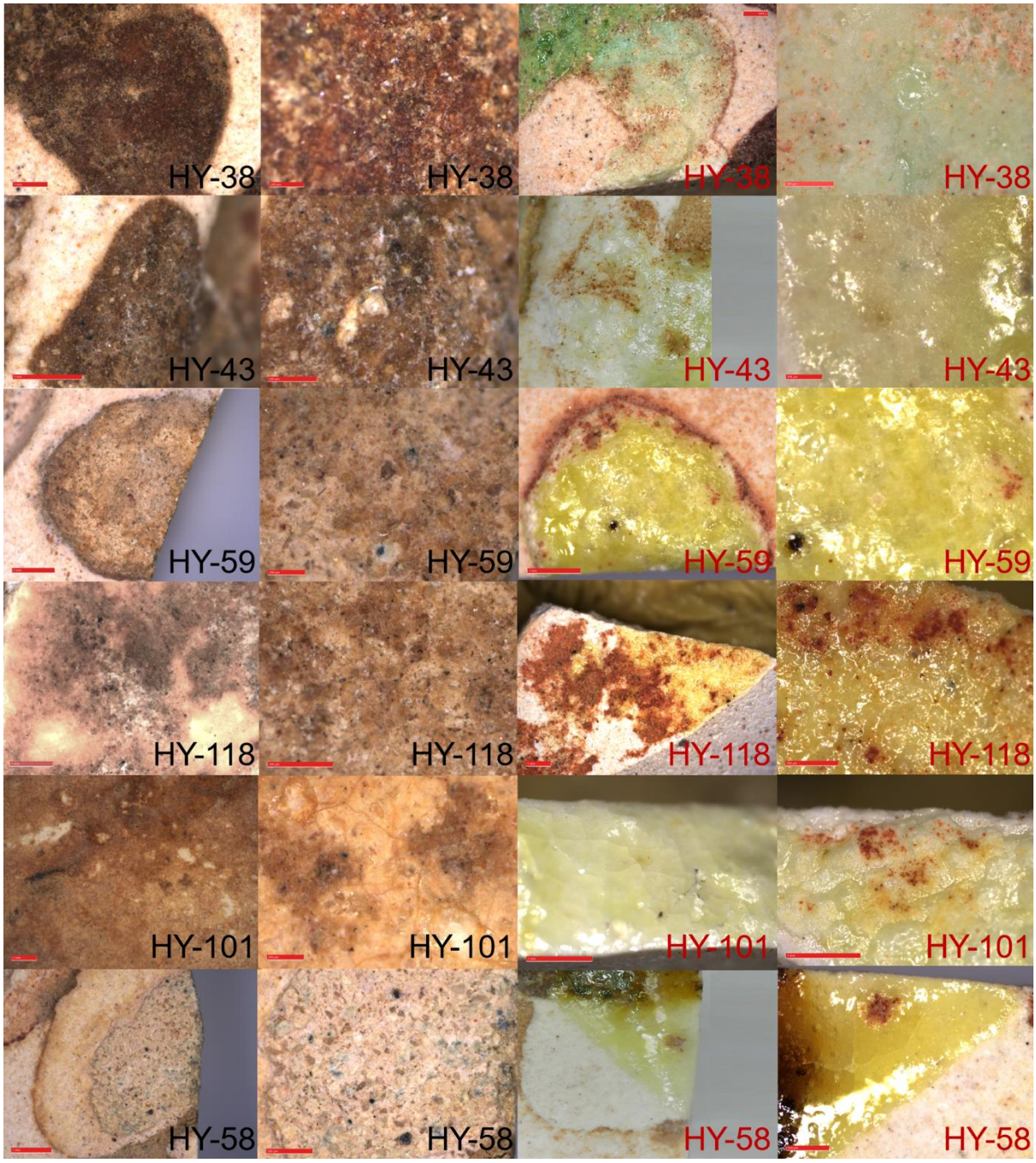


Figure 3. 9 Colour changes of clear glazes before and after the experimental glaze firing, obtained from observation by the optical microscope. Font colours mark samples before experimental glaze firing (black colour) and after firing (red colour).

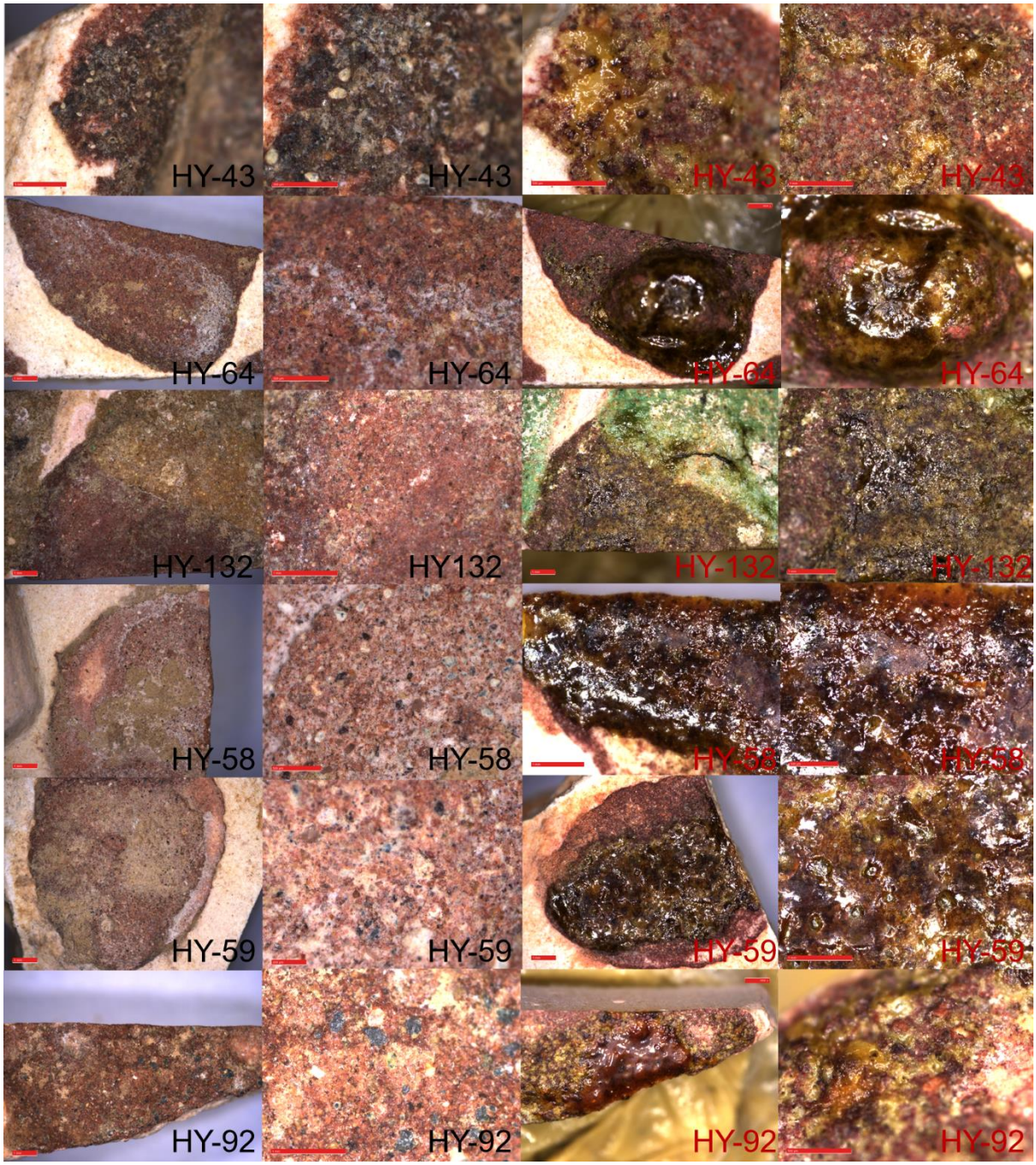


Figure 3. 10 Colour changes of brown glazes before and after the experimental glaze firing, obtained from observation by the optical microscope. Font colours mark samples before experimental glaze firing (black colour) and after firing (red colour).

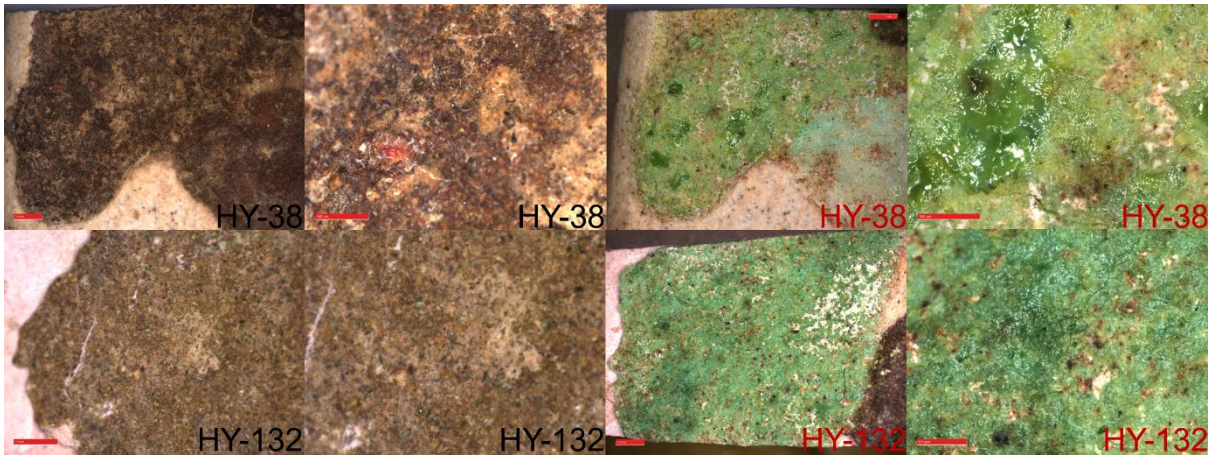


Figure 3. 11 Colour changes of green glazes (HY-38 and HY-132) and before and after the experimental glaze firing. Font colours mark samples before experimental glaze firing (black colour) and after firing (red colour). Photos were obtained from observation by the optical microscope.

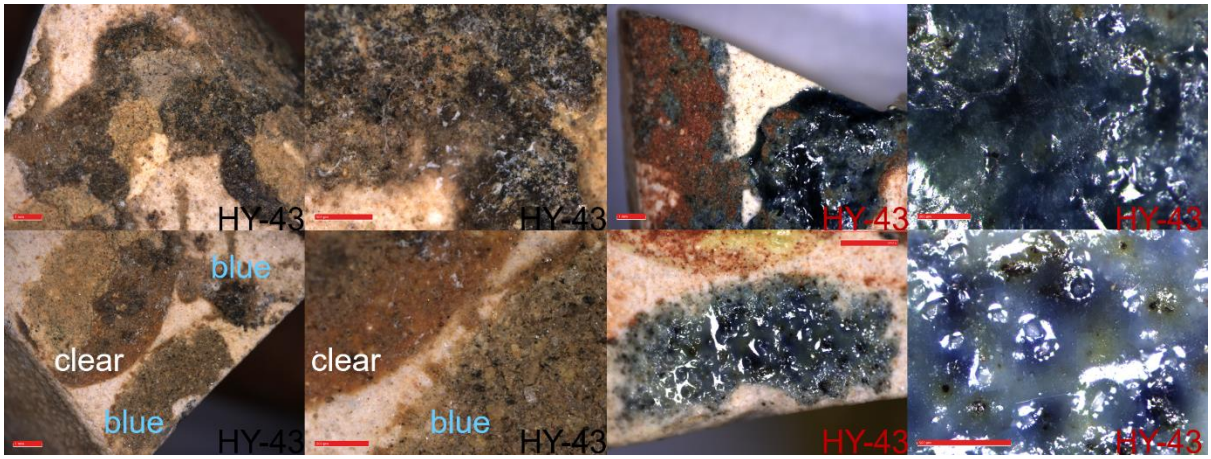


Figure 3. 12 Colour changes of blue glazes (HY-43) before and after the experimental glaze firing. Font colours mark samples before experimental glaze firing (black colour) and after firing (red colour). Photos were obtained from observation by the optical microscope.

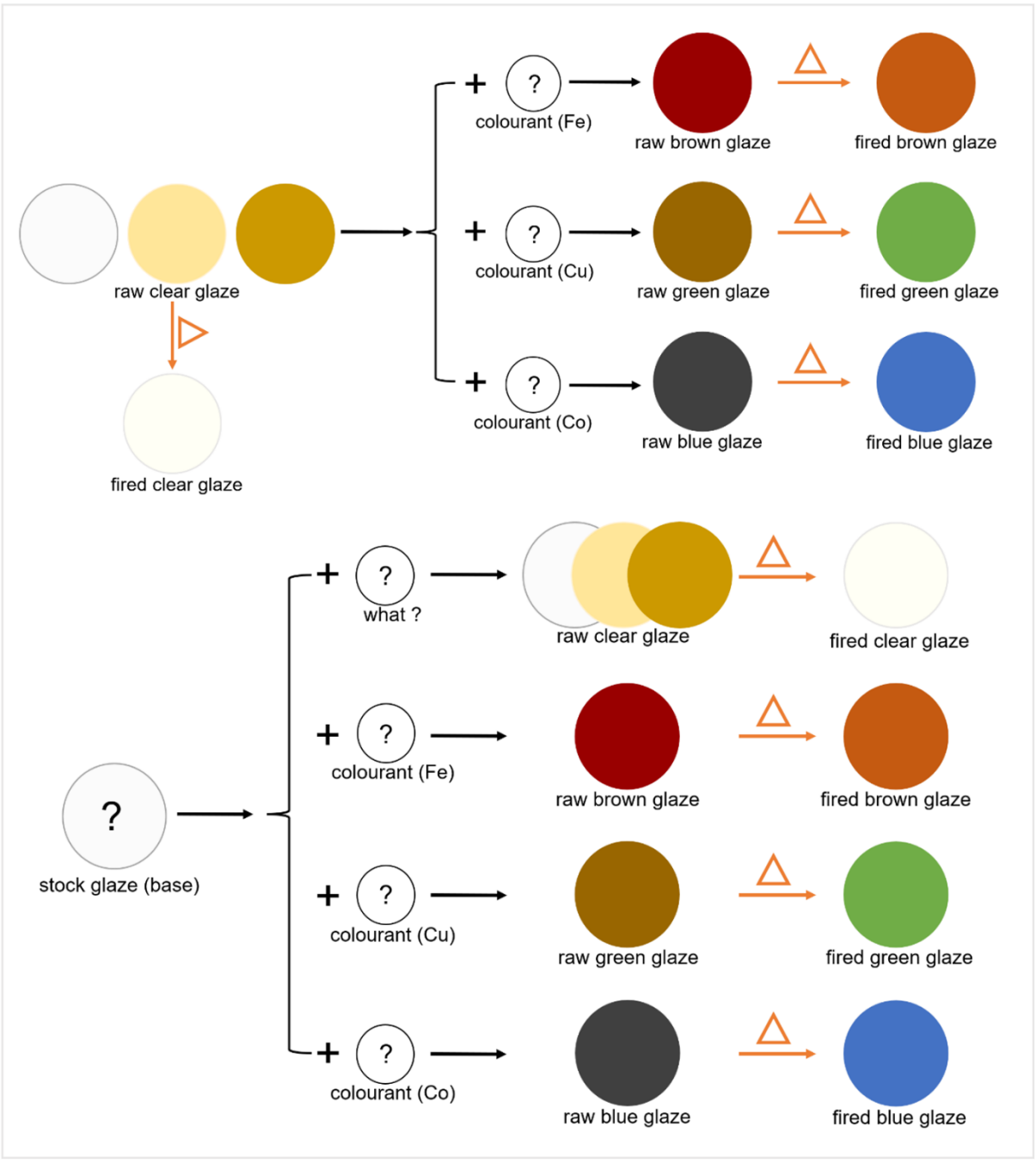


Figure 3. 13 Hypothesis of glaze-making technology.

3.2.2 Establishment of Standards

The colour changes of experimental-fired samples confirm the correspondence between raw and fired colours. The next step is to compare the chemical compositions of raw and fired glazes to establish the classification standard. The brown, green and blue glazes contain some iron, copper and cobalt respectively as their colourants, while clear glaze is a colourless transparent or translucent white or pale honey glaze without a colour agent. The lower concentration of colouring elements, the more transparent of the clear glaze. Therefore, the comparison and discussion of compositions of colourant elements in raw and fired glazes can determine the standards for classification. The compositional data were obtained from almost the same areas of glazes before and after the experimental firing by EDXRF (Appendix 5). The solid colour bars in the Figures (Figure 3. 14, Figure 3. 15 and Figure 3. 16) represent the composition of raw glazes before firing and the striped bars refer to fired glazes after experimental firing. Three colourant elements show a clear predominance in their corresponding glazes.

The standards of clear and blue glazes are relatively straightforward to be confirmed. The determination of blue glazes relies heavily on the cobalt content. The CoO in raw and fired blue glazes is more than 0.3%. The other three glazes contain almost no cobalt (CoO<0.03%) (Appendix 6). The boundary should between 0.03-0.3%. Cobalt is a very efficient colouring agent. In theory, 0.005% of cobalt in glass is sufficient for colouring and mostly 0.1-0.5% CoO in the glaze can show beautiful blue colour (Kerr and Wood, 2004, p.659). Therefore, it would be more reasonable to set the standard at 0.1% CoO rather than 0.3%. In other words, the amount of CoO measured in the glaze to record it as ‘blue’ would be 0.1%.

Compared with high levels of colourant elements in coloured glazes, decreasing colouring agents as much as possible is the aim of the clear glaze. Figure 3. 15 and Figure 3. 16 show

considerable differences between clear glaze, green and blue glazes on CuO and CoO. The contents of copper and cobalt in the clear glaze are both less than 0.03% which is easily distinguished from green and blue glazes. However, the differences between clear and brown glazes are not very distinct. Based on the analysis of experimental-fired samples, Fe_2O_3 in clear glaze varies from 0.1% to 1.6% (Figure 3. 14). Accordingly, Fe_2O_3<1.6% can be regarded as the criteria for clear glaze – higher would be brown. The standard of clear glaze is that CoO and CuO both are less than 0.1%, and Fe_2O_3<1.6%. Remarkably, the lowest Fe_2O_3 in the brown glaze is 2.0% which is close to the highest percentage in the clear glaze (1.6%). When all the raw glaze samples are analysed, it is also possible that unknown raw glaze, clear or brown, contain iron from 1.6% to 2.0%. However, Fe_2O_3 of most clear glazes are less than 1.0%, and Fe_2O_3 of most brown glazes are higher than 2.0% (Figure 3. 14). All sherds have been buried for more than one thousand years. Some dirt contaminated the surface and cannot be removed, such as HY-43 and HY-118 (Figure 3. 9). This contaminant is likely to contain iron and increase the original level of iron content of the clear glaze. Therefore, to match the original uncontaminated raw glaze, low Fe_2O_3 (1.6%) might be more reliable for the discrimination of the clear and brown glazes.

The determination of brown and green glazes is relatively complex because some brown and green glazes contain both high CuO and high Fe_2O_3 (Figure 3. 14 and Figure 3. 16). A single criterion, such as high iron in brown glaze or high copper in green glaze, cannot confirm the type. Therefore, the establishment of the standard of green and brown glazes requires combining compositional and ratio criteria. The compositional criteria of Fe_2O_3 (1.6%) in brown glaze has been established. The green glaze in the firing experiment had CuO of approximately higher than 0.3%. Considering that the number of experimental-fired samples with green glaze is limited, it is possible that the copper content in some raw glaze samples

which were not included in the experimental firing is lower than 0.3%. Also, the study on glasses shows that it is generally accepted that elevated concentrations of these (de)colourant-related elements (over 1000 ppm), such as Cu, suggest that they were deliberately added to the glass (Brems and Degryse, 2014). Based on these two points, higher than 0.1% CuO would be appropriate for the composition criteria of the green glaze.

Some samples have high copper in a brown glaze and high iron in a green glaze. For example, the brown glaze of HY-152 has 0.28% CuO, which is the same as in some of the green glaze samples. Green glazes of the HY-132-3 and HY-38-1 both contain higher iron than copper, 0.73% Fe_2O_3 and 0.29% CuO in HY-38-1 and 0.72% Fe_2O_3 and 0.39% CuO in HY-132-3. Accordingly, the next step is to calculate the ratio of Fe_2O_3/CuO for all raw glazes involved in the experimental firing. The distinction between brown and green glazes was clear, with the lowest Fe_2O_3/CuO of 16.74 for brown glazes and the highest Fe_2O_3/CuO of 2.54 for green glazes (Figure 3. 17). Additionally, the composition of the colouring elements – Fe_2O_3, CoO and CuO, was normalised. The sum of the three elements was considered to 100% and the percentage of these elements was calculated. Figure 3. 18 shows that the brown glazes all contain iron more than 94% of the colouring elements, while the green glazes have a maximum of 71% Fe_2O_3 and a minimum of 28% CuO. To summarise, the standard of brown glaze is Fe_2O_3>1.6% and Fe_2O_3/CuO>16.74. And CuO>0.1% and Fe_2O_3/CuO<16.74 or even lower is the standard of raw green glaze. By combining the above criteria, a process for classifying raw glazes can be established (Figure 3. 19).

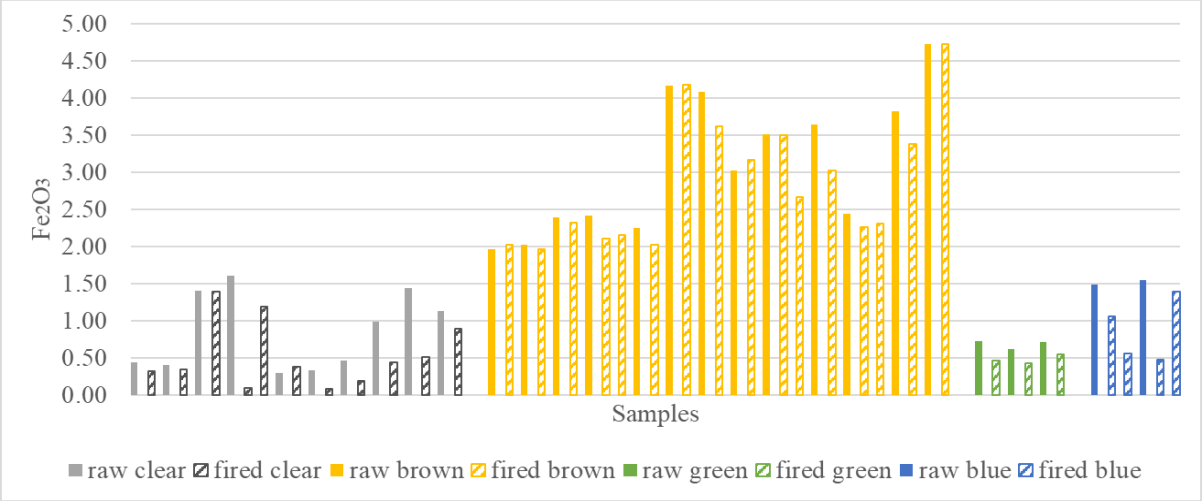


Figure 3. 14 Bar chart of Fe_2O_3 in raw glazes and fired glazes.



Figure 3. 15 Bar chart of CoO in raw and fired glaze.

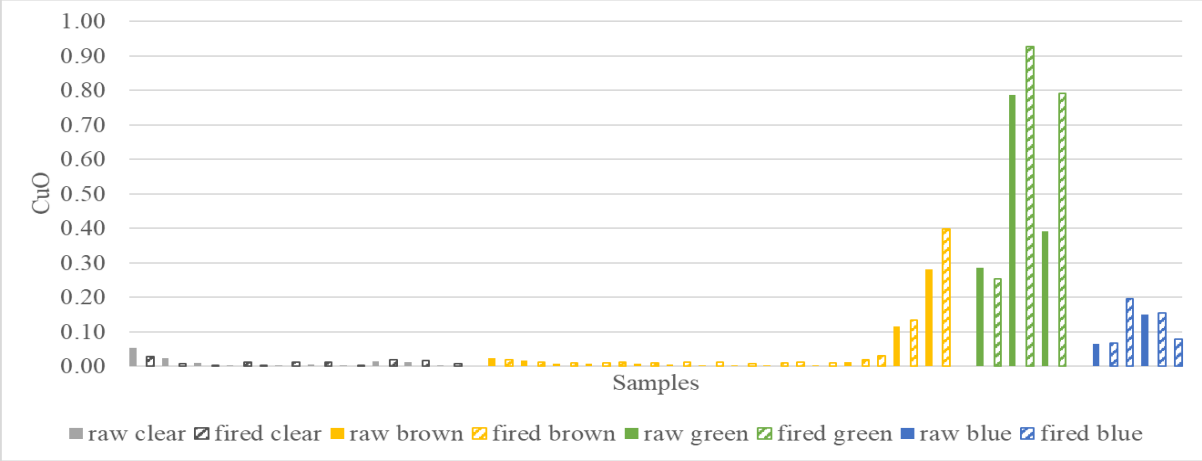


Figure 3. 16 Bar chart of CuO in raw and fired glaze.

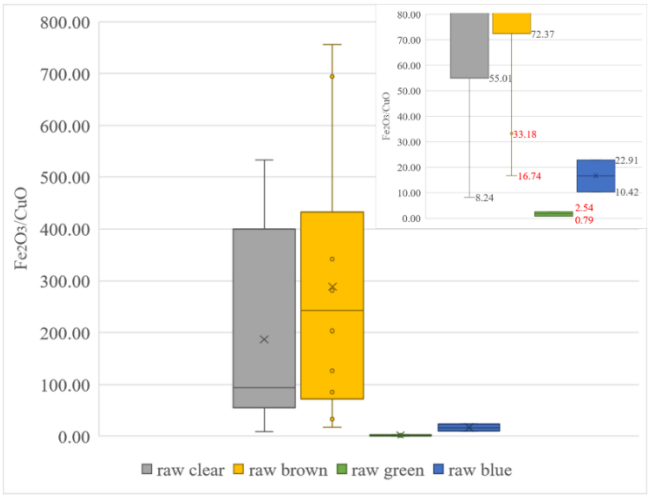


Figure 3. 17 Box plot of Fe_2O_3/CuO in raw glazes.

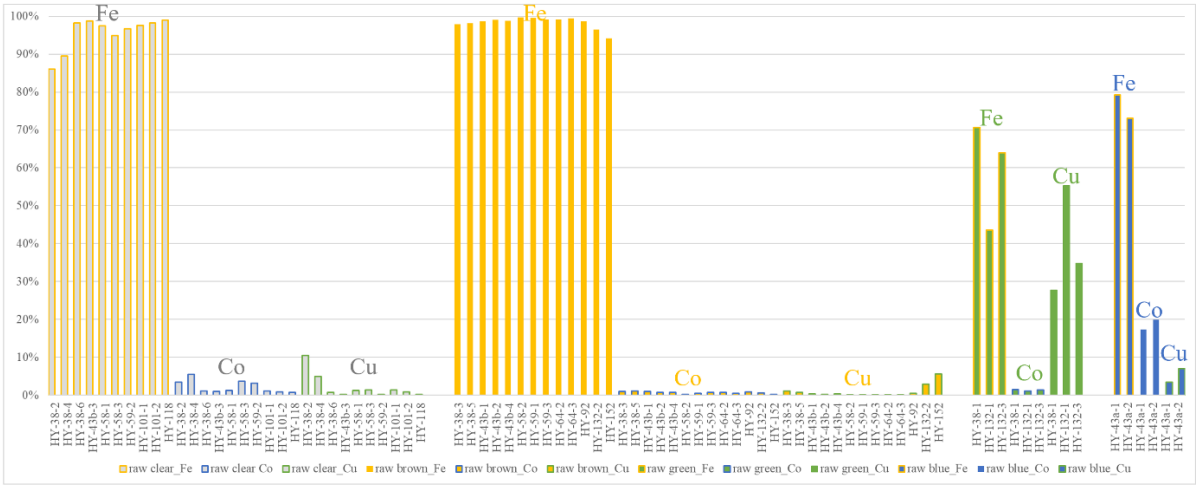


Figure 3. 18 Bar chart of percentages of Fe_2O_3, CuO and CoO in raw glazes.

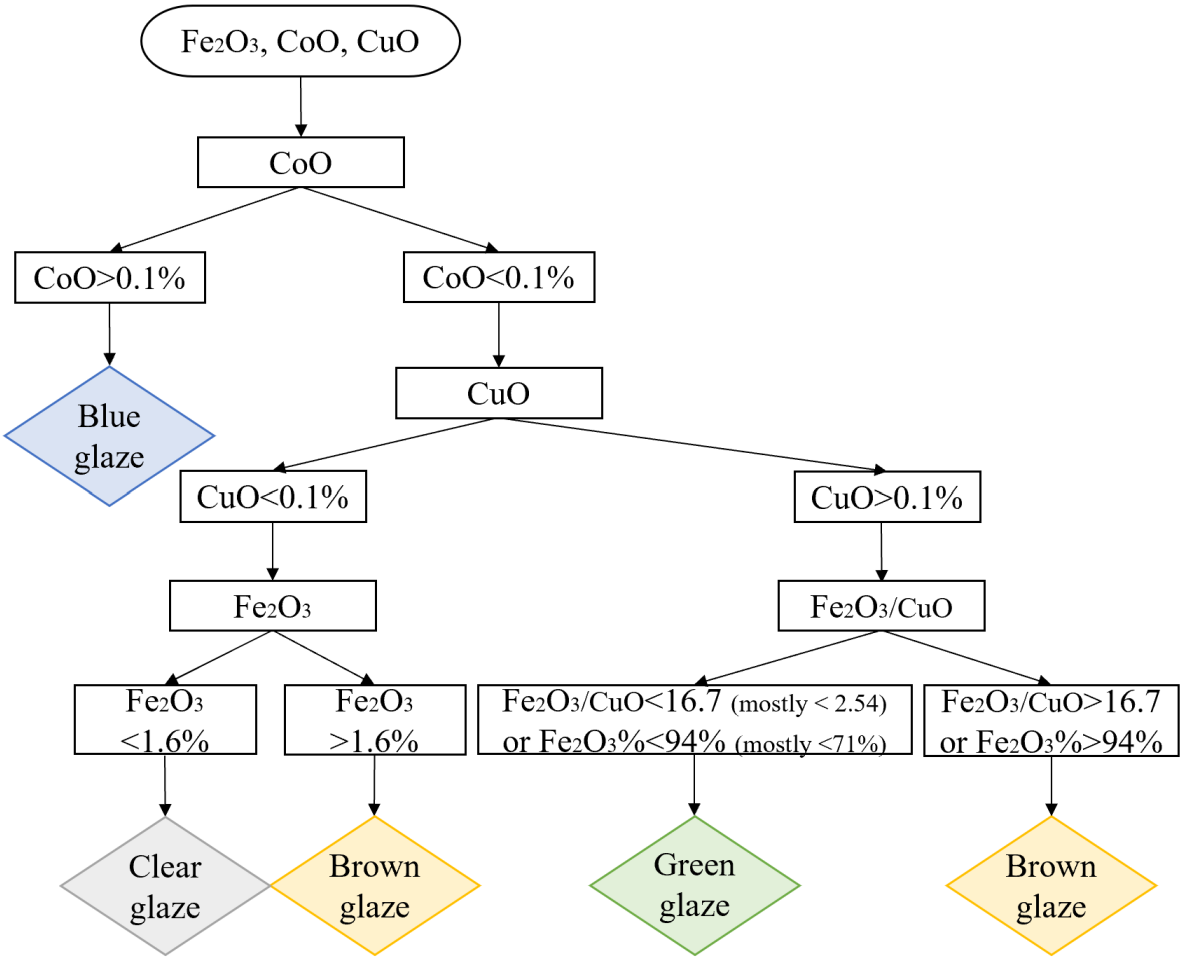


Figure 3. 19 Flow chart of raw glaze classification.

3.3 Classification of Raw Glazes

3.3.1 Special Samples

Some samples are decorated with various spots, strips, and motifs. It has been unknown whether the decorations on the same sherd were painted with the same or different raw glazes. Therefore, all glazes with various decorations on all samples were analysed by EDXRF. To minimise errors, including instrumental error, random error, and the effect of unremovable contaminants, every single pattern is generally tested twice, but in slightly different positions. In total, 663 sets of data were obtained from 66 samples, including 531 tests of glazes or other materials on the body, and 132 tests on cross-sections of bodies (Appendices 7-13). All the data for the possible glaze were classified according to the standards for classification established in section 3.1. Prior to the classification, the first step is to check the PbO in the raw glazes. According to the firing experiments (Chapter 3.1), it is likely that the raw glaze samples include some porcelain glazes and some unidentifiable materials. The compositional results show that thirteen sherds are free of lead.

Six of these samples are covered with red material and the shades of them varied from orange-red to dark red (Figure 3. 20). This material contains high Fe_2O_3 (Appendix 12). And HY-133 contains the highest Fe_2O_3 among these six sherds, 21.27-21.75%. The iron in the orange-red materials of HY-122 and HY-124 is much less than that of HY-133, only 4.72-6.55%. Due to the effect of the cleaning process, Fe_2O_3 in HY-137 and HY-138 is only 2.56-5.26%. The remarkable difference between raw glaze and this red material is that raw glaze was pasted on the body tightly, however, this loose powder dispersed into liquid when they were cleaned by water and ethyl alcohol.

HY-148 is very special among these six red sherds. The red material was pasted on the body stably and did not disperse during the cleaning process. More differently, the blackish red material on the outside of HY-148 is fired glaze which is essentially free of PbO (0.20-0.27%) but has high K_2O (3.50-3.54%), CaO (9.33-9.87%) and MgO (6.01-6.26%). And the sum of SiO_2 and Al_2O_3 reaches up to 70.76-72.62% (HY-148-3 in Figure 3. 20 and Appendix 12). It suggests that this sample might be a fired porcelain sherd with a lime glaze. But confusingly, the compositions of red material on the inside (HY-148-1 in Figure 3. 20) have high PbO (28.71-29.39%) and P_2O_5(41.91-44.31%) and low SiO_2 (10.84-11.7%) and Al_2O_3 (3.60-3.75%), negligible K_2O and MgO (Appendix 9). Based on the chemistry, this material should belong to a raw brown Sancai glaze. In other words, this sherd might be decorated both by lead glaze inside and lime glaze outside. This style has never been found elsewhere.

The other two areas, HY-148-2 and HY-148-4, also show different characteristics even though the texture of them is similar. Compositionally, the dark red material on HY-148-2 is very similar to HY-148-3 and belongs to porcelain glaze. However, it did not mature to a glassy glaze after firing, and the textures of them are very different. The thin-layer red material on HY-148-4 also contains high P_2O_5 (34.95-35.10%) and CaO (15.31-16.21%), low SiO_2 (27.02-27.40%) and Al_2O_3 (11.47-12.03%). And the K_2O and MgO are both lower than HY-148-2 and HY-148-3. Significantly, HY-148-4 have non-negligible PbO (3.19-3.24%) even though it is much lower than HY-148-1. Perhaps, this material here is too thin to obtain the real composition. The lead might be much higher than 3%. To summarise, as Figure 3. 20 shows, two different materials were applied to the same side of this sherd. HY-148-2 and -3 are lime glazes, however, HY-148-1 and -4 might be lead glazes. The existence of glassy porcelain glaze on HY-148-3 proves that this sherd was fired above 1200℃. But the reason for the non-maturation of HY-148-2 has not been known. The lead glaze on HY-148-1 and HY-148-4

might be applied after the high firing. Perhaps, this sherd was a failed trial of a new product, or it just was made by a Tang-dynasty potter's mistake. The red material on these six sherds might be red pigment for enamels used in porcelain or Sancai. Or it is failed raw Sancai glaze due to the lack of some ingredients. No matter what it is, none of these samples could enter the classification process for raw Sancai glazes.

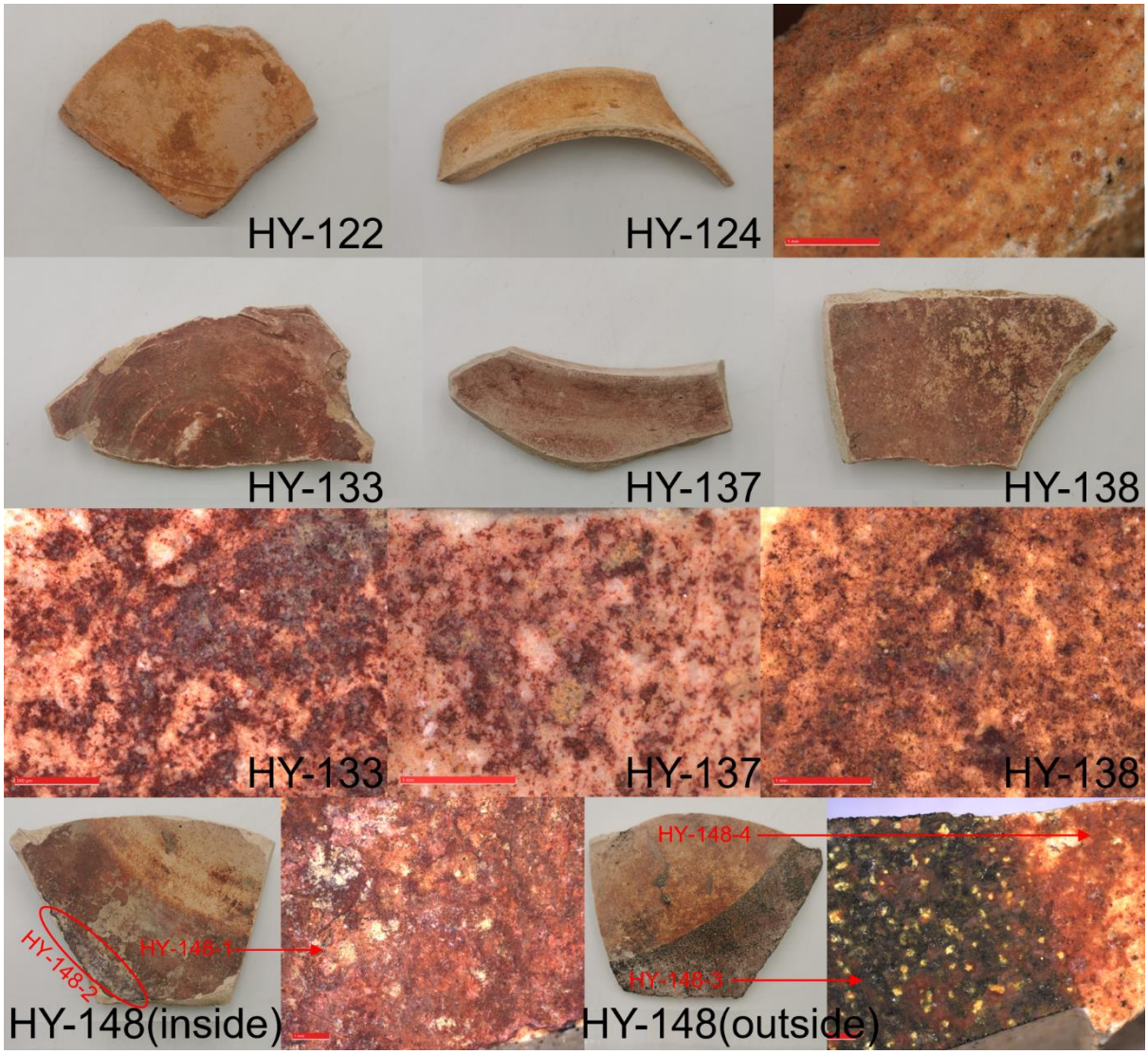


Figure 3. 20 Special samples covered by unknown red materials. Photos of sherds were taken by the author and photos of surfaces were obtained from observation by the optical microscope.

Other special sherds, such as HY-126, -134, -139 and -140, all contain high SiO_2, Al_2O_3, K_2O, and CaO. Presumably, they might be raw porcelain glazes, but the texture of these 'raw glazes' are very coarse. Some big particles can be observed (Figure 3. 21). The most special sample is HY-155 which has the highest CaO (68.17-72.68%) (Appendix 12). It is hard to classify it into raw porcelain glaze. Perhaps, it was contaminated by the presence of limestone or other substances in the burial soil. Or perhaps it was a mistake during glaze preparation by the potter in the Gongyi kiln. These unfired sherds were probably ‘rejects’, thus, it is not surprising that they might include ‘mistakes. The current compositional analysis cannot answer this question now.

The other group of special samples is black material on HY-147 and HY-149. These two sherds are almost identical, both being covered with a thin layer of unknown black material (Figure 3. 21). According to the experimental firing, the black material on HY-149 disappeared after firing and a very thin transparent glaze formed on some areas of this sample (Figure 3. 8). If HY-147 had been fired, the black material would also disappear. What is this black material and how was the thin transparent glaze formed? These questions require more scientific analysis to explore.

In addition, there are two samples, HY-116 and HY-188 which also cannot enter the classification process for raw glazes even though they contain PbO. The special characteristics of these two sherds are not unusual materials like the above samples. They have fired into Sancai sherds with matured clear glazes, but the conditions are different. The size of HY-116 is very small, only around 3 x 2cm (Figure 2. 3 and Figure 2. 4). And the matured clear glaze is a very small strip on it. The whole surface is covered by white slip and the glaze is very colourless clear, so it is very difficult to find the glaze. It is a fired Sancai white clear glaze. An observation error caused a wrong sample collection. HY-188 is also a fired Sancai sherd with

a clear glaze but the whole surface is covered by bright brownish-yellow material. Therefore, it was mistakenly regarded as a raw glaze sample. However, when the surface was observed by the microscope, a shiny clear glaze (Figure 3. 21) is found beneath this brownish-yellow material. Possibly, this is a fired Sancai sherd with clear glaze, but soil and other contaminations adhered to it during burial time. These two Sancai samples also are grouped into special samples (Appendix 12) and are not discussed and analysed in detail in this thesis.

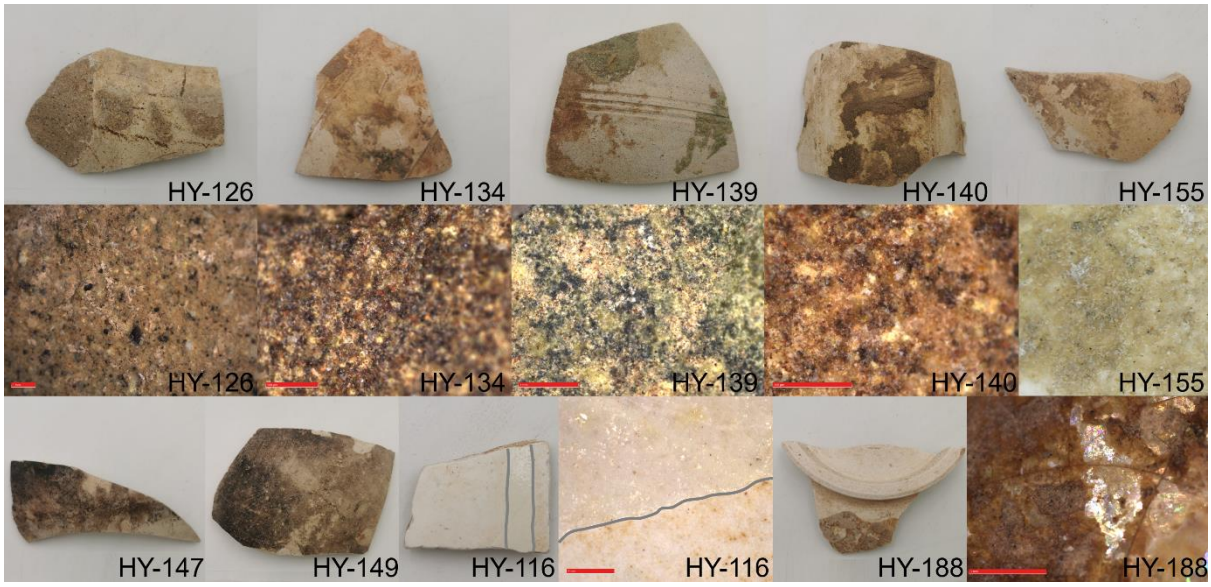


Figure 3. 21 Other special samples. Photos of sherds were taken by the author and photos of surfaces were obtained from observation by the optical microscope.

3.3.2 Raw Coloured Glazes

According to the standards for the classification of raw glazes established in section 3.1, and the analysis of the special samples, it was found that 45 samples (out of 66) are decorated by raw Sancai glazes and without any special materials. HY-148 has special red material and raw brown Sancai glaze together. The other 20 samples include 6 sherds (HY-115, -119, -141, -143, -153, -154) only covered by slip, 14 sherds (HY-116, 122, -124, -126, -133, -134, -137, -

138, -139, -140, -147, -149, -155, -188) only with special materials. Those 45 samples include 17 sherds with a raw clear glaze, 41 sherds with raw brown glaze, 10 sherds with raw green glaze, and 1 sherd with blue glaze (Table 3. 1, Figure 3. 23a). Some samples are monochrome, and others are multi-colour raw glazes (Table 3. 2, Figure 3. 23b). Although there is only one sherd (HY-43) decorated with raw blue glaze, many spots were painted by the raw blue glaze (Figure 3. 22). So, 76 tests by XRF were run on these 32 areas. All data were classified by the standard method and 13 areas were found to be blue glazes were selected (HY-43-7, 43-10, 43-11, 43-17, 43-18, 43-19, 43-20, 43-22, 43-25, 43-28, 43-29, 43-30, 43-32 in Figure 3. 22). After selecting all the raw glazes, the colour combinations of glazes on every sherd were also grouped (Table 3. 2 and Figure 3. 23). Among all 45 samples, five samples (HY-38, -102, -132, -136 and -150) are decorated with clear-brown-green glazes, one sample (HY-43) is painted by clear-brown-blue glazes, seven samples (HY-58, -59, -61, -62, -92, -123, -145) are clear-brown glazed products, three samples are brown-green glazed products (HY-106, -152, -166), and one (HY-146) is a clear-green glazed product. Monochrome sherds are more than multi-coloured sherds, the number of monochromes is 28 including 3 clear glazed samples (HY-101, -117, -118), 24 brown glazed sherds (HY-64, 121 125, 129-131, 135, 148, 151, 172-187) and 1 green glazed sherd.

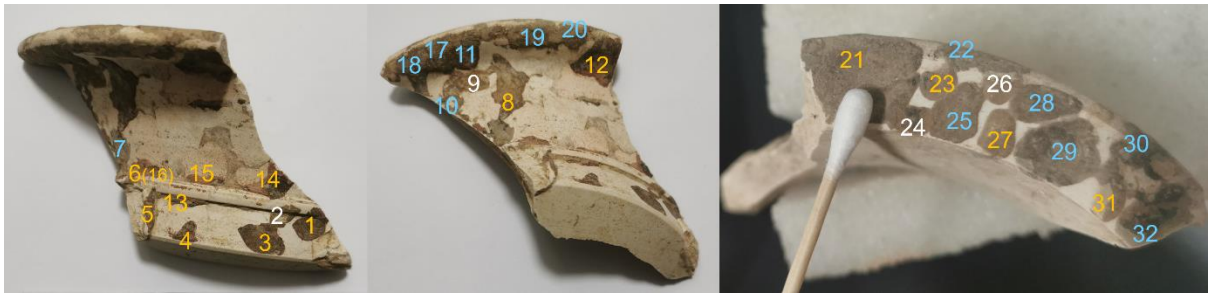


Figure 3. 22 Colours of all glazes on HY-43 sherd, photos taken by the author.

Table 3. 1 Classification of samples

Classification	Samples	Total number of samples	Total number of tests
Raw clear glazes	HY-38, 43, 58, 59, 61, 62, 92, 101, 102, 117, 118, 123, 132, 136, 145, 146, 150	17	139
Raw brown glazes	HY-38, 43, 58, 59, 61, 62, 64, 92, 102, 106, 121, 123, 125, 129, 130, 131, 132, 135, 136, 145, 148, 150, 151, 152, 166, 172,173, 174, 175, 176, 177, 178, 179, 180, 181, 182, 183, 184, 185, 186, 187	41	240
Raw green glaze	HY-38, 102, 106, 127, 132, 136, 146, 150, 152, 166	10	39
Raw blue glaze	HY-43	1	35
Special samples	HY-116, 122, 124, 126, 133, 134, 137, 138, 139, 140, 147, 148, 149, 155, 188	15	44
Slips	HY-101, 115, 116, 117, 118, 119, 130, 131, 137, 141, 143, 146, 151, 153, 154, 155, 166	17	34

Table 3. 2 Colour combinations of samples

Colour combinations	Samples	Total number of samples
Clear + brown + green	HY-38, 102, 132, 136, 150	5

Colour combinations	Samples	Total number of samples
Clear + brown + blue	HY-43	1
Clear + brown	HY-58, 59, 61, 62, 92, 123, 145	7
Brown + green	HY-106, 152, 166	3
Clear + green	HY-146	1
Clear	HY-101, 117, 118	3
Brown	HY-64, 121, 125, 129, 130, 131, 135, 151, 172, 173, 174, 175, 176, 177, 178, 179, 180, 181, 182, 183, 184, 185, 186, 187	24
Green	HY-127	1

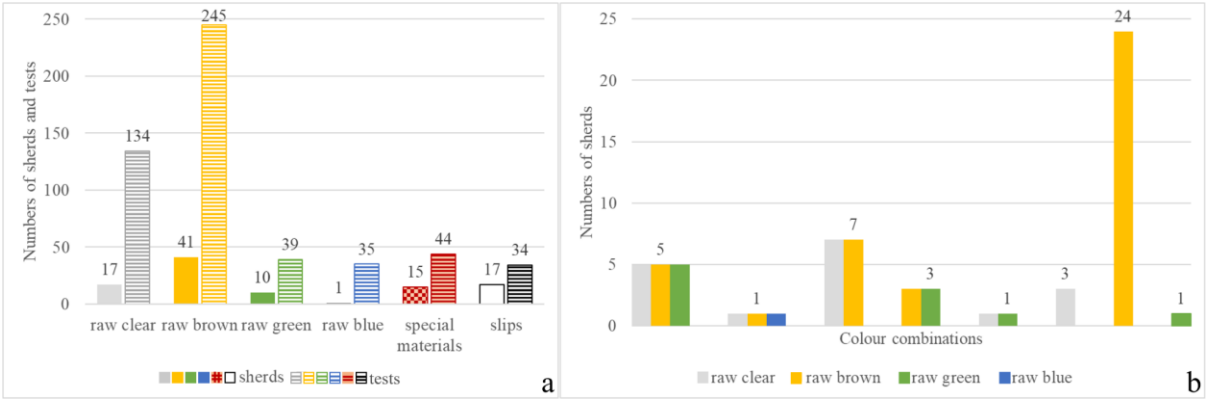


Figure 3. 23 (a) Bar chart of glaze classification. (b) Bar chart of colour combinations of raw glazes.

Chapter 4 Colourants

The colour of fired Sancai glaze is determined by the colourant. Iron gives the glaze brown, yellow or red colours. Copper imparts green colour, and cobalt makes a dark blue colour. Chapter 3 established the classification standard of raw brown, green, and blue glazes. Based on it, the raw coloured glazes were grouped and analysed. The compositional data and mineral characteristics of colourants obtained from EDXRF and ESEM are discussed in this chapter to determine the types, techniques, and origins of iron, copper, and cobalt pigment.

4.1 Iron Brown

Iron is the most common colourant of Chinese glazes. Different valences of iron ions – Fe^{2+} and Fe^{3+}, firing atmosphere, and glaze base - such as lime-alkali and high-lead glaze, all affect the colours after firing. Iron can provide various red, yellow, green, blue, and black hues. Brown Sancai glaze is not a pure 'brown' colour with specific chroma. It refers to all brownish colours, such as light/pale/dark yellow, orange, red and brown. Figure 4. 1 shows that Fe^{3+} ions colour high-lead glaze from straw to dark brown. When Fe_2O_3 (red iron oxide) is dissolved in a high-lead glaze or glass, it will give ivory to straw tones from about 0.5-2.0% by weight, then yellows at 2-3%, on to amber (3-4%), then amber-brown (4-5%), then eventually to black (about 6-8%) (Wood, 1999, p.160).

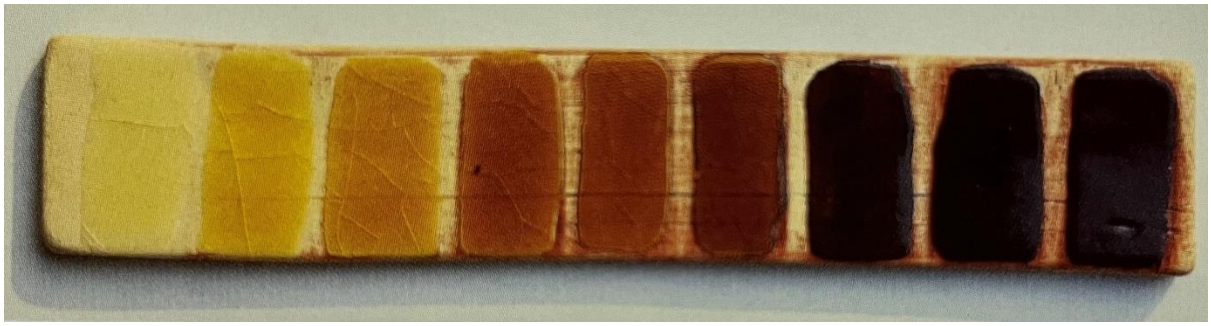


Figure 4. 1 Test bar, showing the effect of adding red iron oxide (Fe_2O_3) in 1% increments to a high-lead glaze, source from Wood (1999, p.161). In these quantities, Fe_2O_3 dissolved in the molten glaze to give Fe^{3+} ions, was fired to 1060℃ in oxidation.

Brown glazes decorate forty-one sherds among all sixty-six samples. The Fe_2O_3[16] of the brown glazes is much higher than that of the others (Figure 4. 2). The average iron content in the brown glaze examined by XRF is 3.51%. The clear glaze has the lowest iron among the four glazes at 0.73%. The green glaze contains a little higher iron than the clear glaze at 0.98%. And iron in the blue glaze is slightly higher than the clear and green glazes at 1.33%. Iron must be the colouring agent of the brown glaze. The following question is what is the raw material of this iron colourant? What is the source of it, e.g., hematite, magnetite, pyrite or other high-iron minerals? The second question is what is the source of iron in clear, green, and blue glazes? Whether this source relates to stock glaze or other colourants? The answers to these questions need to be investigated by the observations and examination of XRF and ESEM.

[16] The form of iron in the Sancai glaze - Fe^{2+}, Fe^{3+} or a mixture of them, is a complex question. Pollard et al. (2017, p.211-212) discussed the forms and equilibrium of Fe (II) and Fe (III), redox reactions and colours of glass/glaze in detail in the book Archaeological Chemistry. In this thesis, one point needs to be aware. EDXRF and ESEM cannot distinguish between the oxidation states of iron. It is an analytical convention to report it as all Fe_2O_3, but it could be mixed Fe(II)/Fe(III).

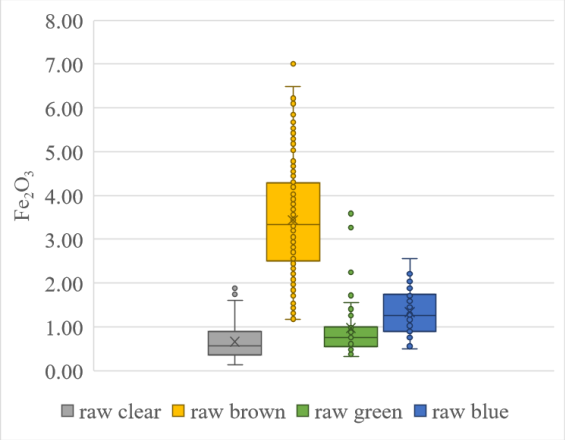


Figure 4. 2 Box plot of Fe_2O_3 in raw glazes

A total of 18 small pieces decorated with brown glazes were prepared for the ESEM analysis. They are HY-38, -43, -58, -59, -61, -62, -64, -92, -102, -106, -121, -123, -129, -130, -132, -136, -151, and -152. Every tested sample contains two kinds of iron-rich particles at the same time. One type is Fe-O-associated particles (Figure 4. 3 and Figure 4. 4), and the other one is Fe-Mg-Si-Al-(K)-O-associated particles. The compositional analysis of these particles (Figure 4. 5) shows that the Fe and O content both are very high, and the highest Fe is 55.57% (Table 4. 1). This widely distributed and easily recognisable Fe-O-associated particles should be from the iron colourant which is a kind of iron oxide. The three most common oxides of iron in their crystalline forms are Fe(III) oxide (Fe_2O_3), Fe(II)/Fe(III) oxide (Fe_3O_4) and Fe(II) oxide (FeO). The key question in the study of iron colourant is the raw material of iron oxide. The colour of the raw brown glaze could offer a clue. The observation by light microscope of all brown glazes shows that these glazes share the same colour – deep red/dark reddish brown (Figure 4. 6). And no other raw glazes, such as blue or green, corresponding to this colour. Among the three oxides of iron, only the colour of Fe_2O_3 is red. Fe_3O_4 is dark grey and FeO is black. Accordingly, the colouring agent of the brown glaze is hematite.

This material is the most common and important ore of iron, and it was used on pottery as early as the Neolithic in China. For example, many of the red-painted wares which were prepared from hematite (α-Fe_2O_3) have been found in the middle Yangtze River valley (MYRV) of China some 8500 and 7800 years ago (Li et al., 2022). Chinese potters continuously used hematite in the following thousands of years. Until the Qing dynasty, hematite red was still applied to enamelled porcelains, such as Doucai (Colomban et al., 2020). Tang Sancai was one of these Chinese ceramics decorated with hematite pigment. Furthermore, the size of this type of iron particle is large, with most of the particles measuring 40-100 μm (Figure 4. 7). The large size of these iron particles suggests that the making of hematite was not particularly fine. Perhaps, hematite ores were ground physically for a short time and added to the stock glaze to produce the raw brown glaze.

Additionally, hematite also was the most widely used red pigment in Chinese wall painting. Li (2002) concluded pigments in Mogao Grottoes and found that hematite was the main red pigment in Mogao Grottoes in Dunhuang from Sixteen Kingdoms (304-439 CE). However, Tang-dynasty Mogao Grottoes show a different use of red pigments. From the early Tang period, red lead (Pb_3O_4) and cinnabar (HgS) from Central Asia started to replace the position of hematite. Until the late Tang, hematite finally was exploited and produced in the Hexi area. Therefore, it became the main pigment again in Mogao Grottoes. Kizil Grottoes, located around 1,000 kilometres west of Mogao Grottoes, prolongedly used red lead (Pb_3O_4) and cinnabar (HgS) from Central Asia. In other words, hematite pigment was different from imported red lead and cinnabar in the Tang dynasty (618-907 CE). It was always a traditional local red pigment in central China. Perhaps, the origin of the hematite applied to Sancai might be Gongyi or other areas in central China.

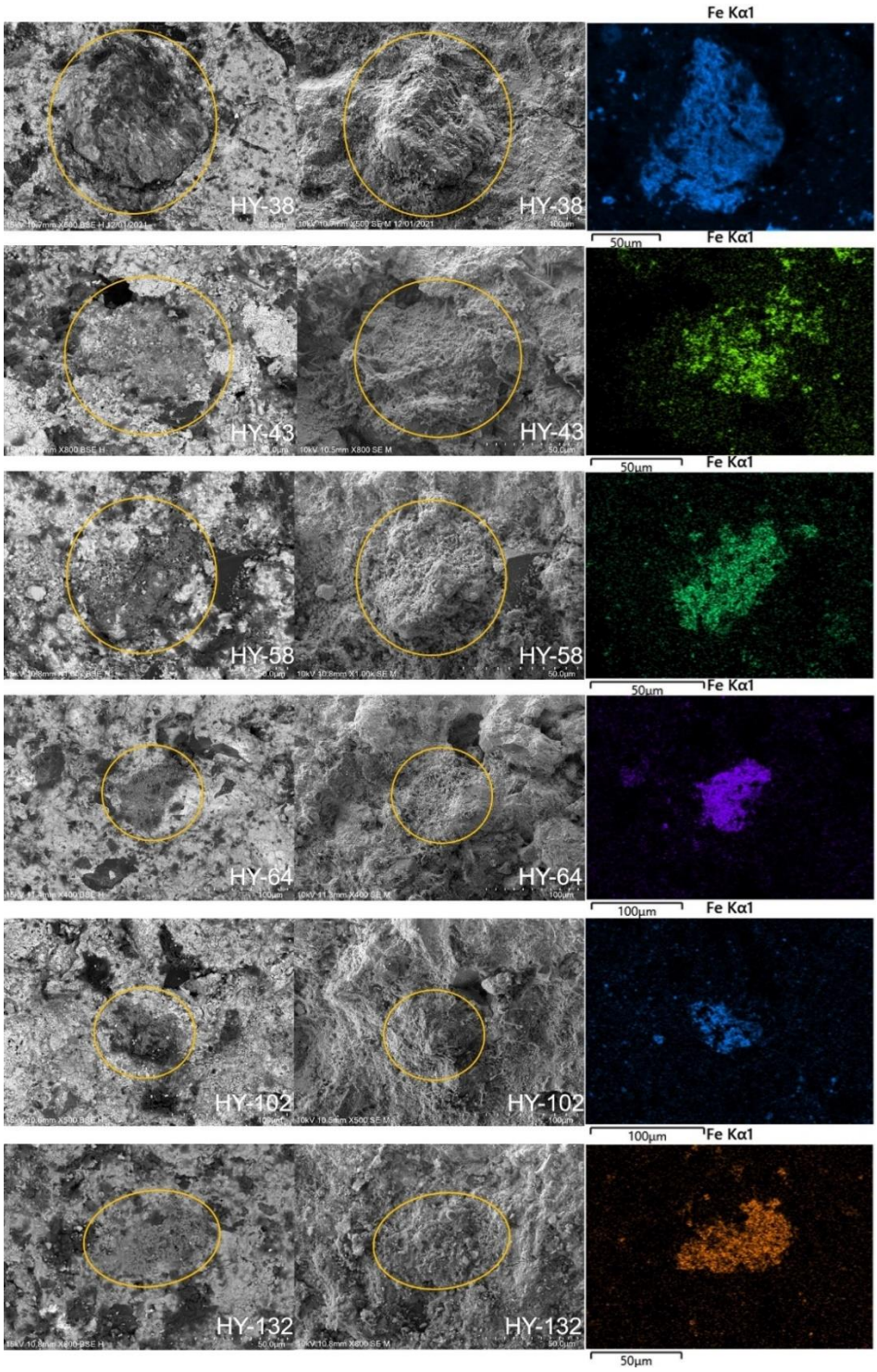


Figure 4. 3 BSE (left), SE[17] (centre) and chemical mapping (right) images of Fe-O-associated particles (yellow circles) in raw brown glazes, obtained from the ESEM.

[17] BSE and SE are abbreviations of Backscattered Electron and Secondary Electron respectively in this thesis.

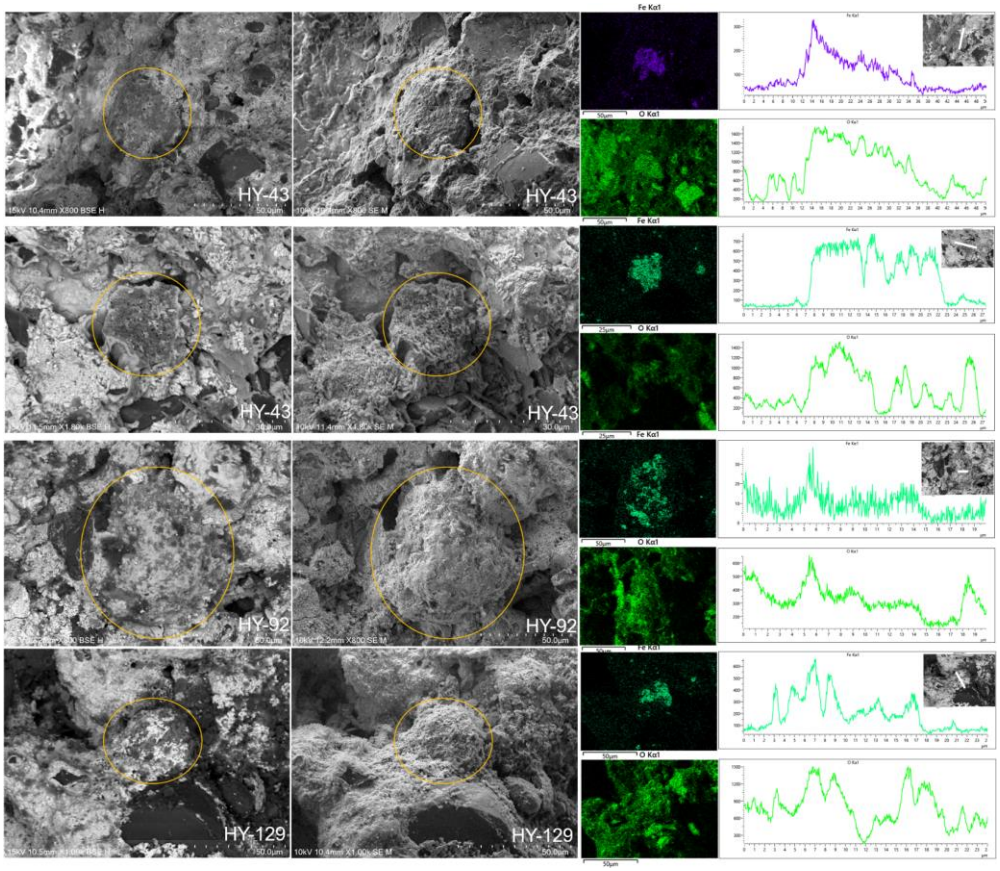


Figure 4. 4 BSE (left), SE (mid-left), chemical mapping (mid-right) images and line scan charts (right) of Fe-O-associated particles (yellow circles) in the raw brown glaze of HY-43, HY-92 and HY-129, obtained from the ESEM.

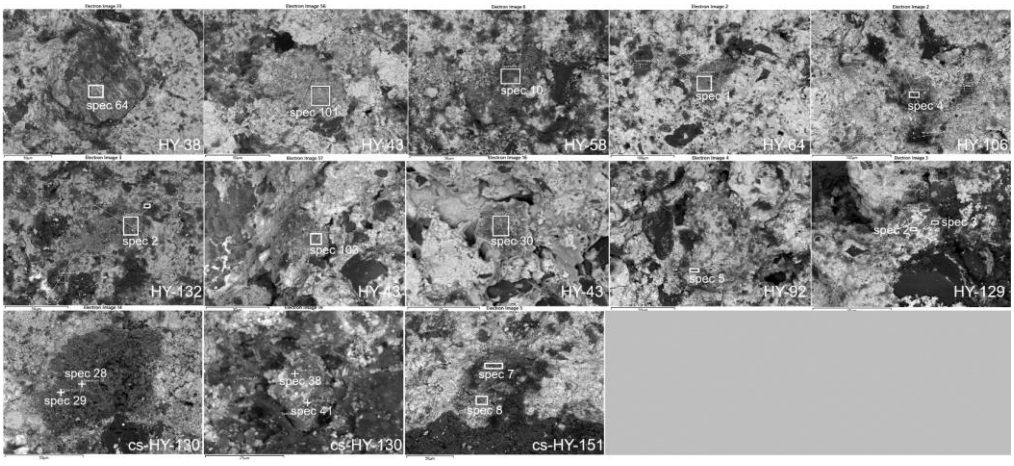


Figure 4. 5 Test areas of Fe-O-associated particles in raw brown glazes, obtained from the ESEM.

Table 4. 1 Chemical compositions of Fe-O-associated particles in raw brown glazes by ESEM[18]

Samples	O	Na	Mg	Al	Si	P	S	Cl	K	Ca	Ti	Mn	Fe	Sn	Pb
HY-38-spec 64	30.21	-	-	6.96	10.19	2.85	-	0.79	1.99	3.22	-	-	17.46	-	26.33
HY-43-spec 101	24.69	-	-	3.65	4.79	4.10	-	1.23	0.66	5.27	-	-	19.86	-	35.74
HY-58-spec 10	25.38	-	0.85	3.07	4.57	0.43	-	0.27	0.52	0.94	-	-	52.14	-	11.84
HY-64-spec 1	26.34	-	-	3.11	4.88	0.77	-	0.42	0.29	1.18	-	-	55.57	-	7.44
HY-102-spec 4	34.67	-	-	8.36	11.20	1.23	2.05	0.32	1.82	6.34	0.38	-	19.33	-	14.30
HY-132-spec 2	27.95	-	-	4.15	5.73	1.25	0.47	0.31	0.66	2.59	-	0.88	46.22	-	9.79
HY-43-spec 103	27.65	-	-	6.65	7.60	3.33	-	1.06	-	2.98	-	-	17.55	-	33.18
HY-43-spec 30	24.06	-	-	2.33	3.35	1.61	-	0.46	-	1.89	-	-	48.83	-	17.46
HY-92-spec 5	25.27	-	-	3.17	5.89	3.16	-	1.00	0.41	2.55	-	-	28.85	-	29.70
HY-129-spec 2	31.20	-	-	7.74	14.24	0.75	-	-	1.00	0.99	-	-	14.91	-	29.18

[18] The test areas are presented in Figure 4. 5.

Samples	O	Na	Mg	Al	Si	P	S	Cl	K	Ca	Ti	Mn	Fe	Sn	Pb
HY-129-spec 3	26.92	-	-	3.97	6.18	0.29	-	0.34	0.53	0.66	0.39	0.79	50.08	-	9.84
HY-130-spec28*[19]	25.82	-	-	4.37	5.58	0.31	-	0.56	0.42	0.93	-	-	47.45	-	14.55
HY-130-spec 29*	25.79	-	-	4.43	5.55	0.36	-	0.54	0.51	0.96	-	-	46.81	-	15.05
HY-130-spec 38*	27.85	-	-	6.00	8.03	0.38	-	0.47	0.78	1.02	-	-	38.33	-	17.14
HY-130-spec 41*	30.52	0.40	0.34	7.84	10.66	0.46	-	0.53	1.38	1.95	-	-	27.90	-	18.01
HY-151-spec 7*	28.81	-	0.60	4.78	7.42	0.70	-	0.21	0.60	1.33	-	-	45.19	2.17	8.21
HY-151-spec 8*	29.45	-	-	5.49	8.00	0.81			0.67	1.29			44.00	1.85	8.44

[19] The data labelled with * refers that they were obtained from the analysis of cross-sections.

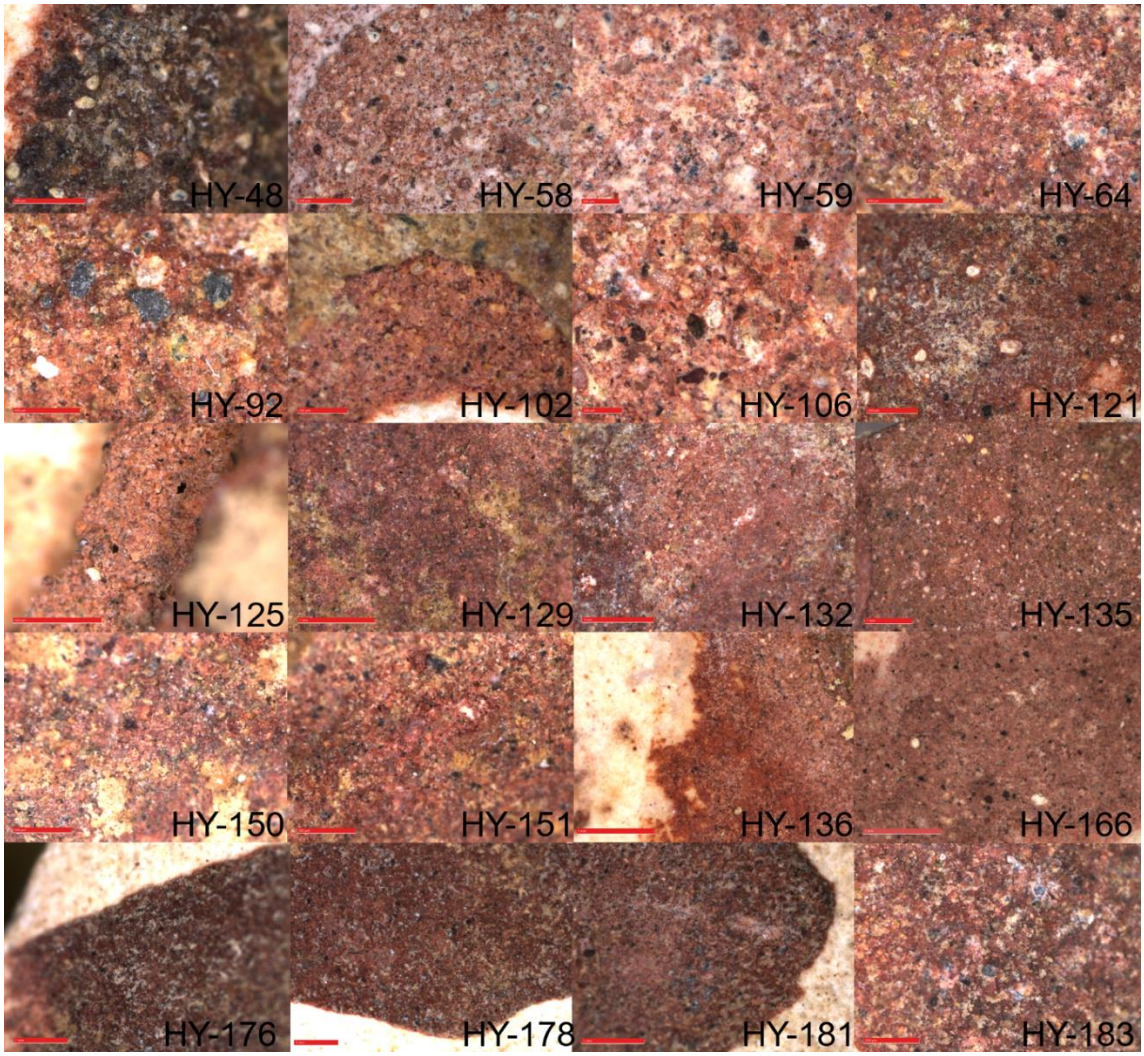


Figure 4. 6 Photos of raw brown glazes in dark red colour, obtained from observation by the optical microscope.

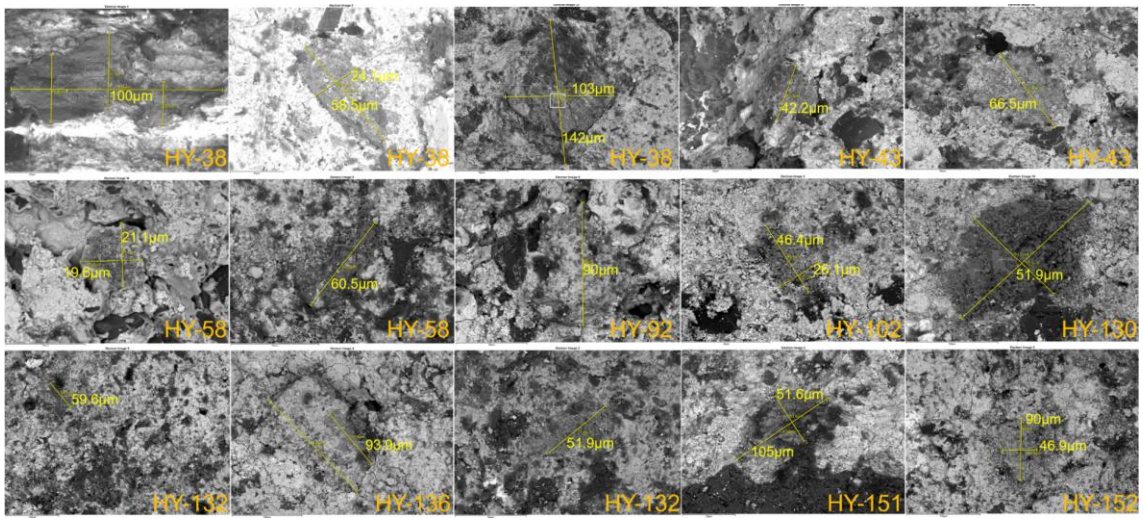


Figure 4. 7 Sizes of iron particles in raw brown glazes, obtained from the ESEM.

Another kind of iron-rich particle is the Fe-Mg-Si-Al-O-associated particles (Figure 4. 8 - Figure 4. 11) and in some cases with K, such as HY-152 (Figure 4. 11). The Fe content of these particles (Figure 4. 12) is much lower than of the Fe-O-associated particles. The lowest content is only 1.51% and the highest is 21.41% by atomic weight (Table 4. 2). Significantly, these particles are also present in the raw clear (Figure 4. 13 and Figure 4. 14), green (Figure 4. 15 and Figure 4. 16) and blue glazes (Figure 4. 17 and Figure 4. 18), which also contain low Fe of 1.52-9.97% (Table 4. 3). The presence of such particles in all four glazes suggests that this iron content is derived from a shared ingredient which might be kaolin clay or a mineral such as a feldspar in the base or stock glaze. Si and Al are the main components of this base or stock glaze and perhaps Fe is an impurity of this Si-Al-rich mineral. And Figure 4. 19a shows a positive correlation between Fe_2O_3 and Al_2O_3 in clear, green, and blue glazes but the brown glaze is an exception due to the additional iron colouring agent. This also proves that opinion – iron in the clear, green and blue glaze from a shared ingredient present as an impurity in the base or stock glaze, such as kaolin clay or felspar etc. The brown glaze is different from other glazes. The sources of iron in the brown glaze are two parts – the iron colourant and impurity in the stock glaze. Remarkably, all raw glazes do not show any correlation between Fe_2O_3 and SiO_2 (Figure 4. 19b). Is this evidence that Al_2O_3 and SiO_2 were provided by different raw materials, and the silica material did not contain Fe_2O_3? This question about SiO_2 will be discussed in Chapter 4.

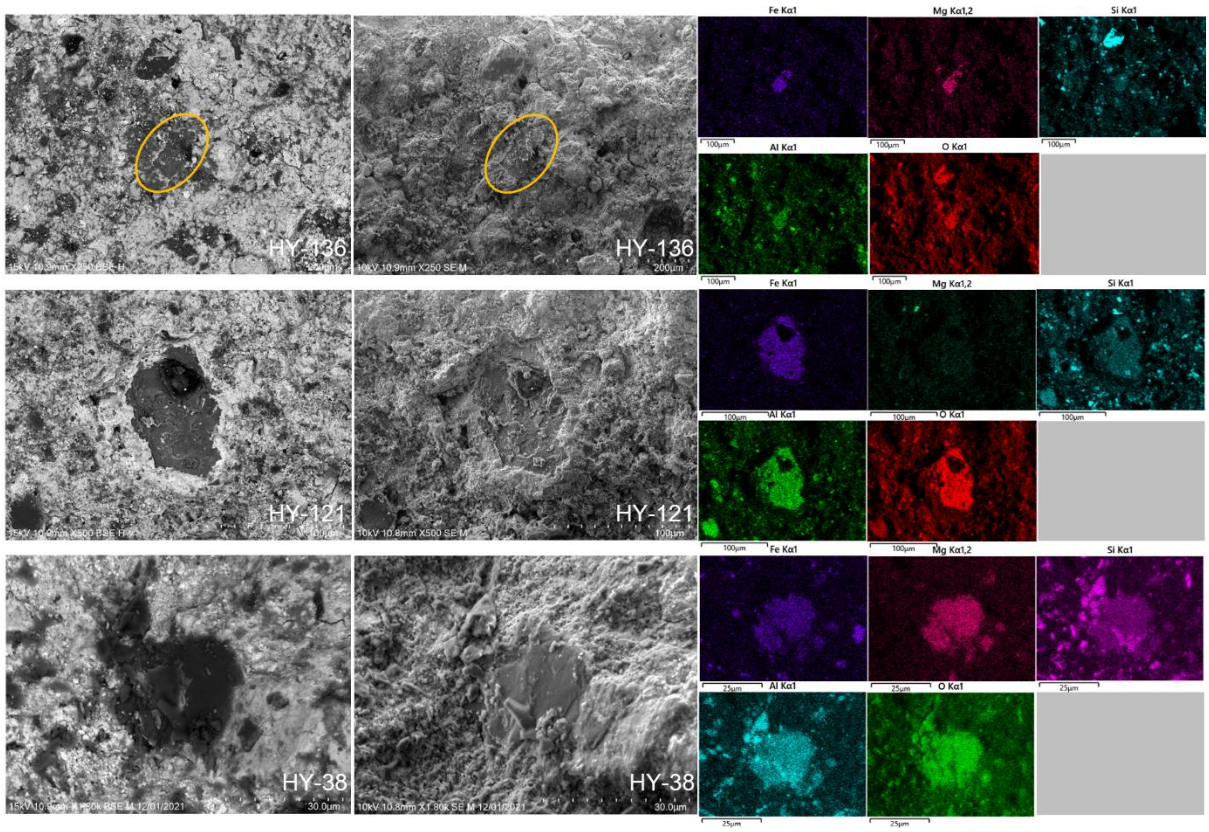


Figure 4. 8 BSE (left), SE (centre) and chemical mapping (right) images of Fe-Mg-Si-Al-O-associated particles in raw brown glazes of HY-136, HY-121, HY-38, obtained from the ESEM.

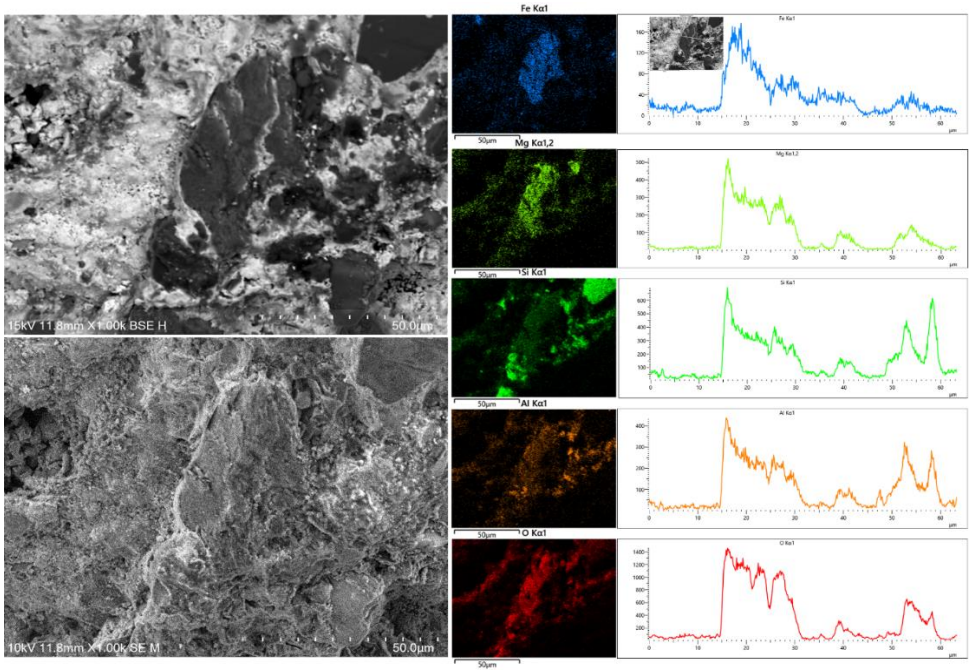


Figure 4. 9 BSE (top left), SE (bottom left), chemical mapping (centre) images and line scan charts (right) of the Fe-Mg-Si-Al-O-associated particle in the brown glaze of HY-123, obtained from the ESEM.

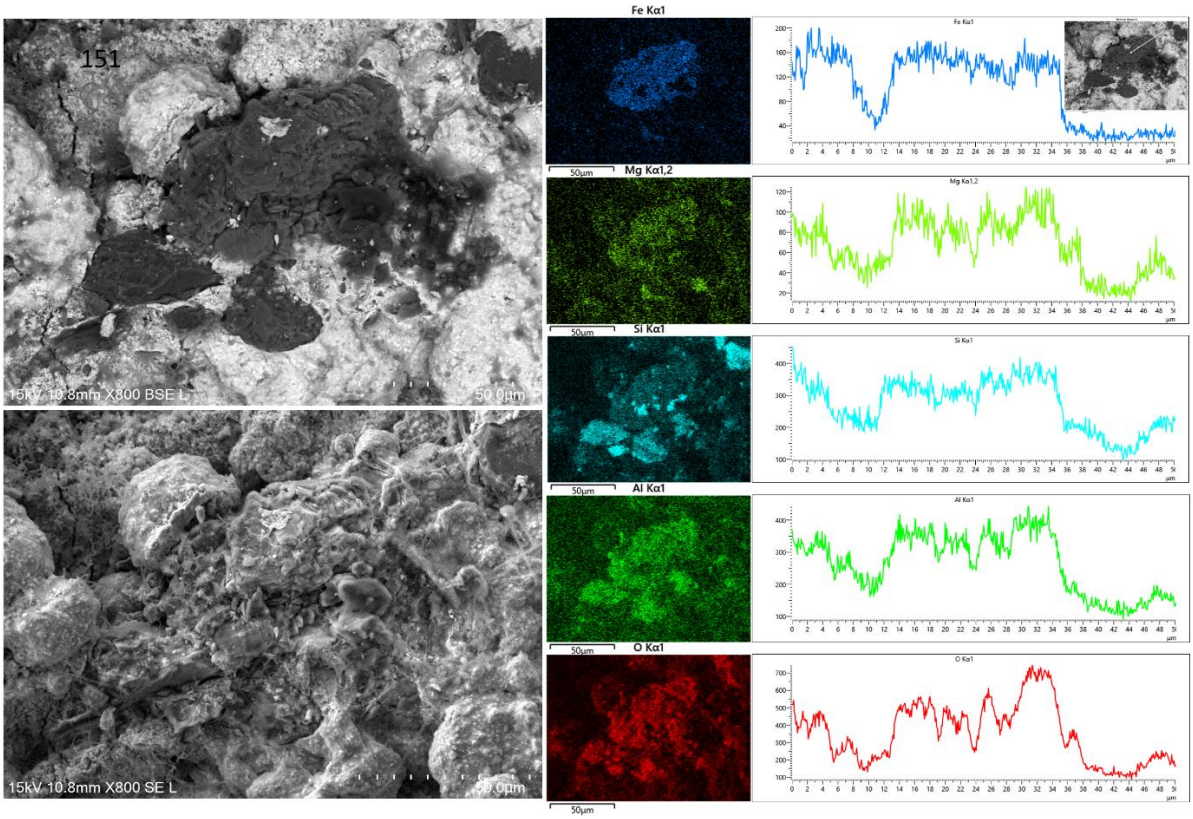


Figure 4. 10 BSE (top left), SE (bottom left), chemical mapping (centre) images and line scan charts (right) of the Fe-Mg-Si-Al-O-associated particle in the brown glaze of HY-151, obtained from the ESEM.

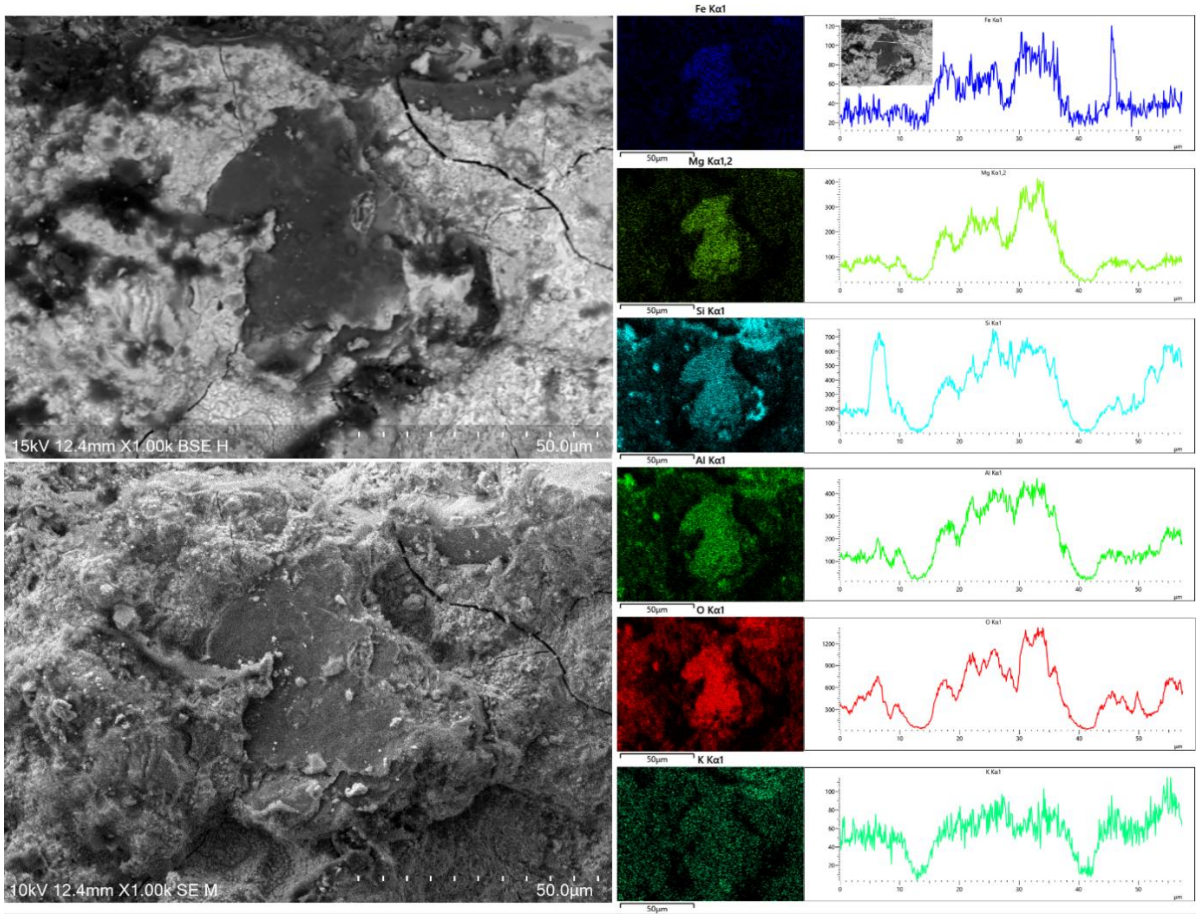


Figure 4. 11 BSE (top left), SE (bottom left), chemical mapping (centre) images and line scan charts (right) of the Fe-Mg-Si-Al-K-O-associated particle in the brown glaze of HY-152, obtained from the ESEM.

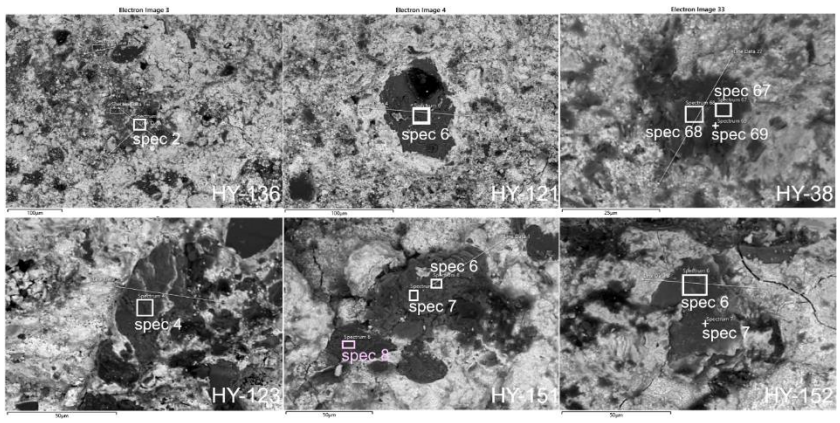


Figure 4. 12 Test areas of iron particles in raw brown glazes, obtained from the ESEM. The area labelled with spec 9 of HY-151 presented a Na-Al-Si-associated particle.

Table 4. 2 Chemical compositions of Fe-Mg-Si-Al-O-associated particles in brown glazes by ESEM[20]

Samples	O	Na	Mg	Al	Si	P	S	Cl	K	Ca	Ti	Fe	Sn	Eu	Pb
HY-136-spec 3	41.43	-	9.91	12.36	16.95	1.36	-	0.26	0.44	1.63	-	4.28	-	-	11.38
HY-121-spec 6	46.22	-	3.81	21.43	19.66	0.87	-	0.43	0.66	1.14	-	-	-	-	5.76
HY-38-spec67	37.90	-	8.03	11.1	13.73	1.15	-	0.26	-	1.54	-	14.15	-	-	12.14
HY-38-spec68	35.39	-	6.66	9.65	12.54	1.71	-	0.49	0.19	2.19	-	12.48	-	-	18.71
HY-38-spec69	38.12	-	8.06	11.29	14.02	0.96	-	0.21	0.26	1.41	-	14.14	-	-	11.53
HY-123-spec 4	40.56	-	9.99	10.05	15.66	1.07	0.74	0.42	1.19	2.01	0.42	9.61	-	-	8.29
HY-151-spec 6	35.80	-	2.59	11.63	12.33	1.38	-	0.37	0.31	1.69	-	21.41	-	1.03	11.47
HY-151-spec 7	36.98	-	3.81	11.97	13.24	1.27	-	0.29	1.03	1.67	-	18.75	-	-	10.99
HY-151-spec 8	42.95	5.57	0.50	10.89	24.00	1.19	-	0.31	0.57	1.37	-	1.51	0.79	-	10.36
HY-152-spec 6	30.29	-	3.72	6.26	9.47	4.44	-	1.28	1.18	4.04	0.39	2.95	-	-	35.98
HY-152-spec 7	45.50	-	7.79	13.92	22.04	0.44	-	-	1.36	0.68	0.47	4.04	-	-	3.77

[20] The tests areas are presented in Figure 4. 12.

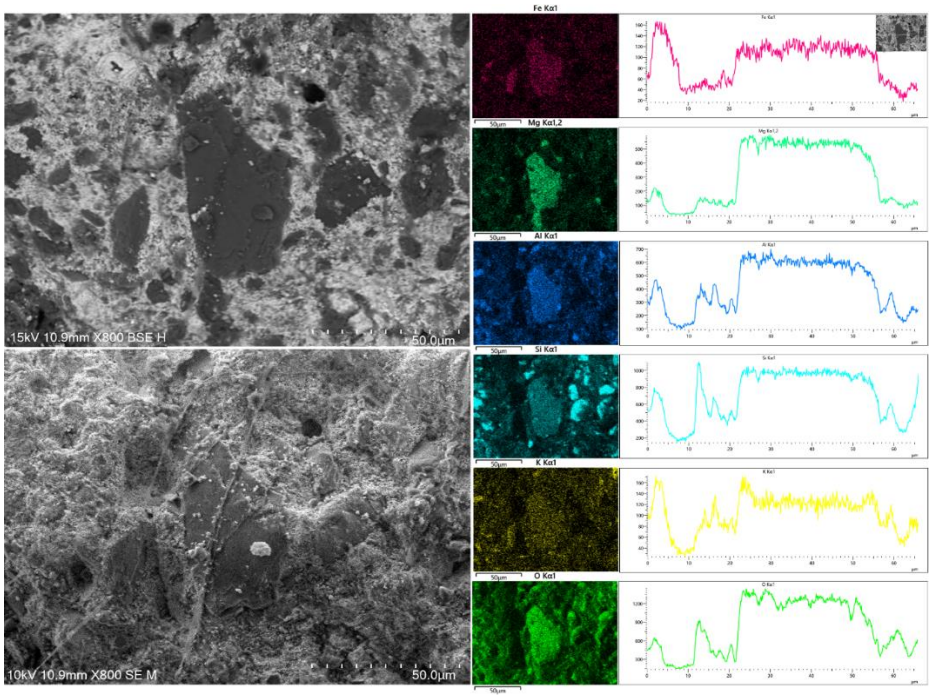


Figure 4. 13 BSE (top left), SE (bottom left), chemical mapping (centre) images and line scan charts (right) of the Fe-Mg-Si-Al-K-O-associated particle in the clear glaze of HY-59, obtained from the ESEM.

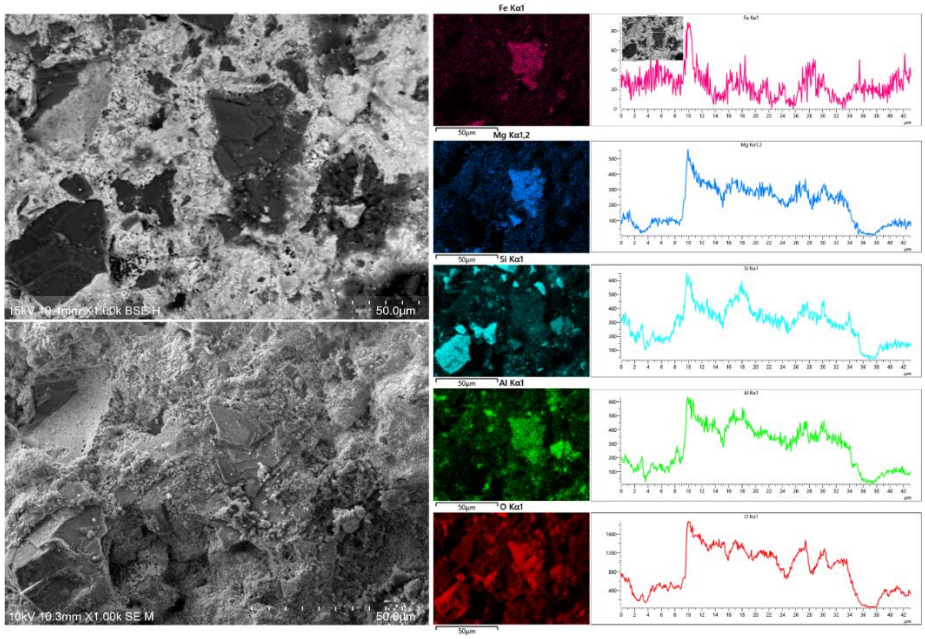


Figure 4. 14 BSE (top left), SE (bottom left), chemical mapping (centre) images and line scan charts (right) of the Fe-Mg-Si-Al-O-associated particle in the clear glaze of HY-123, obtained

from the ESEM.

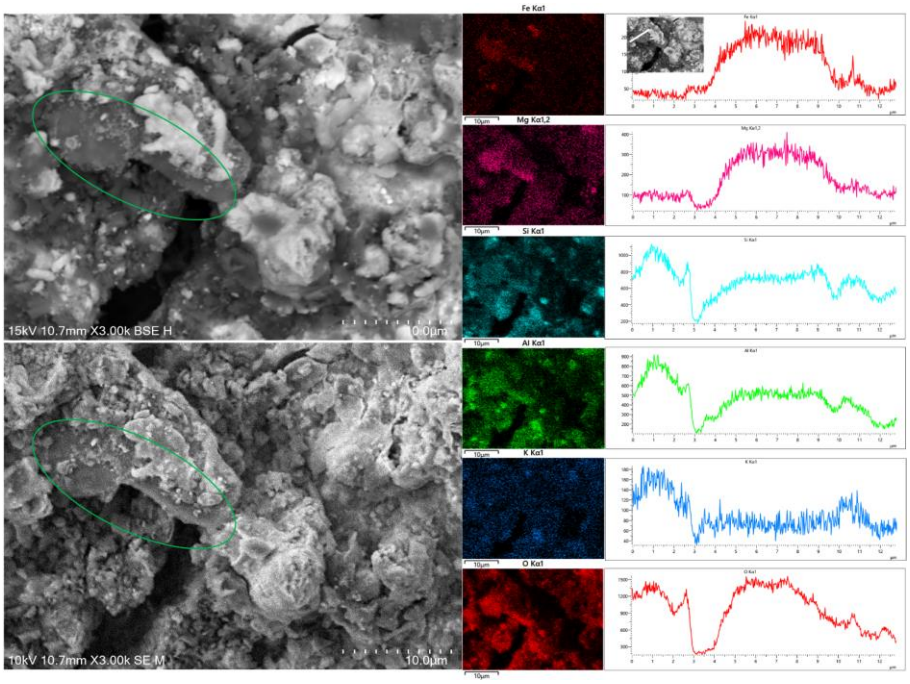


Figure 4. 15 BSE (top left), SE (bottom left), chemical mapping (centre) images and line scan charts (right) of the Fe-Mg-Si-Al-K-O-associated particle (green circles) in the green glaze of HY-38, obtained from the ESEM.

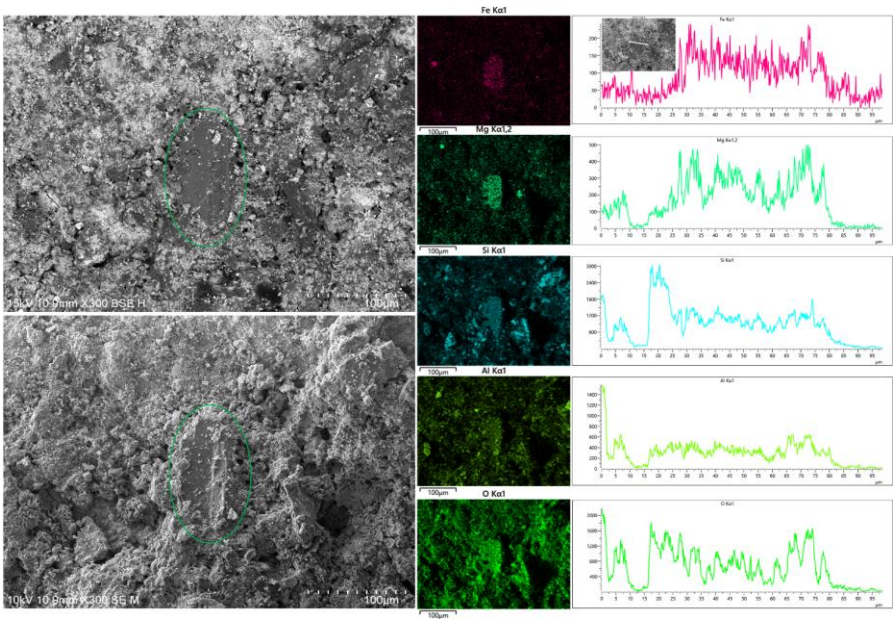


Figure 4. 16 BSE (top left), SE (bottom left), chemical mapping (centre) images and line scan

charts (right) of Fe-Mg-Si-Al-O-associated particle (green circles) in the green glaze of HY-136, obtained from the ESEM.

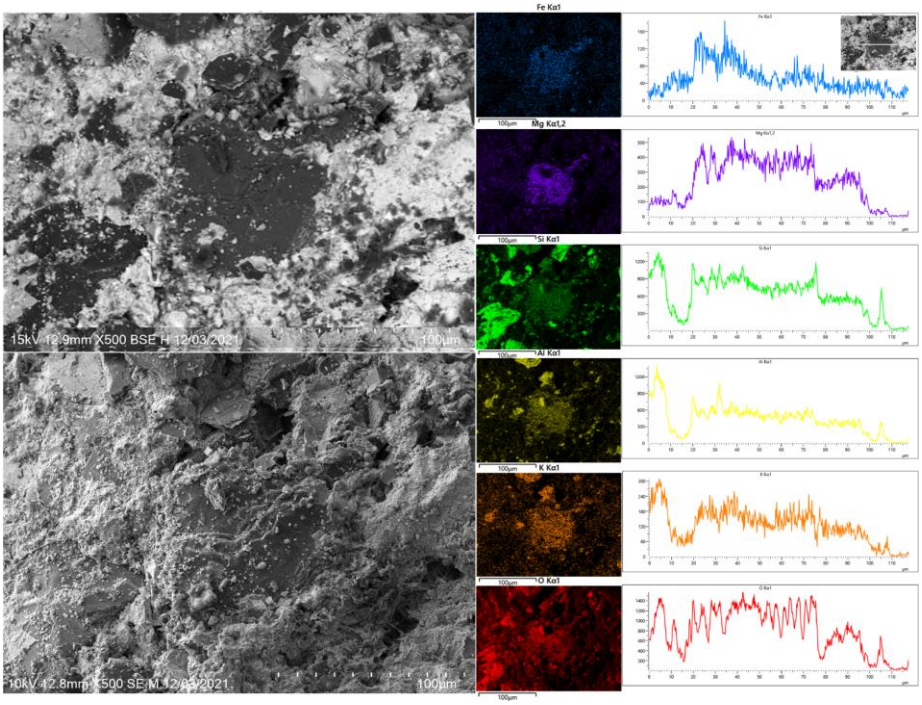


Figure 4. 17 BSE (top left), SE (bottom left), chemical mapping (centre) images and line scan charts (right) of Fe-Mg-Si-Al-K-O-associated particles in the blue glaze of HY-43, obtained from the ESEM.

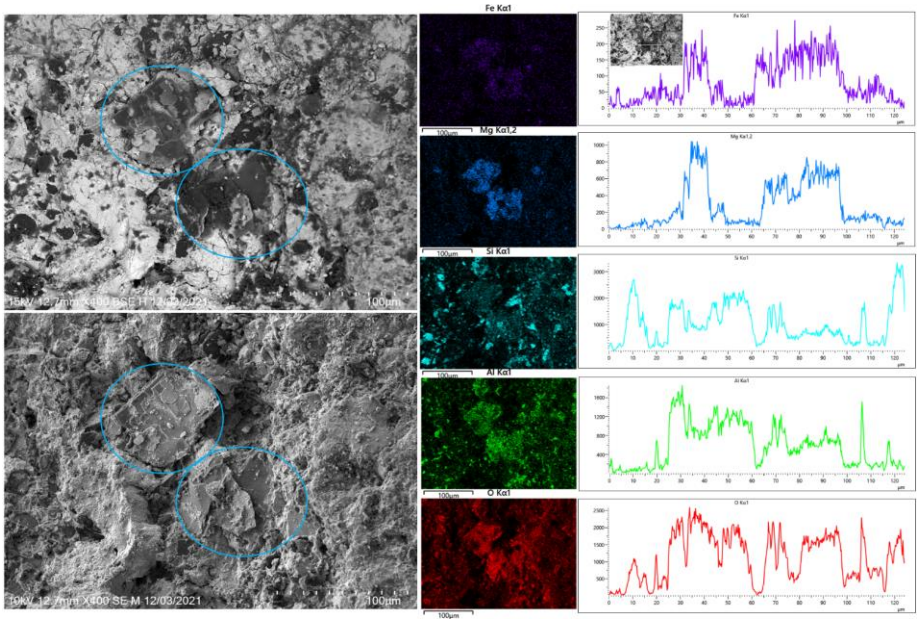


Figure 4. 18 BSE (top left), SE (bottom left) and mapping (centre) images and line scan charts (right) of the Fe-Mg-Si-Al-O-associated particles (blue circles) in the blue glaze of HY-43, obtained from the ESEM.

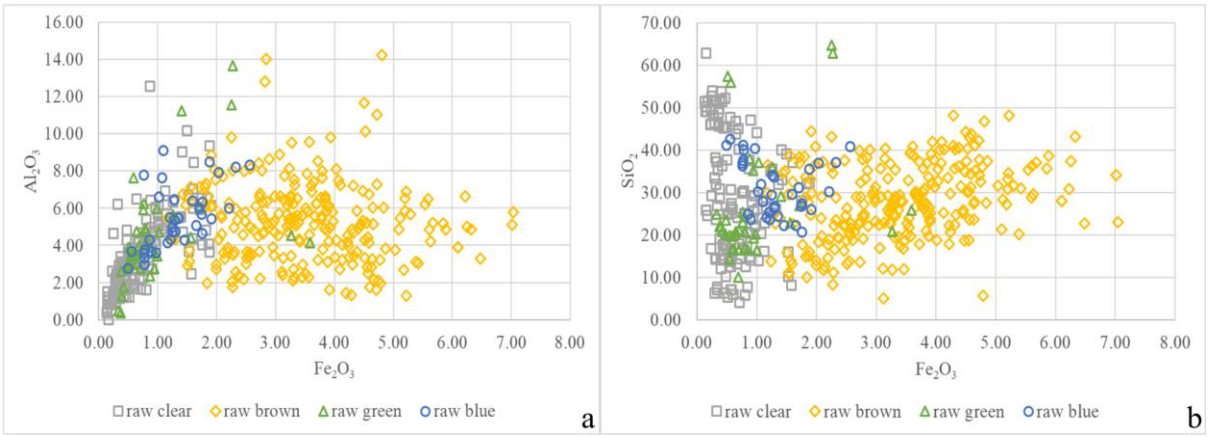


Figure 4. 19 Scatter diagrams of (a) Al_2O_3 and Fe_2O_3 in raw glazes, and of (b) SiO_2 and Fe_2O_3 in raw glazes.

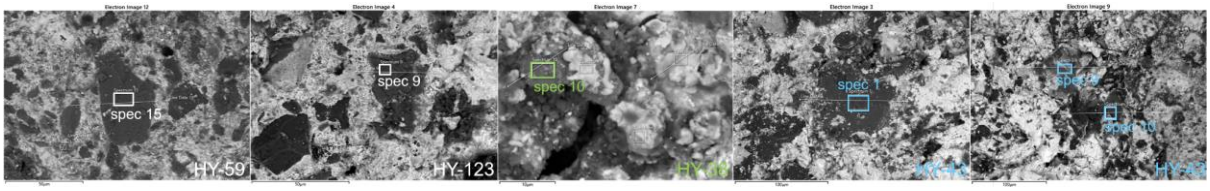


Figure 4. 20 Test areas of Fe-Mg-Si-Al-(K)-O-associated particles in raw clear, green and blue glazes, obtained from the ESEM.

Table 4. 3 Chemical compositions of Fe-Mg-Si-Al-(K)-O-associated particles in clear, green and blue glazes by ESEM[21]

Samples	O	Na	Mg	Al	Si	P	Cl	K	Ca	Ti	Fe	Pb
HY-59-spec 15-clear	40.58	-	9.14	10.38	16.97	0.83	0.35	2.24	1.35	1.65	7.41	9.09
HY-123-spec 9-clear	45.99	-	12.55	17.82	17.99	0.41	-	-	0.39	-	1.52	3.33
HY-38-spec 10-green	35.85	-	5.71	9.73	13.24	2.13	0.43	0.82	2.71	-	9.97	19.40
HY-43-spec 9-blue	34.67	-	7.50	9.46	11.69	2.51	0.75	0.92	2.92	-	5.35	24.22
HY-43-spec 10-blue	32.51	-	8.92	8.78	9.28	1.91	0.62	0.23	2.46	-	9.73	25.56
HY-43-spec 1-blue	61.05	-	6.46	9.40	13.67	0.28	-	2.91	0.50	0.21	1.45	4.08

[21] The test areas are presented in Figure 4. 20.

4.2 Copper Green

Copper-green lead glazed potteries had been already produced in large quantities and been used as burial wares during the Han dynasty (202 BCE-220 CE) (Rawson et al., 1989), earlier than the Tang dynasty (618-907 CE) by around 800 years. The CuO of raw green glaze in the Tang Sancai is 0.24-0.96% (Figure 4. 21) which is much lower than the Fe_2O_3 in the brown glaze, 3.51% on average. It suggests that copper is more efficient and powerful than iron as a colourant. A little addition of this colourant can make a bright green, however, the form of the copper in the glaze is unknown. The discussion in the former section about the red colourant shows that wall painting and ceramic shared the same pigment in the Tang dynasty. The study on green paints of Mogao Grottoes in the Tang dynasty could provide a reference for the exploration of the copper pigment of Sancai. Li (2002) summarised the common pigments used in Mogao Grottoes based on over 600 pigment samples from more than 100 caves. Three green pigments (Figure 4. 21) were used during the Tang dynasty: azurite ($Cu_3(CO_3)_2(OH)_2$), malachite ($Cu_2CO_3(OH)_2$) and atacamite ($Cu_2Cl(OH)_3$). Was one or more of them employed in Sancai glaze? XRF and ESEM analysis will reveal the answer.



Figure 4. 21 Box plot (left)) of CuO in raw glazes and photos (centre and right) of azurite, malachite and atacamite. This azurite ore is from Anhui in China, and malachite ore is from Zaire in Africa. Photos of azurite and malachite ores were obtained from Driscoll et al. (2011).

Photo of atacamite presents sparking deep green crystallised atacamite covering a green malachite matrix, from https://en.wikipedia.org/wiki/Atacamite#/media/File:Atacamite_on_malachite_-_Mt_Gunson_mines,_South_Australia.jpg.

Only a few Cu-rich particles in the green glaze were found in the ESEM examination. Compared with the observation of hematite particles in the brown glaze, it was very difficult to find Cu particles in the green glaze. There might be two reasons - the number of Cu-rich particles is very small, and the size of the particles is too tiny. Three samples - HY-38, -136 and -166, were found to contain identifiable Cu particles. The mapping and line scans show that the Cu particles in HY-166 are only positively correlated with O (Figure 4. 22 and Figure 4. 23). And these Cu-O-associated particles have a regular lamellar and columnar structure (Figure 4. 24), which is very similar to the texture of malachite crystals (Figure 4. 25). The compositional characteristic and specific texture both suggest that the green colourant of HY-166 is malachite. Malachite is a copper carbonate hydroxide mineral, with the formula $Cu_2CO_3(OH)_2$. It was a common green paint in wall painting and was used in the Mogao Grottoes in the Tang dynasty (Li, 2002; Su, 2021). Since C is too light to be tested in the ESEM, only Cu and O would be found in the copper-rich particles of the raw green glaze. After glaze firing, malachite decomposed into CuO ($Cu_2CO_3(OH)_2 \rightarrow 2CuO + CO_2 + H_2O$) and melted into the lead glaze.

A few big distinguishable green grains (Figure 4. 26) in the raw green glaze on HY-166 also proves the use of this green mineral ore - malachite. Some similar green particles were also found in the raw green glaze of HY-132 (Figure 4. 26). It might be malachite, or other green copper minerals. The colour of most raw green glazes is dark brown, and the copper colourant

might be finely ground, therefore, similar green particles have not been found in on other sherds by optical microscope.

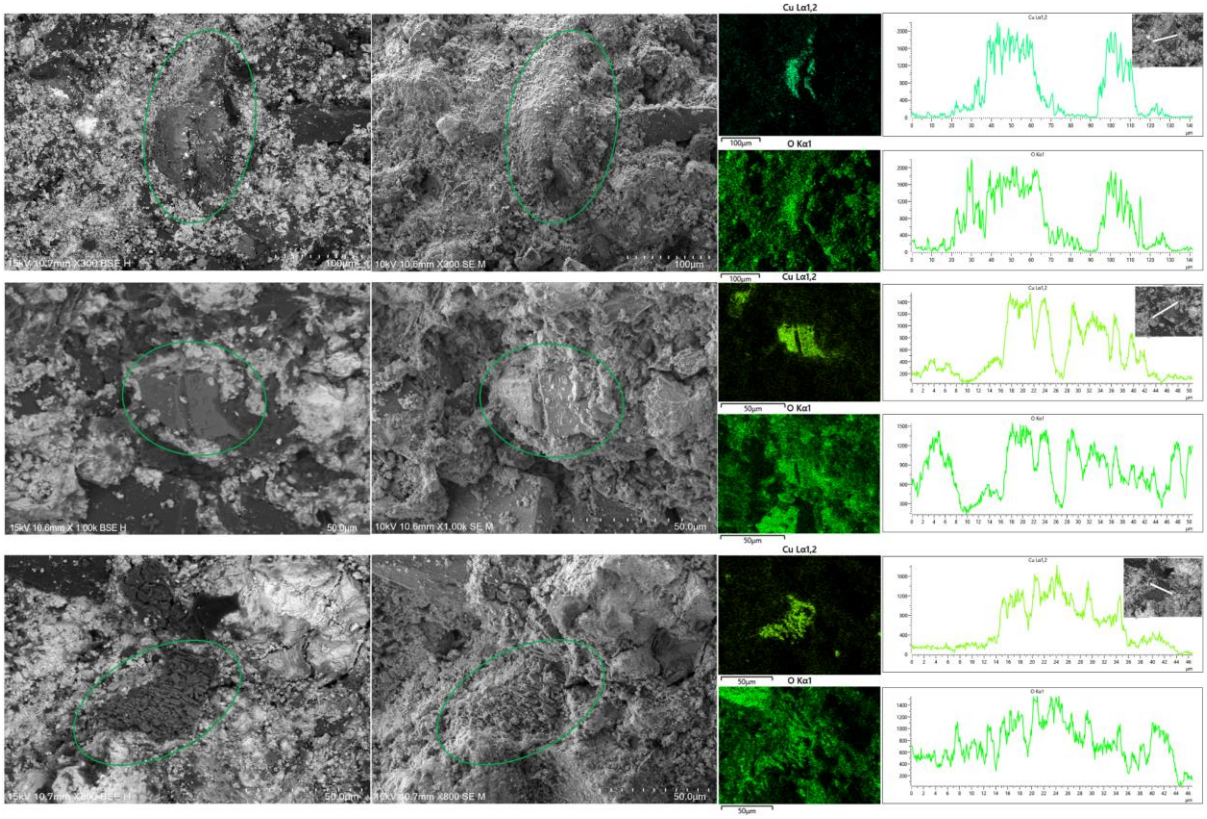


Figure 4. 22 BSE (left), SE (centre left), chemical mapping (centre right) images and line scan charts (right) of Cu-O-associated particles (green circles) in the raw green glazes of HY-166, obtained from the ESEM.

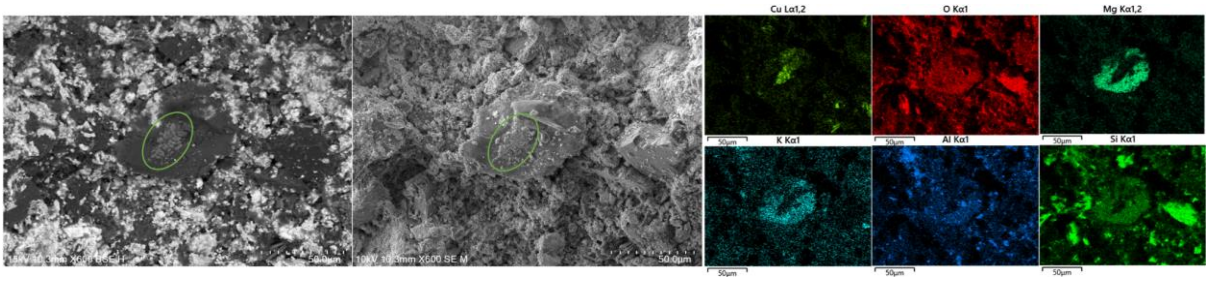


Figure 4. 23 BSE (left), SE (centre) and chemical mapping (right) images of Cu-O-associated particle (green circles) in the raw green glaze of HY-166, obtained from the ESEM.

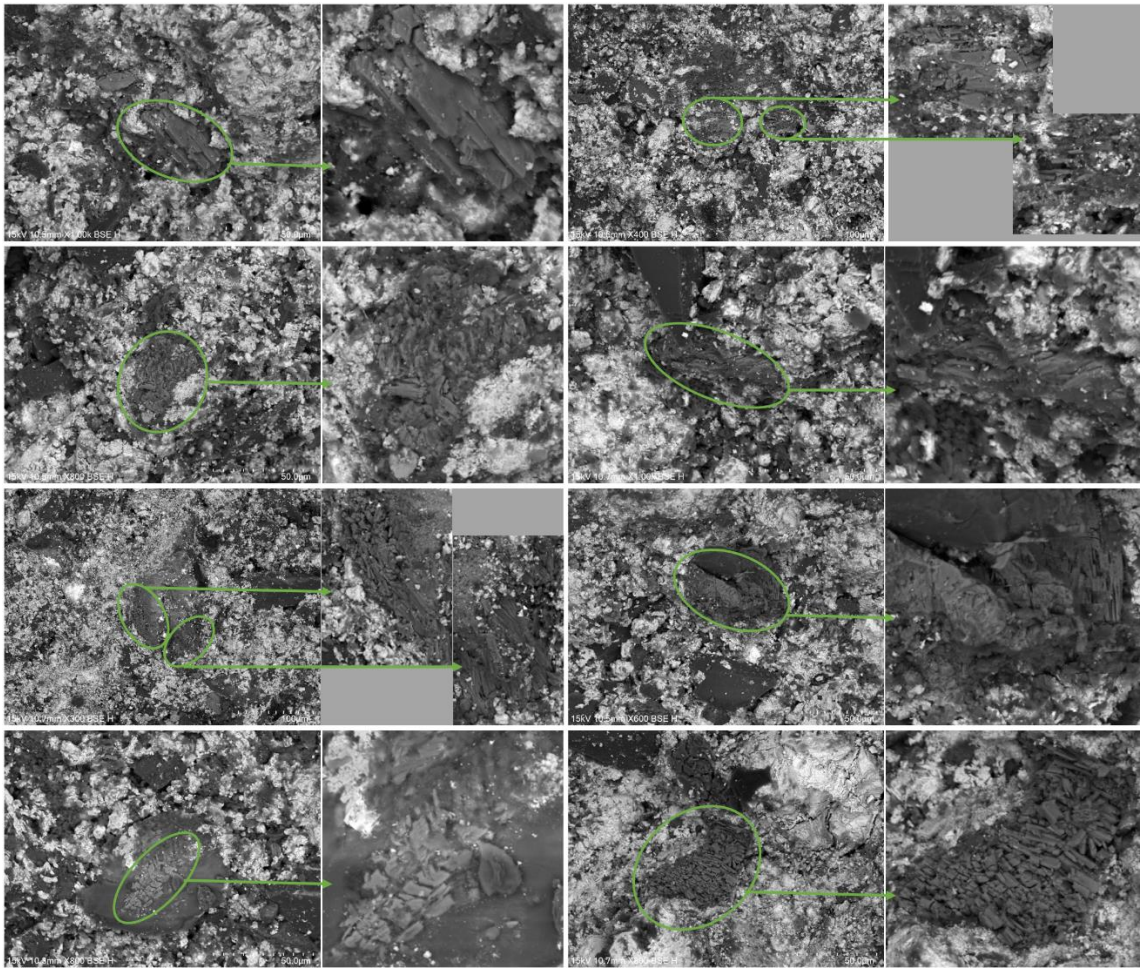


Figure 4. 24 Texture of Cu-O-associated particles in green glazes of HY-166, obtained from the ESEM.

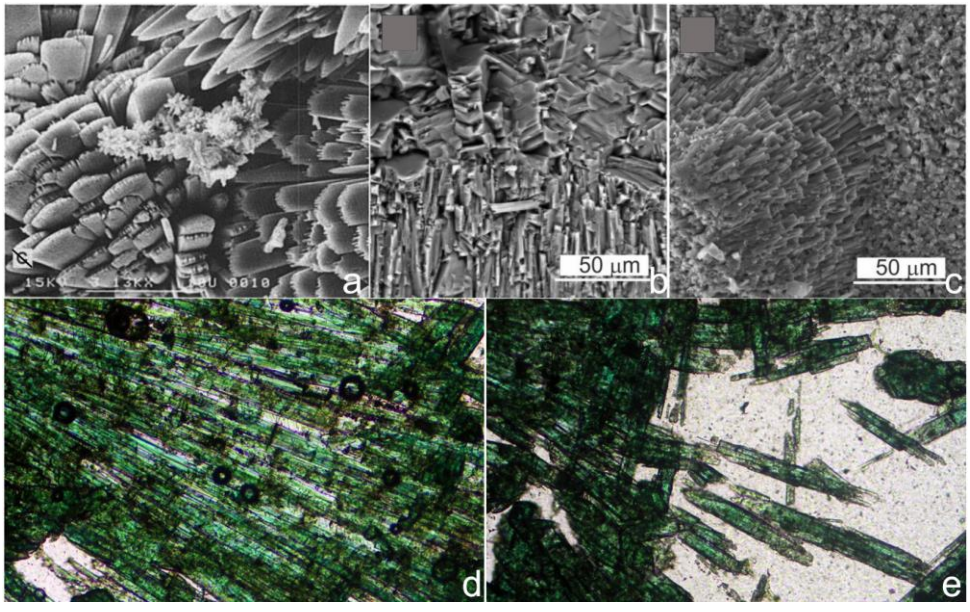


Figure 4. 25 Texture of malachite crystals, from (a) Woods and Garrels (1986), (b) and (c) Bublikova et al. (2022), (d) and (e) https://www.alexstrekeisen.it/english/meta/malachite.php#:~:text=Malachite%20is%20a%20green%2C%20very,as%20mammillary%20aggregates%20as%20well.

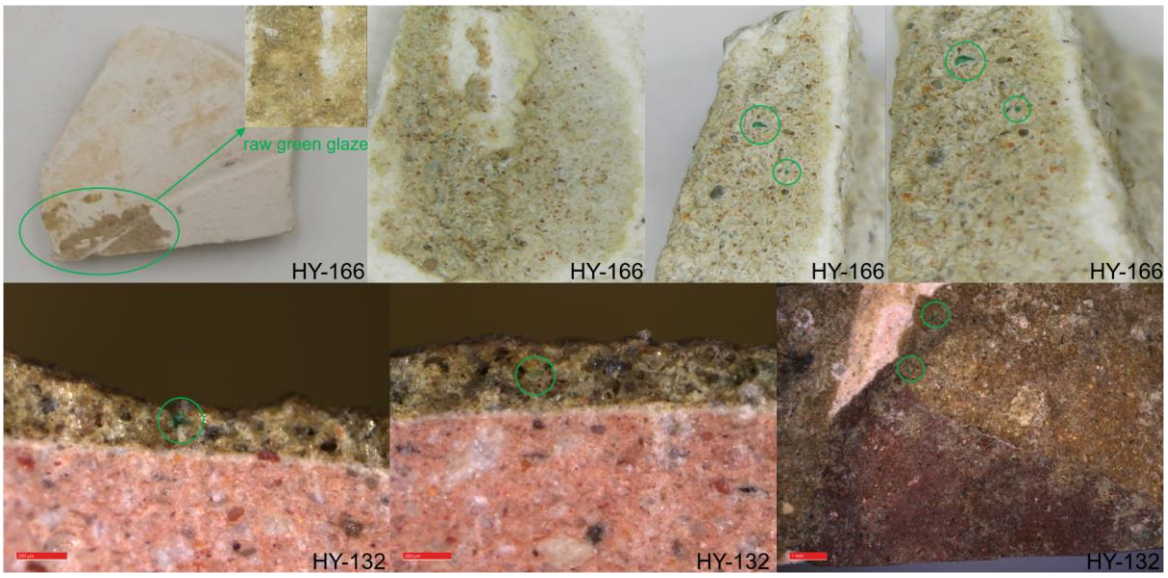


Figure 4. 26 Photos of green grains (green circles) in the raw green glaze of HY-166 and HY-132, obtained from the optical microscope.

The results of HY-136 differ from that of HY-166. The first point is that Cu-rich particles are associated with not only O but also with Si, Al and K (Figure 4. 27). The next important point is that the Cu-Si-Al-K-O-associated particle in HY-136 contains much higher Si (20.81%) and Al (8.99%) than the copper-rich particles in HY-166 (HY-136-spec 28 in Table 4. 4). These characteristics suggest that this colourant of HY-136 possibly is chrysocolla ($(Cu,Al)_2H_2Si_2O_5(OH)_4 \cdot nH_2O$). Chrysocolla is a hydrated copper phyllosilicate mineral. The colours vary from blue-green to green. And the ratio of Si and Al to Cu of this mineral is variable. The element associations – Cu, Si and Al, and compositional data – high Si and Al, obtained from ESEM analysis of HY-136 both proves the use of chrysocolla. Another evidence

of this finding about chrysocolla is that a few tiny pure copper particles have been found in HY-136 (Figure 4. 28 and Figure 4. 29). Neither mapping nor line scans found any associated element with Cu. The Cu content reaches 63.01% and 74.15% (Table 4. 4). The compositions and elemental distribution pattern both suggest that these two grains are natural copper grains associated with chrysocolla. These pure copper particles are unlikely to have grown in the glaze as metallic copper, as is the case with medieval red glass (Kunicki-Goldfinger et al., 2014). First, the chrysocolla colourant of the raw green glaze is natural mineral material rather than fired copper glass. The ruby red colour of medieval glass forms due to the diffusion of oxidised copper into the reduced glass and the nucleation and growth of metallic copper during heat-treatment (Kunicki-Goldfinger et al., 2014). The colourant and glaze are unfired and cannot offer the necessary factors – heating and reducing base, for the growth of metallic copper. Moreover, the metallic copper in the ruby-red glass are nanoparticles (Farges et al., 2006; Colomban et al., 2009). However, the size of pure copper grains in the raw glaze is around 3-5 μm.

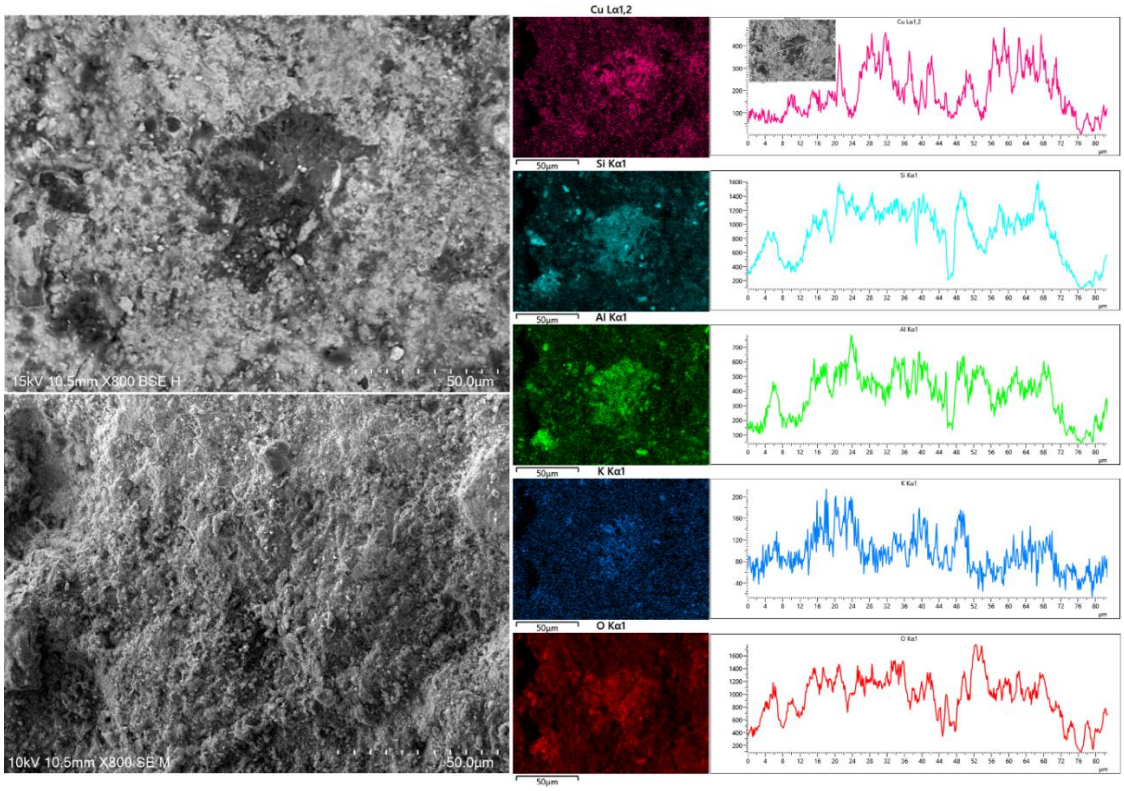


Figure 4. 27 BSE (top left), SE (bottom left), chemical mapping (centre) images and line scan charts (right) of the Cu-Si-Al-K-O-associated particle in the raw green glaze of HY-136, obtained from the ESEM.

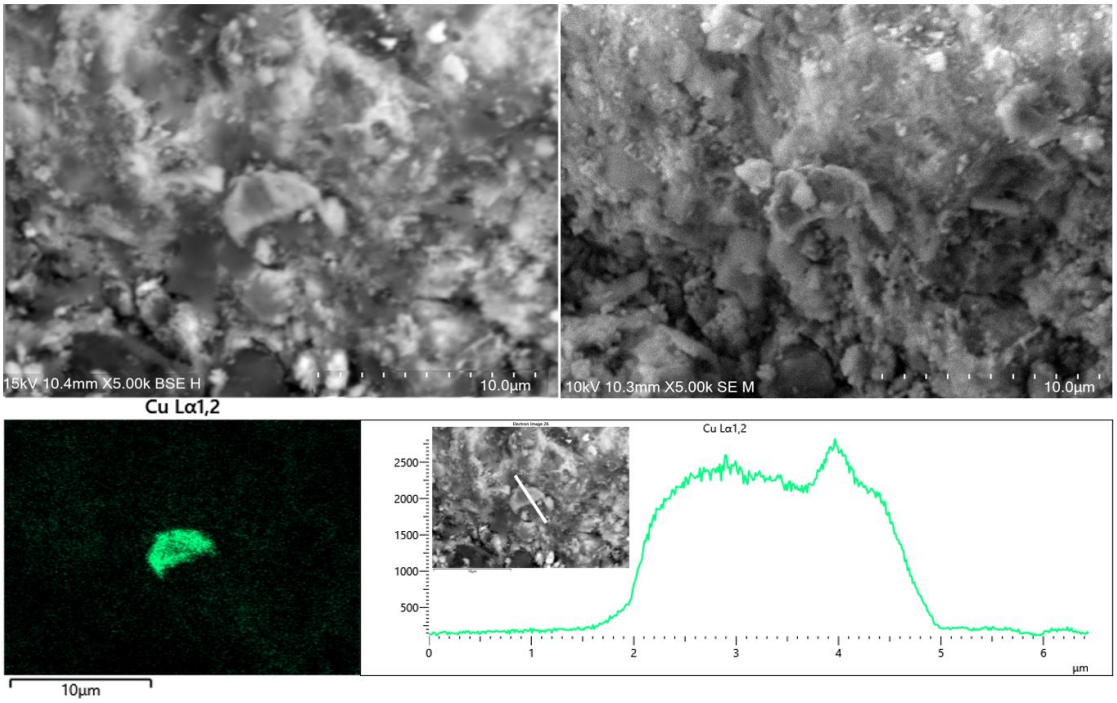


Figure 4. 28 BSE (top left), SE (top right), chemical mapping (bottom left) images and the line scan chart (bottom right) of a pure Cu particle in the raw green glaze of HY-136, obtained from the ESEM.

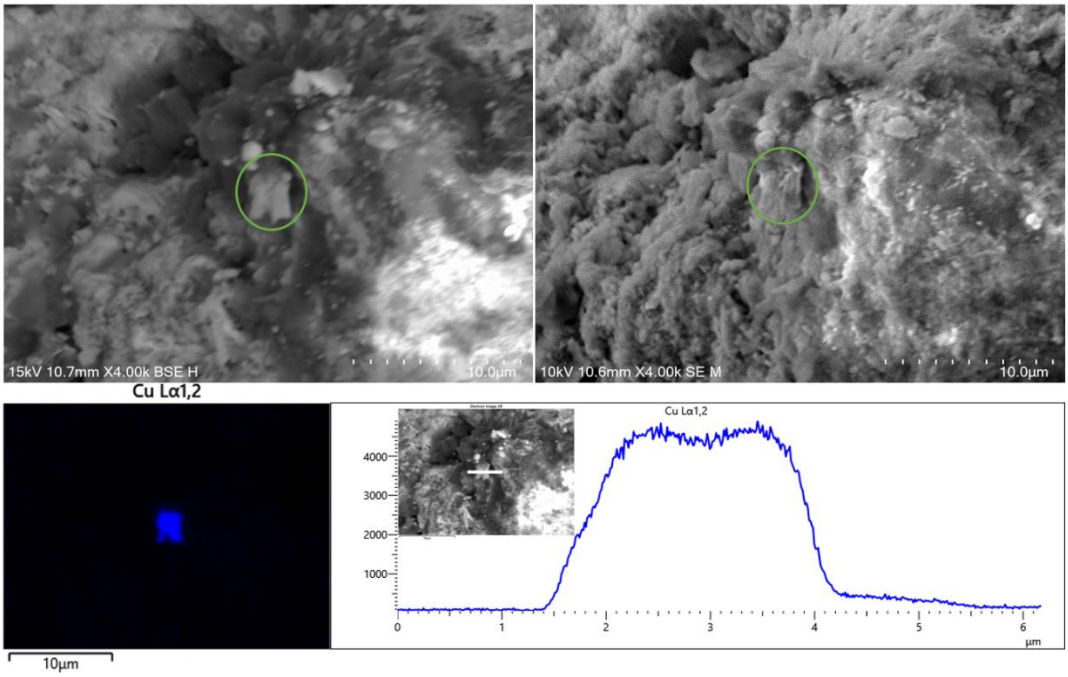


Figure 4. 29 BSE (top left), SE (top right), chemical mapping (bottom left) images and the line scan chart (bottom right) of a pure Cu particle in the raw green glaze of HY-136, obtained from the ESEM.

The green glaze of HY-38 shows significant difference from HY-136 and HY-166 on element association. V, Cu and Pb show the same distribution in some areas (Figure 4. 30 and Figure 4. 31). The first possibility for this special finding is the use of a colourant with V, Cu and Pb, such as mottramite ($PbCu(VO_4)(OH)$). Mottramite is an orthorhombic anhydrous vanadate hydroxide mineral, some of which are green in colour (glass-green, olive-green, and yellow-green etc). No historical accounts or modern scientific analysis mention that mottramite was used in ceramics or in other archaeological materials in China. Moreover, if $PbCu(VO_4)(OH)$ had been used, the molar ratio of Cu to V of these particles would have been

around 1, rather than 1.84 - 2.62 (Table 4. 4, HY-38-spec 7, -8, -9). This material of HY-38 might not be mottramite.

The ‘shapes’ of these Cu-V-Pb-associated ‘particles’ are very strange. They look like shells (Figure 4. 30 and Figure 4. 31) covering the lead-rich area rather than particles (Figure 4. 23 and Figure 4. 27) or minerals with regular texture (Figure 4. 24). The texture of these shells seems to be very homogeneous and dense. They are very different from other colourant particles, but the same as the lead ingredient in the raw glazes. The lead material of all raw glazes is very homogeneous without any particles, which look like fondant on a cake. This suggests that the lead in the Cu-V-Pb-rich areas might be from the background – lead glaze, rather than a Cu-V-Pb material. In other words, the copper material of the raw green glaze on HY-38 only be associated with V. Based on the compositional results of the Cu-V-rich areas (Table 4. 4), it can be found that higher-Cu areas contain higher V (Figure 4. 32). That also confirms this association between Cu and V. The following important question is what is the Cu-V-rich material?

According to the list of minerals recognised by the International Mineralogical Association[22], Cu-V minerals are blossite (α-$Cu(V_2O_7)$), fingerite ($Cu_{11}(VO_4)_6O_2$), mcbirneyite ($Cu_3(VO_4)_2$), molinelloite ($Cu_2(H_2O)(OH)V^{4+}O(V^{5+}O_4)$, stoiberite ($Cu_5(VO_4)_2O_2$)), turanite ($Cu_5(VO_4)_2(OH)_4$), volborthite ($Cu_3V_2O_7(OH)_2$-$2H_2O$) and ziesite β-$Cu_2(V_2O_7)$. It is uncertain that whether a specific Cu-V mineral above was used in Sancai glaze based on current examination. Besides, vanadium can be brought in by the exploitation of some copper minerals. Afify et al. (2022) studied the copper mineralisation in southwestern Sinai in Egypt and found that malachite, azurite, atacamite, chrysocolla, and cuprite occur as disseminations or stratiform,

[22] https://www.mindat.org/chemsearch.php?inc=V%2CCu%2C&exc=&ima=0&sub=Search+for+Minerals

layer-parallel streaks, and lenticular bodies that are intercalated with vanadiferous sandstones. Except for the Cu-V-rich materials, only one pure copper grain was found in HY-38 (Figure 4. 33). The composition results reveal the dominant level of Cu (70.16%) of this particle (HY-38-spec 5 in Table 4. 4), which is almost identical to the associated natural copper particle in HY-136 (HY-136-spec 29 and -spec 33 in Table 4. 4). However, no more findings about copper colourant in the raw glaze of HY-38 were revealed by ESEM analysis. The question of the raw material of this copper colourant does not yet have an answer.

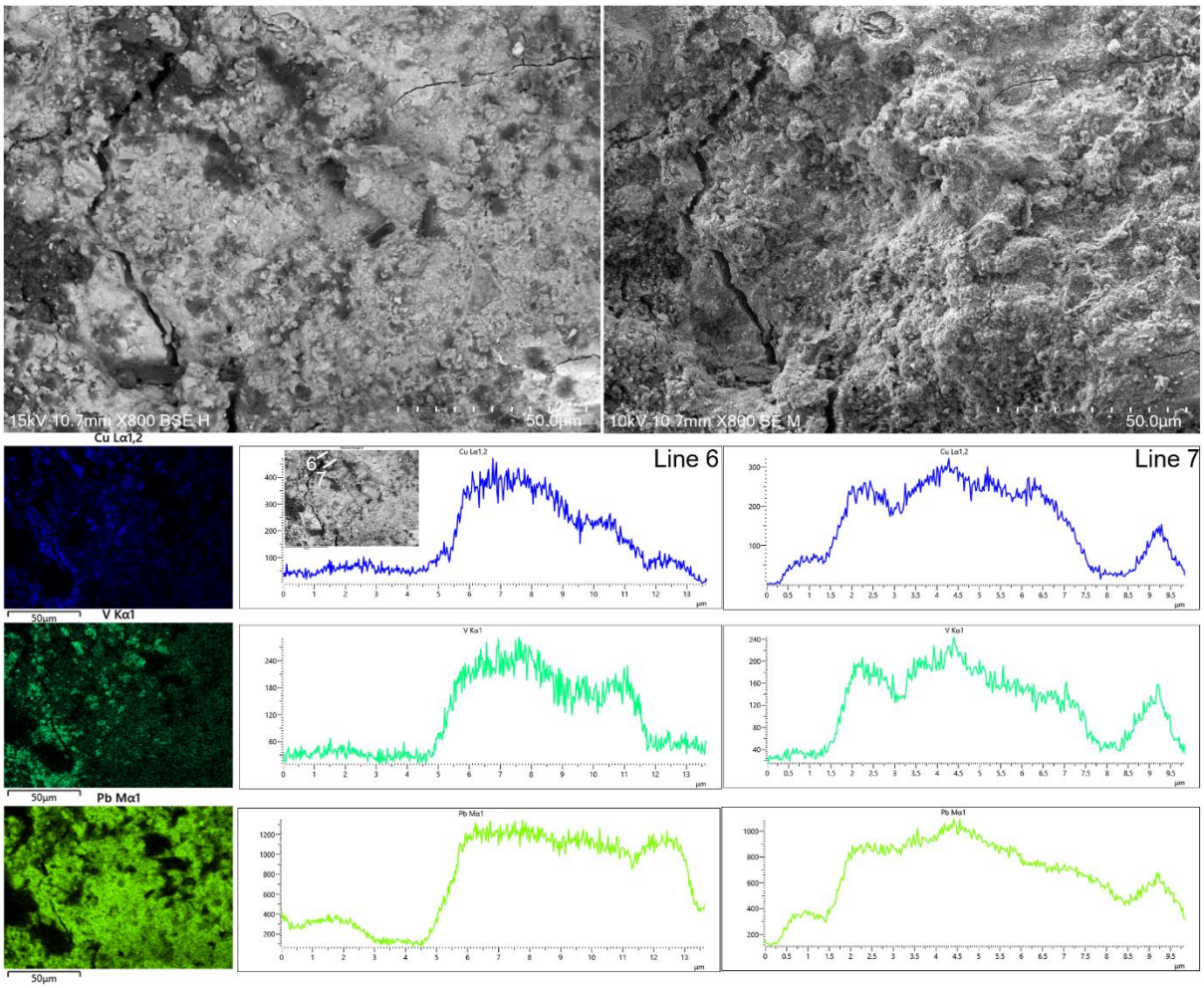


Figure 4. 30 BSE (top left), SE (top right), chemical mapping (bottom left) images and line scan charts (centre and bottom right) of Cu-V-Pb-associated particles in the raw brown glaze of HY-38, obtained from the ESEM. The Cu-V-Pb-rich areas cannot be distinguished from the

high lead areas, which are both very light in the BSE image. The chemical mapping of Cu and V can show the Cu-V-rich 'shells'.

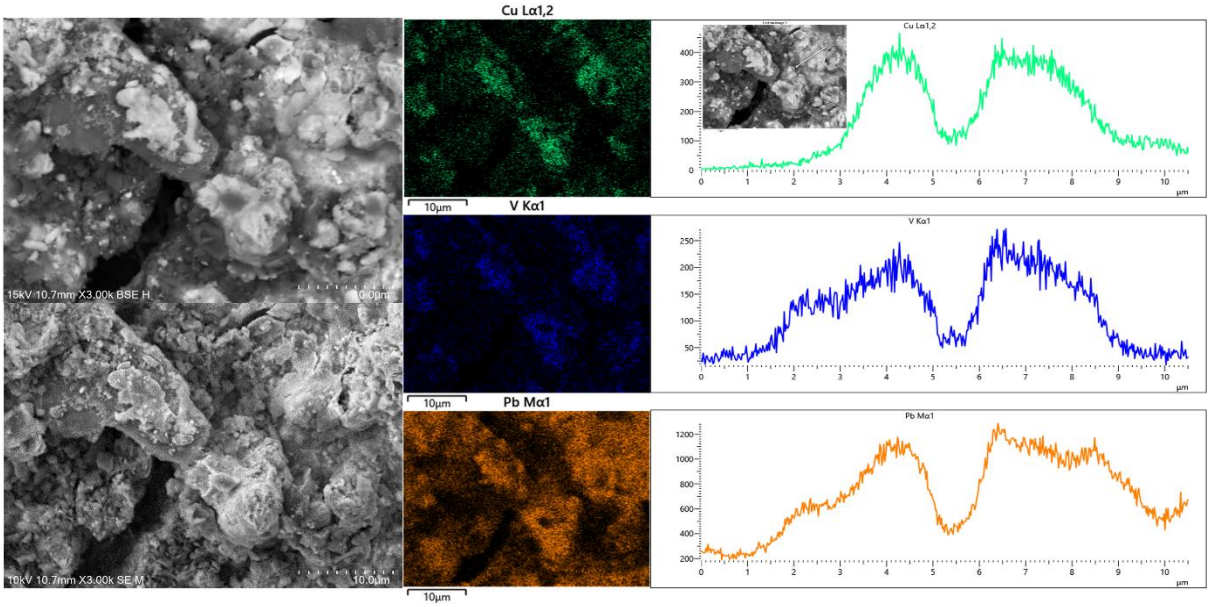


Figure 4. 31 BSE (top let), SE (bottom left), chemical mapping (centre) images and line scan charts (right) of Cu-V-Pb-associated areas in the raw brown glaze of HY-38, obtained from the ESEM.

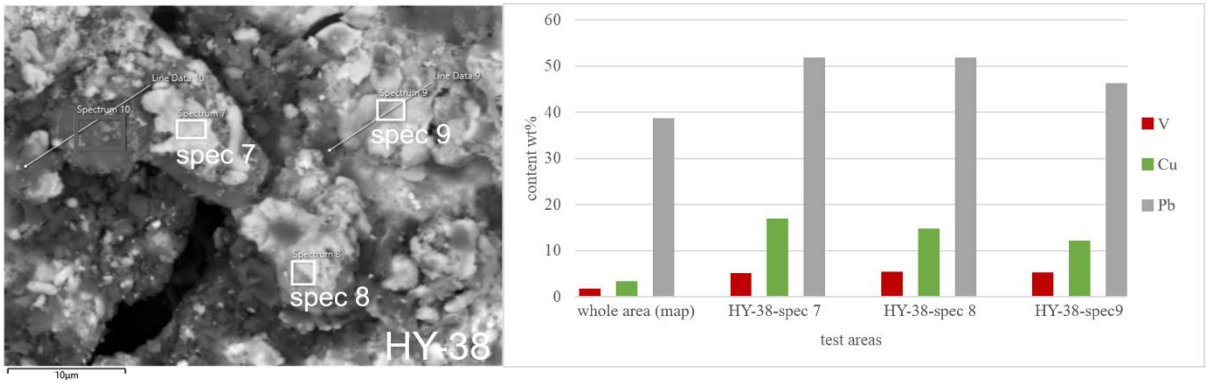


Figure 4. 32 Test area (left) and bar chart (right) of Cu, V and Pb in raw green glazes of HY-38. The image and compositional data were obtained from the ESEM.

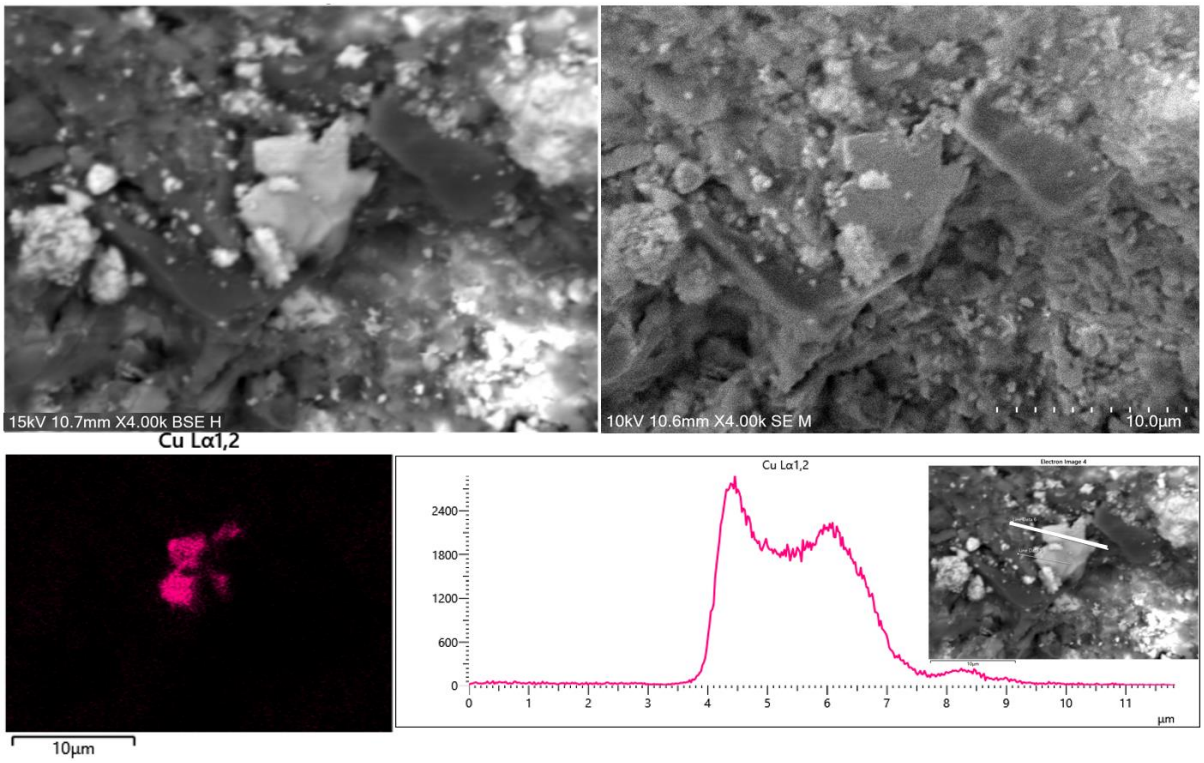


Figure 4. 33 BSE (top left), SE (top right), chemical mapping (bottom left) images and line scan charts (centre and bottom right) of a pure Cu particle in the raw green glaze of HY-38, obtained from the ESEM.

Unlike the use of hematite for the brown glaze, the colourants of the green glaze are more diverse. Possibly, at least two copper ores were used in Gongyi for the green glaze. They were malachite of HY-166 and chrysocolla of HY-136 respectively. The use of these two different materials suggests that potters mastered the chemical changes of these minerals which both would become CuO and show the same green colour in the lead glaze after heating. Therefore, their choice of green colourant need not have been confined to a particular ore. It is uncertain what the chronological order of HY-166 and HY-136 based on the excavation. If they were produced in different periods of the Tang dynasty. That might suggest another possibility - the use of green colourant changed with time. The source and type of the copper green colourant

might be different in different periods, but potters must recognise that the different copper materials made the same final effect.

There is another potential condition about the use of the green colourant. Since some copper mineral – such as malachite, chrysocolla, azurite, cuprite etc. are commonly associated minerals in a natural copper mine. Perhaps, the green colourant was supplied with bag of mixed copper mineral which was pre-treatment and fine-powdered mineral material. The iron colourant – hematite, was collected locally. This might explain the hematite is coarse, but the copper finely ground.

Additionally, potters also found that copper was an efficient colouring agent, much more efficient than iron in the brown glaze. Consequently, much less copper material is added to the glaze than the iron in the brown glaze. The mean values are 3.44% Fe_2O_3 and 0.82% CuO respectively. But the grinding time of the copper colourant might be more than the iron colourant because the sizes of copper-rich particles in the green glaze are much smaller than those of iron-rich particles in the brown glaze. The iron particles in the brown glaze are mostly in the size of 40-100 μm. Some particles are even larger than 100 μm. In comparison, the sizes of copper particles of HY-166 and HY-136 are around 20-60μm. The smallest copper particle is as small as 2μm, and the sizes of most big particles are around 50μm (Figure 4. 34). Rarely, a few particles of copper materials can be recognised on raw green glazes (Figure 4. 26). These big grains are probably exceptions after long-term grinding.

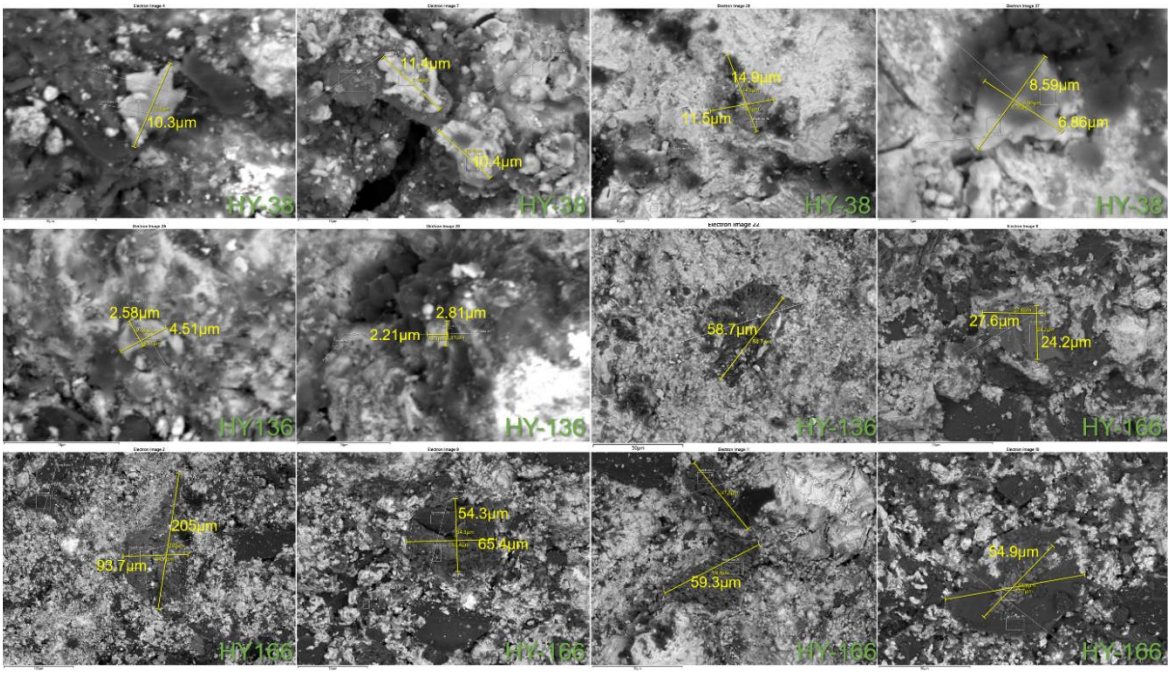


Figure 4. 34 Sizes of Cu-rich particles in raw green glazes, obtained from the ESEM.

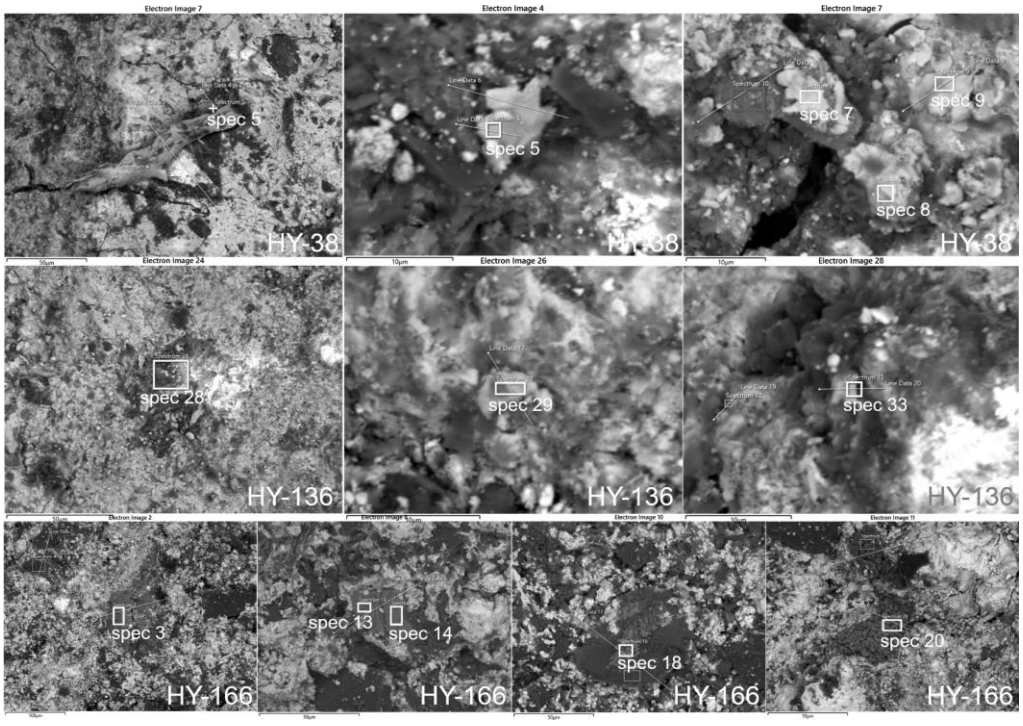


Figure 4. 35 Test areas of Cu-rich particles in raw green glazes, obtained from the ESEM.

Table 4. 4 Chemical compositions of Cu-rich particles in green glazes by ESEM[23]

Samples	O	Na	Mg	Al	Si	P	Cl	K	Ca	Ti	V	Mn	Fe	Cu	Tb	Br	Ba	Pb	n(Cu)/n(V)
HY-38-map 1	34.76	0.44	1.35	5.19	14.90	3.07	0.55	1.65	10.45	-		0.26	1.85	6.15	-	-	-	19.38	-
HY-38-spec 5	21.67	-	-	0.61	1.53	0.67	0.15	-	1.40	-		-	-	70.16	-	-	-	3.82	-
HY-38-map 2	24.02	0.22	-	2.76	5.14	5.00	1.23	0.69	8.62	-	1.33	0.18	1.01	2.04	-	-	-	47.76	1.23
HY-38-map 3	27.51	0.20	0.93	4.42	8.75	3.17	0.70	1.00	6.30	0.17	1.77	-	2.43	3.43	-	-	0.45	38.76	1.55
HY-38-spec 7	18.95	-	-	1.88	3.14	0.68	-	0.32	0.91	-	5.22	-	-	17.04	0.00	-	-	51.86	2.62
HY-38-spec 8	19.62	-	-	1.61	2.84	1.62	-	-	2.18	-	5.44	-	-	14.78	-	-	-	51.91	2.18
HY-38-spec 9	21.71	-	-	2.02	4.31	1.24	-	0.42	5.83	-	5.27	-	0.73	12.15	0.00	-	-	46.31	1.85
HY-136-map 1	26.18	0.19	0.80	3.21	7.67	4.88	1.46	0.87	7.23	-	0.27	-	1.26	2.86	-	-	0.23	42.89	-

[23] The test areas are presented in Figure 4. 35.

Samples	O	Na	Mg	Al	Si	P	Cl	K	Ca	Ti	V	Mn	Fe	Cu	Tb	Br	Ba	Pb	n(Cu)/n(V)
HY-136-spec 28	39.65	-	1.86	8.99	20.81	1.48	0.35	2.16	1.46	-	-	-	0.90	10.31	-	-	-	12.03	-
HY-136-map 2	27.69	-	-	3.66	10.13	4.04	1.19	0.72	5.69	-	0.17	-	0.92	7.59	-	-	-	38.19	-
HY-136-spec 29	25.55	-	-	4.12	4.81	0.16	-	0.51	0.24	-	-	-	-	63.01	-	-	-	1.59	-
HY-136-map 3	31.32	0.29	3.63	4.16	11.39	3.79	1.09	1.01	7.33	0.41	-	-	1.37	4.75	-	-	-	29.48	-
HY-136-spec 33	21.48	-	-	0.65	1.51	0.17	-	-	0.43	-	-	-	-	74.15	-	-	-	1.60	-
HY-166-map 1	22.50	-	0.74	2.48	10.83	-	-	0.62	3.23	-	-	-	0.77	7.36	-	-	-	51.46	-
HY-166-spec 3	20.83	-	-	-	2.94	-	-	-	0.23	-	-	-	-	67.82	-	4.15	-	4.04	-
HY-166-map 2	24.80	-	-	2.66	13.53	-	-	0.65	2.50	-	-	-	0.64	8.23	0.00	-	-	46.99	-
HY-166-spec 13	20.82	-	-	-	4.07	-	-	0.16	0.68	-	-	-	-	59.25	-	2.56	-	12.47	-
HY-166-spec 14	22.52	-	-	1.56	5.00	-	-	0.23	0.81	-	-	-	-	55.40	-	-	-	14.48	-

Samples	O	Na	Mg	Al	Si	P	Cl	K	Ca	Ti	V	Mn	Fe	Cu	Tb	Br	Ba	Pb	n(Cu)/n(V)
HY-166-map 3	24.09	-	-	3.12	12.75	-	-	0.74	2.11	-	-	-	1.00	6.67	0.19	-	-	49.35	-
HY-166-spec 15	26.14	-	-	4.79	7.17	0.24	0.23	0.45	0.38	-	-	-	1.63	46.57	0.03	-	-	12.37	-
HY-166-map 4	29.16	-	2.93	4.21	15.14	-	-	1.75	3.02	-	-	-	0.80	6.47	-	-	-	36.53	-
HY-166-spec 18	33.28	-	8.20	4.78	12.20	-	-	1.10	0.46	-	-	-	-	0.18	-	35.16	-	4.64	-
HY-166-map 5	18.23	-	0.60	1.26	7.20	-	0.73	0.51	4.83	-	-	-	0.41	7.15	-	-	-	59.10	-
HY-166-spec 20	22.93	-	-	1.98	3.70	-	-	0.56	0.64	-	-	-	-	63.90	-	-	-	6.29	-

4.3 Cobalt Blue

The brown and green lead-glazed potteries were produced and used widely in the Han dynasty (202 BCE- 220 CE), but the pottery decorated with cobalt-blue glaze was produced for the first time in the Tang dynasty (618-907 CE) (Li et al., 2017). It is the earliest use of cobalt material in Chinese ceramics. Around the mid to late Tang dynasty, cobalt pigment was applied to high-fired porcelain creatively, which indicates the birth of blue-and-white porcelain. Therefore, the raw material and origin of Tang-dynasty cobalt pigment is not only the key topic of Sancai but also might reveal the birth of Chinese blue-and-white porcelain. As early as 1949, Young (Young, 1949) analysed the blue glaze of Sancai and used 'low' and 'high' to describe the element contents rather than the specific percent. As the very first scholars, Chen et al. (1978) examined two pieces of Sancai blue glaze and demonstrated that the colourant of blue Sancai glaze was cobalt. A comparison of compositions between blue Sancai and Yuan and Ming blue-and-white porcelains was carried out to explore the characteristics of cobalt from the Tang dynasty. All subsequent analyses of cobalt-blue glazes were based on fired wares, such as Wood et al. (2007), Yang et al. (2008) and Li et al. (2017). No scientific analysis of raw blue glaze has ever been published. Among all 66 sherds of this thesis, only one sample, HY-43, was decorated with raw blue glaze. Although only one piece belongs to blue Sancai, this sherd has thirteen glaze spots on it (Figure 4. 36). All blue spots were tested by XRF, and two thin pieces (areas 7, 30 and 32) were cut and analysed by ESEM.



Figure 4. 36 Estimated colours of all raw glazes of HY-43. The colours are predicted based on the compositional results by EDXRF. The small photos in the bottom left present original appearance of HY-43 sherd. Photos were taken by the author.

4.3.1 Cobalt Glass

Smalt or not?

It is difficult to find Co-rich particles/regions in these blue glazes - even more difficult than finding Cu-rich particles in green glazes. The size of cobalt particles is very small and very few particles were found. These identified Co-rich particles can be grouped into two categories according to the elemental distribution. The first category is Co-O-Si-Al-Mg-associated particles (Figure 4. 37 - Figure 4. 40) and some of them also contain K (Figure 4. 41) or Fe (Figure 4. 42). The other category is Co-O-associated particles without any Si and Al (Figure 4. 43). The existence of Co-Si-Al-Mg(-K/Fe)-associated particles is an amazing finding for the blue colourant. This special element distribution matches the characteristics of vitrified material, such as cobalt glass, rather than cobalt ores. Additionally, the texture of these particles shows three characteristics – angular shapes, even surfaces and lamellar structure (Figure 4. 44) which are very similar to cobalt glass (Figure 4. 45 and Figure 4. 46).

The most famous vitrified pigment is smalt which is a potash silicate glassy blue pigment coloured with cobalt which was popular in the 16th and 17th centuries CE in Europe (Mühlethaler and Thissen, 1969). The chemical composition of smalt is complex and can vary considerably since the various ratios of the main components, SiO_2 (65–72%), K_2O (10–21%), and CoO (2–18%) (Daniilia and Minopoulou, 2009). The cobalt in the glass network of smalt exists in the high-spin Co^{2+} state (Altavilla and Ciliberto, 2004). The raw blue glaze is made from a vitrified pigment, but it is not the European smalt. The most important difference between these two blue pigments is that the element distribution of smalt is Co-Si-K but the raw vitrified pigment of Sancai glaze is Co-Si-Al-Mg. Another significant point is the chronology of the smalt. Smalt was widely used in paintings in the 16th and 17th centuries CE in Europe. The earliest known use of smalt in China is probably around the 16th-19th centuries (Xia et al., 2019), and the cases of smalt use in China are in a minority. These two periods are both later than the use of vitrified blue pigment in Sancai by around one thousand years. Despite a few researchers proposing that the earliest use of smalt was a wall painting fragment from Kara Khoto in Central Asia (western Inner Mongolia) in the 11th-13th century CE (Mühlethaler and Thissen, 1969), this date is also much later than the Tang dynasty (618-907 CE). In other words, the vitrified pigment of Sancai glaze is a cobalt glass but not smalt. Traditional inorganic blue pigments in China were mostly lapis lazuli (natural and artificial) and azurite which were totally different from cobalt blue material. Although the glassy cobalt colourant of Sancai blue glaze is not smalt, these two materials share many similar characteristics – vitrified matrix, fine-powdered texture, and mixed environment. Smalt was mixed with other paints, such as lead white. The glassy cobalt colourant was added into the lead glaze to make raw blue glaze. Therefore, research on smalt could provide much insight into the discussion of the cobalt glassy colourant of Sancai based on the similarities, even though they are different materials.

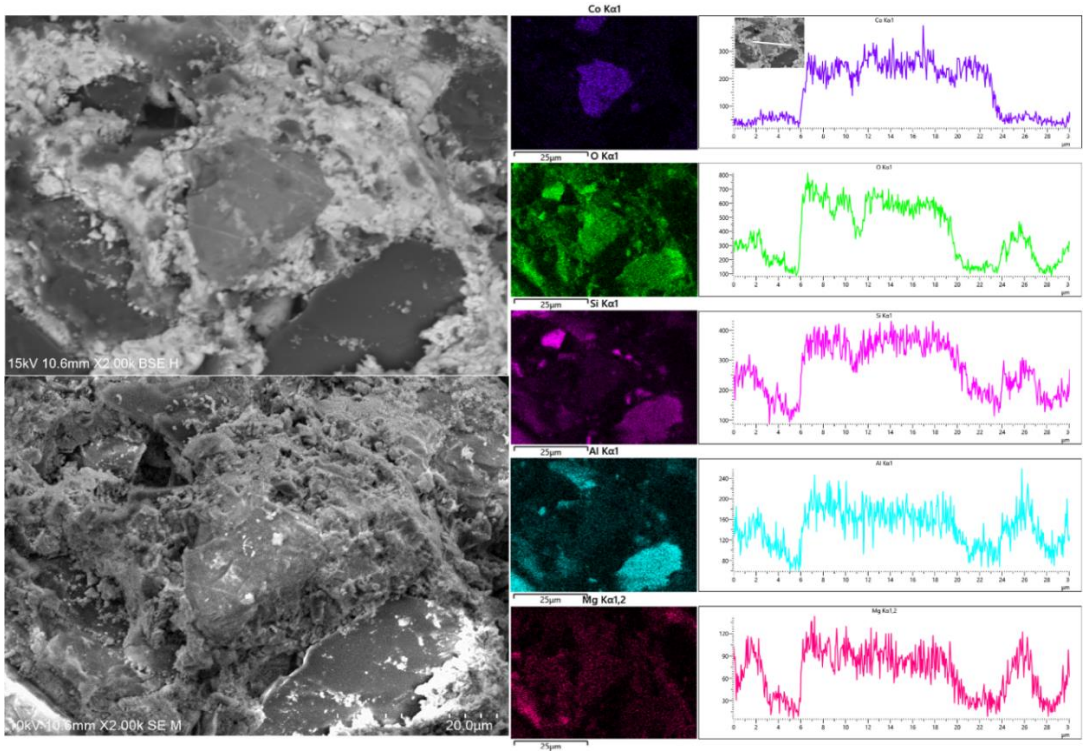


Figure 4. 37 BSE (top left), SE (bottom left), chemical mapping (centre) images and line scan charts (right) of Co-O-Si-Al-Mg associated particles in raw blue glazes of HY-43, obtained from the ESEM.

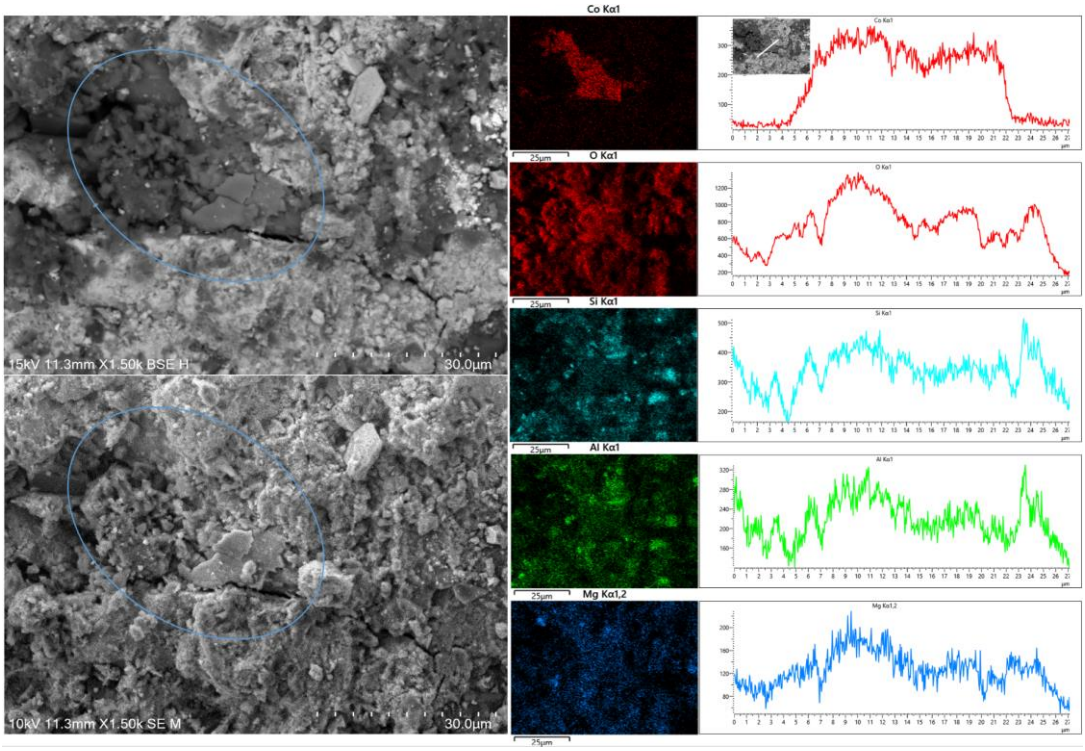


Figure 4. 38 BSE (top left), SE (bottom left), chemical mapping (centre) images and line scan charts (right) of Co-O-Si-Al-Mg associated particles (blue circles) in raw blue glazes of HY-43, obtained from the ESEM.

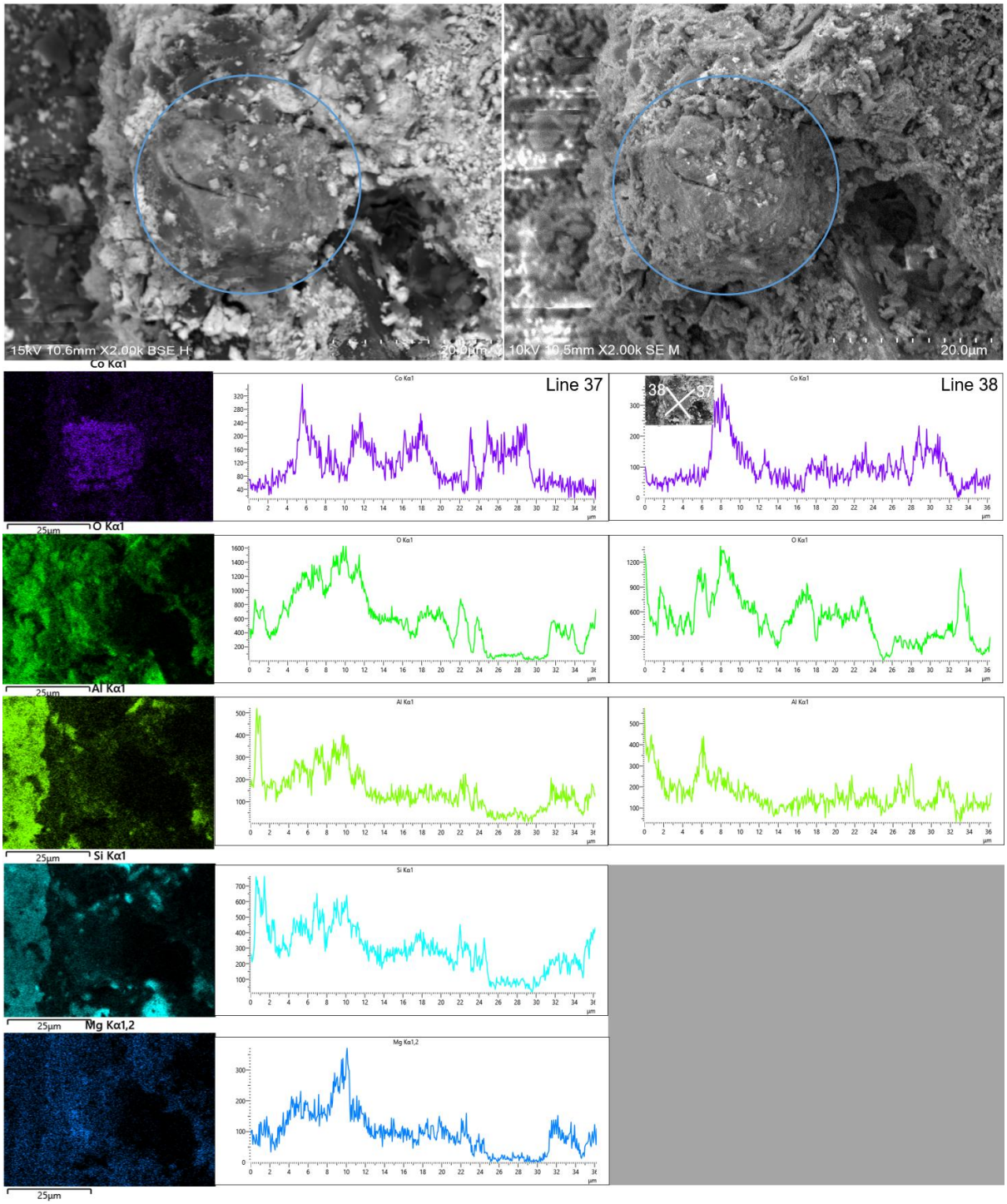


Figure 4. 39 BSE (top left), SE (top right), chemical mapping (bottom left) images and line

scan charts (centre and bottom right) of Co-O-Si-Al-Mg associated particles (blue circles) in raw blue glazes of HY-43, obtained from the ESEM.

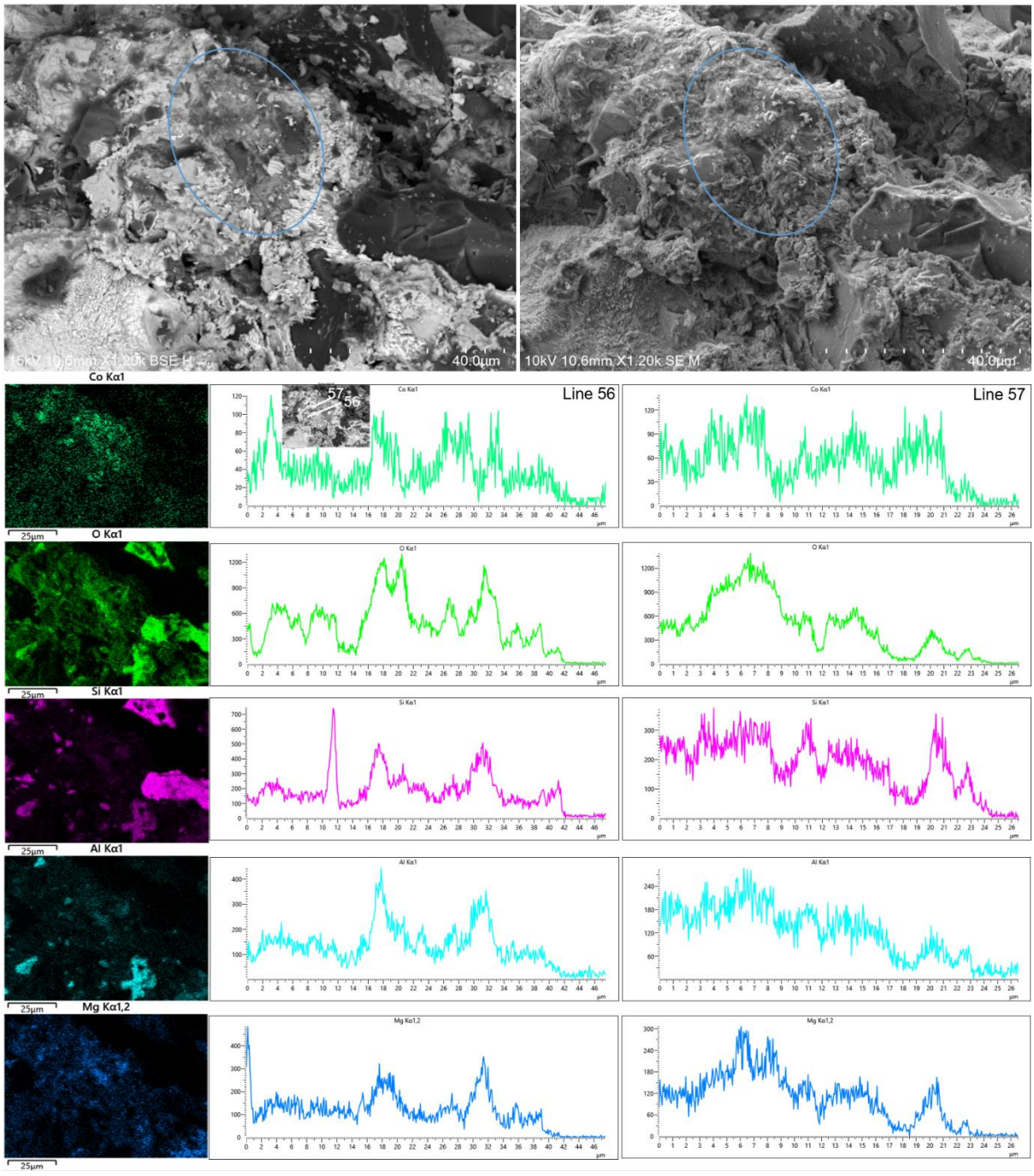


Figure 4. 40 BSE (top left), SE (top right), chemical mapping (bottom left) images and line scan charts (centre and bottom right) of Co-O-Si-Al-Mg associated particles (blue circles) in raw blue glazes of HY-43, obtained from the ESEM.

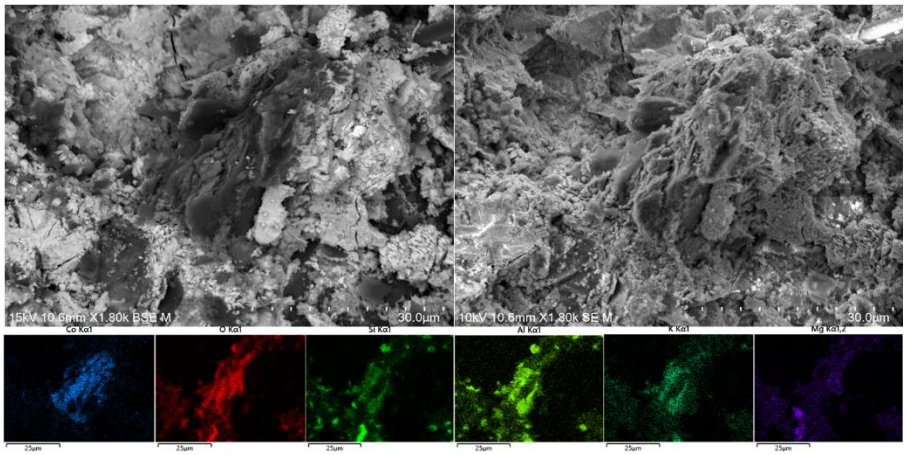


Figure 4. 41 BSE (top left), SE (top right), and chemical mapping (bottom) images the Co-O-Si-Al-K-Mg-associated particle of HY-43, obtained from the ESEM.

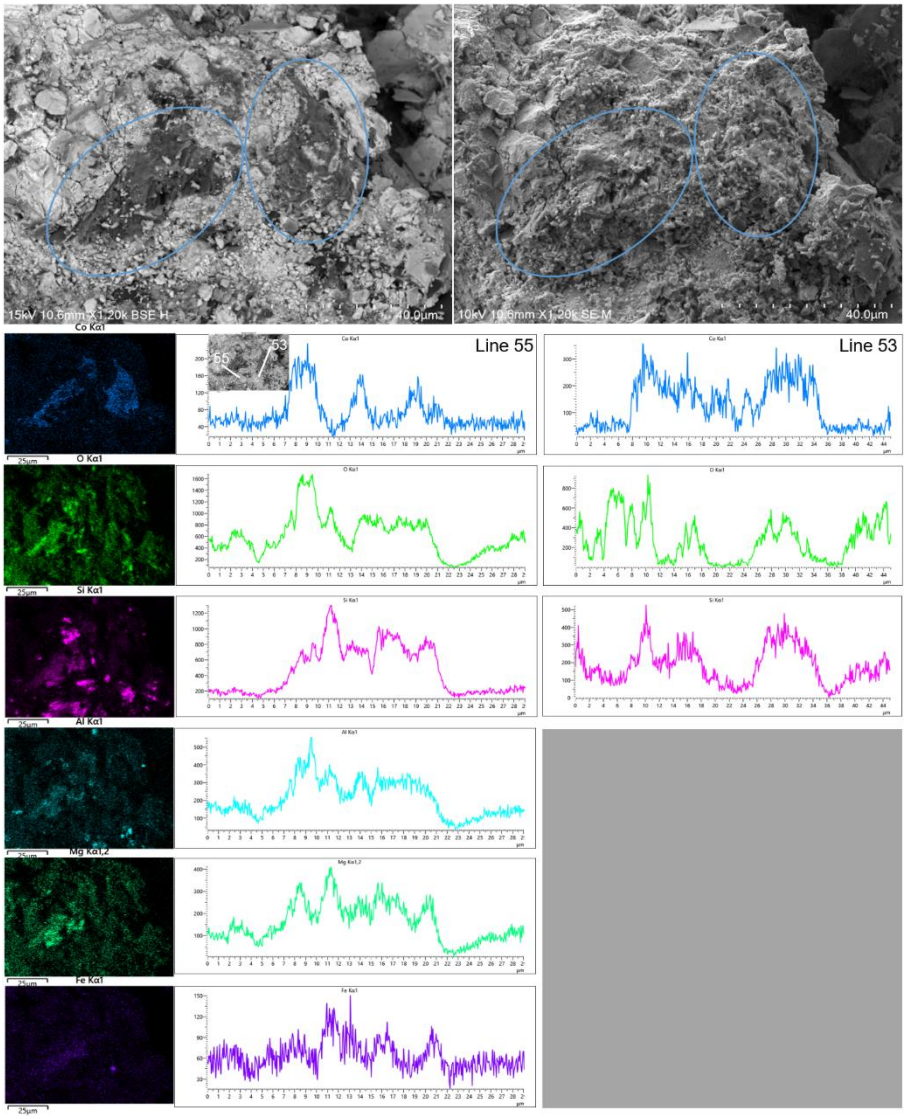


Figure 4. 42 BSE (top left), SE (top right), chemical mapping (bottom left) images and line scan charts (centre and bottom right) of Co-O-Si-Al-Mg-Fe-associated particles (blue circles) in raw blue glazes of HY-43, obtained from the ESEM.

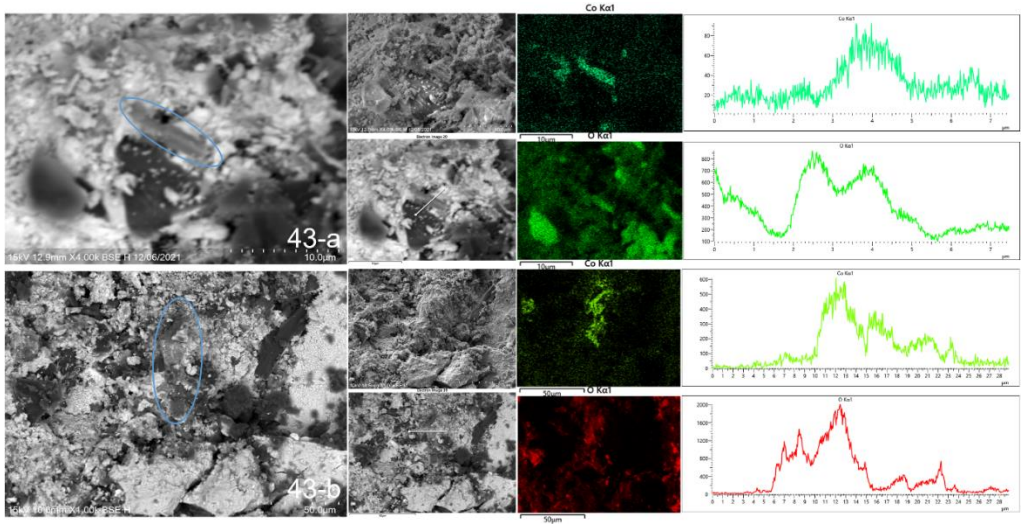


Figure 4. 43 BSE (top left), SE (top right), chemical mapping (bottom left) images and line scan charts (centre and bottom right) of Co-O-associated particles in raw blue glazes of HY-43, obtained from the ESEM.

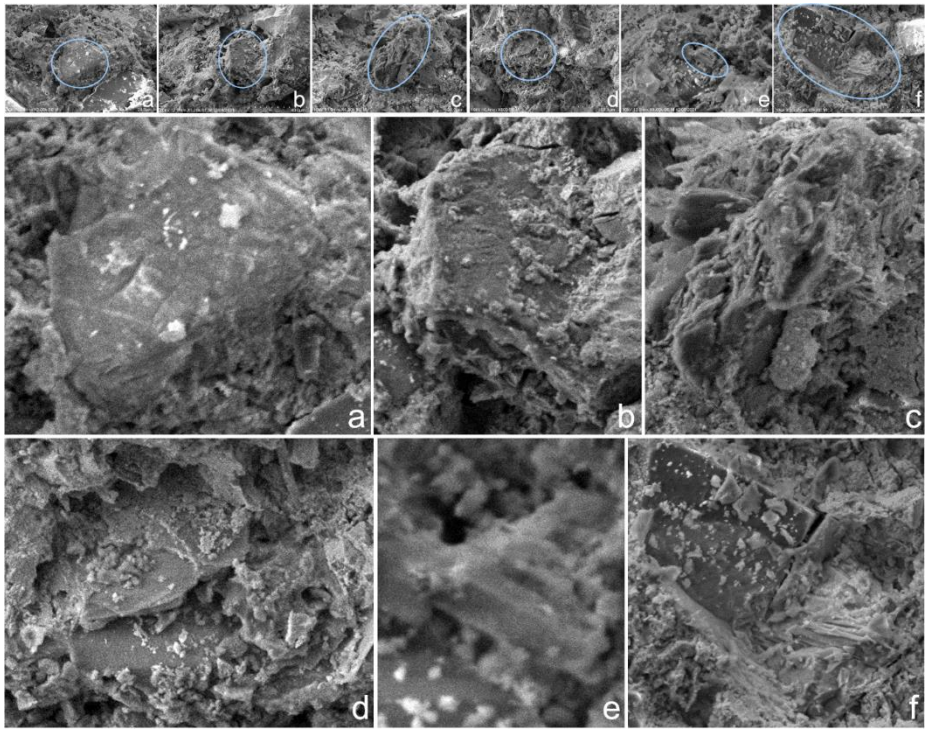


Figure 4. 44 Texture of Co-rich particles in raw blue glazes of HY-43, obtained from the ESEM.

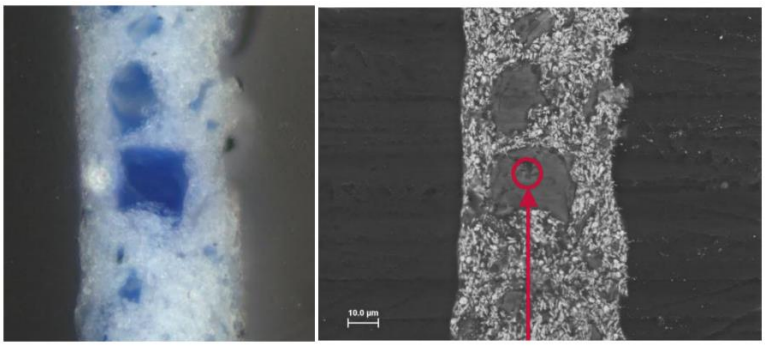


Figure 4. 45 Photo (left) and BSE image (right) of a smalt pigment and lead white in oil in sixteenth- and eighteenth-century paintings, source from (Kugler et al., 2013). The red arrow points to the area of the smalt particle that was analysed and discussed in that paper (Kugler et al., 2013).

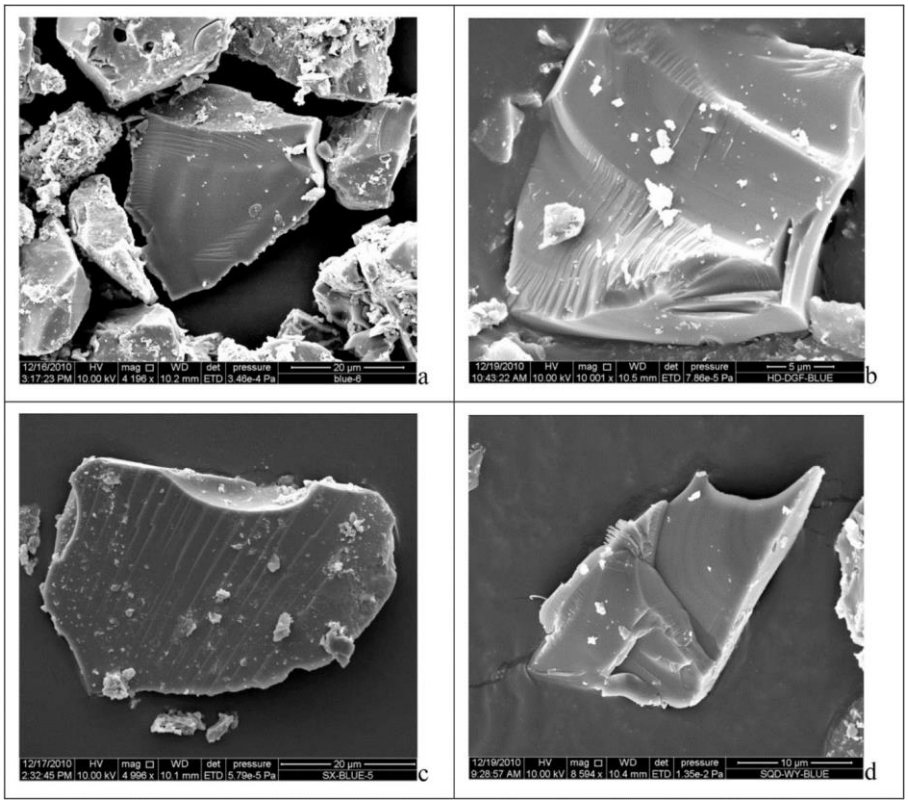


Figure 4. 46 SE images of smalt particles, source from Xia et al. (2019).

Base and flux

The vitrified blue pigment is a pre-treatment cobalt glass material instead of a natural ore. The first research question is about the main ingredients of this pre-treatment material. The base of smalt is silicon. In contrast, the mappings and line scans (Figure 4. 37 - Figure 4. 42) show that the base of the glassy pigment contains Si and Al together. And the atomic weight of Si and Al are very similar (Table 4. 5). Accordingly, the base might be silica-alumina. The flux of smalt is potash and K concentrates on the smalt particles with Si and Co together very distinctly (Figure 4. 47 - Figure 4. 49). K is likely to be lost during weathering (Figure 4. 49). Although K was also found in cobalt-rich particles of raw Sancai glaze, the number of these particles is few. However, the other potential flux element – Mg was found in all Co-Si-Al-associated particles (Figure 4. 37 - Figure 4. 42). Perhaps, K and Mg both acted as the flux of this cobalt glass material. The other possibility is that Mg worked as the flux, and K was brought in the cobalt glass as an impurity.

The following question is whether did the flux contain other elements? B, Na, Mg, P, Ca and Pb all can act as fluxes. But B is too light to be tested by EDXRF and ESEM, and similarly, Na is too light to be detected by EDXRF accurately. Thus, the discussion of flux of this cobalt glass used in Sancai glaze cannot include Na and B in this thesis. Non-negligible P, high Ca and very high Pb were found in all particles (Table 4. 5). However, these three elements are the main ingredients of the glaze. The tiny cobalt-rich particles are surrounded by homogenous fine-powdered Ca-P-Pb materials (light areas in Figure 4. 37 - Figure 4. 43). And some Ca-P-Pb powders are in the surface of cobalt-rich particles. Therefore, the compositional results of cobalt glass might be affected by the Ca-P-Pb material. It is uncertain that whether the cobalt glass utilise Ca, P or Pb flux(es) according to current analysis.

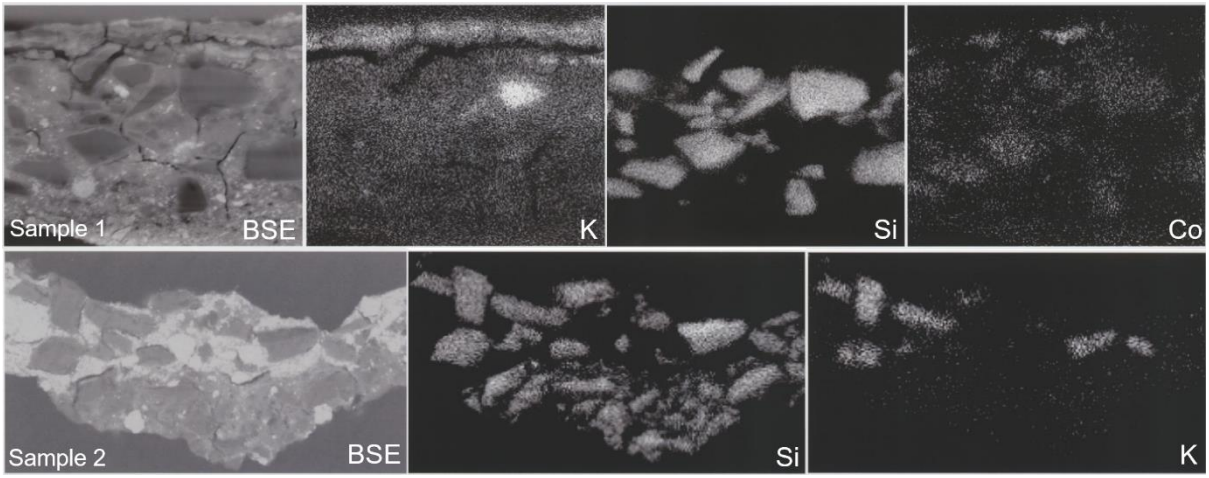


Figure 4. 47 BSE and chemical mapping images of smalt in oil paint, source from Spring et al. (2005).

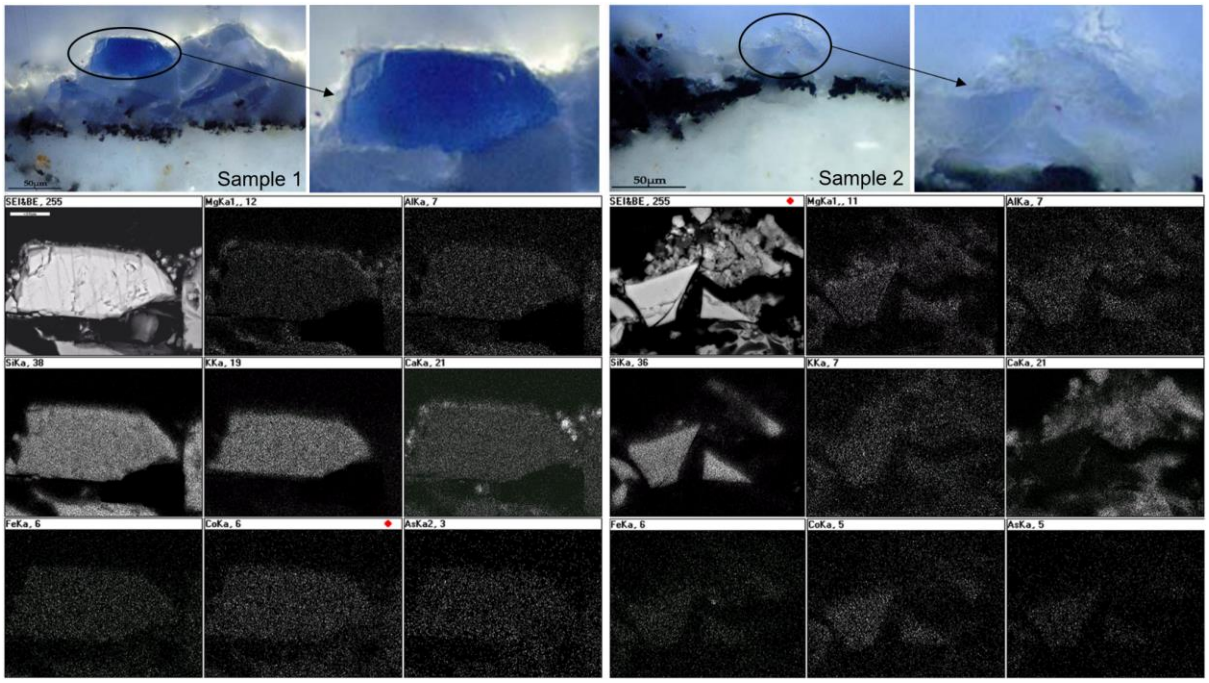


Figure 4. 48 Photos, SE, BSE, and mapping images of smalt in wall paintings in Cyprus, source from Daniilia and Minopoulou (2009).

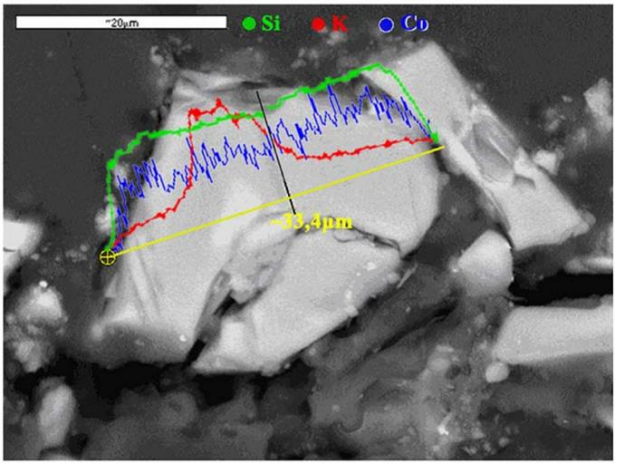


Figure 4. 49 BSE image of a weathered smalt grain with line scan of Si, K and Co, source from Daniilia and Minopoulou (2009).

Possible ore type

Regarding the origin of cobalt ore used in blue and white porcelain, Islamic glazed pottery and smalt, the existence and contents of Co, Mn, Fe, Cu, As, Ni, Zn and S are important to reveal the ore type. The examinations of XRF and ESEM confirmed that the cobalt colourant of the blue glaze contains Fe and Cu. However, Ni, Zn and S were not found. Although some data for Ni (0.01%) and Zn (0.00%) were obtained by XRF, they are too low to be confirmed and are close to the detection limit. Mn and As are special. The content of Mn (0.02-0.03%) is a little higher than the detection limit of XRF (0.01%). The cobalt ore might contain low Mn. As was not calibrated by XRF since the standard, corning glass, does not contain this element. However, two particles showing Mn-Co and As-Co associations were found by ESEM. Based on these findings, it can be inferred that the cobalt ore of blue colourant did not contain Ni, Zn and S, but it might have low Mn. The existence of As needs further discussion. And the relationships between Mn, Fe, Cu and Co also was explored to reveal the possible cobalt ore(s).

Mn

The mean values of MnO in the blue glaze obtained by XRF is only 0.02%, which is equal to the clear glaze and lower than the brown glaze (0.04%) and green glaze (0.03%). And the compositional results of the cobalt particles obtained by ESEM did not include Mn (data labelled with 'spec' in Table 4. 5), but minor Mn was found in some tested areas where the cobalt particles are located (data labelled with 'map' in Table 4. 5). It indicates that the cobalt particle might not contribute to the content of Mn, but the surrounding material is the source of the minor Mn in tested areas. In other words, Mn is certainly an impurity of stock glaze, which explains the reason for the existence of nonnegligible MnO in all glazes, especially in the clear glaze. The key question is whether the stock glaze is the only source of the Mn of the blue glaze. Figure 4. 50 shows the same trend of Mn and Co of a cobalt particle very distinctly. And there are peaks of Mn and Co in the location of cobalt particles. This finding partially contradicts what the compositional ESEM data shows but concerning the size of cobalt particles and weathering of this glassy pigment, this ‘contradiction’ possibly is reasonable. The most of Mn of blue glaze is from stock glaze as an impurity instead of cobalt pigment. simultaneously, this glassy cobalt pigment might contain trace Mn, just it is too low to be tested by most mapping and line scans. Although it cannot be confirmed now that Mn is from the cobalt ore or other components of this pigment, to be sure, the cobalt ore is not a high-manganese type.

In studies of the cobalt pigment used in Chinese ceramics, particularly blue-and-white porcelain, the content of Mn is one of the most critical factors in determining the source of cobalt ore. Many comparative studies on Yuan and Ming blue-and-white porcelains established the central idea of the use of cobalt ore in the 13^{th}-17^{th} century CE. In Yuan and Early Ming dynasties, the low-Mn imported cobalt pigment from the Middle East dominated the production

of blue-and-white porcelain. In the Mid Ming, high-Mn Chinese cobalt became the main trend. In the Late Ming, imported and local materials both were used to decorate the wares (Young, 1956; Zhang et al., 1986; Wen et al., 2007; Cowell and Zhang, 2001; Wen, 2012). Concerning the early blue-and-white porcelains, we reviewed and reanalysed data for Tang and Song blue-and-white porcelains and found that Song-dynasty potters chose domestic high-Mn cobalt ore, however, Tang potters employed imported low-Mn cobalt pigment (Zhang and Pollard, 2022).

Although the published scientific analyses of Sancai show that the manganese of the blue glaze is low (Chen et al., 1978; Zhang et al., 1986; Cheng et al., 2005; Lu et al., 2016; Li et al., 2017), and the cobalt materials used in Tang blue-and-white also have this characteristic (Zhang et al., 1984; Zhang et al., 1986; Zhang et al., 1989; Zhang and Zhang, 2009; Lu et al., 2016; Li et al., 2017,), it cannot be completely concluded that Tang blue-and-white and Sancai shared the same low-Mn cobalt ore. This is because the cobalt pigment used in blue-and-white porcelain was close to cobalt ore powder and it was not fused with calcium glaze after firing. However, the cobalt material of Sancai became a homogeneous glassy glaze after mixing with lead glaze and firing around 800-900℃. The published scientific analysis of fired blue glaze reveals the characteristics of this mixture instead of solo cobalt material. It is not possible to estimate the source of indicative elements. The difficulty can be minimised by the examination of raw blue glaze, especially of cobalt particles. Additionally, considering the confusion of different-colour glazes after firing, the analysis of raw blue glaze also can avoid the possible effect from overlapping glazes. Therefore, the use of low-/no-Mn cobalt colourant on Sancai based on the results of raw glaze can reveal the characteristic of Tang-dynasty cobalt material. Also, it can lay a solid foundation to explore the specific cobalt ore and its origin. Besides, this finding confirms the consistency of cobalt material in Tang blue-and-white porcelain and Sancai.

Subsequently, we re-analysed and compared data for the raw blue glaze of Sancai and blue-and-white porcelains from the Tang to Qing dynasties to explore the differences between Tang-dynasty cobalt and others (Chen et al., 1978; Zhang et al., 1984; Zhang et al., 1986; Zhang et al., 1989; Chen et al., 1995; Cheng et al., 2005; Lu et al., 2016; Li et al., 2017; Spataro et al., 2019). Figure 4. 51 shows low MnO/CoO and high Fe_2O_3/MnO ratios of raw blue glaze, which is different from local high-Mn cobalt pigment used in Song, Mid-Ming and some Yuan blue-and-white porcelains but similar to imported cobalt material in Yuan and Early Ming dynasties. Blue glaze and Tang blue-and-white share the same MnO/CoO. But compared with Tang blue-and-white, the Fe_2O_3/MnO ratios of blue glaze are higher, and its distribution is broader. The levels of Fe_2O_3 in them are almost the same (Figure 4. 51c) so higher Fe_2O_3/MnO and broader distribution caused by lower Mn of blue glaze (Figure 4. 51d). The lower Mn of blue glaze might result from lower concentration of cobalt material instead of different types of ores. The lower content of Co proves that (Figure 4. 51e). Significantly, this slight difference cannot change the group of Tang cobalt material, low-Mn type. Wen (Wen et al., 2007; Wen, 2012) compared many Yuan and Ming blue-and-white porcelains and Islamic Minai ceramics scientifically. Also, they reviewed historical accounts about Islamic cobalt ores. It was found that Kashan (Qamsar) in Iran might have been one of the main sources of cobalt used on Chinese blue-and-white ceramics, especially during the Yuan (1271- 1368 CE), and Early Ming (1368-1424 CE). Did this region offer cobalt pigment to Tang China? Mn is one of the signature elements and the conclusion needs more evidence from others.

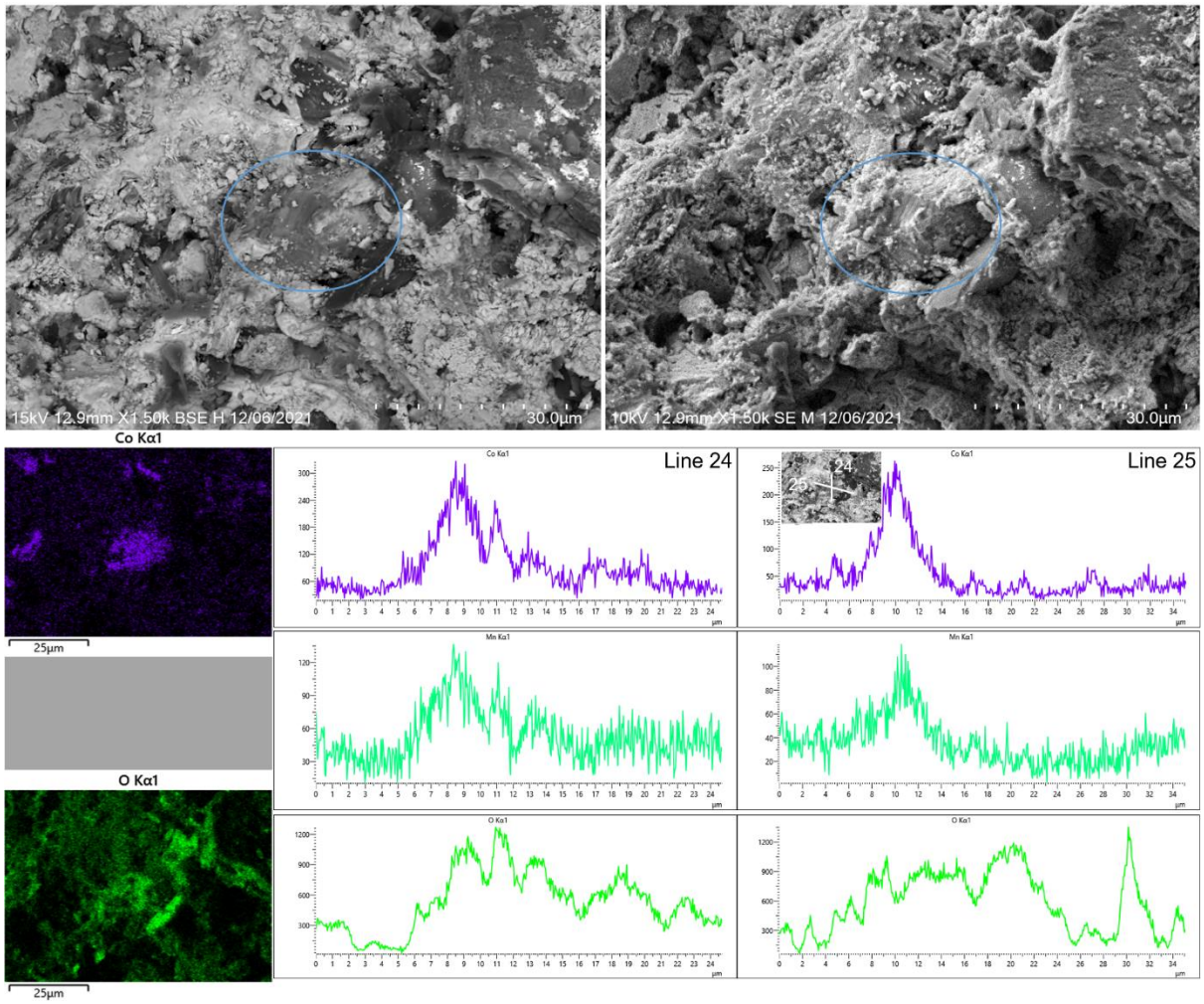


Figure 4. 50 BSE (top left), SE (top right), chemical mapping (bottom left) images and line scan charts (centre and bottom right) of Co-O-Mn-associated particles (blue circles) in raw blue glazes of HY-43, obtained from the ESEM.

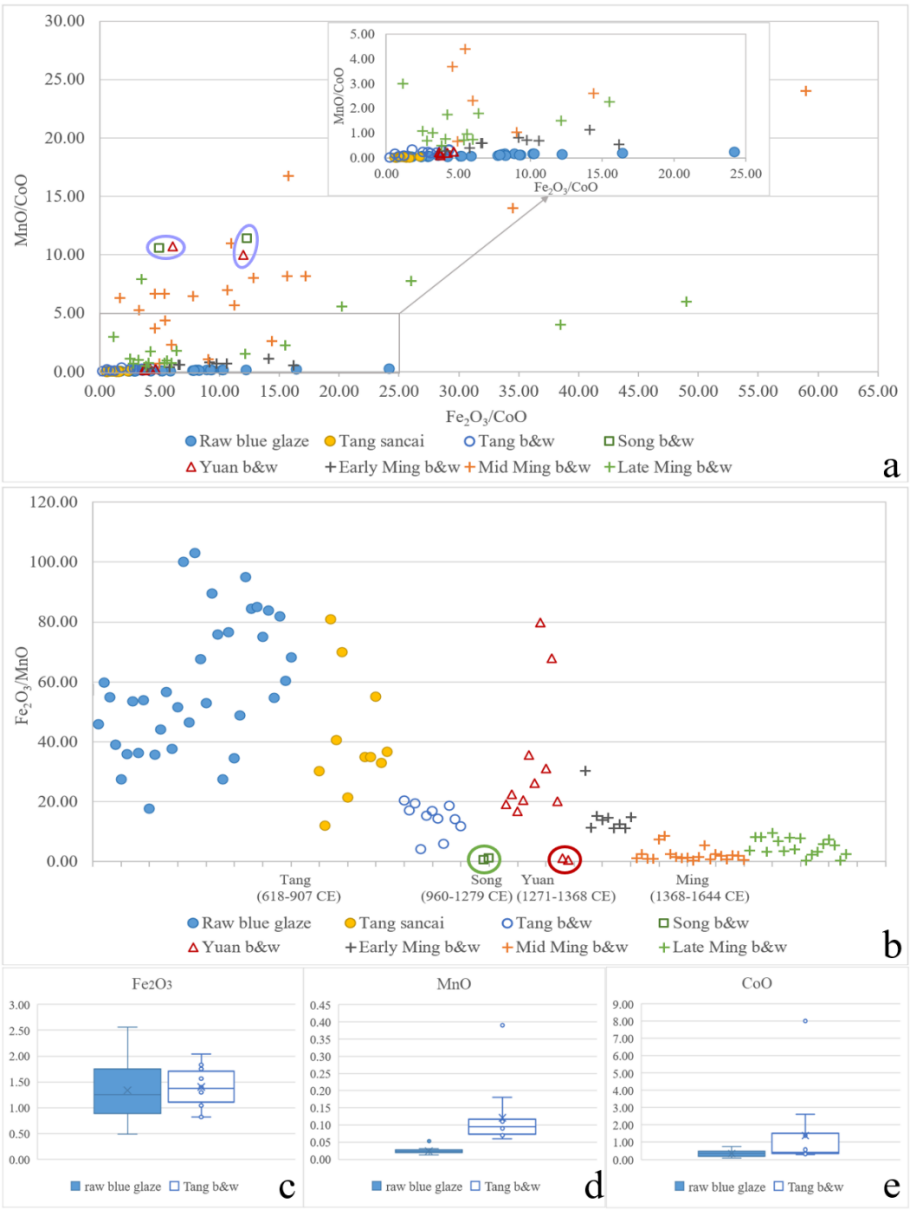


Figure 4. 51 Scatter diagrams of (a) MnO/CoO and (b) Fe_2O_3/MnO ratios, and (c) Fe_2O_3, (d) MnO and (e) CoO contents of blue glaze of Sancai and cobalt pigments used in blue-and-white porcelains from Tang to Ming dynasties. The purple, green and red circles present Song and two Yuan blue-and-white porcelains found in Zhejiang, which were made from local cobalt ore rather than imported material.

Fe

Iron is also one of the signature elements that are crucial to determine the source of cobalt. The Fe_2O_3 of raw blue glaze is higher than clear and green glazes distinctly (Figure 4. 52c). And the association of Fe and Co of cobalt colourant particles were found by line scan and mapping (Figure 4. 42). Although not every single cobalt particle shows this association, distinctly, Fe content of cobalt colourant particles is higher than the whole tested areas where the particles are in Figure 4.53, this evidence confirms the existence of iron in cobalt colourant. As Figure 4. 51b shown, Tang-dynasty cobalt materials, no matter of blue glaze or blue-and-white, show high Fe_2O_3/MnO ratios. This characteristic also was shared by the imported cobalt pigment used in Yuan and Early Ming dynasties. And this pigment was described as a 'high-Fe-low-Mn' type. Regarding 'high-Fe', there are three key questions that need more discussion.

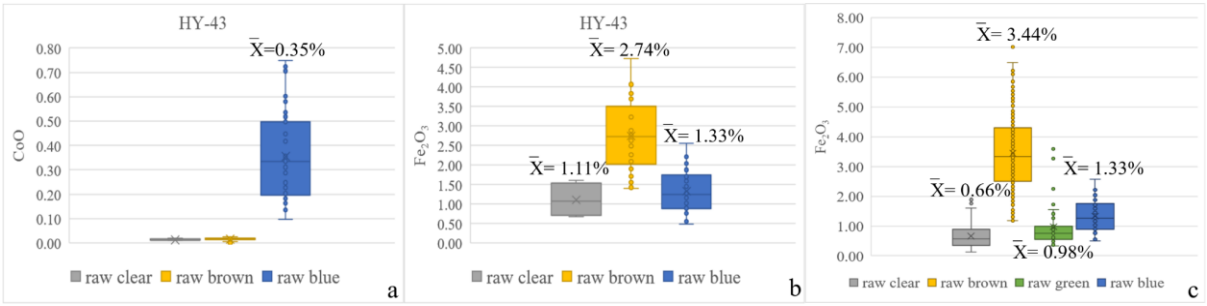


Figure 4. 52 Box plots of (a) CoO and (b) Fe_2O_3 in raw glazes of HY-43 and (c) Fe_2O_3 in different-colour raw glazes of all samples

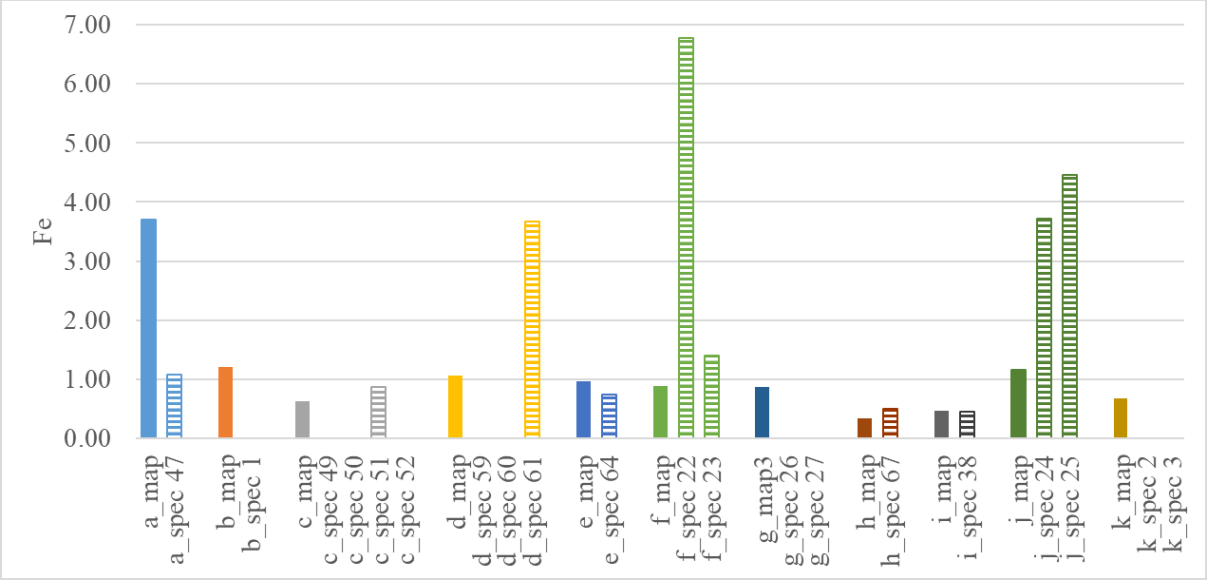


Figure 4. 53 Bar chart of Fe content (atomic weight) of Co-rich particles (cross-striped bars) and in the surrounded background (clear-coloured bars). The compositional data was obtained from ESEM.

The first question is whether all Fe contents were contributed by the cobalt colourant. The brief answer is no. Figure 4. 9 - Figure 4. 11, Figure 4. 14, Figure 4. 16 and Figure 4. 18 show that raw brown, green, blue, and clear glazes all contain Fe-Mg-Si-Al-O-associated particles. It indicates that stock glaze, the shared ingredients of all glazes, contain some Fe. This ingredient contributed to the level of raw blue glaze. The compositional results also prove that (Figure 4. 52). The HY-43 sherd was decorated with 14 brown, 13 blue and 4 clear glaze spots which all were examined by XRF. And the mean values of Fe_2O_3 of blue and clear glazes are 1.33% and 1.11% respectively. Averagely, Fe_2O_3 of all clear glazes on all sherds are 0.66%. These results suggest that prominent Fe_2O_3 in the clear glaze cannot be neglected whether 1.11% of HY-43 or 0.66% of all samples. Certainly, the clear glaze did not contain any colourant. In other words, the un-neglectable Fe_2O_3 might be added into the clear glaze by the stock glaze

as an impurity instead of by potters deliberately. Therefore, it is very likely that the blue glaze also contains Fe_2O_3 at a similar level to the clear glaze.

The second question is how to estimate the contribution of Fe_2O_3 by cobalt colourant? First of all, estimating the possible level of Fe_2O_3 in the stock glaze is necessary. Although it is uncertain whether clear glaze is equal to stock glaze or not, it can be certain that the Fe_2O_3 in the clear glaze is from glaze material instead of any colourant. The Fe_2O_3 in the blue glaze can be regarded as two parts, glaze material and cobalt colourant. Considering only HY-43 contains blue glaze, using the mean Fe_2O_3 of the clear glaze of HY-43 is more reasonable than using the mean Fe_2O_3 of all clear glazes of all sherds. Accordingly, two simplified methods can estimate the iron content of the cobalt colourant. (1) Subtract the mean Fe_2O_3 (1.11%) of the clear glaze from the mean Fe_2O_3 (1.33%) of the blue glaze. The estimated iron from the blue colourant is 0.22% which is lower than CoO (0.35%). (2) Subtract the mean Fe_2O_3 (1.11%) of the clear glaze from every data for Fe_2O_3 of blue glaze[24]. Next, calculate a new mean value of Fe_2O_3 based on all positive results. The Fe_2O_3/MnO ratios of cobalt colourant based on estimated Fe_2O_3 (Figure 4. 54a) are more similar to the imported Yuan cobalt pigment than before (Figure 4. 51b). The result is 0.33%.

The third question is whether Tang-dynasty cobalt material belongs to the ‘high-Fe’ type. Based on those two methods of estimation of Fe_2O_3 in cobalt colourant, the ratio of Fe_2O_3 to CoO of cobalt colourant is around 2:3 and 1:1 respectively. They both suggest that Fe_2O_3 of cobalt colourant is not higher than CoO. Generally, the imported cobalt pigment used in Yuan and Early Ming was described as a ‘high-Fe’ type. However, describing the Tang cobalt

[24] HY-43 contain 13 blue glaze spots and total 35 areas were tested compositionally by XRF. Totally, Fe_2O_3 of 22 areas is higher than 1.11% so 22 positive results were obtained.

material as ‘high-Fe’ is not appropriate. The new Fe_2O_3/CoO also proves that (Figure 4. 54b). Tang cobalt colourant and pigment do not have distinct differences with ‘low-Fe’ cobalt pigment used in Mid-Ming blue-and-white porcelain. Besides that, the atomic weight of Co of cobalt colourant particles is much higher than Fe (Figure 4. 54c). Therefore, the blue glaze of Sancai can be defined as ‘high-Fe low-Mn’ and ‘high Fe_2O_3/MnO’ type. But the Tang cobalt colourant/pigment belongs to a ‘high Fe_2O_3/MnO’ and ‘low-Fe trace-Mn’ type.

Additionally, Figure 4. 54b shows that Fe_2O_3/CoO of fired Tang Sancai from published articles (Chen et al., 1978, Zhang et al., 1986, Cheng et al., 2005, Li et al., 2017) is a little lower than estimated Fe_2O_3/CoO of cobalt colourant in raw blue glaze. Besides the instrument errors, the compositional fluctuation might be another reason. The comparison of Fe_2O_3 between raw glazes and fired glazes reveals that Fe_2O_3 content reduced a little after glaze firing (Figure 4. 55). This reduction is too small to change ideas about cobalt colourant.

Among all Co-Fe-rich particles, one Co-Ti-Fe-O-associated particle is very distinctive (Figure 4. 56). The concentration of Ti is obvious, and the content of Ti is much higher than Fe and Co by atomic weight (f_spec 22 and f_spec 23 in Table 4. 5). Ti reaches to 23.65% and 15.52%. However, Fe is only 6.78% and 1.4% which is a little higher than Co (5.13% and 0.94%). Considering Ti is not a commonly associated element of cobalt ore, the most possibility is that Ti might be from other ingredients of the cobalt glassy pigment, such as kaolinite or felspar etc. The different ingredients of glassy material must be fired or heated together, and Ti might combine with Co during this process.

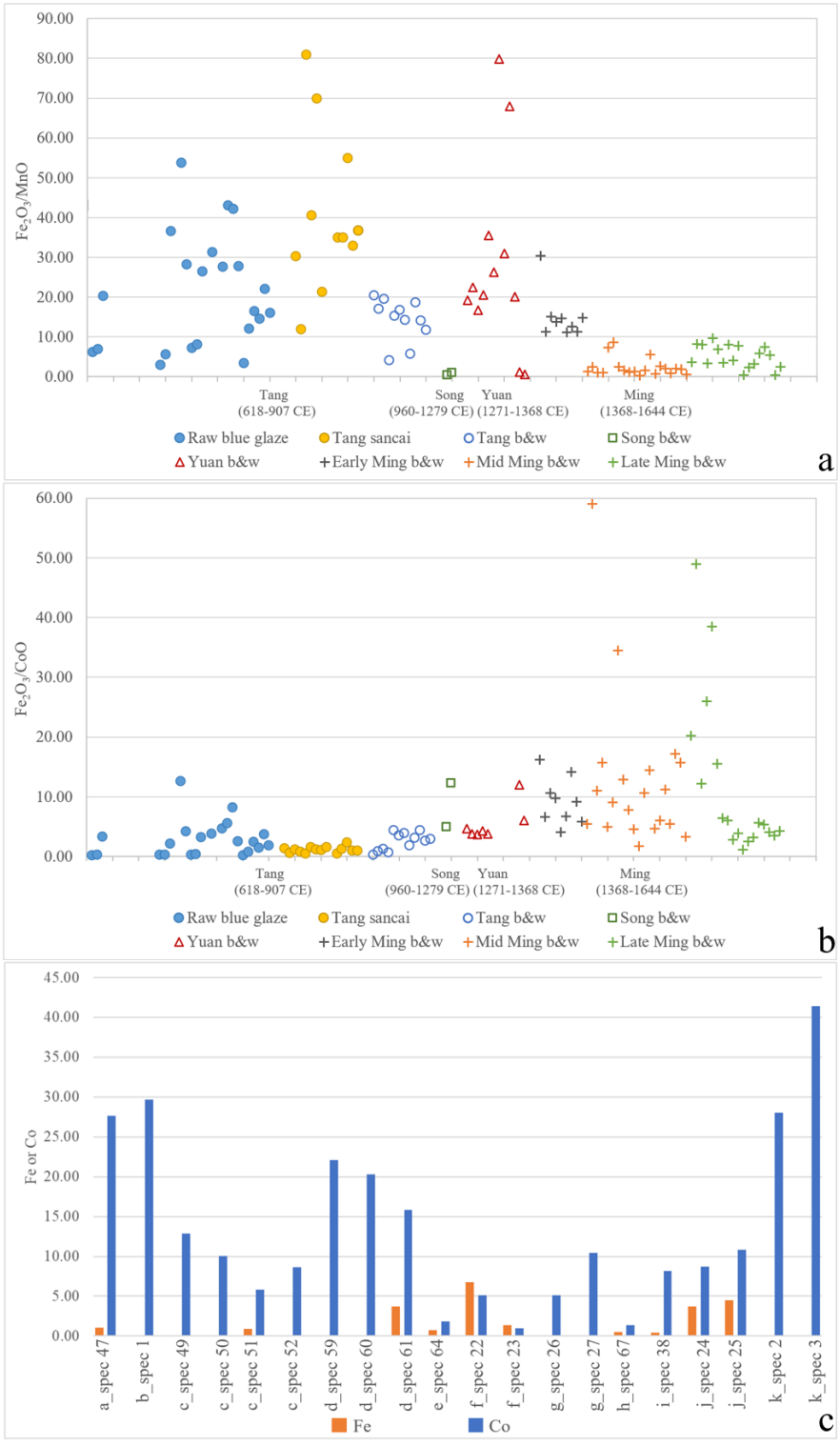


Figure 4. 54 Scatter diagrams of (a) Fe_2O_3/MnO values, and of (b) Fe_2O_3/CoO values of cobalt pigment of raw blue glaze and blue pigments of blue-and-white porcelains. Bar chart of (c) Fe and Co (atomic weight) in cobalt particles.

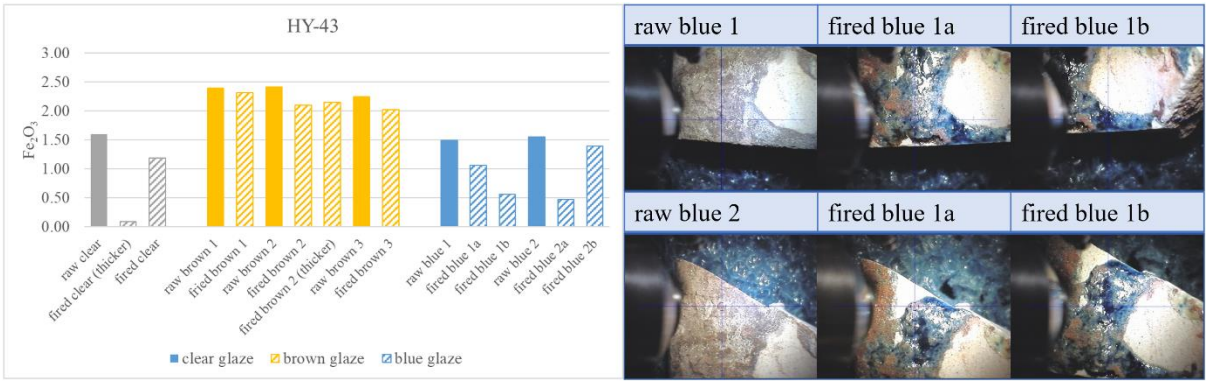


Figure 4. 55 Bar chart of Fe_2O_3 content of raw and fired glazes of the same sherd. The examination was run in the locations of HY-43 before and after glaze firing, and data obtained from XRF analysis

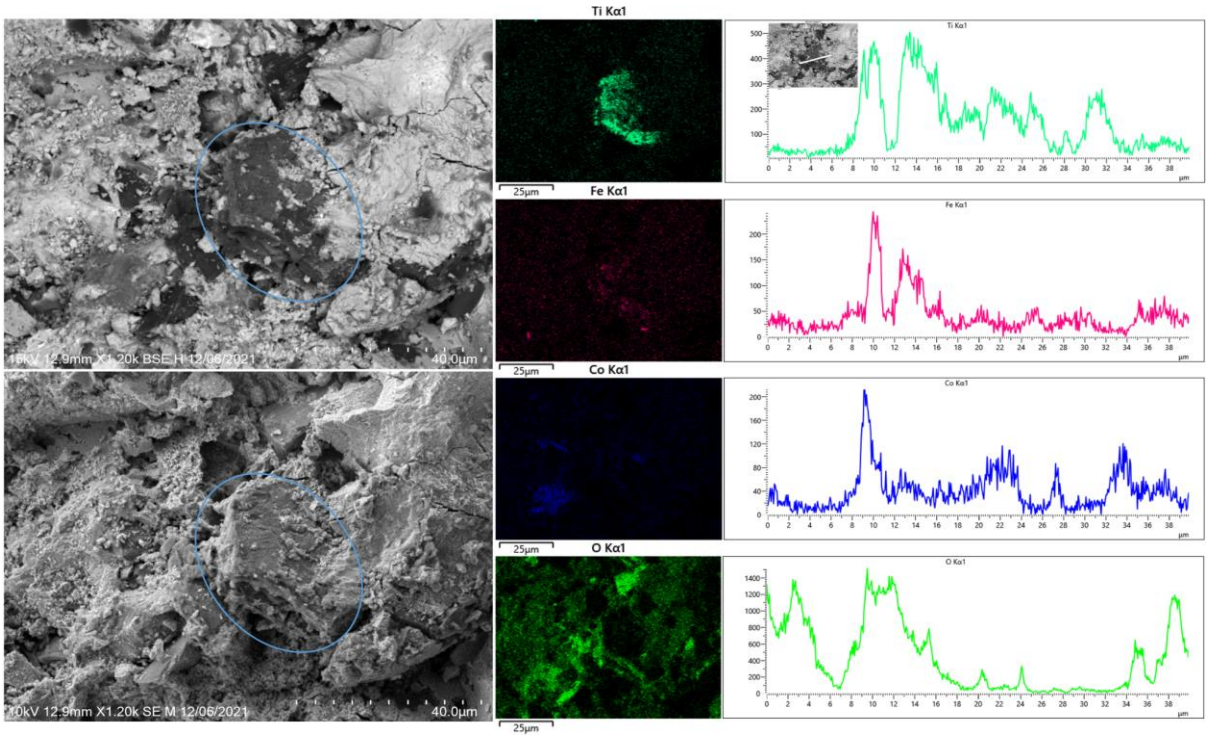


Figure 4. 56 BSE, SE, mapping images and line scan charts of the Co-Ti-Fe-O-associated particle (blue circles) in the raw blue glaze of HY-43, obtained from the ESEM.

As

Another signature element associated with Co in cobalt colourant particles is As. Matin (Matin, 2016; Matin and Pollard, 2017) collected cobalt ores in Kāshān in Iran to process cobalt pigments by physical and chemical methods. They combined chemical compositions, mineral crystals, and historical accounts of cobalt ores and pigments to identify the type of cobalt ores. Cobaltite (CoAsS) and erythrite ($Co_3(AsO_4)_2 \cdot 8H_2O$) were confirmed. Although only one cobalt colourant particle presents the concentration of As by mapping (Figure 4. 57), prominent As was found in many cobalt particles (Figure 4. 58a) and As of particles was higher than of tested areas where particles are located in. Also, As and Co of cobalt particles show a positive correlation (Figure 4. 58b). Therefore, it is most likely that cobalt ore of the blue colourant contains As. But since corning glass standard does not include As, XRF analysis did not quantify As. Table 4. 5 (k_spec 2 and k_spec 3) shows As of the As-Co-associated particle is 6.46% and 4.22%, and the Co of this particle is 28.05% and 41.37%. And only one negligible data (0.58%) for the same particle was obtained by ESEM. These findings suggest that the cobalt ore of the colourant might belong to a ‘low-As’ type and is very similar to erythrite ($Co_3(AsO_4)_2 \cdot 8H_2O$).

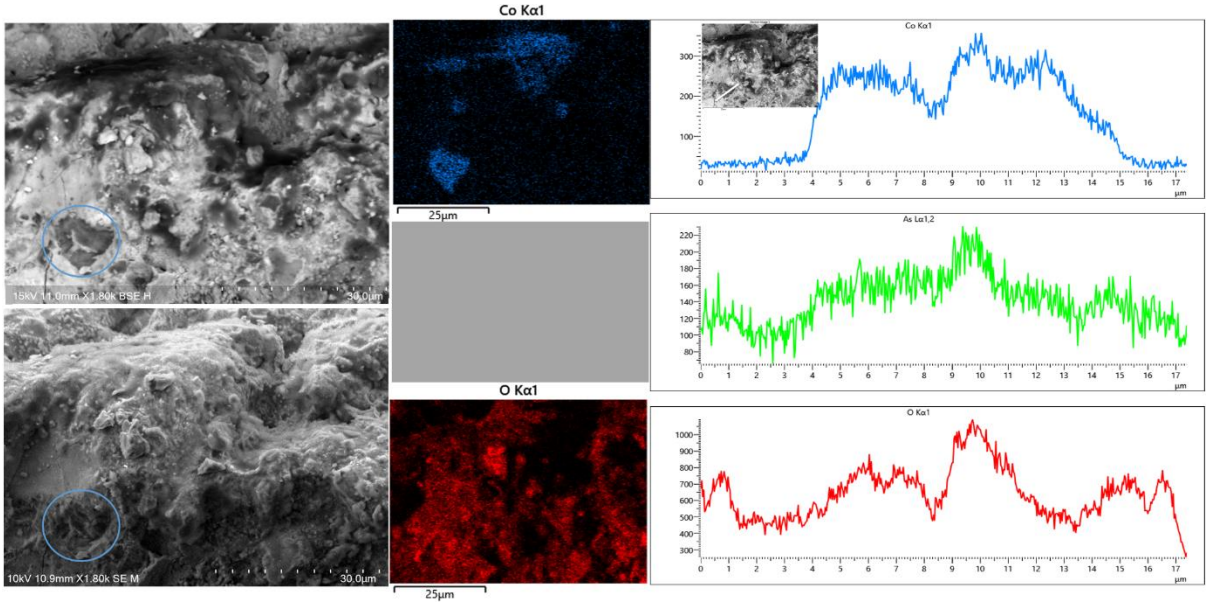


Figure 4. 57 BSE (top left), SE (bottom left), chemical mapping (centre) images and line charts of the Co-As-O-associated particle in the blue glaze of HY-43, obtained from the ESEM.

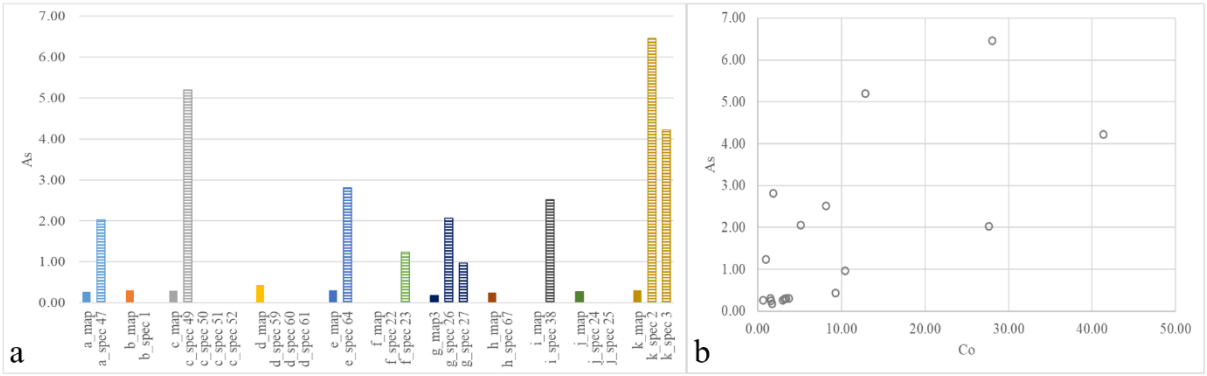


Figure 4. 58 Bar chart of (a) As levels in Co-rich particles and surrounded background. Scatter diagram of (b) As and Co of cobalt particles. The compositional data was obtained from ESEM.

Cu

The discussion about Mn, Fe and As reveals that the cobalt ore of blue colourant belongs to a low-Fe, low-As, trace-Mn and high-Fe_2O_3/MnO ore, might be erythrite ($Co_3(AsO_4)_2 \cdot 8H_2O$) which is one of the confirmed cobalt ores in Kāshān. Based on these findings, it is likely that

Tang potters could obtain imported pigment from Kāshān region. However, the finding about Cu contradicts this viewpoint.

According to a detailed review of historical accounts and rigorous analysis of mine-archaeological examinations, Matin and Pollard (2015) pointed out that an obvious conclusion is that any cobalt pigment containing significant traces of Zn, Cu or Ni did not originate in Kāshān unless pigment processing such as grinding in a brass mortar might have subsequently introduced such traces. However, Cu content in the raw blue glaze is around 0.1% which is much higher than CuO (0.02%) of clear and brown glazes (Figure 4. 59). It not only indicates that the stock glaze did not contain prominent CuO but also suggests that such high CuO of blue glaze is impossible to be introduced by the processing method. In other words, CuO is from the glassy cobalt colourant. The higher Cu of cobalt particles than of tested areas where the particles are in (Figure 4. 60a) also supports this idea. Plus, Figure 4. 60b shows a positive correlation between Cu and Co of cobalt particles. It is confirmable that the glassy cobalt colourant of blue glaze contains low copper. And the ratio of Co to Cu is 3.5:1.

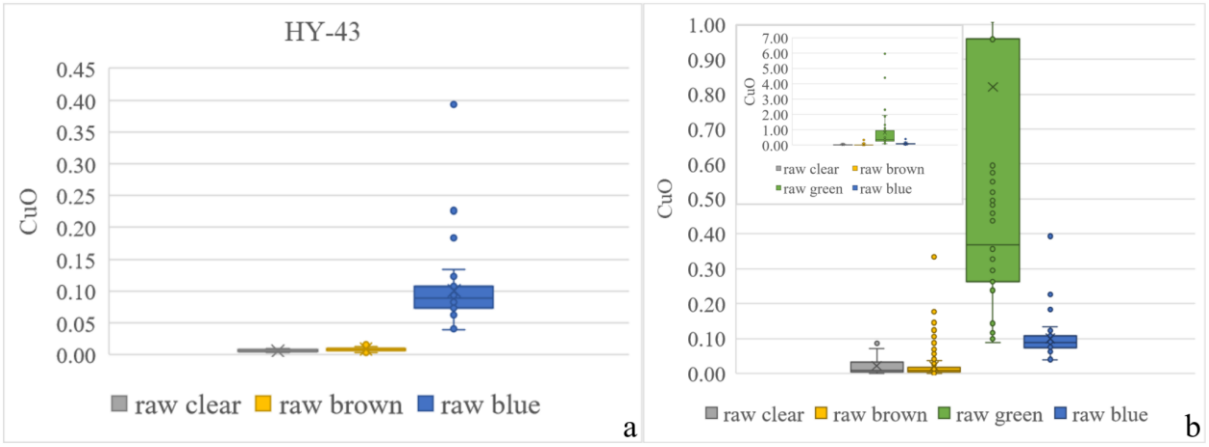


Figure 4. 59 Box plots of (a) CuO in raw glazes of HY-43 and of (b) all raw glazes of all samples.

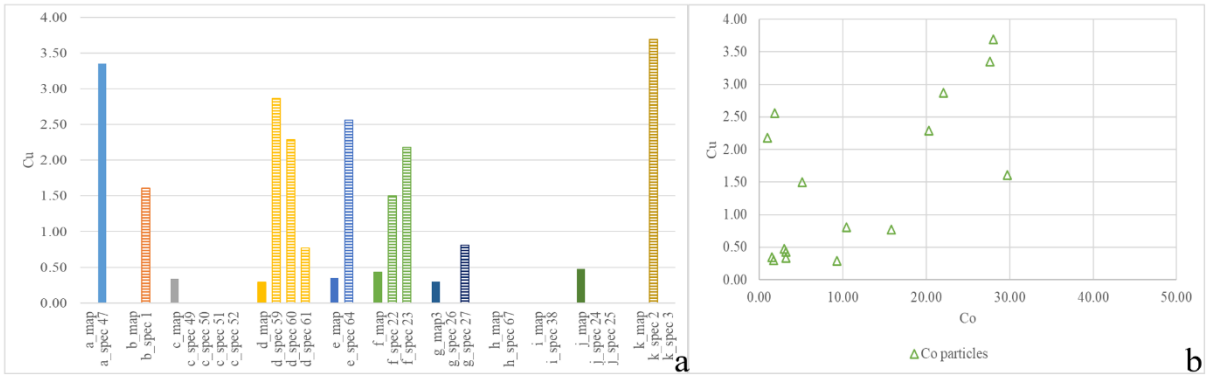


Figure 4. 60 Bar chart of (a) Cu of Co-rich particles and of surrounding areas where the particles are located in. Scatter diagram of (b) Cu and Co of cobalt particles. The compositional data was obtained from ESEM.

Conversely, Yuan-dynasty imported cobalt pigment that did not contain copper. And this remarkable difference between Tang and Yuan materials was recognised and discussed by researchers. Chen et al. (1995), Zhang and Zhang (2009) and Li et al. (2017) found that although Tang and Yuan blue pigments shared low MnO, the existence of CuO distinguished between the different raw materials. Zhang et al. (1986) classified the cobalt materials from the Tang to the Qing dynasties into three types: cobalt ore co-existing with copper (low MnO), cobalt ore co-existing with iron (low MnO and high Fe_2O_3) and cobalt ore co-existing with manganese (high MnO and Fe_2O_3) and proposed that the first type was used in the Tang dynasty, which distinguished it from the Song, Yuan, Ming and Qing ores. This difference has been supported by many scholars (Chen et al., 1995; Cheng et al., 2005; Zhang and Zhang, 2009; Lu et al., 2016; Cheng et al., 2016; Li et al., 2017). They confirmed the existence of copper in Tang cobalt pigment which is also characterised by low manganese and iron. Furthermore, Li et al. (2017) emphasised that this difference suggests no connection between Tang and Yuan blue-and-white. According to these authors, there were two independent origins of China's blue-and-white porcelains, unrelated in time and place.

In my opinion, determining two independent origins of Chinese blue-and-white porcelains based on the difference in CuO is not reliable. The analytical results of raw blue glaze and cobalt colourant particles, such as high Fe_2O_3/MnO, trace MnO, the association of Co and Fe etc. illustrate the big difference between Tang cobalt material and local cobalt pigment used in Song and Mid-Ming dynasties, and the high similarity between it and imported Yuan cobalt pigment. There are two possibilities for copper in cobalt colourant. The first one is that the cobalt ore of this glassy pigment is Co-Fe-Cu-As-Mn co-existing ore. Among these four associated elements, Fe is the highest one but not higher than Co. Cu is the second highest but still low. Mn is a trace element (Figure 4. 61). And the level of As has not been certain. The origin of it was not China and might be a foreign region but not Kāshān. The second possibility is that the cobalt ore did not contain copper, but moderate copper was added to other raw ingredients of the glassy pigment during processing. The cobalt-copper-coloured blue glass was used in Egypt as early as New Kingdom (1570-1069 BCE) (Smirniou and Rehren, 2013). Shortland and Eremin (2006) suggested that copper metal or ore was added to weakly-coloured cobalt-blue glass to enhance its colour. Although New Kingdom Egypt was too far away from Tang China (618-907 CE) chronologically and geographically, this method was possible to be inherited or spread. In comparison, the first possibility is more practical than the other, but the second possibility cannot be eliminated.

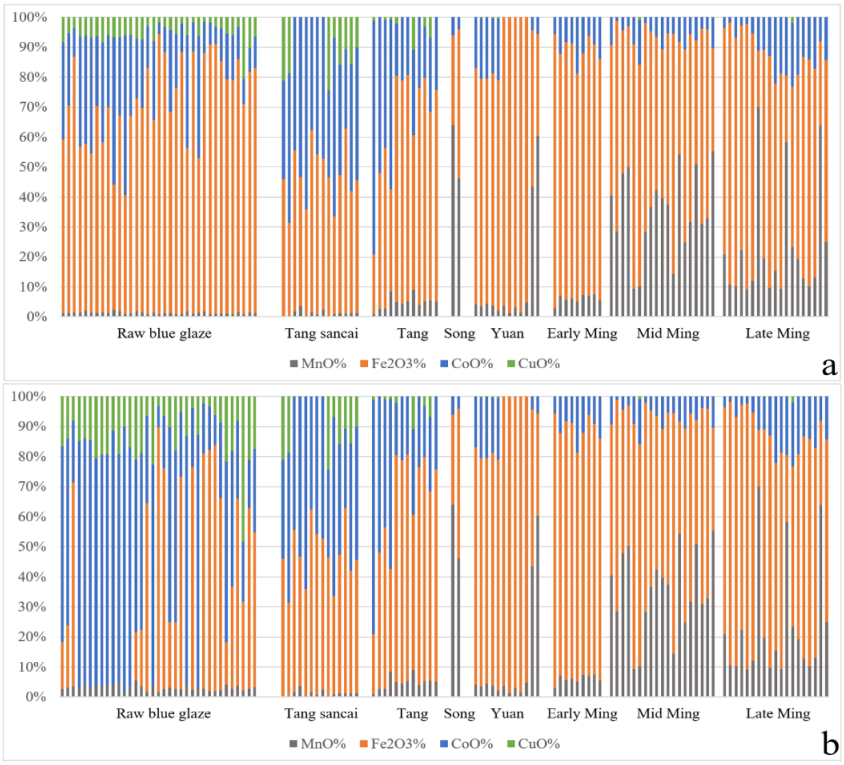


Figure 4. 61 Percentage relationships of CoO, Fe_2O_3, MnO, and CuO of (a) raw blue glaze and of cobalt pigments used in blue ceramics, and of (b) estimated blue colourant of raw blue glaze and cobalt of cobalt pigments used in blue ceramics.

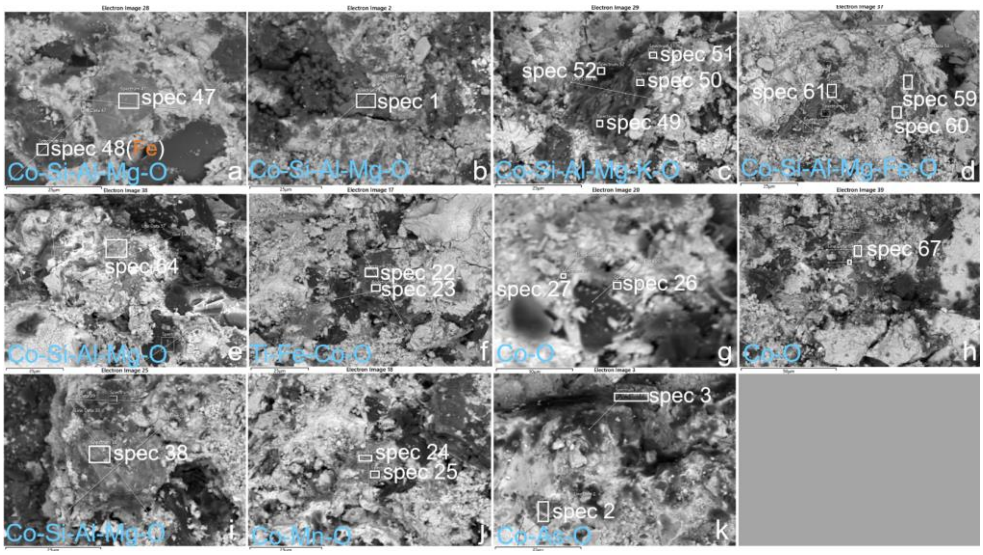


Figure 4. 62 Test areas of Co-rich particles in raw blue glaze, obtained from the ESEM.

Table 4. 5 Chemical compositions of cobalt particles/tested areas

Element	O	Na	Mg	Al	Si	P	S	Cl	K	Ca	Ti	Mn	Fe	Co	Ni	Cu	As	Br	Mo	Ba	Pb
a_map	24.00	0.21	0.74	5.53	8.30	1.50	-	-	1.89	2.53	0.23	2.08	3.70	0.61	-	-	0.27	-	-	-	48.42
a_spec 47	24.92	-	0.67	3.18	7.53	0.82	-	-	0.60	1.27	-	-	1.07	27.64	-	3.35	2.03	-	-	-	26.92
a_spec 48 (Fe)	30.65	-	2.19	6.63	11.34	0.96	-	-	4.14	1.68	0.98	-	17.28	0.93	-	-	-	-	-	-	23.22
b_map	30.75	0.30	0.86	3.13	5.71	3.95	4.39	1.09	1.09	12.61	0.15	-	1.20	3.39	-	-	0.30	-	-	-	31.09
b_spec 1	30.24	-	2.37	5.30	8.02	0.89	1.76	-	0.74	2.92	-	-	-	29.69	-	1.61	-	-	-	-	16.48
c_map	25.35	0.35	0.43	5.72	9.78	1.44	-	-	0.74	4.22	0.24	-	0.63	3.17	-	0.34	0.29	-	-	-	47.31
c_spec 49	34.43	-	-	12.53	11.80	1.74	-	-	2.53	1.49	-	-	-	12.82	-	-	5.20	-	-	-	17.46
c_spec 50	31.81	-	-	9.69	9.92	1.82	0.95	0.97	2.39	7.45	-	-	-	10.03	-	-	-	-	-	-	24.96
c_spec 51	33.57	-	1.75	8.89	12.21	0.96	-	1.80	3.44	13.84	-	-	0.86	5.79	-	-	-	-	-	-	16.87
c_spec 52	38.25	-	-	14.46	16.80	0.68	-	-	8.71	0.87	-	-	-	8.62	-	-	-	-	-	-	11.60
d_map	22.74	-	0.65	4.73	6.87	1.55	-	-	1.40	2.73	0.27	-	1.06	9.26	-	0.29	0.43	-	-	-	48.03
d_spec 59	27.30	-	-	4.22	10.70	0.84	-	0.42	1.02	1.14	-	-	-	22.05	-	2.87	-	-	1.49	-	27.97

Element	O	Na	Mg	Al	Si	P	S	Cl	K	Ca	Ti	Mn	Fe	Co	Ni	Cu	As	Br	Mo	Ba	Pb
d_spec 60	28.32	-	-	3.25	9.01	0.79	3.02	0.48	1.31	2.67	-	-	-	20.30	-	2.29	-	-	-	-	28.55
d_spec 61	28.10	-	2.75	5.09	10.10	1.03	-	0.54	0.77	2.53	-	-	3.67	15.81	-	0.77	-	-	-	-	28.84
e_map	22.85	0.22	0.87	2.69	9.02	2.06	-	0.47	0.72	4.20	-	-	0.96	1.50	-	0.35	0.30	-	-	0.61	53.18
e_spec 64	21.78	-	2.50	3.65	4.54	2.95	-	0.86	0.59	3.94	-	-	0.73	1.84	-	2.56	2.81	-	-	-	51.26
f_map	17.12	0.28	0.64	1.49	4.61	1.82	-	0.53	0.32	3.37	-	-	0.89	3.17	-	0.43	-	-	-	-	65.33
f_spec 22	31.48	-	1.54	2.85	4.26	1.07	-	0.28	0.38	1.51	23.65	-	6.78	5.13	-	1.50	-	-	-	-	19.59
f_spec 23	31.45	-	2.39	4.26	6.89	2.04	-	0.64	1.67	3.18	15.52	-	1.40	0.94	-	2.18	1.24	-	-	-	26.20
g_map	19.25	0.16	0.39	2.28	5.6	1.4	-	-	0.55	2.8	2.76	0.16	0.86	1.66	-	0.3	0.18	-	-	-	61.64
g_spec 26	18.29	-	-	2.42	4.82	2.23	-	-	-	2.15	-	-	-	5.12	-	-	2.06	-	-	-	62.91
g_spec 27	17.40	-	0.34	1.76	4.37	1.36	-	-	0.30	2.05	-	-	-	10.44	-	0.81	0.97	-	-	-	60.21
h_map	19.94	-	0.24	4.37	6.18	1.53	-	-	1.39	2.55	0.30	0.19	0.34	1.59	-	-	0.25	-	-	-	61.14
h_spec 67	44.73	0.76	0.49	17.11	23.64	-	-	-	1.71	0.50	0.38	-	0.50	1.35	-	-	-	-	-	-	8.85
i_map	20.50	-	0.32	3.86	7.80	0.97	-	-	0.84	2.19	0.14	-	0.47	3.01	-	-	-	-	-	-	59.90
i_spec 38	47.73	-	-	-	6.07	1.63	-	0.48	-	1.76	-	-	0.44	8.17	-	-	2.52	4.17	-	-	27.03

Element	O	Na	Mg	Al	Si	P	S	Cl	K	Ca	Ti	Mn	Fe	Co	Ni	Cu	As	Br	Mo	Ba	Pb
j_map	19.58	0.14	0.37	2.43	4.60	1.83	-	-	0.85	3.68	2.90	0.26	1.16	2.94	-	0.48	0.27	-	-	-	58.50
j_spec 24	20.08	-	-	-	7.69	1.62	0.92	0.69	-	2.25	-	-	3.72	8.70	-	-	-	8.75	-	-	45.58
j_spec 25	23.53	-	-	5.07	7.98	1.19	-	0.87	-	1.84	-	-	4.46	10.85	-	-	-	-	-	-	44.22
k_map	24.18	0.65	0.83	2.97	4.61	5.42	-	1.50	0.85	8.88	-	-	0.68	3.74	-	-	0.30	-	-	-	45.40
k_spec 2	21.55	-	-	1.77	2.70	2.07	-	0.78	-	2.42	-	-	-	28.05	1.51	3.69	6.46	-	-	-	28.99
k_spec 3	22.64	-	--	2.13	2.13	1.34	0.58	0.67	0.39	3.63	-	-	-	41.37	-	-	4.22	-	-	-	20.90

4.3.2 Colouring and Weathering

The colour of the raw blue glaze is black (Figure 4. 63) which is the darkest one and different from others. This black colour was given by glassy cobalt colourant. However, the colour of another glassy cobalt material, smalt, is blue (Figure 4. 45 and Figure 4. 48). The following key question is whether black is the true colour of the cobalt colourant. The study of smalt could offer some clues. The pigment was available in different grades from pale grey to deep blue, with the colour being dependent on the cobalt content and particle size (Mühlethaler and Thissen, 1993). Perhaps, Fe, Cu and As darkened the tone of the cobalt colourant and then coloured the raw glaze. Remarkably, the matrix of cobalt colourant is glass, which is likely to be weathered, especially after a one-thousand-year burial. The weathering might change the tune and grade of the original colour.

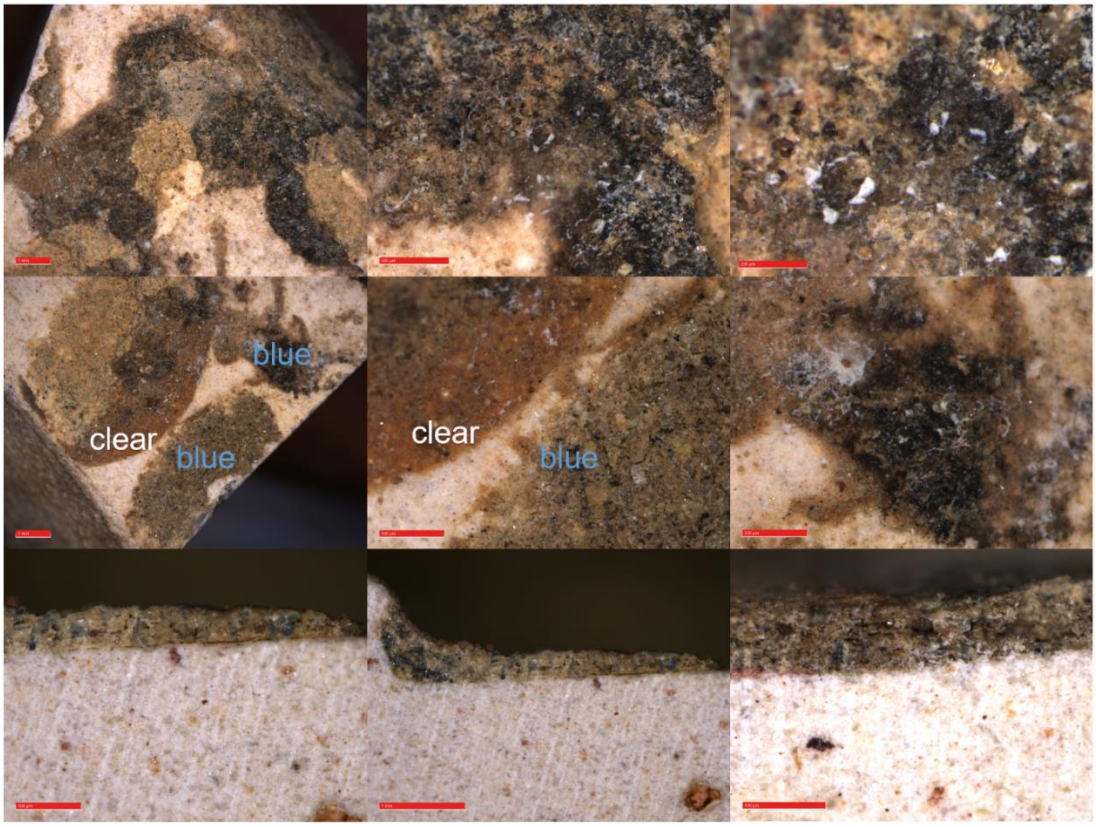


Figure 4. 63 Colours of raw blue glazes, obtained by the optical microscope.

4.3.3 Manufacturing and Applying

Compared with iron and copper colourant particles, cobalt particles are the smallest. Many iron particles of brown glazes are bigger than 100μm. Most copper particles of green glazes are 20-60 μm and a few of them exceed 100μm. However, the size of cobalt particles is around 2-40 μm, and most of them are 20μm approximately (Figure 4. 64). It suggests that the cobalt material was the finest product and that grinding it might take the longest time, and also that Tang-dynasty potters recognised that cobalt was the most efficient one amongst the three colourants. Thus, the amount of added cobalt was the least. The average percentages of Fe_2O_3, CuO and CoO are 3.44%, 0.82% and 0.35%.

The making method of this glassy cobalt pigment can reference the traditional technique of smalt. The manufacturing process of smalt was as follows: the cobalt ore was roasted. The cobalt oxide thereby obtained was melted together with quartz and potash or added to molten glass. When poured into cold water, the blue melt disintegrates into small particles, and these were ground in water mills and elutriated (Mühlethaler and Thissen, 1969). The traditional method of cobalt pigment used in blue-and-white porcelain in China was very different. *Jiangxi Sheng Dazhi · Tao Shu 江西省大志· 陶书* (Wang, 1597) described the processing method as two steps - 'Qiao Qing' (敲青) and 'Tao Qing' (淘青). 'Qiao Qing' refers to smashing cobalt ores, and 'Tao Qing' means grinding and purifying. The smashed ores were ground into small pieces. Next, these pieces were added into the water. A magnet could carry some impurities out, and the fine cobalt pigment was obtained by sedimentation. Besides that, *Tiangong Kaiwu 天工开物* (Song, 1637) also mentioned a calcining procedure – when potters used the cobalt pigment, it was calcined by a charcoal fire. With these traditional processing methods in China

was impossible to produce a glassy matrix. In other words, colourant-making includes outside influences.

Although the details of colourant making are unclear, the basic process can be inferred. Cobalt ore, silicon-alumina base, flux, perhaps with copper, were all ground and mixed up, and fired together to make a glassy material. Next, this glassy pigment was ground to obtain a fine powder. And the colourant powder was added into the stock glaze to produce lead glaze for Sancai. Furthermore, this glassy pigment was possibly used in Tang blue-and-white porcelain. The moderately spreading effect of blue motifs on Tang blue-and-white is similar to the blue decorations on Sancai, but very different from the carefully controlled blue patterns on typical blue-and-white porcelains from Yuan to Qing dynasties (Figure 4. 65). Compared with Yuan and Ming cobalt pigment, the glassy cobalt material used in Tang dynasty contained more flux, which might be the reason for spreading effect. The making of this glassy pigment might happen in a foreign region, possibly the Middle East, but the grinding and applying was finished in the Gongyi kiln in China. The reason for importing glassy pigment rather than cobalt ore cannot be understood based on current evidence. Perhaps, using glassy pigment is a tradition of Islamic potters. Or craftsmen wanted to keep the secret of pigment making. Or maybe carrying this purified material was much more convenient than transporting ores.

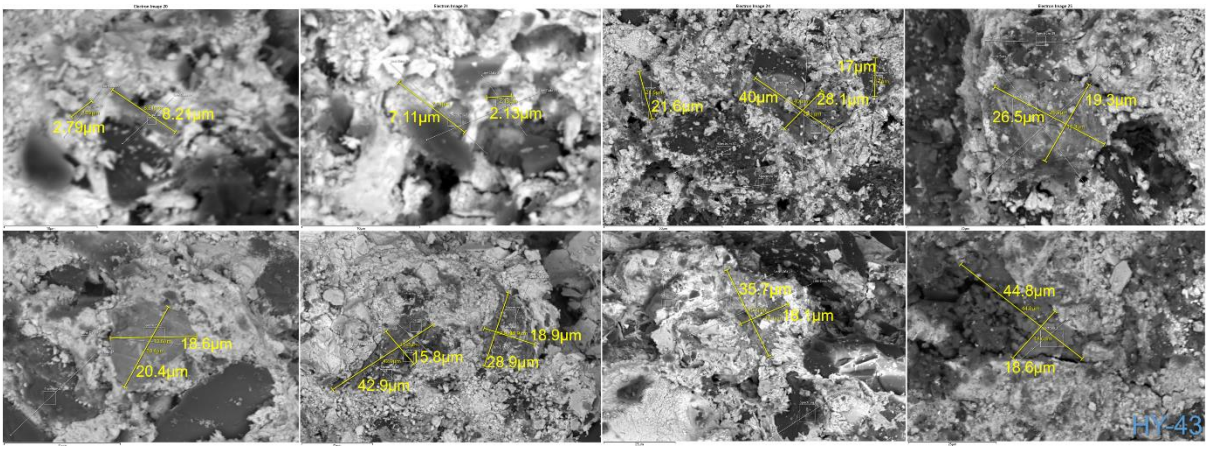


Figure 4. 64 Sizes of Co-rich particles in raw blue glazes, obtained from the ESEM.



Figure 4. 65 Details of blue decorations on ceramics: (a-d) Tang Sancai, from Henan Provincial Institute of Cultural Heritage and Archaeology et al. (2016a, p.130, 160, 232, 262); (e) and (f) Tang blue-and-white porcelains, taken by the author; (g) Yuan blue-and-white porcelain, from https://www.dpm.org.cn/collection/ceramic/227179.html; (h) Ming blue-and-white porcelain, from https://www.dpm.org.cn/collection/ceramic/226869.html.

Chapter 5 Glazes

Chapter 4 discussed iron, copper and cobalt colourants of brown, green and blue glazes respectively. The main elements, except for colourant elements – Fe, Cu and Co, of all raw glazes are very similar. And the dominant tone of most of raw glazes is brown, even though the shades of brown are various. These findings suggest that the four types of raw glazes – clear, brown, green, and blue, shared the same base which can be defined as 'stock glaze'. This chapter aims to explore the recipe of stock glaze and the manufacturing process of raw glazes.

5.1 Stock Glaze Recipe

The sum of main elements (>1%), except for Fe_2O_3, of all raw glazes is 95-98% (Table 5. 1). The clear, brown, green, and blue glazes shared almost same levels of MgO, Al_2O_3, SiO_2, P_2O_5, CaO and PbO. Fired Sancai glaze is a layer of glass which is fused on a fired white body. Al_2O_3 and SiO_2, as the framework of glass, are the most important constituent of glazes like bone for humans. P_2O_5, CaO and PbO work as flux to bring down the melting temperatures of Al_2O_3 and SiO_2, which is 2054℃ and 1710℃ respectively. The other elements in the raw glaze are lower than 1% (Table 5.2). These trace elements were brought in with the main ingredient as 'impurities' instead of being added deliberately by potters. The discussion of the potential association and relation among these elements can reveal the raw materials and recipe of the stock glaze.

Table 5. 1 Mean values of main elements of raw glazes.

Samples	MgO	Al_2O_3	SiO_2	P_2O_5	CaO	PbO	Sum.
body	0.57	35.34	56.23	0.22	1.66	0.13	94.17
clear	0.95	3.38	28.86	25.42	9.79	29.53	97.93
brown	1.50	5.25	27.91	21.95	8.09	29.94	94.63
green	1.00	4.43	26.33	25.73	10.10	29.52	97.11
blue (HY-43)	1.37	5.46	31.11	17.38	7.64	33.14	96.10
clear (HY-43)	1.36	5.20	29.60	22.52	8.80	28.95	96.43
brown (HY-43)	1.62	6.78	30.99	16.80	7.48	30.89	94.56

Table 5. 2 Mean values of trace elements and colourant elements of raw glazes.

Samples	Na_2O	K_2O	TiO_2	V_2O_5	MnO	NiO	ZnO	SrO	SnO_2	Sb_2O_5	BaO	Fe_2O_3	CoO	CuO
body	0.20	2.78	1.28	0.07	0.01	0.00	0.01	0.02	0.01	0.03	0.12	1.33	0.01	0.00
clear	0.49	0.25	0.15	0.06	0.02	0.00	0.01	0.06	0.84	0.06	0.20	0.66	0.01	0.02
brown	0.58	0.50	0.23	0.08	0.04	0.00	0.01	0.06	0.65	0.08	0.23	3.44	0.02	0.02
green	0.29	0.27	0.19	0.06	0.03	0.00	0.02	0.05	0.77	0.13	0.13	0.98	0.01	0.82
blue (HY-43)	0.60	0.58	0.24	0.05	0.02	0.01	0.00	0.05	0.89	0.07	0.25	1.33	0.35	0.10
clear (HY-43)	0.87	0.50	0.22	0.06	0.02	0.00	0.00	0.05	0.86	0.07	0.26	1.11	0.01	0.01
brown (HY-43)	0.84	0.72	0.30	0.05	0.03	0.00	0.01	0.05	0.80	0.02	0.31	2.74	0.02	0.01

5.1.1 Clay or Feldspar?

Silica is the most important glass/glaze-forming constituent. Naturally, it occurs as quartz rock, flint, and sand. It also in combination with other oxides in silicate – a compound involving silica as an important part (Hamer and Hamer, 2015, p.331). Many silicates have been used in ceramics, which include the groups called feldspars, micas, pyroxenes, amphiboles, and zeolites (Hamer and Hamer, 2015, p.338). The content of SiO_2 of clear, brown, and green glazes is around 26-28% on average. The level in the raw blue glaze seems a little higher than the other glazes. However, this 'mean value' of blue glaze is not representative since it was calculated by various blue areas in the same sherd instead of by different sherds. Only one sherd (HY-43) decorated with raw blue glaze was found among all samples. Plus, SiO_2 of clear and brown glazes on HY-43 sherd, are 29.60% and 30.99% respectively, are also higher than the averages of clear glaze (25.60%) and brown glaze (27.91%) calculated by all samples. The raw glazes on the same sherd possibly shared the same stock glaze even though the colours of them are different. In other words, when a stock glaze was finished, colourants would be added in to produce raw coloured glazes. Therefore, the main ingredients of glazes on the same sherd should be the same. For example, if the raw blue glaze of HY-43 contained higher SiO_2 than clear and brown glazes on it, that might suggest blue colourant had higher SiO_2. However, if the SiO_2 in blue, clear, and brown glazes of HY-43 was higher than other samples, this difference was caused by different production batch. Additionally, Al_2O_3 is second only to SiO_2 in importance. In glazes, it is an intermediate oxide and serves to stabilize the combination of fluxes and glass-formers. It is combined with silica in the clay crystal, and it occurs naturally as the crystalline mineral corundum (Hamer and Hamer, 2015, p.6).

Determining the source of SiO_2 and Al_2O_3 is the key research question to be answered in this section. Large numbers of Si-Al-(K/Na)-O-associated grains in raw glazes were found by

the ESEM observation. The element distribution, texture and shapes of these grains are very similar (Figure 5. 1 - Figure 5. 3). It might suggest that these three types of grains were from the same raw material. Compositionally, SiO_2 and Al_2O_3 are the first and second ranking in all elements, around 20% and 50% respectively (Table 5. 3). However, the original composition in the raw material should be higher than the obtained data because lead powder 'contaminated' the tested areas (Figure 5. 4). The mapping did not show a concentration of Pb in these Si-Al-rich grains. And less-contaminated areas of these grains contain very low PbO. For example, only 1.63% PbO was tested in HY-59-spec 14 (Table 5. 3). Thus, we can conclude that the lead was brought in the test areas as 'contamination' rather than from the Si-Al-rich grains themselves. Since all data were normalised automatically during examination, the existence of PbO decreased the percentages of SiO_2 and Al_2O_3. After removing PbO data and re-normalising other elements, Al_2O_3 and SiO_2 are around 20-40% and 50-60% respectively (Table 5. 4). And the real content of K_2O and Na_2O are close to 7-13% and 8-14% for Si-Al-K-O and Si-Al-Na-O grains respectively.

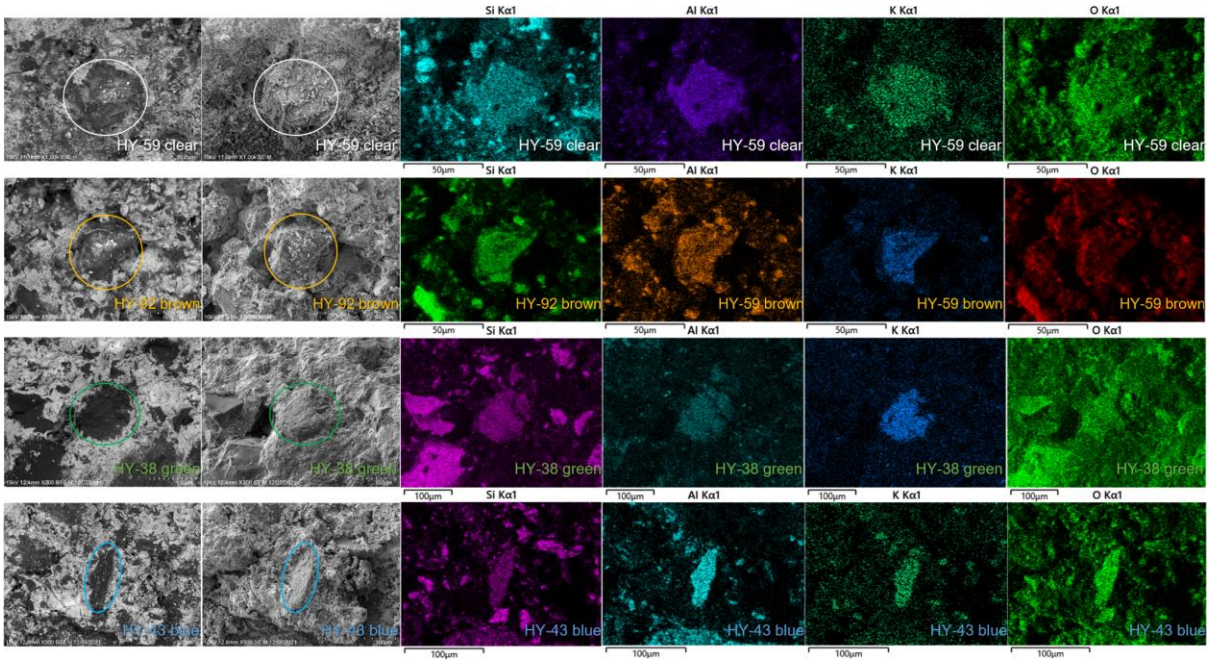


Figure 5. 1 BSE (the first column), SE (the second column), and mapping images (other columns) of Si-Al-K-O-associated particles in raw glazes, obtained from the ESEM.

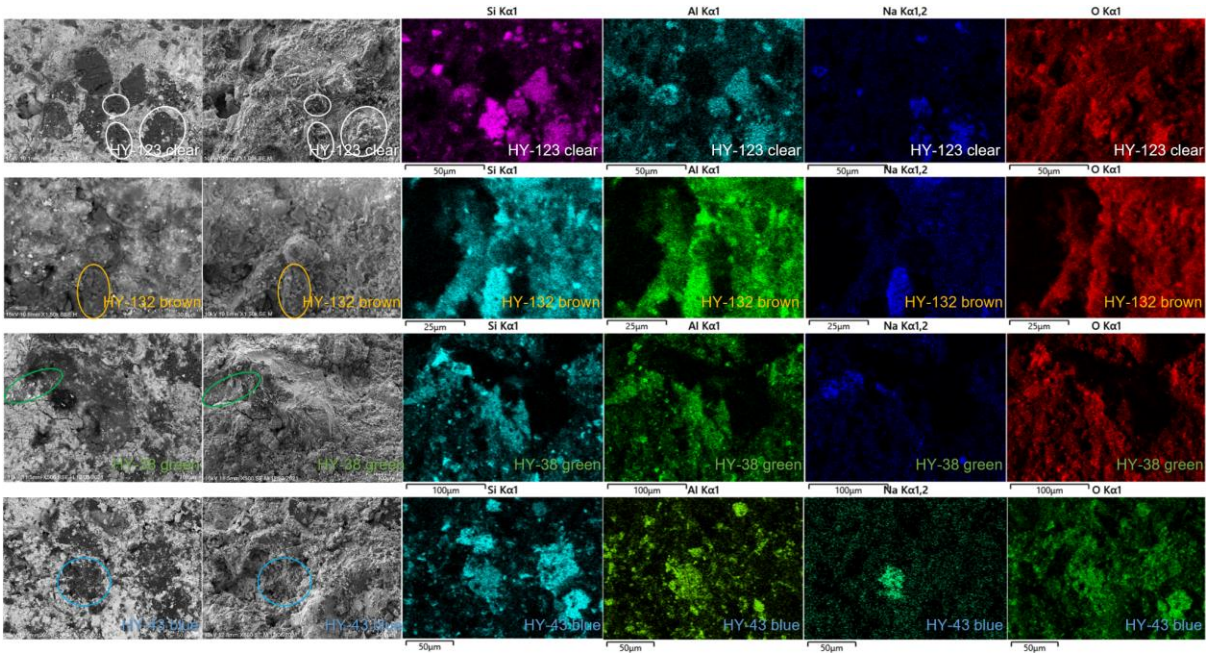


Figure 5. 2 BSE (the first column), SE (the second column) and mapping images (other columns) of Si-Al-Na-O-associated particles in raw glazes, obtained from the ESEM.

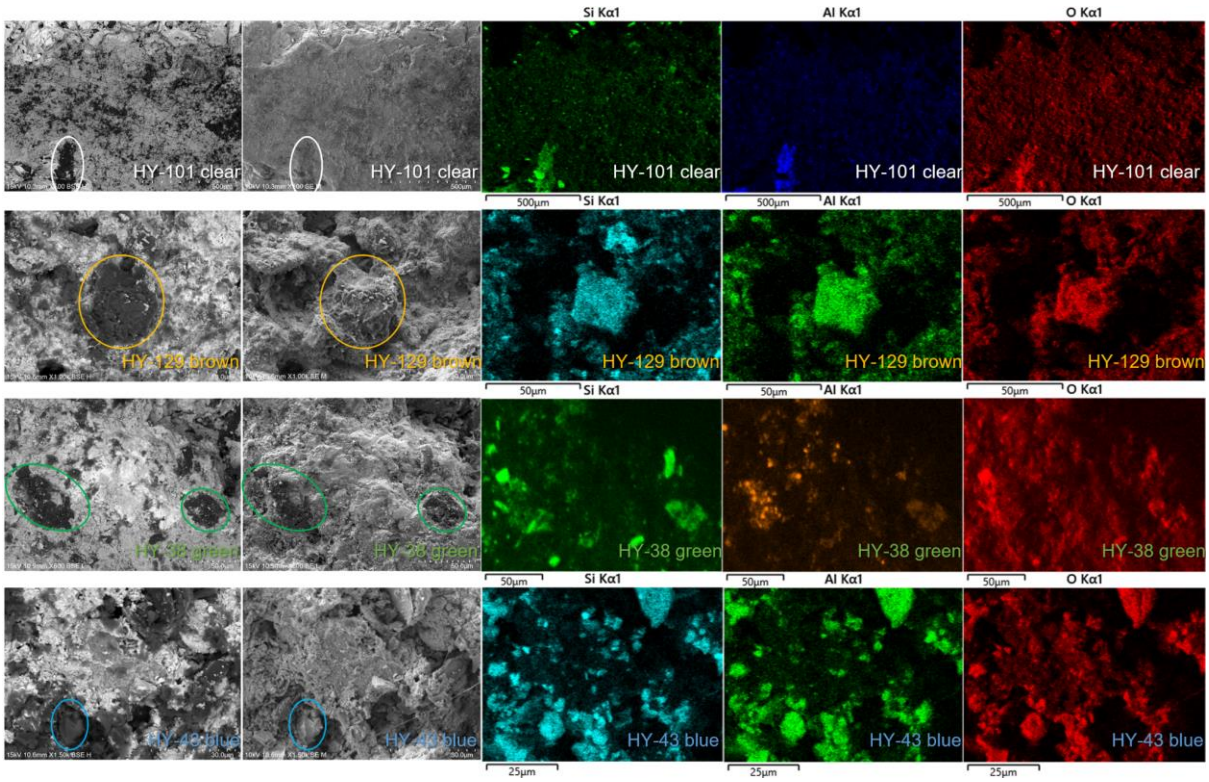


Figure 5. 3 BSE (the first column), SE (the second column) and mapping (other columns) images of Si-Al-O-associated particles in raw glazes, obtained from the ESEM.

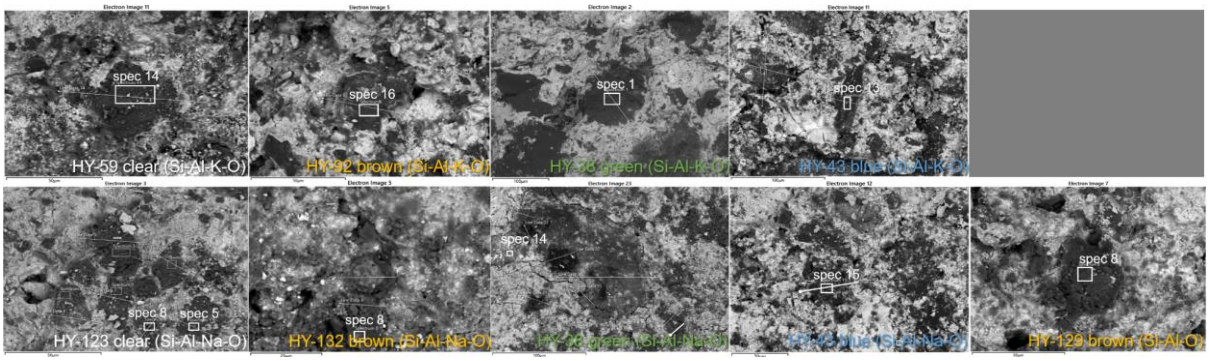


Figure 5. 4 Test areas of Si-Al-(K/Na)-O-associated particles in raw glazes, obtained from ESEM.

Table 5. 3 Chemical compositions of Si-Al-(K/Na)-O-associated particles in raw glazes by ESEM

Particle types	Glaze colours	Samples	Na_2O	MgO	Al_2O_3	SiO_2	P_2O_5	K_2O	CaO	TiO_2	FeO	PbO
Si-Al-K-O	Clear	HY-59-spe 14	1.91	1.31	37.44	49.89	-	6.85	-	0.39	0.57	1.63
	Brown	HY-92-spec 6	0.74	0.88	17.18	48.88	4.81	6.14	2.63	-	-	18.23
	Green	HY-38-spec 1	0.46	0.48	17.17	56.20	2.24	11.93	2.92	-	0.60	7.81
	Blue	HY-43-spec 13	1.17	1.10	33.53	43.91	1.69	7.13	1.01	0.57	0.74	8.98
Si-Al-Na-O	Clear	HY-123-spec 5	10.93	0.68	16.81	49.00	2.59	0.60	1.22	-	-	17.87
	Clear	HY-123-spec 8	6.00	2.01	13.53	35.46	7.54	1.29	5.08	-	1.07	27.16
	Brown	HY-132-spec 8	8.16	0.51	23.99	52.68	2.14	0.52	5.37	-	0.45	5.95
	Green	HY-38-spec 14	6.89	0.81	13.79	36.00	9.30	0.37	4.99	-	-	27.19
	Blue	HY-43-spec 15	10.93	-	19.68	57.29	1.27	0.34	0.99	-	0.46	8.86
Si-Al-O	Brown	HY-129-spec 8	0.38	1.07	31.2	56.62	1.21	2.05	1.17	0.93	0.98	4.24

Table 5. 4 Chemical compositions of Si-Al-(K/Na)-O-associated particles by calculation (PbO removed and re-normalised)

Particle types	Glaze colours	Samples	Na_2O	MgO	Al_2O_3	SiO_2	P_2O_5	K_2O	CaO	TiO_2	FeO
Si-Al-K-O	Clear	HY-59-spe 14	1.94	1.33	38.06	50.72	-	6.96	-	0.40	0.58
	Brown	HY-92-spec 6	0.91	1.08	21.14	60.15	5.92	7.56	3.24	-	-
	Green	HY-38-spec 1	0.50	0.52	18.66	61.09	2.43	12.97	3.17	-	0.65
	Blue	HY-43-spec 13	1.29	1.21	36.91	48.33	1.86	7.85	1.11	0.63	0.81
Si-Al-Na-O	Clear	HY-123-spec 5	13.36	0.83	20.55	59.89	3.17	0.73	1.49	-	-
	Clear	HY-123-spec 8	8.34	2.79	18.80	49.26	10.48	1.79	7.06	-	1.49
	Brown	HY-132-spec 8	8.70	0.54	25.57	56.14	2.28	0.55	5.72	-	0.48
	Green	HY-38-spec 14	9.55	1.12	19.12	49.90	12.89	0.51	6.92	-	-
	Blue	HY-43-spec 15	12.01	0.00	21.63	62.98	1.40	0.37	1.09	-	0.51
Si-Al-O	Brown	HY-129-spec 8	0.40	1.12	32.63	59.21	1.27	2.14	1.22	0.97	1.02

The use of a high-Si-Al material associating with K or Na also was proved by XRF analysis. Figure 5. 5 shows a positive correlation between Al_2O_3 and SiO_2 of raw glazes. And Figure 5. 6b presents a direct positive correlation between K_2O and Al_2O_3. Almost no samples deviate much from this relationship. And if a straight line to the Al_2O_3-K_2O data was fitted in, it will go through the origin. In other words, all the K_2O and Al_2O_3 is provided by one material. The lack of obvious structure in the relationship between Na_2O and Al_2O_3 might be caused by the method errors (Figure 5. 6 a). Sodium is too light to be tested accurately by XRF. The discussion about sodium cannot be included here.

Additionally, this material contains trace Fe_2O_3 and TiO_2 (Table 5. 4) as impurities. Except for the deviation of Fe_2O_3 of brown glaze, other Fe_2O_3 vs. Al_2O_3 and Fe_2O_3 vs. K_2O, and all TiO_2 vs. Al_2O_3 and TiO_2 vs. K_2O_3 of raw glazes keep almost perfect positive correlation (Figure 5. 7 and Figure 5. 8). And these relationships pass through the origin. This reveals that the source of all K_2O, TiO_2 in all glazes and all Fe_2O_3 in clear, green, and blue glazes is the same one – the high-Si-Al material. The reason for the deviation of iron from brown glaze is the use of an additional iron colourant.

The subsequent question is whether all Si is also provided by this high-Si-and-Al material containing some K and trace Fe and Ti? Two findings suggest a negative answer. The first finding is the relation between Al and Si. As shown by the red triangles in Figure 5. 5, many samples, no matter which colour, contain much higher silicon than the samples near the fitted line. The other direct evidence is from the observation by ESEM. A large number of Si-O-associated particles were found in the raw glazes (Figure 5. 9). To summarise, there are two sources of silicon. One source is a high-Si-and-Al material, such as clay, feldspar etc. The other one is a high/pure-Si material.

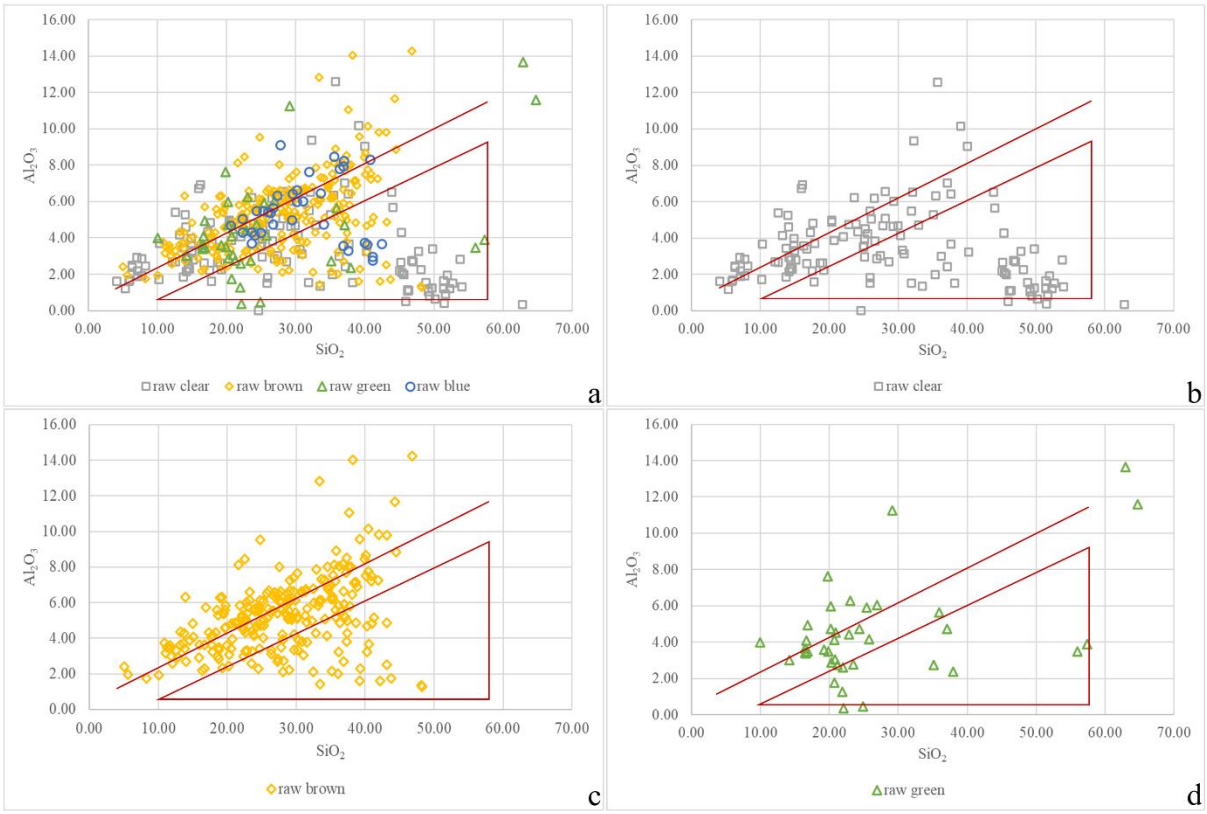


Figure 5. 5 Scatter diagrams of Al_2O_3 to SiO_2 of (a) all raw glazes, (b) raw clear glaze, (c) raw brown glaze and (d) raw green glaze, data from XRF. The data in red triangle belongs to the high-Si group.

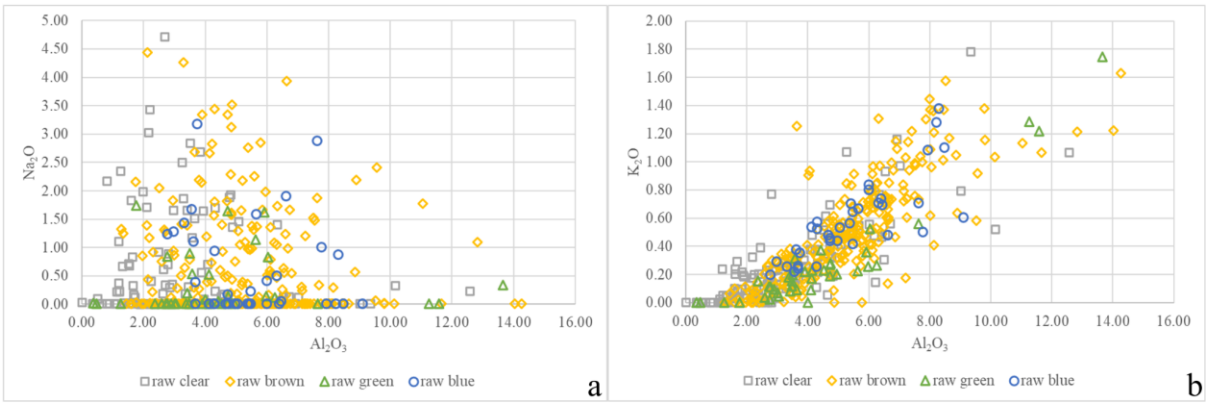


Figure 5. 6 Scatter diagrams of (a) Na_2O to Al_2O_3 and (b) K_2O to Al_2O_3 of raw glazes.

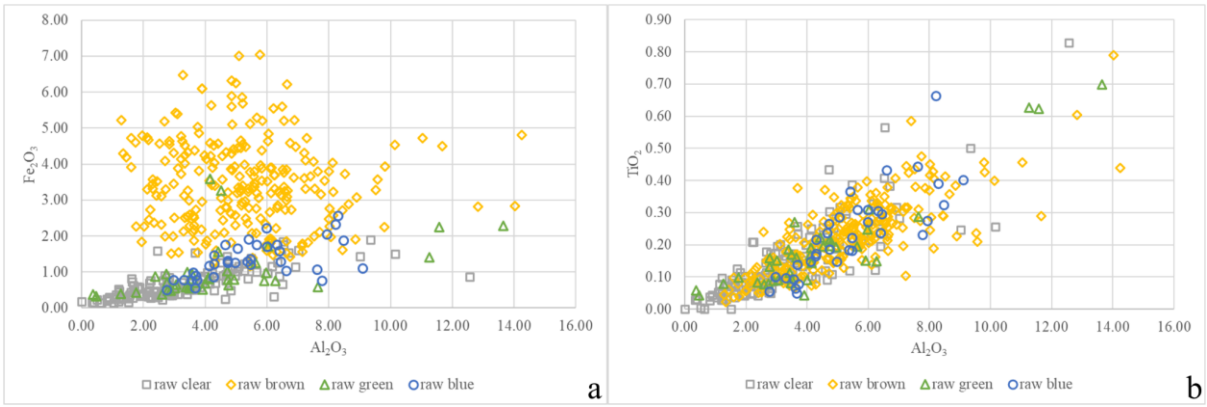


Figure 5. 7 Scatter diagrams of (a) Fe_2O_3 to Al_2O_3 and (b) TiO_2 to Al_2O_3 of raw glazes.

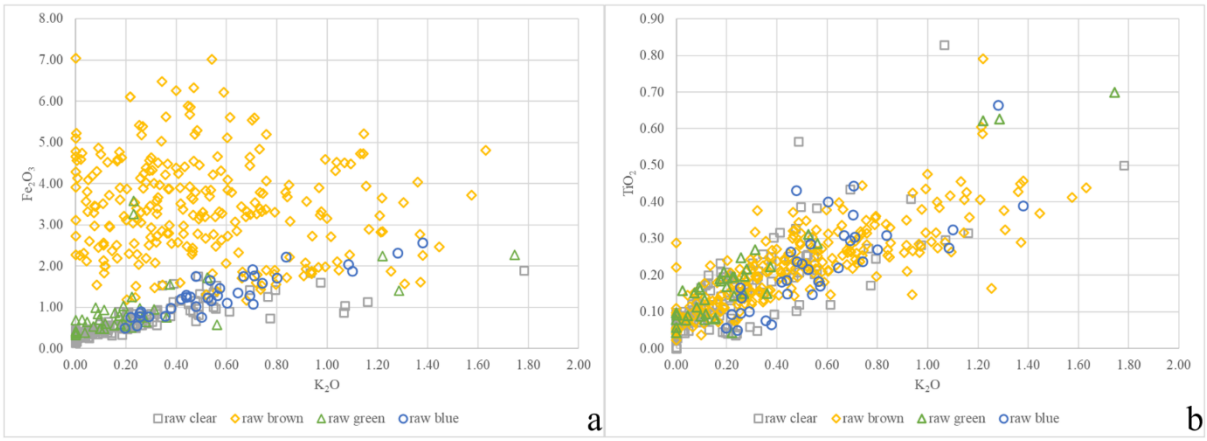


Figure 5. 8 Scatter diagrams of (a) Fe_2O_3 to K_2O and (b) TiO_2 to K_2O of raw glazes.

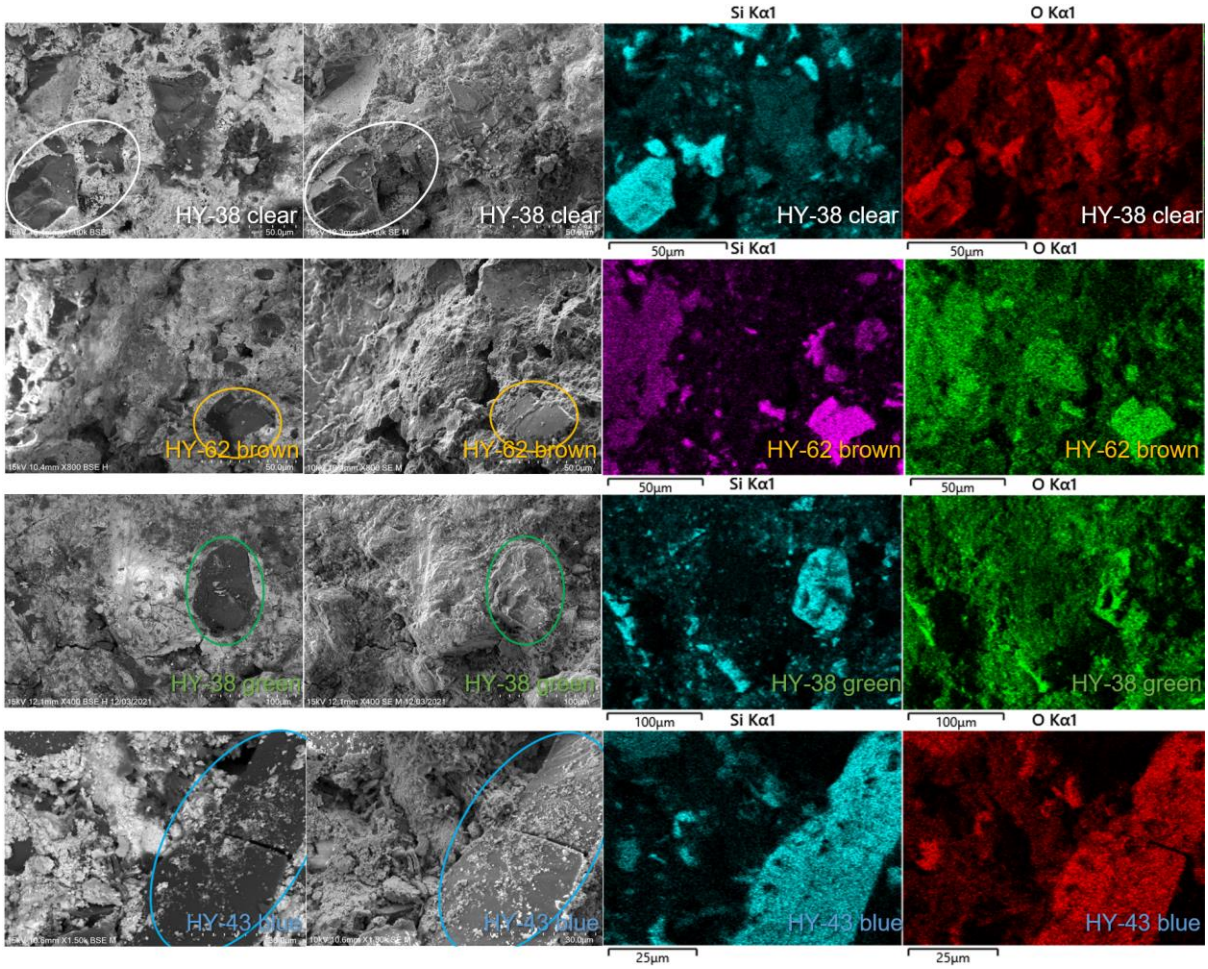


Figure 5. 9 SEM (the first column), SE (the second column) and mapping (other columns) images of Si-O-associated particles in raw glazes, obtained from ESEM.

Common raw materials used in ceramic industry containing high Si and Al, some K and trace Fe and Ti are feldspar and kaolinitic clay. Accordingly, three hypotheses can be proposed. Hypothesis 1 is the use of feldspar. Calculations[25] are performed using the theoretical formula of potassium feldspar ($K_2O \cdot Al_2O_3 \cdot 6SiO_2$).

[25] These calculations are inspired by Pollard et al. (2007, pp.158-159). Pollard used weight percentages of theoretical composition of minerals to assume the contribution of oxides by specific mineral, but I used the molar weight to do the calculation. The results are the same. For examples, theoretical composition of sericite is $K_2O \cdot 3Al_2O_3 \cdot 6SiO_2 \cdot 2H_2O$. A porcelain body contains 3.47% K_2O. Assuming all K_2O comes from sericite to calculate how much SiO_2 is contributed by sericite. His method is to calculate the theoretical weight percentage

1) Calculate the amount of substance n(Al_2O_3) of raw glazes by dividing m(Al_2O_3) obtained from XRF by its molar mass M (Al_2O_3).

   n (Al_2O_3) = m (Al_2O_3) / M (Al_2O_3)

2) According to the formula of potassium feldspar ($K_2O \cdot Al_2O_3 \cdot 6SiO_2$), the amount of substance n(K_2O) is equal to the n(Al_2O_3).

   n (K_2O) = n (Al_2O_3)

3) Estimate theoretical value m'(K_2O) provided by the feldspar.

   m' (K_2O) = n (K_2O) * M (K_2O)

4) Obtain the difference Δm (K_2O) between practical data m(K_2O) and theoretical values m'(K_2O) provided by feldspar.

   Δm (K_2O) = m (K_2O) - m' (K_2O)

The previous discussion has already shown that all K_2O and Al_2O_3 were brought in the raw glazes by the same material. Therefore, the m' (K_2O) (Figure 5. 10 b) should be almost equal to the m (K_2O) tested by XRF (Figure 5. 10 a). However, the result shows that ΔK_2O is much less than 0, and most of ΔK_2O is from -1.57% to -5.28% (Figure 5. 10 c). The ΔK_2O is too big to be explained by the difference between theoretical formula and practical constituent. It can be concluded that hypothesis 1 is invalid.

of K_2O and SiO_2 in sericite: M(K2O)/M(sericite)x100%=11.8% and M(SiO_2)/M(sericite)x100%=45.2%, the predicted %SiO_2=45.2%/11.8%x3.47%=13.3%. My method is to calculate amount of substance of %SiO_2 = 3.47%/M(K_2O)x6=22.10%, the predicted %Si_2O=22.10%x60.08=13.3.

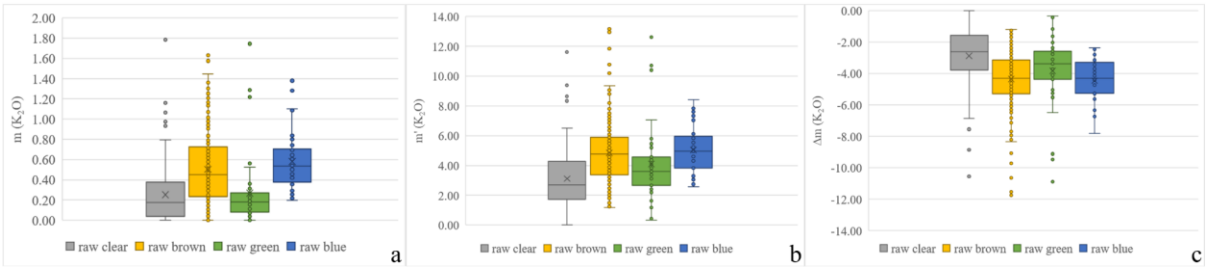


Figure 5. 10 Box plots of (a) m (K_2O), (b) m' (K_2O) and (c) Δm (K_2O) of raw glazes. The calculation is based on hypothesis 1: feldspar.

Considering low K_2O in raw glazes, it might be an associated constituent or impurities, rather than the main ingredient of the high-Si-and-Al material. Hypothesis 2 is the use of kaolinitic clay. It is the idealised clay mineral and is high in aluminium oxide content and with few alkaline impurities (Hamer and Hamer, 2015, p.199). Gongyi is rich with this clay mineral (Henan Provincial Institute of Cultural Heritage and Archaeology et al., 2016b, p.2). The theoretical formula of kaolinitic clay is $Al_4(Si_4O_{10})(OH)_8$ or $Al_2O_3{\cdot}2SiO_2{\cdot}2H_2O$ which does not contain K, Na and Fe. A similar calculation used for hypothesis 1 also is applied for hypothesis 2. However, the target is not to predict the content of K_2O, nor other impurities. This calculation aims to explore the SiO_2 content provided by the other source of silicon rather than to verify the use of kaolinitic clay.

1) Calculate n(Al_2O_3) of raw glazes by dividing m(Al_2O_3) from XRF by its molar mass M(Al_2O_3)

   n (Al_2O_3) = m (Al_2O_3) / M (Al_2O_3)

2) Double n(Al_2O_3) to get n(SiO_2)

   n (SiO_2) = 2n (Al_2O_3)

3) Estimate theoretical values m'(SiO_2) from kaolinitic clay.

   m' (SiO_2) = n (SiO_2) * M (SiO_2)

4) Obtain the difference Δm (SiO_2) (Figure 5. 11 a) between data m (SiO_2) tested by XRF (Figure 5. 11a) and theoretical m' (SiO_2) contributed by kaolinitic clay (Figure 5. 11b). Theoretically, this difference is close to SiO_2 from the other source – the high/pure-Si material.

$\Delta m\ (SiO_2) = m\ (SiO_2) - m'\ (SiO_2)$

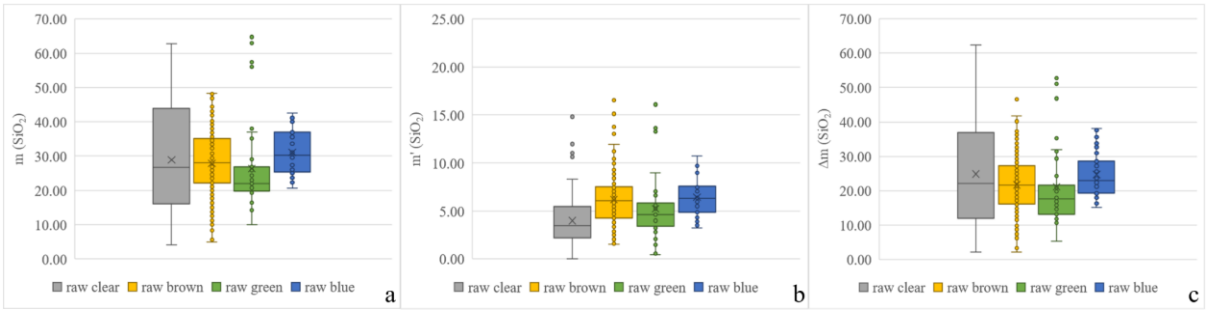


Figure 5. 11 Box plots of (a) m (SiO_2), (b) m' (SiO_2) and (c) Δm (SiO_2) of raw glazes. The calculation is based on hypothesis 2: kaolinitic clay.

Theoretically, pure clay is 47% silica but in practice the ranges of SiO_2 and Al_2O_3 vary for clays in different places. And clay used by different batches of products might not be totally the same. The level of main and trace elements may fluctuate a little. A theoretical value cannot represent all materials. A more practical method is the use of the data for body materials. That is hypothesis 3: body material. Using the same kaolinitic clay for body and in glaze is a tradition in ceramic production. It makes similar thermal expansion properties of body and glaze to avoid too much cracking. To be close to the practice, the body and raw glaze of every sherd was linked. To be more precise, every body was regarded as a 'body material'. The average compositions of bodies calculated by all sherds was not used. For instance, the prediction of raw glazes on HY-43 was calculated based on the body composition of HY-43. The calculation is as follow:

1) Calculate the amount of substance n1(Al_2O_3) and n2(SiO_2) of bodies by dividing m(Al_2O_3) and m(SiO_2) both obtained from XRF by its molar mass.

   n1 (Al_2O_3) = m (Al_2O_3) / M (Al_2O_3)

   n2 (SiO_2) = m (SiO_2) / M(SiO_2)

2) Calculate the amount of substance n(Al_2O_3) of raw glazes by dividing m(Al_2O_3) by its molar mass.

   n (Al_2O_3) = m (Al_2O_3) / M (Al_2O_3)

3) Estimate theoretical value m'(SiO_2) obtained from body material (Figure 5. 12 b) by n(Al_2O_3) times the ratio of n2/n1 and times M(SiO_2).

   m' (SiO_2) = n (Al_2O_3) *(n2/n1) * M (SiO_2)

4) Obtain the difference Δm (SiO_2) (Figure 5. 12c) between data m(SiO_2) tested by XRF (Figure 5. 12 a) and theoretical value m'(SiO_2) provided by the body material (Figure 5. 12b). The Δm (SiO_2) should equal to quartz from the high/pure-Si source.

   Δm (SiO_2) = m (SiO_2) – m' (SiO_2)

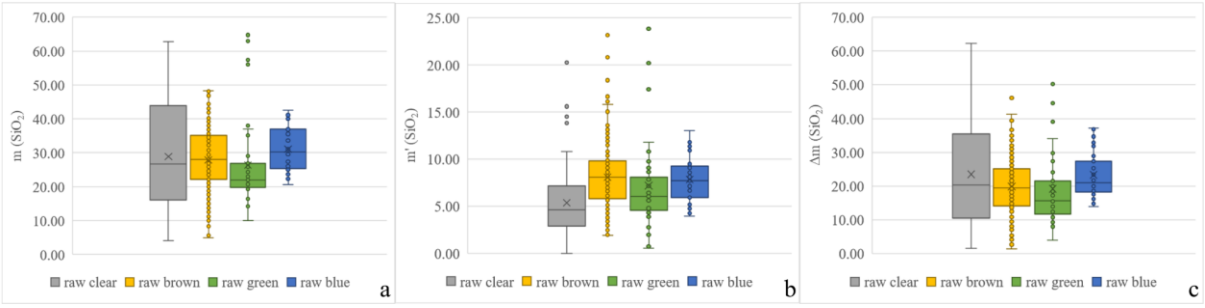


Figure 5. 12 Box plots of (a) m (SiO_2), (b) m' (SiO_2) and (c) Δm (SiO_2) of raw glazes. The calculation is based on hypothesis 3: body material.

Compared with theoretical kaolinitic clay, the body material offered a little more SiO_2 (Figure 5. 11b and Figure 5. 12b). It suggests that clay used for body contains higher SiO_2. This calculation also can be used to estimate the difference between XRF data and theoretical values

of K_2O, Fe_2O_3 and TiO_2 by replacing SiO_2 with K_2O, Fe_2O_3 and TiO_2. If body material was added into glaze recipe as the source of high-Si-and-Al ingredient, the Δm (K_2O), Δm (Fe_2O_3) and Δm (TiO_2) should be around zero since all these impurities are brought in glaze by that high-Si-and-Al material. The calculation processes are as follow:

K_2O:

$n1\ (Al_2O_3) = m\ (Al_2O_3) / M\ (Al_2O_3)$

$n2\ (K_2O) = m\ (K_2O) / M(K_2O)$

$n\ (Al_2O_3) = m\ (Al_2O_3) / M\ (Al_2O_3)$

$m'\ (K_2O) = n\ (Al_2O_3) *(n2/n1) * M\ (K_2O)$

$\Delta m\ (K_2O) = m\ (K_2O) – m'\ (K_2O)$

Fe_2O_3:

$n1\ (Al_2O_3) = m\ (Al_2O_3) / M\ (Al_2O_3)$

$n2\ (Fe_2O_3) = m\ (Fe_2O_3) / M(Fe_2O_3)$

$n\ (Al_2O_3) = m\ (Al_2O_3) / M\ (Al_2O_3)$

$m'\ (Fe_2O_3) = n\ (Al_2O_3) *(n2/n1) * M\ (Fe_2O_3)$

$\Delta m\ (Fe_2O_3) = m\ (Fe_2O_3) – m'\ (Fe_2O_3)$

TiO_2:

$n1\ (Al_2O_3) = m\ (Al_2O_3) / M\ (Al_2O_3)$

$n2\ (TiO_2) = m\ (TiO_2) / M(TiO_2)$

$n\ (Al_2O_3) = m\ (Al_2O_3) / M\ (Al_2O_3)$

$m'\ (TiO_2) = n\ (Al_2O_3) *(n2/n1) * M\ (TiO_2)$

$\Delta m\ (TiO_2) = m\ (TiO_2) – m'\ (TiO_2)$

Only one sherd, HY-43, contains raw blue glaze but many sherds were decorated by raw clear, brown, and green glazes. To make the comparison more reliable, data for all raw glazes of HY-43 were added into this comparison (Figure 5. 13). The data labelled with 43 can be regarded as an example of one production batch. The results of Δm (K_2O) and Δm (TiO_2) prove the use of body material perfectly. Almost all data for Δm (K_2O) and Δm (TiO_2) are very close to the zero line (Figure 5. 13 a and b). Figure 5. 13c shows the data for Δm (Fe_2O_3) of all raw glazes is higher than zero. Δm (Fe_2O_3) of raw brown glaze is much higher than zero, which is caused by the iron colourant. Why are Δm (Fe_2O_3) of other glazes higher than zero? Whether it suggests a little higher Fe_2O_3 in raw glaze than in body?

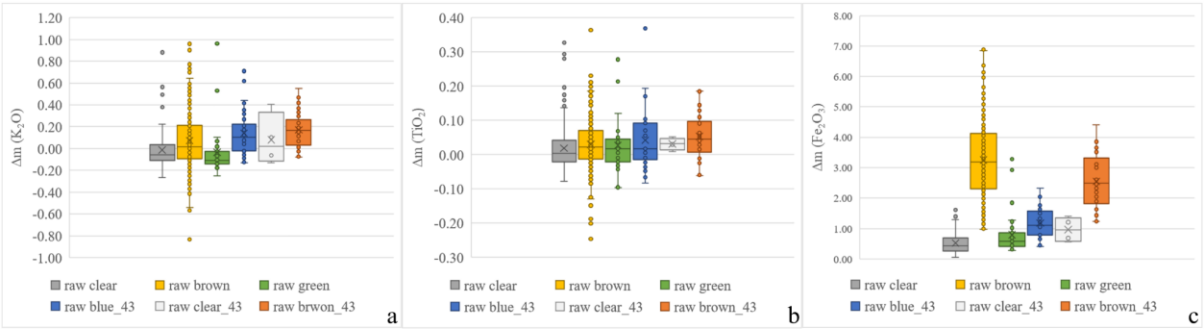


Figure 5. 13 Box plots of (a) Δm (K_2O), (b) ΔTiO_2 and (c) ΔFe_2O_3 of all raw glazes and of blue, clear, and brown glazes of HY-43

Figure 5. 14a and c reveal two confusing findings. Fe_2O_3 of bodies is nearly equal to that of raw blue glaze, and a little higher than that in the raw clear and green glazes. But, obviously, TiO_2 of bodies is higher than of raw glazes. The second is Fe_2O_3/TiO_2 ratios of clear, green, and blue glazes is much higher than that of bodies. Noticeably, the comparison among original data for elements is not reliable since the amount and proportion of this clay in body and glaze is different. The only constituent of bodies is this clay, but the glaze recipe included several ingredients. The level of iron in the raw glaze might be reduced since all compositional results are normalised. The direct comparison of Fe_2O_3 and TiO_2 contents in bodies and glazes is not

reliable. Hence, the ratios of Fe_2O_3, TiO_2 to Al_2O_3 were calculated to explore the levels of these elements in bodies and glazes. It is assumed that all Al_2O_3 and TiO_2 in the glazes both came from the clay. Therefore, the ratios of TiO_2/Al_2O_3 should be the same. Figure 5. 14e evidences this assumption. Figure 5. 14d shows higher Fe_2O_3/Al_2O_3 in raw clear, green, and blue glaze than in bodies. Accordingly, the reason for higher ratios of Fe_2O_3/TiO_2 of raw glazes than of bodies is due to higher Fe_2O_3 in the glazes. The same clay was employed for the body and the glaze, and the same proportion of TiO_2 was contributed by this clay. Why are the levels of Fe_2O_3 different?

Obviously, the iron colourant in the brown glaze caused much higher Δm (Fe_2O_3) (Figure 5. 13c). The significant finding is that the Δm (Fe_2O_3) of colourless clear glaze is also above zero. In other words, the stock glaze without any colourant has higher Fe_2O_3 than the bodies. There are two possibilities. First, the clay might be purified before making bodies but used directly in glaze. Perhaps the potters had realised that some iron in glazes did not change the colours. Thus, to simplify the manufacturing process, the clay was collected and used directly. In contrast, the same level of iron could tint the body. And to make a whiter body, some purification measures were taken. The TiO_2 levels of all glazes are the same, which suggests that the processing has not removed TiO_2. Δm (TiO_2) remained around zero. The other possibility is that other ingredients of stock glaze, perhaps flux or quartz, also contain some iron impurities. According to Figure 5. 14b, the first possibility is closer to the evidence for the practice of Sancai production. Fe_2O_3 and TiO_2 of raw glazes presents positive correlation but the data of the bodies are disordered. If the clay was not purified, Fe_2O_3 and TiO_2 of bodies should keep a positive correlation. As the black rectangular points in Figure 5. 14b shown, Fe_2O_3 varies considerably when TiO_2 is at the same level, which ought to be caused by cleaning of the body materials. For example, when the TiO_2 is 1.2%, the Fe_2O_3 varied from 0.7-2.5%

Figure 5. 14b. If no cleaning or purifying process was accepted, the Fe_2O_3 and TiO_2 of the bodies should show the similar positive correlation with Fe_2O_3 and TiO_2 of clear, green, and blue glazes. When the TiO_2 content of the bodies is 1.2%, the Fe_2O_3 should concentrate on a narrow range.

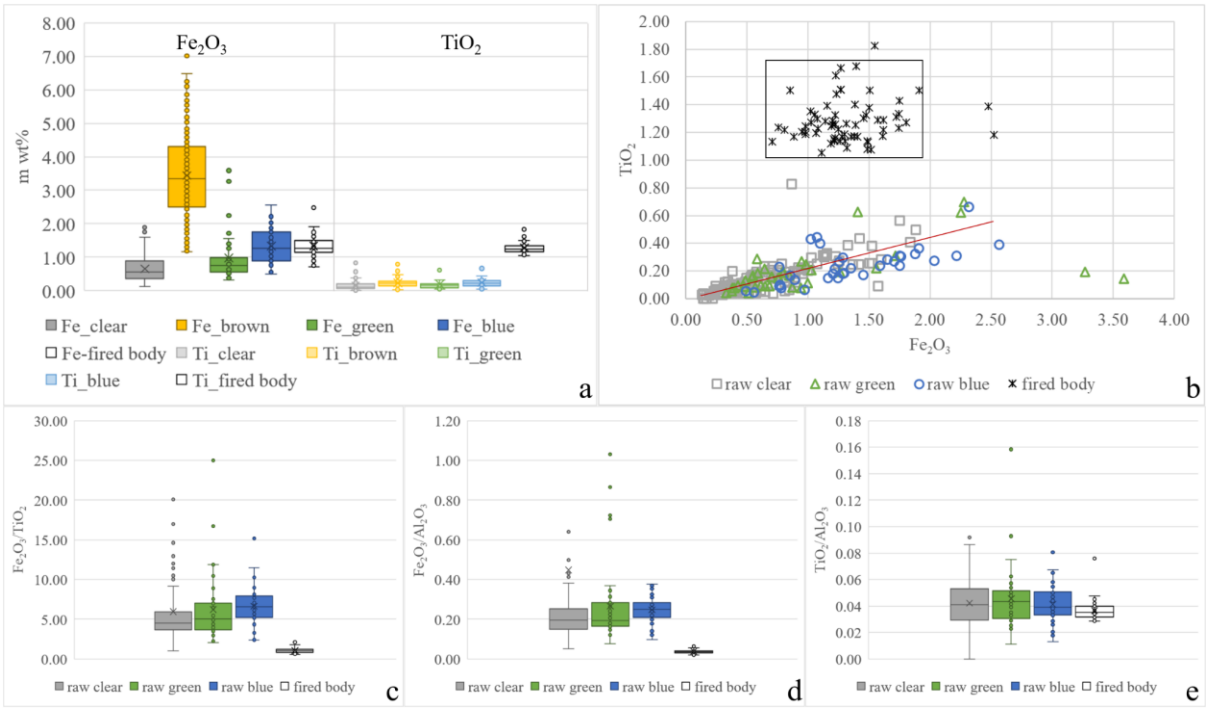


Figure 5. 14 (a) Box plot of Fe_2O_3 and TiO_2 of raw glazes and of fired bodies. (b) Scatter diagram of TiO_2 to Fe_2O_3 of raw clear, green, and blue glazes. Box plots of (c) Fe_2O_3/TiO_2 ratios, (d) Fe_2O_3/Al_2O_3 ratios and (e) TiO_2/Al_2O_3 ratios of raw clear, green, blue glaze and fired bodies.

This un-purified clay used in raw glaze contains many Fe-rich particles, excluding iron colourant grains. Mostly, Fe is associated with Mg, Al, Si, K and O. No matter whether in brown, green, blue, or clear, a majority of Fe-Mg-Si-Al-(K)-O-associated grains were found in the raw glazes (Figure 5. 15[26]). Only one example of Ti-Fe-associated particles in raw blue

[26] Detailed mapping images are presented in Chapter 4.1 (Figures 4.8-4.11 and 4.13-4.16)

glazes was observed (Figure 5. 16). Most of Ti-rich particles only show the presence of Ti (Figure 5. 17), and the Ti content is very high (Table 5. 5). To avoid the 'contamination' from the lead powder, the analytical results of Ti-rich particles (Figure 5.18) was re-calculated (Table 5. 6).

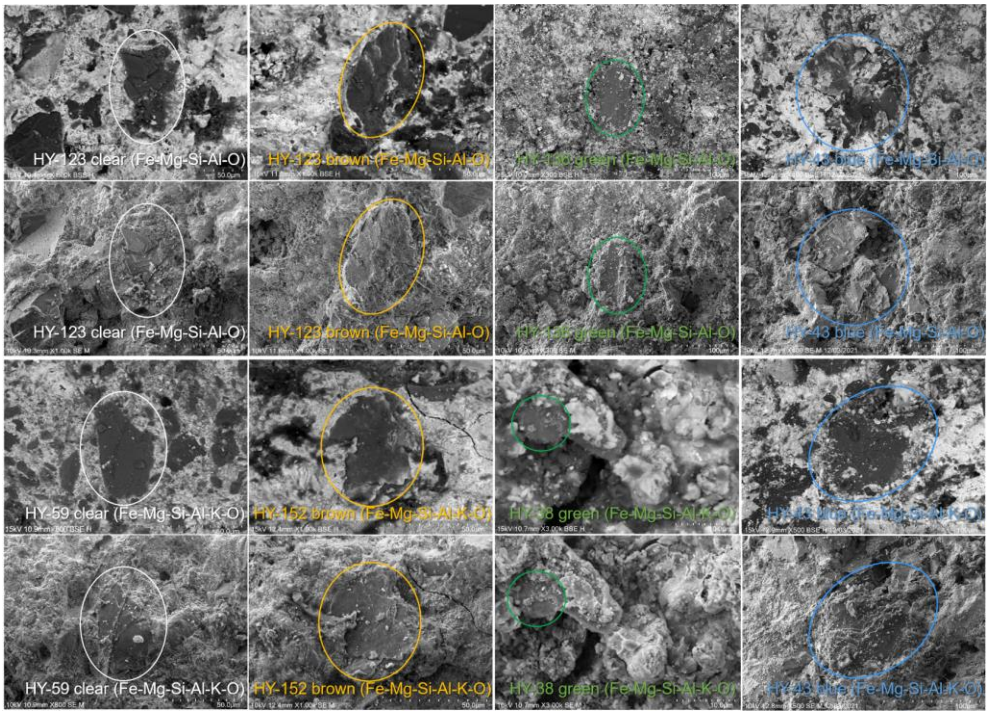


Figure 5. 15 BSE (the first and third rows) and SE (the second and fourth rows) images of Fe-Si-Al-O-associated particles and Fe-Mg-Si-Al-K-O-associated particles in raw glazes, obtained from ESEM.

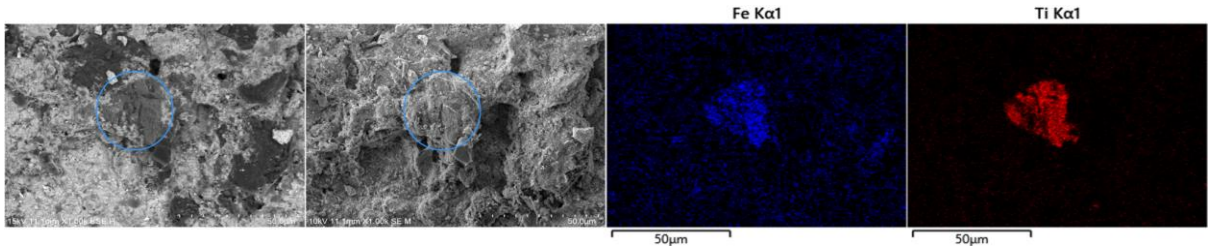


Figure 5. 16 BSE (left), SE (centre left) and mapping (right) images of Fe-Ti-associated particle in blue glaze of HY-43

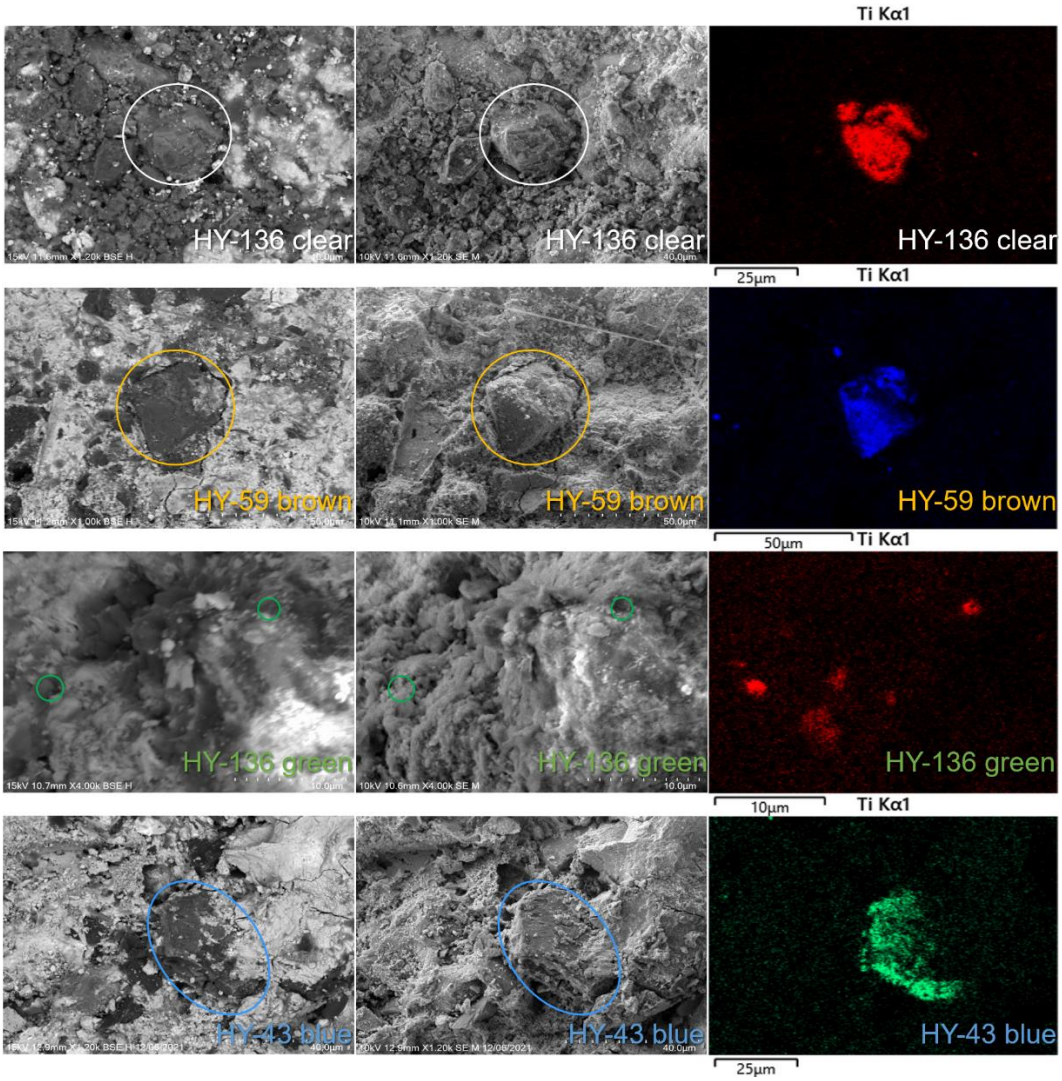


Figure 5. 17 BSE (left column), SE (central column) and mapping (right column) images of Ti-rich particles in raw glazes, obtained from the ESEM.

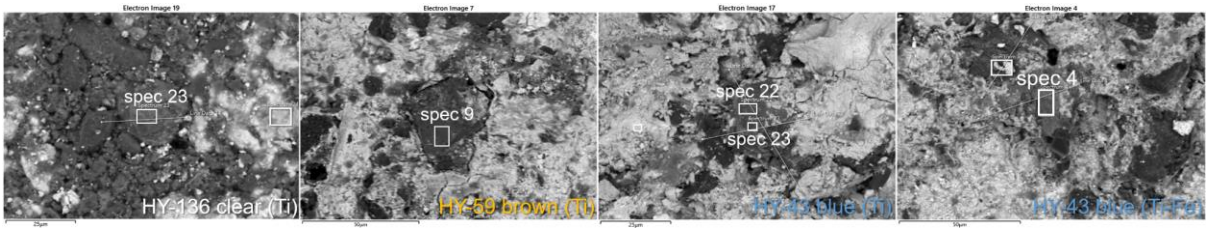


Figure 5. 18 Test areas of Ti-rich particles in raw glazes, obtained from the ESEM.

Table 5. 5 Chemical compositions of Ti-rich particles in raw glazes

Samples	Glaze colours	Particle types	Na_2O	MgO	Al_2O_3	SiO_2	P_2O_5	K_2O	CaO	TiO_2	MnO	FeO	CoO	CuO	As_2O_3	PbO
HY-136 spec 23	Clear	Ti	0.35	1.91	7.78	14.66	1.74	0.92	2.49	62.03	-	1.92	-	-	-	6.01
HY-59 spec 9	Brown	Ti	-	1.87	7.17	14.46	4.82	2.27	5.92	30.71	-	3.69	-	-	-	28.14
HY-43 spec 22	Blue	Ti	-	2.55	5.39	9.11	2.45	0.46	2.11	39.45	-	8.72	6.52	1.88	-	21.10
HY-43 spec 23	Blue	Ti	-	3.97	8.04	14.75	4.68	2.01	4.45	25.89	-	1.80	1.19	2.73	1.64	28.22
HY-43 spec 4	Blue	Ti-Fe	-	1.32	4.20	9.18	0.69	0.45	0.56	51.67	1.82	27.93	-	-	-	2.17

Table 5. 6 Chemical compositions of Ti-rich particles (remove Pb and re-normalised) in raw glaze

Oxide	Glaze colours	Particle types	Na_2O	MgO	Al_2O_3	SiO_2	P_2O_5	K_2O	CaO	TiO_2	MnO	FeO	CoO	CuO	As_2O_3
HY-136 spec 23	Clear	Ti	0.37	2.04	8.29	15.63	1.86	0.98	2.65	66.13	-	2.05	-	-	-
HY-59 spec 9	Brown	Ti	-	2.64	10.11	20.39	6.80	3.20	8.35	43.31	-	5.20	-	-	-

Oxide	Glaze colours	Particle types	Na_2O	MgO	Al_2O_3	SiO_2	P_2O_5	K_2O	CaO	TiO_2	MnO	FeO	CoO	CuO	As_2O_3
HY-43 spec 22	Blue	Ti	-	3.24	6.85	11.58	3.12	0.58	2.68	50.17	-	11.09	8.29	2.39	-
HY-43 spec 23	Blue	Ti	-	5.58	11.30	20.73	6.58	2.83	6.25	36.39	-	2.53	1.67	3.84	2.30
HY-43 spec 4	Blue	Ti-Fe	-	1.35	4.29	9.38	0.71	0.46	0.57	52.82	1.86	28.55	-	-	-

All raw glazes discussed in this thesis were made in the Tang dynasty. However, it is not possible to find raw/unfired bodies because unfired bodies can soften in water and re-used with the original raw materials. To learn more about the clay in Gongyi, I collected some kaolin stones in a modern Sancai kiln in Luoyang (Figure 5. 19). These stones are various shades of grey and were analysed by ESEM (Figure 5. 20 and Table 5. 7). Although the collection date of these kaolin stones is far removed from the Tang dynasty (618-907 CE) by more than one thousand years, this difference is very short in geological term. This comparison can therefore still reveal some typical characteristics of the clay. The obvious and important characteristic is high alumina, approximately 43-58%, higher than typical china clay at 44% (Hamer and Hamer, 2015, p.65). Shen et al. (2019) also found the high alumina contents in Sancai glazes, which implies that it is highly like to have been added to the glaze recipe deliberately in the form of clay. The use of high-Al clay in Gongyi ceramics is a tradition, not only in Sancai, but also in Tang blue-and-white porcelain (Zhang et al., 1986; Chen et al., 1995). Furthermore, some potassium was found in this clay. This characteristic matches the scientific results of raw glazes by ESEM and XRF. Also, trace titanium and iron were analysed.



Figure 5. 19 Photo of kaolinitic clay in a modern Sancai kiln in Luoyang, taken by the author. Luoyang is situated about 54 kilometres as the crow flies to the west of Gongyi.

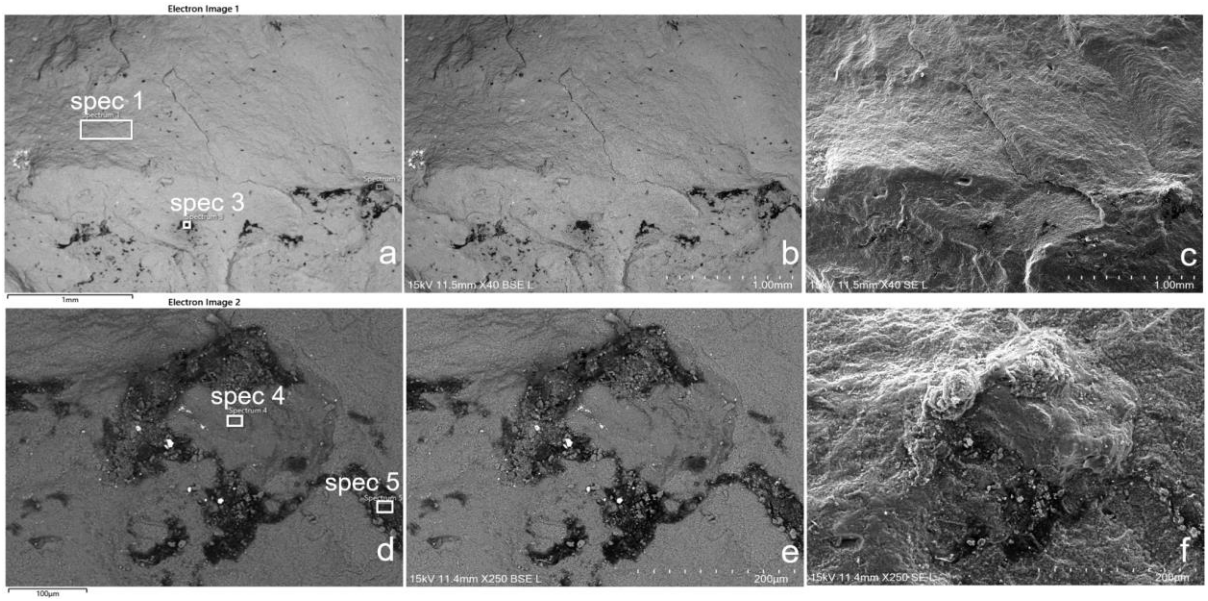


Figure 5. 20 (a and d) Test areas, (b and e) BSE and (c and f) SE images of kaolinitic clay, obtained from the ESEM.

Table 5. 7 Chemical compositions of kaolinitic clay collected in Luoyang by ESEM

Samples	Na_2O	MgO	Al_2O_3	SiO_2	P_2O_5	SO_3	K_2O	CaO	TiO_2	FeO	Ho_2O_3	MoO_3
map	0.43	0.56	49.53	46.91	-	-	1.45	0.50	0.62	-	-	-
spec 1	-	0.88	49.87	46.30	-	-	1.18	0.46	0.60	-	0.72	-
spec 2	0.56	0.69	44.48	46.08	-	1.01	2.57	1.77	1.14	1.69	-	-
spec 3	1.15	0.68	43.49	42.92	0.98	0.00	4.23	2.21		0.94	-	1.94
spec 4	0.39	0.45	58.43	37.85	-	-	1.34	0.45	0.65	0.44	-	-
spec 5	0.45	0.80	44.54	47.38	-	0.95	1.76	1.77	1.46	0.91	-	-
Mean values	0.60	0.68	48.39	44.57	0.98	0.65	2.09	1.19	0.89	1.00	0.72	1.94

5.1.2 Flint and Sand?

Kaolinitic clay provided all the Al and some Si to the stock glaze and a high/pure-silica material was added into the glaze to bring the other silica. Many Si-O-associated grains were found by ESEM observation (Figure 5. 21), the compositions of which are almost pure SiO_2 (Table 5. 8 and Table 5. 9). The key question is what is the source of the pure SiO_2 constituent? and why was the silica added into the stock glaze?

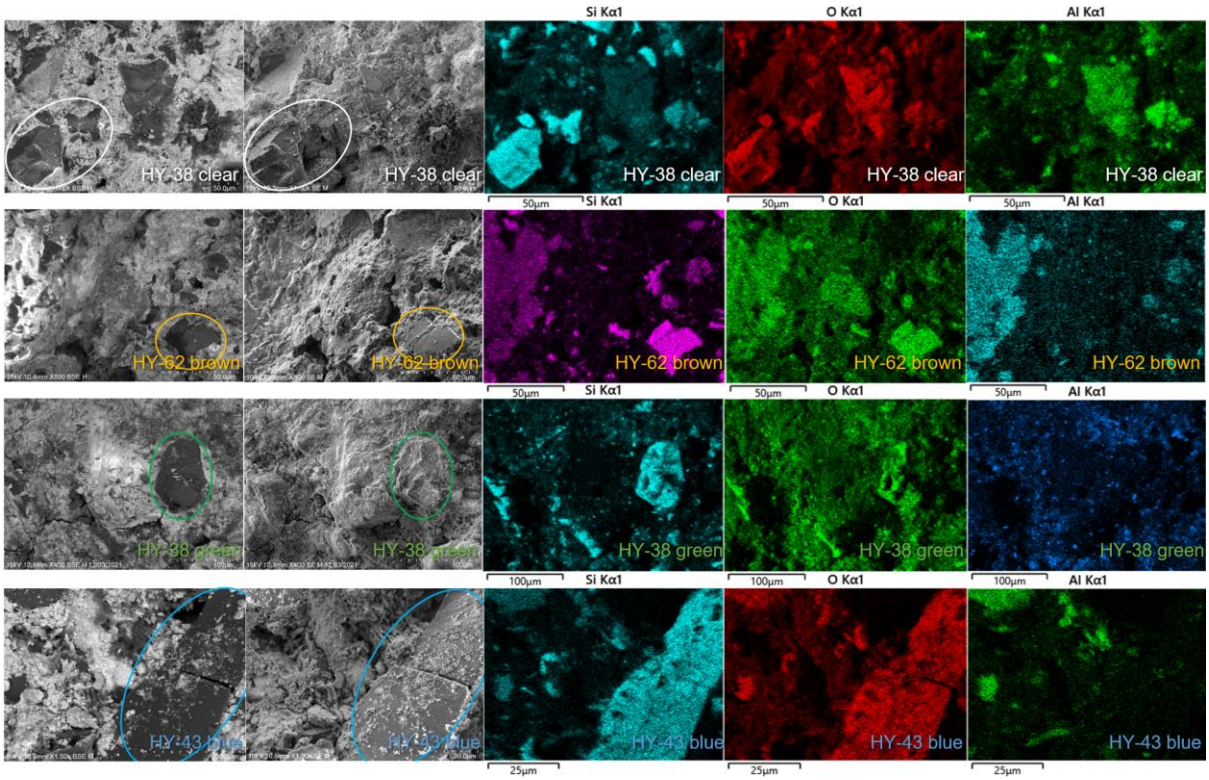


Figure 5. 21 BSE (the first column), SE (the second column) and mapping (other columns) images of Si-O-associated particles in raw glazes, obtained from ESEM.

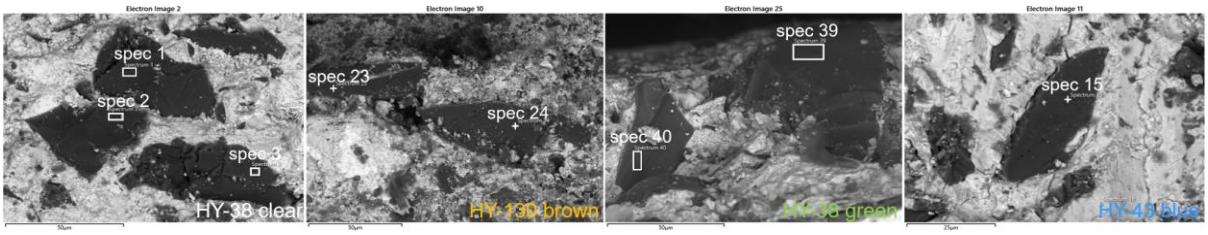


Figure 5. 22 Test areas of Si-O-associated particles in raw glazes, developed from ESEM.

Table 5. 8 Chemical compositions of Si-O-associated particles in raw glazes by ESEM

Glaze colours	Samples	Al_2O_3	SiO_2	P_2O_5	K_2O	CaO	FeO	PbO
Clear	HY-38 spec 1	2.40	83.63	-	0.27	0.82	-	12.88
	HY-38 spec 2	2.72	81.83	-	0.23	0.95	-	14.28
	HY-38 spec 3	3.75	74.60	1.26	0.34	1.30	-	18.75
Brown	HY-130 spec 23	5.57	79.82	0.96	0.49	1.31	0.74	10.86
	HY-130 spec 24	4.54	85.48	-	0.50	0.99	0.55	7.94
Green	HY-38 spec 15	5.10	76.19	2.72	0.53	1.80	-	13.4
Blue	HY-43 spec 39	8.54	85.83	-	0.32	0.63	-	4.69

Table 5. 9 Calculated compositions of Si-O-associated particles of raw glazes by ESEM. The data was normalised after decreasing P_2O_5 and PbO

Glaze colours	Samples	Al_2O_3	SiO_2	K_2O	CaO	FeO
Clear	HY-38 spec 1	2.75	95.99	0.31	0.94	-
	HY-38 spec 2	3.17	95.46	0.27	1.11	-
	HY-38 spec 3	4.69	93.26	0.43	1.63	-
Brown	HY-130 spec 23	6.34	90.79	0.56	1.49	0.84
	HY-130 spec 24	4.93	92.85	0.54	1.08	0.60
Green	HY-38 spec 15	6.10	91.10	0.63	2.15	-
Blue	HY-43 spec 39	8.96	90.05	0.34	0.66	-

Silica, the glassy substance, is the most important constituent of glazes. It occurs naturally as quartz rock, flint, and sand. It also occurs in combination with other oxides in silicates. Quartz rock is the purest occurrence being 99% silica and only 1% impurity (Hamer and Hamer, 2015, p.331). However, the quartz in raw glazes contains some Al and Ca. It is probably not a quartz rock. The BSE and SE images present the flat surface and conchoidal fracture that indicates a glassy nature (Figure 5. 23 - Figure 5. 26). These characteristics match flint. Flint is cryptocrystalline native silica containing less than 5% impurity. It varies in colour from light to dark brown and black (Figure 5. 27) (Hamer and Hamer, 2015, p.142). In some samples, some black glassy grains can be recognised by the naked eyes (Figure 5. 28). Possibly, therefore, they are ground flint grains.

Raw flint is hard and therefore difficult to grind. However, calcination renders the flint crumbly and brittle and breaks the existing weak bonds between the micro-crystals enabling grinding to break down the flint into an exceedingly fine powder (Hamer and Hamer, 2015, pp.142-143). And remarkably, the calcination turns the flint from its native dark colour to white. In the modern ceramic industry, flint is purchased as a white powder for introduction into bodies and glazes. This might explain why black flints was only found in a few samples rather than in all. Most of the raw glazes might contain brown or white flint grains which is difficult to be recognised by the naked eye. The existence of black flint grains in raw glazes suggest that the processing method in the Tang-dynasty Gongyi kiln was not perfect. Those samples showed in Figure 5. 28 might be defective products.

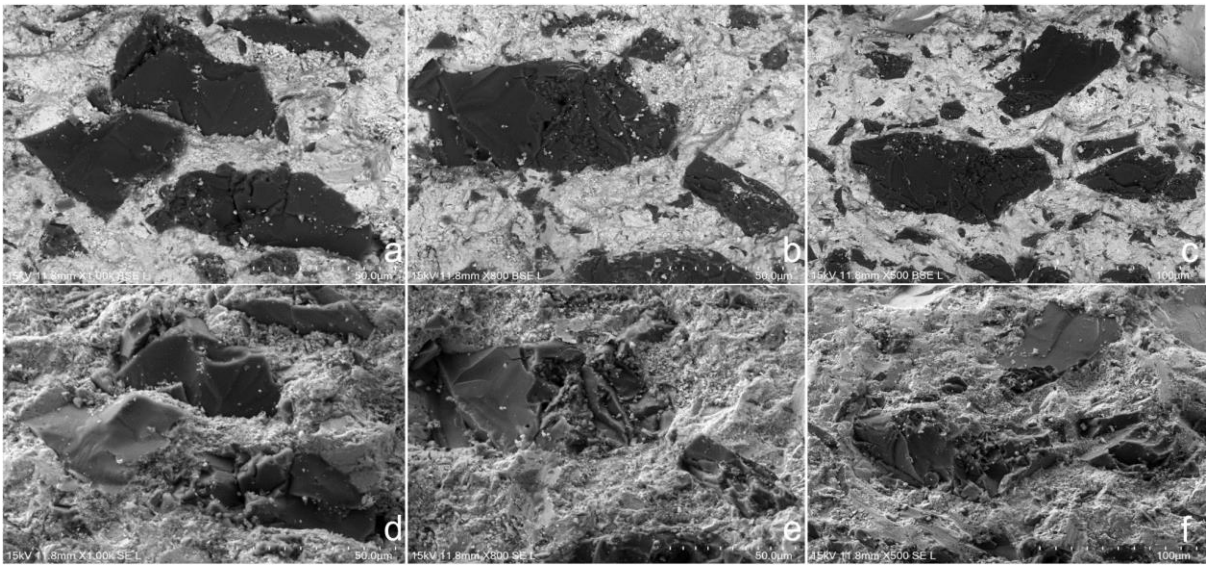


Figure 5. 23 BSE (a-c) and SE (d-f) images of possible flint grains in raw clear glaze of HY-38, obtained from ESEM.

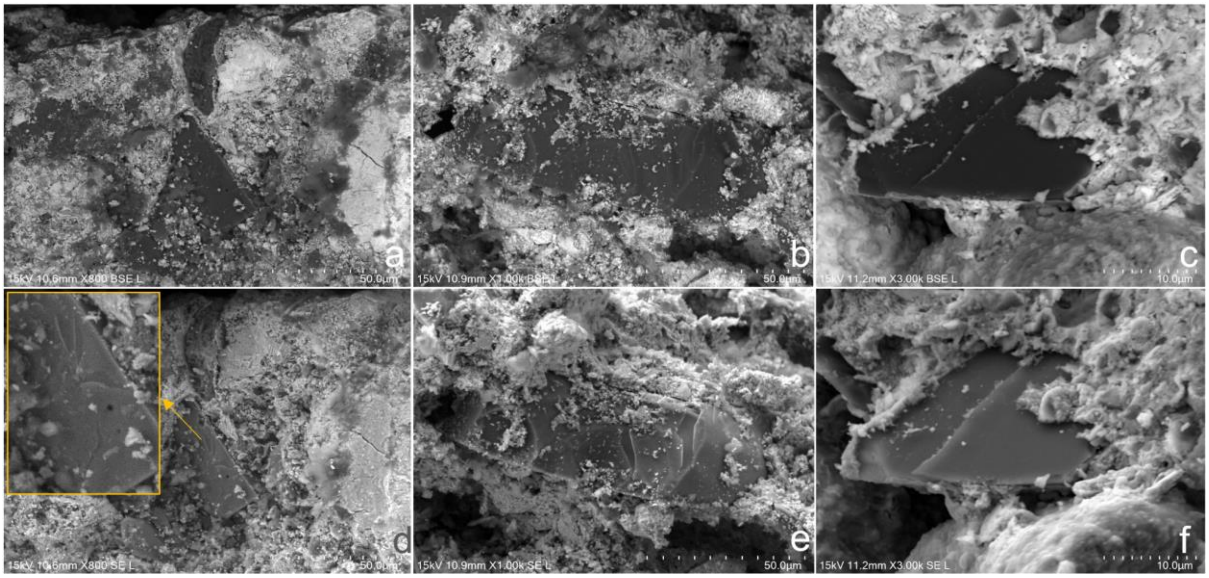


Figure 5. 24 (a-c) BSE and (c-f) SE images of possible flint grains in raw brown glaze of HY-130, obtained from ESEM.

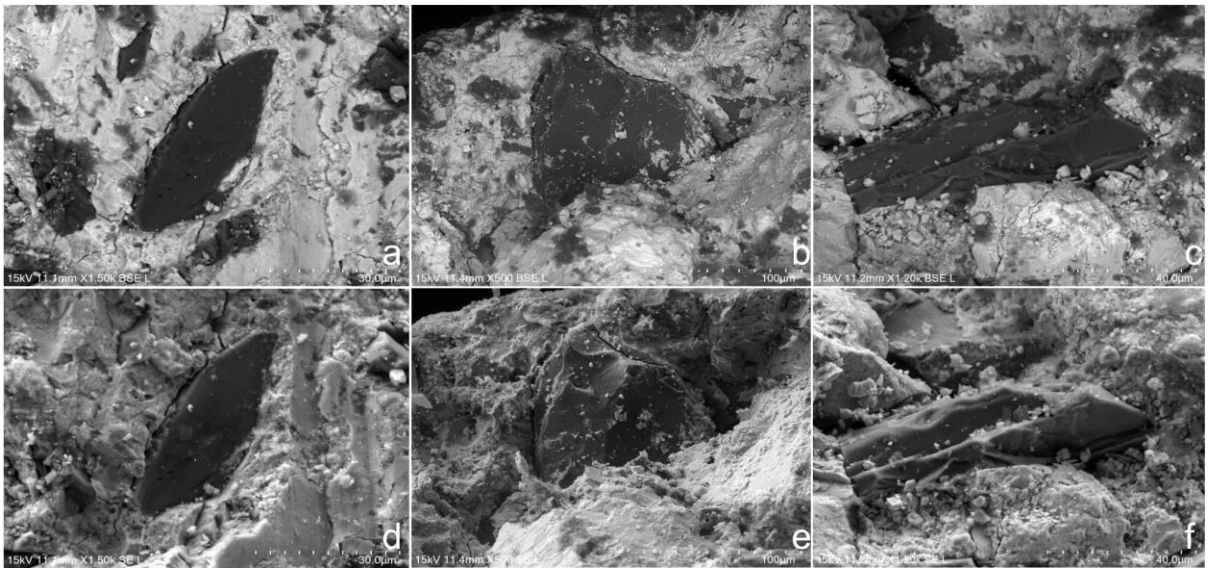


Figure 5. 25 (a-c) BSE and (c-f) SE images of possible flint grains in raw green glaze of HY-38, obtained from ESEM.

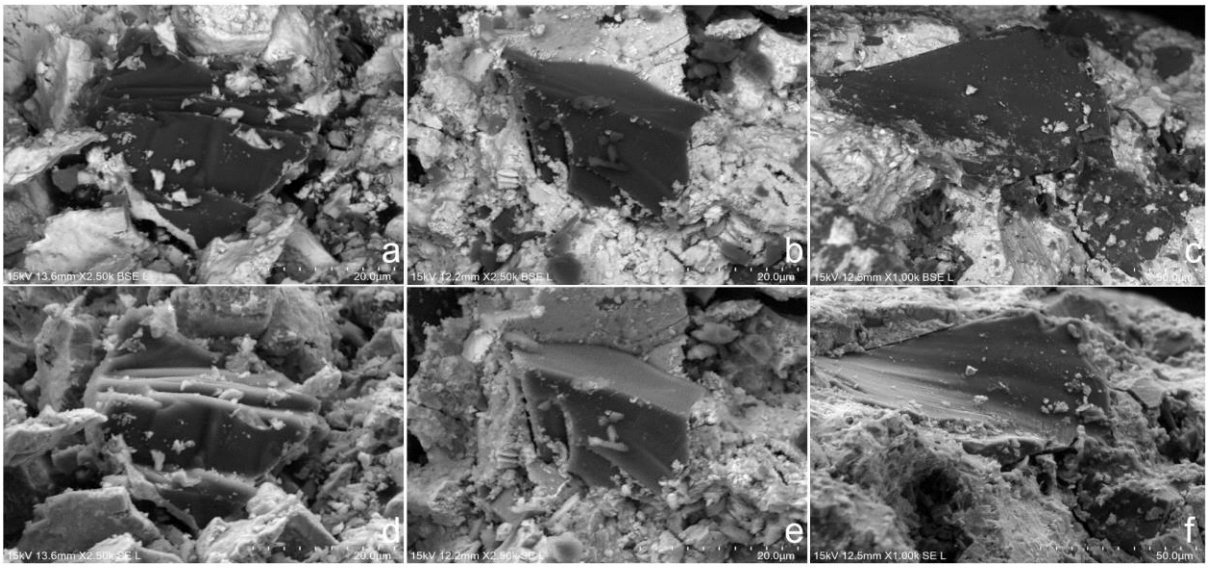


Figure 5. 26 (a-c) BSE and (c-f) SE images of possible flint grains in raw blue glaze of HY-43, obtained from ESEM.

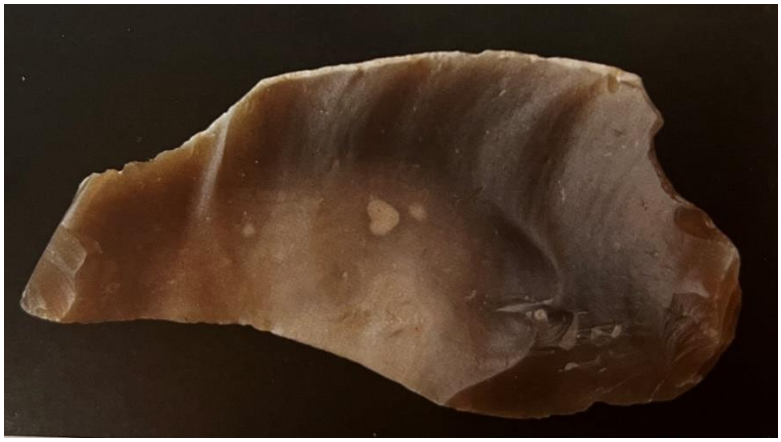


Figure 5. 27 Photo of a flint, from Hamer and Hamer, 2015 (p.142).

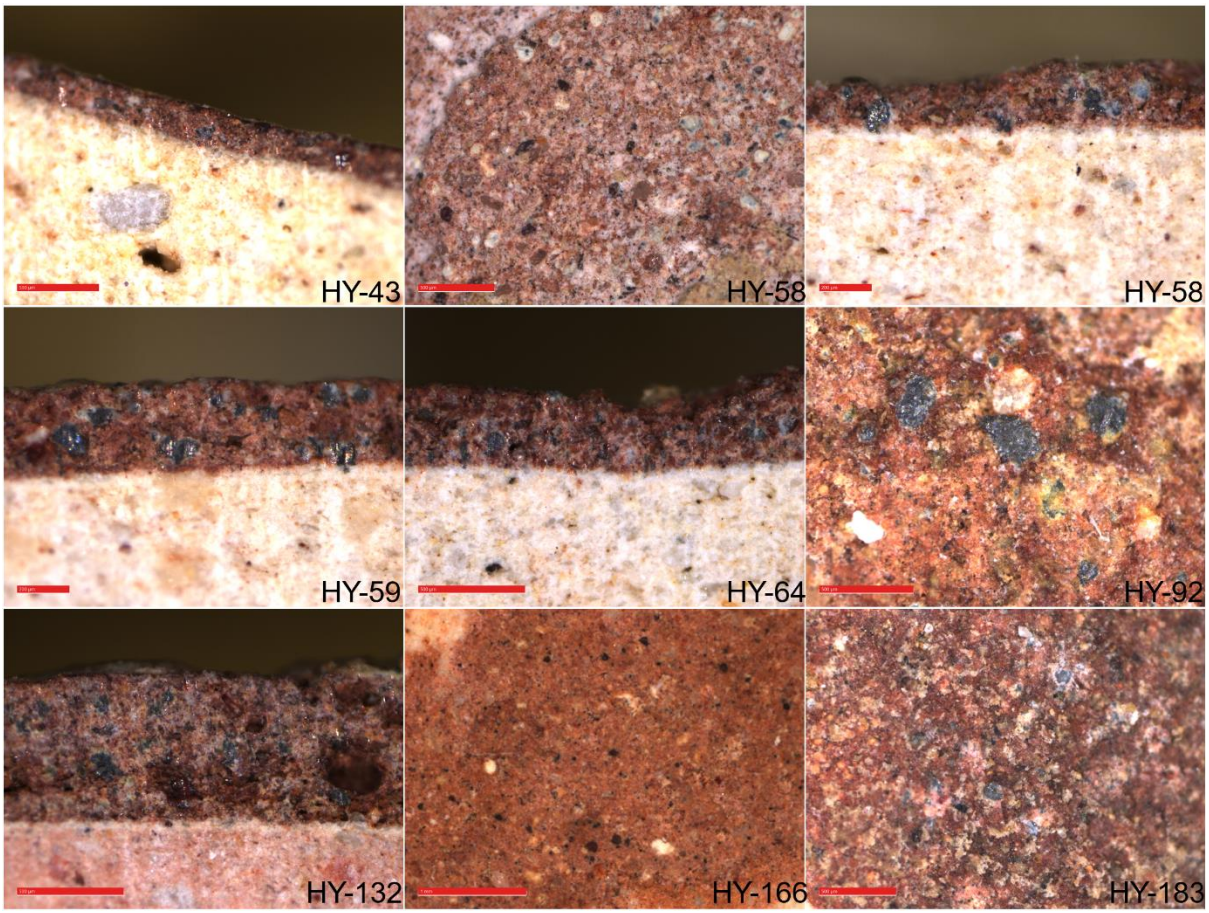


Figure 5. 28 Photos of possible black flint grains in raw brown glazes, obtained from the optical microscope.

Most quartz grains in the raw glazes did not show layers, conchoidal fracture or glassy nature (Figure 5. 29 - Figure 5. 32). The main tone of colours is (semi-)transparent, white, milky, and pale yellow. And a large number of high/pure-silica grains can be observed by optical microscope (Figure 5. 33). Presumably, they are sands. The shapes of sand grains are not so sharp as those of flints. A few round particles were found (Figure 5. 29). Compared with flint, sand is not so pure. It varies in composition from pure silica to a mixture of silica, calcium compounds (shells), clay and soluble salts (Hamer and Hamer, 2015, p.320). The compositional analysis found high alumina in some sand grains (Figure 5. 34 and Table 5. 10). This finding confirms the use of sand in raw glazes. As a natural ground quartz, sand is also hard and difficult to grind. Therefore, Chinese potters generally first heat it to around 1000℃. The volumetric expansion reaches to 2-4%. Next, rapid cooling was carried out. This method can break the quartz sand (Li and Guo, 2012, p.18). The broken sand and flint grains have different sizes (Figure 5. 35). The size of the large grains is greater than 100μm and the small ones are only around 20μm (Figure 5. 35). Relatively, the amount and size of quartz is large. It is easy to be found in the raw glaze (Figure 5. 36 - Figure 5. 39).

After identifying the sources and manufacturing method of the quartz, the next central question is why potters added high/pure-silica materials into raw glazes? Kaolinitic clay can offer silicon to the raw glaze, so why did potters not use it alone? The key point is aluminium. Definitely, kaolinitic clay contributed high silica to the glaze, but at the same time, high aluminium was also brought in. A simplified calculation can be proposed. If all SiO_2 in glaze was only provided by kaolinitic clay, same as the body material, how much Al_2O_3 would be brought into the glaze? The mean SiO_2 and Al_2O_3 of bodies are 56.23% and 35.34 % respectively. The ratio of SiO_2 to Al_2O_3 is 1.59. The estimated Al_2O_3 contents of the glazes by using the mean SiO_2 of 1.59 are 16.10% (clear glaze), 17.55% (brown glaze), 16.56% (green

glaze) and 19.56% (blue glaze). Generally, in ceramic production, most glazes contain between 5-15% aluminium oxide, and this is easily dissolved in the glaze. Amounts in excess of this separate from the molten mass during cooling to give a crystalline opacity and a matt surface. Alumina matts can be very greyish, of poor opacity, pin-holed and with a tendency to crawl[27] (Hamer and Hamer, 2015, p.7). Obviously, the estimated aluminium is higher than the normal scale. Moreover, too much alumina can raise the melting point too high. Although silica also can increase the melting temperature, it is only half as effective as aluminium oxide in its power to raise a melting point (Hamer and Hamer, 2015, p.8). Therefore, for purposes of glaze fit, potters accepted extra silica which increase the resistance to abrasion of the final glaze and improve its glassiness.

The last question about silica is why mix two sources of quartz – flint and sand? For example, flint and sand grains were both found in the glazes (Figure 5.33). Besides the availability of two sources of quartz, one advantage perhaps was recognised by Gongyi potters in the Tang dynasty. Flint should melt more easily than quartz but a mixture of the two will probably be found to melt more easily than either alone because of the phenomenon of interaction (Hamer and Hamer, 2015, p.311).

[27] The glaze defect characterised by the way the glaze parts and rolls back on itself leaving a bald patch of body (Hamer and Hamer, 2015,p.93).

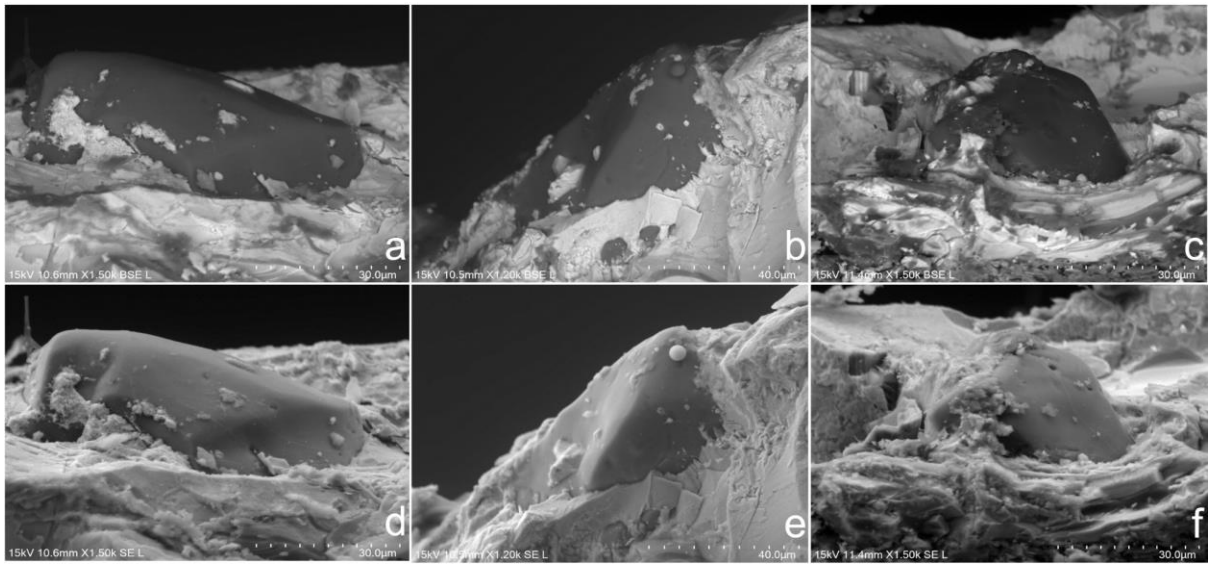


Figure 5. 29 (a-c) BSE and (c-f) SE images of sand grains in raw clear glaze of HY-101, obtained from ESEM.

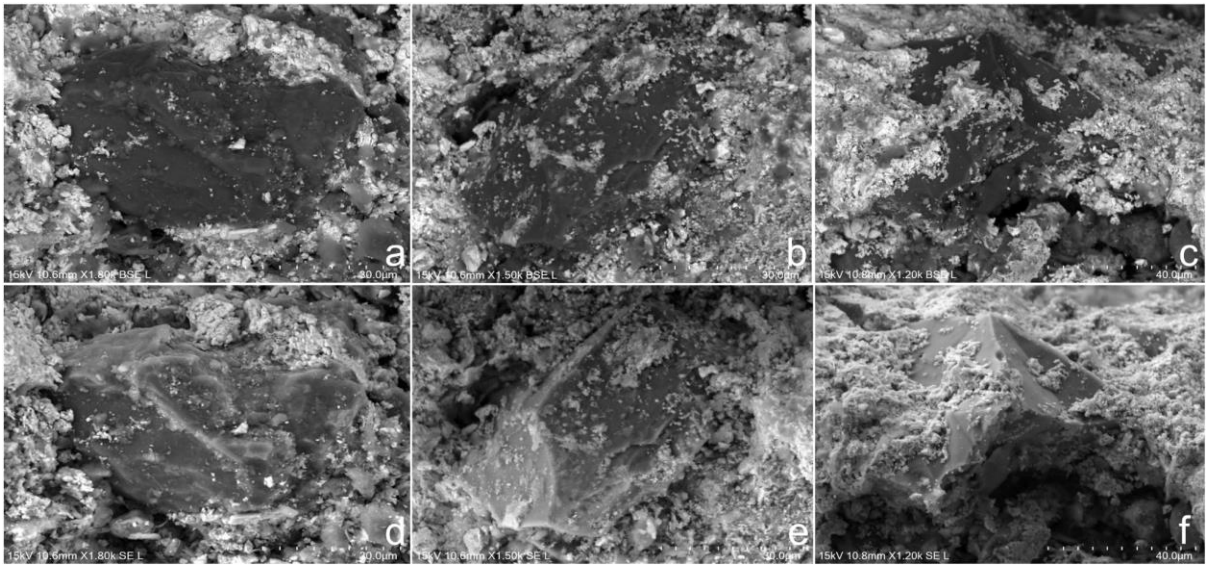


Figure 5. 30 (a-c) BSE and (c-f) SE images of sand grains in raw brown glaze of HY-130, obtained from ESEM.

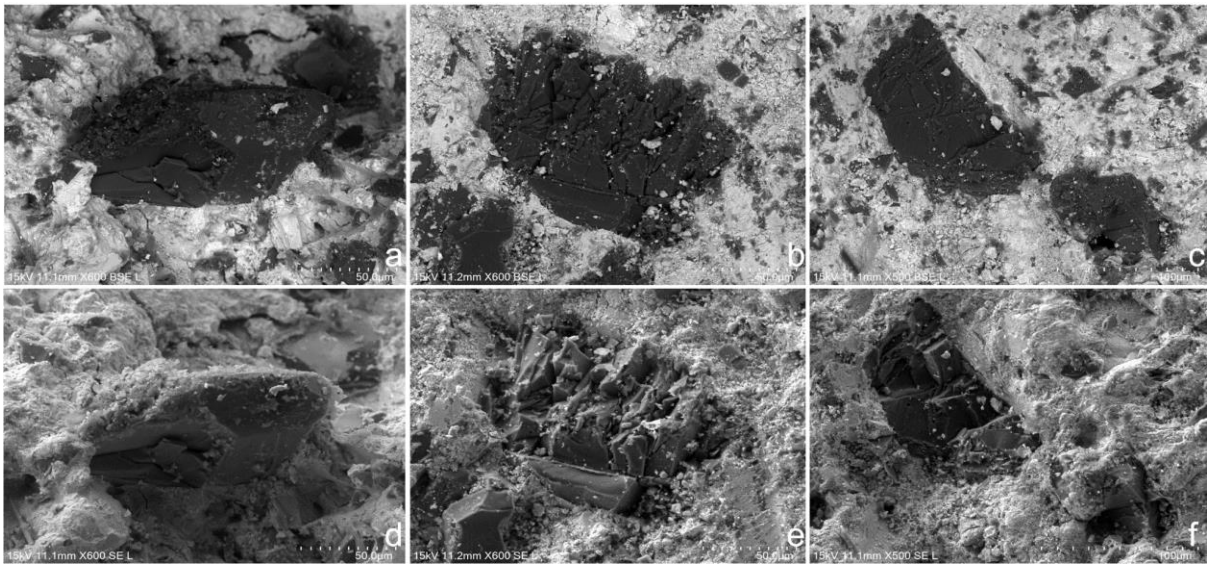


Figure 5. 31 (a-c) BSE and (c-f) SE images of sand grains in raw green glaze of HY-38, obtained from ESEM.

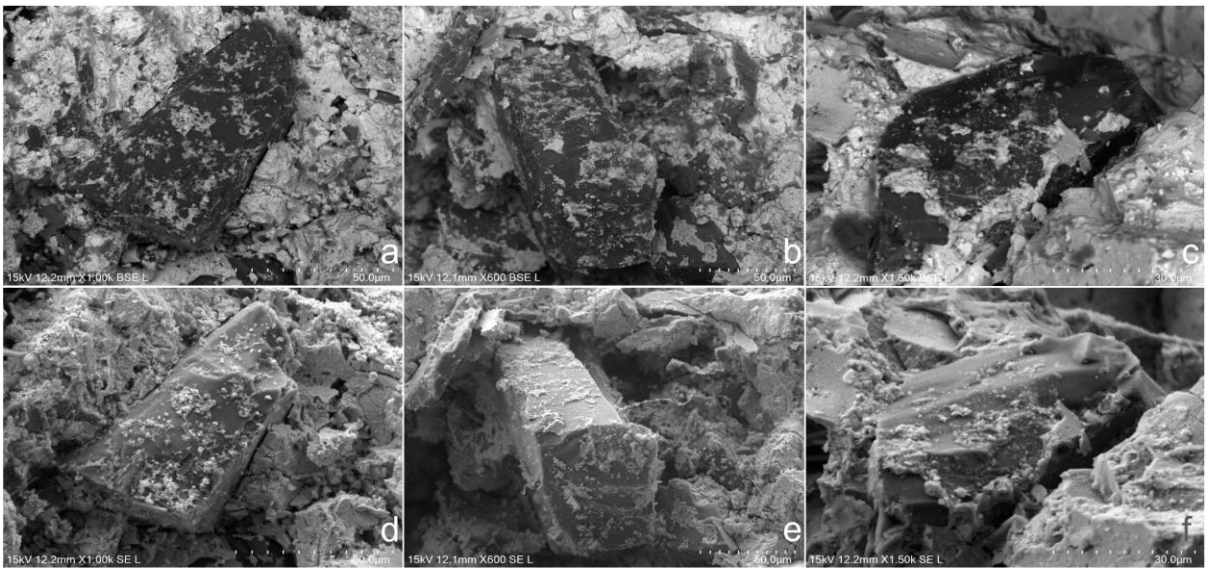


Figure 5. 32 (a-c) BSE and (c-f) SE images of sand grains in raw blue glaze of HY-43, obtained from ESEM.

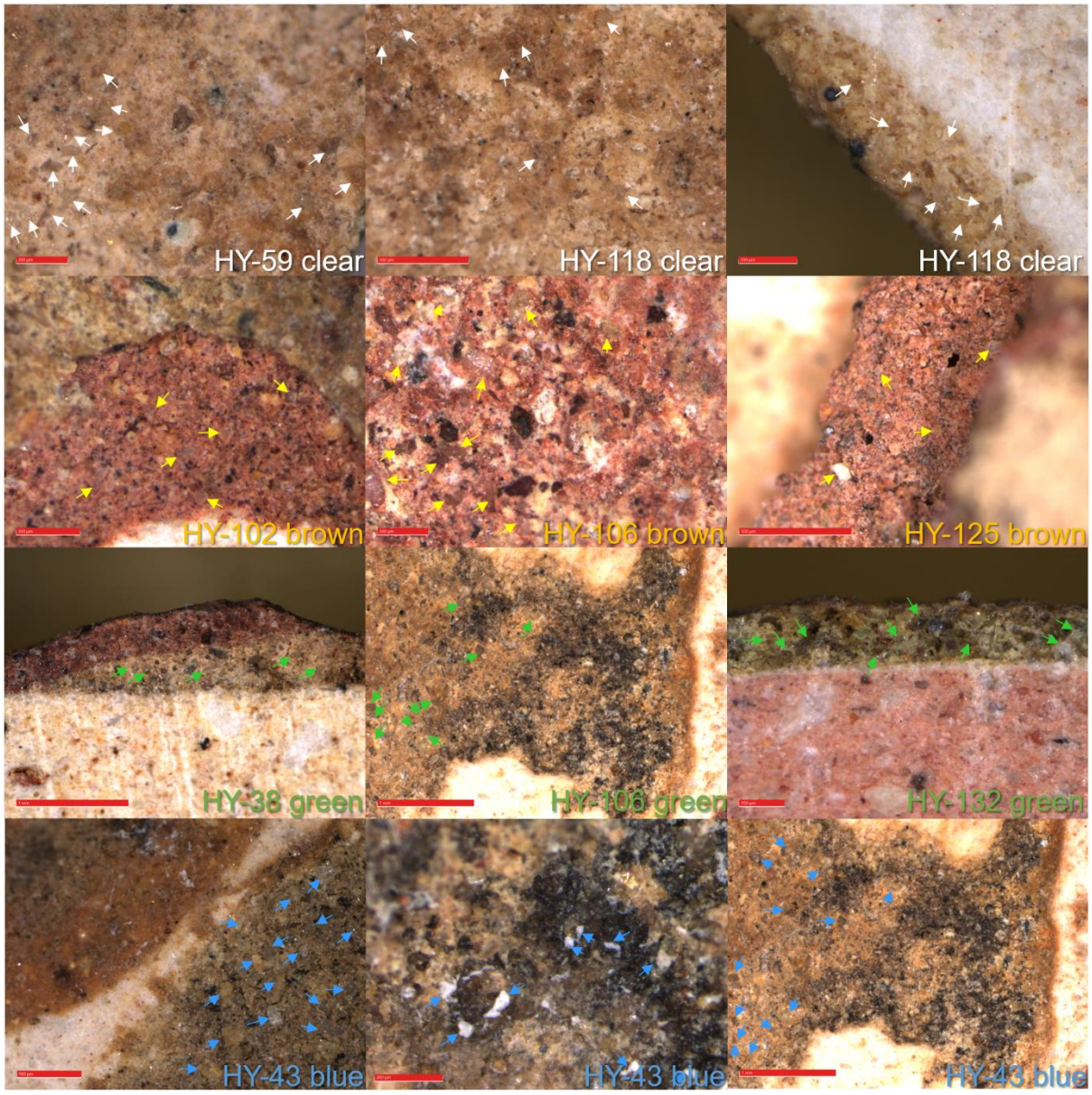


Figure 5. 33 Photos of flint and sand in raw glaze. The arrows identify flint and sand grains in the raw glazes, developed from the optical microscope.

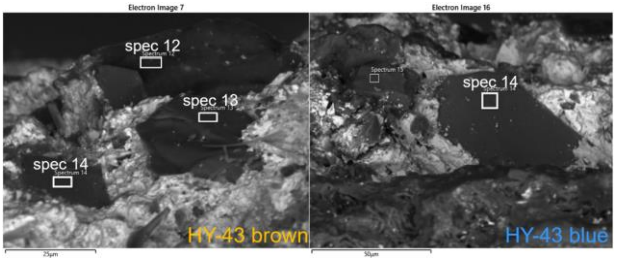


Figure 5. 34 Test areas of high-Al particles in raw brown and blue glazes, obtained from ESEM.

Table 5. 10 Chemical compositions of high-Al particles in raw brown and blue glazes by ESEM

Samples	Glaze colours	Na_2O	MgO	Al_2O_3	SiO_2	P_2O_5	K_2O	CaO	FeO	CuO	PbO
HY-43 spec 12	Brown	-	-	70.47	19.86	-	0.46	0.46	0.88	4.52	3.36
HY-43 spec 13	Brown	-	-	48.82	43.77	-	0.38	0.39	-	3.04	3.59
HY-43 spec 14	Brown	-	-	71.08	15.38	0.69	0.44	2.96	-	5.06	4.39
HY-43 spec 14	Blue	-	-	67.07	21.79	0.66	0.74	0.62	-	4.33	4.79

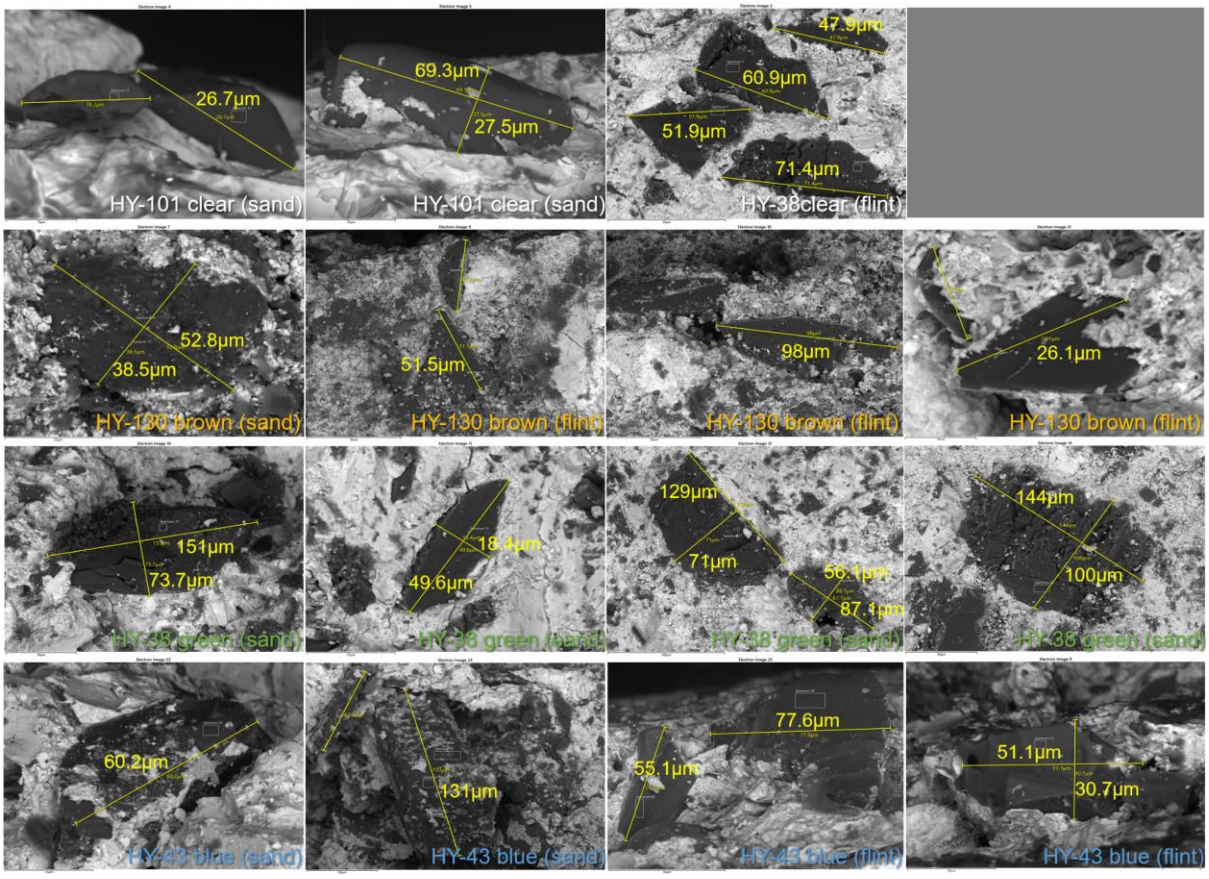


Figure 5. 35 Sizes of flint and sand grains in raw glazes, developed from ESEM.

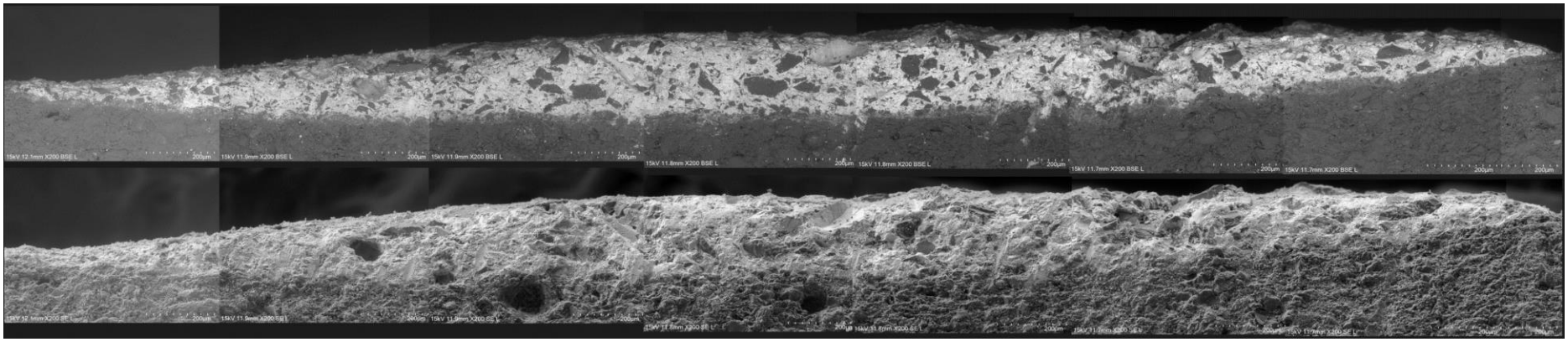


Figure 5. 36 BSE (top) and SE (bottom) images of clear glaze layer of HY-38, obtained from ESEM.

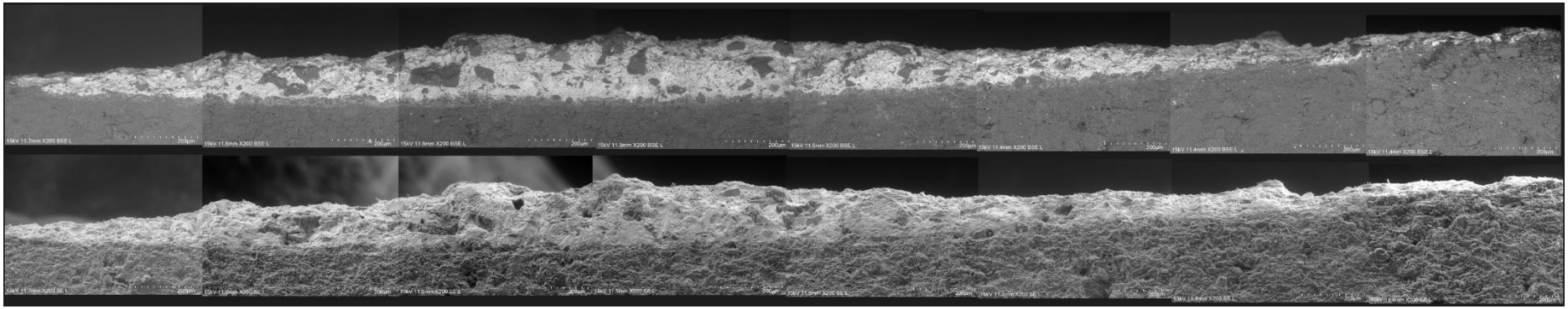


Figure 5. 37 BSE (top) and SE (bottom) images of brown glaze layer of HY-38, obtained from ESEM.

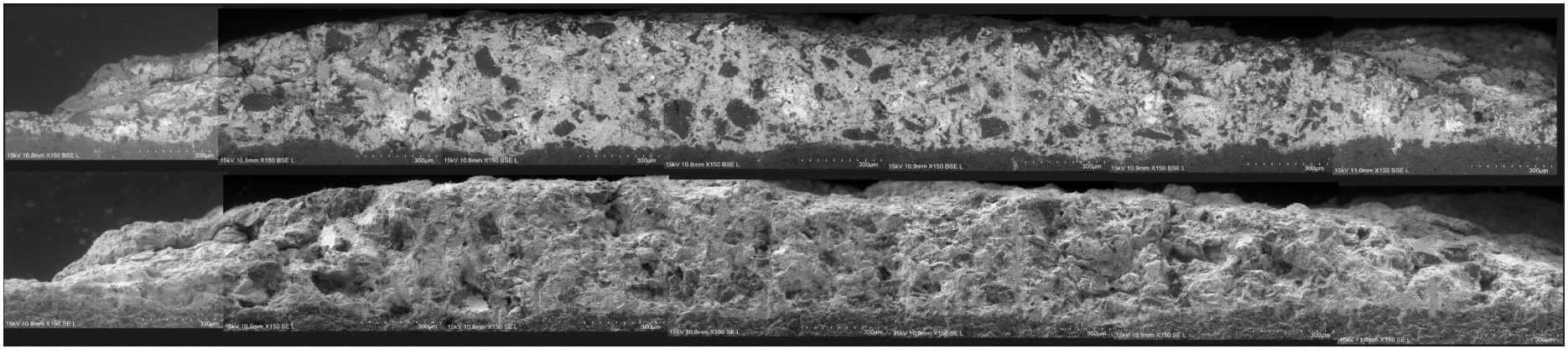


Figure 5. 38 BSE (top) and SE (bottom) images of green glaze layer of HY-38, obtained from ESEM.

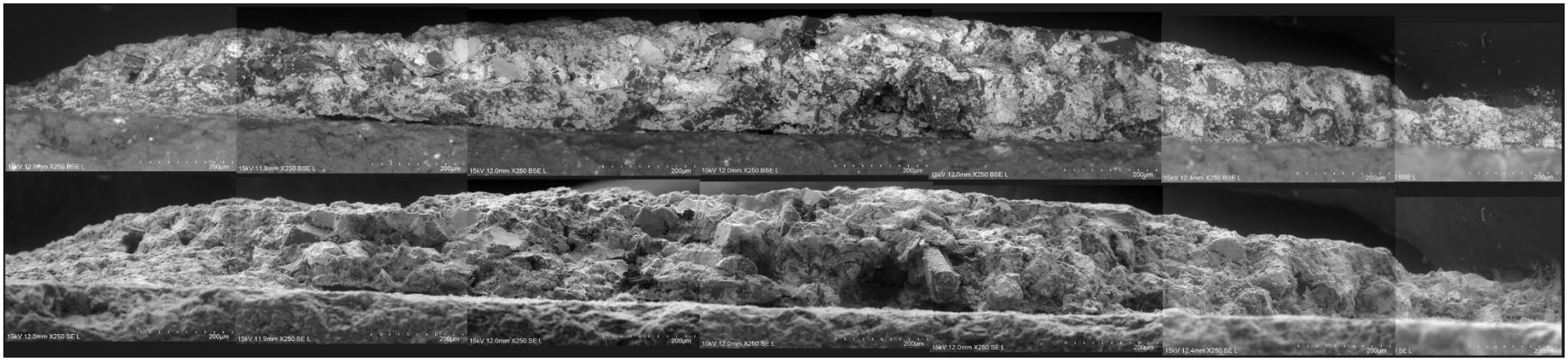


Figure 5. 39 BSE (top) and SE (bottom) images of blue glaze layer of HY-43, obtained from ESEM.

5.1.3 Ash or Mineral?

The melting points of silica and aluminium are too high for a kiln and so fluxes are mixed with them to bring down the melting temperature and promote glaze fusion. Many RO and R_2O compounds can work as a flux, such as CaO, MgO, PbO, Na_2O and K_2O, etc. For Sancai glaze, it is generally accepted that lead is the main flux. The compositional analysis by XRF reveals high CaO and P_2O_5 of raw glazes. Specifically, the weight percent of P_2O_5 content is only a little less than PbO (Figure 5. 40). High P_2O_5 (around 30%) is not common in ceramic glazes. Contamination is a possibility, but I choose to consider it as a deliberately added material for the following reasons:

1) The raw glazes on all sherds contain similar level of high P_2O_5 around 30-40%. However, these samples were excavated in different strata at different places in the same big town at different times – 2002-4 and 2015 respectively.
2) The slips (powder materials) on sherds did not contain high P_2O_5. The average of P_2O_5 in slips is only 0.3%.
3) No P-Fe association was found. If high phosphorus was caused by vivianite ($Fe^{2+}{}_3(PO_4)_2 \bullet 8(H_2O)$) contamination, the high-P areas should contain high Fe.
4) All samples were packaged into independent sample bags and cleaned by ethyl alcohol before every XRF test.

Also, high P_2O_5 was not produced by instrumental error. Some Gongyi white porcelain sherds were analysed using the same instrument in the same lab on the same day as the raw glaze samples, but the white porcelain results did not show high P_2O_5. For example, the P_2O_5 (30.86%, labelled with HY-152-2-2 in Appendix 9) in raw brown glaze of HY-152 was obtained at 14:15 on the 27th of May in 2021. The fired glaze of a Gongyi white porcelain sherd was tested at 17:16 on the same day. The P_2O_5 is 0.67%.). Furthermore, pyromorphite ($Pb_5(PO_4)Cl$) is less

likely to be used to bring in high P_2O_5 because most of Ca-P-Pb areas only show the association between these three elements.

Based on the above discussion, I suggest that high P_2O_5 was not caused by contamination, instrumental error, or a specific high-Pb-and-P mineral. However, this finding of high P_2O_5 is different from previous scientific analysis of fired Sancai products, no matter whether excavated from Gongyi or other tombs and sites. For instance, Chang et al. (2020) analysed Sancai products from five kilns including 19 Gongyi sherds. Most samples only contained 0.1-0.3% P_2O_5. Could the high P_2O_5 reported here be lost on firing? The brief answer is no. In the experimental glaze firing, the compositional results of raw and fired glazes on the same sherds both show high P_2O_5 even though the contents decreased (Appendix 6). In other words, the raw glazes retain P_2O_5 after glaze firing. However, my lab work shows that three fired Sancai sherds unearthed from the same place as the samples of raw glaze did contain high P_2O_5 - 44.99% and 17.05% in two green glazes, and 8.75% in a blue glaze[28]. The fired sherd with 17.05% P_2O_5 was excavated from the same stratum (T0231:⑦) with HY-38 which decorated with raw clear, brown, and green glazes (Table 3.2 and Appendix 2). Two possibilities can be proposed – maybe these raw glazed sherds were made in error (excess P_2O_5), or the raw materials used by the Gongyi potters had some changes in a specific period. Many questions about phosphorus cannot be answered now, but no matter what possibility matches the practice in the Tang-dynasty Gongyi kiln, P_2O_5 can be accepted as a component of the raw glaze in this thesis.

[28] 160 fired Gongyi Sancai sherds and 66 raw glazed sherds were analysed at the same time with the same instrument in the same lab at Northwest University by this author. Due to the word limitation, the examination and discussion of fired sherds was not presented in this thesis.

The phosphorus might be from a phosphorus-rich material which was deliberately added to the stock glaze by the Gongyi potters[29]. One significant point must be noted – most of the sherds discussed in this thesis were excavated from trash pits. They were flawed products and thrown away, and these sherds have been buried underground for more than a thousand years. The weathering and some contamination cannot be avoided. Thus, the compositional results obtained from EDXRF and ESEM cannot precisely reveal the original levels of every constituent of the Sancai glaze.

The high Ca-P-Pb material is homogeneous and looks like the fondant of a cake. Many different-size particles, including quartz and colourant grains etc., were embedded in the 'fondant'. This form was observed in every test of all glazes (Figure 5. 41). However, Ca-P and Pb might not originate from the same material, because the high-Pb areas do not contain high Ca and P. As Figure 5. 41 shown, the light high-lead area in HY-130 brown glaze (yellow circle) was only characterised by high lead – the calcium and phosphorus were the same as the immediate background. This distribution – light high-Pb areas and Ca-P-association, were found in every sample. It can be confirmed that the raw material for the lead is different from that of calcium and phosphorus. The 'association' of Ca, P and Pb was possibly made by a fine blending of powders. Does it suggest that Ca and P belong to the same raw material? Unlike the kaolinite or quartz grains, no Ca-P-associated particles were found by ESEM observation. Generally, glaze is made into a liquid to be applied. After the evaporation of water, the Ca-P material attaches to the body as a fine powder. The positive correlation suggests that Ca and P came from the same ingredient (Figure 5. 42a). What is this Ca-P material?

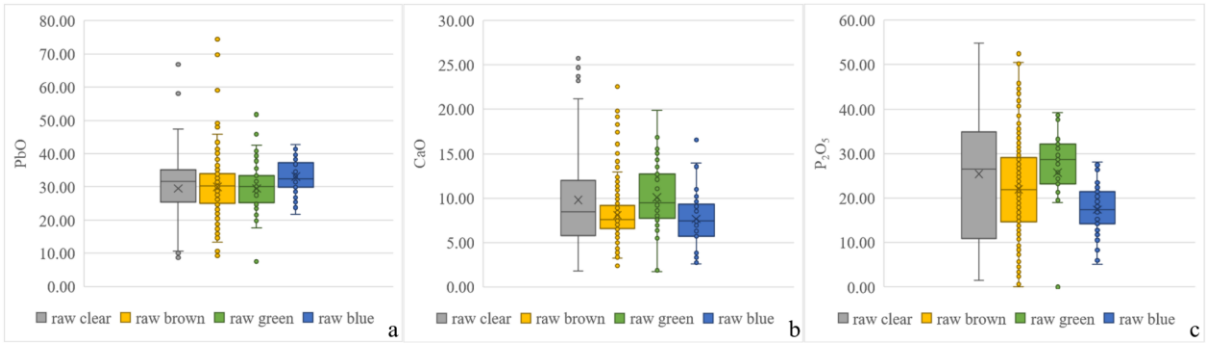


Figure 5. 40 Box plots of (a) PbO, (b) CaO, (c) P_2O_5 of raw glazes

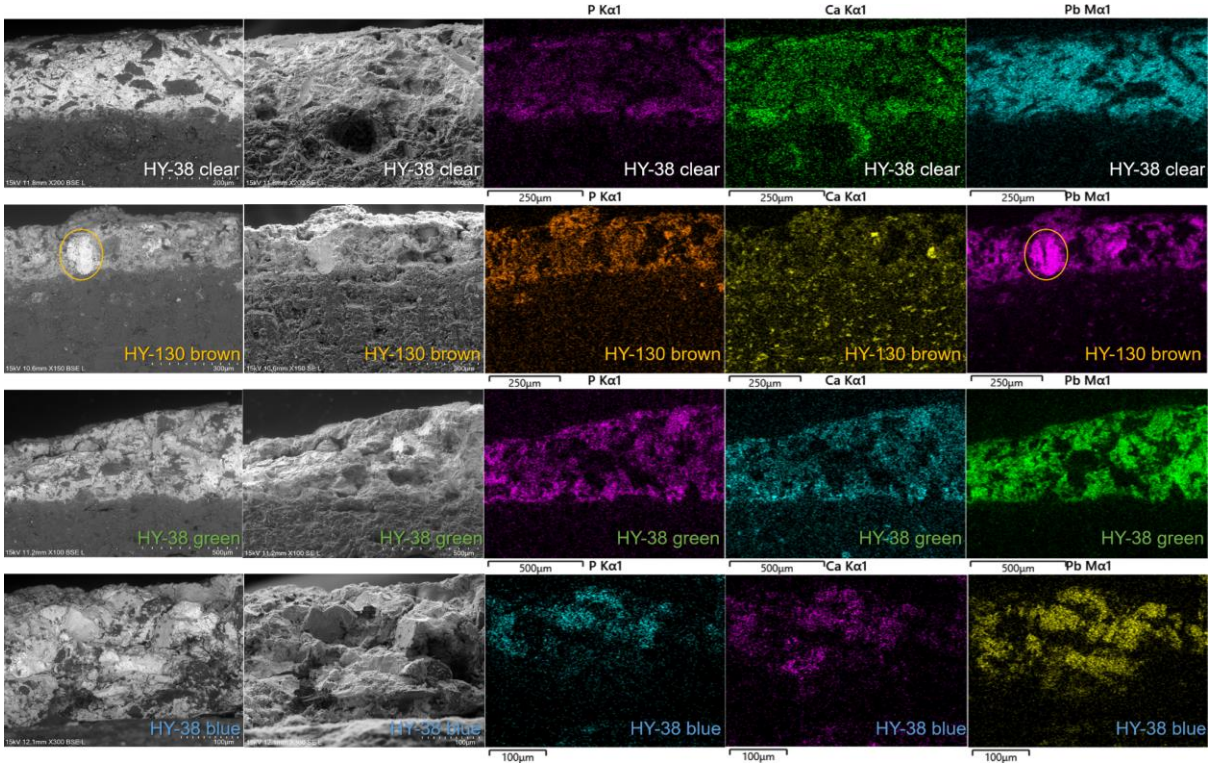


Figure 5. 41 BSE (the first column), SE (the second column) and mapping (the other columns) images of glaze layers. Yellow circle presents the high-lead area. Images obtained from ESEM.

A typical high-Ca-and-P powder is bone ash. It is one source of calcium phosphate and is used in European porcelain bodies as a flux to make a very white body. Tite and Bimson (1991) analysed English bone porcelain and found a scatter of calcium phosphate particles, typically about 10 μm across. There are two differences. Firstly, this high-Ca-and-P material was used

in the raw Sancai glaze instead of in the bodies. The averages of CaO and P_2O_5 of the Sancai bodies are very low, only 1.66% and 0.22% respectively. The other difference is that no Ca-P-associated particles were found in the raw glazes by ESEM analysis.

Usually, bone ash was made from cattle bones. A typical bone analysis of bone ash would be calcium oxide 55%, phosphorus oxide 40%, with the remainder composed of fluorine, silica, and alkaline oxides. An acceptable formula for bone ash is $Ca_3(PO_4)_2$ otherwise expressed as between $3CaO \cdot P_2O_5$ up to $13CaO \cdot 4P_2O_5$ (Hamer and Hamer, 2015, p.33). Whichever formula it is, the ratio of n(CaO) to n(P_2O_5) is around 3. Moreover, in the modern ceramic industry, the materials offering high Ca and P together are phosphorite ($Ca_3(PO_4)_2$ and apatite ($3Ca_3(PO_4)_2 \cdot Ca(Cl,F)_2$) (Hamer and Hamer, 2015, p.268). The ratio of n(CaO) to n(P_2O_5) of rocks are also around 3.3. But the molar ratio of raw glazes is only around 1 (Figure 5. 42b), much lower than bone ash, phosphorite and apatite. The following key question is that is this molar ratio of CaO to P_2O_5 of raw glazes based on XRF results reliable? The answer might be negative. The P_2O_5 of Corning glass D is 3.93% (Adlington, 2017). However, the two tests of this glass by XRF shows a higher result – 5.52% - 6.20% (Appendix 4), and the average is 5.92%. Accordingly, the phosphorus content in raw glazes obtained from the XRF might be higher than the real values. It is a limitation of XRF analysis, rather than an instrumental error or mistake. The use or absence of bone ash or natural minerals cannot be verified based on current scientific analysis.

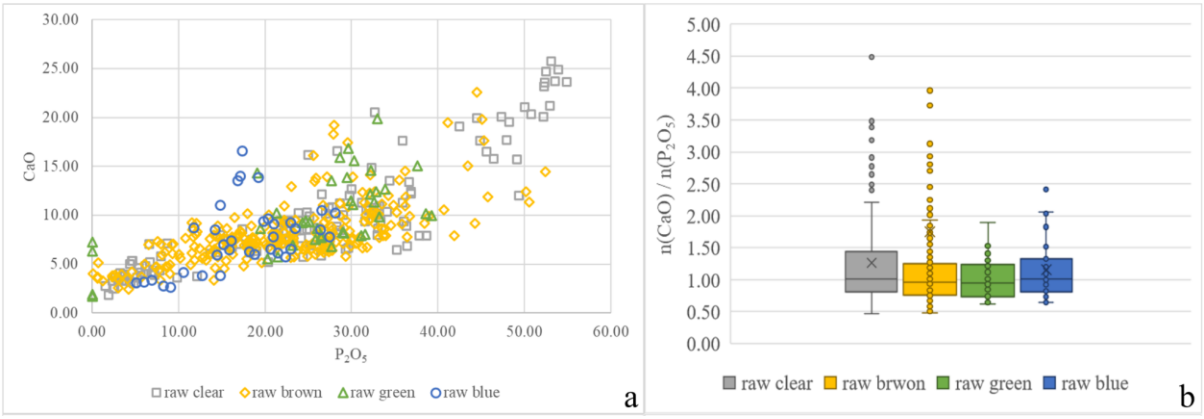


Figure 5. 42 (a) Scatter diagram of CaO to P_2O_5 of raw glazes. (b) Box plot of n(CaO)/n(P_2O_5) ratios of raw glazes

Are there any other common high phosphorous materials used in ceramic making? Plant ash and wood ash were both widely employed to produce glazes in ancient China. Surprisingly, some special remains in the raw glaze might suggest the potential use of wood ash in Sancai glaze. As shown in Figure 5. 43 - Figure 5. 45, some curly and fibre-shaped particles were included in the Pb and Ca-P powders. The surfaces show regular stripes. This texture is almost the same as archaeological wood and charcoal fragments (Figure 5. 52). Possibly, the special remains were charcoal or unfired wood, which can be regarded as evidence for the use of wood ash. However, the compositional results contradict this finding. The levels of P_2O_5 in raw glazes are too high to be explained by wood ash alone. Whether other material(s) was used independently or added to the raw glazes to contribute more phosphorus? This question cannot be answered now since the XRF test cannot offer a reliable result of P_2O_5.

If the wood ash was applied to make the raw Sancai glazes, perhaps, the wood was not burned totally to be transformed into a fine powder, and these ‘big fibres’ remained. Additionally, the high-Ca and high-P particles near the wood remains (yellow and pink circles in Figure 5. 45) are also a piece of evidence for this semi-burning. Undoubtedly, Ca and P are

the main elements in this artificial material. The high Pb might be caused by mixing it with lead powder. Some clusters of lead powder on these wood remains are recognisable (green circles in Figure 5. 45). Tiny particles of lead powder attached on the surfaces of the wood remain, and large clusters of lead might separate from the surfaces after the evaporation of water. If these remains were burned totally to a fine Ca-P powder, they would be very well mixed with lead powder as in other samples (Figure 5. 41). The concentration of Cl in some wood remains perhaps was due to the burial environment. Groundwater contains Cl^- and many kinds of metal cations.

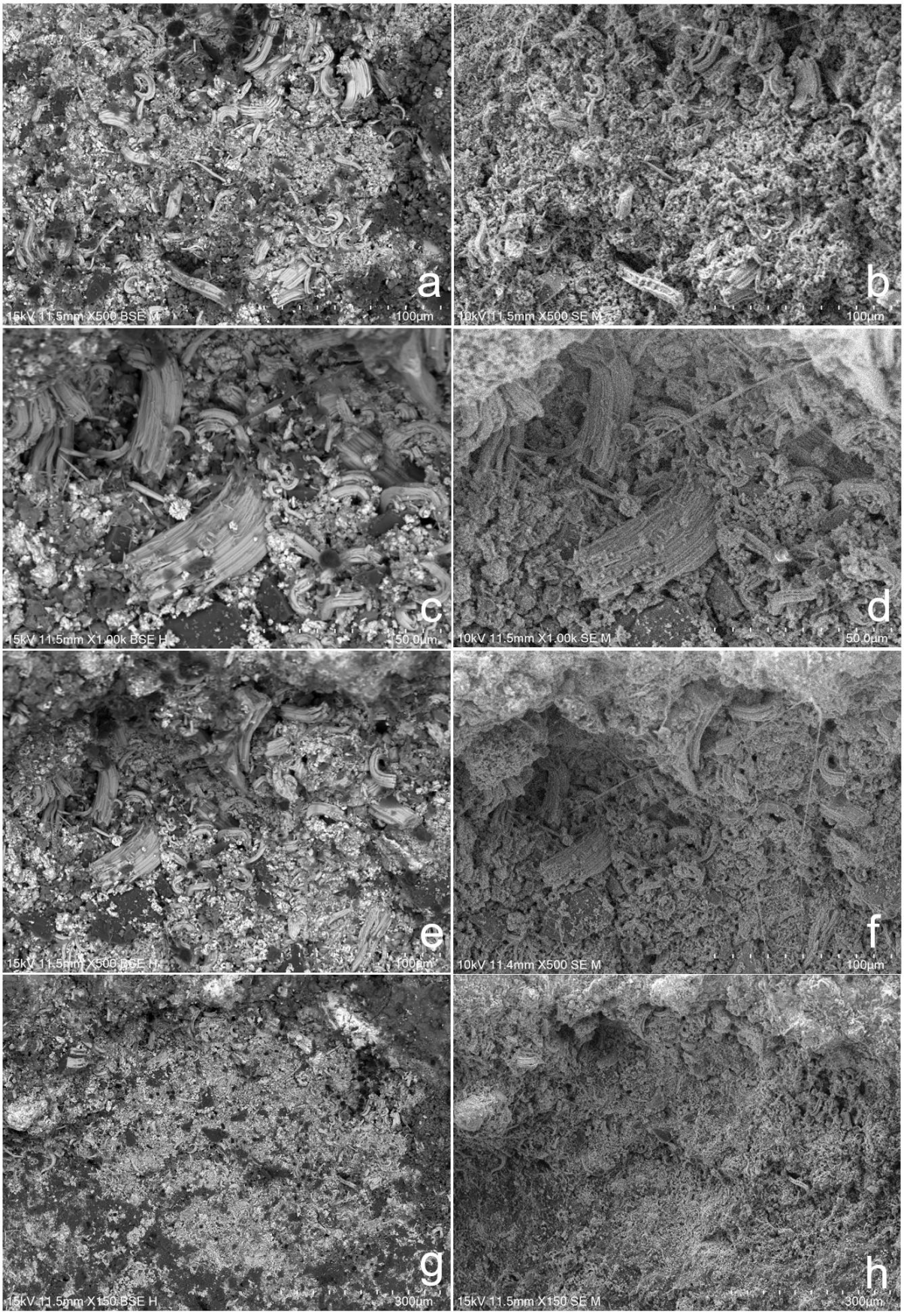

a
15kV 11.5mm X500 BSE M
100µm
b
10kV 11.5mm X500 SE M
100µm
c
15kV 11.5mm X1.00k BSE H
50.0µm
d
10kV 11.5mm X1.00k SE M
50.0µm
e
15kV 11.5mm X500 BSE H
100µm
f
10kV 11.4mm X500 SE M
100µm
g
15kV 11.5mm X150 BSE H
300µm
h
15kV 11.5mm X150 SE M
300µm

Figure 5. 43 BSE (left) and SE (right) images of unknow curl materials in the raw brown glaze of HY-62, obtained from ESEM.

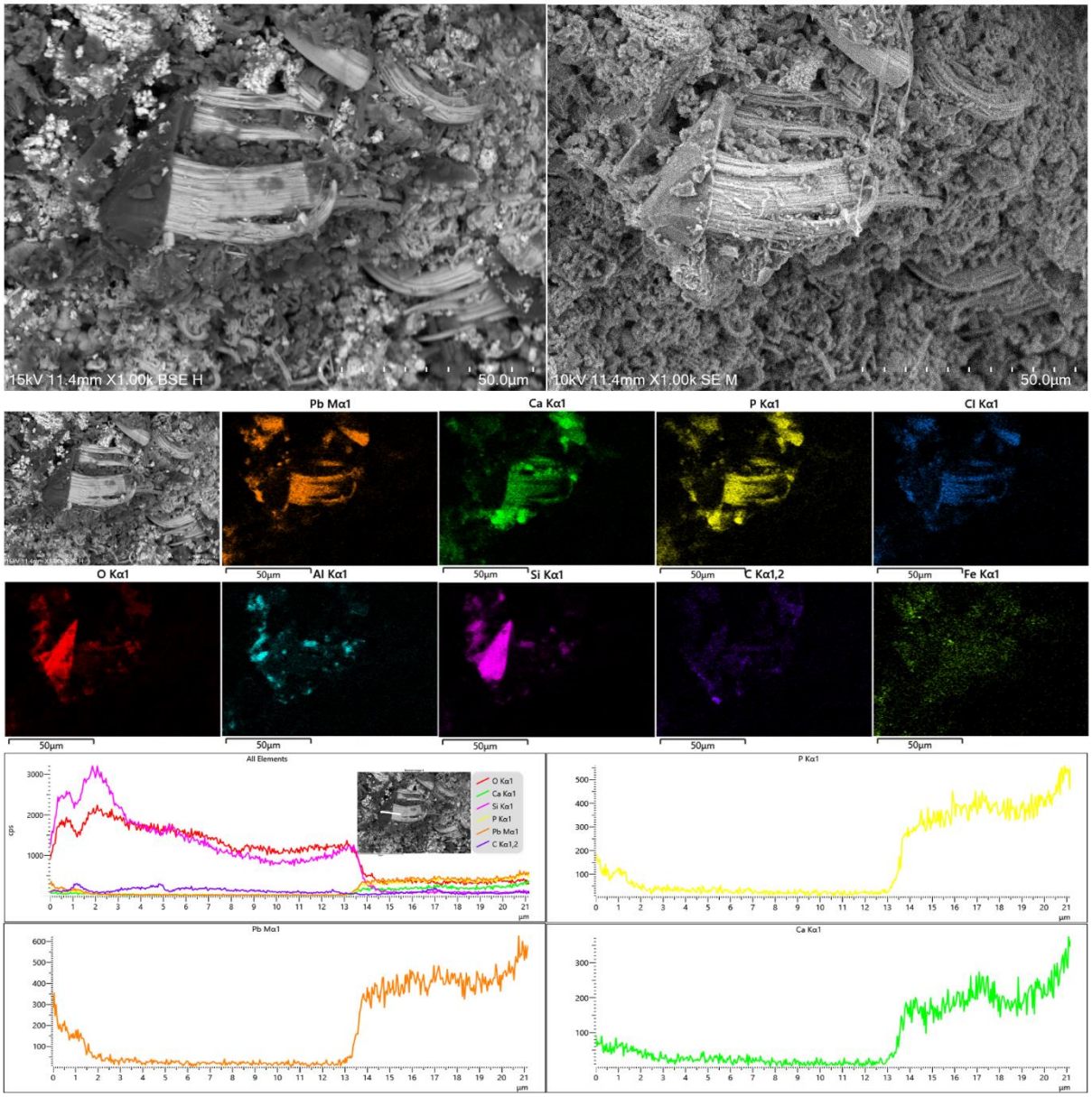


Figure 5. 44 BSE (top left), SE (top right), mapping (centre) and line scan (bottom) images of unknown curl ‘grains’ in raw brown glaze of HY-62, obtained from ESEM.

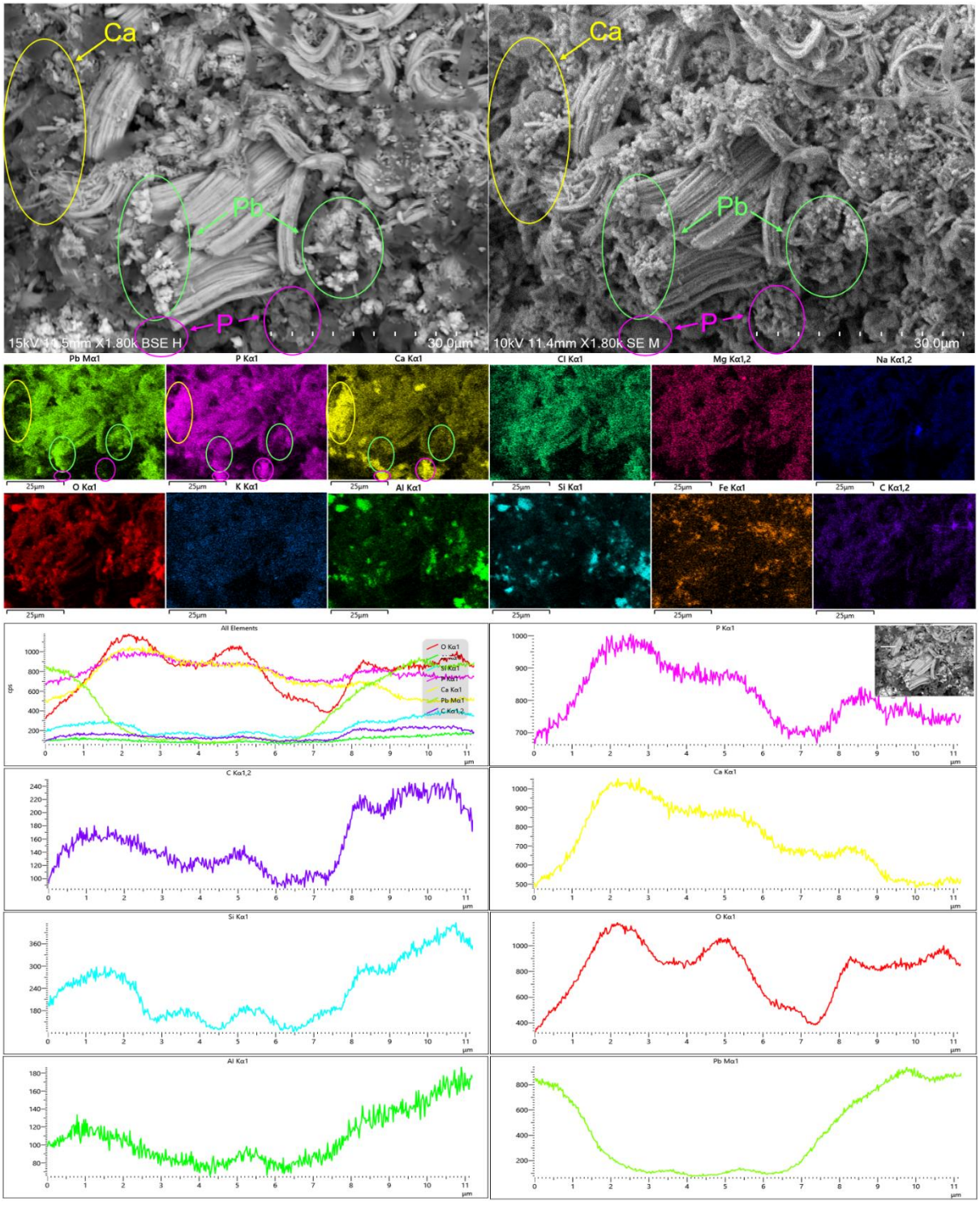


Figure 5. 45 BSE (top left), SE (top right), mapping (centre) and line scan (bottom) images of unknown curl ‘grains’ in raw brown glaze of HY-62, obtained from ESEM.

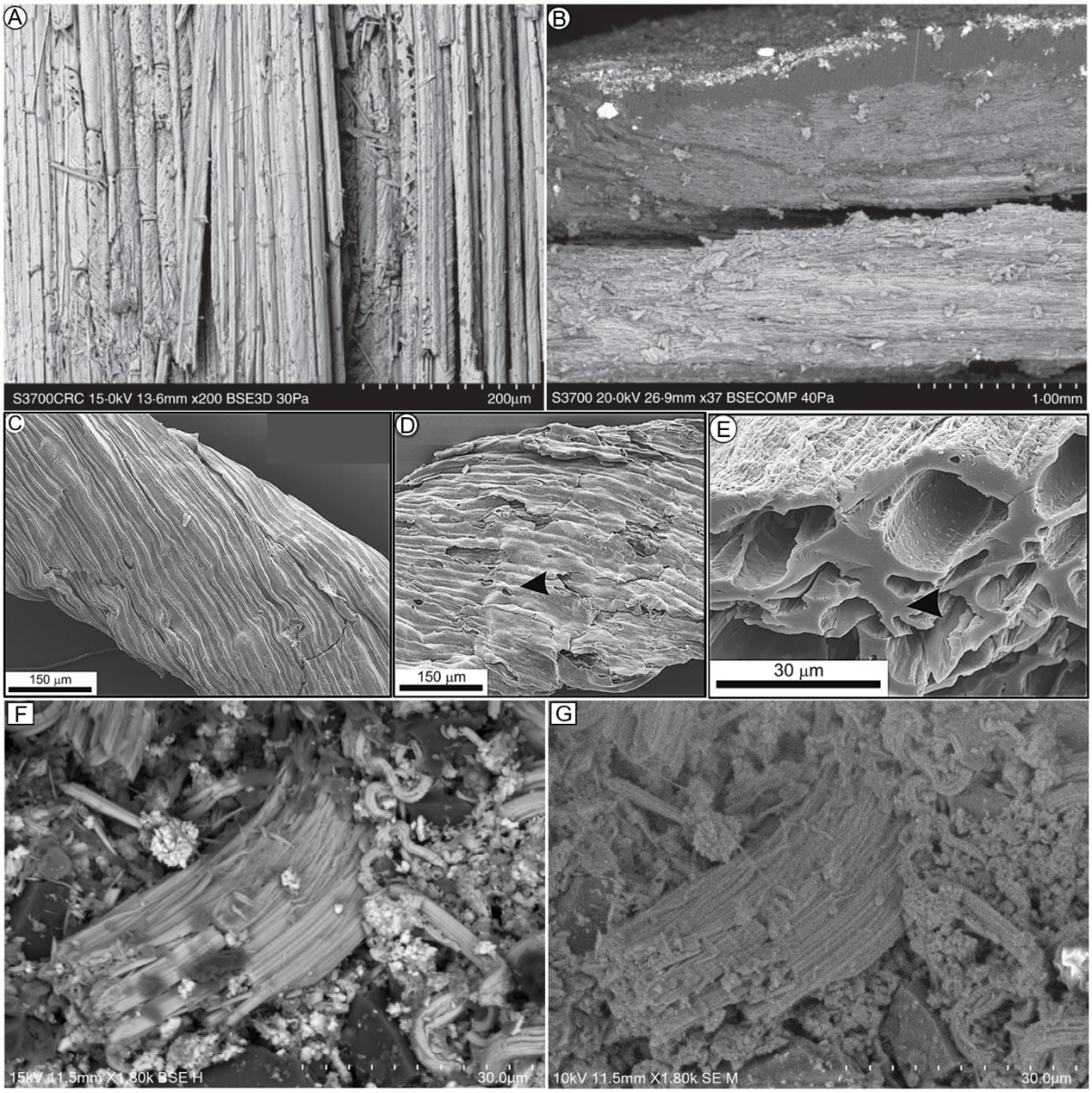


Figure 5. 46 BSE (A, B and F) and SE (C, D and E) images of (A and B) archaeological wood, (C, D and E) charcoal fossils, and (F and G) special remains in raw glazes of Gongyi Sancai. Variable pressure scanning electron microscope images of (A) a tangential longitudinal section of mineral-replaced wood, and (B) a tangential longitudinal section of desiccated wood from a funerary Table in a Jericho Bronze Age tomb. A and B are cited from Cartwright (2015). SE images of (C, D and E) charcoal fossils of from Ludford Lane, obtained from Glasspool et al. (2004).

The next key question is what is the source of calcium? Although no Ca-P-associated particles were found, many Ca-rich particles were observed in all raw glazes by ESEM (Figure 5. 47). A confusing finding is that these particles only show the concentration of Ca. It is impossible to use a simple substance containing only Ca. Additionally, an association of Ca, C and O was also found in a few particles (Figure 5. 48). This matches the element distribution of $CaCO_3$. Therefore, those Ca-rich particles shown in Figure 5. 47 might be CaO or $CaCO_3$. Perhaps, since C is too light to be tested, the chemical mapping of particles in Figure 5. 47 did not obtain the C result. The other possibility of the lack of C result might be the decomposition of calcium carbonate during one-thousand-year burial. There is no direct evidence to prove this viewpoint. It is uncertain whether these particles shown in Figure 5. 47 is $CaCO_3$ or CaO. But it is certain that the level of Ca is very high (Table 5. 11).

There are two ways to bring Ca into wood ash. The first is the calcination of limestone. Burning limestone and ferns together to make plant ash was used as early as the Southern Song dynasty (1127-1279 CE) or even earlier (Xiong, 1995). $CaCO_3$ is transformed to CaO after heating. The calcium content was brought in glaze by the plant ash. The other way to bring Ca is from the plant itself. Misra et al. (1993) prepared various wood ashes at different temperatures from several wood species, such as aspen, yellow poplar white oak etc. and analysed them. The authors found low-temperature (around 500℃) ash produced from the wood appears to contain predominantly calcium carbonate. However, at higher temperatures (around 1300℃), the content changes to predominantly calcium oxide (Misra et al., 1993).

Whichever way it was applied, CaO and $CaCO_3$ are both possible to be found in raw glazes. But the finding of Ca-Mg-C-O-associated particles directs the answer to this question about Ca source (Figure 5. 49 and Figure 5. 50). This particle is impossible to be brought by natural wood. It is more likely to be from a mineral ore. The common Ca-Mg mineral ore is dolomite

($CaMg(CO_3)_2$). But three findings contradict the use of Ca-Mg mineral ore. Firstly, MgO and CaO in all glazes do not have a positive correlation (Figure 5. 51). Additionally, MgO contents in raw glazes are much lower than CaO. On average, there is 0.79% MgO in clear glaze, 1.00% in green glaze, 1.37% in blue glaze an 1.50% in brown glaze. The mean value of CaO is 8.92%. The last finding is that the number of Ca-Mg-C-O-associated particles is very small, much fewer than C-O-associated particles. Thus, the Mg content was not contributed by a deliberately added Mg ore. It might be from limestone because most natural limestones contain small amounts of Mg.

If Tang-dynasty potters did use a wood ash for glaze making, the wood might be fired with limestone together to produce the ash. However, the wood species is unknown. Different places have a very large number of various plants. And plant species, the nature of soil where the plant grows, and application of appropriate chemistry and technology are some of the factors which influence both qualitative and quantitative determination of components of ash (Babayemi et al., 2010). Although the current P_2O_5 content obtained from XRF is higher than its real value, the levels of it in all raw glazes are very similar. That is, the real levels of P_2O_5 in all raw glazes are very stable. Potters might fix a specific proportion of limestone to wood to make a stable ash. The current ratio of P_2O_5 to CaO is around 2:1 of all glazes, and the real ratio should be lower than it. The confirmation of the use of wood ash and the ratio of P_2O_5 to CaO both need further scientific analysis. The use of this high-P wood ash was a tradition in the Gongyi kiln. (Ling et al., 2005; Li, 2019) found it in white porcelain, and Spataro et al. (2019) revealed its use in Tang blue-and-white porcelain. If the future work verifies the existence of wood ash in Sancai glaze recipe, the potential shared ingredients of Sancai and other ceramics in the Gongyi kiln can be explored.

Furthermore, one point needs clarification. The body material, kaolinitic clay, also contains low CaO. A simplified calculation was applied to estimate the CaO offered by the kaolinitic clay. Firstly, the ratio of CaO to Al_2O_3 was obtained for every body. Then, this ratio multiplied by the Al_2O_3 content of the raw glazes on the same sherd gives the m'(CaO) originating from the kaolinitic clay in the glaze. Finally, the difference between the real m(CaO) obtained by XRF and estimated the m'(CaO) from kaolinitic clay was calculated. This difference is the amount of Ca contributed by the limestone (Δm (CaO) in Figure 5. 52a). CaO from kaolinitic clay (m'(CaO)) is too little to affect the correlation of CaO and P_2O_5 and consequently the ratio of limestone to wood. The same correlation shown in Figure 5. 52b (P_2O_5- Δm (CaO) and Figure 5. 52c (P_2O_5-CaO) can prove this point.

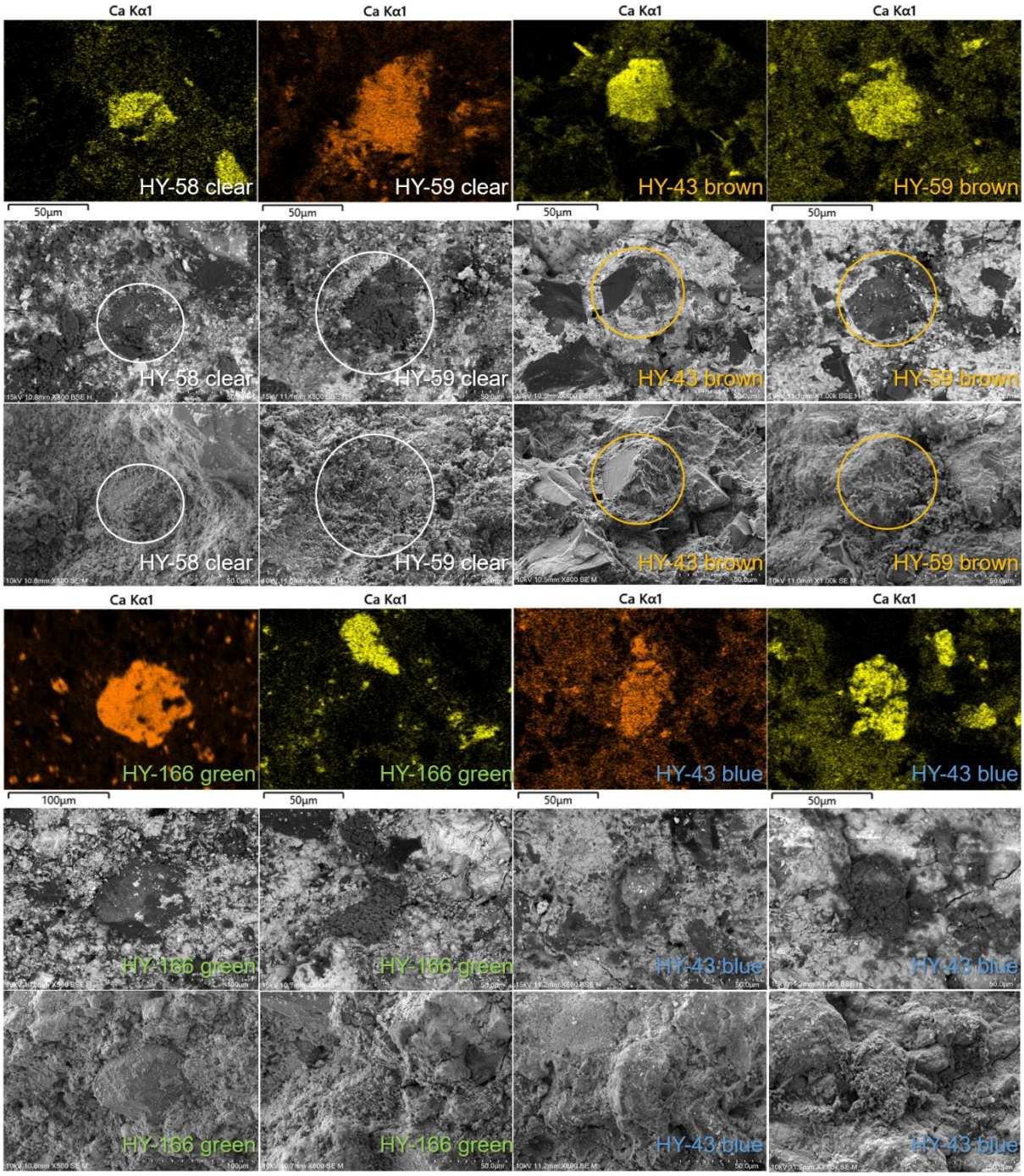


Figure 5. 47 Mapping (the first and fourth row), BSE (the second and fifth row) and SE (the third and sixth) images of Ca-rich particles in raw glazes, obtained from ESEM.

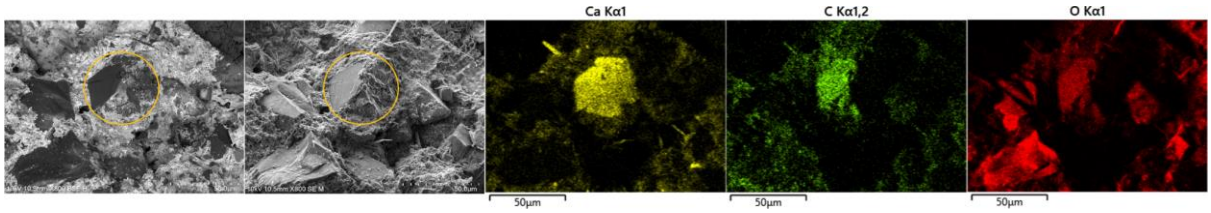


Figure 5. 48 BSE (the first one from the left), SE (the second one from the left) and mapping (the others) images of possible CaCO3 particles, obtained from ESEM.

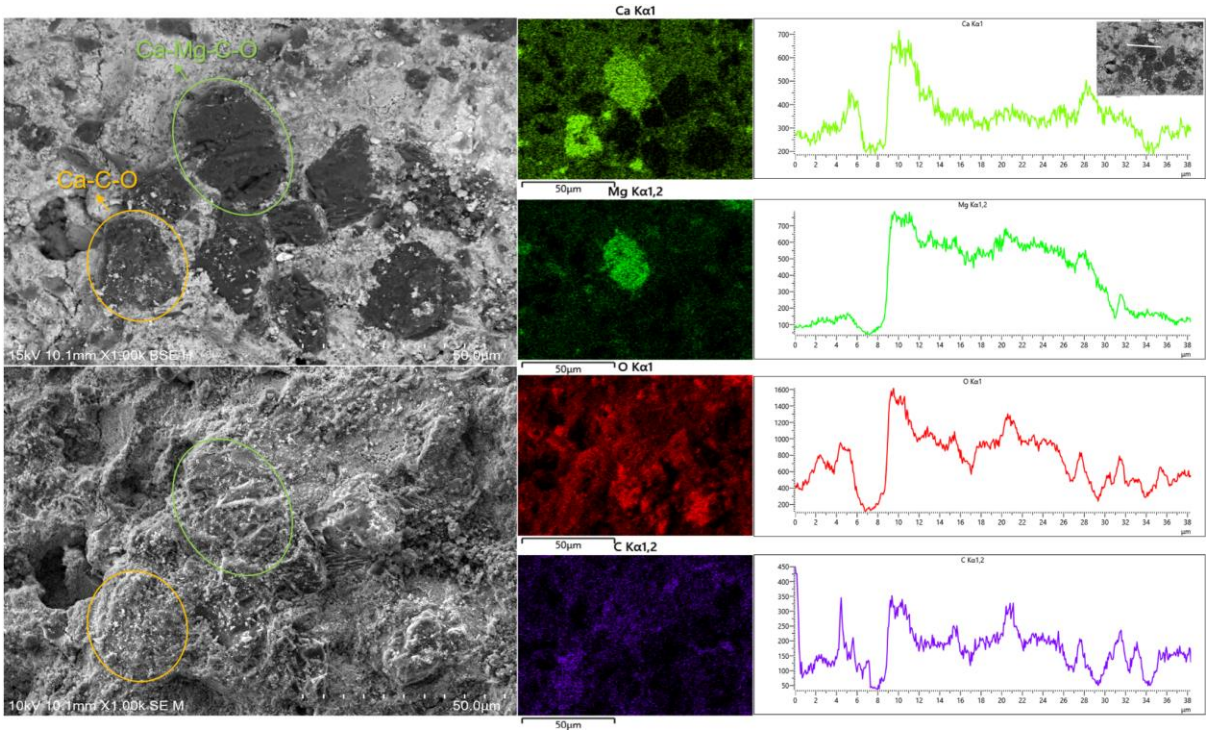


Figure 5. 49 BSE (top left), SE (bottom left), mapping (centre), line scan (right) images of Ca-Mg-C-O-associated particles in clear glaze of HY-123, obtained from ESEM.

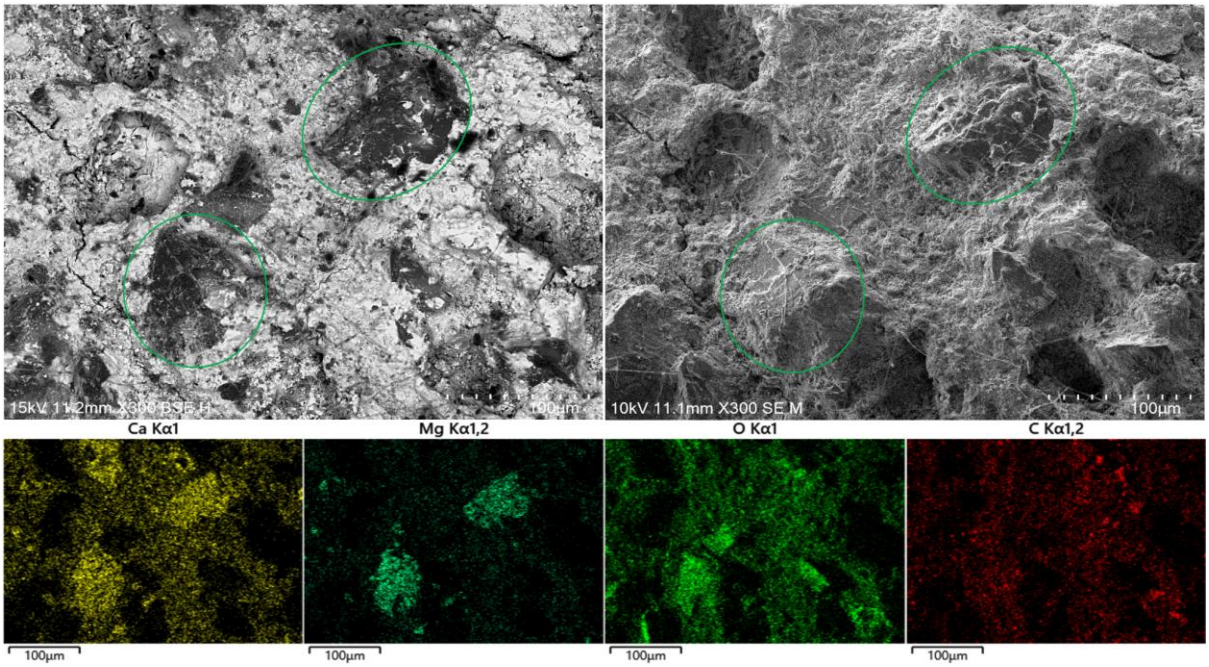


Figure 5. 50 BSE (top left), SE (top right) and mapping (bottom) images of Ca-Mg-C-O-associated particles in raw green glaze of HY-106, obtained from ESEM.

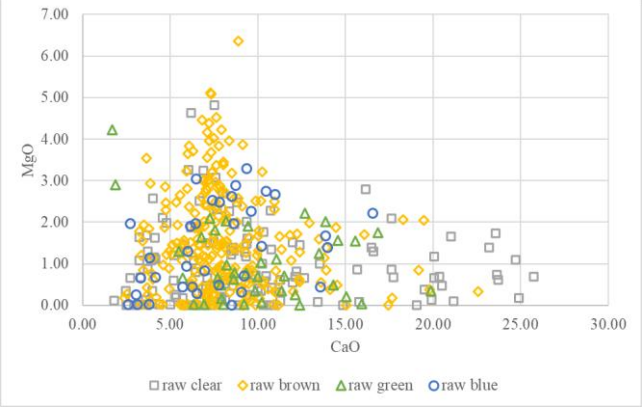


Figure 5. 51 Scatter diagrams of MgO to CaO of raw glazes.

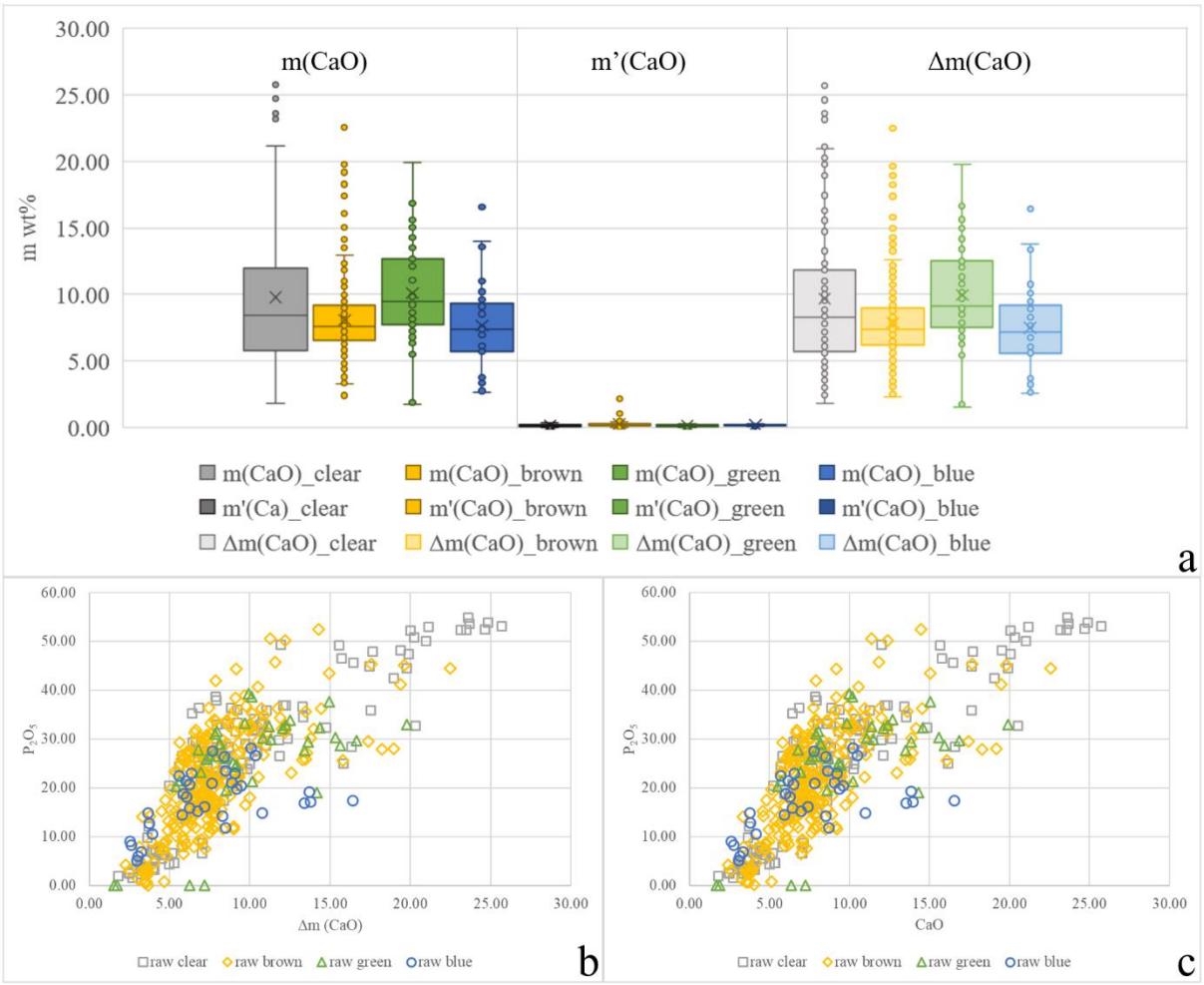


Figure 5. 52 (a) Box plot of m(CaO), m'(CaO) and Δm(CaO) of raw glazes. Scatter diagrams of (b) P_2O_5 to Δm (CaO) and (c) P_2O_5 to CaO of raw glazes.

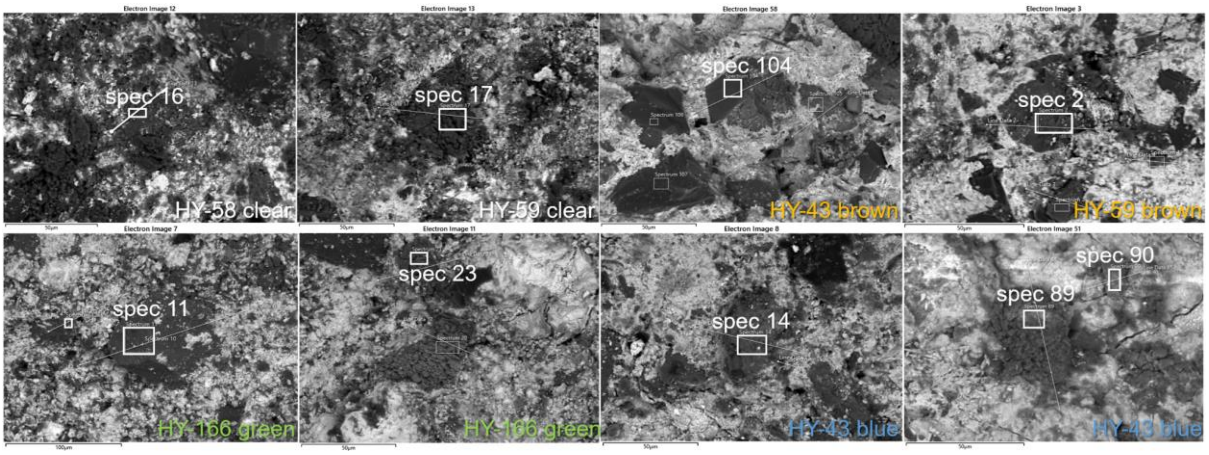


Figure 5. 53 Test areas of Ca-rich particles in raw glazes, obtained from ESEM.

Table 5. 11 Chemical compositions of Ca-rich particles in raw glazes by ESEM.

Glaze colours	Samples	Na_2O	MgO	Al_2O_3	SiO_2	P_2O_5	SO_3	K_2O	CaO	FeO	CuO	PbO
Clear	HY-58 spec 16	-	2.24	8.26	15.25	3.08	-	0.85	53.28	1.07	-	15.51
	HY-59 spec 17	-	0.88	1.21	2.42	0.46	-	-	93.38	-	-	1.66
Brown	HY-43 spec 104	-	1.13	6.06	3.95	0	-	-	83.69	-	-	4.81
	HY-59 spec 2	0.51	1.86	9.73	16.7	2.41	-	0.81	54.1	0.9	-	12.2
Green	HY-166 spec 10	3.5	5.48	5.76	10.62	-	1.14	1.6	65.24	-	-	6.07
	HY-166 spec 21	-	1.22	1.34	5.95	-	-	-	46.6	-	3.05	41.85
Blue	HY-43 spec 14	0.59	2.49	5.17	9.35	1.68	0.81	0.95	71.72	0.88	-	6.07
	HY-43 spec 89	0.72	3.1	14.15	27.3	0.88	-	2.08	47.11	1.39	-	3.27
	HY-43 spec 90	0.42	2.90	9.56	18.22	33.10	0.00	1.29	28.35	1.21	-	4.96

5.1.4 Which Lead?

Lead acts as the main flux of Sancai glaze - the content of all raw glazes is very similar, fluctuating around 30% (Figure 5. 40a). Based on the discussion in the last section, the lead material has separate source. In the modern pottery industries, since lead and compounds of

lead are poisonous, lead frits are generally used by potters. This frit is any prepared mineral that contains lead oxide and silica as the main constituents in a fused form, which was developed during the first half of the 20th century. An investigation of a traditional Sancai kiln in Henan was carried out by me. This kiln is located in the countryside of Luoyang, the neighbour city of Gongyi. The owner of it said that they used the traditional method to produce Sancai products. The glaze recipe is a secret, but the colours of the raw glaze liquid revealed a significant clue. The raw glaze labelled as 'red (brown)' and 'white (clear)' both show an orange colour (Figure 5. 54). The slight difference is that the raw clear glaze is a light orange, and the raw brown glaze is dark orange. Accordingly, the raw material is Pb_3O_4, red lead, and the dark orange of the raw brown glaze was caused by iron colourant.

Prior to this research, no unfired glaze has been available for study, and previous publications focused on the compositional analysis and lead isotopes study of fired glaze. Cui et al. (2010a) and Lingtong et al. (2022) have proposed the constituents of the Sancai glaze PbO-SiO_2-Al_2O_3 system. It is generally accepted that the source of lead varies in different places, such Yaozhou (Huangbao) in Shaanxi and Gongyi in Henan (Cui et al., 2010a; Shen et al., 2019; Henderson et al., 2020; Wang and Yang, 2021). No publication has discussed and confirmed the raw material of the lead. Only Wenjie (2021) proposed that slag from lead-smelting might be made into a transparent base glaze. However, this author did not give any discussion or scientific results to prove this viewpoint. One potential factor which cannot be ignored is that the colour of slag is usually very dark and impurities in slag are high. These both might increase the opacity and darken the colour of Sancai glaze. The use of slag is not very likely. So, what is the source of the raw lead?



Figure 5. 54 Photos of (a) a potter who is decorating a Sancai body in a traditional Sancai kiln in Henan and of (b-e) lead oxides and lead. Photo (a) was taken by the author, (b) is from https://en.wikipedia.org/wiki/Lead(II,IV)_oxide#/media/File:Red_lead.jpg, (c) is from https://en.wikipedia.org/wiki/Lead_dioxide#/media/File:Lead_dioxide.jpg, (d) is from https://en.wikipedia.org/wiki/Lead(II)_oxide#/media/File:Oxid_olovnat%C3%BD.JPG, and (e) is from https://en.wikipedia.org/wiki/Lead#/media/File:Lead_electrolytic_and_1cm3_cube.jpg

The ESEM examination shows that the texture of lead in the raw glazes is a fine powder which surround many different-size particles. This indicates that the lead material is very soft, and it was ground to a fine powder. The glaze layer looks like fondant on the cake (Figure 5. 55). The discussion in chapter 5.1.3 has proved that Pb had its own independent source even though it shared a similar distribution with Ca and P. The high-Pb without high Ca and P confirms this point. For example, neither the light circle on a round dark particle in HY-101 nor the light area in HY-130 show the clear concentration of Ca and P (Figure 5. 56). No other association of Pb and any element was found. But lead is unlikely to be used in glazes as a simple substance. Possibly, Pb is associated with some elements, but the mapping results did not show it clearly. For examples, the element might be too light, such as C. Or many

constituents contain the element, such as O, which causes the identification of it in lead area against the background to be difficult. The common lead oxides and carbonate compounds are PbO, PbO_2, Pb_3O_4， $PbCO_3$ and $2PbCO_3 \cdot Pb(OH)_2$. Additionally, no S or Cl was found to be associated with Pb. Thus, lead sulfide ores and lead chloride or chlorate are unlikely to have been used in the raw glaze.

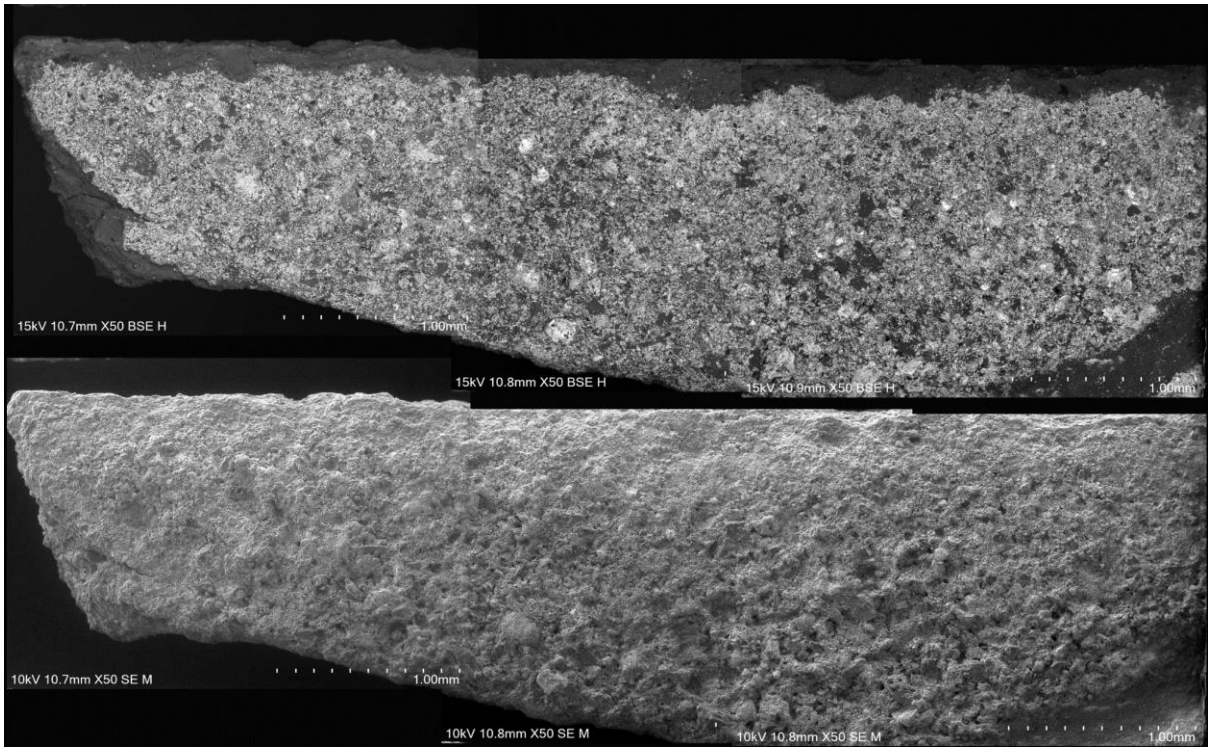


Figure 5. 55 BSE (top) and SE (bottom) images of the green-glaze surface of HY-166, obtained from ESEM.

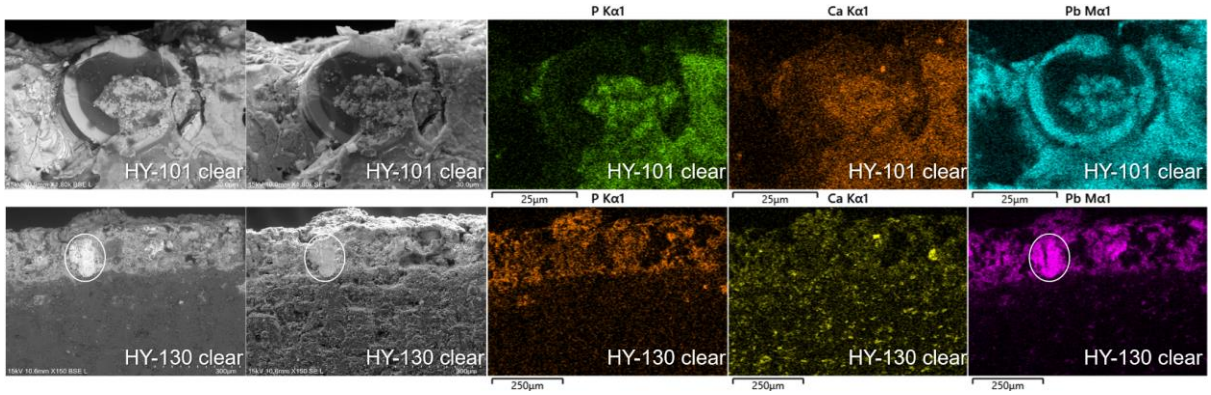


Figure 5. 56 BSE (the first column), SE (the second column) and mapping (the other columns) images of high-Pb areas of clear glazes of HY-101 and HY-130

The colours of those lead compounds and raw glazes could offer clues (Figure 5. 54 b-e). Besides the lead flux, other main ingredients of the stock glaze are kaolinitic clay, quartz, and Ca-P-rich material (might wood ash). The colours of these materials are normally white, milky, and grey, and the colour of the raw clear glaze should be close to the stock glaze since the clear glaze does not contain any colourant. The colours of raw clear glazes are white and transparent (Figure 5. 57) which are the final colour by mixing those four main ingredients – kaolinitic clay, quartz, Ca-P-rich material, and lead flux. Therefore, PbO, PbO_2, Pb_3O_4 can be removed from the possible source of lead because PbO is yellow, PbO_2 is black and Pb_3O_4 is an orange colour. Lead material owning the highest possibility is $PbCO_3$ and $2PbCO_3{\cdot}Pb(OH)_2$ because they are white in colour. Which lead was used by the Tang-dynasty potters?

The earliest example of lead-based white pigment was as early as the eighth century BCE in China. It was a white cosmetic residue excavated from Liangdaicun in North China (Han et al., 2022). From Qin (221-206 BCE) to Tang (618-907 CE) dynasties, white lead was also widely used as a pigment in potteries and frescos, such as the Terra-cotta Warriors (Li, 1983) and murals in Tang tombs (Zhang, 2001). Many Chinese historical accounts record the use and trade of this white pigment (Xu, 2006). It was named as Qian-bai (white lead 铅白), Bai-qian-

fen (white lead powder 白铅粉), Hu-fen (powder of Hu 胡粉[30]), Shao-fen (powder of Shao 韶粉[31]) and so on.

In modern chemistry, white lead or ceruse refers to $2PbCO_3 \cdot Pb(OH)_2$. It occurs naturally as hydrocerussite (Figure 5. 58), a hydrate of lead carbonate. The smooth mixture of this mineral allowed it to be used as pigment and cosmetics. Also, it can be synthesised based on minerals and acid. According to Schafer (1956)'s description, white lead forms readily when lead is exposed to moist air and some heat, but greater quantities are produced, and the process accelerated by the action of fumes of acetic acid. However, in ancient China, white lead can be referred to hydrocerussite ($(PbCO_3)_2 \cdot Pb(OH)_2$) and cerussite ($PbCO_3$), and also as a mixture of these two main lead carbonates (Zhou, 2012; Han et al., 2022). $PbCO_3$ occurs naturally as the mineral cerussite (Figure 5. 58). It is very brittle, and the Mohs hardness is 3-3.75 which is very close to that of hydrocerussite, at 3.5. The similar colour and texture of hydrocerussite and cerussite might be the reasons for sharing the same identification in ancient China. $PbCO_3$ was also found to be used as a cosmetic and a pigment - for example, the Dunhuang Frescoes (Geist et al., 1987) and the makeup powder residues containing 83% $PbCO_3$ unearthed from an Eastern-Han tomb (Xu and Zhou, 1983).

The current analysis in this thesis cannot confirm that the raw lead is hydrocerussite, cerussite or a mixture of them. But the scientific and archaeological results and discussions reveal that the raw lead is the 'white lead' in the Gongyi potters' mind, and this raw material

[30] In ancient China, 'Hu 胡' or 'Hu people 胡人' was generally used to refer to the foreigner and outsider. Narrow identification of Hu people in Tang dynasty is Caucasian people from the Central and Western Asia.

[31] 'Shao-fen 韶粉' is named by the provenance. It was produced in Chenzhou and Shaozhou, both in southern China.

is very pure. The compositional data obtained from the high-Pb areas reaches up to 60-80%, even though the lead powder in these areas were mixed up with kaolinitic clay and ash (Figure 5. 59 and Table 5. 12). Also, the texture of it is a very fine powder, and no particle or grain of metallic lead was observed (Figure 5. 60). The raw lead material must have been carefully ground before adding into the stock glaze.

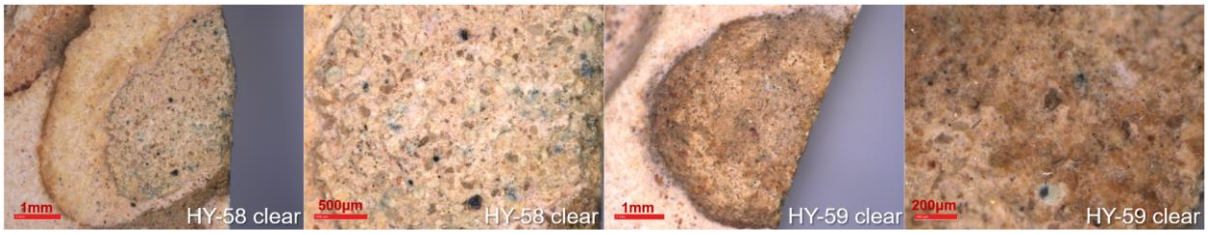


Figure 5. 57 Photos of colours of different raw glaze

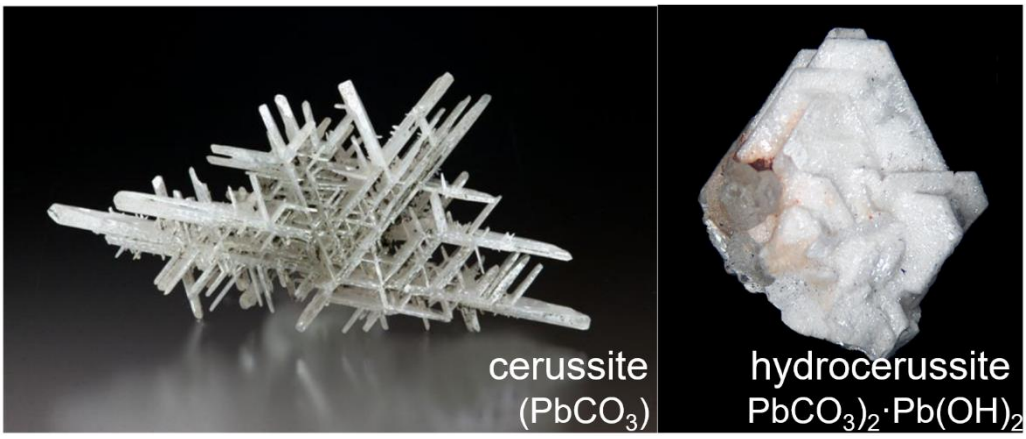


Figure 5. 58 Photos of cerussite and hydrocerussite, from https://www.mindat.org/min-934.html and from https://www.mindat.org/min-1969.html

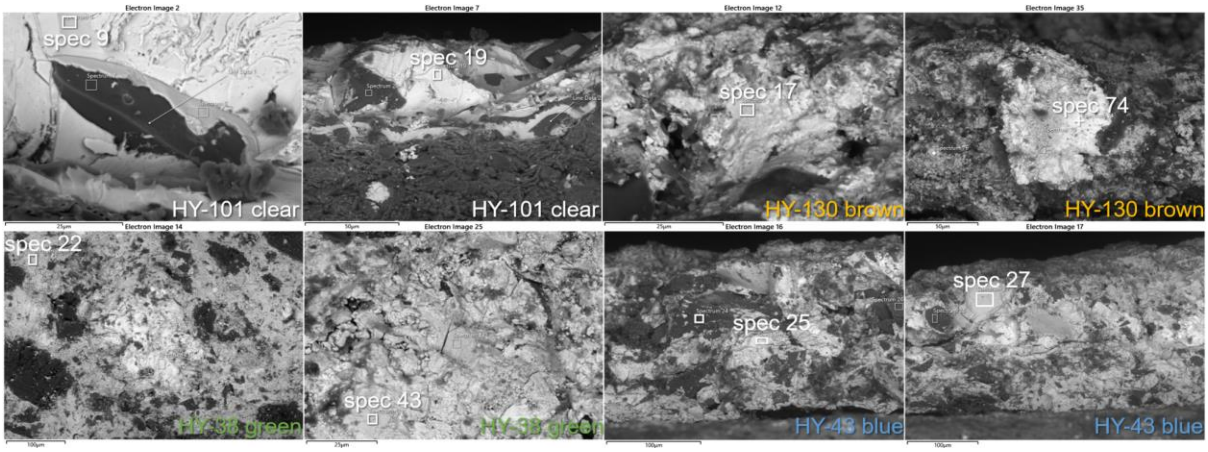


Figure 5. 59 Test areas of high-Pb areas in raw glazes, developed from ESEM.

Table 5. 12 Chemical compositions of high-Pb areas in raw glazes by ESEM

Glaze colours	Samples	Na_2O	Al_2O_3	SiO_2	P_2O_5	K_2O	CaO	CuO	PbO
Clear	HY-101 spec 9	0.61	10.23	21.00	-	1.22	1.75	-	65.19
	HY-101 spec 19	-	4.90	10.15	-	0.48	2.96	-	81.51
Brown	HY-130 spec 17	-	27.48	6.32	-	-	1.71	-	64.48
	HY-130 spec 74	-	10.02	5.26	-	0.35	0.44	0.58	83.35
Green	HY-38 spec 22	-	3.60	9.98	5.63	-	5.39	-	75.40
	HY-38 spec 43	-	3.75	7.63	1.49	-	4.58	-	82.56
Blue	HY-43 spec 25	-	19.94	13.16	-	0.80	1.84	-	64.27
	HY-43 spec 27	-	20.59	11.90	11.53	0.77	9.62	-	44.19

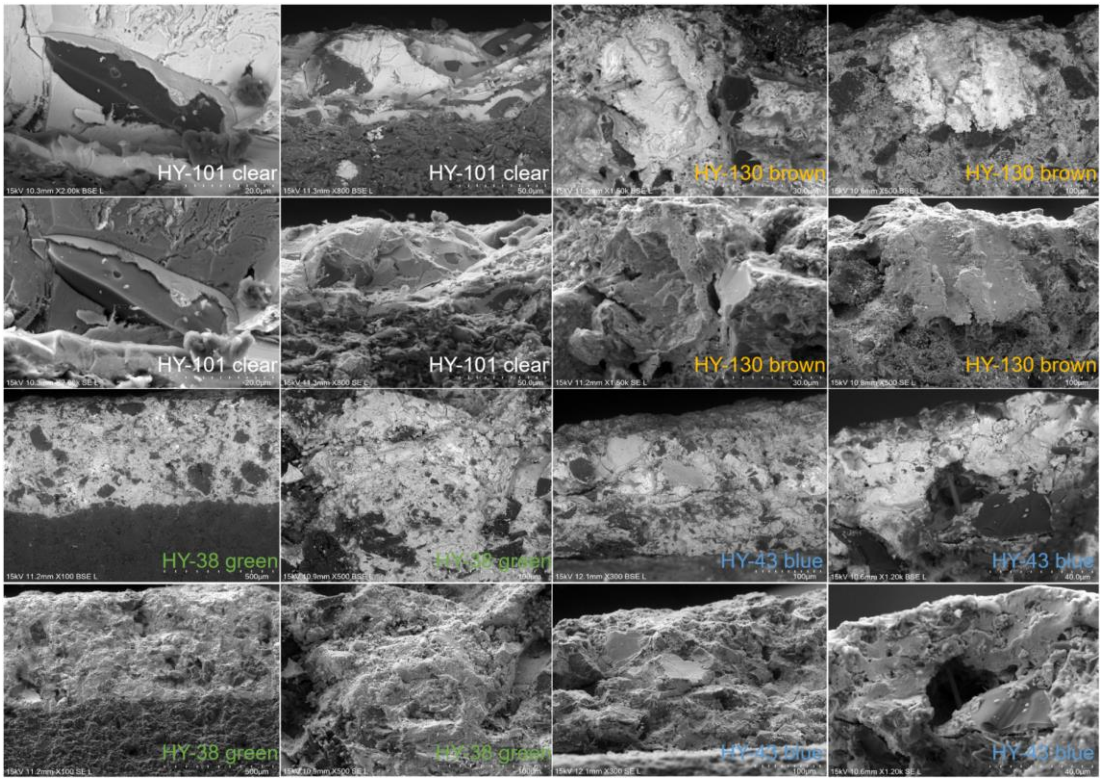


Figure 5. 60 BSE (the first and third rows) and SE (the second and fourth rows) images of high-Pb areas (light areas) of raw glazes, obtained from ESEM.

5.2 Glaze Making

5.2.1 From Raw Materials to Stock Glaze

According to the function of the materials, the important ingredients of the glaze are glass/glaze-former, flux and colourant. The glaze-former and flux constituent of the stock glaze is also the base of all coloured glazes. Chapter 5.1 has revealed the raw materials of the stock glaze. The next research question is how to process these materials to make the stock glaze? Based on the scientific analysis of fired glazes, the Pb-Si-Al system has been proposed (Cui et al., 2010a; Lingtong et al., 2022). However, the results and discussion of the raw glazes reveal that the system of the stock glaze is (Si+Al)-(Ca+P)-Pb, and based on the compositional data obtained from XRF, the ratio of these three constituents is around 1:1:1 (Figure 5. 61). In practice, the proportion of Ca+P might be lower than the other constituents due to the limitation of XRF on analysing phosphorus. The distribution of glaze data in the ternary plot is centralised and focused (Figure 5. 62a). It indicates that the proportion of the three constituents was carefully controlled by the potters.

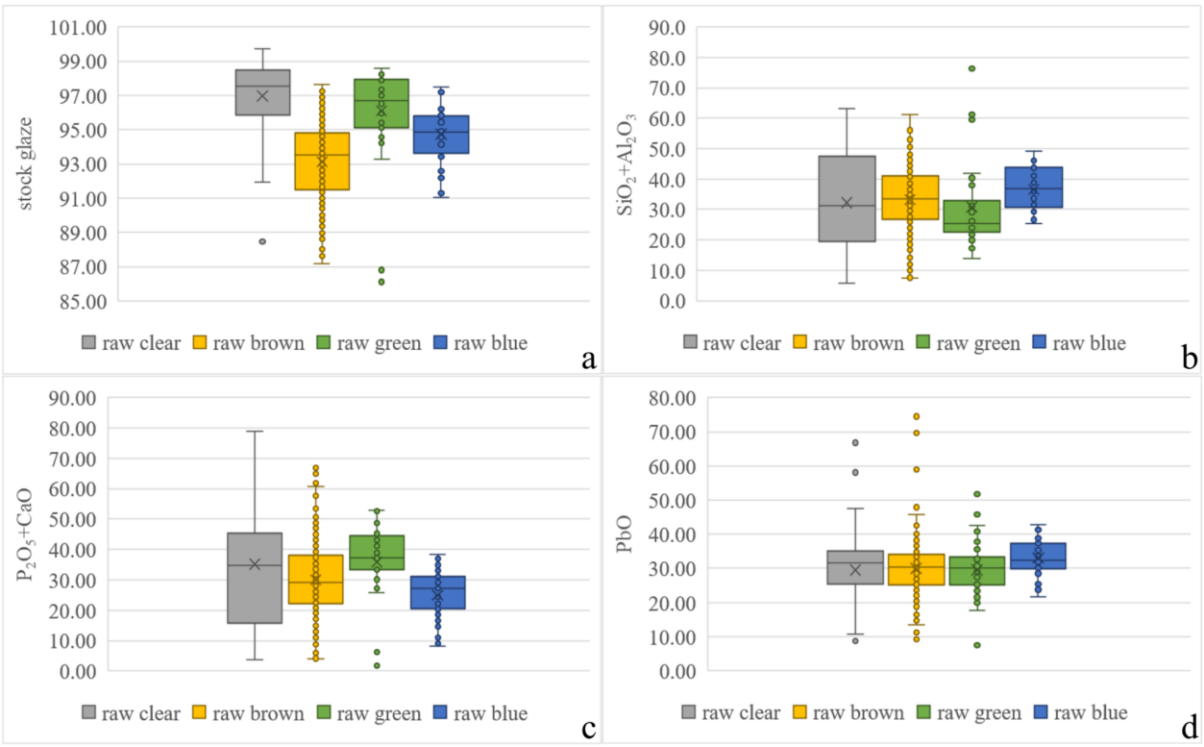


Figure 5. 61 Box plots of (a) weight percentage of stock glaze, (b) the sum of SiO_2 and Al_2O_3, (c) P_2O_5 and CaO, and (d) PbO of raw glazes.

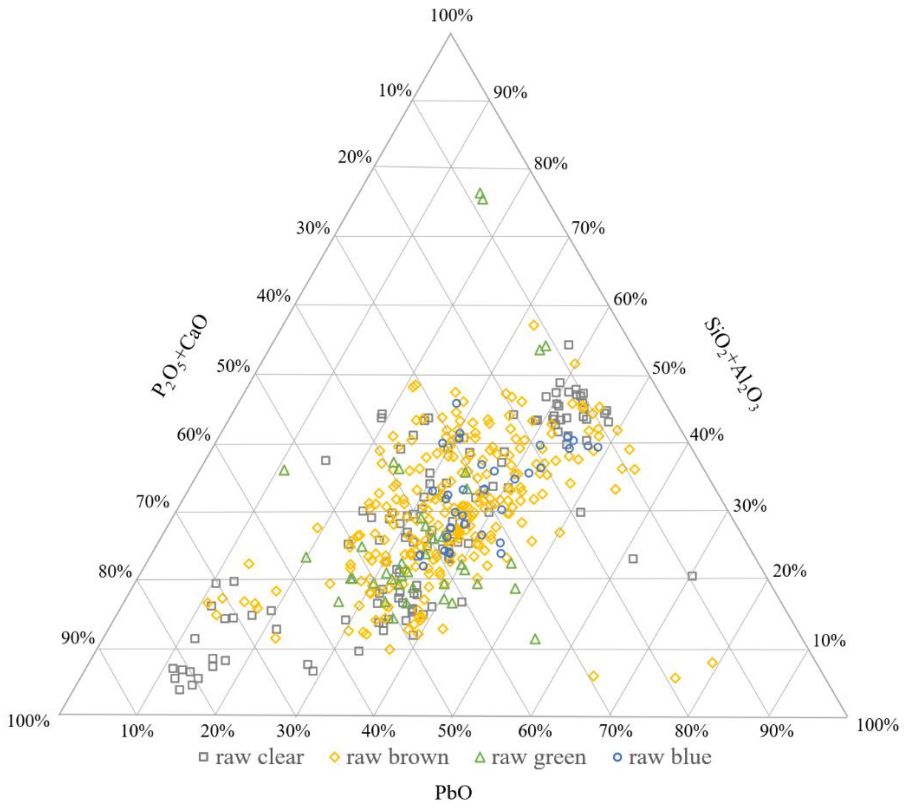


Figure 5. 62 Ternary plot of PbO, the sum of P_2O_5 and CaO, and the sum of SiO_2 and Al_2O_3 of raw glazes.

Si and Al act as the framework of the glaze, like the bone for human body. It has two sources, one-part local kaolinitic clay and two-parts flint and sand (Figure 5. 63). The kaolinitic clay is same as the material used in the body, which was exploited locally in Gongyi. The only difference between the kaolinitic clay and body material is that the clay used in the glaze is less purified than in the body. The body material was purified to decrease the concentration of the colouring impurity – iron before using. However, the kaolinitic clay might be added directly into the raw glaze after simple grinding. The use of flint and sand both aim to bring in a considerable quantity of silica. Flint is purer than sand, but sand is more available than flint. Sometimes, some sand grains brought in a little impurity, aluminium. These two quartz materials are too hard to be ground. The processing method is heating followed by rapid cooling. These hard flints and sands would break up into small particles. Tang potters might have recognised that a mixture of flint and quartz could provide extra fusion in a glaze when substituted for the single type. Thus, they were added into the glaze recipe together.

Ca, P and Pb work as the flux, but their sources are different. Pb was made from white lead. This white lead refers to $PbCO_3$ and $2PbCO_3 \cdot Pb(OH)_2$, which is different from the modern conception in chemistry and mineralogy. It is uncertain whether this white lead is a natural mineral or a synthesised material. They are both very brittle and soft which could be ground easily. The amount of lead material was kept in the same proportion in different glazes, which is equal to the sum of kaolinitic clay, flint, and sand. Also, a calcium-and-phosphorus-rich material was added into the glaze in an uncertain fixed proportion. This high-Ca-and-P material might be wood ash or other uncertain ash or mineral. If a wood ash was applied to the glaze making to import Ca and P, they might originate from two raw ingredients. Ca was contributed

by limestone and P was offered by the wood. These two raw ingredients were mixed up in a fixed proportion and calcined together. The limestone contains magnesium as a low impurity. However, the type of wood cannot be determined from the composition of the wood ash, because the making of wood ash included some chemical reactions, such as calcination, which might cause potential loss or changes to some elements in the wood. Also, it is uncertain whether the wood brought any inorganic impurity into the ash.

To summarise, the manufacturing process of the stock glaze can be divided into five steps (Figure 5. 64). The first four steps did not have a fixed order. The details are as follows:

1) Grind the local kaolinitic clay to a fine powder.
2) Break up the flint and sand by heating and rapid cooling.
3) Produce the Ca-and-P-rich material. For example, a wood ash can be made by mixing limestone and wood and calcining them together.
4) Grind the white lead to a fine powder.
5) Mix up all the materials and add water to the mixture to make up the stock glaze liquid.

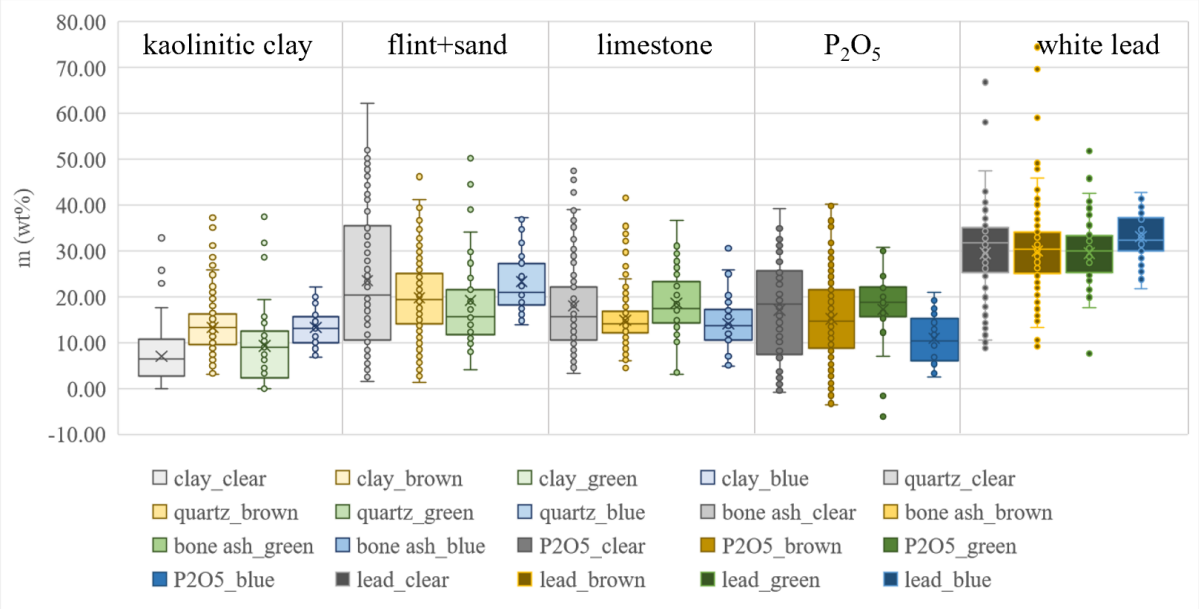


Figure 5. 63 Box plot of main ingredients of stock glaze.

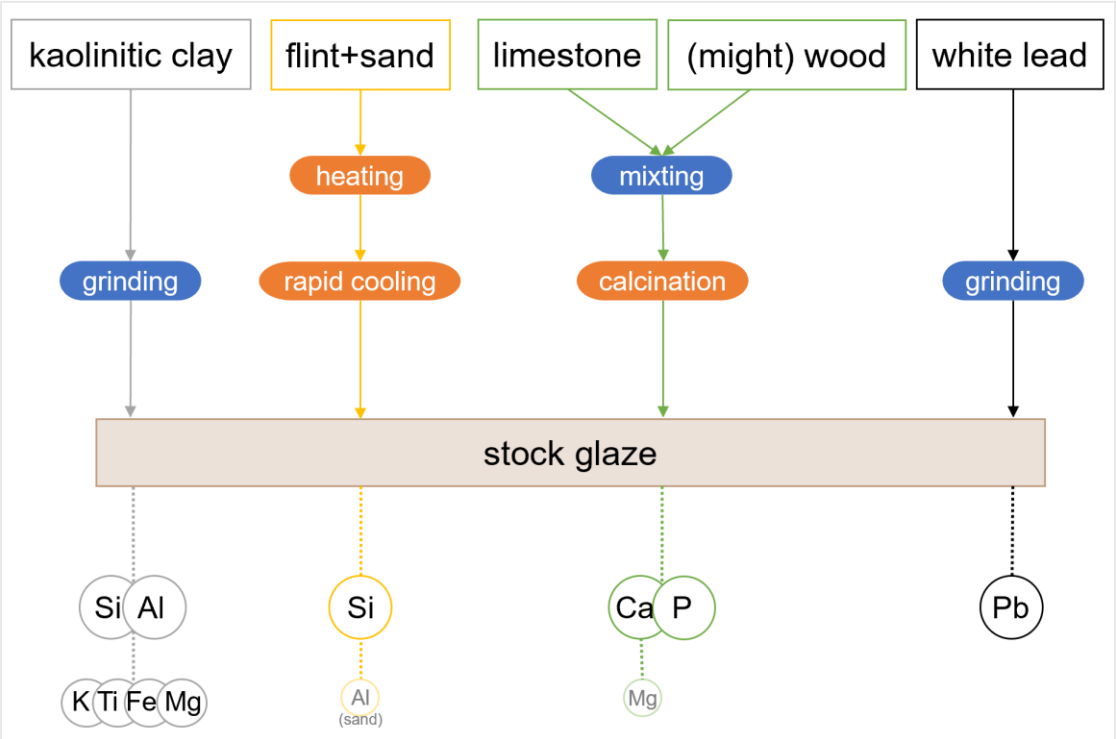


Figure 5. 64 The manufacturing process of stock glaze.

5.2.2 From Stock Glaze to Coloured Glazes

No constituents in the raw clear glaze are obviously higher than in other glazes. It indicates that the raw clear glaze had no other ingredients than the stock glaze - in other words, when the stock glaze was made, it could be used as the raw clear glaze. The other coloured glazes were produced by adding a colourant into the stock glaze. Compositionally, the content of the colourant is very low. The mean value of iron is 3.44%, and that of Co and Cu are both lower than 1%. The iron colourant added to the brown glaze is lower than 3.44% since the stock glaze contains some iron as an impurity of the kaolinitic clay. The simplified method of estimating the amount of colourant is to subtract the content of iron found in the stock glaze – in other words, that in the raw clear glaze, from the iron tested in the brown glaze. The result is 2.78%. In summary, the content of colourants in the glaze recipe is around 3% hematite for the brown

glaze, 1% green minerals, such as malachite, chrysocolla and atacamite etc. for green glaze and 1% glassy blue pigment, perhaps cobalt glass, for the blue glazes.

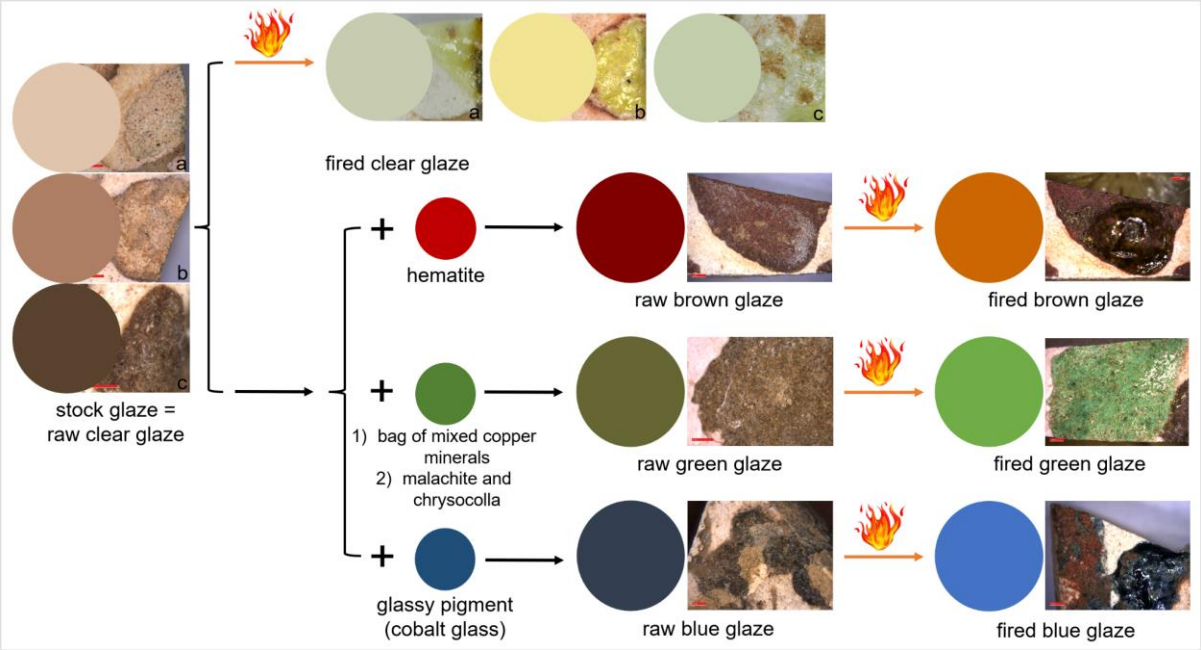


Figure 5. 65 Manufacturing process of coloured glazes.

Chapter 6 Conclusions and Future Work

The Tang dynasty witnessed the peak and glory of Chinese lead glaze and the earliest use of cobalt pigment on Chinese ceramics. The Gongyi kiln was the largest Sancai factory which had advanced technology and might have controlled the imported cobalt material in the Tang dynasty. Thus, Gongyi Sancai is the perfect sample to explore the technology Tang lead glaze and colourants. However, the published studies focus on the fired Sancai wares due to the lack of the finding of raw Sancai glazes. This thesis analysed 66 raw glazed sherds from the official excavation in 2002-4 and 2015 in the Gongyi kiln site. It is the first time that direct evidence of the raw materials and processing methods have been obtained from the scientific analysis of the raw Sancai glazes.

The raw clear glaze worked as the shared base of the brown, green, and blue Sancai glazes. The system of the stock glaze is (Si+Al)-(Ca+P)-Pb, and the ratio of these three constituents is around 1:1:1. The proportion of these constituents was carefully controlled by the potters. Si and Al act as the framework of the glaze, like the bone for human body. It has two sources, one-part local kaolinitic clay and two-parts flint and sand. The kaolinitic clay is same as the material used in the body, which was exploited locally in Gongyi. It might be added directly into the raw glaze after simple grinding. The use of flint and sand both aim to bring in a considerable quantity of silica. In the modern ceramic industry, the aim of the use of a mixture of different quartz is to provide extra and more fusion in a glaze than the single type. Perhaps, Tang potters had recognised that. These two quartz materials are too hard to be ground. The

processing method is heating followed by rapid cooling. These hard flints and sands would break up into small particles.

The white lead ($PbCO_3$ and $2PbCO_3 \cdot Pb(OH)_2$) and a Ca-and-P-rich material were the fluxes of the Sancai glaze. It is uncertain whether this white lead is a natural mineral or a synthesised material. They are both very brittle and soft which could be ground easily. The amount of lead material was kept in the same proportion in different glazes, which is equal to the sum of kaolinitic clay, flint, and sand. Also, the sum of calcium and phosphorus might be added into the glaze in the same proportion. If Ca and P are both from a wood ash, they might originate from two raw materials which were mixed up in a fixed proportion and calcined together. The X-ray fluorescence (XRF) analysis indicates a P_2O_5 to CaO ratio in this material of approximately 2:1. However, it is worth noting that the practical ratio could potentially be lower due to the initially lower P_2O_5 content in the raw glazes. Ca was contributed by limestone and P was offered by the wood. However, since the calcination might change the composition of the original wood, the type of wood cannot be determined based on current analysis.

The brown, green, and blue Sancai glazes were produced based on the raw clear glaze (stock glaze). Approximately, 3% hematite, 1% copper mineral(s), and 1% cobalt glass were added to the raw clear glaze respectively to make the iron-brown, copper-green, and cobalt-blue glazes. Hematite pigment was always a traditional local red pigment in China and was also applied to the mural paintings in the Tangy dynasty, such as the Mogao Grottoes. Compared with the hematite, copper green and cobalt blue pigments were ground for much longer term to be tiny fine powder. Malachite and chrysocolla were both confirmed to be used in the raw green glazes. Since some copper mineral – such as malachite, chrysocolla, azurite, cuprite etc. are commonly associated minerals in a natural copper mine. Perhaps, the green colourant was supplied with bag of mixed copper mineral which was pre-treatment and fine-powdered

mineral material. The iron colourant – hematite, was collected locally. This might explain the hematite is coarse, but the copper finely ground. The other possibility is that malachite and chrysocolla were both separately added to the clear glaze to make the green glaze. Gongyi potters might have realised that different copper ores can make the same green colour after firing.

The type and the origin of cobalt pigment is a core question of Tang Sancai and Chinese blue-and-white porcelain. Gongyi and Liquanfang were the only two kilns producing blue Sancai among six Sancai kilns (Gongyi, Liqunanfang, Yaohzou, Hunyuan, Xing, and Qionglai). However, only Gongyi created and produced blue-and-white porcelain in the Tang dynasty, later than blue Sancai. Thus, the research on cobalt colourant can give partial answer of the birth of Chinese blue-and-white porcelain. The analysis reveals that the cobalt blue colourant is cobalt glass which was fluxed by Mg or Mg and K together. This is the earliest glassy cobalt pigment based on current research, which was earlier by around one thousand years than the use of smalt. The original cobalt ore of the cobalt glass used in Sancai might be a low-iron, trace-manganese (high-Fe_2O_3/MnO), low-copper, uncertain-arsenic, no-nickel, no-zinc cobalt ore. Some characteristics of the ore of this cobalt glassy pigment is similar to the Yuan-Dynasty (1271-1368 CE) blue-and-white porcelain but the cobalt mine used in Tang Sancai was not in Kāshān. Although the production and trade of Tang blue-decorated ceramics (blue sancai and blue-and-white porcelain) were halted with the collapse of the Tang Empire (618-907 CE), a few Song blue-and-white still shimmered in southern China. Whether or not this blue glimmer in the Song Dynasty (960-1279 CE) inspired potters in the Mongol Empire is another story.

This research has some unavoidable limitations and also proposes many new research questions. Due to the limits of XRF and SEM-EDS, B, C and Na cannot be detected. However, B and Na are significant flux. It is uncertain whether they were used in the Sancai glaze and

the cobalt glass. C is significant for the determination of minerals, such as calcium oxide and calcium carbonate. Additionally, the valence of elements cannot be obtained by these two methods. Thus, it is unclear that the colouring mechanism of Sancai glazes - for example, the balance between Fe(II) an Fe(III) in the fired brown glaze. The other study to be done in the future is the quantitative study of the archaeological findings of burial Sancai and later Tang and Song blue-and-white porcelains. More than 4,000 Tang tombs have been involved in this research. The availability – time, location, the status of owners, distance to sancai kilns etc., of blue Sancai and Tang blue-and-white porcelain will be discussed based on the statistical work. Also, the organisation of the Gongyi and Liquanfang kilns will be explored by a comparison study and a lot of literary references.

Bibliography

ABE, Y., HARIMOTO, R., KIKUGAWA, T., YAZAWA, K., NISHISAKA, A., KAWAI, N., YOSHIMURA, S. & NAKAI, I. 2012. Transition in the use of cobalt-blue colorant in the New Kingdom of Egypt. *Journal of Archaeological Science,* 39**,** 1793-1808.

ADLINGTON, L. W. 2017. The Corning archaeological reference glasses: new values for" old" compositions. *Papers from the Institute of Archaeology,* 27**,** 1-8.

AFIFY, A., OSMAN, R., WANAS, H. & KHATER, T. 2022. Mineralogical and geochemical studies of copper mineralization in the Paleozoic sedimentary section in southwestern Sinai, Egypt. *Ore Geology Reviews,* 147**,** 104994.

ALLAN, J. W. 1991. *Islamic ceramics,* Oxford, Ashmolean Museum.

ALTAVILLA, C. & CILIBERTO, E. 2004. Decay characterization of glassy pigments: an XPS investigation of smalt paint layers. *Applied Physics A,* 79**,** 309-314.

BABAYEMI, J., DAUDA, K., NWUDE, D. & KAYODE, A. 2010. Evaluation of the composition and chemistry of Ash and. *J. Appl. Sci,* 10**,** 1820-1824.

BREMS, D. & DEGRYSE, P. 2014. Trace Element Analysis in Provenancing R oman Glass-Making. *Archaeometry,* 56**,** 116-136.

BUBLIKOVA, T., BALITSKY, V. & SETKOVA, T. 2022. Physical and chemical properties of geomaterials. *Experiment in Geosciences,* 28**,** 127-140.

BURAVLEV, I. Y., GELMAN, E., LAPO, E., PIMENOV, V. & MARTYNENKO, A. 2022. Three-colored Sancai glazed ceramics excavated from Bohai sites in Primorye (Russia). *Journal of Archaeological Science: Reports,* 41**,** 103346.

CARTWRIGHT, C. R. 2015. The principles, procedures and pitfalls in identifying archaeological and historical wood samples. *Annals of Botany,* 116**,** 1-13.

CHANG, D., CUI, J., SONG, Y., ZHAO, Z., QUAN, R. & ZHANG, L. 2023. International Trade of Lead for Glazed Tile Production in Ancient East Asia. *Archaeometry***,** 1-22.

CHANG, D., MA, R., CUI, J., ZHANG, L., SHI, Z., GONG, G. & LEI, Y. 2021. Circulation of Tang Sancai wares and lead materials in the two capital cities of the Tang empire. *Ceramics International,* 47**,** 10147-10152.

CHANG, D., MA, R., ZHANG, L., CUI, J. & LIU, F. 2020. Characterizing the chemical composition of Tang Sancai wares from five Tang dynasty kiln sites. *Ceramics International,* 46**,** 4778-4785.

CHEN, Y., WEN, R. & WANG, T. 2020. The origins of low-fire polychrome glazed pottery in China. *Antiquity,* 94**,** e30.

CHENG, H. S., ZHANG, B., ZHU, D., YANG, F., SUN, X. & GUO, M. 2005. Some new results of PIXE study on Chinese ancient porcelain. *Nuclear Instruments and Methods in Physics Research Section B: Beam Interactions with Materials and Atoms,* 240**,** 527-531.

CHENG, H.S.承焕生, SUN, X.M.孙新民, GUO, M.S.郭木森, ZHU, D.朱丹 & LIN, J.W.林家炜. 2016. Tang qinghua chandi de PIXE yanjiu 唐青花产地的 PIXE 研究 PIXE study on the provenance of Chinese ancient porcelain. *In:* 河南文物考古研究院, H. P. I. O. C. H. A. A., 中国文化遗产研究院, C. A. O. C. H. & PROPERTIE 日本奈良文化财研究所, N. N. R. I. F. C. (eds.) *Gongyi huangye yao 巩义黄冶窑 Gongyi Huangye Kiln* Beijing 北京: Kexue chubanshe 科学出版社 Science Press

CHEN, Y.C.陈尧成, ZHANG, F.K.张福康, ZHANG, X.W.张筱薇, JIANG, Z.Y.蒋忠义 & LI, D.J.李德金. 1995. Tangdai qinghuaci yong guliao laiyuan yanjiu 唐代青花瓷用钴料来源研究 An Investigation on the sources of cobalt pigment used in Tang blue-and-white *Zhongguo taoci 中国陶瓷 China Ceramics* 43-47.

CHEN, Y.C.陈尧成, GUO, Y.Y.郭演仪 & ZHANG, Z.G.张志刚. 1978. Lidai qinghua ciqi he qinghua seliao de yanjiu 历代青花瓷器和青花色料的研究 The study of blue-and-white porcelain and cobalt pigment from different dynasties *Guisuanyan xuebao 硅酸盐学报 Journal of Chinese Ceramic Society***,** 225-241+323-327.

CHEN, Y.T.陈彦堂 2021. Linzi chutu zhanguo qianyou taolei ji xiangguan wenti yanjiu 临淄出土战国铅釉陶罍及相关问题研究 Research of Warring-States lead-glazed Lei excavated from Linzi. *Zhongyuan wenwu 中原文物 Cultural Relics of Central China*, 95-96.

CHEN, X.S.陈显双 & LIAO, Q.Q 廖启清. 1986. Sichuan pujiang wuxing zhen songmu qingli ji 四川浦江五星镇宋墓清理记 Findings of the Song tomb in Wuxing of Pujiang in Sichuan. *Kaogu yu wenwu 考古与文物 Archaeology and Cultural Relics*.

COLOMBAN, P., KIRMIZI, B., ZHAO, B., CLAIS, J.-B., YANG, Y. & DROGUET, V. 2020. Investigation of the pigments and glassy matrix of painted enamelled qing dynasty chinese porcelains by noninvasive on-site raman microspectrometry. *Heritage,* 3**,** 915-940.

COLOMBAN, P., TOURNIE, A. & RICCIARDI, P. 2009. Raman spectroscopy of copper nanoparticle-containing glass matrices: ancient red stained-glass windows. *Journal of Raman Spectroscopy: An International Journal for Original Work in all Aspects of Raman Spectroscopy, Including Higher Order Processes, and also Brillouin and Rayleigh Scattering,* 40**,** 1949-1955.

COWELL, M. & ZHANG, F. K. 2001. *Catalogue of Late Yuan and Ming Ceramics in the British Museum,* London, the British Museum Press.

CUI, J., LEI, Y., JIN, Z., HUANG, B. & WU, X. 2010a. Lead isotope analysis of Tang Sancai pottery glazes from Gongyi kiln, Henan Province and Huangbao kiln, Shaanxi Province. *Archaeometry,* 52**,** 597-604.

CUI, J., REHREN, T., LEI, Y., CHENG, X., JIANG, J. & WU, X. 2010b. Western technical traditions of pottery making in Tang Dynasty China: chemical evidence from the Liquanfang Kiln site, Xi'an city. *Journal of Archaeological Science,* 37**,** 1502-1509.

DANIILIA, S. & MINOPOULOU, E. 2009. A study of smalt and red lead discolouration in Antiphonitis wall paintings in Cyprus. *Applied Physics A,* 96**,** 701-711.

DONG, J.Q.董俊卿, LI, Q.H.李青会 & YAN, X.严鑫. 2015. Jiyu OCT chengxiang jishu dui changjian taoci wenwu duanmian jiegou de wusun fenxi 基于 OCT 成像技术对常见陶瓷文物断面结

构的无损分析 Non-destructive analysis of the cross sections of ceramics by OCT technology. *Ziran zazhi 自然杂志 Chinese Journal of Nature* 37**,** 325-331.

DRISCOLL, R., HAGEMAN, P., BENZEL, W., DIEHL, S., ADAMS, D., MORMAN, S. & CHOATE, L. 2011. Assessment of the geoavailability of trace elements from minerals in mine wastes: analytical techniques and assessment of selected copper minerals. *US Geological Survey Scientific Investigations Report.*

DU, W.杜文 2011. Zhongguo gudai youtao fazhan mailuo ji guancang juyao 中国古代釉陶发展脉络及馆藏举要 Development and collection of ancient glazed wares in China. *Shoucang 收藏 Collections***,** 78-87.

FARGES, F., ETCHEVERRY, M.-P., SCHEIDEGGER, A. & GROLIMUND, D. 2006. Speciation and weathering of copper in "copper red ruby" medieval flashed glasses from the Tours cathedral (XIII century). *Applied Geochemistry,* 21**,** 1715-1731.

FENG, X., FENG, S., SHA, Y. & JAKŠIĆ, M. 2005. Study on the provenance and elemental distribution in the glaze of Tang Sancai by proton microprobe. *Nuclear Instruments and Methods in Physics Research Section B: Beam Interactions with Materials and Atoms,* 231**,** 553-556.

FENG, X.M.冯先铭. 1959. Henan gongxian guyaozhi diaocha jiyao 河南巩县古窑址调查纪要 Briefs of investigation of ancient kilns in Gongxian, Henan. *Wenwu 文物 Cultural Relics***,** 56-58.

GAN, F.X.干福熹. 2016. *Zhongguo gudai boli jishu fazhanshi 中国古代玻璃技术发展史 The Technological History of Chinese Ancient Glass* Shanghai 上海, Shanghai kexue jishu chubanshe 上海科学技术出版社 Shanghai Science and Technology Publisher.

GAN, F.X.干福熹, CHENG, H.S.承焕生, HU, Y.Q.胡永庆, MA, B.马波 & GU, D.H.顾冬红 2009. Henan xichuan xujialing chutu zhongguo zuizao de qingtingyan bolizhu de yanjiu 河南淅川徐家岭出土中国最早的蜻蜓眼玻璃珠的研究 Chinese Earliest Glass Beads Excavated from Xichuan Xujialing Tomb in Henan Province. *Zhongguo kexue 中国科学: E 辑 Science in China, Series E, Engineering and Materials Science***,** 787-792.

GEIST, R.盖特斯, 罗瑟福., JIANG, Z.Q.江致勤 & WANG, J.Y.王进玉 1987. Zhongguo yanliao de chubu yanjiu 中国颜料的初步研究. *Dunhuang yanjiu 敦煌研究 Dunhuang Research,* 1**,** 98-100.

GELMAN, E. I. 2006. Trade ceramics from Bohai sites of Russian Primor'e. *Beyond the Steppe and the Sown.* Brill.

GLASSPOOL, I. J., EDWARDS, D. & AXE, L. 2004. Charcoal in the Silurian as evidence for the earliest wildfire. *Geology,* 32**,** 381-383.

GONG, G.Q.龚国强 & HE, S.L.何岁利 2003. Tang changan cheng daming gong taiye chi yizhi fajue jianbao 唐长安城大明宫太液池遗址发掘简报 Excavation report of Taiye Pool of Daming Palace in Tang-dynasty Chang'an. *Kaogu 考古 Archaeology***,** 967-986+1060+2.

GUAN, L.关林, GUO, M.S 郭木森, YANG, J.K 杨军凯 & XIN, L.辛龙 2012. Xi'an yangjiaweiqiang chutu tangdai taociqi 西安杨家围墙出土唐代陶瓷器 The Tang ceramics unearthed from Yangjiaweiqiang in Xi'an *Shoucangjie 收藏界 Collection World* 107-110.

HAI, Q.海清 2015. Shanxi beiqi shiqi chutu taozhi qimin yanjiu 山西北齐时期出土陶质器皿研究 Research on Northern-Qi pottery vessels excavated from Shanxi. *Wenwu shijie 文物世界 Journal of Chinese Antiquity***,** 25-27.

HAMER, F. & HAMER, J. 2015. *The Potter's Dictionary of Materials and Techniques,* London, Bloomsbury Academic.

HAN, B., ZHANG, B., CHONG, J., SUN, Z. & YANG, Y. 2022. Beauty and chemistry: the independent origins of synthetic lead white in east and west Eurasia. *Humanities and Social Sciences Communications,* 9**,** 1-12.

Henan Museum 河南省博物馆. 1972. Henan anyang beiqi fancui mu fajue jianbao 河南安阳北齐范粹墓发掘简报 Excavation report of Norther-Qi Fancui tomb in Anyang, Henan. *Wenwu 文物 Cultural Relics***,** 47-57+86.

Henan Provincial Institute of Cultural Heritage and Archaeology 河南省文物考古研究所, Cultural Relics Institute of China 中国文化遗产研究院 & Nara National Research Institute for Cultural Properties 日本奈良文化财研究所. 2009. *Gongyi baiheyao kaogu xinfaxian 巩义白河窑考古新发现 The New Archaeological Discovery at Baihe Kiln in Gongyi* Zhengzhou 郑州, Daxiang chubanshe 大象出版社 Elephant Press.

Henan Provincial Institute of Cultural Heritage and Archaeology 河南省文物考古研究所, Cultural Relics Institute of China 中国文物研究所 & Nara National Research Institute for Cultural Properties 日本奈良文化财研究所. 2005. *Huangye yao kaogu xin faxian 黄冶窑考古新发现 The New Archaeological Discovery at Huangye Kiln Site* Zhengzhou 郑州, Daxiang chubanshe 大象出版社 Elephant Press.

Henan Provincial Institute of Cultural Heritage and Archaeology 河南省文物考古研究所, Cultural Relics Institute of China 中国文化遗产研究院 & Nara National Research Institute for Cultural Properties 日本奈良文化财研究所. 2016a. *Gongyi huangye yao (xia) 巩义黄冶窑 (下) Gongyi Huangye Kiln (II),* Beijing 北京, Kexue chubanshe 科学出版社 Science Press.

Henan Provincial Institute of Cultural Heritage and Archaeology 河南省文物考古研究所, Cultural Relics Institute of China 中国文化遗产研究院 & Nara National Research Institute for Cultural Properties 日本奈良文化财研究所. 2016b. *Gongyi huangyeyao (shang) 巩义黄冶窑 (上) Gongyi Huangye Kiln (I)* Beijing 北京, Kexue chubanshe 科学出版社 Science Press.

HENDERSON, J., MA, H., CUI, J., MA, R. & XIAO, H. 2020. Isotopic investigations of Chinese ceramics. *Archaeological and Anthropological Sciences,* 12**,** 1-13.

JIANG, X.Y.蒋玄佁. 1959. Gudai de liuli 古代的琉璃 Ancient glaze. *Wenwu 文物 Cultural Relics***,** 8-10.

JIA, M.Z.贾忠敏 & JIA, Y.L.贾永禄. 1987. Hebei sheng neiqiu xian xingyao diaocha jianbao 河北省内丘县邢窑调查简报 The survey report of Xing Kiln Site in Neiqiu, Hebei *Wenwu 文物 Cultural Relics* 1-10.

JI, J.G.冀金刚. 2001. Jieshao yipi yuandai liuli youtao yong he taozhi jiaju 介绍一批元代琉璃釉陶俑和陶制家具 Introduction of some glazed figures and furniture. *Wenwu chunqiu 文物春秋***,** 64-70.

KANG, B.Q.康葆强, WANG, S.W.王时伟, DUAN, H.Y.段鸿莺, CHEN, T.M.陈铁梅 & MIAO, J.M.苗建民. 2013. Gugong shenwu men liuli wa niandai he chandi de chubu yanjiu 故宫神武门琉璃瓦年代和产地的初步研究 Preliminary research on the manufacture location glazed tiles for the Forbidden City's Gate of Divine Prowess (Shenwu men). *Gugong xuekan 故宫学刊 Journal of Gugong Studies,* 2**,** 234-241.

KERR, R. & WOOD, N. 2004. *Science and Civilisation in China, Volume 5 Part 12, Ceramic Technology*, Cambridge: Cambridge University Press.

KUGLER, V., SPRING, M. & HUDSON, J. 2013. Quantitative SEM-EDX Analysis of Smalt Pigment Under Variable Pressure Conditions. *Proc Microsc Microanal,* 19**,** 1428-9.

KUNICKI-GOLDFINGER, J. J., FREESTONE, I. C., MCDONALD, I., HOBOT, J. A., GILDERDALE-SCOTT, H. & AYERS, T. 2014. Technology, production and chronology of red window glass in the medieval period–rediscovery of a lost technology. *Journal of Archaeological Science,* 41**,** 89-105.

LANG, J.F.郎剑锋 & CUI, J.F.崔剑锋. 2017. 临淄战国齐墓出土釉陶罍的风格与产地——兼论我国铅釉陶的起源问题 Style and provenance of glazed Lei excavated from Warring-States Qi tomb in Linzi – the origin of Chinese lead-glazed pottery. *Huaxia kaogu 华夏考古 Huaxia Archaeology***,** 95-101.

LEI, Y., FENG, S., FENG, X. & CHAI, Z. 2007. A provenance study of Tang sancai from Chinese tombs and relics by INAA. *Archaeometry,* 49**,** 483-494.

LEI, Y.雷勇. 2007. Tang sancai de yiqi zhongzi huohua fenxi qi zai liangjing diqu fazhan guiji de yanjiu 唐三彩的仪器中子活化分析其在两京地区发展轨迹的研究 Research on the development of Tang sancai in capital cities by INAA. *Gugong Bowuyuan yuankan 故宫博物院院刊 Palace Museum Journal* 86-127+158.

LEI, Y.雷勇, FENG, S.L.冯松林, FENG, X.Q.冯向前, FAN, D.Y.范东宇, XU, Q.徐清, SHA, Y.沙因, CHENG, L.程琳, JIANG, J.姜捷, GAO, Z.X.禚振西 & ZHANG, S.L.张松林. Dianxing yaozhi chutu tang sancai de zhongzi huohua fenxi yu yanjiu 典型窑址出土唐三彩的中子活化分析与研究 Research on Tang sancai excavated from kilns by INAA analysis. Di shier jie quanguo hewuli dahui ji diqi jie huiyuan daibiao dahui lunwen zhaiyao ji 第十二届全国核物理大会暨第七届会员代表大会论文摘要集 Conference Proceedings of 12th CNPN'2004 2004.

LEI, Y.雷勇, FENG, S.L.冯松林, FENG, X.Q.冯向前 & GUO, H.T.郭洪涛. 2005. Tang gongling aifei mu chutu tang sancai de zhongzi huohua fenxi he chandi yanjiu 唐恭陵哀妃墓出土唐三彩的中子活化分析和产地研究 Provenance study of Tang sancai excavated from Queen Ai tomb in Gongling by INAA. *Zhongyuan wenwu 中原文物 Cultural Relics of Central China,* 1**,** 86-89.

LI, B., ZHAO, J., GREIG, A., COLLERSON, K. D., FENG, Y., SUN, X., GUO, M. & ZHUO, Z. 2006. Characterisation of Chinese Tang sancai from Gongxian and Yaozhou kilns using ICP-MS trace element and TIMS Sr–Nd isotopic analysis. *Journal of Archaeological Science,* 33**,** 56-62.

LI, B., ZHAO, J., GREIG, A., COLLERSON, K. D., ZHUO, Z. & FENG, Y. 2005. Potential of Sr isotopic analysis in ceramic provenance studies: characterisation of Chinese stonewares. *Nuclear Instruments and Methods in Physics Research Section B: Beam Interactions with Materials and Atoms,* 240**,** 726-732.

LI, T., LI, G., LI, Z., WU, T., TIAN, H., SHAN, S. & WANG, L. 2022. Surface treatment of red painted and slipped wares in the middle Yangtze River valley of Late Neolithic China: multi-analytical case analysis. *Heritage Science,* 10**,** 188.

LI, W. D., LU, X. K., LUO, H. J., SUN, X. M., LIU, L. H., ZHAO, Z. W. & GUO, M. S. 2017. A Landmark in the History of Chinese Ceramics: The Invention of Blue-and-white Porcelain in the Tang Dynasty (618–907 AD). *STAR: Science & Technology of Archaeological Research,* 3**,** 358-365.

LINGTONG, Y., YUE, Z., BO, M., HEYANG, S., LI, L. & XIANGQIAN, F. 2022. The coordination structure and optical property of iron ions in the traditional lead glazes. *Journal of Molecular Structure***,** 132593.

LING, X.凌雪, MAO, Z.W.毛振伟, FENG, M.冯敏, HU, Y.W.胡耀武, WANG, C.S 王昌燧 & LIU, H.M.刘洪淼. 2005. Gongyao tangdai zaoqi baoci de EDXRF xiansaomiao fenxi 巩窑唐代早期白瓷的 EDXRF 线扫描分析 Line scanning analysis of white porcelain from Gong kiln in early Tang dynasty by energy disperse X-Ray fluorescence. *Guangpuxue yu guangpu fenxi 光谱学与光谱分析 Spectroscopy and Spectral Analysis,* 25**,** 1145-1150.

LI, Y.D.李亚东. 1983. Qinyong caihui yanliao ji qindai yanliao shikao 秦俑彩绘颜料及秦代颜料史考 Research on the painted pigments of the terracotta warriors and the history of the pigments in the Qin Dynasty. *Kaogu yu wenwu 考古与文物 Archaeology and Cultural Relics***,** 62-65.

LI, G.Z.李国桢 & GUO, Y.Y.郭演仪. 2012. *Zhongguo mingci gongyi jichu 中国名瓷工艺基础 Technological Bases of Famous Chinese Porcelains,* Hangzhou 杭州, Zhejiang daxue chubanshe 浙江大学出版社 Zhejiang University Press.

LI, J.Z.李家治 1998. *Zhongguo kexue jishu shi taoci juan 中国科学技术史·陶瓷卷 The Science History of China · Ceramics,* Beijing 北京, Kexue chubanshe 科学出版社 Science Press.

LI, Z.X.李最雄. 2002. Dunhuang mogaoku tangdai huihua yanliao fenxi yanjiu 敦煌莫高窟唐代绘画颜料分析研究 Research on Tang-dynasty pigments of Mogao Caves in Dunhuang. *Dunhuang yanjiu 敦煌研究 Dunhuang Research***,** 11-18+110.

LI, Z.Y.李知宴. 1972. Tan fancui mu chutu de ciqi 谈范粹墓出土的瓷器 Porcelains from Fancui tomb. *Kaogu 考古 Archaeology***,** 53-55.

LI, X.李鑫. 2019. Suitang wudai shiqi baici zhici jishu de chuangxin liubian yu chuanbo 隋唐五代时期白瓷制瓷技术的创新, 流变与传播 Technological innovation and spreading of white

porcelain in Sui, Tang and Five dynsties. *Nanfang wenwu 南方文物 Cultural Relics in Southern China***,** 258-265.

LI, T.C.李铁锤. 2011. Shengdong er shenmi de sichuan song sancai yaoyong 生动而神秘的四川宋三彩陶俑 Vivid and mysterious Song sancai figures found in Sichuan. *Wenwu jianding yu jianshagn 文物鉴定与鉴赏 Identification and Appreciation to Cultural Relics***,** 48-51.

LI, T.C.李铁锤. 2013. Meilun meihuan de qiongyao gaowen tang sancai 美轮美奂的邛窑高温唐三彩 Beautiful high-fired Tang sancai excavated from Qiong kiln. *Shoucangjie 收藏界 Collection World***,** 34-38.

LU, X.K.鲁晓珂, LI, W.D.李伟东, SUN, X.M.孙新民, LUO, H.J.罗宏杰, LIU, L.H.刘兰华, ZHAO, Z.W.赵志文, GUO, M.S.郭木森 & XU, J.M.徐霁明. 2016. Tang qinghua de chansheng 唐青花的产生 The origin of Tang blue-and-white porcelain. *In:* 河南省文物考古研究院, H. P. I. O. C. H. A. A., 中国文化遗产研究院, C. A. O. C. H. & 日本奈良文化财研究所, N. N. R. I. F. C. P. (eds.) *Gongyi Huangye yao 巩义黄冶窑 Gongyi Huangye Kiln* Beijing 北京: Kexue chubanshe 科学出版社 Science Press

MA, B., LIU, L., FENG, S., XU, Q. & FENG, X. 2014. Analysis of the elemental composition of Tang Sancai from the four major kilns in China using EDXRF. *Nuclear Instruments and Methods in Physics Research Section B: Beam Interactions with Materials and Atoms,* 319**,** 95-99.

MATIN, M. 2016. *Revisiting the origins of Islamic glazed pottery: a technological examination of 8th-10th century AD ceramics from Islamic lands.* University of Oxford.

MATIN, M. & POLLARD, A. M. 2017. From Ore to Pigment: A description of the Minerals and an Experimental Study of Cobalt Ore Processing from the Kāshān Mine, Iran. *Archaeometry,* 59**,** 731-746.

MATIN, M. & POLLARD, M. 2015. Historical accounts of cobalt ore processing from the Kashan mine, Iran. *Iran,* 53**,** 171-183.

MA, D.Z.马得志 & ZHANG, Z.L.张正龄. 1958. Xi'an jiaoqu sange tangmu de fajue jianbao 西安郊区三个唐墓的发掘简报 Excavation report of three Tang tombs in the suburb of Xi'an *Kaoguu tongxun 考古通讯（考古）Archaeology* 42-52.

MIAO, J. M.苗建民 & LUO, S.L.陆寿麟. 2001. Zhongzi huohua fenxi he zhuchengfen fenxi dui tang sancai chandi wenti de yanjiu 中子活化分析和主成份分析对唐三彩产地问题的研究 The provenance of Tang sancai by INAA and PCA *Dongnan wenhua 东南文化 Southeast Culture* 83-93.

MISRA, M. K., RAGLAND, K. W. & BAKER, A. J. 1993. Wood ash composition as a function of furnace temperature. *Biomass and Bioenergy,* 4**,** 103-116.

MÜHLETHALER, B. & THISSEN, J. 1969. Smalt. *Studies in Conservation,* 14**,** 47-61.

MÜHLETHALER, B. & THISSEN, J. 1993. Artists Pigments. A Handbook of their History and Characteristics, Vol. 2. *National Gallery of Art, Washington***,** 113.

POLLARD, A. M., HERON, C. & ARMITAGE, R. A. 2017. *Archaeological Chemistry,* Cambridge, The Royal Society of Chemistry.

RAWSON, J., TITE, M. & HUGHES, M. 1989. The export of Tang sancai wares: some recent research. *Transactions of the Oriental Ceramic Society,* 52**,** 39-61.

RUAN, P.E.阮平尔 1990. Zhejiang longquan xian chutu songdai qinghuaci 浙江龙泉县出土宋代青花瓷 Song blue-and-white porcelains excavated from Longquan in Zhejiang. *Nanfang wenwu 南方文物 Cultural Relics in Southern China***,** 120-120.

SCHAFER, E. H. 1956. The early history of lead pigments and cosmetics in China. *T'oung Pao,* 44**,** 413-438.

SCHAFER, E. H. 1963. *The golden peaches of Samarkand: a study of T'ang exotics,* Univ of California Press.

Shaanxi Museum 陕西省博物馆 1972. Tang zheng rentai mu fajue jianbao 唐郑仁泰墓发掘简报 The excavation report of Zheng Rentai Tang Tomb *Wenwu 文物 Cultural Relics* 33-41.

Shaanxi Provincial Institute of Archaeology 陕西省考古研究院 2008. *Tang changan liquanfang sancai yaozhi 唐长安醴泉坊三彩窑址 The Kiln Site of Tricolor-Glazed Pottery at Liquanfang In Chang'an Capital City of Tang Dynasty* Beijing 北京, Wenhua chubanshe 文化出版社 Cultural Relics Press.

SHAN, D.山丹. 2019. Liao sancai yu qidan wenhua 辽三彩与契丹文化 Liao sancai and the culture of Khitay. *Taoci yanjiu 陶瓷研究 Ceramic Studies,* 34**,** 7-11.

SHEN, J. Y., HENDERSON, J., EVANS, J., CHENERY, S. & ZHAO, F. Y. 2019. A study of the glazing techniques and provenances of Tang sancai glazes using elemental and lead isotope analyses. *Archaeometry,* 61**,** 358-373.

SHEN, L.H.沈丽华, ZHU, Y.S.朱岩石 & WANG, Y.汪盈. 2015. Hebei zanhuangxian beiwei liyi fufu mu 河北赞皇县北魏李翼夫妇墓 Northern-Wei Liyi couple tomb in Zanhuang, Heibei. *Kaogu 考古 Archaeology***,** 64-77.

SHI, R.Y.石若瑀, WEN, R.温睿, GAO, X.高翔, WANG, W.X.王文轩, BAO, L.G.宝力格, ZHAO, X.F.赵学锋, LI, Z.X.李梓轩, CAO, K.曹昆, XIAO, W.肖薇 & LI, Y.L.李昱龙 2021. Yuandai ducheng liuli wa youceng de EDXRF he SEM-EDS fenxi 元代都城琉璃瓦釉层的 EDXRF 和 SEM-EDS 分析 X-ray fluorescence spectroscopy combined withe SEM-EDS analysis to glaze composition of glazed tiles in Yuan dynasty. *Guangpu xue yu guangpu fenxi 光谱学与光谱分析 Spectroscopy and Spectral Analysis*, 41**,** 3808.

SHORTLAND, A. & EREMIN, K. 2006. The analysis of second millennium glass from Egypt and Mesopotamia, part 1: new WDS analyses. *Archaeometry,* 48**,** 581-603.

SMIRNIOU, M. & REHREN, T. 2013. Shades of blue–cobalt-copper coloured blue glass from New Kingdom Egypt and the Mycenaean world: a matter of production or colourant source? *Journal of Archaeological Science,* 40**,** 4731-4743.

SONG, Y.S.宋应星. 1637. Tian gong kai wu 天工开物. *In:* YANG, W.Z.杨维增 (ed.). Beijing 北京: Zhonghua shuju 中华书局 Zhonghua Book Company.

SPATARO, M., WOOD, N., MEEKS, N., MEEK, A. & PRIESTMAN, S. 2019. Pottery technology in the Tang dynasty (ninth century ad): archaeometric analyses of a Gongyi sherd found at Siraf, Iran. *Archaeometry,* 61**,** 574-587.

SPRING, M., HIGGITT, C. & SAUNDERS, D. 2005. Investigation of pigment-medium interaction processes in oil paint containing degraded smalt. *National Gallery Technical Bulletin,* 26**,** 56-70.

SU, B. 2021. Wall painting materials and techniques of the Mogao grottoes. *Conservation and Painting Techniques of Wall Paintings on the Ancient Silk Road***,** Springer, 253-263.

SUN, X.M.孙新民. 2006. Lvelun liao sancai yu sang song sancai de yitong 略论辽三彩与唐, 宋三彩的异同 Discussion about the similarities and differences of Liao, Tang and Song sancai wares. *Caoyuan wenwu 草原文物 Steppe Cultural Relics***,** 75-77.

SUN, F.X.孙福喜, YANG, J.K.杨军凯, SUN, W.孙武 & FENG, J.冯健. 2004. Xian nanjiao tangmu (M31) fajue jianbao 西安南郊唐墓（M31）发掘简报 Excavation report of Tang tomb M31 in the southern Xian. *Wenwu 文物 Cultural Relics* 31-61.

TANG, C.P.唐昌朴 1980. Jiangxi jizhou yao faxian song yuan qinghuaci 江西吉州窑发现宋元青花瓷 Song and Yuan blue-and-white porcelains found in Jizhou kiln in Jiangxi. *Wenwu 文物 Cultural Relics***,** 4.

TANG, X.M.唐雪梅, YU, L.于璐, LI, H.李合 & DING, Y.Z.丁银忠. 2022. Nanjing dabaoen si chutu liuli jiancai de fenlei ji chengen fenxi 南京大报恩寺出土琉璃建材的分类及成分分析 Grouping and compositional analysis of glazed materials of the Grand Bao'en temple in Nanjing. *Gugong bowuyuan yuankan 故宫博物院院刊 Palace Museum Journal,* 244**,** 101-142.

The Institute of Archaeology CASS 1974. Tang qinglong si yizhi fajue jianbao 唐青龙寺遗址发掘简报 The excavation of Qinglong temple. *Kaogu 考古 Archaeology* 322-327+349-350+321.

TIAN, T.田雨 2002. Shanxi hunyuan xian jiezhuang tangdai ciyao 山西浑源县界庄唐代瓷窑 Tang-dynasty kiln in Jiezhuang of hunyuan, Shanxi. *Kaogu 考古 Archaeology*, 60-68.

TITE, M. & BIMSON, M. 1991. A technological study of English porcelains. *Archaeometry,* 33**,** 3-27.

WANG, H. & YANG, G. 2021. Provenance study of Sancai Glazed Pottery excavated in Longhai Royal Tomb of Bohai state by composition and statistical analysis. *Forest Chemicals Review***,** 373-382.

WANG, H.T.王会田 & CUI, J.J.崔建军. 2008. Shandong zibo shi linzi qu faxian yizuo zhanguo muzang 山东淄博市临淄区发现一座战国墓葬 A Warring-States tomb found in Linzi District of Zibo of Shandong. *Kaogu 考古 Archaeology***,** 95-96.

WANG, D.H.王冬华. 2012. Xi'an faxian de cizhou yao sancai qi 西安发现的磁州窑三彩器 Sancai wares found in Cizhou kiln in Xi'an. *Shoucang 收藏 Collections***,** 64-66.

WANG, W.D.王卫丹 2011. Song jin yuan sancai zhen de fenlei yu chandi 宋金元三彩枕的分类与产地 Grouping and provenance of Song, Jin and Yuan sancai pillows. *Shoucang 收藏 Collections***,** 64-71.

WANG, T.T.王天艺. 2018. 汉代复色低温铅釉陶器初探 Research on Han-dynasty low-firing lead-glazed two-coloured potteries. *Kaogu yu wenwu 考古与文物 Archaeology and Cultural Relics***,** 78-88.

WANG, Z.M.王宗沐 1597. Jiang-xi sheng da zhi 江西省大志 The great gazette of Jiang-xi province. Taibei 台北: Chengwen chubanshe 成文出版社 Cheng Wen Press.

WANG, X.M.王小蒙 2018. Liangjing diqu tang sancai de fazhan ji gongyi tezheng 两京地区唐三彩的发展及工艺特征 Development and manufacture of Tang sancai in two capitals. *Shoucang 收藏 Collections***,** 78-81.

WANG, H.M.王洪敏, PAN, W.B.潘伟斌 & ZHU, T.Q.朱铁权 2011. Anyang beichao mu chutu qianyoutao de fenxi yanjiu 安阳北朝墓出土铅釉陶的分析研究 Analysis of lead-glazed potteries excavated from Northern-dynasties tombs in Anyang. *Zhongguo guojia bowuguan guankan 中国国家博物馆馆刊 Journal of National Museum of China***,** 128-133.

WANG, Y.王熠 & TIAN, W.L.田卫丽 2010. Handai qianyoutao fazhan zongshu 汉代铅釉陶发展综述 Review of Han-Dynasty Lead Glazed Pottery *Wenbo 文博 Relics and Museology* 17-23.

WANG, W.B.王蔚波 2011. Tang gongling chutu youtao beihou de gushi 唐恭陵出土釉陶背后的故事 Appreciation on Glazed Potteries Unearthed from Gong Mausoleum in Luoyang *Shoucang 收藏 Collections* 58-63.

WATSON, O. 2014. Revisiting Samarra: the rise of Islamic glazed pottery. *Beiträge zur Islamischen Kunst und Archäologie,* 4**,** 123-142.

WEI, J.魏坚. 2008a. *Yuanshangdu (shang) 元上都（上）Shangdu Site of the Yuan Dynasty (I),* Beijing 北京, Zhongguo dabaike quanshu chubanshe 中国大百科全书出版社 Encyclopedia of China Publishing House.

WEI, J.魏坚. 2008b. *Yuanshangdu (xia) 元上都（下）Shangdu Site of the Yuan Dynasty (II),* Beijing 北京, Zhongguo dabaike quanshu chubanshe 中国大百科全书出版社 Encyclopedia of China Publishing House.

WEN, R. 2012. *The cobalt blue pigment used on Islamic ceramics and chinese blue-and-white porcelains.* Oxford University.

WEN, R., WANG, C., MAO, Z., HUANG, Y. & POLLARD, A. 2007. The chemical composition of blue pigment on Chinese blue-and-white porcelain of the Yuan and Ming dynasties (AD 1271–1644). *Archaeometry,* 49**,** 101-115.

WENJIE, L. 2021. Pottery-Making in Ancient China. *In:* XIAOYUAN, J. (ed.) *A New Phase of Systematic Development of Scientific Theories in China.* Shanghai Shanghai Jiao Tong University Press.

WOOD, N. 1999. *Chinese glazes: Their origins, chemistry, and recreation*, University of Pennsylvania Press.

WOOD, N., DOHERTY, C. & ROSSER-OWEN, M. A technological study of Iraqi imitations of Chinese Changsha wares and Chinese Sancai wares found at Samarra. ISAC, 2009 Shanghai. Shanghai Science and Technology Press, 154-180.

WOOD, N., TITE, M. S., DOHERTY, C. & GILMORE, B. 2007. A technological examination of ninth-tenth century AD Abbasid blue-and-white ware from Iraq , and its comparison with eighth century AD Chinese blue-and-white sancai ware. *Archaeometry,* 49**,** 665-684.

WOODS, T. L. & GARRELS, R. M. 1986. Phase relations of some cupric hydroxy minerals. *Economic Geology,* 81**,** 1989-2007.

XIA, Y., XI, N., HUANG, J., WANG, N., LEI, Y., FU, Q. & WANG, W. 2019. Smalt: an under-recognized pigment commonly used in historical period China. *Journal of Archaeological Science,* 101**,** 89-98.

XIONG, Y.F.熊燕飞. 1995. Caomuhui zai youliao peizhi zhong de yingyong 草木灰在釉料配制中的应用 The use of plant ash in glaze recipe. *Jingdezhen taoci 景德镇陶瓷 Jingdezhen Ceramics,* 5**,** 17-18.

XUE, D.X.薛东星. 2002. Yaozhou yao tang sancai 耀州窑唐三彩 Tang sancai of Yaozhou kiln. *Wenbo 文博 Relics and Museolgy***,** 50-53.

XU, W.Y.徐位业 & ZHOU, G.X.周国信. 1983. Anhui shouxian donghan mu chutu baifen fenxi 安徽寿县东汉墓出土白粉分析 Analysis of the white powder excavated from a Donghan tomb in Shouxian, Anhui. *Kaogu 考古 Archaeology***,** 1139-1140.

XU, Y.徐勇. 2006. Wantang wudai dunhuang diqu suoyong yanliao yanjiu 晚唐五代敦煌地区所用颜料研究 Research of pigments used in Dunhuang in late Tang and Five dynasties. *Dunhuangxue jikan 敦煌学辑刊 Journal of Dunhuang Studies***,** 80-84.

YANG, Y.杨勇, JI, Y.冀勇, LI, G.X.李国霞, ZHAO, W.J 赵维娟, SUN, H.W.孙洪巍, GAO, Z.Y.高正耀, GUO, M.郭敏, XIE, J.Z.谢建忠, LI, R.W.李融武 & ZHAO, Q.Y.赵青云. 2008. Huangyeyao he yaozhouyao tangsancai zhiwen yuansu de duoyuan tongji fenxi 黄冶窑和耀州窑唐三彩指纹元素的多元统计分析 Study on the fingerprint elements of Tang tri-color pottery of Huangye kiln and Yaozhou kiln by muktivariate statistical analysis. *Xinyang shifan xueyuan xuebao (ziran kexue ban) 信阳师范学院学报:（自然科学版）Journal of Xinyang Normal University(Natural Science Edition)* 21**,** 190.

YANG, H.Q.杨海青 & ZHAO, X.C.赵小灿. 2015. Sanmenxia miaodigou chutu de tang song sancai qi 三门峡庙底沟出土的唐宋三彩器 Tang and Song sancai unearthed in Miaodigou in Sanmenxia. *Shoucangjia 收藏家 Collector***,** 49-51.

YAO, Q.姚庆. 2017. Beijing longquanwu yao liao sancai taoci 北京龙泉务窑辽三彩陶瓷 Liao sancai made by Longqianwu kiln in Beijing. *Shoucangjia 收藏家 Collector***,** 38-40.

YE, Z.M.叶喆民. 2011. *Zhongguo taoci shi 中国陶瓷史 History of Chinese Pottery and Porcelain,* Beijing 北京, Shenghuo dushu xinzhi sanlian shudian 生活·读书·新知三联书店 SDX Joint Publishing Company.

YONG, L., SONGLIN, F., XIANGQIAN, F., DONGYU, F., QING, X., YIN, S., LIN, C., ZHIFANG, C., JIE, J. & ZHENXI, Z. 2005. Study on the compositional differences of Tang Sancai from different kilns by INAA. *Journal of archaeological science,* 32**,** 183-191.

YOUNG, S. 1956. An analysis of Chinese blue-and-white. *Oriental Art,* 2**,** 43-47.

YOUNG, W. J. 1949. Discussion of Some Analyses of Chinese Underglaze Bllue and Underglaze Red. *Far Eastern Ceramic Bulletin,* 2**,** 99-111.

ZHANG, Y. & POLLARD, A. M. 2022. The archaeological and scientific analysis of blue-decorated ceramics in the Tang and Song dynasties. *Archaeometry,* 64**,** 1394-1410.

ZHANG, C.张冲 & ZHANG, W.W.张伟伟. 2020. Zibo shi bowuguan cang boshandajie yao jin sancai shixing qi 淄博市博物馆藏博山大街窑金三彩狮形器 Jin sancai lion-shaped wares made by Boshandajia kiln in Zibo Museum. *Wenwu tiandi 文物天地 Cultural Relics World,* 3**,** 66-71.

ZHANG, J.L.张建林 & MA, Z.J.马志军. 2000. Bieju tese d jindai sancai qi 别具特色的金代三彩器 Special Jin sancai. *Shoucangjia 收藏家 Collector***,** 4-7.

ZHANG, Z.G.张志刚, GUO, Y.Y.郭演仪 & CHEN, Y.C.陈尧成. 1986. Tangdai qinghuaci yu sancai gulan 唐代青花瓷与三彩钴兰 Tang blue-and-white porcelain and cobalt pigment used on Tang sancai wares *Jingdezhen taoci xuebao 景德镇陶瓷学报 Journal of Jingdezhen Ceramic Institute* 99-107.

ZHANG, Z.G.张志刚, GUO, Y.Y.郭演仪, CHEN, Y.C.陈尧成, ZHANG, P.S.张浦生 & ZHU, J.朱戢. 1989. Tangdai qinghua ciqi yantao 唐代青花瓷器研讨 Research on blue-and-white porcelain of Tang dynasty *Jingdezhen taoci xuebao 景德镇陶瓷学报 Journal of Jingdezhen Ceramic Institute* 11.

ZHANG, Z.G.张志刚, LUO, Z.Z.罗宗真, GUO, Y.Y.郭演仪 & CHEN, Y.C.陈尧成. 1984. Yangzhou tangcheng chutu qinghuaci de ceding jiqi zhongyao yiyi 扬州唐城出土青花瓷的测定及其重要意义 The scientific analysis of Tang blue-and-white porcelain excavated from Yangzhou Tang city site *Wenwu 文物 Cultural Relics* 56-59.

ZHANG, Z.G.张志刚 & ZHANG, P.S.张浦生. 2009. Qianshuo tang qinghuaci keji jianding 浅说唐青花瓷科技鉴定 The scientific analysis of Tang blu-and-white porcelain *Shoucang jie 收藏界 Collection World***,** 69-73.

ZHANG, Q.X.张群喜. 2001. Tangmu bihua yanliao de fenxi yu yanjiu 唐墓壁画颜料的分析与研究 Research of pigments on murals in Tang tombs. *In:* 周天游 (ed.) *Tangmu bihua yanjiu wenji 唐墓壁画研究文集 Collection of Reserches on Murals in Tang Tombs.* Sanqin chubanshe 三秦出版社 Sanqin Press.

ZHANG, C.H.张长海, JING, X.T.靖晓亭 & WANG, J.王江. 2022. 山西大同开源美域北魏砖室墓发掘简报 Excavation report of Northern-Wei brick-chamber tomb in Kaiyuanmeiyu of Datong, Shanxi. *Huaxia kaogu 华夏考古 Huaxia Archaeology*, 37-41.

ZHAO, K.M.赵康民. 1985. Lintong tang qingshan si sheli taji jingshi qingliji 临潼唐庆山寺舍利塔基精室清理记 Findings of the chamber of dagoba of Tang-dynasty Qingshan temple in Lintong. *Wenbo 文博 Relics and Museolgy*, 12-37.

ZHAO, Z.W.赵志文. 2011. Henan gongyi shi baihe yao yizhi fajue jianbao 河南巩义市白河窑遗址发掘简报 Excavation report of the Baihe kiln site in Gongyi, Henan. *Huaxia kaogu 华夏考古 Huaxia Archaeology*, 26-86.

ZHOU, D.周到. 1964. Henan puyang beiqi liyun mu chutu de ciqi he muzhi 河南濮阳北齐李云墓出土的瓷器和墓志 Northern-Qi porcelains and gravestone of Liyun tomb in Puyang, Henan. *Kaogu 考古 Archaeology* 482-484+412.

ZHOU, G.X.周国信. 2012. Zhongguo xibei diqu gudai bihua caisu zhong de hanqian baise yanliao 中国西北地区古代壁画彩塑中的含铅白色颜料 White lead-based pigments on the murals in the Northwest China. *Wenwu baohu yu kaogu kexue 文物保护与考古科学 Sciences of Conservation and Archaeology*, 24, 95-103.

ZHU, B.Q.朱伯谦. 1980. Zhejiang liangchu taji chutu song qinghuaci 浙江两处塔基出土宋青花瓷 Song blue-and-white porcelains excavated from two Pagoda foundations in Zhejiang. *Wenwu 文物 Cultural Relics*, 1-3.

ZI, Y.紫玉. 2011. Tang sancai de jiemeihua —— yiyu sancai 唐三彩的姊妹花——异域三彩 Twins of Tang sancai – exotic sancai. *Shoucangjie 收藏界 Collection World*, 65-68.

Appendices

Appendix 1 Description of samples unearthed from the Gongyi kiln site (II and III areas) in 2002-2004

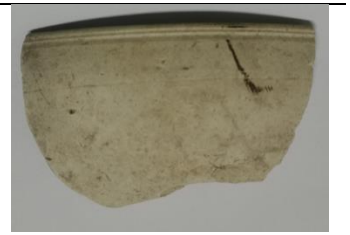
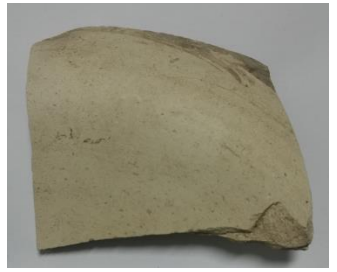
Original numbers	Numbers	Bodies	Shapes	Inside surfaces	Photos of inside	Outside surfaces	Photos of outside
II 区 T4H15	HY-101	white, hard, and heavy	bowl sherd with foot	yellowish brown glaze		foot: unglazed, central area: white slip, edge: yellowish brown glaze	
II 区 T4H15	HY-102	whitey, hard and heavy	pot sherd	unglazed，unglazed		edge: reddish brown glaze, middle area: yellowish brown spot-shape, one yellowish brown strip, one red strip	

Original numbers	Numbers	Bodies	Shapes	Inside surfaces	Photos of inside	Outside surfaces	Photos of outside
						and some unclear glaze/pollutant with irregular shape	
II ☒ T4H15	HY-106	white	sherd	reddish brown spot-shape and yellowish-brown spot-shape glaze		reddish brown glaze	
II ☒ T4H15	HY-115	pinkish	sherd	white slip, a small brown spot (possible fired glaze)		white slip (some areas are unglazed which looks like motif)	

Original numbers	Numbers	Bodies	Shapes	Inside surfaces	Photos of inside	Outside surfaces	Photos of outside
III 区 T6 (0706)H81	HY-116	pinkish	sherd	unglazed		white slip, fired transparent stripe-shape glaze	
III 区 T6 (0706)H81	HY-117	white	sherd	unglazed		yellowish brown glaze on white slip	

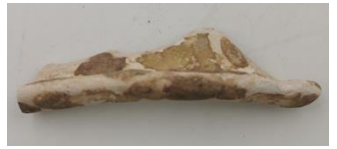
Original numbers	Numbers	Bodies	Shapes	Inside surfaces	Photos of inside	Outside surfaces	Photos of outside
III 区 T6 (0706)H81	HY-118	white	sherd	unglazed		yellowish brown glaze on white slip	
II 区 T4H15	HY-119	yellowish	bowl sherd	white slip		middle area and edge: thick white slip	

Appendix 2 Description of samples unearthed from the Gongyi kiln site in 2015

Original numbers	Numbers	Bodies	Shapes	Inside surfaces	Photos of inside	Outside surfaces	Photos of outside
T0231:⑦	HY-38	white	sherd, edge	big and small brown spot-shape glaze		unglazed, no slip	
2015GZHI T0231:⑥	HY-43	white	sherd, edge	unglazed, no slip		black irregular-shape glaze, brown irregular-shape glaze, no slip	
T0231:⑦	HY-58	white	sherd	small white spot-shape glaze, big reddish-brown spot-shape glaze		unglazed, no slip	

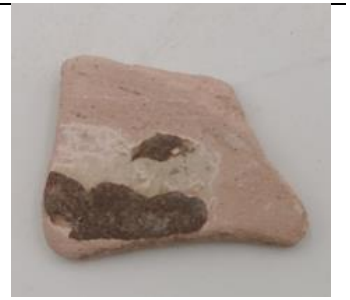
Original numbers	Numbers	Bodies	Shapes	Inside surfaces	Photos of inside	Outside surfaces	Photos of outside
T0231:⑦	HY-59	white	sherd	small white spot-shape glaze, big reddish-brown spot-shape glaze		unglazed, no slip	
2015GZHZ ☒ T0332H7	HY-61	white	sherd	unglazed		brown spot-shape thin glaze (some brown areas are dyed by the lost glaze)	
	HY-62	white	sherd	unglazed		brown spot thin glazes, many of them are peeled off	

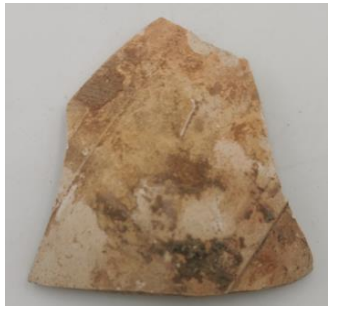
Original numbers	Numbers	Bodies	Shapes	Inside surfaces	Photos of inside	Outside surfaces	Photos of outside
T0131:⑥	HY-64	white	sherd	unglazed		brown spot glaze	
2015GZH I ☒ T0331	HY-92	white	sherd	unglazed		irregular-shape reddish brown decoration	

Original numbers	Numbers	Bodies	Shapes	Inside surfaces	Photos of inside	Outside surfaces	Photos of outside
T0131:⑭	HY-121	white	sherd	unglazed		reddish brown spot-shape glaze, main parts were peeled off	
T0131:⑭	HY-122	pinkish	sherd	unglazed		thin red powder (possible soil/pigment)	
T0131:⑭	HY-123	white	sherd, edge	reddish brown glaze, yellowish brown glaze		reddish brown spot-shape glaze, yellowish brown/white spot-shape glaze	

Original numbers	Numbers	Bodies	Shapes	Inside surfaces	Photos of inside	Outside surfaces	Photos of outside
T0331 下⑥	HY-124	yellowish	sherd, edge	unglazed		thin red powder (possible soil/pigment)	
T0237	HY-125	white	fragment, foot	unglaze		reddish brown irregular-shape glaze	
T0236③	HY-126	greyish	sherd	unglazed		coarse yellowish grey spot-shape material on the body	

Original numbers	Numbers	Bodies	Shapes	Inside surfaces	Photos of inside	Outside surfaces	Photos of outside
T0131①	HY-127	yellowish	sherd	unglazed		dark green glaze on white slip	
T0131:⑥	HY-129	white	fragment, foot	unglaze		reddish brown spot-shape glaze	

Original numbers	Numbers	Bodies	Shapes	Inside surfaces	Photos of inside	Outside surfaces	Photos of outside
T0131:⑥	HY-130	pinkish	sherd, edge	reddish brown glaze on the white slip		reddish brown glaze on the white slip	
T0333C1	HY-131	pinkish	sherd	white slip		reddish brown glaze on white slip	
T0333C1	HY-132	pinkish	sherd	unglazed, no slip		reddish brown spot-shape glaze and yellowish-brown spot-shape glaze on white slip	

Original numbers	Numbers	Bodies	Shapes	Inside surfaces	Photos of inside	Outside surfaces	Photos of outside
T0231:⑦	HY-133	white	sherd	unglazed		red material (possible soil/pigment)	
T0231:⑦	HY-134	yellowish	sherd	unglazed		yellowish and black material (possible soil or pollutant)	
T0332:⑥下	HY-135	white	sherd	yellowish brown glaze		reddish brown strip-shape glaze	

Original numbers	Numbers	Bodies	Shapes	Inside surfaces	Photos of inside	Outside surfaces	Photos of outside
T0332:⑥下	HY-136	white	sherd	yellowish brown glaze		reddish brown strip-shape glaze; white spot-shape glaze, yellowish brown glaze	
T0231:⑨	HY-137	greyish	sherd	thin red material		possibly covered with white slip	
T0231:⑨	HY-138	white	sherd, edge	thin red material		unglazed，unglazed	

Original numbers	Numbers	Bodies	Shapes	Inside surfaces	Photos of inside	Outside surfaces	Photos of outside
T0237:⑦	HY-139	yellowish	sherd	unglazed		irregular-shape dark green material and reddish-brown material	
T0237:⑦	HY-140	white	sherd	unglazed		irregular-shape yellowish brown material	
T0131 北	HY-141	white	sherd, edge	edge area: covered with white slip; lower area: unglazed		white slip	

Original numbers	Numbers	Bodies	Shapes	Inside surfaces	Photos of inside	Outside surfaces	Photos of outside
T0131 北	HY-143	white	sherd	unglazed		white slip	
?	HY-145	white	sherd	reddish brown material on fired white glaze		yellowish brown material on white slip	
T0331:⑧	HY-146	white	sherd, edge	yellowish brown glaze		covered with yellowish brown glaze	
T0331:⑧	HY-147	white	sherd	unglazed		thin black material (possible soot)	

Original numbers	Numbers	Bodies	Shapes	Inside surfaces	Photos of inside	Outside surfaces	Photos of outside
T0331:⑧	HY-148	white	sherd	half area: covered with red material; the other half: unglazed		half area: black material with a little gloss (possible fired glaze), the other half: thin red material	
T0331:⑧下	HY-149	white	sherd, edge	unglazed		thin black material (possible soot)	
T0331:⑧下	HY-150	white	sherd	unglazed		irregular-shape reddish brown and yellowish-brown glaze	

Original numbers	Numbers	Bodies	Shapes	Inside surfaces	Photos of inside	Outside surfaces	Photos of outside
T0331:⑧下	HY-151	greyish	sherd	strip-shape reddish brown glaze		unglazed	
T0331:⑧下	HY-152	white	bowl sherd with foot	spot-shape reddish brown glaze; the colour of one spot is darker than the other one		unglazed	
T0131：①	HY-153	pinkish	sherd	white slip		white slip	

Original numbers	Numbers	Bodies	Shapes	Inside surfaces	Photos of inside	Outside surfaces	Photos of outside
T0131：①	HY-154	pinkish	sherd	little white slip		white slip	
T0131：①	HY-155	greyish yellow	sherd	unglazed		small area: white slip; big area: yellow glaze	
T0131：①	HY-166	white	sherd	pink material		white slip	

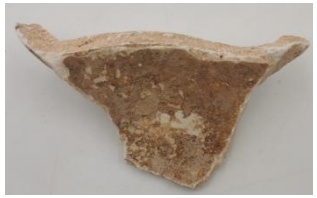
Original numbers	Numbers	Bodies	Shapes	Inside surfaces	Photos of inside	Outside surfaces	Photos of outside
2015GZHI☒T0131:⑥	HY-172	white	sherd, edge	unglazed		neck area: covered with reddish brown glaze, v-shap and circle reddish brown glaze	
2015GZHI☒T0131:⑥	HY-173	white	sherd, edge	unglazed		reddish brown glaze	
2015GZHI☒T0131:⑥	HY-174	white	sherd, edge	unglazed		neck area: reddish brown glaze, v-shap and circle reddish brown glaze	

Original numbers	Numbers	Bodies	Shapes	Inside surfaces	Photos of inside	Outside surfaces	Photos of outside
2015GZHI ☒ T0131:⑥	HY-175	white	sherd, neck	unglazed		reddish brown glaze	
2015GZHI ☒ T0131:⑥	HY-176	white	sherd, edge	unglazed		neck area: reddish brown glaze, v-shap and circle reddish brown glaze	
2015GZHI ☒ T0131:⑥	HY-177	white	sherd	unglazed		spot-shape reddish brown glaze	

Original numbers	Numbers	Bodies	Shapes	Inside surfaces	Photos of inside	Outside surfaces	Photos of outside
2015GZHI ⊠ T0131:⑥	HY-178	white	sherd	unglazed		spot-shape reddish brown glaze	
2015GZHI ⊠ T0131:⑥	HY-179	white	sherd	unglazed		spot-shape reddish brown glaze	
2015GZHI ⊠ T0131:⑥	HY-180	white	sherd	unglazed		spot-shape reddish brown glaze	

Original numbers	Numbers	Bodies	Shapes	Inside surfaces	Photos of inside	Outside surfaces	Photos of outside
2015GZHI ☒ T0131:⑥	HY-181	white	sherd	unglazed		spot-shape reddish brown glaze	
2015GZHI ☒ T0131:⑥	HY-182	white	sherd	unglazed		small spot-shape reddish brown glaze, v-shape, and circle reddish brown glaze	
2015GZHI ☒ T0131:⑥	HY-183	white	sherd	unglazed		small-spot reddish-brown glaze, circle reddish brown glaze	

Original numbers	Numbers	Bodies	Shapes	Inside surfaces	Photos of inside	Outside surfaces	Photos of outside
2015GZHI ☒ T0131:⑥	HY-184	white	sherd	unglazed		small-spot reddish-brown glaze, circle reddish brown glaze	
2015GZHI ☒ T0131:⑥	HY-185	white	sherd with foot	unglazed		abdomen: spot-shape reddish brown glaze, foot: unglazed, leg: reddish brown glaze	
2015GZHI ☒ T0131:⑥	HY-186	white	sherd	unglazed		irregular reddish-brown spots and some black spots	

Original numbers	Numbers	Bodies	Shapes	Inside surfaces	Photos of inside	Outside surfaces	Photos of outside
2015GZHI ☒ T0131:⑥	HY-187	white	sherd	unglazed		irregular reddish-brown spots and some black spots	
2015GZHI ☒ T0131:⑥	HY-188	white	sherd with foot circle	yellowish brown glaze		yellowish brown glaze	

Appendix 3 The scientific methods of Tang Sancai in publications

References	Samples	Test areas	Methods	Tested elements
Buravlev et al.2022	Bohai: 30	body and glaze	p-XRF	Si. Al, Fe, Ti, Pb, Cu, Mn, Zn, Mg, Sb, Sn, P, S, Zr, Nb, Hf, Bi, Cd, V, Cr, Ni, Ca, Na, K
Yan et al. 2022	Yaozhou: 5; Liquanfang: 5	glaze	EDXRF, XAFS	Na2O, MgO, Al2O3, SiO2, K2O, CaO, Fe2O3, CuO, PbO2
Wang & Yang 2021	Longhai royal tomb of Baohai State: 4	body, glaze	WDXRF, EDXRF	PbO, CuO, SiO2, TiO2, Al2O3, Fe2O3, MnO, MgO, CaO, Na2O, K2O, P2O5, Ba, Co, Cr, Cu, Ca, Nv, Ni, Pb, Rb, Sr, V, Y, Zn, Zr
Chang et al. 2021	Tomb: 13; residence of Juyi, Bai (772-846) in Luoyang: 9; Taiye Pond, Daming Palace: 9	body, glaze	MC-ICP-MS: lead isotope, EDXRF	Na2O, MgO, Al2O3, SiO2, P2O5, K2O, CaO, TiO2, MnO, Fe2O3
Chang et al. 2020	Gongyi: 19; Liquanfang: 29; Yaozhou: 17; Xing:4; Qionglai: 14	body, glaze	EDXRF	Na2O, MgO, Al2O3, SiO2, K2O, CaO, TiO_2, Fe2O3, CuO, ZnO, SnO2, PbO2

References	Samples	Test areas	Methods	Tested elements
Shen et al. 2019	Gongyi: 10; Yaozhou: 10; Tomb: 9	glaze	LA-ICP-MS: rare earth elements, lead isotope	
Ma et al. 2014	Gongyi: 33; Yaozhou: 49; Liquanfang: 85; Xing: 7	body	EDXRF	Na2O, MgO, Al2O3, SiO2, P2O5, K2O, CaO, TiO2, Cr2O3, MnO, Fe2O3, CuO, ZnO, Rb2O, SrO, Y2O3, ZrO2
Cui et al. 2010	Liquanfang: 29	body, glaze, slip	LA-ICP-AES: trace elements, SEM-EDS	18 elements in the bodies--Al, Fe, Mg, Ca, Na, K, Ti, Mn, Ba, Sr, Cu, Zn, Sr, Ce, La, Y, Yb, Zr
Cui et al. 2010	Gongyi 10; Yaozhou: 9	glaze	MC-ICP-MS: lead isotope	Pb
Yang et al. 2008	Yaozhou: 2	glaze	NAA	La , Ce, Nd , Sm , Eu , Tb , Yb , Lu, Na, Sc, Cr, Fe, Co, Ni, Zn, As, Se, Rb, Sr, Zr, Mo, Sb, Cs, Ba, Hf, Ta, W, Th, U
Yang et al. 2008	Gongyi: 18; Yaozhou: 5	body		
Xia & Wang 2008	Luoyang : 5		thermoluminescence dating	

References	Samples	Test areas	Methods	Tested elements
Dong et al. 2008	Gongyi: 18	body, glaze	PIXE	Na2O , MgO , SiO2 , K2O, TiO2, CaO, CuO, CoO, PbO
Wood et al. 2007	Sancai:7; Abbasid blue-and-white glazed earthenware: 8	body, glaze	XRF, SEM-EDS/-WDS	SiO2, Na2O, CaO, MgO, Al2O3, FeO, PbO, CuO, SnO2, CoO, MnO, ZnO, NiO, As2O5, Cr2O3, BaO
Junko et al. 2007	Gongyi: 7		XRF, XRD	SiO2, Al2O3, CaO, PbO, K2O, Fe2O3, TiO2, MnO, CoO, CuO
Lei et al. 2007	Xing: 7; Tomb: 130	body	INAA	Fe, Na, K, Ce, Nd, Eu, Tb, Yb, Lu, Hf, Ta, Th, Sc, Cr, Co, Rb, Cs, Ba, La, Sm and U
Lei 2007	Gongyi: 36; Yaozhou:51; Liquanfang: 85; Xing: 7; Tombs: 67; Sites: 30	body	INAA	Ce, Nd, Eu, Tb, Yb, Lu, Hf, Ta, Th, Sc, Cs, La, Sm, U
Li et al. 2006	Gongyi: 7; Yaozhou: 7		ICP-MS: trace elements, TIMS: Sr-Nd isotopes	

References	Samples	Test areas	Methods	Tested elements
Li et al. 2006		body	INAA	29-La, Ce, Nd, Sm, Eu, Tb, Yb, Lu, Na, Sc, Cr, Fe, Co, Ni, Zn, As, Se, Rb, Sr, Zr, Mo, Sb, Cs, Ba, Hf, Ta, W, Th, U
Feng et al. 2005	Gongyi: 1; Yaozhou: 1; Liquanfang: 1	glaze	PIXE	Al2O3, SiO2, K2O, CaO, Ti(ppm), Fe2O3, Cu(ppm), PbO
Lei et al. 2005	Gongyi: 36; Yaozhou: 51; Liquanfang: 85	body	INAA	Fe, Na, K, Ce, Nd, Eu, Tb, Yb, Lu, Hf, Ta, Th, Sc, Cr, Co, Rb, Cs, Ba, La, Sm, and U
Cheng et al. 2005	Gongyi:9; Yangzhou: 6	body, glaze		Al2O3, SiO2, P2O5, K2O, CaO, TiO2, MnO, Fe2O3, CoO, PbO
Li et al. 2005	Yaozhou:7	body	ICP-MS: trace elements; TIMES: Sr isotopic compositions	Li, Be, Sc, Ti, V, Cr, Co, Ni, Cu, Zn, Ga, Rb, Sr, Y, Zr, Nb, Sn, Cs, Ba, La, Ce, Pr, Nd, Sm, Eu, Gd, Tb, Dy, Ho, Er, Tm, Yb, Lu, Hf, Ta, W, Tl, Pb, Th, U
Lei et al. 2005	Gongling tomb: 7	body	INAA	Na, K, Fe, Ba, La, Sm, U, Ce, Nd, Eu, Yb, Lu, Hf, Ta, Th, Se, Sc, Cr, Co, Rb, Cs
Lei 2004	Lihui tomb	body	SRXRF, NAA	

References	Samples	Test areas	Methods	Tested elements
Lei 2004		body	INAA	24--As, Ba, Ce, Co, Cr, Cs, Eu, Fe, Hf, K, La, Lu, Na, Nd, Rb, Sb, Sc, Sm, Ta, Tb, Th, U, Yb, Zr
Lei 2002	Gongyi: 31; Yaozhou: 51	body	SRXRF	K, Ti , Cr , Mn , Fe , Zn , Rb , Sr , Y , Zr， Ti, Ca , Cu , Ga , Pb， Nb
Miao & Lu 2001	Gongyi: 48; Yaozhou: 15; Xianyang site: 9; Luoyang tombs:24; Luoyang site: 8; Hubei Museum: 5, Nanjing Museum: 6; Yangzhou Museum: 5; Qianling Museum: 10	body	INAA	As, Ba, Ce, Co, Cr, Cs, Eu, Fe, Hf, K, La, Lu, Na, Nd, Rb, Sb, Sc, Sm, Ta, Tb, Th, U, Yb, Zr
Miao & Lu 2001	Gongyi: 48; Yaozhou: 15	body		As, Ba, Ce, Co, Cr, Cs, Eu, Fe, Hf, K, La, Lu, Na, Nd, Rb, Sb, Sc, Sm, Ta, Tb, Th, U, Yb, Zr
Lang et al. 1998	Yaozhou: 10: Xian tombs: 29; Luoyang tombs:7	glaze	XRF	K/Si, Ca/Si, K/Ca, Fe/Ti, Rb/Ti, Sr/Ti, Rb/Sr

References	Samples	Test areas	Methods	Tested elements
Xia 1993	Luoyang: 5		thermoluminescence dating	
Miao et al. 1992	Gongyi: 10; Yaozhou: 5; Luoyang: 3		INAA, thermoluminescence dating	As, Ba, Co, Cr, Cs, Hf, Rb, Sc, Ta, Th, U, Zr, Ce, Eu, La, Lu, Nd, Sm, Tb, Yb, Sb, Zn
Miao & Lu 1990	Gongyi: 5; Palace Museum: 1; Yaozhou: 4; unknown: 3		thermoluminescence dating	

Appendix 4 Two tests of corning glasses B, C and D[32]

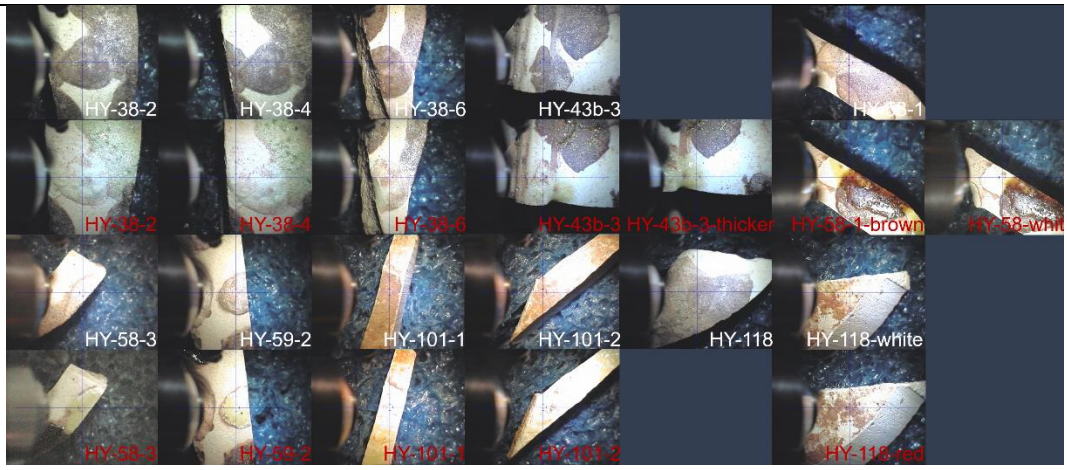
Glasses	Na_2O	MgO	Al_2O_3	SiO_2	P_2O_5	K_2O	CaO	TiO_2	V_2O_5	MnO	Fe_2O_3	CoO	NiO	CuO	ZnO	SrO	SnO_2	Sb_2O_5	BaO	PbO
B-1	6.38	0.83	4.60	68.29	0.95	1.16	11.26	0.13	0.04	0.26	0.46	0.05	0.10	3.57	0.27	0.03	0.10	0.30	0.36	0.86
B-2	5.32	0.92	4.98	69.03	1.06	1.19	11.42	0.13	0.04	0.27	0.47	0.05	0.10	3.61	0.27	0.03	0.02	0.00	0.23	0.86
B-3	5.25	0.19	4.74	69.89	1.02	1.18	11.52	0.14	0.04	0.27	0.47	0.05	0.10	3.65	0.27	0.03	0.05	0.00	0.28	0.87
B-4	7.02	0.98	4.59	68.31	0.93	1.11	11.11	0.14	0.04	0.26	0.46	0.05	0.09	3.52	0.26	0.02	0.02	0.00	0.26	0.84
B-5	6.20	0.91	4.79	68.60	0.99	1.11	11.14	0.13	0.04	0.26	0.45	0.05	0.09	3.52	0.26	0.02	0.10	0.16	0.34	0.84
B-6	5.09	1.22	4.94	69.22	0.99	1.19	11.61	0.14	0.04	0.27	0.48	0.05	0.10	3.66	0.27	0.03		0.01	0.29	0.87
C-1	2.40	5.78	1.65	49.56	0.00	1.79	4.61	0.44	0.25	0.04	0.25	0.12	0.01	1.18	0.03	0.14	0.64	0.01	0.72	30.38
C-2	1.62	2.24	1.29	51.03	0.00	1.81	4.91	0.50	0.25	0.03	0.25	0.12	0.01	1.26	0.03	0.15	0.81	0.00	0.79	32.89
C-3	0.45	5.22	1.27	48.95	0.00	1.91	4.96	0.53	0.27	0.04	0.26	0.13	0.01	1.26	0.04	0.15	0.64	0.29	0.79	32.83
C-4	0.55	5.42	3.33	48.22	0.00	1.94	4.83	0.49	0.26	0.04	0.32	0.12	0.02	0.91	0.03	0.14	0.63	0.01	0.55	32.20
C-5	1.62	3.24	2.02	49.14	0.00	1.94	4.92	0.54	0.27	0.04	0.27	0.12	0.01	0.93	0.03	0.15	0.70		0.81	33.37

[32] These two examinations were run on the 14th of April and 25th of June in 2021. The numbers in the labels refer to different testing areas.

Glasses	Na_2O	MgO	Al_2O_3	SiO_2	P_2O_5	K_2O	CaO	TiO_2	V_2O_5	MnO	Fe_2O_3	CoO	NiO	CuO	ZnO	SrO	SnO_2	Sb_2O_5	BaO	PbO
C-6	0.84	6.24	2.34	47.73	0.00	1.84	4.81	0.50	0.28	0.05	0.26	0.12	0.01	0.91	0.03	0.14	0.72	0.08	0.68	32.41
D-1	0.41	5.31	5.57	55.50	5.85	12.14	13.03	0.31	0.01	0.36	0.42	0.01	0.03	0.30	0.08	0.06	0.10	0.01	0.13	0.38
D-2	0.70	5.01	5.31	56.09	5.75	12.06	12.88	0.30	0.02	0.36	0.41	0.01	0.03	0.30	0.08	0.06	0.04	0.00	0.23	0.38
D-3	0.27	4.82	5.76	55.59	5.94	12.23	13.13	0.30	0.01	0.37	0.42	0.01	0.03	0.30	0.08	0.06	0.06	0.01	0.22	0.38
D-4	0.93	4.71	5.35	55.71	5.85	12.10	12.98	0.31	0.02	0.36	0.42	0.01	0.03	0.30	0.08	0.06	0.07	0.18	0.15	0.38
D-5	0.29	4.96	5.21	56.03	5.85	12.24	13.10	0.30	0.02	0.37	0.41	0.01	0.03	0.31	0.08	0.06	0.07	0.14	0.14	0.39
D-6	0.10	4.29	5.48	56.66	5.52	12.41	13.33	0.32	0.02	0.37	0.44	0.01	0.03	0.31	0.08	0.06	0.00	0.00	0.17	0.39
B1	7.88	0.27	4.63	69.19	0.88	1.05	10.81	0.14	0.04	0.24	0.41	0.05	0.09	3.19	0.23	0.02	0.00	0.00	0.15	0.72
B2	7.08	0.89	4.55	69.24	0.91	1.05	10.91	0.13	0.04	0.24	0.42	0.05	0.09	3.19	0.23	0.02	0.00	0.01	0.26	0.71
B3	9.07	1.23	4.48	67.23	1.01	1.02	10.63	0.14	0.04	0.24	0.41	0.05	0.08	3.14	0.23	0.02	0.01	0.04	0.23	0.70
B4	7.89	0.81	4.75	68.40	1.04	1.06	10.82	0.13	0.04	0.24	0.41	0.05	0.09	3.17	0.23	0.02	0.03	0.00	0.13	0.71
B5	6.38	0.32	4.59	70.09	1.12	1.10	10.96	0.14	0.03	0.25	0.42	0.05	0.09	3.23	0.24	0.02	0.04	0.01	0.23	0.73
C1	1.62	3.79	2.50	49.35	0.00	2.30	5.64	0.57	0.28	0.04	0.33	0.12	0.01	0.95	0.03	0.13	0.49	0.02	0.59	31.24

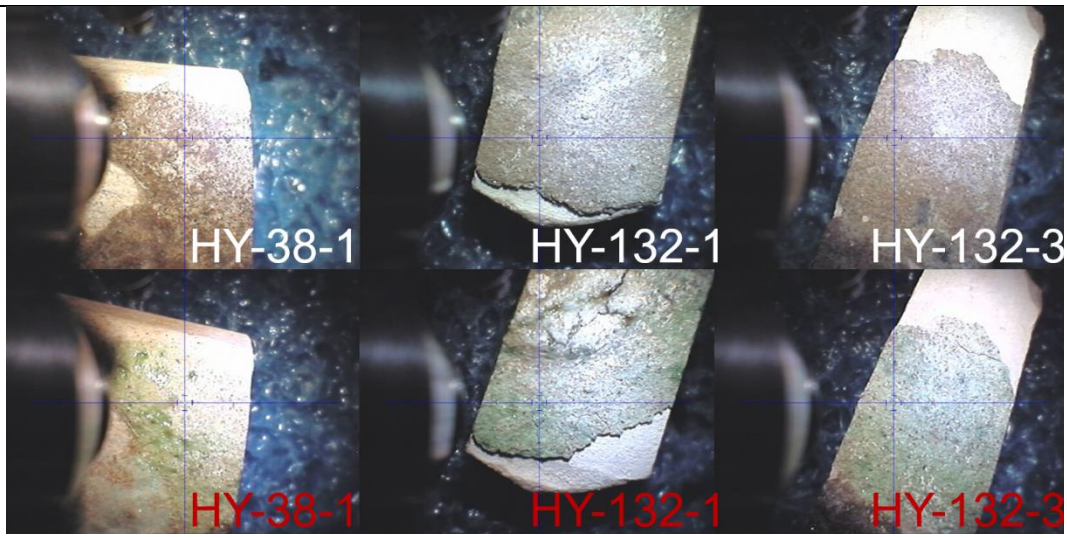
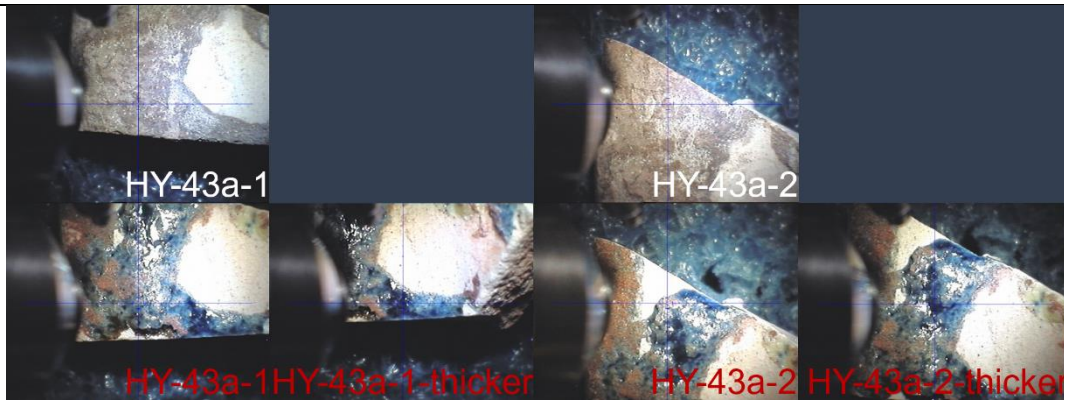
Glasses	Na_2O	MgO	Al_2O_3	SiO_2	P_2O_5	K_2O	CaO	TiO_2	V_2O_5	MnO	Fe_2O_3	CoO	NiO	CuO	ZnO	SrO	SnO_2	Sb_2O_5	BaO	PbO
C2	2.05	4.23	1.97	49.36	0.00	2.30	5.49	0.56	0.28	0.03	0.34	0.13	0.01	0.94	0.04	0.13	0.63	0.19	0.52	30.82
C3	0.08	3.28	2.29	50.69	0.00	2.37	5.70	0.61	0.28	0.04	0.34	0.13	0.01	0.98	0.04	0.14	0.56	0.02	0.61	31.84
C4	2.07	3.72	2.25	49.41	0.00	2.31	5.56	0.64	0.26	0.04	0.33	0.13	0.01	0.96	0.04	0.13	0.59	0.00	0.56	31.01
C5	0.55	3.35	1.85	50.22	0.00	2.30	5.66	0.63	0.28	0.04	0.34	0.13	0.01	0.98	0.04	0.14	0.59	0.04	0.71	32.15
D1	0.92	5.24	4.95	56.98	6.15	11.72	12.28	0.28	0.02	0.32	0.36	0.01	0.03	0.26	0.07	0.04	0.04	0.01	0.04	0.29
D2	0.79	6.08	5.12	56.32	5.89	11.68	12.26	0.27	0.02	0.33	0.37	0.01	0.03	0.26	0.07	0.04		0.06	0.11	0.30
D3	0.85	5.31	5.23	56.49	6.13	11.74	12.34	0.27	0.02	0.33	0.37	0.01	0.03	0.26	0.07	0.04	0.00	0.04	0.15	0.32
D4	1.31	5.15	4.86	56.73	6.01	11.75	12.33	0.28	0.01	0.33	0.37	0.01	0.03	0.26	0.07	0.05	0.02	0.01	0.12	0.31
D5	0.60	5.20	5.20	56.69	6.20	11.81	12.51	0.28	0.02	0.33	0.37	0.01	0.03	0.27	0.07	0.05	0.00	0.01	0.07	0.32

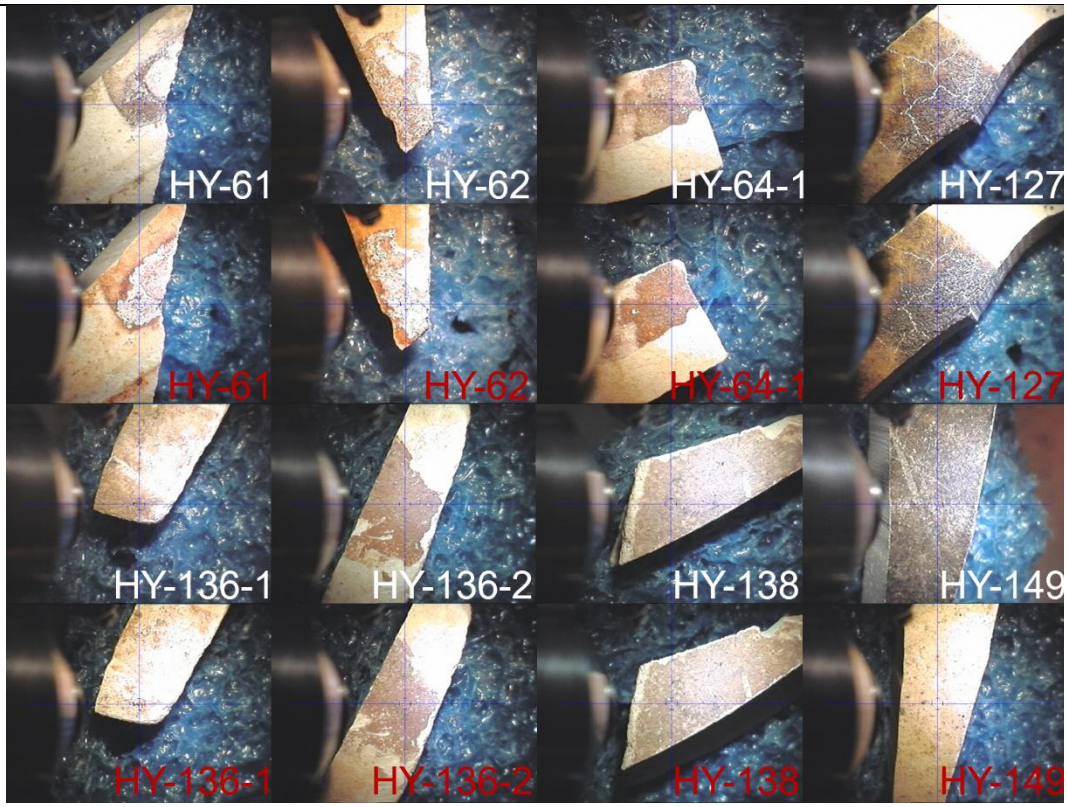
Appendix 5 EDXRF testing areas of samples for experimental glaze firing[33]

Labels	Photos
Clear glazes[34]	

[33] All images from EDXRF examination. Font colours distinguishes original raw pieces (white labels) from fired pieces (red labels). All labels including '-thicker' refer to the data obtained from the thick-glaze areas.

[34] The testing area HY-58-1 should be white after glaze firing due to low colourant contents, 0.3% Fe_2O_3, no CuO and CoO (Appendix F). However, the next reddish brown raw glaze splashed to HY-58-1. Thus, the content of fired clear glaze was tested in 'HY-58-white' area and the original area HY-58-1 is marked as 'HY-58-brown' after firing.

Brown glazes	
Green glazes	
Blue glazes	

Others	HY-61 HY-62 HY-64-1 HY-127 HY-61 HY-62 HY-64-1 HY-127 HY-136-1 HY-136-2 HY-138 HY-149 HY-136-1 HY-136-2 HY-138 HY-149

Appendix 6 Chemical compositions of samples for experimental glaze firing[35]

Samples	Na_2O	MgO	Al_2O_3	SiO_2	P_2O_5	K_2O	CaO	TiO_2	V_2O_5	MnO	Fe_2O_3	CoO	NiO	CuO	ZnO	SrO	SnO_2	Sb_2O_5	BaO	PbO
HY-38-1	0.01	1.07	4.98	19.08	37.76	0.18	13.01	0.17	0.08	0.04	0.73	0.02	0.00	0.29	0.01	0.03	0.21	0.01	0.25	22.08
HY-38-1	2.90	2.17	3.59	22.12	27.58	0.09	12.12	0.08	0.04	0.01	0.47	0.01	0.00	0.25	0.00	0.04	0.47	0.03	0.33	27.72
HY-38-2	1.78	1.60	3.66	19.93	40.14	0.10	10.13	0.17	0.06	0.02	0.45	0.02	0.00	0.05	0.01	0.04	0.22	0.02	0.23	21.39
HY-38-2	0.01	0.01	2.41	30.10	28.88	0.00	8.49	0.10	0.05	0.02	0.32	0.01	0.00	0.03	0.00	0.04	0.49	0.07	0.27	28.70
HY-38-3	0.09	1.60	6.61	20.34	32.28	0.39	16.85	0.19	0.03	0.03	1.97	0.02	0.00	0.02	0.01	0.03	0.18		0.26	19.11
HY-38-3	0.01	0.70	5.38	23.61	29.84	0.39	15.63	0.13	0.03	0.02	2.02	0.01	0.00	0.02	0.00	0.04	0.32	0.12	0.29	21.44
HY-38-4	1.27	2.05	2.92	32.53	31.28	0.15	10.90	0.08	0.03	0.02	0.41	0.03	0.00	0.02	0.01	0.03	0.17	0.01	0.24	17.85
HY-38-4	0.01	1.29	2.74	33.61	31.02	0.13	10.85	0.08	0.04	0.02	0.35	0.01	0.00	0.01	0.01	0.03	0.27		0.17	19.38
HY-38-5	1.59	0.35	4.98	22.37	35.78	0.32	10.68	0.19	0.08	0.03	2.02	0.02		0.02	0.01	0.04	0.29	0.02	0.11	21.10
HY-38-5	0.01	1.57	4.46	24.31	34.19	0.42	10.48	0.15	0.06	0.02	1.96	0.02	0.00	0.01	0.00	0.03	0.20	0.06	0.27	21.78
HY-38-6	0.81	2.55	5.99	27.50	28.29	0.62	10.95	0.33	0.11	0.04	1.41	0.02	0.00	0.01	0.01	0.04	0.23		0.28	20.85

[35] Font colours distinguishes original unfired pieces (black colour) from fired pieces (red colour).

Samples	Na_2O	MgO	Al_2O_3	SiO_2	P_2O_5	K_2O	CaO	TiO_2	V_2O_5	MnO	Fe_2O_3	CoO	NiO	CuO	ZnO	SrO	SnO_2	Sb_2O_5	BaO	PbO
HY-38-6	2.67	3.25	6.13	30.04	24.06	0.87	11.52	0.31	0.08	0.03	1.40	0.01	0.00	0.00	0.01	0.03	0.20		0.16	19.25
HY-43a-1	1.13	0.01	7.35	30.15	25.63	0.67	8.36	0.25	0.07	0.03	1.49	0.33	0.01	0.07	0.01	0.03	0.32	0.07	0.19	23.86
HY-43a-1	1.11	0.01	4.59	39.54	13.41	0.33	4.95	0.13	0.04	0.02	1.06	0.33	0.01	0.07	0.00	0.03	0.46	0.07	0.36	33.48
HY-43a-1	3.55	0.02	2.77	39.47	10.37	0.00	3.18	0.11	0.03	0.01	0.57	0.69	0.02	0.20		0.04	0.50	0.10	0.33	38.06
HY-43a-2	0.29	0.44	8.56	36.65	17.82	0.69	8.21	0.26	0.06	0.03	1.55	0.42	0.01	0.15	0.01	0.03	0.31	0.04	0.32	24.16
HY-43a-2	0.99	0.52	1.98	31.99	18.49	0.00	3.94	0.05	0.01	0.01	0.48	0.53	0.02	0.16		0.05	0.42	0.13	0.26	39.96
HY-43a-2	0.65	1.24	10.74	40.93	12.16	1.01	5.29	0.39	0.05	0.02	1.39	0.30	0.01	0.08	0.00	0.03	0.30		0.39	25.02
HY-43b-1	1.83	0.60	5.98	22.07	32.76	0.34	10.07	0.19	0.16	0.03	2.39	0.02	0.00	0.01	0.01	0.04	0.17	0.11	0.31	22.94
HY-43b-1	0.95	2.92	4.19	26.73	27.34	0.09	8.68	0.13	0.09	0.02	2.32	0.03	0.00	0.01	0.00	0.05	0.21	0.10	0.21	25.94
HY-43b-2	0.94	1.01	9.05	30.14	24.44	0.61	8.15	0.29	0.10	0.02	2.42	0.02	0.00	0.01	0.01	0.04	0.24	0.00	0.27	22.26
HY-43b-2	0.50	0.52	5.30	31.48	23.85	0.27	8.06	0.15	0.07	0.02	2.11	0.02	0.00	0.01	0.00	0.04	0.26		0.47	26.90

Samples	Na_2O	MgO	Al_2O_3	SiO_2	P_2O_5	K_2O	CaO	TiO_2	V_2O_5	MnO	Fe_2O_3	CoO	NiO	CuO	ZnO	SrO	SnO_2	Sb_2O_5	BaO	PbO
HY-43b-2-thicker[36]	1.89	1.53	4.01	29.04	18.09	0.02	5.27	0.12	0.04	0.02	2.15	0.02	0.00	0.01	0.00	0.04	0.53	0.14	0.37	36.72
HY-43b-3	0.01	3.00	9.12	38.19	20.41	0.93	9.54	0.31	0.04	0.02	1.60	0.02	0.00	0.00	0.01	0.03	0.13	0.02	0.26	16.37
HY-43b-3-thicker	4.76	3.02	1.00	30.09	13.62	0.00	3.32	0.04	0.02	0.01	0.09	0.01	0.00	0.01		0.04	0.50	0.15	0.29	43.02
HY-43b-3	0.19	1.26	6.61	41.09	16.87	0.36	7.20	0.22	0.03	0.01	1.19	0.01	0.00	0.00	0.01	0.03	0.23	0.12	0.41	24.17
HY-43b-4	0.53	0.46	6.80	28.87	29.29	0.52	10.83	0.22	0.07	0.02	2.25	0.02	0.00	0.01	0.00	0.03	0.23	0.13	0.13	19.62
HY-43b-4	1.13	1.00	6.29	34.08	18.84	0.31	7.21	0.14	0.05	0.02	2.03	0.02		0.01	0.00	0.04	0.35		0.23	28.28
HY-58-1	0.57	0.38	3.36	62.57	4.26	0.00	2.55	0.05	0.02	0.06	0.30	0.00	0.00	0.00	0.01	0.03	0.29	0.14	0.17	25.25
HY-58-1-white	3.03	1.54	0.80	46.23	7.59	0.00	4.60	0.04	0.04	0.01	0.38		0.00	0.01	0.00	0.05	0.43	0.08	0.55	34.63
HY-58-1-brown	2.30	3.63	1.91	37.10	11.69	0.00	4.34	0.08	0.02	0.01	2.12	0.01	0.00	0.01	0.00	0.05	0.40	0.12	0.17	36.03

[36] All labels with '-thicker' refer to the data obtained from same sample and same glaze with the former sample, but the thickness of glaze layer in this area is bigger than the former.

Samples	Na_2O	MgO	Al_2O_3	SiO_2	P_2O_5	K_2O	CaO	TiO_2	V_2O_5	MnO	Fe_2O_3	CoO	NiO	CuO	ZnO	SrO	SnO_2	Sb_2O_5	BaO	PbO
HY-58-2	0.02	0.20	8.43	41.56	1.80	0.43	3.89	0.28	0.06	0.03	4.17	0.01	0.00	0.01	0.01	0.06	0.41		0.33	38.32
HY-58-2	0.02	3.11	4.72	31.37	12.10	0.00	5.21	0.20	0.09	0.03	4.17	0.02	0.00	0.01	0.00	0.07	0.49	0.05	0.32	38.05
HY-58-3	0.04	0.27	4.67	61.52	1.27	0.07	3.39	0.09	0.02	0.03	0.34	0.01	0.01	0.01	0.01	0.04	0.38		0.13	27.73
HY-58-3	2.27	1.02	0.75	50.20	3.01	0.00	2.57	0.03	0.02	0.01	0.09	0.00	0.00	0.01	0.00	0.05	0.58	0.12	0.39	38.88
HY-59-1	0.02	1.61	8.57	40.35	12.11	0.29	5.42	0.20	0.05	0.03	4.08	0.02	0.00	0.00	0.01	0.05	0.35	0.12	0.22	26.50
HY-59-1	0.53	2.97	3.37	30.73	12.82	0.00	4.61	0.12	0.04	0.03	3.62	0.02		0.01	0.00	0.06	0.52	0.29	0.33	39.93
HY-59-2	1.89	2.61	4.17	40.65	18.77	0.24	6.27	0.15	0.10	0.02	0.47	0.02	0.00	0.00	0.01	0.04	0.26		0.21	24.19
HY-59-2	4.34	0.17	0.64	40.17	15.83	0.00	4.59	0.04	0.07	0.01	0.19	0.01	0.00	0.00		0.04	0.46	0.09	0.18	33.17
HY-59-3	1.48	1.61	8.90	36.32	17.82	0.68	7.37	0.22	0.10	0.04	3.02	0.02		0.00	0.00	0.04	0.22		0.20	21.99
HY-59-3	0.83	0.22	6.39	40.73	13.35	0.45	4.89	0.17	0.10	0.03	3.16	0.02	0.00	0.01	0.00	0.04	0.37		0.36	28.91
HY-61	0.98	1.74	2.88	7.11	53.47	0.17	23.49	0.06	0.01	0.01	0.49	0.01	0.00	0.01	0.05	0.02	0.12	0.01	0.17	9.20
HY-61	1.14	0.40	2.27	7.44	54.32	0.09	21.65	0.04	0.01	0.01	0.57	0.01	0.00	0.01	0.05	0.02	0.15	0.01	0.13	11.69
HY-62	0.81	1.34	2.83	8.10	54.13	0.19	23.52	0.05	0.01	0.00	0.46	0.00	0.00	0.01	0.03	0.02	0.06	0.01	0.18	8.27

Samples	Na_2O	MgO	Al_2O_3	SiO_2	P_2O_5	K_2O	CaO	TiO_2	V_2O_5	MnO	Fe_2O_3	CoO	NiO	CuO	ZnO	SrO	SnO_2	Sb_2O_5	BaO	PbO
HY-62	0.91	0.54	2.22	7.53	54.12	0.05	21.74	0.04	0.01	0.01	0.53	0.00	0.00	0.01	0.02	0.02	0.13	0.03	0.16	11.94
HY-64-1	0.88	0.50	8.03	33.29	24.66	0.55	7.10	0.22	0.10	0.02	3.15	0.02	0.00	0.00	0.00	0.06	0.18	0.13	0.26	20.85
HY-64-1	1.24	1.39	6.40	32.13	27.79	0.47	7.48	0.19	0.09	0.02	3.17	0.02	0.00	0.00	0.01	0.06	0.16		0.36	19.02
HY-64-2	3.11	1.53	6.23	31.30	25.95	0.22	5.81	0.14	0.15	0.02	3.50	0.03	0.00	0.00	0.01	0.06	0.25	0.07	0.19	21.43
HY-64-2	1.55	1.91	2.65	27.84	18.80	0.00	5.07	0.11	0.14	0.03	3.50	0.03	0.00	0.01	0.00	0.07	0.18	0.04	0.58	37.52
HY-64-2-thicker	3.30	2.08	1.51	34.31	15.71	0.00	3.75	0.03	0.08	0.02	2.66	0.02	0.00	0.01	0.00	0.06	0.49		0.24	35.76
HY-64-3	0.15	1.91	7.17	32.17	23.02	0.49	6.57	0.19	0.15	0.04	3.65	0.02	0.00	0.00	0.01	0.05	0.34	0.08	0.29	23.71
HY-64-3	0.96	0.59	1.77	33.37	16.94	0.00	5.23	0.09	0.08	0.02	3.02	0.02	0.00	0.01	0.00	0.06	0.50		0.76	36.61
HY-92	1.27	2.00	5.91	20.03	33.40	0.38	8.89	0.22	0.08	0.03	2.44	0.02	0.00	0.01	0.01	0.06	0.26	0.07	0.35	24.57
HY-92-1	2.19	0.02	4.13	21.71	27.72	0.08	6.12	0.14	0.07	0.03	2.26	0.03	0.00	0.02		0.06	0.44		0.47	34.53
HY-92-1-thicker	0.02	1.49	3.60	17.71	26.35	0.00	5.41	0.17	0.03	0.03	2.30	0.03	0.00	0.03	0.00	0.05	0.55	0.06	0.49	41.68
HY-101-1	1.30	2.95	8.86	29.01	25.46	0.68	7.96	0.27	0.04	0.02	0.99	0.01	0.00	0.01	0.01	0.03	0.30	0.02	0.34	21.76

Samples	Na_2O	MgO	Al_2O_3	SiO_2	P_2O_5	K_2O	CaO	TiO_2	V_2O_5	MnO	Fe_2O_3	CoO	NiO	CuO	ZnO	SrO	SnO_2	Sb_2O_5	BaO	PbO
HY-101-1	0.02	0.02	3.29	35.98	16.64	0.00	4.07	0.09	0.03	0.02	0.45	0.01	0.00	0.02	0.00	0.05	0.43	0.09	0.45	38.36
HY-101-2	0.01	0.01	8.46	28.87	27.96	0.76	8.96	0.31	0.04	0.02	1.44	0.01	0.00	0.01	0.01	0.04	0.28	0.01	0.23	22.57
HY-101-2	0.21	0.02	3.92	35.64	16.52	0.00	4.43	0.13	0.02	0.02	0.51	0.01	0.00	0.02	0.00	0.05	0.41	0.03	0.42	37.64
HY-118-1	0.68	0.37	7.62	42.54	15.81	0.72	8.95	0.35	0.14	0.03	1.14	0.01	0.00	0.00	0.01	0.02	0.27		0.29	21.09
HY-118-red	2.86	2.60	13.88	48.41	2.54	0.85	7.14	0.40	0.08	0.07	2.31	0.02	0.00	0.01	0.01	0.02	0.12	0.02	0.23	18.45
HY-118-white	2.27	0.02	3.91	48.05	8.96	0.00	4.48	0.17	0.06	0.02	0.89	0.01	0.00	0.01	0.01	0.03	0.33	0.05	0.18	30.58
HY-127	1.68	3.18	12.00	66.87	0.00	1.14	1.84	0.54	0.02	0.06	1.91	0.02	0.01	4.31	0.10	0.01	0.03	0.04	0.16	6.10
HY-127-1	2.95	3.74	10.05	67.88	0.00	0.84	1.62	0.46	0.02	0.05	1.71	0.02	0.01	4.20	0.11	0.01	0.05	0.04	0.26	5.99
HY-132-1	0.75	0.08	5.86	23.77	34.46	0.18	10.22	0.12	0.06	0.02	0.62	0.02	0.00	0.79	0.01	0.03	0.22	0.06	0.19	22.56
HY-132-1	2.21	1.20	2.25	21.63	31.24	0.00	8.83	0.06	0.05	0.02	0.43	0.01	0.00	0.93	0.01	0.04	0.37		0.13	30.60
HY-132-2	0.01	0.71	6.79	21.86	23.09	0.37	18.09	0.29	0.07	0.04	3.82	0.02	0.00	0.12	0.01	0.05	0.26	0.09	0.10	24.23
HY-132-2	0.12	0.02	6.34	26.76	17.89	0.00	9.77	0.22	0.05	0.02	3.37	0.02	0.00	0.13	0.00	0.05	0.49	0.06	0.30	34.39
HY-132-3	0.01	1.11	6.69	23.00	32.42	0.28	13.07	0.12	0.04	0.03	0.72	0.02		0.39	0.01	0.03	0.26		0.26	21.53

Samples	Na_2O	MgO	Al_2O_3	SiO_2	P_2O_5	K_2O	CaO	TiO_2	V_2O_5	MnO	Fe_2O_3	CoO	NiO	CuO	ZnO	SrO	SnO_2	Sb_2O_5	BaO	PbO
HY-132-3	1.98	1.64	2.69	23.56	29.63	0.00	10.35	0.06	0.04	0.02	0.55	0.01	0.00	0.79	0.01	0.04	0.39	0.07	0.21	27.97
HY-136-1	0.51	3.78	7.86	34.60	25.29	0.61	9.44	0.23	0.04	0.02	0.91	0.02	0.00	0.06	0.01	0.04	0.11	0.01	0.49	15.99
HY-136-1	0.01	0.81	6.06	30.36	34.35	0.28	10.57	0.20	0.04	0.01	0.82	0.01	0.00	0.06	0.01	0.04	0.04	0.03	0.26	16.05
HY-136-2	0.72	1.54	3.98	29.66	26.46	0.03	7.98	0.13	0.12	0.02	2.94	0.02	0.00	0.05	0.01	0.04	0.19		0.55	25.58
HY-136-2	5.03	1.76	1.89	22.69	33.38	0.00	8.53	0.11	0.12	0.03	2.92	0.02		0.04	0.01	0.03	0.18	0.07	0.56	22.64
HY-138	1.60	3.08	25.65	50.03	0.72	3.37	6.49	1.12	0.07	0.05	6.83	0.02	0.00	0.00	0.01	0.02	0.00	0.05	0.15	0.74
HY-138-1	0.16	3.45	25.47	50.83	0.83	3.41	6.85	1.18	0.07	0.05	6.80	0.02	0.00	0.00	0.01	0.02	0.01	0.05	0.09	0.71
HY-149	0.33	3.77	28.31	52.03	0.39	5.14	6.74	1.16	0.06	0.02	1.65	0.01	0.00	0.00	0.01	0.03	0.12	0.06	0.13	0.05
HY-149-1	0.79	3.37	30.80	51.87	0.21	5.01	5.22	1.15	0.05	0.01	1.30	0.00	0.00	0.00	0.01	0.03		0.02	0.12	0.04
HY-152	3.65	2.30	5.65	12.68	16.81	0.00	6.94	0.11	0.05	0.03	4.72	0.01	0.00	0.28	0.01	0.05	0.63	0.11	0.49	45.48
HY-152-1	2.50	0.02	2.54	30.32	15.02	0.00	3.84	0.06	0.02	0.02	4.73	0.01	0.00	0.40	0.00	0.03	0.56	0.07	0.47	39.41
average																				

Appendix 7 Chemical compositions of bodies

Samples	Na_2O	MgO	Al_2O_3	SiO_2	P_2O_5	K_2O	CaO	TiO_2	V_2O_5	MnO	Fe_2O_3	CoO	NiO	CuO	ZnO	SrO	SnO_2	Sb_2O_5	BaO	PbO
HY-38	0.37	1.29	33.77	55.79	0.55	2.78	2.15	1.40	0.07	0.02	1.39	0.01	0.00	0.00	0.01	0.03	0.02	0.07	0.16	0.12
HY-43	0.58	1.66	37.09	53.12	0.33	2.99	1.05	1.33	0.06	0.00	1.06	0.01	0.00	0.00	0.01	0.04	0.09	0.00	0.31	0.28
HY-58	0.53	0.71	34.94	56.22	0.55	2.53	0.74	1.39	0.08	0.01	1.16	0.01	0.00	0.00	0.01	0.03	0.00	0.07	0.27	0.76
HY-59	0.03	0.80	35.93	54.08	1.07	3.25	0.99	1.68	0.09	0.00	1.39	0.01	0.00	0.00	0.01	0.03	0.05	0.00	0.27	0.31
HY-61	0.34	0.26	35.98	55.85	1.51	3.47	0.93	1.31	0.07	0.01	1.59	0.01	0.00	0.00	0.02	0.03			0.11	0.11
HY-62	0.01	0.19	34.70	54.81	2.94	3.98	1.41	1.45	0.07	0.02	1.78	0.01	0.00	0.00	0.02	0.03			0.13	0.15
HY-64	0.01	1.41	34.32	53.86	0.66	4.25	3.88	1.53	0.08	0.01	1.29	0.01	0.00	0.00	0.01	0.03			0.09	0.22
HY-92	0.01	1.41	34.32	53.86	0.66	4.25	3.88	1.53	0.08	0.01	1.29	0.01	0.00	0.00	0.01	0.03			0.09	0.22
HY-101	0.01	0.14	35.25	60.82	0.04	2.42	0.31	1.29	0.07	0.00	1.04	0.01	0.00	0.00	0.01	0.02			0.15	0.12
HY-102	0.01	0.18	33.61	60.14	0.15	2.34	0.94	1.41	0.08	0.01	2.52	0.01	0.00	0.00	0.01	0.03			0.10	0.20
HY-106	0.10	0.40	37.05	58.06	0.07	2.23	0.72	1.70	0.07	0.00	1.29	0.01	0.00	0.01	0.01	0.03			0.05	0.11
HY-115	0.01	0.31	34.28	57.52	0.09	2.75	2.76	1.20	0.06	0.01	2.57	0.01	0.00	0.00	0.01	0.04			0.05	0.10

Samples	Na_2O	MgO	Al_2O_3	SiO_2	P_2O_5	K_2O	CaO	TiO_2	V_2O_5	MnO	Fe_2O_3	CoO	NiO	CuO	ZnO	SrO	SnO_2	Sb_2O_5	BaO	PbO
HY-116	0.01	0.13	34.82	60.61	0.01	2.22	0.64	1.53	0.08	0.00	1.53	0.01	0.00	0.00	0.01	0.02			0.08	0.02
HY-117	0.07	0.38	36.88	57.96	0.03	2.55	0.32	1.32	0.08	0.00	1.47	0.01	0.00	0.00	0.01	0.03			0.11	0.09
HY-118	0.01	0.60	36.12	58.39	0.01	2.52	1.00	1.40	0.09	0.00	1.53	0.01	0.00	0.00	0.01	0.03			0.06	0.16
HY-119	0.26	0.27	33.79	59.12	0.04	2.48	1.66	1.52	0.08	0.01	1.94	0.01	0.00	0.00	0.01	0.03			0.12	0.03
HY-121	0.01	0.22	37.09	58.84	0.06	2.26	0.53	1.07	0.06	0.00	1.13	0.01	0.00	0.00	0.01	0.02			0.17	0.01
HY-122	0.01	0.77	37.74	57.27	0.02	2.29	0.75	1.11	0.06	0.00	1.34	0.01	0.00	0.00	0.01	0.02			0.18	0.01
HY-123	0.01	0.74	37.21	57.20	0.02	2.47	0.93	1.20	0.06	0.00	1.31	0.01	0.00	0.00	0.01	0.02			0.12	0.02
HY-124	0.01	0.51	35.44	57.74	0.05	2.35	2.60	1.17	0.06	0.01	1.23	0.01	0.00	0.00	0.01	0.02			0.16	0.02
HY-125	0.01	0.28	36.84	58.73	0.10	2.30	0.45	1.26	0.07	0.00	0.77	0.01	0.00	0.00	0.00	0.01			0.19	0.57
HY-126	0.07	0.35	36.54	59.02	0.03	2.25	0.44	1.09	0.06	0.00	1.54	0.01	0.00	0.00	0.01	0.02			0.10	0.01
HY-127	0.06	0.00	34.37	59.97	0.00	1.97	0.38	1.21	0.06	0.01	1.08	0.00	0.00	0.17	0.01	0.01			0.12	1.78
HY-129	0.04	0.41	36.73	58.24	0.07	2.25	0.90	1.16	0.06	0.01	1.32	0.01	0.00	0.00	0.01	0.01			0.07	0.05
HY-130	0.01	0.74	38.26	55.82	0.02	2.50	1.19	1.19	0.06	0.00	1.40	0.01	0.00	0.00	0.01	0.02			0.13	0.05

Samples	Na_2O	MgO	Al_2O_3	SiO_2	P_2O_5	K_2O	CaO	TiO_2	V_2O_5	MnO	Fe_2O_3	CoO	NiO	CuO	ZnO	SrO	SnO_2	Sb_2O_5	BaO	PbO
HY-131	0.03	0.60	38.27	55.78	0.13	2.73	0.63	1.29	0.07	0.01	1.83	0.01	0.00	0.00	0.01	0.02			0.17	0.06
HY-132	0.12	0.71	38.57	55.81	0.05	2.54	0.78	1.15	0.07	0.00	1.51	0.01	0.00	0.01	0.01	0.02			0.17	0.05
HY-133	0.06	0.39	35.86	59.06	0.04	2.69	0.39	1.27	0.07	0.00	1.41	0.01	0.00	0.00	0.01	0.02			0.07	0.02
HY-134	0.11	0.64	34.26	59.32		2.05	2.70	1.26	0.07	0.01	1.00	0.00	0.00	0.00	0.01	0.01			0.11	0.01
HY-135	0.01	0.48	38.27	56.81	0.11	2.55	0.47	1.10	0.06	0.00	1.51	0.01	0.00	0.00	0.01	0.02			0.14	0.06
HY-136	0.81	1.56	35.04	57.01	0.04	2.68	1.24	1.31	0.08	0.00	1.64	0.01	0.00	0.00	0.01	0.02			0.12	0.13
HY-137	0.13	0.37	34.63	59.80	0.04	2.33	0.62	1.33	0.06	0.01	1.74	0.01	0.00	0.00	0.01	0.02			0.08	0.02
HY-138	0.03	0.16	35.66	60.89	0.03	2.18	0.34	1.19	0.07	0.00	0.90	0.00	0.00		0.01	0.02			0.09	0.03
HY-139	0.01	0.02	34.19	61.21	0.02	2.57	0.56	1.31	0.06	0.01	1.09	0.00	0.00	0.00	0.01	0.02			0.10	0.01
HY-140	0.28	0.70	33.59	60.41	0.03	2.20	1.95	1.21	0.05	0.00	1.00	0.00	0.00	0.00	0.01	0.01			0.11	0.01
HY-141	0.01	0.16	38.47	56.67	0.04	2.32	1.06	1.18	0.06	0.01	1.38	0.01	0.00	0.00	0.01	0.02			0.07	0.03
HY-143	0.05	0.82	35.44	60.73	0.01	1.93	0.24	1.24	0.07	0.00	0.82	0.00	0.00	0.00	0.01	0.01			0.07	0.01
HY-145	0.18	0.51	35.88	59.67	0.03	2.13	0.41	1.24	0.07	0.00	1.27	0.01	0.00	0.00	0.01	0.01			0.08	0.16

Samples	Na_2O	MgO	Al_2O_3	SiO_2	P_2O_5	K_2O	CaO	TiO_2	V_2O_5	MnO	Fe_2O_3	CoO	NiO	CuO	ZnO	SrO	SnO_2	Sb_2O_5	BaO	PbO
HY-146	0.10	0.50	37.43	57.87	0.01	2.51	0.61	1.16	0.07	0.01	1.29	0.00	0.00	0.00	0.01	0.02			0.10	0.02
HY-147	0.01	0.60	37.73	58.21	0.03	2.07	0.31	1.19	0.07	0.00	1.43	0.00	0.00	0.00	0.01	0.02			0.05	0.02
HY-148	0.01	0.15	34.80	61.96	0.03	1.87	0.32	1.28	0.06	0.01	1.23		0.00	0.00	0.01	0.01			0.13	0.01
HY-149	0.01	0.19	37.75	58.00	0.06	2.17	0.64	1.16	0.06	0.00	1.23	0.00	0.00	0.00	0.01	0.02			0.11	0.01
HY-150	0.14	0.30	37.18	57.05	0.01	2.34	1.59	1.17	0.06	0.00	1.24	0.01	0.00	0.00	0.01	0.02			0.10	0.03
HY-151	0.05	0.40	36.04	60.00	0.04	2.03	0.67	1.23	0.06	0.00	1.00	0.01	0.00	0.00	0.01	0.02			0.06	0.02
HY-152	0.38	0.74	37.87	57.00	0.03	2.35	0.59	1.14	0.07	0.00	1.21	0.00	0.00	0.00	0.01	0.02			0.04	0.02
HY-153	0.04	0.28	38.15	57.55	0.00	2.41	0.50	1.27	0.07	0.00	1.21	0.01	0.00	0.00	0.01	0.01			0.16	0.06
HY-154	0.20	0.50	38.10	56.98	0.05	2.42	0.61	1.31	0.07	0.00	1.22	0.01	0.00	0.00	0.01	0.01			0.14	0.05
HY-155	0.05	0.21	40.03	56.24	0.01	2.12	0.44	1.19	0.06	0.00	1.30	0.01	0.00	0.00	0.01	0.02			0.11	0.01
HY-166	0.01	0.50	35.98	59.10	0.01	2.29	0.76	1.28	0.07	0.01	1.33	0.01	0.00	0.00	0.00	0.01			0.14	0.10
HY-172	0.25	1.17	35.61	52.60	0.17	3.65	3.74	1.28	0.06	0.01	1.14	0.01	0.00	0.00	0.01	0.02	0.00	0.06	0.17	0.06
HY-173	0.89	0.75	35.36	53.19	0.28	4.21	2.02	1.22	0.06	0.01	1.62	0.02	0.00	0.00	0.01	0.03	0.00	0.02	0.25	0.08

Samples	Na_2O	MgO	Al_2O_3	SiO_2	P_2O_5	K_2O	CaO	TiO_2	V_2O_5	MnO	Fe_2O_3	CoO	NiO	CuO	ZnO	SrO	SnO_2	Sb_2O_5	BaO	PbO
HY-174	0.01	1.30	37.23	54.48	0.04	2.45	1.23	1.23	0.06	0.01	1.74	0.01	0.00	0.00	0.01	0.02	0.00	0.01	0.15	0.03
HY-175	0.50	0.89	33.80	53.73	0.10	3.95	3.81	1.61	0.07	0.02	1.23	0.01	0.00	0.00	0.01	0.03		0.04	0.12	0.08
HY-176	0.52	0.77	33.35	53.84	0.08	4.95	3.37	1.33	0.06	0.02	1.48	0.01	0.00	0.00	0.02	0.02		0.03	0.12	0.05
HY-177	0.61	0.74	24.07	50.17	0.71	5.85	13.74	1.83	0.09	0.01	1.54	0.01	0.00	0.00	0.02	0.03	0.01	0.04	0.17	0.36
HY-178	1.00	0.23	34.04	56.36	0.08	2.54	3.02	1.51	0.07	0.00	0.86	0.01	0.00	0.00	0.01	0.02	0.01	0.02	0.10	0.12
HY-179	0.28	0.60	36.77	54.82	0.21	2.80	1.62	1.32	0.06	0.01	1.22	0.01	0.00	0.00	0.01	0.02		0.04	0.15	0.05
HY-180	0.59	0.91	34.14	55.99	0.06	2.53	3.18	1.21	0.07	0.02	0.95	0.01	0.00	0.00	0.01	0.02		0.03	0.15	0.14
HY-181	1.01	0.85	28.10	50.73	0.45	4.49	11.70	1.23	0.06	0.01	1.08	0.01	0.00	0.00	0.02	0.02	0.00	0.04	0.10	0.11
HY-182	0.01	0.53	35.01	53.59	0.10	3.61	3.99	1.48	0.07	0.02	1.23	0.01	0.00	0.00	0.01	0.02	0.00	0.05	0.17	0.12
HY-183	0.01	0.95	36.53	52.82	0.22	3.74	2.87	1.26	0.06	0.01	1.22	0.01	0.00	0.00	0.01	0.02		0.04	0.08	0.15
HY-184	0.40	1.06	32.56	51.83	1.67	5.29	3.09	1.33	0.06	0.01	1.74	0.01	0.00	0.00	0.02	0.02	0.00	0.02	0.09	0.80
HY-185	1.44	0.77	34.85	53.20	0.70	4.17	2.12	1.35	0.06	0.01	1.02	0.01	0.00	0.00	0.01	0.02		0.04	0.11	0.13
HY-186	0.01	0.41	39.00	55.79	0.01	2.89	0.39	1.16	0.06	0.01	1.50	0.01	0.00	0.00	0.01	0.02			0.13	0.02

Samples	Na_2O	MgO	Al_2O_3	SiO_2	P_2O_5	K_2O	CaO	TiO_2	V_2O_5	MnO	Fe_2O_3	CoO	NiO	CuO	ZnO	SrO	SnO_2	Sb_2O_5	BaO	PbO
HY-187	0.01	0.31	38.81	56.12	0.05	2.77	0.39	1.19	0.06	0.00	1.63	0.01	0.00	0.00	0.01	0.02			0.11	0.02
HY-188	0.29	0.29	37.93	58.41	0.05	2.11	0.26	1.15	0.06	0.00	0.72	0.01	0.00	0.00	0.01	0.01			0.11	0.05
man values	0.20	0.57	35.34	56.23	0.22	2.78	1.66	1.28	0.07	0.01	1.33	0.01	0.00	0.00	0.01	0.02	0.01	0.03	0.12	0.13

All values are averaged by two tests.

Appendix 8 Chemical compositions of clear glazes

Samples	Na_2O	MgO	Al_2O_3	SiO_2	P_2O_5	K_2O	CaO	TiO_2	V_2O_5	MnO	Fe_2O_3	CoO	NiO	CuO	ZnO	SrO	SnO_2	Sb_2O_5	BaO	PbO
HY-38-1-1	1.86	0.40	3.30	14.97	32.93	0.10	10.01	0.16	0.15	0.04	0.59	0.01	0.00	0.04	0.01	0.06	0.85	0.01	0.61	33.87
HY-38-1-2	3.03	2.01	2.17	14.21	36.03	0.02	9.38	0.07	0.07	0.04	0.32	0.02	0.00	0.02	0.01	0.05	0.74	0.29	0.39	31.14
HY-38-4-1	0.19	0.01	2.62	19.07	33.25	0.07	10.93	0.10	0.08	0.04	0.38	0.01	0.00	0.01	0.01	0.05	0.76		0.50	31.90
HY-38-4-2	2.68	0.34	3.84	26.64	27.01	0.21	10.17	0.13	0.02	0.03	0.56	0.01	0.00	0.00	0.01	0.05	0.68		0.59	27.01
HY-38-6-1	1.18	0.52	3.58	25.01	28.32	0.14	8.17	0.16	0.11	0.03	0.53	0.01	0.00	0.00	0.01	0.05	0.83	0.03	0.54	30.80
HY-38-6-2	3.43	1.48	2.21	17.51	33.35	0.07	9.36	0.09	0.08	0.02	0.45	0.01	0.00	0.00	0.01	0.05	0.68		0.53	30.67
HY-38-7-1	0.23	1.30	4.32	17.25	28.38	0.32	16.59	0.20	0.04	0.03	0.84	0.01	0.00	0.01	0.01	0.06	0.81	0.06	0.63	28.91
HY-38-7-2	1.36	2.79	4.89	20.35	25.01	0.45	16.15	0.25	0.06	0.04	1.07	0.01	0.00	0.01	0.00	0.06	0.70	0.00	0.60	26.20
HY-38-13-1	0.01	1.46	2.68	12.62	36.87	0.13	12.39	0.18	0.06	0.04	0.57	0.01	0.00	0.02	0.00	0.06			0.04	32.88
HY-38-13-2	0.01	0.82	2.33	14.39	36.86	0.09	12.22	0.10	0.07	0.02	0.43	0.01	0.00	0.02	0.00	0.05			0.02	32.55
HY-38-13-3	0.01	0.08	2.30	14.63	36.67	0.03	13.41	0.07	0.03	0.02	0.30	0.02	0.00	0.02	0.01	0.05			0.08	32.27
HY-38-15-1	0.01	0.32	3.12	30.88	28.69	0.13	11.21	0.20	0.03	0.03	0.38	0.01	0.00	0.05	0.01	0.05			0.03	24.87

Samples	Na_2O	MgO	Al_2O_3	SiO_2	P_2O_5	K_2O	CaO	TiO_2	V_2O_5	MnO	Fe_2O_3	CoO	NiO	CuO	ZnO	SrO	SnO_2	Sb_2O_5	BaO	PbO
HY-38-15-2	0.01	0.66	4.97	20.34	30.00	0.32	12.67	0.19	0.10	0.04	0.89	0.01	0.00	0.09	0.01	0.07			0.06	29.57
HY-38-15-3	0.01	0.68	4.15	30.37	26.56	0.38	12.12	0.25	0.03	0.06	0.78	0.01	0.00	0.05	0.01	0.05				24.49
HY-38-16-1	0.31	0.47	3.45	13.77	32.68	0.26	20.51	0.15	0.02	0.04	0.56	0.01	0.00	0.07	0.01	0.06			0.03	27.59
HY-38-16-2	0.01	1.00	3.56	16.27	34.44	0.12	13.55	0.17	0.02	0.03	0.54	0.01	0.00	0.05	0.00	0.06			0.03	30.15
HY-38-16-3	0.12	2.09	1.71	10.22	35.90	0.08	17.65	0.12	0.03	0.02	0.49	0.01	0.00	0.07	0.00	0.06			0.02	31.40
HY-38-18-1	0.01	0.42	6.18	26.58	27.73	0.48	10.79	0.33	0.04	0.04	1.16	0.01	0.00	0.01	0.01	0.05			0.01	26.17
HY-38-18-2	1.46	1.76	5.09	28.18	24.85	0.41	10.32	0.32	0.07	0.03	1.15	0.01	0.00	0.01	0.01	0.05			0.04	26.27
HY-38-18-3	0.01	0.72	5.47	25.95	25.11	0.50	9.87	0.39	0.12	0.03	1.33	0.01	0.00	0.01	0.00	0.06			0.01	30.41
HY-38-18-4	0.01	0.20	4.73	22.85	29.04	0.39	10.04	0.30	0.10	0.03	1.13	0.01	0.00	0.01	0.00	0.06				31.10
HY-38-18-5	0.01	0.01	2.20	45.08	17.01	0.18	7.07	0.21	0.05	0.02	0.69	0.01	0.00	0.01	0.01	0.05			0.10	27.31
HY-38-18-6	0.01	1.01	6.54	28.10	23.86	0.49	10.24	0.56	0.07	0.03	1.75	0.01	0.00	0.01	0.01	0.06				27.25
HY-38-20-1	0.01	0.12	3.71	17.92	35.91	0.17	11.28	0.23	0.08	0.04	0.71	0.01	0.00	0.05	0.01	0.06			0.03	29.67
HY-38-20-2	0.56	0.61	3.88	20.75	31.22	0.30	11.27	0.16	0.08	0.04	0.84	0.01	0.00	0.10	0.00	0.06			0.08	30.03

Samples	Na_2O	MgO	Al_2O_3	SiO_2	P_2O_5	K_2O	CaO	TiO_2	V_2O_5	MnO	Fe_2O_3	CoO	NiO	CuO	ZnO	SrO	SnO_2	Sb_2O_5	BaO	PbO
HY-38-20-3	0.14	2.28	4.53	25.25	27.39	0.52	10.73	0.25	0.06	0.04	1.25	0.01	0.00	0.09	0.01	0.06			0.01	27.40
HY-38-22-1	0.18	1.31	3.35	30.62	28.63	0.15	8.46	0.09	0.06	0.01	0.56	0.01	0.00	0.02	0.00	0.05			0.00	26.48
HY-38-22-2	0.01	1.23	2.00	35.33	25.15	0.06	8.50	0.07	0.04	0.02	0.35	0.03	0.00	0.02	0.01	0.05			0.03	27.10
HY-38-22-3	0.01	0.67	1.54	38.20	23.63	0.03	8.46	0.08	0.05	0.02	0.31	0.01	0.00	0.03	0.01	0.05			0.05	26.87
HY-43-2-1	1.70	0.48	4.33	24.19	24.88	0.22	8.55	0.19	0.09	0.01	0.68	0.01	0.00	0.00	0.01	0.05	0.94	0.14	0.59	32.94
HY-43-2-2	1.64	1.95	3.94	25.12	26.06	0.26	8.68	0.15	0.06	0.01	0.79	0.01	0.00	0.01	0.01	0.05	0.78	0.01	0.36	30.10
HY-43-24-1	0.01	1.61	5.50	31.96	21.77	0.55	9.40	0.25	0.05	0.02	1.37	0.01	0.00	0.01	0.00	0.05			0.01	27.44
HY-43-24-2	0.12	1.40	7.03	37.12	17.38	0.97	8.58	0.28	0.04	0.02	1.60	0.02	0.00	0.00	0.00	0.05			0.07	25.31
HY-58-1-1	2.17	1.07	0.83	51.68	2.37	0.00	3.25	0.03	0.02	0.01	0.19	0.01	0.00	0.00	0.01	0.05	0.98	0.01	0.63	36.71
HY-58-1-2	1.71	1.11	2.10	45.40	7.12	0.12	4.17	0.08	0.03	0.02	0.44	0.01	0.00	0.01	0.01	0.05	0.94	0.01	0.81	35.86
HY-58-1-3	1.99	2.58	1.98	45.68	7.01	0.03	4.02	0.10	0.17	0.02	0.37	0.01	0.00	0.01	0.01	0.07	0.74	0.01	0.52	34.69
HY-58-3-1	2.34	0.67	1.25	49.75	3.11	0.00	3.33	0.03	0.02	0.02	0.23	0.00	0.00	0.01	0.01	0.05	1.12	0.01	0.68	37.36
HY-58-3-2	0.22	0.60	1.13	46.41	6.66	0.03	5.22	0.05	0.04	0.02	0.30	0.00	0.00	0.00	0.02	0.06	1.01	0.03	0.48	37.74

Samples	Na_2O	MgO	Al_2O_3	SiO_2	P_2O_5	K_2O	CaO	TiO_2	V_2O_5	MnO	Fe_2O_3	CoO	NiO	CuO	ZnO	SrO	SnO_2	Sb_2O_5	BaO	PbO
HY-58-5-1	0.22	1.16	1.23	52.30	3.24	0.05	4.08	0.10	0.02	0.03	0.47	0.00	0.00	0.00	0.01	0.07	1.00	0.00	0.54	35.51
HY-58-5-2	2.50	2.11	3.25	47.80	5.42	0.26	4.59	0.15	0.06	0.04	0.56	0.00	0.00	0.00	0.00	0.06	0.73		0.40	32.06
HY-58-5-3	0.23	1.21	12.58	35.72	20.38	1.07	5.23	0.83	0.26	0.01	0.87	0.01	0.00	0.01	0.01	0.07	0.33	0.01	0.84	20.34
HY-58-7-1	1.11	0.66	1.21	49.17	1.54	0.00	2.73	0.03	0.00	0.03	0.17	0.01	0.01	0.01	0.01	0.07	1.12	0.15	0.53	41.45
HY-58-7-2	0.01	0.88	2.75	46.79	3.79	0.13	3.73	0.05	0.09	0.03	0.65	0.01	0.00	0.01	0.01	0.07	1.09	0.11	0.72	39.10
HY-58-8-1	0.01	1.08	1.13	46.23	7.20	0.00	3.91	0.08	0.05	0.02	0.35	0.00	0.00	0.00	0.01	0.06			0.17	39.70
HY-58-8-2	0.01	0.48	2.25	48.14	6.59	0.05	7.06	0.05	0.03	0.01	0.28	0.00	0.00	0.00	0.01	0.07			0.00	34.96
HY-58-12-1	1.65	1.68	3.41	49.79	5.21	0.11	3.64	0.08	0.05	0.03	0.37	0.00	0.00	0.00	0.00	0.05				33.92
HY-58-12-2	0.01	0.01	2.81	53.84	4.80	0.00	3.03	0.05	0.03	0.02	0.41	0.00	0.00	0.01	0.02	0.04			0.15	34.77
HY-58-14-1	0.23	0.26	1.22	51.42	4.61	0.00	5.33	0.05	0.06	0.01	0.42	0.00	0.00	0.00	0.00	0.07			0.01	36.31
HY-58-14-2	0.33	0.19	1.65	51.41	4.64	0.04	5.34	0.07	0.04	0.01	0.28	0.00	0.00	0.00	0.00	0.06				35.94
HY-58-16-1	0.67	0.01	1.31	54.05	3.03	0.04	3.41	0.07	0.02	0.02	0.26	0.00	0.00	0.01	0.01	0.05				37.05
HY-58-16-2	0.01	0.01	0.90	51.70	3.75	0.00	3.28	0.04	0.12	0.02	0.29	0.00	0.00	0.01	0.01	0.05			0.03	39.76

Samples	Na_2O	MgO	Al_2O_3	SiO_2	P_2O_5	K_2O	CaO	TiO_2	V_2O_5	MnO	Fe_2O_3	CoO	NiO	CuO	ZnO	SrO	SnO_2	Sb_2O_5	BaO	PbO
HY-58-17-1	0.01	0.11	0.35	62.81	1.89	0.00	1.81	0.03	0.02	0.02	0.15	0.00	0.00	0.00	0.01	0.04				32.74
HY-58-17-2	0.01	0.01	0.65	50.17	4.45	0.00	3.17	0.00	0.03	0.02	0.14	0.00	0.00	0.00	0.02	0.06			0.12	41.14
HY-58-22-1	0.01	3.25	3.25	40.23	13.61	0.28	6.04	0.15	0.07	0.02	0.70	0.00	0.00	0.01	0.01	0.07			0.01	32.26
HY-58-22-2	0.01	0.34	1.56	48.83	6.80	0.07	3.99	0.08	0.05	0.02	0.36	0.00	0.00	0.01	0.01	0.06			0.08	37.74
HY-58-24-1	0.34	1.99	2.71	47.03	6.19	0.17	4.78	0.09	0.03	0.02	0.90	0.00	0.00	0.01	0.00	0.07			0.05	35.64
HY-58-24-2	0.01	0.01	1.10	46.19	4.34	0.00	5.02	0.05	0.03	0.02	0.24	0.01	0.00	0.00	0.00	0.07				42.91
HY-59-2-1	0.01	0.14	4.67	27.74	22.11	0.46	8.15	0.22	0.13	0.03	0.92	0.02	0.00	0.01	0.01	0.09	0.98	0.01	0.42	33.90
HY-59-2-2	1.41	2.70	6.34	35.48	14.87	0.77	8.00	0.27	0.10	0.02	1.26	0.01	0.00	0.00	0.00	0.08	0.64	0.29	0.52	27.24
HY-59-3-1	1.51	1.88	3.66	37.70	14.32	0.24	6.19	0.15	0.08	0.02	0.50	0.01	0.00	0.00	0.00	0.07	0.81	0.01	0.43	32.43
HY-59-3-2	4.72	4.63	2.69	28.71	18.16	0.14	6.18	0.10	0.10	0.02	0.38	0.01	0.00	0.00	0.00	0.06	0.87	0.00	0.49	32.74
HY-59-7-1	0.71	0.13	1.52	52.71	2.70	0.01	3.62	0.07	0.02	0.01	0.25	0.00	0.00	0.00	0.01	0.07	0.00	0.00	0.00	38.16
HY-59-7-2	0.01	1.65	1.94	51.94	3.39	0.03	3.25	0.04	0.02	0.01	0.38	0.00	0.00	0.00	0.01	0.06	0.00	0.00	0.06	37.19
HY-59-10-1	2.84	3.24	3.52	24.91	25.30	0.22	6.91	0.12	0.13	0.02	0.51	0.02	0.00	0.01	0.01	0.08	0.00	0.00	0.05	32.13

Samples	Na_2O	MgO	Al_2O_3	SiO_2	P_2O_5	K_2O	CaO	TiO_2	V_2O_5	MnO	Fe_2O_3	CoO	NiO	CuO	ZnO	SrO	SnO_2	Sb_2O_5	BaO	PbO
HY-59-10-2	0.01	4.82	6.02	29.35	18.52	0.56	7.52	0.21	0.11	0.02	0.96	0.01	0.00	0.00	0.00	0.07	0.00	0.00	0.08	31.71
HY-61-4-1	0.83	0.73	1.63	4.10	54.88	0.24	23.63	0.04	0.01	0.01	0.71	0.00	0.00	0.01	0.06	0.04	0.00	0.00	0.02	13.06
HY-61-4-2	0.01	1.65	2.46	8.22	50.05	0.39	21.04	0.09	0.02	0.01	1.57	0.01	0.00	0.02	0.07	0.05	0.00	0.00	0.01	14.34
HY-61-5-1	0.01	1.40	1.62	5.88	52.28	0.20	23.19	0.06	0.01	0.01	0.81	0.00	0.00	0.01	0.06	0.04	0.00	0.00	0.02	14.39
HY-61-5-2	0.37	0.61	1.21	5.35	53.57	0.24	23.70	0.04	0.01	0.01	0.52	0.00	0.00	0.02	0.06	0.04	0.00	0.00	0.00	14.27
HY-61-7-1	0.01	0.37	5.27	13.98	48.21	1.07	19.53	0.30	0.02	0.01	1.03	0.01	0.00	0.04	0.05	0.04	0.00	0.00	0.03	10.04
HY-61-7-2	0.01	0.87	6.92	16.17	44.87	1.16	17.63	0.32	0.03	0.01	1.13	0.01	0.00	0.07	0.05	0.04	0.00	0.00	0.03	10.69
HY-61-8-1	0.00	0.10	1.91	7.73	52.93	0.18	21.17	0.04	0.01	0.01	0.33	0.00	0.00	0.02	0.04	0.03	0.00	0.00		15.48
HY-61-8-2	0.88	0.67	2.81	14.45	47.91	0.77	17.72	0.17	0.02	0.04	0.73	0.01	0.00	0.03	0.07	0.07	0.00	0.00	0.02	13.62
HY-61-9-1	0.01	1.39	1.85	13.76	45.62	0.22	16.49	0.08	0.02	0.01	0.53	0.00	0.00	0.02	0.03	0.05	0.00	0.00	0.03	19.89
HY-61-9-2	0.01	1.17	9.36	32.30	31.57	1.78	9.35	0.50	0.05	0.03	1.88	0.01	0.00	0.02	0.05	0.06	0.00	0.00	0.16	11.69
HY-61-10-1	0.01	0.13	5.40	12.59	44.49	0.49	19.92	0.12	0.01	0.01	0.81	0.01	0.00	0.01	0.04	0.04	0.00	0.00	0.00	15.93
HY-61-10-2	0.18	0.01	4.60	14.12	42.46	0.61	19.08	0.12	0.01	0.01	0.90	0.01	0.00	0.02	0.05	0.04	0.00	0.00	0.00	17.78

Samples	Na_2O	MgO	Al_2O_3	SiO_2	P_2O_5	K_2O	CaO	TiO_2	V_2O_5	MnO	Fe_2O_3	CoO	NiO	CuO	ZnO	SrO	SnO_2	Sb_2O_5	BaO	PbO
HY-62-3-1	0.00	1.73	2.39	6.29	52.38	0.20	23.57	0.04	0.01	0.00	0.46	0.00	0.00	0.01	0.03	0.03	0.00	0.00		12.85
HY-62-3-2	0.01	0.68	2.84	7.74	50.80	0.23	20.36	0.06	0.01	0.01	0.84	0.00	0.00	0.01	0.03	0.03				16.34
HY-62-4-1	0.01	1.18	4.15	13.18	47.35	0.48	20.07	0.10	0.01	0.01	0.66	0.00	0.00	0.01	0.04	0.03				12.72
HY-62-4-2	0.00	1.09	1.89	7.08	52.53	0.19	24.70	0.04	0.01	0.00	0.57	0.00	0.00	0.01	0.03	0.03			0.00	11.82
HY-62-5-1	0.00	0.18	2.20	7.13	53.91	0.32	24.91	0.05	0.01	0.00	0.57	0.00	0.00	0.01	0.03	0.04			0.01	10.63
HY-62-5-2	0.17	0.69	1.68	5.95	53.07	0.29	25.75	0.06	0.01	0.00	0.61	0.00	0.00	0.01	0.03	0.04			0.01	11.63
HY-92-3	0.29	0.26	2.86	26.90	22.79	0.09	9.40	0.12	0.08	0.02	0.34	0.01	0.00	0.04	0.00	0.09			0.29	36.41
HY-92-4-1	0.61	0.01	2.65	18.70	31.73	0.23	10.64	0.14	0.05	0.01	0.75	0.01	0.00	0.01	0.00	0.08			0.12	34.26
HY-92-4-2	0.41	0.70	2.24	19.18	32.00	0.20	10.47	0.21	0.05	0.02	0.76	0.03	0.00	0.01	0.01	0.08			0.11	33.55
HY-101-1-1	0.35	0.21	2.93	14.14	37.89	0.08	7.92	0.09	0.07	0.02	0.40	0.01	0.00	0.03	0.01	0.07			0.89	34.90
HY-101-1-2	0.01	0.15	2.69	12.12	38.66	0.00	7.88	0.10	0.05	0.02	0.40	0.01	0.00	0.03	0.01	0.07			0.40	37.40
HY-101-2-1	0.01	0.01	3.42	16.73	36.38	0.16	8.89	0.11	0.06	0.01	0.50	0.01	0.00	0.02	0.00	0.06			0.19	33.45
HY-101-2-2	1.92	0.59	4.83	17.61	33.02	0.19	8.00	0.11	0.04	0.01	0.48	0.01	0.00	0.02	0.01	0.06			0.22	32.89

Samples	Na_2O	MgO	Al_2O_3	SiO_2	P_2O_5	K_2O	CaO	TiO_2	V_2O_5	MnO	Fe_2O_3	CoO	NiO	CuO	ZnO	SrO	SnO_2	Sb_2O_5	BaO	PbO
HY-101-3-1	0.70	0.40	2.80	15.17	36.42	0.00	6.85	0.08	0.05	0.01	0.44	0.01	0.00	0.02	0.01	0.07			0.38	36.60
HY-101-3-2	0.01	0.80	2.61	16.72	35.23	0.00	6.45	0.06	0.07	0.02	0.23	0.01	0.00	0.01	0.01	0.07			0.72	36.98
HY-102-1-1	0.01	0.58	3.61	14.88	34.09	0.18	10.38	0.14	0.04	0.02	0.89	0.01	0.00	0.06	0.01	0.06			0.06	34.99
HY-102-1-2	0.08	1.34	3.97	14.87	32.91	0.21	10.78	0.20	0.04	0.02	0.88	0.01	0.00	0.06	0.00	0.06			0.03	34.54
HY-102-2-1	0.01	1.62	0.82	49.40	5.66	0.00	4.12	0.04	0.01	0.02	0.23	0.01	0.00	0.05	0.01	0.05				37.94
HY-102-2-2	0.10	0.01	0.51	45.95	7.77	0.00	4.37	0.00	0.02	0.03	0.22	0.01	0.00	0.06	0.01	0.06			0.22	40.65
HY-102-3	1.88	2.48	4.78	23.88	28.28	0.33	8.82	0.21	0.03	0.01	0.94	0.01	0.00	0.02	0.01	0.05				28.27
HY-117-1-1	0.01	0.35	1.05	49.18	2.60	0.00	2.47	0.04	0.02	0.01	0.14	0.00	0.01	0.01	0.01	0.04			0.10	43.96
HY-117-1-2	0.01	0.01	0.40	51.54	2.40	0.00	2.50	0.03	0.01	0.01	0.13	0.00	0.01	0.00	0.01	0.04				42.88
HY-117-2-1	0.01	1.50	6.51	43.85	8.69	0.30	7.11	0.23	0.05	0.02	0.65	0.00	0.00	0.00	0.01	0.03			0.05	30.98
HY-117-2-2	0.02	1.46	4.29	45.32	7.93	0.11	5.82	0.09	0.06	0.02	0.48	0.00	0.00	0.00	0.01	0.03			0.08	34.27
HY-118-1-1	0.01	0.01	2.44	37.18	18.82	0.00	5.91	0.10	0.10	0.02	0.33	0.01	0.00	0.00	0.01	0.03				35.04
HY-118-1-2	0.01	0.08	3.00	36.26	16.17	0.04	6.74	0.09	0.10	0.02	0.42	0.00	0.00	0.00	0.01	0.03			0.00	37.03

Samples	Na_2O	MgO	Al_2O_3	SiO_2	P_2O_5	K_2O	CaO	TiO_2	V_2O_5	MnO	Fe_2O_3	CoO	NiO	CuO	ZnO	SrO	SnO_2	Sb_2O_5	BaO	PbO
HY-123-2-1	0.68	0.01	1.53	31.90	26.50	0.04	5.83	0.09	0.09	0.03	0.32	0.02	0.00	0.04	0.00	0.11			0.07	32.72
HY-123-2-2	0.01	0.01	1.82	25.93	29.35	0.10	6.49	0.11	0.10	0.03	0.59	0.01	0.00	0.04	0.01	0.11			0.06	35.24
HY-123-3-1	1.83	2.52	1.61	17.78	29.67	0.10	6.66	0.07	0.11	0.02	0.43	0.01	0.00	0.07	0.00	0.12			0.09	38.92
HY-123-3-2	0.02	1.30	1.36	33.51	12.11	0.00	3.73	0.03	0.03	0.02	0.30	0.00	0.00	0.06	0.00	0.09			0.02	47.42
HY-123-5-1	0.01	0.28	4.24	25.61	26.25	0.38	6.92	0.18	0.08	0.02	0.96	0.01	0.00	0.03	0.00	0.08			0.08	34.85
HY-123-5-2	0.01	1.08	4.72	32.95	19.00	0.69	6.33	0.43	0.07	0.02	1.42	0.01	0.00	0.04	0.01	0.09			0.00	33.12
HY-123-7-1	1.65	1.50	2.96	25.15	27.50	0.23	7.26	0.17	0.11	0.01	0.59	0.01	0.00	0.04	0.00	0.11			0.01	32.70
HY-123-7-2	0.01	0.01	5.05	26.07	26.52	0.49	7.42	0.21	0.08	0.01	1.01	0.02	0.00	0.04	0.00	0.10			0.03	32.91
HY-123-8-1	0.70	3.07	4.08	22.01	26.70	0.38	7.61	0.22	0.09	0.02	0.97	0.02	0.00	0.07	0.00	0.10			0.11	33.85
HY-123-8-2	0.13	0.67	6.53	32.15	21.86	0.93	7.12	0.41	0.08	0.02	1.84	0.01	0.00	0.05	0.00	0.09			0.10	28.00
HY-132-8-1	0.01	1.31	4.65	29.26	33.06	0.06	8.64	0.09	0.03	0.02	0.24	0.01	0.00	0.05	0.00	0.03			0.12	22.41
HY-132-8-2	0.01	0.01	6.23	23.59	32.30	0.14	14.86	0.12	0.02	0.02	0.32	0.01	0.00	0.03	0.00	0.03			0.37	21.94
HY-136-1-1	0.01	1.52	4.68	29.96	29.78	0.34	11.99	0.15	0.03	0.01	0.75	0.01	0.00	0.07	0.01	0.03			0.08	20.57

Samples	Na_2O	MgO	Al_2O_3	SiO_2	P_2O_5	K_2O	CaO	TiO_2	V_2O_5	MnO	Fe_2O_3	CoO	NiO	CuO	ZnO	SrO	SnO_2	Sb_2O_5	BaO	PbO
HY-136-1-2	0.01	0.01	3.03	27.39	32.59	0.19	10.32	0.20	0.12	0.02	0.58	0.01	0.00	0.09	0.01	0.03			0.04	25.37
HY-145-1-1	0.03	0.03	0.01	24.61	3.62	0.00	3.97	0.00	0.03	0.07	0.17	0.01	0.01	0.01	0.03	0.19			0.42	66.80
HY-145-1-2	0.03	0.02	1.51	25.88	9.79	0.00	3.64	0.00	0.05	0.05	0.15	0.01	0.01	0.01	0.03	0.17			0.56	58.08
HY-146-2-1	0.92	0.56	2.48	6.28	49.34	0.00	11.99	0.06	0.01	0.01	0.30	0.01	0.00	0.02	0.00	0.04			0.11	27.87
HY-146-2-2	0.01	0.08	2.94	7.02	46.47	0.06	15.78	0.12	0.01	0.01	0.34	0.01	0.00	0.01	0.01	0.05			0.05	27.02
HY-146-3-1	0.01	0.66	3.68	10.26	52.19	0.34	20.05	0.26	0.03	0.01	1.52	0.01	0.00	0.00	0.01	0.05			0.22	10.68
HY-146-3-2	0.13	0.86	6.71	15.98	49.15	0.56	15.68	0.38	0.03	0.02	1.52	0.01	0.00	0.01	0.02	0.05			0.16	8.73
HY-150-2-1	0.01	1.53	5.28	35.08	22.85	0.53	7.48	0.30	0.15	0.04	1.22	0.01	0.00	0.02	0.00	0.06			0.09	25.34
HY-150-2-2	0.07	2.31	6.42	37.63	24.19	0.47	7.66	0.19	0.13	0.04	0.88	0.01	0.00	0.02	0.00	0.04			0.09	19.86
HY-150-4-1	0.01	1.27	9.03	40.04	22.40	0.79	9.26	0.25	0.08	0.03	1.42	0.01	0.00	0.06	0.01	0.05			0.22	15.08
HY-150-4-2	0.33	2.26	10.16	39.08	22.49	0.52	8.37	0.26	0.08	0.03	1.50	0.02	0.00	0.07	0.01	0.05			0.07	14.71
HY-150-9-1	0.01	0.17	2.67	45.20	24.40	0.13	5.71	0.11	0.14	0.02	0.45	0.01	0.00	0.00	0.01	0.04			0.02	20.91
HY-150-9-2	0.01	0.01	5.67	44.07	20.84	0.55	6.43	0.20	0.21	0.03	1.00	0.01	0.00	0.01	0.00	0.04			0.10	20.82

Samples	Na_2O	MgO	Al_2O_3	SiO_2	P_2O_5	K_2O	CaO	TiO_2	V_2O_5	MnO	Fe_2O_3	CoO	NiO	CuO	ZnO	SrO	SnO_2	Sb_2O_5	BaO	PbO
Mean values	0.49	0.95	3.38	28.86	25.42	0.25	9.79	0.15	0.06	0.02	0.66	0.01	0.00	0.02	0.01	0.06	0.84	0.06	0.20	29.53

Appendix 9 Chemical compositions of brown glazes

Samples	Na_2O	MgO	Al_2O_3	SiO_2	P_2O_5	K_2O	CaO	TiO_2	V_2O_5	MnO	Fe_2O_3	CoO	NiO	CuO	ZnO	SrO	SnO_2	Sb_2O_5	BaO	PbO
HY-38-2-1	2.15	1.71	3.87	14.52	32.10	0.17	12.24	0.13	0.07	0.07	2.19	0.02	0.00	0.02	0.01	0.06	0.77	0.00	0.47	29.44
HY-38-2-2	0.87	0.63	3.00	18.62	31.31	0.11	12.35	0.11	0.04	0.06	2.50	0.02	0.00	0.01	0.00	0.05	0.78	0.00	0.37	29.15
HY-38-5-1	4.26	1.26	3.30	12.59	31.46	0.11	9.34	0.18	0.13	0.09	2.14	0.02	0.00	0.01	0.01	0.06	0.76	0.01	0.44	33.84
HY-38-5-2	1.83	0.52	2.96	12.83	32.89	0.11	10.25	0.14	0.27	0.06	1.99	0.03	0.00	0.00	0.00	0.06	0.71	0.01	0.71	34.62
HY-38-8-1	1.39	1.58	3.41	20.53	25.77	0.38	13.49	0.27	0.07	0.06	2.55	0.02	0.00	0.01	0.01	0.06	0.68	0.02	0.75	28.96
HY-38-8-2	1.17	0.56	2.19	16.34	32.68	0.09	12.38	0.10	0.06	0.03	2.45	0.02	0.00	0.01	0.01	0.06	0.73	0.00	0.78	30.35
HY-38-9-1	0.01	0.67	14.03	38.23	12.11	1.22	8.31	0.79	0.14	0.08	2.84	0.01	0.00	0.01	0.01	0.05			0.10	21.39
HY-38-9-2	0.01	0.30	3.33	26.38	26.71	0.16	11.05	0.18	0.14	0.13	2.51	0.02	0.00	0.01	0.00	0.06				29.01
HY-38-9-3	0.01	0.61	3.48	27.85	23.34	0.07	8.16	0.15	0.10	0.05	2.98	0.02	0.00	0.01	0.00	0.05				33.12
HY-38-12-1	0.01	0.85	3.63	17.68	27.99	0.28	19.19	0.17	0.04	0.07	2.19	0.02	0.00	0.03	0.00	0.06			0.07	27.73
HY-38-12-2	0.01	1.15	4.97	22.22	25.89	0.46	13.78	0.30	0.08	0.06	2.29	0.01	0.00	0.03	0.00	0.06			0.02	28.66
HY-38-12-3	0.01	1.70	4.57	22.21	25.59	0.46	16.10	0.37	0.05	0.08	2.44	0.02	0.00	0.03	0.00	0.05			0.03	26.28

Samples	Na_2O	MgO	Al_2O_3	SiO_2	P_2O_5	K_2O	CaO	TiO_2	V_2O_5	MnO	Fe_2O_3	CoO	NiO	CuO	ZnO	SrO	SnO_2	Sb_2O_5	BaO	PbO
HY-38-14-1	0.16	2.50	6.63	27.74	22.20	0.66	10.96	0.38	0.07	0.06	1.86	0.01	0.00	0.01	0.01	0.06			0.00	26.70
HY-38-14-2	1.29	1.07	2.71	13.97	36.30	0.12	11.90	0.11	0.05	0.03	2.00	0.02	0.00	0.01	0.00	0.05			0.00	30.39
HY-38-14-3	0.01	0.85	5.65	23.96	27.18	0.60	13.91	0.38	0.03	0.06	2.07	0.01	0.00	0.01	0.00	0.06			0.07	25.15
HY-38-17-1	0.01	0.55	2.29	16.73	35.56	0.08	13.61	0.12	0.04	0.04	3.45	0.02	0.00	0.04	0.00	0.06			0.05	27.34
HY-38-17-2	0.01	0.37	2.34	19.31	32.14	0.14	14.14	0.13	0.02	0.03	2.37	0.02	0.00	0.05	0.00	0.06			0.00	28.85
HY-38-17-3	0.01	0.34	3.32	22.91	31.85	0.25	10.95	0.13	0.03	0.02	3.13	0.03	0.00	0.03	0.00	0.06			0.02	26.94
HY-38-21-2	1.80	0.59	4.31	18.32	32.44	0.25	10.33	0.22	0.07	0.03	2.04	0.02	0.00	0.02	0.01	0.06			0.01	29.48
HY-38-21-3	0.01	1.98	5.42	27.25	23.03	0.49	12.95	0.34	0.03	0.05	2.79	0.02	0.00	0.01	0.00	0.06				25.57
HY-38-21-4	1.82	0.95	4.70	24.85	27.21	0.37	9.69	0.25	0.08	0.04	2.80	0.02	0.00	0.01	0.00	0.06			0.03	27.12
HY-43-1-1	0.48	3.20	4.65	24.20	21.22	0.36	7.37	0.16	0.09	0.03	2.79	0.02	0.00	0.01	0.01	0.06	0.81	0.01	0.49	34.05
HY-43-1-2	0.08	0.39	5.66	24.62	22.09	0.55	8.95	0.23	0.09	0.02	2.76	0.02	0.00	0.01	0.01	0.07	0.63	0.01	0.80	33.02
HY-43-3-1	2.85	1.63	5.79	24.62	22.26	0.44	9.53	0.19	0.07	0.02	2.49	0.01	0.00	0.01	0.00	0.06	0.69	0.06	0.37	28.91
HY-43-3-2	1.98	2.06	5.96	28.77	21.30	0.65	8.08	0.40	0.06	0.02	2.33	0.02	0.00	0.00	0.00	0.05	0.62	0.01	0.54	27.17

Samples	Na_2O	MgO	Al_2O_3	SiO_2	P_2O_5	K_2O	CaO	TiO_2	V_2O_5	MnO	Fe_2O_3	CoO	NiO	CuO	ZnO	SrO	SnO_2	Sb_2O_5	BaO	PbO
HY-43-4-1	0.36	1.21	5.36	19.50	28.69	0.46	9.95	0.32	0.08	0.02	2.36	0.02	0.00	0.01	0.00	0.06	0.71		0.54	30.35
HY-43-4-2	2.29	0.85	4.83	20.62	25.65	0.58	9.67	0.27	0.07	0.03	2.63	0.02	0.00	0.01	0.00	0.07	0.74	0.01	0.40	31.26
HY-43-5-1	1.48	2.72	7.54	35.34	9.20	0.98	7.01	0.38	0.05	0.04	3.32	0.01	0.00	0.01	0.01	0.05	0.83	0.01	0.52	30.51
HY-43-5-2	0.29	1.45	8.14	36.79	11.57	1.21	9.21	0.41	0.06	0.04	3.23	0.02	0.00	0.01	0.00	0.06	0.73	0.12	0.34	26.33
HY-43-5-3	1.20	0.27	7.24	29.03	13.61	0.74	7.58	0.44	0.06	0.04	3.32	0.02	0.00	0.01	0.01	0.06	0.89	0.01	0.65	34.82
HY-43-6-1	1.09	1.43	12.83	33.39	12.74	1.21	5.63	0.60	0.08	0.02	2.82	0.02	0.00	0.01	0.01	0.05	0.57	0.00	0.42	27.07
HY-43-6-2	1.87	1.30	7.64	30.10	12.43	0.73	6.60	0.31	0.04	0.03	3.79	0.02	0.00	0.01	0.00	0.05	0.86	0.01	0.95	33.24
HY-43-8-1	0.56	3.02	6.55	26.90	17.93	0.74	7.18	0.27	0.05	0.03	3.77	0.02	0.00	0.01	0.00	0.04	0.87	0.06	0.79	31.22
HY-43-8-2	1.24	2.19	6.59	23.20	20.90	0.60	8.20	0.29	0.07	0.03	2.73	0.02	0.00	0.01	0.00	0.05	0.90		0.41	32.55
HY-43-9-1	0.01	1.99	5.52	24.01	20.01	0.56	8.81	0.25	0.07	0.02	1.40	0.02	0.00	0.02	0.01	0.06	0.94	0.01	0.50	35.78
HY-43-9-2	0.54	0.86	6.14	24.74	21.43	0.76	9.39	0.31	0.08	0.03	1.90	0.01	0.00	0.02	0.01	0.06	0.84	0.02	0.62	32.23
HY-43-12-1	1.53	1.77	7.50	40.13	1.24	0.76	3.26	0.28	0.02	0.03	4.07	0.01	0.00	0.01	0.01	0.05	0.95	0.01	0.80	37.56
HY-43-12-2	3.93	1.84	6.64	36.89	2.38	0.60	3.78	0.21	0.03	0.03	3.84	0.01	0.00	0.01	0.01	0.05	1.10	0.01	0.40	38.25

Samples	Na_2O	MgO	Al_2O_3	SiO_2	P_2O_5	K_2O	CaO	TiO_2	V_2O_5	MnO	Fe_2O_3	CoO	NiO	CuO	ZnO	SrO	SnO_2	Sb_2O_5	BaO	PbO
HY-43-13-1	1.31	0.39	5.58	35.73	9.00	0.48	4.96	0.26	0.04	0.03	3.79	0.00	0.00	0.01	0.02	0.06			0.17	38.19
HY-43-13-2	1.73	2.37	6.34	35.28	13.82	0.64	6.07	0.32	0.04	0.03	2.85	0.01	0.00	0.00	0.00	0.05				30.45
HY-43-14-1	0.01	0.11	3.64	16.65	32.00	0.21	9.56	0.15	0.08	0.02	2.30	0.02	0.00	0.01	0.00	0.07			0.09	35.05
HY-43-14-1	0.01	0.52	4.60	19.77	29.30	0.32	9.49	0.20	0.11	0.02	2.09	0.02	0.00	0.00	0.00	0.07			0.08	33.42
HY-43-15-1	1.65	1.19	5.17	22.06	21.84	0.34	7.38	0.23	0.05	0.02	2.86	0.01	0.00	0.01	0.00	0.06			0.08	37.04
HY-43-15-2	0.01	0.26	7.24	41.89	2.37	0.60	3.71	0.31	0.03	0.03	4.10	0.00	0.00	0.00	0.01	0.06			0.07	39.31
HY-43-15-3	1.77	0.76	11.05	37.64	3.42	1.13	3.96	0.46	0.05	0.04	4.73	0.01	0.00	0.01	0.01	0.05			0.27	34.65
HY-43-16-1	0.01	0.44	6.24	29.40	16.14	0.53	6.83	0.16	0.04	0.03	3.69	0.01	0.00	0.01	0.01	0.05			0.11	36.30
HY-43-16-2	0.01	1.85	6.50	27.46	15.94	0.54	6.60	0.28	0.06	0.03	3.84	0.02	0.00	0.01	0.00	0.05			0.00	36.82
HY-43-21-1	0.01	1.61	8.44	39.90	16.14	1.01	7.80	0.29	0.04	0.03	2.72	0.03	0.00	0.00	0.00	0.06			0.02	21.90
HY-43-21-2	0.01	2.01	8.65	40.10	14.76	1.17	6.92	0.36	0.04	0.04	2.89	0.03	0.00	0.00	0.00	0.05			0.10	22.86
HY-43-23	0.01	1.52	8.06	36.27	17.29	0.97	8.18	0.29	0.03	0.02	1.97	0.02	0.00	0.01	0.00	0.05			0.01	25.28
HY-43-23-1	0.31	2.00	7.12	38.42	17.56	0.84	7.60	0.25	0.03	0.02	1.72	0.01	0.00	0.01	0.00	0.05			0.08	23.97

Samples	Na_2O	MgO	Al_2O_3	SiO_2	P_2O_5	K_2O	CaO	TiO_2	V_2O_5	MnO	Fe_2O_3	CoO	NiO	CuO	ZnO	SrO	SnO_2	Sb_2O_5	BaO	PbO
HY-43-23-2	1.67	3.69	6.75	34.66	18.35	0.73	7.33	0.31	0.03	0.02	1.43	0.01	0.00	0.01	0.00	0.05				24.96
HY-43-26-1	0.01	2.51	5.99	32.58	17.97	0.72	10.16	0.26	0.04	0.01	1.60	0.02	0.00	0.01	0.00	0.06			0.00	28.05
HY-43-26-2	0.01	1.45	5.92	36.93	18.47	0.66	7.67	0.25	0.05	0.02	1.71	0.01	0.00	0.01	0.01	0.05			0.07	26.68
HY-43-27-1	0.01	0.94	7.15	38.65	16.96	0.80	8.01	0.20	0.08	0.02	1.56	0.01	0.00	0.01	0.00	0.05			0.20	25.37
HY-43-27-2	0.34	2.50	7.70	37.19	16.20	1.04	7.59	0.27	0.03	0.03	2.11	0.01	0.00	0.01	0.00	0.05			0.00	24.92
HY-43-31-1	0.51	1.55	6.12	28.74	22.21	0.79	8.21	0.34	0.05	0.02	1.81	0.01	0.00	0.02	0.01	0.06			0.03	29.52
HY-43-31-2	0.01	3.96	8.02	34.54	17.16	1.09	8.38	0.42	0.04	0.03	2.27	0.02	0.00	0.01	0.01	0.05			0.01	23.99
HY-58-2-1	2.68	0.85	3.66	40.53	4.07	0.28	3.47	0.17	0.06	0.03	4.38	0.03	0.00	0.00	0.01	0.06	0.93	0.02	0.59	38.19
HY-58-2-2	1.62	1.94	4.85	38.67	0.65	0.45	3.52	0.26	0.03	0.03	5.89	0.02	0.00	0.01	0.01	0.06	1.03	0.01	0.34	40.61
HY-58-4-1	0.01	2.47	4.91	31.48	8.79	0.43	4.77	0.21	0.06	0.03	4.41	0.02	0.00	0.01	0.01	0.06	1.28	0.25	0.58	40.23
HY-58-4-2	0.96	1.48	5.46	28.32	12.94	0.60	5.76	0.21	0.09	0.05	5.12	0.01	0.00	0.01	0.01	0.06	1.08	0.01	0.72	37.13
HY-58-6-1	1.58	0.42	4.85	36.33	0.65	0.61	3.69	0.15	0.02	0.03	5.61	0.02	0.00	0.00	0.01	0.08	1.12	0.01	0.98	43.83
HY-58-6-2	1.37	2.94	5.66	31.62	2.63	0.48	3.87	0.20	0.04	0.03	5.29	0.01	0.00	0.00	0.01	0.06	1.27	0.73	0.40	43.40

Samples	Na_2O	MgO	Al_2O_3	SiO_2	P_2O_5	K_2O	CaO	TiO_2	V_2O_5	MnO	Fe_2O_3	CoO	NiO	CuO	ZnO	SrO	SnO_2	Sb_2O_5	BaO	PbO
HY-58-9-1	0.01	2.85	5.16	41.21	8.55	0.56	4.72	0.26	0.05	0.04	4.66	0.02	0.00	0.01	0.00	0.06			0.11	31.72
HY-58-9-2	0.01	3.03	6.25	27.06	18.67	0.79	6.92	0.36	0.11	0.03	3.31	0.03	0.00	0.01	0.00	0.08			0.05	33.30
HY-58-10-1	0.01	5.09	5.67	25.96	19.87	0.51	7.33	0.22	0.12	0.04	3.19	0.02	0.00	0.00	0.00	0.08			0.05	31.82
HY-58-10-2	0.01	6.36	6.15	23.22	18.40	0.97	8.90	0.26	0.13	0.04	3.90	0.03	0.00	0.00	0.00	0.08			0.06	31.49
HY-58-11-1	0.01	2.29	4.67	40.24	7.41	0.58	4.76	0.21	0.06	0.03	4.32	0.02	0.00	0.00	0.01	0.05			0.10	35.24
HY-58-11-2	0.01	1.26	4.95	32.32	14.51	0.45	5.71	0.22	0.07	0.03	3.93	0.00	0.00	0.00	0.00	0.06			0.08	36.38
HY-58-13-1	0.01	3.84	6.93	34.87	11.66	1.09	7.80	0.26	0.09	0.05	4.48	0.03	0.00	0.01	0.00	0.07			0.05	28.77
HY-58-13-2	0.01	3.45	7.28	34.12	12.00	1.14	8.03	0.32	0.08	0.04	4.72	0.03	0.00	0.00	0.00	0.06			0.01	28.70
HY-58-13-3	0.01	3.19	8.52	37.31	11.59	1.58	8.52	0.41	0.09	0.04	3.72	0.02	0.00	0.01	0.00	0.07			0.06	24.88
HY-58-13-4	0.01	2.86	6.75	31.38	14.55	0.99	7.87	0.32	0.10	0.04	4.58	0.02	0.00	0.00	0.01	0.07				30.46
HY-58-13-5	0.01	3.23	6.21	35.37	8.12	0.70	5.92	0.22	0.05	0.05	5.54	0.02	0.00	0.00	0.00	0.06			0.06	34.43
HY-58-13-6	0.01	2.10	5.10	34.20	7.56	0.54	7.33	0.30	0.05	0.04	7.01	0.02	0.00	0.00	0.00	0.08			0.03	35.62
HY-58-15-1	0.26	1.51	6.49	28.79	11.52	0.71	6.16	0.24	0.08	0.06	5.59	0.02	0.00	0.01	0.00	0.06			0.07	38.43

Samples	Na_2O	MgO	Al_2O_3	SiO_2	P_2O_5	K_2O	CaO	TiO_2	V_2O_5	MnO	Fe_2O_3	CoO	NiO	CuO	ZnO	SrO	SnO_2	Sb_2O_5	BaO	PbO
HY-58-15-2	0.01	2.82	5.14	25.84	16.21	0.49	5.98	0.28	0.10	0.04	4.45	0.01	0.00	0.02	0.01	0.06			0.22	38.29
HY-58-18-1	0.02	4.52	6.55	30.79	10.80	0.76	7.62	0.32	0.08	0.03	5.20	0.02	0.00	0.00	0.00	0.07			0.00	33.20
HY-58-18-2	0.64	2.96	6.54	25.79	15.55	0.76	7.60	0.35	0.13	0.03	3.37	0.02	0.00	0.01	0.01	0.07			0.27	35.90
HY-58-19-1	1.40	4.38	4.55	22.29	20.99	0.54	7.23	0.27	0.15	0.04	4.22	0.02	0.00	0.01	0.00	0.09			0.16	33.67
HY-58-19-2	0.01	3.72	6.02	27.90	14.18	0.69	6.31	0.27	0.09	0.04	4.64	0.01	0.00	0.00	0.00	0.07			0.08	35.98
HY-58-20-1	0.01	3.37	7.33	33.63	16.75	0.94	7.64	0.42	0.12	0.03	1.82	0.01	0.00	0.01	0.00	0.07			0.10	27.75
HY-58-20-2	0.01	3.56	6.63	29.59	18.37	0.74	7.10	0.25	0.10	0.03	1.52	0.01	0.00	0.01	0.00	0.06			0.08	31.93
HY-58-21-1	0.01	0.82	6.89	34.56	11.87	1.15	6.79	0.41	0.09	0.05	5.22	0.02	0.00	0.01	0.00	0.07			0.15	31.88
HY-58-21-2	0.01	3.87	8.02	37.94	12.09	1.37	9.15	0.45	0.11	0.05	2.76	0.01	0.00	0.01	0.00	0.08			0.82	23.26
HY-58-23-1	0.01	3.84	7.20	35.70	9.33	1.03	6.07	0.32	0.08	0.04	4.31	0.00	0.00	0.01	0.00	0.07			0.21	31.77
HY-58-23-2	0.01	2.88	8.11	35.56	14.29	1.36	7.82	0.43	0.10	0.04	4.03	0.02	0.00	0.01	0.01	0.09			0.12	25.13
HY-58-25-1	0.01	2.34	7.87	32.93	14.08	1.30	7.99	0.38	0.11	0.04	3.54	0.02	0.00	0.01	0.00	0.08			0.04	29.27
HY-58-25-2	0.17	4.46	6.05	27.54	15.66	0.73	6.81	0.24	0.10	0.02	4.84	0.02	0.00	0.01	0.00	0.08				33.28

Samples	Na_2O	MgO	Al_2O_3	SiO_2	P_2O_5	K_2O	CaO	TiO_2	V_2O_5	MnO	Fe_2O_3	CoO	NiO	CuO	ZnO	SrO	SnO_2	Sb_2O_5	BaO	PbO
HY-58-26-1	0.01	2.99	6.66	29.04	17.58	0.85	6.89	0.29	0.10	0.03	3.08	0.01	0.00	0.01	0.00	0.06			0.05	32.34
HY-58-26-2	0.01	3.21	5.83	21.81	21.46	0.71	7.42	0.29	0.16	0.03	3.54	0.01	0.00	0.02	0.00	0.08			0.24	35.19
HY-59-1-1	3.44	2.77	4.31	17.33	23.30	0.33	7.12	0.20	0.14	0.02	3.40	0.02	0.00	0.00	0.00	0.08	0.98	0.08	0.40	36.09
HY-59-1-2	1.06	3.97	5.12	22.58	19.01	0.47	7.25	0.32	0.13	0.03	3.23	0.02	0.00	0.01	0.00	0.08	0.90	0.14	0.48	35.20
HY-59-1-3	0.98	4.02	5.40	22.90	18.64	0.49	7.49	0.31	0.13	0.03	3.22	0.02	0.00	0.00	0.00	0.08	0.96	0.01	0.48	34.85
HY-59-1-4	0.93	2.27	4.56	19.66	21.80	0.32	7.49	0.19	0.12	0.03	3.58	0.02	0.00	0.01	0.00	0.08	1.02		0.45	37.47
HY-59-4-1	2.25	1.46	5.60	19.64	18.58	0.43	7.72	0.23	0.14	0.03	3.37	0.02	0.00	0.01	0.00	0.08	1.09		0.58	38.77
HY-59-4-2	2.77	3.38	5.40	19.36	21.11	0.51	8.03	0.23	0.15	0.02	3.31	0.02	0.00	0.01	0.00	0.08	0.88		0.61	34.13
HY-59-5-1	0.01	0.20	4.99	37.39	4.58	0.40	4.20	0.24	0.05	0.04	6.25	0.02	0.00	0.01	0.01	0.07			0.14	41.43
HY-59-5-2	0.01	1.88	4.28	37.40	7.35	0.33	4.70	0.16	0.05	0.04	4.51	0.00	0.00	0.01	0.01	0.07			0.08	39.13
HY-59-6-1	1.67	2.65	5.85	33.19	10.21	0.47	5.58	0.22	0.05	0.03	5.20	0.02	0.00	0.00	0.00	0.07			0.06	34.73
HY-59-6-2	0.01	1.31	5.18	35.69	6.06	0.46	4.99	0.16	0.04	0.03	5.85	0.02	0.00	0.01	0.01	0.09				40.09
HY-59-8-1	0.01	3.65	6.64	30.79	10.07	0.59	6.01	0.18	0.06	0.05	6.22	0.02	0.00	0.00	0.00	0.07				35.62

Samples	Na_2O	MgO	Al_2O_3	SiO_2	P_2O_5	K_2O	CaO	TiO_2	V_2O_5	MnO	Fe_2O_3	CoO	NiO	CuO	ZnO	SrO	SnO_2	Sb_2O_5	BaO	PbO
HY-59-8-2	0.01	4.16	5.56	26.67	15.75	0.46	7.13	0.24	0.11	0.03	3.66	0.02	0.00	0.00	0.00	0.07			0.15	35.96
HY-59-9-1	0.01	5.11	6.58	26.84	16.32	0.70	7.32	0.26	0.10	0.03	3.25	0.02	0.00	0.00	0.00	0.07			0.04	33.35
HY-59-9-2	0.01	0.84	5.20	30.18	18.20	0.47	6.37	0.24	0.10	0.03	4.55	0.02	0.00	0.00	0.00	0.07			0.09	33.62
HY-59-11-1	2.19	3.54	5.20	37.13	2.95	0.45	3.64	0.20	0.03	0.04	5.68	0.02	0.00	0.00	0.00	0.08			0.14	38.71
HY-59-11-2	0.44	1.55	4.86	43.18	3.11	0.47	3.44	0.14	0.03	0.04	6.33	0.02	0.00	0.01	0.01	0.09			0.11	36.19
HY-61-1-1	0.01	0.17	3.14	11.09	45.34	0.35	17.66	0.13	0.01	0.02	1.54	0.01	0.00	0.02	0.04	0.04			0.00	20.43
HY-61-1-2	0.01	0.27	3.43	13.81	38.47	0.23	9.19	0.07	0.02	0.02	2.54	0.02	0.00	0.05	0.03	0.04			0.03	31.78
HY-61-1-3	1.57	2.74	4.29	13.78	33.93	0.24	7.89	0.08	0.02	0.01	1.24	0.01	0.00	0.03	0.03	0.04			0.03	34.08
HY-61-2-1	0.01	0.39	3.50	11.22	40.66	0.24	10.57	0.08	0.02	0.02	2.28	0.02	0.00	0.03	0.05	0.04			0.01	30.84
HY-61-2-2	0.47	0.38	6.31	13.93	45.12	1.31	19.80	0.32	0.02	0.01	1.57	0.01	0.00	0.02	0.06	0.04			0.05	10.58
HY-61-2-3	0.12	1.34	2.89	15.87	50.56	0.24	11.37	0.16	0.03	0.05	1.51	0.01	0.00	0.02	0.08	0.07			0.02	15.65
HY-61-2-4	0.01	1.69	6.29	18.95	45.79	0.85	11.85	0.33	0.05	1.13	2.21	0.01	0.00	0.02	0.07	0.06			0.01	10.67
HY-61-3-1	0.39	2.05	4.06	15.11	41.17	0.94	19.47	0.15	0.02	0.02	1.87	0.01	0.00	0.01	0.05	0.05			0.01	14.62

Samples	Na_2O	MgO	Al_2O_3	SiO_2	P_2O_5	K_2O	CaO	TiO_2	V_2O_5	MnO	Fe_2O_3	CoO	NiO	CuO	ZnO	SrO	SnO_2	Sb_2O_5	BaO	PbO
HY-61-3-2	0.30	0.33	3.64	15.95	44.53	1.25	22.58	0.16	0.01	0.02	1.88	0.01	0.00	0.01	0.06	0.05				9.22
HY-61-6-1	0.01	2.30	8.45	22.57	36.20	1.37	10.95	0.29	0.03	0.03	1.62	0.01	0.00	0.08	0.08	0.06			0.02	15.92
HY-61-6-2	0.01	0.01	4.02	17.67	43.50	0.91	15.06	0.26	0.03	0.04	1.76	0.01	0.00	0.09	0.09	0.07			0.00	16.49
HY-62-1-1	0.01	1.88	4.35	13.20	52.45	0.42	14.46	0.19	0.03	0.03	1.59	0.00	0.00	0.02	0.08	0.06			0.10	11.15
HY-62-1-2	0.01	1.28	4.83	14.97	50.20	0.54	12.39	0.21	0.03	0.11	1.81	0.01	0.00	0.02	0.07	0.05			0.08	13.39
HY-64-1-1	0.99	2.42	6.67	26.04	20.07	0.72	6.98	0.23	0.11	0.02	3.26	0.02	0.00	0.00	0.00	0.10			0.09	32.27
HY-64-1-2	1.08	2.99	6.25	28.82	21.57	0.84	7.21	0.27	0.11	0.03	3.68	0.03	0.00	0.00	0.01	0.10			0.09	26.92
HY-64-2-1	0.98	1.53	5.50	24.57	23.10	0.68	7.36	0.26	0.10	0.03	3.32	0.02	0.00	0.00	0.00	0.09			0.07	32.38
HY-64-2-2	0.01	0.82	6.37	26.71	22.31	0.97	7.60	0.28	0.10	0.03	3.23	0.02	0.00	0.00	0.00	0.10			0.03	31.42
HY-64-3-1	0.01	1.21	3.43	24.67	26.76	0.30	6.19	0.22	0.15	0.02	4.33	0.03	0.00	0.00	0.00	0.11			0.03	32.54
HY-64-3-2	0.05	1.92	2.97	22.38	27.33	0.29	6.59	0.15	0.14	0.03	4.31	0.03	0.00	0.00	0.00	0.11			0.00	33.70
HY-64-4-1	0.01	0.53	2.84	27.34	27.10	0.30	7.30	0.15	0.08	0.02	4.63	0.04	0.00	0.00	0.01	0.11			0.04	29.49
HY-64-4-2	0.01	0.01	2.72	28.17	26.64	0.26	6.45	0.15	0.09	0.02	3.30	0.02	0.00	0.00	0.00	0.10			0.01	32.03

Samples	Na_2O	MgO	Al_2O_3	SiO_2	P_2O_5	K_2O	CaO	TiO_2	V_2O_5	MnO	Fe_2O_3	CoO	NiO	CuO	ZnO	SrO	SnO_2	Sb_2O_5	BaO	PbO
HY-64-5-1	0.01	1.90	6.13	33.38	18.89	0.68	6.97	0.23	0.08	0.03	3.20	0.02	0.00	0.00	0.00	0.09			0.07	28.33
HY-64-5-2	0.54	2.61	6.80	32.43	18.00	0.94	6.77	0.27	0.07	0.02	2.73	0.02	0.00	0.00	0.00	0.09			0.06	28.64
HY-64-6-1	0.19	1.46	5.04	29.34	21.39	0.55	6.62	0.22	0.11	0.02	3.19	0.01	0.00	0.00	0.00	0.10			0.00	31.75
HY-64-6-2	0.01	0.77	5.16	28.94	21.06	0.57	8.27	0.18	0.10	0.03	3.31	0.02	0.00	0.00	0.00	0.11			0.03	31.42
HY-64-7-1	0.01	0.01	3.34	29.69	23.36	0.27	5.72	0.12	0.11	0.03	4.24	0.03	0.00	0.00	0.00	0.10			0.07	32.89
HY-64-7-2	0.01	0.62	3.11	26.39	26.10	0.27	6.28	0.14	0.14	0.02	3.89	0.03	0.00	0.00	0.00	0.10			0.04	32.86
HY-64-8-1	0.40	0.17	5.21	29.45	21.43	0.73	7.08	0.32	0.09	0.03	3.39	0.03	0.00	0.00	0.01	0.11			0.05	31.51
HY-64-8-2	1.10	1.46	5.28	31.35	21.61	0.85	7.16	0.25	0.08	0.03	3.98	0.03	0.00	0.00	0.01	0.11			0.03	26.69
HY-92-1-1	0.01	2.52	1.95	10.03	38.94	0.11	9.90	0.10	0.05	0.02	1.84	0.02	0.00	0.01	0.01	0.09			0.07	34.35
HY-92-1-2	0.01	0.31	5.31	22.18	27.67	0.56	8.41	0.32	0.04	0.02	2.48	0.02	0.00	0.01	0.00	0.07			0.01	32.56
HY-92-2-1	0.01	0.16	3.69	13.65	33.12	0.32	10.10	0.38	0.05	0.02	2.73	0.02	0.00	0.01	0.00	0.09			0.13	35.51
HY-92-2-2	0.01	2.39	3.63	13.17	32.69	0.29	9.12	0.22	0.06	0.02	2.51	0.02	0.00	0.01	0.00	0.10			0.61	35.15
HY-92-2-3	0.01	0.01	2.57	12.04	33.53	0.20	11.17	0.24	0.06	0.02	3.11	0.01	0.00	0.01	0.00	0.09				36.92

Samples	Na_2O	MgO	Al_2O_3	SiO_2	P_2O_5	K_2O	CaO	TiO_2	V_2O_5	MnO	Fe_2O_3	CoO	NiO	CuO	ZnO	SrO	SnO_2	Sb_2O_5	BaO	PbO
HY-92-5-1	0.01	0.01	3.43	11.71	29.62	0.32	10.90	0.25	0.15	0.03	3.27	0.02	0.00	0.01	0.00	0.10			1.59	38.57
HY-92-5-2	1.29	1.11	5.06	25.26	18.97	0.69	6.66	0.28	0.05	0.03	4.44	0.02	0.00	0.01	0.01	0.08			0.15	35.87
HY-102-1-1	0.01	0.31	4.30	32.80	14.12	0.28	6.52	0.19	0.06	0.04	4.03	0.02	0.00	0.07	0.01	0.05			0.00	37.20
HY-102-1-2	0.01	0.89	2.71	36.90	11.36	0.05	4.96	0.08	0.03	0.04	4.09	0.00	0.00	0.06	0.01	0.06				38.77
HY-102-2-1	0.76	0.91	4.96	22.68	29.18	0.32	8.71	0.20	0.04	0.02	2.58	0.02	0.00	0.04	0.01	0.05			0.05	29.47
HY-102-2-2	0.01	1.36	4.52	22.44	31.03	0.23	7.68	0.17	0.04	0.03	3.05	0.01	0.00	0.05	0.01	0.05			0.03	29.28
HY-106-1-1	0.01	1.22	2.02	36.10	17.53	0.02	4.79	0.06	0.02	0.01	2.26	0.01	0.00	0.09	0.01	0.04			0.00	35.80
HY-106-1-2	0.02	0.02	2.21	29.00	15.26	0.00	4.57	0.09	0.03	0.02	2.73	0.00	0.00	0.11	0.01	0.06			0.05	45.83
HY-106-2-1	0.44	0.01	2.15	35.15	5.74	0.00	3.65	0.11	0.00	0.04	4.66	0.02	0.00	0.05	0.00	0.04			0.00	47.91
HY-106-2-2	0.02	0.27	1.60	39.15	3.05	0.00	2.55	0.10	0.02	0.03	3.92	0.02	0.00	0.04	0.00	0.04			0.04	49.15
HY-121-1-1	0.01	0.42	4.88	21.05	34.56	0.52	9.00	0.35	0.10	0.03	3.83	0.04	0.00	0.01	0.01	0.12			0.13	24.94
HY-121-1-2	0.01	0.97	3.34	18.76	33.66	0.31	7.92	0.23	0.09	0.03	4.01	0.03	0.00	0.00	0.00	0.12			0.12	30.38
HY-123-1-1	0.01	0.47	3.27	23.59	27.38	0.18	6.24	0.11	0.13	0.02	4.63	0.04	0.00	0.04	0.00	0.10			0.03	33.75

Samples	Na_2O	MgO	Al_2O_3	SiO_2	P_2O_5	K_2O	CaO	TiO_2	V_2O_5	MnO	Fe_2O_3	CoO	NiO	CuO	ZnO	SrO	SnO_2	Sb_2O_5	BaO	PbO
HY-123-1-2	1.32	0.01	2.67	27.30	24.91	0.26	5.79	0.15	0.11	0.03	5.18	0.03	0.00	0.04	0.00	0.10			0.01	32.09
HY-123-2-1	0.02	1.43	2.83	18.74	31.80	0.16	6.71	0.13	0.09	0.02	4.55	0.03	0.00	0.04	0.00	0.11				33.34
HY-123-2-2	0.29	0.26	3.10	20.26	29.06	0.27	7.14	0.20	0.08	0.02	5.38	0.04	0.00	0.05	0.00	0.13			0.01	33.70
HY-123-3	0.01	0.90	5.60	27.90	22.09	0.66	7.12	0.34	0.08	0.03	3.45	0.02	0.00	0.01	0.00	0.08			0.09	31.63
HY-123-3-1	0.02	0.02	1.60	42.18	14.06	0.10	3.35	0.04	0.02	0.01	4.71	0.03	0.00	0.00	0.00	0.07			0.33	33.46
HY-123-3-2	0.01	1.24	3.05	31.01	19.62	0.25	5.12	0.10	0.04	0.05	5.42	0.03	0.00	0.01	0.00	0.09			0.14	33.82
HY-123-4-1	0.02	0.45	3.27	22.64	27.49	0.34	7.28	0.13	0.08	0.02	6.48	0.03	0.00	0.04	0.01	0.12			0.10	31.49
HY-123-4-2	0.01	0.28	3.97	20.74	30.05	0.41	7.54	0.15	0.10	0.03	4.24	0.03	0.00	0.03	0.00	0.12			0.10	32.21
HY-123-1-1	0.01	0.34	6.12	29.88	19.01	0.92	7.22	0.28	0.07	0.03	1.92	0.01	0.00	0.11	0.01	0.09			0.14	33.85
HY-123-1-2	0.01	1.05	6.07	33.25	18.19	0.79	6.74	0.36	0.07	0.03	1.90	0.01	0.00	0.15	0.00	0.10			0.14	31.14
HY-123-4-1	0.01	0.01	4.32	22.65	26.48	0.52	7.43	0.22	0.09	0.02	1.31	0.01	0.00	0.04	0.00	0.11			0.29	36.49
HY-123-4-2	1.38	0.91	5.51	28.95	20.82	0.91	7.73	0.35	0.07	0.03	2.08	0.01	0.00	0.05	0.00	0.10			0.07	31.02
HY-123-6-1	0.01	2.86	8.00	37.61	15.18	1.45	7.62	0.37	0.06	0.02	2.47	0.01	0.00	0.04	0.01	0.09			0.05	24.16

Samples	Na_2O	MgO	Al_2O_3	SiO_2	P_2O_5	K_2O	CaO	TiO_2	V_2O_5	MnO	Fe_2O_3	CoO	NiO	CuO	ZnO	SrO	SnO_2	Sb_2O_5	BaO	PbO
HY-123-6-2	0.01	0.26	5.46	29.86	23.22	0.68	7.40	0.27	0.09	0.02	1.17	0.01	0.00	0.05	0.01	0.10			0.09	31.29
HY-125-1-1	0.09	0.81	5.31	18.70	26.90	0.36	9.32	0.24	0.13	0.04	4.48	0.02	0.00	0.01	0.00	0.09			0.06	33.44
HY-125-1-2	0.01	1.35	4.18	17.86	27.67	0.36	8.82	0.29	0.14	0.03	4.22	0.02	0.00	0.01	0.00	0.08			0.08	34.87
HY-129-1-1	0.01	0.70	8.01	27.58	23.17	0.62	8.06	0.25	0.11	0.03	3.79	0.02	0.00	0.00	0.01	0.08			0.05	27.51
HY-129-1-2	0.19	0.01	4.83	24.52	17.91	0.20	5.55	0.15	0.10	0.02	3.87	0.00	0.00	0.01	0.00	0.07			0.01	42.55
HY-130-1-1	0.01	1.45	14.26	46.84	0.73	1.63	5.11	0.44	0.03	0.04	4.81	0.00	0.00	0.00	0.01	0.04				24.61
HY-130-1-2	0.01	1.14	11.66	44.35	0.09	1.07	4.03	0.29	0.03	0.04	4.50	0.01	0.00	0.00	0.01	0.06			0.08	32.63
HY-131-1-1	0.01	2.06	2.45	20.22	27.92	0.11	18.28	0.09	0.02	0.03	3.52	0.02	0.00	0.02	0.01	0.06				25.19
HY-131-1-2	0.01	0.01	3.23	17.86	29.54	0.13	17.43	0.08	0.02	0.04	3.72	0.02	0.00	0.02	0.00	0.05			0.04	27.80
HY-132-2-1	0.13	0.49	5.73	16.87	36.24	0.26	14.54	0.19	0.03	0.03	3.06	0.03	0.00	0.07	0.00	0.05			0.22	22.06
HY-132-2-2	0.51	1.40	6.01	22.79	30.15	0.42	13.91	0.21	0.04	0.06	3.51	0.03	0.00	0.08	0.00	0.05			0.08	20.77
HY-132-2-1	0.01	3.21	5.59	18.49	35.25	0.29	10.27	0.20	0.04	0.04	3.46	0.03	0.00	0.11	0.01	0.04			0.45	22.52
HY-132-2-2	0.01	0.01	5.84	19.71	36.74	0.37	9.88	0.21	0.04	0.05	3.88	0.03	0.00	0.12	0.01	0.04			0.14	22.92

Samples	Na_2O	MgO	Al_2O_3	SiO_2	P_2O_5	K_2O	CaO	TiO_2	V_2O_5	MnO	Fe_2O_3	CoO	NiO	CuO	ZnO	SrO	SnO_2	Sb_2O_5	BaO	PbO
HY-132-4-1	0.01	1.66	8.13	21.63	31.49	0.41	11.25	0.19	0.04	0.03	2.58	0.02	0.00	0.09	0.00	0.04			0.99	21.45
HY-132-4-2	0.07	0.58	9.53	24.78	28.67	0.58	11.21	0.24	0.03	0.05	3.28	0.03	0.00	0.03	0.00	0.04			0.13	20.76
HY-132-6-1	0.79	2.09	6.11	25.17	25.90	0.41	8.20	0.21	0.05	0.03	3.90	0.03	0.00	0.05	0.00	0.03			0.73	26.28
HY-132-6-2	1.05	1.31	6.33	19.18	31.67	0.43	10.05	0.24	0.11	0.03	2.78	0.03	0.00	0.07	0.00	0.05			3.51	23.17
HY-135-1-1	0.60	1.80	4.49	22.48	32.37	0.30	10.05	0.12	0.09	0.02	2.70	0.03	0.00	0.05	0.01	0.03			0.07	24.80
HY-135-1-2	0.76	0.84	2.58	23.50	33.79	0.03	8.60	0.07	0.13	0.02	2.32	0.02	0.00	0.05	0.01	0.03			0.08	27.15
HY-136-1-1	0.79	0.84	3.49	18.73	34.88	0.05	11.01	0.11	0.13	0.02	2.60	0.02	0.00	0.06	0.00	0.03			0.01	27.22
HY-136-1-2	0.01	0.33	3.61	19.94	34.30	0.11	12.01	0.07	0.13	0.02	2.56	0.03	0.00	0.06	0.01	0.03			0.06	26.72
HY-145-1-1	0.02	0.53	5.30	28.61	22.25	0.43	9.30	0.24	0.07	0.05	2.98	0.00	0.00	0.03	0.01	0.07				30.11
HY-145-1-2	0.01	0.20	3.90	28.05	23.51	0.22	9.52	0.21	0.07	0.04	6.10	0.03	0.00	0.03	0.00	0.06			0.11	27.93
HY-145-1-3	0.01	0.20	3.90	28.05	23.51	0.22	9.52	0.21	0.07	0.04	6.10	0.03	0.00	0.03	0.00	0.06			0.11	27.93
HY-148-1-1	0.02	0.01	3.60	11.70	44.31	0.04	9.17	0.09	0.03	0.02	2.12	0.02	0.00	0.01	0.00	0.05			0.10	28.71
HY-148-1-2	0.02	4.22	3.75	10.84	41.91	0.08	7.92	0.10	0.03	0.02	1.54	0.01	0.00	0.01	0.00	0.04			0.13	29.39

Samples	Na_2O	MgO	Al_2O_3	SiO_2	P_2O_5	K_2O	CaO	TiO_2	V_2O_5	MnO	Fe_2O_3	CoO	NiO	CuO	ZnO	SrO	SnO_2	Sb_2O_5	BaO	PbO
HY-150-1-1	2.82	1.86	4.23	23.77	27.79	0.18	6.41	0.14	0.23	0.03	3.90	0.02	0.00	0.00	0.01	0.05			0.08	28.50
HY-150-1-2	0.01	1.19	4.13	23.91	29.91	0.24	6.84	0.18	0.24	0.02	3.54	0.02	0.00	0.00	0.00	0.04			0.05	29.68
HY-150-3-1	0.01	0.03	5.80	37.75	26.65	0.33	7.62	0.15	0.13	0.04	3.97	0.03	0.00	0.01	0.02	0.05			0.08	17.34
HY-150-3-2	0.01	0.61	6.88	38.87	22.75	0.47	8.61	0.31	0.11	0.04	3.62	0.02	0.00	0.01	0.00	0.04			0.02	17.64
HY-150-5-1	0.01	2.56	9.80	43.13	15.58	1.38	8.63	0.46	0.05	0.04	2.25	0.01	0.00	0.01	0.01	0.04				16.04
HY-150-5-2	0.57	1.48	8.86	44.49	16.94	1.05	8.08	0.38	0.06	0.03	1.91	0.01	0.00	0.01	0.00	0.04			0.02	16.07
HY-150-6-1	0.01	1.12	6.63	31.30	28.21	0.13	7.24	0.23	0.17	0.01	2.98	0.01	0.00	0.01	0.00	0.05			0.02	21.88
HY-150-6-2	0.09	0.01	6.44	38.10	25.83	0.49	6.01	0.29	0.14	0.02	3.14	0.01	0.00	0.00	0.00	0.04			0.04	19.34
HY-150-8-1	0.01	0.77	7.75	40.45	18.59	1.00	7.72	0.48	0.15	0.05	3.15	0.01	0.00	0.01	0.00	0.04			0.07	19.75
HY-150-8-2	0.01	1.95	5.84	36.18	20.32	0.40	6.65	0.27	0.13	0.03	4.38	0.01	0.00	0.01	0.01	0.04			0.07	23.70
HY-150-10-1	0.01	1.25	7.52	40.88	19.50	0.99	7.93	0.44	0.11	0.05	1.99	0.02	0.00	0.01	0.00	0.04			0.10	19.17
HY-150-10-2	0.24	0.44	7.15	38.55	22.27	0.72	7.61	0.30	0.14	0.03	1.79	0.02	0.00	0.01	0.01	0.04			0.16	20.52
HY-150-11-1	0.01	0.67	6.19	35.03	26.18	0.31	8.55	0.32	0.14	0.03	1.48	0.01	0.00	0.09	0.01	0.05			0.17	20.76

Samples	Na_2O	MgO	Al_2O_3	SiO_2	P_2O_5	K_2O	CaO	TiO_2	V_2O_5	MnO	Fe_2O_3	CoO	NiO	CuO	ZnO	SrO	SnO_2	Sb_2O_5	BaO	PbO
HY-150-11-2	0.01	1.80	5.51	36.48	26.93	0.20	8.41	0.19	0.12	0.02	1.18	0.02	0.00	0.10	0.01	0.05			0.14	18.82
HY-150-12-1	0.08	0.01	5.07	28.84	30.53	0.28	7.10	0.16	0.13	0.02	3.34	0.02	0.00	0.00	0.02	0.04			0.18	24.16
HY-150-12-2	0.27	1.56	3.80	30.87	29.33	0.04	5.81	0.15	0.08	0.02	3.80	0.03	0.00	0.00	0.01	0.04			0.04	24.15
HY-151-1-1	3.52	1.50	4.87	21.32	26.36	0.00	7.95	0.29	0.08	0.07	5.09	0.02	0.00	0.01	0.00	0.06				28.86
HY-151-1-2	0.02	0.02	5.77	22.97	24.43	0.00	6.52	0.22	0.07	0.05	7.04	0.02	0.00	0.02	0.01	0.07			0.14	32.64
HY-152-1-1	0.03	0.03	1.77	8.28	7.63	0.00	4.36	0.04	0.03	0.05	2.27	0.03	0.01	0.15	0.02	0.08			0.77	74.46
HY-152-1-2	0.03	1.50	2.41	5.02	11.84	0.00	5.38	0.05	0.07	0.04	3.12	0.02	0.01	0.18	0.01	0.08			0.54	69.71
HY-152-1-3	0.85	0.63	1.97	5.60	16.49	0.00	9.76	0.06	0.06	0.02	4.78	0.00	0.00	0.33	0.01	0.07			0.34	59.03
HY-152-2-1	0.01	2.40	7.41	29.57	26.56	1.22	7.10	0.59	0.05	0.03	3.65	0.02	0.00	0.10	0.00	0.04			0.07	21.19
HY-152-2-2	0.01	0.01	5.44	26.27	30.86	0.83	7.41	0.34	0.05	0.02	3.78	0.01	0.00	0.09	0.00	0.04			0.07	24.73
HY-166-1-1	0.02	0.01	10.13	40.43	13.59	1.04	6.55	0.40	0.10	0.04	4.52	0.01	0.00	0.03	0.00	0.06			0.13	22.92
HY-166-1-2	0.02	0.51	9.81	42.02	8.38	1.15	6.22	0.43	0.07	0.05	3.94	0.01	0.00	0.03	0.01	0.05			0.06	27.25
HY-172-1	2.05	1.20	2.51	43.11	7.87	0.01	3.37	0.05	0.06	0.03	4.56	0.03	0.00	0.01	0.01	0.05	0.65	0.04	0.53	33.86

Samples	Na_2O	MgO	Al_2O_3	SiO_2	P_2O_5	K_2O	CaO	TiO_2	V_2O_5	MnO	Fe_2O_3	CoO	NiO	CuO	ZnO	SrO	SnO_2	Sb_2O_5	BaO	PbO
HY-172-2	1.32	0.63	1.28	48.26	9.02	0.00	4.01	0.04	0.06	0.04	5.22	0.04	0.00	0.00	0.02	0.04	0.40		0.50	29.10
HY-172-3	0.51	1.60	4.73	25.26	25.40	0.19	6.57	0.11	0.12	0.03	3.22	0.04	0.00	0.00	0.00	0.06	0.51	0.27	0.39	31.01
HY-172-4	1.24	0.18	1.34	48.15	4.20	0.00	2.40	0.02	0.01	0.03	4.29	0.02	0.00	0.00	0.02	0.04	0.61	0.07	0.65	36.71
HY-173	0.22	1.83	2.29	24.49	31.28	0.05	6.68	0.08	0.05	0.02	3.32	0.03	0.00	0.01	0.00	0.06	0.42	0.07	0.44	28.67
HY-174-1	2.16	0.25	1.73	43.76	9.38	0.02	7.04	0.08	0.06	0.03	4.59	0.03	0.00	0.01	0.01	0.04	0.50		0.36	29.96
HY-174-2	3.34	1.16	4.72	23.16	24.78	0.37	7.00	0.16	0.15	0.03	2.99	0.03	0.00	0.00	0.00	0.06	0.63	0.01	0.42	30.98
HY-174-3	1.36	0.44	6.12	33.60	23.78	0.37	6.39	0.14	0.16	0.03	3.88	0.04	0.00	0.00	0.01	0.07	0.17	0.02	0.56	22.87
HY-174-4	0.60	2.36	6.09	29.00	23.29	0.52	7.65	0.23	0.06	0.03	2.67	0.03	0.00	0.00	0.00	0.06	0.51	0.18	0.51	26.22
HY-175-1	2.66	1.93	4.15	34.42	13.19	0.17	5.40	0.07	0.11	0.04	4.58	0.02	0.00	0.00	0.01	0.05	0.60	0.03	0.72	31.84
HY-175-2	2.41	3.02	9.57	39.23	6.52	0.92	6.96	0.21	0.10	0.04	3.57	0.01	0.00	0.00	0.01	0.04	0.35	0.04	0.17	26.83
HY-176-1	0.65	0.17	3.34	30.24	25.52	0.13	7.10	0.12	0.09	0.03	4.52	0.03	0.00	0.00	0.00	0.07	0.39		0.45	27.15
HY-176-2	0.01	0.52	1.44	33.45	30.89	0.07	7.72	0.06	0.06	0.02	4.19	0.04	0.00	0.01	0.01	0.05	0.17	0.08	0.21	21.00
HY-176-3	0.95	0.88	2.98	11.88	36.40	0.07	7.75	0.15	0.12	0.04	3.46	0.05	0.00	0.01	0.02	0.07	0.33	0.09	0.62	34.16

Samples	Na_2O	MgO	Al_2O_3	SiO_2	P_2O_5	K_2O	CaO	TiO_2	V_2O_5	MnO	Fe_2O_3	CoO	NiO	CuO	ZnO	SrO	SnO_2	Sb_2O_5	BaO	PbO
HY-177	2.19	0.52	3.81	37.33	15.21	0.09	7.59	0.10	0.20	0.03	4.86	0.03	0.00	0.01	0.01	0.04	0.36	0.14	0.32	27.17
HY-178	1.39	0.01	2.11	28.09	33.23	0.07	7.74	0.07	0.06	0.02	3.30	0.03	0.00	0.00	0.01	0.05	0.25	0.07	0.28	23.21
HY-179	0.73	1.71	4.21	28.00	30.00	0.24	7.44	0.12	0.10	0.02	3.41	0.03	0.00	0.00	0.00	0.05	0.30		0.27	23.33
HY-180	1.42	2.48	3.23	40.24	15.53	0.01	5.35	0.09	0.13	0.03	4.14	0.03	0.00	0.00	0.01	0.04	0.34	0.17	0.41	26.38
HY-181	4.44	1.66	2.12	32.50	20.46	0.03	10.03	0.09	0.25	0.03	4.75	0.04	0.00	0.00	0.01	0.05	0.20	0.02	0.37	22.98
HY-182-1	2.19	2.57	8.90	35.75	14.54	0.64	8.90	0.23	0.17	0.03	3.07	0.02	0.00	0.00	0.01	0.04	0.24	0.01	0.20	22.50
HY-182-2	3.13	2.79	4.85	40.99	7.93	0.09	7.06	0.15	0.06	0.02	4.29	0.02	0.00	0.00	0.01	0.04	0.43	0.00	0.37	27.79
HY-182-3	0.92	1.09	2.30	39.31	22.98	0.04	5.70	0.08	0.30	0.03	3.57	0.03	0.00	0.00	0.01	0.05	0.26	0.06	0.38	22.90
HY-182-4	0.02	0.97	7.21	40.86	14.22	0.18	4.62	0.10	0.09	0.01	3.61	0.02	0.00	0.00	0.01	0.04	0.28		0.37	27.38
HY-183	3.34	2.21	3.90	30.28	27.14	0.13	6.40	0.10	0.13	0.02	2.95	0.03	0.00	0.00	0.00	0.04	0.25		0.21	22.84
HY-184-1	0.51	1.09	3.22	36.15	24.74	0.17	6.63	0.10	0.10	0.04	4.77	0.04	0.00	0.00	0.01	0.05	0.21		0.29	21.88
HY-184-2	0.34	0.51	5.19	29.46	30.19	0.30	7.65	0.13	0.06	0.02	2.93	0.03	0.00	0.00	0.01	0.06	0.22		0.34	22.56
HY-185	0.06	1.45	5.11	30.19	27.61	0.33	7.95	0.15	0.11	0.03	3.66	0.03	0.00	0.00	0.00	0.06	0.26		0.22	22.78

Samples	Na_2O	MgO	Al_2O_3	SiO_2	P_2O_5	K_2O	CaO	TiO_2	V_2O_5	MnO	Fe_2O_3	CoO	NiO	CuO	ZnO	SrO	SnO_2	Sb_2O_5	BaO	PbO
HY-186-1-1	0.40	1.28	4.20	29.66	29.78	0.36	8.34	0.21	0.06	0.03	5.63	0.04	0.00	0.01				0.34	0.17	19.49
HY-186-1-2	0.12	2.70	3.76	31.57	27.84	0.34	8.18	0.17	0.06	0.04	5.03	0.03	0.00	0.01				0.29	0.07	19.79
HY-187-1-1	0.01	0.01	4.42	23.67	35.86	0.29	9.10	0.24	0.07	0.04	4.56	0.03	0.00	0.01				0.26	0.14	21.28
HY-187-1-2	1.19	1.38	4.03	25.17	33.55	0.26	8.65	0.14	0.07	0.04	4.13	0.03	0.00	0.01				0.37	0.15	20.85
Mean values	0.58	1.50	5.25	27.91	21.95	0.50	8.09	0.23	0.08	0.04	3.44	0.02	0.00	0.02	0.01	0.06	0.16	0.02	0.21	29.94

Appendix 10 Chemical compositions of green glazes

Samples	Na_2O	MgO	Al_2O_3	SiO_2	P_2O_5	K_2O	CaO	TiO_2	V_2O_5	MnO	Fe_2O_3	CoO	NiO	CuO	ZnO	SrO	SnO_2	Sb_2O_5	BaO	PbO
HY-38-3-1	1.64	1.90	4.73	24.38	24.67	0.27	9.44	0.20	0.07	0.15	0.80	0.01	0.00	0.27	0.00	0.05	0.71	0.01	0.65	30.05
HY-38-3-2	1.62	0.76	5.91	25.42	25.15	0.36	9.32	0.15	0.06	0.04	0.76	0.01	0.00	0.37	0.01	0.05	0.83	0.26	0.51	28.43
HY-38-10-1	0.01	0.34	2.88	20.27	32.58	0.10	11.37	0.09	0.06	0.02	0.48	0.01	0.00	0.44	0.00	0.05			0.04	31.24
HY-38-10-2	0.01	0.34	2.60	22.02	33.22	0.04	9.85	0.08	0.04	0.01	0.38	0.01	0.00	0.36	0.00	0.05			0.10	30.90
HY-38-10-3	0.84	0.70	2.77	23.50	29.96	0.11	11.49	0.13	0.04	0.03	0.49	0.01	0.00	0.30	0.00	0.05			0.02	29.54
HY-38-11-1	0.01	1.75	3.38	16.59	29.63	0.18	16.85	0.18	0.04	0.02	0.59	0.01	0.00	0.14	0.00	0.06			0.03	30.53
HY-38-11-2	0.89	2.01	3.49	19.88	29.47	0.20	13.86	0.17	0.02	0.01	0.55	0.01	0.00	0.11	0.01	0.06			0.02	29.23
HY-38-11-3	0.14	0.03	4.74	20.19	28.65	0.28	15.94	0.22	0.04	0.03	0.64	0.01	0.00	0.11	0.00	0.05			0.10	28.82
HY-38-19-1	0.52	1.11	4.12	20.72	30.15	0.17	11.06	0.19	0.04	0.03	0.80	0.01	0.00	0.27	0.00	0.06			0.00	30.74
HY-38-19-2	0.01	2.22	3.01	14.19	33.90	0.07	12.69	0.15	0.06	0.03	0.54	0.01	0.00	0.30	0.01	0.06			0.01	32.72
HY-38-19-3	0.54	1.54	3.58	19.23	30.27	0.31	15.57	0.27	0.03	0.06	0.95	0.01	0.00	0.13	0.01	0.06			0.01	27.44
HY-102-1-1	0.02	0.48	4.52	20.90	19.06	0.23	14.30	0.20	0.06	0.03	3.27	0.04	0.00	1.01	0.02	0.05			0.02	35.79

Samples	Na_2O	MgO	Al_2O_3	SiO_2	P_2O_5	K_2O	CaO	TiO_2	V_2O_5	MnO	Fe_2O_3	CoO	NiO	CuO	ZnO	SrO	SnO_2	Sb_2O_5	BaO	PbO
HY-102-1-2	0.01	0.02	4.15	25.80	24.32	0.23	9.22	0.14	0.09	0.03	3.59	0.02	0.00	0.60	0.02	0.05			0.09	31.62
HY-102-2-1	0.06	0.97	4.42	22.84	28.92	0.37	8.21	0.22	0.06	0.03	1.56	0.01	0.00	1.10	0.03	0.05			0.09	31.04
HY-102-2-2	0.83	0.78	6.03	26.88	26.01	0.52	8.66	0.31	0.05	0.02	1.72	0.01	0.00	0.46	0.03	0.05			0.05	27.58
HY-106-1-1	0.02	0.02	4.10	16.64	31.58	0.09	8.05	0.17	0.05	0.01	0.84	0.02	0.00	0.27	0.04	0.04			0.09	37.97
HY-106-1-2	0.02	0.16	3.65	16.47	31.11	0.09	7.92	0.16	0.05	0.02	0.70	0.01	0.00	0.26	0.02	0.04			0.03	39.30
HY-106-2-1	1.75	2.03	1.76	20.76	29.09	0.00	8.17	0.10	0.03	0.02	0.42	0.01	0.00	0.24	0.04	0.04			0.00	35.56
HY-106-2-2	0.01	1.63	0.47	24.85	27.72	0.00	6.79	0.04	0.02	0.02	0.33	0.01	0.00	0.26	0.04	0.04			0.00	37.77
HY-106-3-1	0.02	0.02	0.36	22.09	23.20	0.00	6.94	0.06	0.02	0.02	0.37	0.01	0.00	0.96	0.06	0.05			0.05	45.77
HY-106-3-2	0.02	0.49	1.27	21.92	26.48	0.00	7.91	0.08	0.02	0.02	0.40	0.01	0.00	0.58	0.04	0.04			0.02	40.72
HY-127-1	0.01	2.90	11.58	64.73	0.00	1.22	1.88	0.62	0.02	0.05	2.25	0.01	0.00	5.96	0.13	0.02			0.00	8.61
HY-127-2	0.34	4.22	13.66	62.90	0.00	1.74	1.70	0.70	0.04	0.06	2.28	0.01	0.00	4.39	0.09	0.02			0.00	7.85
HY-132-1-1	0.20	0.25	3.42	16.48	32.19	0.08	12.12	0.11	0.06	0.01	1.00	0.01	0.00	0.52	0.01	0.06			0.09	33.40
HY-132-1-2	0.01	1.24	4.94	16.87	27.70	0.20	13.50	0.19	0.09	0.02	0.79	0.01	0.00	0.48	0.01	0.07			1.76	32.12

Samples	Na_2O	MgO	Al_2O_3	SiO_2	P_2O_5	K_2O	CaO	TiO_2	V_2O_5	MnO	Fe_2O_3	CoO	NiO	CuO	ZnO	SrO	SnO_2	Sb_2O_5	BaO	PbO
HY-132-5-1	0.01	0.21	3.48	16.82	37.66	0.12	15.03	0.09	0.04	0.03	0.61	0.01	0.00	0.55	0.01	0.04			0.02	25.26
HY-132-5-2	0.12	0.01	6.26	23.02	32.85	0.27	12.38	0.15	0.05	0.02	0.76	0.02	0.00	0.50	0.01	0.04			0.07	23.48
HY-132-7-1	0.01	1.03	3.05	20.87	38.63	0.04	10.18	0.09	0.03	0.02	0.65	0.02	0.00	0.36	0.01	0.04			0.10	24.86
HY-132-7-2	0.01	0.69	2.76	21.21	39.28	0.02	9.98	0.16	0.03	0.02	0.70	0.01	0.00	0.33	0.01	0.04			0.02	24.73
HY-136-1-1	0.01	0.66	2.73	35.16	21.46	0.11	5.72	0.08	0.14	0.04	0.94	0.01	0.00	1.94	0.03	0.03			0.05	30.87
HY-136-1-2	0.01	1.30	2.37	37.99	20.32	0.16	5.51	0.08	0.16	0.03	0.87	0.01	0.00	1.86	0.04	0.03			0.03	29.24
HY-146-1-1	0.01	1.56	11.26	29.12	32.27	1.29	14.57	0.63	0.06	0.01	1.41	0.01	0.00	0.12	0.01	0.04			0.05	7.58
HY-146-1-2	0.01	0.34	7.64	19.81	32.97	0.56	19.90	0.29	0.03	0.01	0.58	0.00	0.01	0.09	0.01	0.05			0.12	17.57
HY-150-7-1	0.01	0.66	4.72	37.05	26.47	0.19	7.72	0.21	0.19	0.02	1.03	0.01	0.00	0.12	0.00	0.05			0.02	21.51
HY-150-7-2	1.14	1.81	5.63	35.97	25.81	0.22	7.54	0.20	0.23	0.02	1.26	0.01	0.00	0.10	0.01	0.05			0.16	19.85
HY-152-3-1	0.14	0.62	5.97	20.17	19.50	0.26	8.61	0.25	0.05	0.03	0.98	0.02	0.00	0.58	0.01	0.08			0.26	42.46
HY-152-3-2	0.08	0.07	4.00	9.99	21.35	0.00	10.22	0.09	0.05	0.03	0.68	0.02	0.02	1.33	0.02	0.11			0.18	51.78
HY-166-1-1	0.02	2.10	3.47	55.99	0.00	0.15	7.26	0.08	0.00	0.03	0.57	0.00	0.00	1.94	0.07	0.03			0.22	28.07

Samples	Na_2O	MgO	Al_2O_3	SiO_2	P_2O_5	K_2O	CaO	TiO_2	V_2O_5	MnO	Fe_2O_3	CoO	NiO	CuO	ZnO	SrO	SnO_2	Sb_2O_5	BaO	PbO
HY-166-1-2	0.02	0.01	3.91	57.37	0.00	0.22	6.35	0.04	0.01	0.02	0.51	0.00	0.00	2.31	0.02	0.03			0.10	29.06
Mean values	0.29	1.00	4.43	26.33	25.73	0.27	10.10	0.19	0.06	0.03	0.98	0.01	0.00	0.82	0.02	0.05	0.77	0.13	0.13	29.52

Appendix 11 Chemical compositions of blue glazes

Samples	Na_2O	MgO	Al_2O_3	SiO_2	P_2O_5	K_2O	CaO	TiO_2	V_2O_5	MnO	Fe_2O_3	CoO	NiO	CuO	ZnO	SrO	SnO_2	Sb_2O_5	BaO	PbO
HY-43-7-1	0.06	0.83	6.45	33.64	15.20	0.69	6.96	0.30	0.08	0.03	1.29	0.72	0.03	0.18	0.01	0.05	0.88	0.00	0.24	32.36
HY-43-7-2	0.17	0.94	4.73	34.09	14.46	0.46	5.93	0.26	0.05	0.02	1.25	0.43	0.02	0.10	0.00	0.05	0.98	0.23	0.42	35.40
HY-43-7-3	0.50	0.31	6.32	27.33	21.02	0.71	9.08	0.30	0.05	0.03	1.76	0.20	0.00	0.08	0.00	0.06	0.78	0.01	0.44	31.03
HY-43-7-4	3.18	0.66	3.73	40.00	6.90	0.36	3.33	0.08	0.04	0.02	0.78	0.52	0.02	0.09	0.00	0.05	1.05	0.01	0.98	38.21
HY-43-7-5	1.28	0.01	2.97	41.12	6.01	0.29	3.15	0.10	0.03	0.03	0.77	0.50	0.02	0.08	0.00	0.05	1.19	0.07	0.93	41.39
HY-43-10-1	1.11	0.25	3.62	40.35	5.10	0.38	3.08	0.06	0.03	0.03	0.97	0.71	0.02	0.13	0.00	0.07	1.00	0.01	0.34	42.76
HY-43-10-2	2.88	1.96	7.62	31.94	15.84	0.71	6.45	0.44	0.06	0.02	1.07	0.36	0.01	0.10	0.00	0.05	0.58	0.06	0.63	29.19
HY-43-10-3	1.01	0.67	7.78	36.37	10.56	0.50	4.16	0.23	0.07	0.02	0.76	0.45	0.01	0.11	0.01	0.06	0.89	0.00	0.63	35.70
HY-43-10-4	1.90	0.45	6.62	30.15	18.18	0.48	6.27	0.43	0.15	0.02	1.02	0.35	0.01	0.09	0.00	0.06	0.64	0.01	0.95	32.22
HY-43-11-1	1.23	0.01	2.76	41.12	9.07	0.20	2.62	0.05	0.03	0.03	0.49	0.58	0.02	0.08	0.00	0.05	0.99	0.15	0.87	39.63
HY-43-11-2	0.40	0.44	3.69	23.66	22.41	0.26	5.70	0.14	0.06	0.03	0.89	0.36	0.01	0.09	0.01	0.05	0.78	0.26	0.74	40.04
HY-43-11-3	0.01	1.96	3.67	42.49	8.28	0.24	2.75	0.05	0.03	0.01	0.56	0.75	0.02	0.08	0.00	0.05			0.18	38.86

Samples	Na_2O	MgO	Al_2O_3	SiO_2	P_2O_5	K_2O	CaO	TiO_2	V_2O_5	MnO	Fe_2O_3	CoO	NiO	CuO	ZnO	SrO	SnO_2	Sb_2O_5	BaO	PbO
HY-43-11-4	0.01	3.05	9.11	27.82	20.68	0.60	6.51	0.40	0.06	0.02	1.10	0.45	0.01	0.10	0.00	0.05			0.00	30.04
HY-43-17-1	0.01	0.28	5.48	25.33	23.00	0.42	6.53	0.18	0.05	0.03	1.20	0.34	0.01	0.12	0.00	0.05			0.05	36.91
HY-43-17-2	0.01	1.30	4.97	29.51	18.77	0.44	6.00	0.15	0.05	0.02	1.25	0.42	0.01	0.13	0.00	0.05			0.11	36.81
HY-43-18-1	1.59	2.48	5.66	26.70	20.97	0.67	7.81	0.31	0.06	0.02	1.75	0.30	0.01	0.06	0.00	0.05			0.12	31.45
HY-43-18-2	0.01	1.91	4.28	24.95	21.48	0.26	6.15	0.17	0.05	0.02	0.86	0.35	0.01	0.11	0.00	0.06			0.01	39.35
HY-43-19-1	0.01	2.62	8.23	37.03	14.26	1.28	8.53	0.66	0.06	0.02	2.32	0.10	0.00	0.04	0.00	0.05			0.00	24.78
HY-43-19-2	0.01	0.70	5.41	26.06	22.98	0.70	9.22	0.36	0.07	0.03	1.91	0.19	0.01	0.07	0.00	0.06			0.06	32.16
HY-43-20-2	0.01	2.27	5.37	26.37	20.38	0.57	9.61	0.18	0.05	0.02	1.29	0.52	0.01	0.08	0.00	0.04			0.09	33.14
HY-43-20-2	0.01	0.01	4.30	23.64	26.40	0.53	8.53	0.21	0.05	0.01	1.22	0.29	0.00	0.09	0.00	0.05			0.03	34.61
HY-43-22-1	0.42	1.39	6.00	31.10	17.15	0.80	13.97	0.27	0.04	0.02	1.71	0.18	0.00	0.04	0.00	0.06			0.03	26.81
HY-43-22-2	1.43	1.15	3.31	37.64	12.75	0.26	3.82	0.10	0.03	0.03	0.77	0.54	0.02	0.08	0.00	0.05			0.12	37.91
HY-43-22-3	0.01	2.66	8.48	35.57	14.80	1.10	11.00	0.32	0.04	0.02	1.88	0.20	0.00	0.04	0.00	0.05			0.03	23.78
HY-43-22-4	1.68	0.02	3.56	36.89	14.81	0.22	3.78	0.09	0.03	0.02	0.76	0.60	0.02	0.09	0.01	0.05			0.09	37.27

Samples	Na_2O	MgO	Al_2O_3	SiO_2	P_2O_5	K_2O	CaO	TiO_2	V_2O_5	MnO	Fe_2O_3	CoO	NiO	CuO	ZnO	SrO	SnO_2	Sb_2O_5	BaO	PbO
HY-43-25-1	0.88	2.89	8.30	40.77	11.75	1.38	8.73	0.39	0.05	0.05	2.57	0.31	0.01	0.04	0.00	0.05			0.07	21.75
HY-43-25-2	0.01	2.52	7.94	36.93	16.07	1.08	7.41	0.27	0.04	0.02	2.03	0.17	0.00	0.04	0.00	0.05			0.00	25.40
HY-43-28-1	0.01	0.45	5.99	30.18	16.88	0.84	13.55	0.31	0.04	0.03	2.22	0.13	0.00	0.08	0.00	0.06			0.01	29.22
HY-43-28-2	0.01	2.22	5.06	22.29	17.40	0.53	16.57	0.28	0.06	0.02	1.65	0.21	0.00	0.07	0.00	0.06			0.03	33.53
HY-43-29-1	0.01	0.48	4.13	24.06	27.46	0.54	7.78	0.15	0.04	0.02	1.16	0.23	0.00	0.08	0.00	0.06			0.04	33.76
HY-43-29-2	0.01	1.96	4.74	26.76	23.50	0.44	8.62	0.19	0.06	0.02	1.30	0.25	0.01	0.10	0.00	0.06			0.02	31.97
HY-43-30-1	0.01	3.29	6.40	29.57	19.80	0.74	9.36	0.24	0.04	0.03	1.59	0.20	0.00	0.06	0.00	0.06			0.13	28.48
HY-43-20-2	0.23	1.66	5.47	24.38	19.22	0.64	13.86	0.22	0.05	0.02	1.35	0.16	0.00	0.39	0.00	0.07			0.02	32.25
HY-43-32-1	0.01	1.42	4.66	20.61	28.14	0.48	10.21	0.24	0.08	0.03	1.75	0.17	0.00	0.23	0.00	0.06			0.08	31.83
HY-43-32-2	0.95	2.74	4.30	22.32	26.57	0.57	10.49	0.17	0.04	0.02	1.45	0.18	0.00	0.12	0.00	0.06			0.09	29.93
Mean	0.60	1.37	5.46	31.11	17.38	0.58	7.64	0.24	0.05	0.02	1.33	0.35	0.01	0.10	0.00	0.05	0.89	0.07	0.25	33.14

Appendix 12 Chemical compositions of special samples

Samples	Na_2O	MgO	Al_2O_3	SiO_2	P_2O_5	K_2O	CaO	TiO_2	V_2O_5	MnO	Fe_2O_3	CoO	NiO	CuO	ZnO	SrO	SnO_2	Sb_2O_5	BaO	PbO
HY-122-1-1	0.01	2.73	16.77	63.06	0.11	4.22	5.42	0.83	0.06	0.10	6.55	0.04	0.00	0.00	0.01	0.04				0.03
HY-122-1-2	0.01	4.46	16.79	61.83	0.18	4.06	5.11	0.90	0.05	0.11	6.37	0.04	0.00	0.00	0.01	0.04				0.04
HY-124-1-1	0.02	4.68	16.66	59.45	0.21	3.49	8.95	1.11	0.06	0.08	5.07	0.02	0.00	0.00	0.01	0.04			0.07	0.07
HY-124-1-2	0.07	4.84	16.84	60.33	0.19	3.45	8.15	1.07	0.05	0.07	4.72	0.02	0.00	0.00	0.01	0.04			0.08	0.06
HY-126-1-1	0.01	2.45	26.38	55.56	0.35	3.64	7.50	1.23	0.06	0.02	2.43	0.01	0.00	0.01	0.01	0.03			0.12	0.18
HY-126-1-2	0.01	2.79	24.99	56.28	0.35	3.47	8.15	1.06	0.05	0.03	2.51	0.01	0.00	0.00	0.01	0.03			0.10	0.15
HY-133-1-1	0.01	3.25	20.96	39.42	2.27	3.69	6.40	1.25	0.09	0.12	21.75	0.09	0.00	0.01	0.00	0.02			0.35	0.30
HY-133-1-2	0.01	2.33	21.21	39.11	2.07	3.36	8.49	1.24	0.10	0.11	21.27	0.08	0.00	0.01	0.01	0.02			0.29	0.29
HY-134-1-1	0.11	2.99	14.35	61.70	0.46	4.47	10.41	0.70	0.04	0.07	4.56	0.03	0.00	0.00	0.01	0.02			0.05	0.01
HY-134-1-2	0.18	2.47	14.99	62.63	0.29	4.46	8.76	0.71	0.04	0.07	5.30	0.03	0.00	0.00	0.01	0.03			0.00	0.03
HY-137-1-1	0.01	1.34	33.42	53.86	0.18	2.64	2.22	1.43	0.07	0.02	4.55	0.02	0.00	0.01	0.01	0.02			0.17	0.04
HY-137-1-2	0.10	1.35	30.96	54.77	0.23	2.78	2.66	1.57	0.08	0.03	5.26	0.02	0.00	0.00	0.01	0.02			0.10	0.05

Samples	Na_2O	MgO	Al_2O_3	SiO_2	P_2O_5	K_2O	CaO	TiO_2	V_2O_5	MnO	Fe_2O_3	CoO	NiO	CuO	ZnO	SrO	SnO_2	Sb_2O_5	BaO	PbO
HY-138-1-1	0.01	3.40	26.14	52.11	2.79	3.90	5.23	1.24	0.06	0.04	4.15	0.02	0.00	0.00	0.01	0.02			0.10	0.80
HY-138-1-2	0.42	3.16	31.39	51.74	0.39	3.66	3.64	1.20	0.06	0.03	3.33	0.01	0.00	0.00	0.01	0.02			0.19	0.77
HY-138-2-1	0.01	2.69	25.31	57.34	1.25	2.51	5.47	1.01	0.07	0.03	2.56	0.01	0.00	0.01	0.01	0.01			0.08	1.64
HY-138-2-2	0.34	3.26	23.81	56.00	0.85	2.83	7.25	1.05	0.07	0.03	2.60	0.01	0.00	0.01	0.01	0.02			0.01	1.87
HY-139-1-1	0.01	5.86	14.34	53.87	0.37	3.78	14.49	0.93	0.04	0.09	5.69	0.02	0.00	0.00	0.01	0.03			0.09	0.37
HY-139-1-2	0.36	7.56	13.68	54.97	0.29	3.79	13.06	0.83	0.03	0.08	4.97	0.02	0.00	0.00	0.01	0.02			0.05	0.27
HY-139-2-1	0.01	5.50	15.67	58.57	0.42	5.35	9.39	0.83	0.06	0.06	3.78	0.01	0.00	0.00	0.01	0.02			0.13	0.19
HY-139-2-2	0.49	6.71	15.89	57.04	0.44	5.02	9.24	0.83	0.05	0.05	3.89	0.01	0.00	0.00	0.01	0.02			0.06	0.25
HY-139-3-1	0.23	4.07	20.40	60.15	0.31	4.08	6.61	1.00	0.05	0.04	2.74	0.01	0.00	0.00	0.01	0.02			0.11	0.18
HY-139-3-2	0.94	3.52	23.34	58.03	0.12	4.26	5.86	1.07	0.05	0.03	2.47	0.01	0.00	0.00	0.01	0.02			0.14	0.12
HY-139-4-1	0.01	8.43	14.45	56.66	0.38	4.95	10.36	0.82	0.05	0.06	3.57	0.01	0.00	0.00	0.01	0.02			0.00	0.23
HY-139-4-2	0.01	8.52	15.00	56.06	0.31	4.72	10.27	0.83	0.06	0.07	3.76	0.01	0.00	0.00	0.01	0.02			0.14	0.21
HY-140-1-1	0.72	3.67	15.48	62.05	0.17	4.19	7.62	0.81	0.04	0.08	4.85	0.02	0.00	0.00	0.02	0.02			0.00	0.25

Samples	Na_2O	MgO	Al_2O_3	SiO_2	P_2O_5	K_2O	CaO	TiO_2	V_2O_5	MnO	Fe_2O_3	CoO	NiO	CuO	ZnO	SrO	SnO_2	Sb_2O_5	BaO	PbO
HY-140-1-2	0.01	3.83	15.78	62.38	0.30	4.22	7.42	0.78	0.06	0.07	4.87	0.02	0.00	0.00	0.01	0.02			0.00	0.22
HY-147-1-1	0.92	1.87	30.76	52.96	0.41	6.12	2.68	1.12	0.07	0.01	1.75	0.01	0.00	0.01	0.01	0.02			0.07	1.21
HY-147-1-2	0.05	3.29	26.18	54.70	0.89	5.89	4.26	1.05	0.07	0.02	2.16	0.01	0.00	0.01	0.02	0.02			0.05	1.32
HY-148-2-1	0.22	5.35	12.96	60.50	3.07	2.80	7.26	0.84	0.05	0.09	6.51	0.02	0.00	0.00	0.01	0.02			0.00	0.28
HY-148-2-2	0.01	6.84	11.24	56.35	4.98	2.80	8.61	0.75	0.04	0.10	7.17	0.03	0.00	0.01	0.00	0.03			0.11	0.92
HY-148-3-1	0.41	6.24	14.08	57.54	2.62	3.54	9.33	0.70	0.04	0.09	5.08	0.02	0.00	0.01	0.00	0.02			0.07	0.20
HY-148-3-2	0.01	6.01	13.81	56.95	3.82	3.50	9.87	0.73	0.04	0.08	4.87	0.02	0.00	0.01	0.00	0.02			0.00	0.27
HY-148-4-1	0.01	1.93	11.47	27.02	35.10	1.57	16.21	0.58	0.03	0.02	2.71	0.01	0.00	0.01	0.01	0.03			0.10	3.19
HY-148-4-2	0.01	1.97	12.03	27.40	34.95	1.68	15.31	0.66	0.04	0.03	2.56	0.01	0.00	0.01	0.01	0.03			0.08	3.24
HY-149-1-1	0.05	4.85	25.70	52.21	0.60	5.89	7.28	1.26	0.06	0.02	1.82	0.01	0.00	0.00	0.01	0.02			0.17	0.04
HY-149-1-2	0.67	3.27	25.87	52.48	0.53	5.76	7.68	1.22	0.06	0.02	2.17	0.01	0.00	0.00	0.02	0.02			0.16	0.05
HY-151-1-1	0.37	1.90	32.54	52.44	0.12	7.79	2.27	1.16	0.05	0.01	1.14	0.01	0.00	0.00	0.01	0.02			0.14	0.01
HY-151-1-2	0.01	1.89	31.42	52.70	0.13	8.19	2.92	1.17	0.06	0.01	1.28	0.01	0.00	0.00	0.01	0.02			0.20	0.01

Samples	Na_2O	MgO	Al_2O_3	SiO_2	P_2O_5	K_2O	CaO	TiO_2	V_2O_5	MnO	Fe_2O_3	CoO	NiO	CuO	ZnO	SrO	SnO_2	Sb_2O_5	BaO	PbO
HY-155-1-1	0.01	3.72	6.50	17.10	2.01	1.21	68.17	0.19	0.01	0.01	0.80	0.00	0.00	0.00	0.00	0.03			0.02	0.21
HY-155-1-2	0.07	2.82	5.31	15.48	1.35	1.06	72.68	0.15	0.01	0.02	0.73	0.00	0.00	0.00	0.00	0.04			0.03	0.24
HY-116-wg-1	0.01	0.01	7.15	71.15	0.00	0.45	0.48	0.25	0.00	0.00	0.21	0.01	0.00	0.02	0.00	0.02			0.06	20.19
HY-116-wg-2	0.14	0.24	8.60	67.65	0.00	0.54	0.44	0.30	0.01	0.00	0.25	0.00	0.00	0.02	0.00	0.02			0.00	21.79
HY-188-wg-1	0.55	1.60	14.27	62.28	0.05	6.40	1.25	0.11	0.01	0.00	0.17	0.00		0.00	0.00	0.01	0.16	0.02	0.19	12.92
HY-188-wg-2	0.01	2.01	14.28	61.76	0.00	6.35	1.35	0.12	0.00	0.00	0.15	0.00	0.00	0.00		0.01	0.17	0.04	0.25	13.50

Appendix 13 Chemical compositions of slips

Samples	Na_2O	MgO	Al_2O_3	SiO_2	P_2O_5	K_2O	CaO	TiO_2	V_2O_5	MnO	Fe_2O_3	CoO	NiO	CuO	ZnO	SrO	SnO_2	Sb_2O_5	BaO	PbO
HY-101-s-1	2.75	0.45	30.78	55.58	0.22	7.88	0.08	1.19	0.07	0.00	0.67	0.00	0.00	0.00	0.01	0.02			0.13	0.18
HY-101-s-2	2.27	0.15	31.04	56.18	0.10	7.97	0.12	1.14	0.06	0.00	0.68	0.01	0.00	0.00	0.01	0.02			0.14	0.09
HY-115-s-1	0.01	0.46	33.28	54.88	0.08	5.45	2.54	1.26	0.06	0.01	1.74	0.01	0.00	0.00	0.02	0.04			0.06	0.09
HY-115-s-2	0.43	0.24	33.28	55.55	0.00	4.91	2.06	1.42	0.07	0.01	1.79	0.01	0.00	0.00	0.02	0.04			0.06	0.09
HY-116-s-1	0.01	0.01	31.74	54.28	0.00	1.86	1.30	1.36	0.07	0.01	0.92	0.01	0.00	0.00	0.01	0.03			0.09	8.30
HY-116-s-2	0.17	0.76	34.66	53.66	0.00	1.85	1.42	1.45	0.07	0.00	0.85	0.01	0.00	0.00	0.01	0.02			0.06	5.00
HY-117-s-1	0.45	0.01	32.30	54.88	0.82	6.24	1.28	1.42	0.10	0.00	0.73	0.01	0.00	0.00	0.02	0.03			0.11	1.60
HY-117-s-2	0.01	0.01	33.47	53.93	0.93	6.68	1.19	1.60	0.11	0.00	0.75	0.01	0.00	0.00	0.02	0.03			0.08	1.18
HY-118-s-1	0.01	0.10	35.49	54.33	0.61	5.28	0.51	1.55	0.10	0.00	0.74	0.01	0.00	0.00	0.02	0.02			0.09	1.15
HY-118-s-2	0.01	0.21	33.69	53.27	1.49	6.49	0.80	1.60	0.11	0.00	0.73	0.01	0.00	0.00	0.03	0.03			0.06	1.47
HY-119-s-1	0.02	0.01	35.85	57.84	0.27	2.36	1.16	1.47	0.08	0.01	0.68	0.00	0.00	0.00	0.01	0.03			0.16	0.08
HY-119-s-2	0.19	0.29	34.35	58.53	0.48	2.33	1.33	1.51	0.09	0.00	0.67	0.00	0.00	0.00	0.01	0.03			0.08	0.10

Samples	Na_2O	MgO	Al_2O_3	SiO_2	P_2O_5	K_2O	CaO	TiO_2	V_2O_5	MnO	Fe_2O_3	CoO	NiO	CuO	ZnO	SrO	SnO_2	Sb_2O_5	BaO	PbO
HY-130-s-1	0.01	0.62	35.96	54.34	0.45	2.69	0.95	1.32	0.18	0.01	1.27	0.01	0.00	0.00	0.01	0.04			0.14	2.00
HY-130-s-2	0.01	0.32	36.41	54.25	0.54	2.68	1.09	1.34	0.16	0.00	1.24	0.01	0.00	0.00	0.01	0.04			0.11	1.81
HY-131-s-1	0.01	1.09	31.08	54.68	0.73	6.45	2.57	1.46	0.10	0.01	1.31	0.01	0.00	0.00	0.03	0.04			0.19	0.23
HY-131-s-2	0.01	0.12	33.88	55.52	0.21	5.66	1.44	1.31	0.08	0.01	1.32	0.01	0.00	0.00	0.02	0.03			0.18	0.19
HY-137-s-1	0.01	1.00	32.68	56.76	0.12	4.68	2.78	1.02	0.05	0.01	0.65	0.00	0.00	0.01	0.01	0.01			0.15	0.05
HY-137-s-2	0.28	2.13	30.96	56.35	0.20	5.20	2.75	1.03	0.05	0.01	0.81	0.00	0.00	0.00	0.01	0.01			0.13	0.06
HY-141-s-1	1.35	0.55	28.02	58.30	0.09	6.56	2.70	1.24	0.06	0.01	0.94	0.00	0.00	0.00	0.01	0.02			0.09	0.07
HY-141-s-2	0.76	0.40	32.32	57.82	0.07	4.39	1.68	1.26	0.06	0.00	1.00	0.00	0.00	0.00	0.01	0.02			0.13	0.05
HY-143-s-1	0.17	0.47	34.51	57.52	0.00	3.12	0.72	1.07	0.06	0.00	0.60	0.01	0.00	0.00	0.01	0.01			0.11	1.61
HY-143-s-2	0.01	0.75	34.07	56.89	0.05	3.26	1.17	1.15	0.06	0.00	0.65	0.00	0.00	0.00	0.01	0.01			0.14	1.79
HY-146-s-1	0.01	1.13	35.47	53.93	1.58	3.01	1.86	1.23	0.08	0.01	1.47	0.01	0.00	0.00	0.02	0.02			0.08	0.10
HY-146-s-2	0.39	0.42	36.47	55.15	1.01	2.67	1.06	1.20	0.06	0.01	1.34	0.01	0.00	0.00	0.01	0.02			0.10	0.08
HY-151-s-1	2.82	1.16	34.01	53.67	0.05	5.95	0.17	1.04	0.05	0.00	0.96	0.00	0.00	0.00	0.01	0.02			0.09	0.01

Samples	Na_2O	MgO	Al_2O_3	SiO_2	P_2O_5	K_2O	CaO	TiO_2	V_2O_5	MnO	Fe_2O_3	CoO	NiO	CuO	ZnO	SrO	SnO_2	Sb_2O_5	BaO	PbO
HY-151-s-2	1.51	0.06	34.79	55.20	0.04	6.20	0.15	1.01	0.05	0.00	0.83	0.00	0.00	0.00	0.01	0.01			0.11	0.02
HY-153-s-1	0.47	0.70	36.75	57.45	0.04	1.87	0.40	1.27	0.08	0.00	0.65	0.01	0.00	0.00	0.00	0.01			0.18	0.10
HY-153-s-2	0.01	0.57	37.31	57.32	0.02	1.98	0.39	1.28	0.07	0.00	0.77	0.01	0.00	0.00	0.00	0.02			0.15	0.11
HY-154-s-1	0.26	0.50	36.96	56.71	0.00	2.00	1.01	1.26	0.07	0.01	0.87	0.01	0.00	0.00	0.01	0.02			0.26	0.06
HY-154-s-2	0.01	0.32	36.61	57.16	0.02	2.07	1.28	1.30	0.07	0.00	0.87	0.01	0.00	0.00	0.01	0.02			0.18	0.07
HY-155-s-1	0.00	2.60	32.69	55.76	0.05	3.44	2.78	1.30	0.06	0.01	1.01	0.01	0.00	0.00	0.00	0.02			0.14	0.11
HY-155-s-2	0.01	1.43	31.27	53.94	0.13	3.63	6.95	1.26	0.07	0.00	1.07	0.01	0.00	0.00	0.00	0.02			0.09	0.11
HY-166-s-1	0.01	0.35	36.14	56.03	0.02	2.69	1.52	1.27	0.07	0.01	1.23	0.01	0.00	0.03	0.01	0.02			0.03	0.58
HY-166-s-2	0.01	0.39	36.42	56.17	0.02	2.64	1.05	1.34	0.07	0.01	1.23	0.01	0.00	0.01	0.01	0.01			0.08	0.54